


THE UNIVERSITY *of* EDINBURGH

This thesis has been submitted in fulfilment of the requirements for a postgraduate degree (e. g. PhD, MPhil, DClinPsychol) at the University of Edinburgh. Please note the following terms and conditions of use:

- This work is protected by copyright and other intellectual property rights, which are retained by the thesis author, unless otherwise stated.
- A copy can be downloaded for personal non-commercial research or study, without prior permission or charge.
- This thesis cannot be reproduced or quoted extensively from without first obtaining permission in writing from the author.
- The content must not be changed in any way or sold commercially in any format or medium without the formal permission of the author.
- When referring to this work, full bibliographic details including the author, title, awarding institution and date of the thesis must be given.

# The Rise of Placental Mammals: The Anatomy and Phylogeny of the South American Native Ungulates with a Focus in the Order Litopterna

**Hans P. Püschel**




Thesis submitted for the degree of Doctor of Philosophy

School of Geosciences

University of Edinburgh

**2023**

## Fósiles

*Dinosaurios*
La glacial ceniza arponea de pie el páramo
pero en el parpadeo ingrávido de las plumas
y las pesadas extremidades se enraízan
huesos que duran como divinidades

Sin prisa el frío rueda en el espacio
las nubes gritan en silencio calcinadas
musgos hambrientos devoran el terror del reptil
mientras las piedras esquivan los rayos del sol

*Mamíferos*
A tientas se sueña a sí misma la vida
en la honda noche del tiempo echan pelo los árboles
cambian la voz las estrellas como dientes todavía no nacidos
lo invisible olfatea en los caminos su lugar entre las cosas

En el humo unos pasos rasgan pronto la placenta del aire
una criatura que aún apenas tiene nombre trama
sin saberlo una cosmogonía desenfrenada
calladamente el crujido de una rama multiplica al mundo

*Humanos*
Los cielos se han colmado de figuras
en la gruta del oído se pinta el canto de dioses o de pájaros
los animales de palabras cambian como los bosques bajo el fuego
y donde solo había una choza la agitación de gentes innumerables

El sol llueve afilado como las dagas del arado
semidormidos sepulcros se desvisten bajo el hielo fundido
y en el barro disuelto piedra de la que un día también asomaremos
un murmullo intemporal de helechos movidos por el viento

Stephan Puschel

17/05/2022

Florida, BioBío

## Fossils

*Dinosaurs*
The glacial ash harpoons the moor
but in the weightless blink of feathers
and heavy extremities bones everlasting
as deities set down roots

The cold wheels through space unhurried
the clouds, charred, scream in silence
starving mosses devour the reptile's terror
while the rocks dodge the sun's rays

*Mammals*
Blindly life dreams herself into being
in the deep night of time trees put out hairs
the stars' voices change like unborn teeth
the invisible sniffs along the paths for its place among things

In the smoke, steps quickly rip through the placenta of the air
a creature which has hardly yet been named plots
unaware a wild cosmogony
quietly the snap of a branch multiplies the world

*Humans*
The heavens have overflowed with figures
in the cave of the ear the song of gods or of birds is painted
the animals of words change like the forests under the fire
and where there once was only a hut the tumult of innumerable people

The sun rains sharp like a plow's daggers
half-asleep tombs undress under the molten ice
and in the dissolved mud, rock from which we one day will also surface
a timeless murmur of ferns moved by the wind

Stephan Puschel

17/05/2022

Florida, BioBío

# Abstract

Placentals are the most preeminent mammalian lineage today in terms of diversity and distribution over the world, having over 6000 recognised extant and recently extinct species. The timing for the origin and diversification of Placentalia, and its relationship with the Cretaceous-Palaeogene (K/Pg) mass extinction event, is one of the key questions in palaeontology. Different hypotheses have been proposed over the years for the inter and intraordinal diversification of placentals, each one with a distinct time and a rate component that make them identifiable if tested. Testing these hypotheses has been hindered by the limited knowledge of the "archaic" Palaeogene placental mammals that lived after the K/Pg mass extinction event. Among "archaic" Palaeogene mammals from different landmasses, those from South America stand out because of their particular biogeographic history. Indeed, it is only after the K/Pg mass extinction event that eutherians are found in the South American fossil record, probably the result of crossing in a single or multiple events from North America in the latest Cretaceous or early Palaeogene. Among these mammalian immigrants, there were placentals that gave rise to endemic groups, including Xenarthra and five or maybe six ancient "ungulate" orders known as the South American Native Ungulates (SANUs): Xenungulata, Notoungulata, Litopterna, Pyrotheria, Astrapotheria, and Notopterna (the latter usually included within Litopterna). SANUs were first discovered by Charles Darwin in the 19$^{th}$ century who immediately was puzzled by their bizarre anatomy, a feeling shared by Richard Owen one of the most prominent comparative anatomists of all time. To these "ungulate" orders a couple of families/subfamilies of "condylarths" (i.e., a wastebasket group of "archaic" ungulates) can be added: Didolodontidae, traditionally linked to Litopterna, and Kollpaninae, considered to be part of Mioclaenidae, a group of primitive ungulates otherwise known from North America. Interestingly, two SANUs orders, Litopterna and Astrapotheria, crossed from South America to Antarctica probably at some point between the late Palaeocene and the early Eocene.

The phylogenetic position of the SANUs in the placental tree has been controversial over the years, but recently thanks to molecular evidence it was determined that Notoungulata and Litopterna are sister taxa, and that both are closely related to Perissodactyla (the odd-toed hoofed mammal group including horses and rhinos). However, how the rest of SANUs fit in the placental tree, and if SANUs effectively form a monophyletic group (i.e., Meridiungulata)

are still open questions. In order to resolve the affinities of SANUs in the placental tree and the timing of their diversification, we first have to understand and determine the composition and affinities of each one of the SANU orders. Much research attention has been already given to the most diverse SANU order, Notoungulata, in detriment of the second most diverse order, Litopterna. Therefore, the main goal of this thesis is to determine the interfamilial relationships within Litopterna and the timing of its familial diversification. In order to achieve this goal, a deep understanding of modern phylogenetic methods and litoptern anatomy must be marshalled.

Therefore, in Chapter 2 I first applied cutting-edge Bayesian phylogenetic methods to a case study, estimating the divergence-times of hominins and exploring trends in human evolution. Quantifying speciation times during evolution is fundamental as it provides a timescale to test for the correlation between key evolutionary transitions and extrinsic factors like climatic or environmental change. I applied a Total Evidence Dating approach for the first time to a hominin phylogeny to estimate divergence times under different topological hypotheses. The time scaled phylogenies were subsequently used to perform ancestral state reconstruction of body mass and phylogenetic encephalization quotient (PEQ), an index that determines relative brain size considering body mass and phylogeny. The divergence time estimates are consistent with other recent studies that analysed extant species. The origin of *Homo* most likely occurred between 4.30 and 2.56 Ma. The ancestral state reconstructions show a general trend towards a smaller body mass before the emergence of *Homo*, followed by a trend towards a greater body mass within *Homo*. PEQ estimations display a general trend of gradual but accelerating evolution of larger brain sizes relative to body sizes over time (i.e., encephalization). The obtained results provide a rigorous temporal framework for human evolution. In addition, this chapter allowed me to test the impact that different interpretations of the phylogenetic affinities of a lineage have in the divergence-time estimations for the different species within that lineage, which is particularly important in the phylogeny of litopterns considering how uncertain their early affinities are.

In Chapter 3 I describe a new macraucheniine macraucheniid litoptern, *Micrauchenia saladensis* gen. et sp. nov. from the late Miocene (Huayquerian SALMA) and applied some of the phylogenetic methods described in chapter 2 to this important litoptern family, the Macraucheniidae. *Micrauchenia saladensis* is the first litoptern from the Bahía Inglesa Formation, Chile. The specimen includes a partial mandible, cervical and thoracic vertebrae fragments, and portions of the forelimbs (a scapula fragment, an ulna-radius fragment, seven

carpals, three metapodials, two proximal phalanges and four intermediate phalanges). The postcranial anatomy of *Micrauchenia saladensis* is consistent with terrestrial and cursorial locomotion, which suggests an allochthonous position of this specimen within the marine Bahía Inglesa Formation. The fusion of the ulna and radius and the presence of a radial aliform expansion aligns *Micrauchenia* with other macraucheniines, with which it shares these features. The fusion of the ulna and radius is interpreted as a cursorial specialisation, and the aliform expansion as an adaptation for strong flexion movements and to resist higher transverse stresses during locomotion. In addition, *Micrauchenia saladensis* is the smallest member of the subfamily Macraucheniinae. To test the systematics and phylogenetics of this new species, previously published morphological matrices of macraucheniids were expanded by adding one dental and eight postcranial characters, and scoring *Micrauchenia saladensis*. I performed maximum parsimony and Bayesian phylogenetic analyses, the latter applied for the first time in a macraucheniid phylogeny. These analyses confirm *Micrauchenia saladensis* as a member of the subfamily Macraucheniinae, although with uncertain affinities within this subfamily.

Finally, in Chapter 4 I addressed the monophyly, interfamilial relationships and timing of the familial diversification of the order Litopterna with phylogenetic methods. Based on a large collaborative matrix currently being built by the Palaeocene Mammal Working Group for exploring the affinities within Placentalia, I built a new morphological matrix with 954 dental and mandibular characters, that included the more complete and earliest members of the five well-established litoptern families: Adianthidae, Anisolambdidae, Macraucheniidae, Proterotheriidae and Sparnotheriodontidae. I also included families with controversial affinities and sometimes considered to be part of Litopterna: Protolipternidae, Indaleciidae, and Notonychopidae. The last two are often grouped as members of the order Notopterna. In addition, I included North American mioclaenids, South American kollpanines and didolodontids, and early members of the SANU orders Notoungulata, Xenungulata and Astrapotheria. I conducted maximum parsimony and undated and tip-dated Bayesian phylogenetic analyses. The obtained trees from the various analyses mostly agree showing protolipternids, didolodontids and kollpanines at the stem of a monophyletic group composed of the SANU orders, and finding Litopterna as monophyletic group composed of the families Adianthidae, Anisolambdidae, Macraucheniidae, Proterotheriidae and Sparnotheriodontidae. The trees differ in the position of the group formed by Indaleciidae and Notonychopidae, which is sometimes closely related to Litopterna and at other times closely related to Notoungulata, and also in the precise interfamilial affinities of Adianthidae and Macraucheniidae within

Litopterna. The tip-dated Bayesian tree suggests that the migration from North America occurred in the earliest Palaeocene, the origin of Litopterna was in the late Palaeocene, and the migration of litopterns to Antarctica occurred in the early to middle Eocene. These results suggest that (1) didolodontids, protolipternids and kollpanines should be considered early SANUs, but not particularly closely related to any order, (2) considering the uncertainty in the exact position of the monophyletic group formed by Indaleciidae and Notonychopidae, these families should be excluded from Litopterna and potentially grouped in the order Notopterna as previously proposed, and (3) Litopterna is composed of five families (i.e., Adianthidae, Anisolambdidae, Macraucheniidae, Proterotheriidae and Sparnotheriodontidae) which form a monophyletic unit with an origin probably in the early Palaeocene.

Overall, this thesis provides new insights about the tempo and mode of evolution of placental mammals through the use of cutting-edge phylogenetic methods. Crucially, this thesis as a whole represents a major step in our understanding of the anatomy and phylogenetic affinities of Darwin's enigmatic South American ungulates.

# Lay summary

Mammals are ubiquitous and a key component in our modern fauna, being extremely diverse in terms of body size, locomotion and mode of life. They occupy a diverse array of ecological niches and are present on every continent on Earth. Among different mammalian lineages, placentals (i.e., mammals carrying the foetus for an extended period of development so as to give birth to relatively well-developed young) are particularly diverse, having over 6000 recognized extant and recently extinct species. However, mammals were smaller and filled a limited range of niches before the asteroid impact that ~66 Ma marked the Cretaceous-Palaeogene (K/Pg) boundary and a mass extinction event that wiped out non-avian dinosaurs, among other lineages. It was only after this event that placentals fully diversified and filled the empty niches left by non-avian dinosaurs. The exact timing of this diversification and the evolutionary relationships of the different placental orders is hindered by our limited knowledge of the "archaic" placentals that evolved during the first ~10 – 15 Ma of the Palaeogene. Among the different continents, South America stands out because placentals seem to have arrived around K/Pg boundary probably from North America, giving rise to peculiar endemic placental groups, including Xenarthra (encompasses modern sloths, anteaters and armadillos) and five or maybe six currently extinct ancient "ungulate" (hooved) orders known as the South American Native Ungulates (SANUs): Xenungulata, Notoungulata, Litopterna, Pyrotheria, Astrapotheria, and Notopterna (usually included within Litopterna). SANUs were first discovered by Charles Darwin in the 19$^{th}$ century who immediately was puzzled by their bizarre anatomy, a feeling shared by Richard Owen one of the most prominent comparative anatomists of all time. To these orders of SANUs, the families of "archaic" ungulates Didolodontidae and Kollpaninae of uncertain affinities can be added. Among SANUs, litopterns and astrapotheres are also known to have reached Antarctica during the Palaeogene at least ~55 Ma.

Thanks to recent studies of DNA and other molecular evidence remarkably preserved in fossils, we know that litopterns and notoungulates were closely related to perissodactyls, a group that includes modern horses, tapirs and rhinos. However, these studies did not clarify the evolutionary relationships of the other four SANU orders, so the relationships of most SANUs in the placental tree are still controversial and it is still an open question if SANUs form a single major group or a series of distantly related lineages. In order to understand the diversification

of SANUs and its timing, we also have to understand the species that compose each SANU order and their affinities. In this thesis I focused in the order Litopterna with the objective of resolving the family tree and origin times of this group.

In the first chapter of my thesis, I concentrated on testing cutting-edge phylogenetic methods in a placental case study, the human evolutionary tree. I estimated the timing of divergence of the different species that form part of the human lineage (hominins) and explored trends in body size and encephalization (i.e., how brain size scales with respect to body size) in human evolution. I applied a tip-dating Bayesian method that allows the incorporation of molecular, morphological and stratigraphic data of extinct and extant species directly (i.e., as tips in the tree) in order to estimate these divergence-times in different hypotheses for the affinities of controversial hominins. I also used algorithms that allowed the ancestral state reconstruction of body size and encephalization. Among other divergence events, I was able to determine that the origin of our genus, the genus *Homo*, most likely occurred between 4.30 and 2.56 Ma. I also determined that before the emergence of *Homo* there was a general trend towards a smaller body mass among hominins, whilst after the emergence, there was a trend towards a greater body mass. In contrast, relative brain size showed a general trend of gradual but accelerating increases over human evolution.

In my second chapter, I examined the anatomy of litopterns and applied similar phylogenetic methods to the litoptern family Macraucheniidae. Macraucheniidae owns its name to *Macrauchenia* (“big neck" in Greek) discovered by Darwin and described by Owen, which convergently resembles a large camel due to its elongated neck, a feature shared by other members of the family. I describe a new macraucheniid *Micrauchenia saladensis* gen. et sp. nov. from ~ 8 – 6 Ma (late Miocene) from the marine Bahía Inglesa Formation, Chile, being the first litoptern described for that formation and among the smallest macraucheniids known. The specimen included a partial mandible, but mostly postcranial elements, in particular vertebrae from the neck and thorax, and elements of the forelimbs. The anatomy of *M. saladensis* is consistent with a terrestrial and cursorial locomotion (i.e, adapted to run) which suggests that the specimen incidentally arrived to its place of deposition in this marine formation. I also investigated the evolutionary relationships of *M. saladensis* by expanding previous datasets by adding postcranial characters and performing different phylogenetic analyses. *Micrauchenia saladensis* was recovered consistently among a subfamily of the most derived macraucheniids (Macraucheniinae), although with uncertain affinities within this subfamily.

In the third chapter of my thesis, I focused on resolving the evolutionary relationships of early litopterns and determining the time they originated by using similar phylogenetic methods as those exposed in the previous two chapters. I first built a new morphological matrix that incorporated dental and mandibular anatomical data that I collected by making detailed observations on specimens in museum collections around the world. The matrix of data primarily included early litopterns from different families, but it also incorporated early members of all other orders of SANUs (except Pyrotheria), "archaic" ungulates from South America such as didolodontids and kollpaniines, and also some "archaic" ungulates from North America that have been previously linked with SANUs. I conducted different phylogenetic analyses including tip-dating finding Litopterna consistently as a monophyletic group composed of the families Adianthidae, Anisolambdidae, Macraucheniidae, Proterotheriidae and Sparnotheriodontidae. Didolodontids and kollpaniines were not found as a component of this order, being early divergent lineages that are closely related to all SANUs orders, but not to any in specific. The results of the tip-dating analyses showed that the migration of SANUs from North America most likely occurred just after K/Pg mass extinction, the origin of Litopterna was during the Palaeogene at ~ 57.3 Ma, and that the migration of litopterns to Antarctica occurred ~11 Ma later in the Palaeogene.

Overall, this thesis provides new insights about the tempo and mode of evolution of placental mammals through the use of cutting-edge phylogenetic methods. Crucially, this thesis as a whole represents a major step in our understanding of the anatomy and phylogenetic affinities of Darwin's enigmatic South American ungulates.

# Author's declaration

I declare that the thesis has been composed by myself and that the work has not be submitted for any other degree or professional qualification. I confirm that the work submitted is my own, except where work which has formed part of jointly-authored publications has been included. My contribution and those of the other authors to this work have been explicitly indicated below. I confirm that appropriate credit has been given within this thesis where reference has been made to the work of others.

The work presented in Chapter 2 was previously published in Püschel *et al.* (2021*a*) as "Divergence-time estimates for hominins provide insight into encephalization and body mass trends in human evolution" by Hans P. Püschel (myself), Ornella C. Bertrand, Joseph E. O'Reilly, René Bobe, Thomas A. Püschel. This study was conceived and designed by myself and Thomas A. Püschel. Ornella C. Bertrand compiled the body mass and ECV dataset. Joseph E. O'Reilly provided methodological support. I carried out all the mentioned analyses and wrote an initial draft with the support and constructive criticism of Thomas A. Püschel. All the authors contributed with the interpretation of the final results and gave feedback in order to improve the writing of the submitted version of this work.

The work presented in Chapter 3 is currently in press (Püschel *et al.* 2023) as "Anatomy and phylogeny of a new small macraucheniid (Mammalia: Litopterna) from the Bahía Inglesa Formation (late Miocene), Atacama Region, Northern Chile" by Hans P. Püschel (myself), Jhonatan Alarcón-Muñoz, Sergio Soto-Acuña, Raúl Ugalde, Sarah L. Shelley and Stephen L. Brusatte. I conceived and designed the study. Jhonatan Alarcón-Muñoz and Sergio Soto-Acuña prepared SGO.PV.21700 and took the final pictures of the specimen. I prepared all the figures and received assistance in three figures from Jhonatan Alarcón-Muñoz (Figs. 3.3, 3.5 and 3.9) and Raúl Ugalde (Fig. 3.2). Raúl Ugalde provided the stratigraphic context of SGO.PV.21700. I examined SGO.PV.21700 anatomy, took the specimens measurements, conducted the phylogenetic analyses and wrote an initial manuscript. All the authors contributed with the interpretation of the final results and gave feedback in order to improve the writing of the submitted version of this work.

Hans Püschel Rouliez

August 2022

# Acknowledgments

How to summarise these past four years of PhD? Chaotic. Tumultuous. Hectic. Probably those three words fall short. At the beginning of 2019 when I was starting my PhD full of energy and optimism, not even in my worst nightmares would I have thought that one year later a global pandemic would put in check our civilization. Overnight, our way of living, our way of relating to each other, and among other things, our way of doing research, completely changed. The entire plan of research that I set in 2019 and months of preparation for important museum visits were shattered in a single stroke. Adapting to these sudden changes required resilience and flexibility to modify my course of action, and doing not necessarily what I planned and wanted to do, but what it was possible to do in these circumstances. In this context, completing my PhD was particularly challenging and most likely not possible without the support of many people that help me through these complex times.

First, I would like to thank my supervisors Steve Brusatte, Sarah Shelley and Tom Williamson for their support over these four years. I am very grateful to Steve for accepting me into his lab and giving me the opportunity to contribute to the Palaeogene Mammal Working Group (PalM) with the scoring of SANUs. Being part of this mammal research group has been an intense and entertaining learning experience that I really enjoyed and am grateful for. More broadly, I enjoyed being part of Steve's Edinburgh lab for its vibrant research environment and activities arranged by Steve to engage with the work of other lab members or external guest researchers. In many ways, Steve has set an excellent example for me if I ever form my own lab. I thank Sarah for her help with mammalian anatomy and for being always there for me when I needed to discuss any interesting anatomical problem. I thank Tom for his help with mammalian anatomy and North American Palaeocene mammals, and for welcoming me to New Mexico for amazing mammalian fieldwork trips. It is a shame that the pandemic only allowed two of these trips. In addition, I would like to thank John Wible, Fernando Perini and Ornella Bertrand from the PalM team for their support. I am very grateful to John for his help and patience with me and other students while explaining mammalian anatomy in such long but entertaining video call meetings. Even though John was not my supervisor, I feel that unofficially he was.

I would like to thank my fellow PhD students and members of the PalM team, Zoi Knigopoulou, Paige dePolo and Sofía Holpin for their support over these years and for contributing to a stimulating research environment. When I started this PhD, you were 6 months ahead of me and in our first mammal meeting I will never forget how ignorant I felt about early placental mammals in comparison with you, that already had a good grasp of the overall picture and of your groups of interest. That feeling of ignorance was a driver for me to try to catch up as fast as possible with you, and for that, I am very grateful. Special thanks to Paige for taking the time during her 2022 AMNH visit to take pictures of specimens very important for my contribution to the PalM team and also for my PhD. I also would like to thank the various members (past and present) of the Edinburgh Palaeontology Lab. Thanks to Rachel Wood, Michaela Johnson, Greg Funston, Davide Foffa, Tom Challands, Julia Schwab, Natalia Jagielska, and Sherri Donaldson for contributing on a stimulating research environment.

Thanks to my fellow PhD students at the Grant Building for your good company over these years. Also, I would like to thank the staff of the School of Geosciences, and in particular, the PGR office for their support over these years. Among all these people, special thanks to Sophie Ramette for really caring and for her proactive attitude in finding answers and solutions for any problem that I had.

From my Chilean colleagues, I would like to thank Jhonny Alarcón and Sergio Soto for their research support during the pandemic, particularly when I couldn't travel to Chile to examine *Micrauchenia*. Special thanks to Jhonny for working hard to get the best pictures, and for taking most of the pictures and videos that made the study presented in Chapter 3 of this thesis possible.

I would like to thank Gabriela Schmidt, Leonardo Lobo, Andy McGrath, Guillaume Billet (MNHN), Alejandro Kramarz, Vanessa Rhue (YPM VPPU), Óscar Rojas Mondaca (MUHNCAL-KM), Pip Brewer (NHMUK), and Bárbara Vera for sharing photographs/3D models/old publications of important specimens that improved the anatomical comparisons of this study. I am particularly grateful to Agustín Martinelli and Pablo Ortiz, who even took new photographs from the MACN and PVL collections respectively to assist me in my studies. I thank Christian de Muizon for accepting a cast exchange arranged by me and Thomas Williamson, which allow me to examine excellent casts of some of the fossils of "condylarths" from Tiupampa. I would thank Javier Gelfo for helping me in finding the material I needed to

see in the MLP collections, and also for picking me up at Ezeiza airport. I also thank Gabriela Schmidt for the interesting discussions about dental anatomy in macraucheniids.

I thank the curators of the following institutions for their kind assistance during my museum visits: Daniel Brinkman (YPM VPPU), Agustín Martinelli and Laura Chornogubsky (MACN), Guillaume Billet (MNHN), Marcelo Reguero (MLP), Susana Bargo (MLP), Gabriel Aguirre and Marcelo Sanchez-Villagra (PIMUZ), and David Rubilar-Rogers (SGO.PV). I also would like to the following reviewers and editors of the published version of some of the chapters of this thesis for helpful comments that improved the original manuscripts: Gabriela Schmidt, François Pujos and Darin Croft (Chapter 3), and Mana Dembo and Fredrik Ronquist (Chapter 2). To anyone that I have forgotten, my sincere apologies.

My PhD research was funded by the National Agency for Research and Development (ANID)/ PFCHA/Doctorado en el extranjero Becas Chile/2018-72190003. I also received travel grants from the Palaeontological Association (PalAss) and the Society of Vertebrate Paleontology (SVP) for attending conferences.

In closing, I would like to thank the most important people in my life. First, I thank my parents Denise and Jorge for their love and support, for showing me with their example the values of perseverance and diligence, and for always encouraging me to pursue the studies that I liked most. I wouldn't have done a PhD without you. I thank my brothers Stephan and Thomas for their love and support during my life, and for many times acting as mentors for their younger brother. I thank Stephan for the poem at the beginning of this thesis, and I thank Thomas for the interesting scientific conversations that we have had since we were kids, and more recently for being the best possible collaborator. I thank Vilma for her support during my childhood. I thank my friend, Mario, for being there when I needed him and for those entertaining football matches. Last and foremost, I thank my beloved and kindhearted wife Ale who almost five years ago joined me on this European adventure moving with me to the UK to fulfil my dream of becoming a palaeontologist. Ale, your love and support over these years have been crucial for finishing this PhD, and for that and all the laughs and good times, I am forever grateful.

# Contents

**Abstract** ..... i

**Lay summary** ..... v

**Author's declaration** ..... viii

**Acknowledgments** ..... ix

**Contents** ..... xii

**List of Figures** ..... xvi

**List of Tables** ..... xviii

**Institutional Abbreviations** ..... xix

**Chapter 1 Introduction** ..... 1

**Origin of Placentalia** ..... 4

**Mirorder Meridiungulata: antecedents of a hypothesized monophyly** ..... 7

**Outline of Research** ..... 16

**Chapter 2 Divergence-time estimates for hominins provide insight into encephalization and body mass trends in human evolution** ..... 20

**Introduction** ..... 21

**Methods** ..... 23

Data collection and Total Evidence analyses ..... 23

Evaluating the prior sensitivity of divergence-time estimates ..... 25

Estimating PEQ using a PGLS regression ..... 26

PEQ and body mass ancestral character state reconstructions ..... 27

Measuring uncertainty in the ML ancestral character state reconstructions ..... 27

Measuring the relationship between ACSR of brain mass and body mass ..... 27

**Results** ..... 28

**Discussion** ..... 36

**Data availability** ..... 40

**Code availability** ..... 40

**Chapter 3 Anatomy and phylogeny of a new small macraucheniid (Mammalia: Litopterna) from the Bahía Inglesa Formation (late Miocene), Atacama Region, Northern Chile ..... 41**

**Introduction ..... 42**

**Geographic and geologic context ..... 45**

**Paleoenvironmental conditions of Bahía Inglesa Formation ..... 46**

**Material and methods ..... 47**

Description and comparison ..... 47

Character dataset and taxa included ..... 50

Phylogenetic analyses ..... 51

Systematic palaeontology ..... 53

**Descriptions and comparisons ..... 55**

Skull ..... 55

Postcranial elements ..... 57

Vertebrae ..... 57

Thoracic limbs ..... 70

**Phylogenetic results ..... 96**

**Discussion ..... 98**

Skeletal Anatomy, Locomotion, and Paleobiological Inferences ..... 98

Body Mass ..... 105

Macraucheniid Diversity in the Late Miocene ..... 107

Phylogenetic Considerations ..... 108

**Conclusions ..... 112**

**Chapter 4 New phylogeny of Litopterna (Mammalia) and "archaic" Palaeogene ungulates enlightens their relationships and evolution ..... 114**

**Introduction ..... 115**

Families currently recognised of Litopterna and their phylogenetic relationships ..... 123

Families of SANUs with controversial affinities and that are sometimes placed within Litopterna ..... 132

Other groups of interest ..... 140

**Taxon sampling ..... 143**

Families currently recognised in the Order Litopterna (Ameghino 1889) ..... 146

Family Adianthidae (Ameghino 1891*a*) ..... 146

Family Anisolambdidae (Soria 2001) ..... 149

Family Macraucheniidae (Gervais 1855) ..... 152

Family Proterotheriidae (Ameghino 1887) ..... 160

Family Sparnotheriodontidae (Soria 1980*a*) ..... 163

Families that are sometimes placed within Litopterna but that have been considered to be part of the order Notopterna (Soria 1984*b*) ..... 166
Family Indaleciidae (Soria 1989*b*) ..... 166
Family Notonychopidae (Soria 1989*a*) ..... 166
Other families that are sometimes placed within Litopterna ..... 168
Family Protolipternidae (Cifelli 1983a) ..... 168
Family Didolodontidae (Scott 1913) ..... 171
Other groups of interest ..... 174
Order Astrapotheria (Lydekker 1894) ..... 174
Order Notoungulata (Roth 1903) ..... 175
Order Xenungulata (Paula Couto 1952) ..... 176
Subfamily Kollpaniinae (Marshall *et al.* 1990) ..... 179
North American Mioclaenidae ..... 182
Arctocyonidae (Root of the tree) ..... 185
**Methods ..... 185**
Dental nomenclature ..... 185
Character sampling ..... 186
Testing different hypotheses for the paraconid of notoungulates ..... 187
Maximum parsimony analyses ..... 187
Undated Bayesian analyses ..... 187
Tip-dated Bayesian analyses ..... 188
**Results ..... 192**
Maximum parsimony analyses ..... 192
Bayesian analyses ..... 197
**Discussion ..... 202**
Early origins of SANUs, kollpanines, didolodontids and protolipternids ..... 202
About the status of the families Didolodontidae and Protolipternidae ..... 204
Interordinal affinities among the SANU orders ..... 207
Interfamilial affinities of Litopterna: Macraucheniidae and Adianthidae ..... 210
Interfamilial affinities of Litopterna: Proterotheriidae, Anisolambdidae and Sparnotheriodontidae ..... 213
Sparnotheriodontidae and an Antarctic voyage ..... 217
Macroevolutionary trends in litoptern evolution ..... 221
**Conclusions ..... 222**

**Chapter 5 Synthesis & Conclusions ..... 225**
**Summary of Key Findings ..... 226**
**Future directions ..... 228**
Hominin phylogenetics ..... 228
Anatomy, biology and phylogeny of Macraucheniidae ..... 229

Phylogeny of Litopterna and early SANUs phylogeny ..... 230

**References ..... 232**

**Appendices ..... 291**

**Appendix C2 ..... 291**

Resource 1: Supplementary Tables ..... 291

Resource 2: Supplementary Figures ..... 291

Resource 3: Püschel *et al.* (2021) article "Divergence-time estimates for hominins provide insight into encephalization and body mass trends in human evolution" ..... 292

Resource 4: Püschel *et al.* (2022) article "Reply to: Modelling hominin evolution requires accurate hominin data" ..... 292

**Appendix C3 ..... 292**

Resource 1: Supplementary Tables ..... 292

Resource 2: Character list and supplementary tables in relation to the phylogenetic aspect of this study ..... 292

Resource 3: Nexus file with the script for the undated Bayesian analysis ..... 293

Resource 4: Nexus file with the script for the tip-dated Bayesian analysis ..... 293

Resource 5: Additional figures. ..... 293

**Appendix C4 ..... 293**

Resource 1: Table S1. Valid genera of Litopterna and relevant South American native ungulate (SANU) recorded during the South American land mammal ages (SALMAs) in the Cenozoic 293

Resource 2: List of characters and character states ..... 293

Resource 3: Matrix with scores for hypothesis 1 regarding *Simpsonotus* paraconid ..... 293

Resource 4: Matrix with scores for hypothesis 2 regarding *Simpsonotus* paraconid ..... 293

Resource 5: List of synapomorphies and autapomorphies ..... 293

Resource 6: Additional tip-dated Bayesian phylogenetic analyses results ..... 293

# List of Figures

**Figure 1.1** Hypotheses on the ecological radiation of Mammaliformes (**a**), and the placental divergence hypotheses (**b**). ..... 5
**Figure 1.2** Matthew's phylogenetic hypothesis of the origin of SANUs and their relationship with other ungulates. ..... 12
**Figure 1.3** Simpson's hypothesis about the origin of SANUs and simple reconstructions. ..... 13
**Figure 1.4** Paleogeographic maps of the Caribbean (**a**) and the southern oceans (**b**) during the latest Cretaceous (70 Ma). ..... 13
**Figure 2.1** Alternative topological hypotheses tested in the TED analyses. ..... 22
**Figure 2.2** Summary diagram of important palaeoclimatic and hominin evolution events plotted next to the four obtained consensus phylogenies and time divergence estimates. ..... 29
**Figure 2.3** Body mass ancestral character state reconstructions (ACSR) for each species mapped onto the four consensus time-calibrated phylogenies. ..... 33
**Figure 2.4** PEQ ancestral character state reconstructions (ACSR) for each species mapped onto the four consensus time-calibrated phylogenies. ..... 34
**Figure 2.5** Boxplots of (**a-d**) body mass (kg) and (**e-h**) PEQ ancestral character state reconstructions (ACSR) per node based on a sample of 9002 time-calibrated posterior trees for each of the tested hypothesis. ..... 35
**Figure 3.1** Geographic distribution of late Miocene sites yielding macraucheniids. ..... 44
**Figure 3.2** Bahía Salado locality and stratigraphy. **a**. context map of the Bahía Salado locality, at the central coast of Atacama Region, Northern Chile. ..... 46
**Figure 3.3** Skeletal reconstruction of *Micrauchenia saladensis* (SGO.PV.21700) in left lateral view, with preserved elements in dark grey. ..... 49
**Figure 3.4** Mandible of *Micrauchenia saladensis* (SGO.PV.21700). ..... 56
**Figure 3.5** Atlas of *Micrauchenia saladensis* compared with atlases of other macraucheniids. ..... 59
**Figure 3.6** Axis of *Micrauchenia saladensis* (SGO.PV.21700). ..... 63
**Figure 3.7** Fifth and seventh cervical vertebrae (C5 and C7) of *Micrauchenia saladensis* (SGO.PV.21700). ..... 68
**Figure 3.8** Second thoracic vertebra (T2) of *Micrauchenia saladensis* (SGO.PV.21700). ..... 69

**Figure 3.9** Left scapula, and ulna-radius and manus articulated of *Micrauchenia saladensis* (SGO.PV.21700). ..... 73
**Figure 3.10** Left ulna-radius and articulated carpals of *Micrauchenia saladensis* (SGO.PV.21700). ..... 74
**Figure 3.11** Left scaphoid of *Micrauchenia saladensis* compared with scaphoids of other macraucheniids. ..... 77
**Figure 3.12** Right lunate of *Micrauchenia saladensis* compared with lunates of other macraucheniids. ..... 78
**Figure 3.13** Left cuneiform of *Micrauchenia saladensis* compared with cuneiforms of other macraucheniids. ..... 81
**Figure 3.14** Left pisiform of *Micrauchenia saladensis* compared with pisiforms of other macraucheniids. ..... 82
**Figure 3.15** Left magnum of *Micrauchenia saladensis* compared with magnums of other macraucheniids. ..... 84
**Figure 3.16** Right unciform of *Micrauchenia saladensis* compared with unciforms of other macraucheniids. ..... 86
**Figure 3.17** Metacarpals of *Micrauchenia saladensis* (SGO.PV.21700) and *Macrauchenia patachonica* (MNHN.F.PAM75). ..... 89
**Figure 3.18** Proximal phalanges of the manus of *Micrauchenia saladensis* (SGO.PV.21700). ..... 93
**Figure 3.19** Intermediate phalanges of *Micrauchenia saladensis* (SGO.PV.21700). ..... 95
**Figure 3.20** Maximum parsimony phylogenies of Macraucheniidae. ..... 97
**Figure 3.21** Bayesian phylogenies of Macraucheniidae. ..... 99
**Figure 3.22** Restoration of *Micrauchenia saladensis* in the late Miocene coast of Bahía Salado, Northern Chile. ..... 105
**Figure 4.1** Phylogenies of the order Litopterna illustrating its interordinal relationships (**a-b**) and its interfamilial relationships (**b-d**). ..... 118
**Figure 4.2** Diversity of litoptern and associated early SANUs families expressed as the number of genera. ..... 122
**Figure 4.3** Dental nomenclature used in the text and in the characters. ..... 189
**Figure 4.4** Most parsimonious trees (MPTs) from the maximum parsimony analyses. ..... 196
**Figure 4.5** Bayesian phylogenies of Litopterna from the undated analysis. ..... 199
**Figure 4.6** Tip-dated Bayesian phylogenetic analyses. ..... 200

# List of Tables

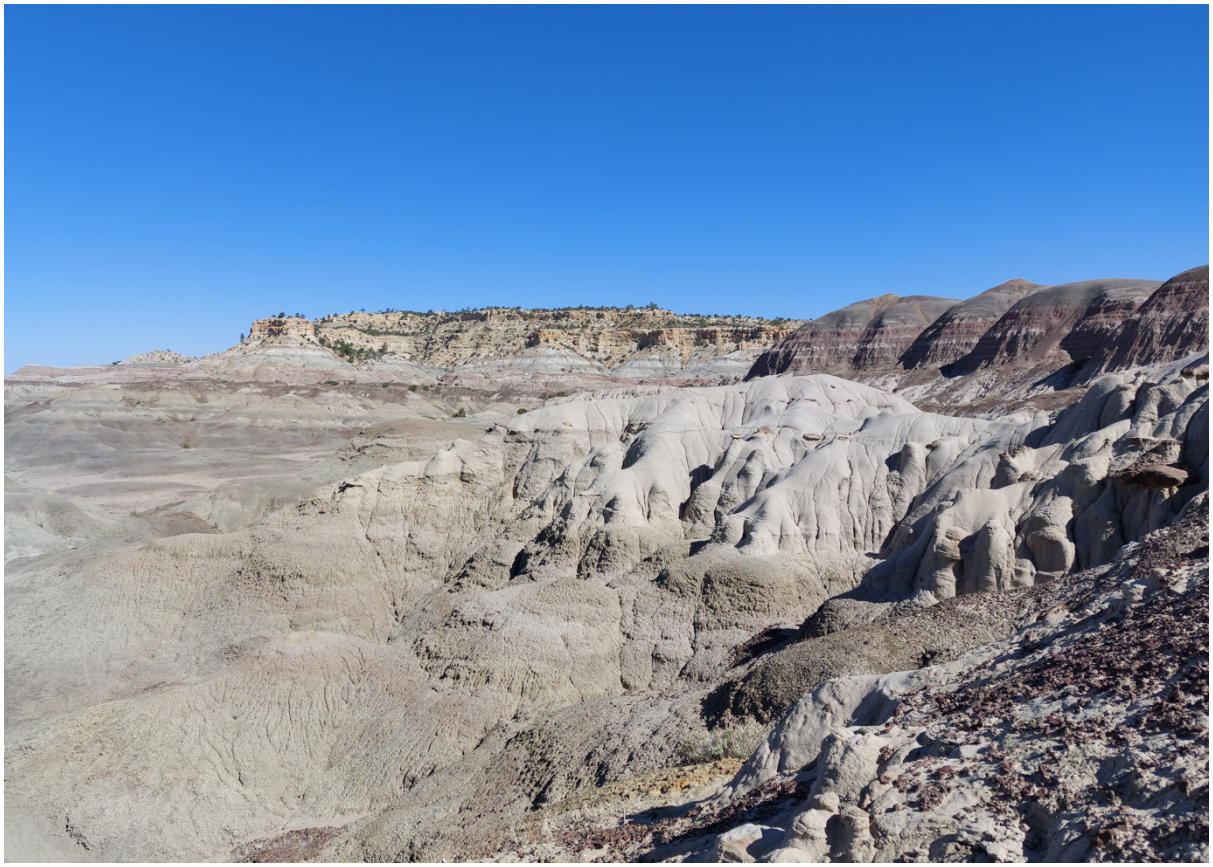
**Table 1.1** Current taxonomy of SANUs' orders up to a familial level and their main proposed phylogenetic affinities and controversies. ..... 9
**Table 2.1** Divergence times mean and 95% highest posterior density interval (HPD) in Ma for the different phylogenetic hypotheses in Fig. 1.1..... 31
**Table 4.1** Summary of the main taxonomic proposals for early SANUs ("condylarths"), Litopterna and Notopterna..... 117
**Table 4.2** Previous phylogenetic analyses that included Litopterna and Didolodontidae .... 121
**Table 4.3** SALMAs' lower and upper limits in Ma. ..... 190
**Table 4.4** Divergence-times mean for each Bayesian analysis, the total mean and total maximum and minimum ages..... 201
**Table 4.5** New taxonomic proposal for the orders Litopterna and Notopterna. ..... 212

# Institutional Abbreviations

**ACM**, Pratt Museum, Amherst College, Amherst, USA; **AMNH**, American Museum of Natural History, New York, USA; **CICYTTP PV**, Centro de Investigaciones Científicas y Transferencia de Tecnología a la Producción, Diamante, Entre Ríos, Argentina; **DGM**, Divisão de Geología e Mineralogía do Departamento Nacional da Produção Mineral, Rio de Janeiro, Brazil (also **DNPM**)**; FMNH P**, Field Museum of Natural History, Paleontology collection, Chicago, USA; **GM**, Colecciones paleontológicas del Departamento de Geociencias, Universidad Nacional de Colombia, Bogotá; **IMMH**, Idaho Museum of Natural History, Pocatello, Idaho; **KU**, Museum of Natural History, University of Kansas, Lawrence; **MACN PV A**, Museo Argentino Ciencias Naturales "Bernardino Rivadavia", Colección Ameghino, Buenos Aires, Argentina; **MACN PV**, Museo Argentino Ciencias Naturales "Bernardino Rivadavia", Colección Nacional de Paleontología Vertebrados, Buenos Aires, Argentina; **MAS PALEO- VERT**, Museo de Ciencias Naturales y Antropológicas "Profesor Antonio Serrano" de Paraná, Entre Ríos; **MCL**, Museu de Ciências Naturais da Pontificia Universidade Católica de Minas Gerais, Paleontological collection, Belo Horizonte, Brazil; **MNRJ**, Museu Nacional e Universidade Federal do Rio de Janeiro, Rio de Janeiro, Brazil; **MHNC**, Museo de Historia Natural "Alcide d'Orbigny", Cochabamba, Bolivia; **MLP**, Museo de La Plata, La Plata, Argentina; **MNHN-Bol**, Departamento de Paleontología, Museo Nacional de Historia Natural, La Paz, Bolivia; **MNHN.F**, Museum National d'Histoire Naturelle, Palaeontological collection, Paris, France; **MPCN**, Museo Paleontológico y de Ciencias Naturales "Alejandro C. Berro", Mercedes, Soriano, Uruguay; **MPEF- PV**, Colección del Paleontología del Museo Paleontológico "Egidio Feruglio", Trelew, Argentina; **MUHNCAL-KM,** Museo de Historia Natural y Cultural del Desierto de Atacama, Calama, Chile; **MUSM**, Departamento de Paleontología de Vertebrados, Museo de Historia Natural, Universidad Mayor de San Marcos, Lima, Perú; **NHMUK PV**, Natural History Museum, Vertebrate Palaeontology Collection, London, UK; **NMMNH**, New Mexico Museum of Natural History and Science, Albuquerque; **NMS**, National Museum of Scotland, UK; **PIMUZ**, Paleontological Institute and Museum, University of Zurich; PVL, Fundación Miguel Lillo, Vertebrate Paleontology Collection, Tucumán, Argentina; **SGO.PV**, Vertebrate Paleontology Collection, Museo Nacional de Historia Natural, Santiago, Chile; **SPSM**, St. Paul Science Museum, Minnesota , USA; **UALP**, University of Arizona Laboratory of Paleontology, Tucson, USA; **UATF-V**, Vertebrate

Paleontology Collections, Universidad Autónoma Tomás Frías, Potosí, Bolivia; **UCMP**, University of California Museum of Paleontology, Berkeley, USA; **UMVP**, University of Minnesota, Vertebrate Paleontology Collection, Minneapolis, USA; **UNPSJB-PV**, Universidad Nacional Patagónica San Juan Bosco, Comodoro Rivadavia, Argentina; **USNM**, United States National Museum, USA; **YPFB Pal**, Yacimientos Petrolíferos Fiscales Bolivianos, Colección Paleontología, Santa Cruz, Bolivia; **YPM VPPU**, Yale Peabody Museum, Vertebrate Paleontology Princeton University Collection, Yale, USA;

# Chapter 1 Introduction



West Flank of Torreon Wash, New Mexico. May 2022

Placentals are the most successful mammalian lineage today in terms of diversity and distribution over the world, having over 6000 recognized extant and recent extinct species (Burgin *et al.* 2018). They are distinguished from marsupials, because their gestational period is longer, giving birth to a comparatively well-developed progeny, and not for the presence of placenta (Renfree 2010). The numbers of placentals has been increasing because of new discoveries every year, although with some biases linked to taxonomic, geographic and geopolitical factors (Reeder *et al.* 2007; Jones & Safi 2011). These numbers are only overshadowed by the increasing rates of extinction due to "anthropic" pressures on the environment (Pimm *et al.* 2014). Similarly, during their evolutionary history, placentals have faced different environmental threats to their survival, and one of these events, the Cretaceous-Palaeogene (K/Pg) mass extinction event, is directly linked to their current success. Although mammals had at least two ecological radiations during the Mesozoic in the early to middle Jurassic and the late Cretaceous (Grossnickle *et al.* 2019), it was not until the K/Pg mass extinction event, 66 Ma when placentals radiated and started to fill the ecological niches we are familiar with today. The extinction of dinosaurs also is widely considered to have allowed mammals to reach much larger body sizes (Alroy 1998; Smith *et al.* 2010; Slater 2013; Lyson *et al.* 2019) and increase their taxonomic diversity (Grossnickle & Newham 2016). However, trends in ecomorphological disparity display a more complex pattern without a clear increase in disparity immediately after the K/Pg (Wilson 2013; Grossnickle & Newham 2016; Benevento *et al.* 2019). Similarly, when we consider their phylogeny there are still ongoing debates about the tempo and mode of the placental radiation.

There are three main hypotheses of ordinal origination and diversification within Placentalia: the explosive model, the short fuse model and the long fuse model (Archibald & Deutschman 2001). All of these hypotheses have a distinct time and a rate component that make them identifiable if tested. Therefore, many studies over the last 20 years, with the assistance of molecular techniques, have been trying to determine which one of these hypothesis fits better with what is observed in the fossil record and is at the same time congruent with the molecular evidence (e.g. Springer *et al.* 2017; Phillips and Fruciano 2018). However, far from a consensus, most of these studies have focused on the fossil members of the modern orders which date from the early Eocene onwards, thus leaving a big gap on the study of "archaic" Palaeocene mammals which lived during the first ~10 million years after the K/Pg event. This gap is problematic because it represents an omission of putative and/or stem placental species in the placental tree, which evolved in the time period immediately

following the mass extinction, thus probably generating a misinterpretation of early placental evolution.

The reason underlying the omission of these early Palaeocene placental mammals is mainly because they are considered "archaic" and they lack morphologies that clearly defined them as members of extant placental orders (Rose 2006). Nevertheless, resolving their phylogenetic position will undoubtedly improve our understanding of the early evolution of placental mammals. Recently, some efforts have been done in that direction studying the phylogenetic relationships between Palaeocene placental mammals using a new morphological data matrix including 130 Palaeogene taxa (Halliday & Goswami 2016*a*, *b*; Halliday *et al.* 2016, 2017, 2019). However, although methodologically strong, the data matrix used in these studies showed phylogenetic relationships that seem wrong contradicting well-supported molecular taxa (Foley *et al.* 2016; Springer *et al.* 2017), raising questions about how the matrix was constructed. Hence, a major revision of the phylogenetic relationship between Palaeogene, particularly Palaeocene placental mammals, is still required.

"Archaic" Palaeogene mammals inhabited all continents, although South America stands out for its particular biogeographic history and unusual relatively well-preserved fossil faunas. During most of its Cenozoic history, South America was isolated from the rest of the continents developing a large diversity of unique and peculiar mammals, including xenarthrans and five ancient "ungulate" orders Xenungulata, Notoungulata, Litopterna, Pyrotheria and Astrapotheria, known as the extinct South American Native Ungulates (SANUs). Two additional "archaic ungulate" groups are also known from South America: Didolodontidae (Simpson 1934) and Kollpaniinae (Muizon & Cifelli 2000), which have been historically linked to "Condylarthra", a probable paraphyletic group of early Cenozoic ungulate mammals mainly from the Northern Hemisphere. Simpson (1944) was the first in noticing the relevance of SANUs for understanding ubiquitous trends in macroevolution like the "explosive" evolution (i.e., a sudden diversification or radiation particularly early in the evolutionary history of a taxon, surviving afterwards few lineages that become permanent within the group). *"Among many examples of such an explosive phase of evolution, that of the native South American ungulates is unhackneyed […]. At the beginning of the Tertiary their ancestor were […] scattered, small local groups of obscure and diminutive animals […]. The earliest well-known mammalian fauna in South America, the Casamayoran [middle Eocene], presents the unusual and fascinating spectacle of such a great deployment still in its quantum phase, although nearing the end of it. Intragroup variation is enormous, intergroup variation is also*

*unusually great in some cases, the ungulate population is protean almost beyond parallel, and there are so many transitional types, some of them quite plainly adaptively unstable, that the taxonomic problem seems almost hopeless."* (Simpson 1944, p. 214).

Since Simpson's (1944) assertion, multiple new discoveries of early SANUs in early Palaeocene sites in Bolivia and Argentina have improved our knowledge of early SANUs evolution (Pascual *et al.* 1978; Bonaparte *et al.* 1993; Muizon & Cifelli 2000), although considering the incompleteness of most fossil remains of this period, the taxonomic problem still seems extremely difficult. However, we now count with different phylogenetic methods that can greatly help with determine SANUs phylogenetic affinities, including the currently more traditional maximum parsimony approach (Goloboff & Catalano 2016) and also the relatively new Bayesian methods that include a tip-dating approach using relaxed-clock models (Ronquist *et al.* 2012*b*). The latter approach also allows to estimate the divergence times of different lineages which can be potentially linked paleoclimatic records and provide aid in important biogeographic questions. In addition, important advances in molecular techniques such as collagen and ancient DNA extraction in the last decades are providing important information about SANUs affinities in the Placental tree (Buckley 2015; Welker *et al.* 2015; Westbury *et al.* 2017).

## Origin of Placentalia

The placental diversification has been historically considered to be driven by the opening of empty ecospaces or niches left by the sudden extinction of non-avian dinosaurs, a scenario consistently supported by the evidence found in the fossil record (Alroy 1999). It is indeed another of the key examples given by Simpson (1944) for the process known as "explosive evolution" described in his revolutionary book "Tempo and mode in evolution". Considering the broad time scale of macroevolutionary processes and the impossibility of running experiments as is common at microevolutionary level, disentangling how placentals diversified give us a unique opportunity to understand and make hypotheses about general trends in evolution of life, or at minimum, about vertebrate evolution. Historically, hypotheses of mammalian radiation have been classified into two groups; a) ecological diversity hypotheses that includes all Mammaliformes, and b) placental divergence hypotheses, that are focused in the timing of placental diversification (Grossnickle *et al.* 2019; Fig. 1.1). Considering the latter, there are three main hypotheses of ordinal origination and

diversification within Placentalia: the explosive model, the short fuse model and the long fuse model (Archibald & Deutschman 2001).

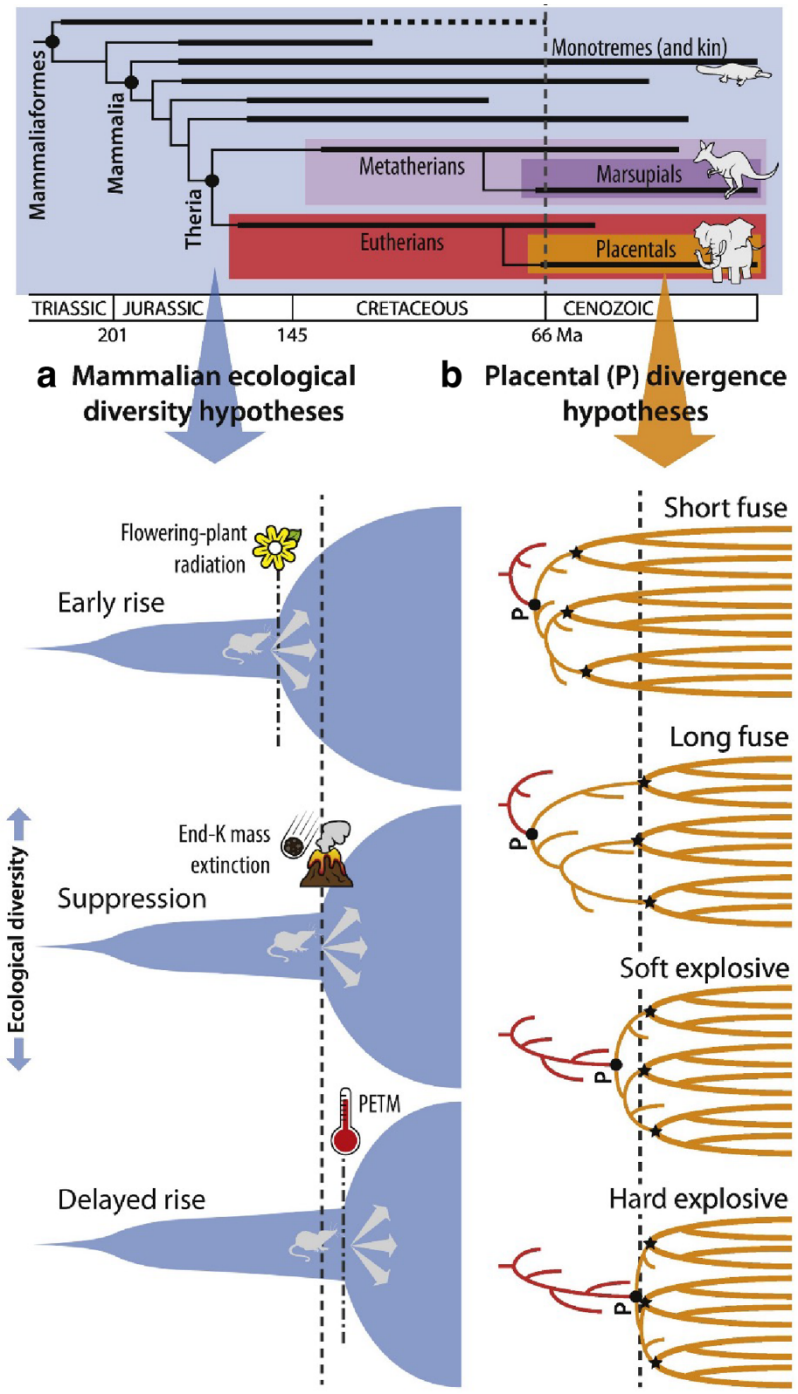



**Figure 1.1** Hypotheses on the ecological radiation of Mammaliformes (**a**), and the placental divergence hypotheses (**b**). Abbreviations: *P*, Placentalia (placental orders as stars); *K*, Cretaceous; Ma, millions of years ago; *PETM*, Palaeocene–Eocene Thermal Maximum. Extracted and edited from Grossnickle *et al.* 2019.

The explosive model states (Fig. 1.1b, "Hard explosive") that most of the interordinal origination and diversification of placentals happened right after or during the first 10 Ma after the K/Pg mass extinction event,66 Ma. It is probably the oldest model and it has been promoted

by prominent palaeontologists like Simpson (1944). It comes mainly from the direct observation of the fossil record and the apparent absence of crown placentals in the Late Cretaceous (Wible *et al.* 2009). This model has been supported by many subsequent studies (e.g. Carroll 1997; Alroy 1999; Wible *et al.* 2007; Davies *et al.* 2017), including some recent studies using molecular clocks (O'Leary *et al.* 2013), although not without some criticism (see for e.g. Dos Reis *et al.* 2014).

The short fuse model (Figure 1.1b) considers that most interordinal and intraordinal origination and diversification occurred considerably before the K/Pg boundary (i.e., during the Late Cretaceous). This model is based on relatively recent molecular studies that using a molecular clock were able to calculate ordinal divergence times that are tens of millions of years older than what the fossil record suggests. This would be explained by many ghost lineages and a poor Late Cretaceous fossil record (Springer 1997; Kumar & Hedges 1998; Eizirik 2001; Bininda-Emonds *et al.* 2007). However, there were voices that called for caution, emphasising the need of reliable calibrations with a molecular clock that allows rate variation between taxa (e.g. Alroy 1999; Benton 1999; Bromham *et al.* 1999; Dos Reis *et al.* 2012). Furthermore, there is no evidence for a Late Cretaceous eutherian poor preservation rate (Foote *et al.* 1999; Davies *et al.* 2017).

The long fuse model (Fig. 1.1b) is an intermediate solution between the two previously described models. This model states that intraordinal diversification definitely occurred after the K/Pg limit, even though the interordinal was long before (i.e., within the Late Cretaceous). Unlike the short fuse, this model does not contradict the fossil record and has found support in recent studies which use relaxed clocks and multiple fossil calibrations with soft bounds e.g. (Meredith *et al.* 2011; Dos Reis *et al.* 2012, 2014; Foley *et al.* 2016; Tarver *et al.* 2016; Springer *et al.* 2017).

Although the hard explosive and the short fuse models have been practically discarded, a recently proposed model based on molecular studies has re-fuelled the debate: the soft explosive model (Figure 1.1b). This model is similar to its predecessor, but includes the possibility that some of the interordinal diversification occurred shortly before the K/Pg boundary (Phillips 2016; Phillips & Fruciano 2018). The discussion of which one of these hypotheses is the most adequate to explain modern mammalian diversity has been long and it does not show any sign of reaching a consensus (e.g., Springer *et al.* 2017, 2019; Phillips & Fruciano 2018). An important part of the problem is related to the fact that most studies have

been practically ignoring the evidence from the "archaic" Palaeogene mammals, especially those living during the first ~10 million years of the Palaeocene. This is highly problematic, because Palaeocene mammals evolved immediately after the K/Pg boundary and not including them is likely having an effect on the resultant rates of evolution calculated for extant mammal lineages, such as overestimating the inter and intraordinal divergence times.

In consequence, a major revision of the phylogenetic relationships between Palaeogene, in particular Palaeocene placental mammals is still required in order to better understand the earliest placental radiation. The origin and affinities of SANUs with other placentals are an important part of this debate. Solving the phylogenetic relationships of early placental mammals is one of the main objectives of the interdisciplinary team called the Palaeogene Mammal Working Group (PalM) to which I have been contributing during my PhD project with the anatomical scoring of a representative sample of SANUs in large placental matrix. Even if SANUs did not leave any extant relatives, understanding their evolution has puzzled palaeontologists for more than a century.

## Mirorder Meridiungulata: antecedents of a hypothesized monophyly

The current state of knowledge, proposed affinities and controversies are exposed in Table 1.1, so it can be used as a guide while reading this section. The history of the classification and phylogenetic relationships of SANUs has been complex since their discovery by Charles Darwin of the first species: *Toxodon platensis* and *Macrauchenia patachonica.* Now well-known to be a Pleistocene notoungulate and litoptern respectively, Darwin was immediately perplexed by their peculiar anatomy and size (Darwin 1839). Owen (1837, 1840) who first received the specimens, tentatively described both as referable to the order "Pachydermata", a now obsolete order that grouped rhinoceroses, elephants, tapirs and hippopotamuses together. Lydekker (1893) grouped the three SANUs discovered by then, Litopterna, Toxodontia (Notoungulata) and Astrapotheria, as suborders of "Ungulata". Later, he suggested that they all shared a "common ancestral stock" belonging to "Condylarthra" and likely with a North American origin (Lydekker 1896). Roth (1903) shared a similar view, suggesting that SANUs were part of a group confined to South America and distinct from ungulates of other continents. In contrast, Ameghino (1906) believed that SANUs were ancestral to many modern lineages from other continents, from proboscideans to primates. However, apart from Argentina, contemporary authors discredited his views arguing that many

of the proposed similarities were mere convergences. One of these authors was Scott (1910), whom while studying SANUs from the Argentinean Santa Cruz (early Miocene) reaffirmed the uniqueness of this assemblage of mammals. They were, in his opinion, very different from North American mammals, not just in terms of families or genera, but also in terms of orders. He also had views similar to Lydekker, in the sense of thinking that all SANUs, maybe with the exception of Pyrotheria and Astrapotheria, had a common ancestor.

Even though Toxodontia (Notoungulata) had a more specialized ear region in in comparison with Litopterna (Scott 1910), Scott (1912) found a series of skeletal and dental features that united these taxa. Osborn (1910) fully agreed with this view and in his classification of Mammalia included within the cohort "Ungulata" the superorder Notoungulata that comprised all the SANUs, indirectly acknowledging the monophyly of the group. Schlosser (1911) meanwhile characterised SANUs into two groups: Litopterna as a suborder of the order "Ungulata", while astrapotheres and pyrotheres were suborders within the order Notoungulata. Matthew (1915*a*) agreed with a "condylarth" origin for SANUs but doubted their monophyly instead proposing that they have a diverse range of affinities with different "condylarth" groups. (Fig..2).

Later, Simpson (1945) proposed a superorder called Protoungulata, which included the orders "Condylarthra" (North American "condylarths" plus didolodontids), Litopterna, Notoungulata, Astrapotheria and Tubulidentata (with some doubts), but excluding Pyrotheria of uncertain affinities. However, subsequently he was also of the opinion that all SANUs, including Pyrotheria, were derived from generalized North American "condylarths" that crossed to South America during the late Cretaceous or early Palaeocene, although not necessarily originating from one ancestral form (Simpson 1948). He later included to this group Xenungulata (Simpson 1978, 1980), a new order of South American ungulates discovered in Itaboraí, Brazil (Paula Couto 1952). Simpson believed that after the early arrival of these generalized "condylarths" by sweepstakes dispersal from North America, all SANUs including the "condylarth" didolontids evolved "in situ" in South America (Simpson 1951, 1978; Figure 1.3). Later, Patterson and Pascual (1972) supported the North American origin of South American ungulates, although in two consecutive invasions. The first one from a "condylarth", ancestral to all South American ungulates (except Notoungulata), and the second from an early member of Notoungulata, which evolved in North America.

**Table 1.1** Current taxonomy of SANUs' orders up to a familial level and their main proposed phylogenetic affinities and controversies. The names in bold indicate a current taxonomic controversy.

| Mirorder | Order | Suborder | Family | Main proposed affinities and controversies |
|---|---|---|---|---|
| | "Condylarthra" | | **Didolodontidae**<br>Mioclaenidae | "Condylarthra" member of Protoungulata (Simpson 1945).<br>"Condylarthra" order of the grandorder Ungulata (McKenna 1975; McKenna and Bell 1997).<br>"Condylarthra" order of the superoder Meridungulata (Soria 1988).<br>Mioclaenidae and Didolodontidae within the order Panameriungulata (Muizon and Cifelli 2000).<br>Didolodontidae classified within Laurasiatheria as a stem eungulates (O'Leary *et al.* 2013). |
| Meridiungulata | Litopterna | | Adianthidae<br>**Anisolambdidae**<br>Macraucheniidae<br>Proterotheriidae<br>Protolipternidae<br>**Sparnotheriodontidae** | Litopterna member of "Pachydermata" (Owen 1837, 1840).<br>Litopterna suborder of "Ungulata" (Lidekker 1893).<br>Litopterna order of the superorder Notoungulata within the cohort "Ungulata" (Osborn 1910).<br>Litopterna as a suborder of the order "Ungulata" (Schlosser 1911).<br>Litopterna member of Protoungulata (Simpson 1945).<br>Litopterna order of the mirorder Meridiungulata, a subrank of the grandorder Ungulata (McKenna 1975; McKenna and Bell 1997).<br>Litopterna order of the superorder Meridiungulata (Soria 1988).<br>Litopterna within the order Panameriungulata (Muizon and Cifelli 2000).<br>Notoungulata and Litopterna were sister taxa closely related with the North American phenacodontids (Horovitz 2004).<br>Litopterna classified alongside "condylarths" within Laurasiatheria as a stem eungulates (O'Leary *et al.* 2013).<br>Litopterna closely related to Notoungulata forming a monophyletic unit with Perissodactyla called Panperissodactyla (Buckley 2015; Welker *et al.* 2015).<br>Close relationship between Litopterna and Perissodactyla based on aDNA (Westbury *et al.* 2017).<br>Sparnotheriodontids are didolodontids according to Cifelli (1983*a*).<br>Anisolambdidae is a subfamily of Proterotheriidae according to Cifelli (1983*a*) and Villafañe *et al.* (2006). |
| | **Notopterna** | | **Amilnedwardsiidae** | |

| | | | |
|---|---|---|---|
| | | **Indaleciidae** | Indaleciidae is a subfamily of Adianthidae according to Bond and Vucetich (1983). |
| | | **Notonychopidae** | Notopterna order of the superorder Protoungulata including 3 families: Amilnedwardsiidae, Indaleciidae, and Notonychopidae (Soria 1988).<br>Notopterna considered invalid and its members within Litopterna (e.g., McKenna and Bell 1997). |
| Notoungulata | Notioprogonia | Henricosborniidae | |
| | | Notostylopidae | |
| | | Perutheriidae | |
| | Toxodontia | Homalodotheriidae | Notoungulata member of "Pachydermata" (Owen 1837, 1840). |
| | | Isotemnidae | Toxodontia (Notoungulata) suborder of "Ungulata" (Lidekker 1893). |
| | | Leontiniidae | Toxodontia (Notoungulata) order of the superorder Notoungulata within the cohort "Ungulata"(Osborn 1910). |
| | | Notohippidae | Notoungulata member of Protoungulata (Simpson 1945). |
| | | Toxodontidae | Notoungulata order of the mirorder Meridiungulata, a subrank of the grandorder Ungulata (McKenna 1975; McKenna and Bell 1997). |
| | Typotheria | Archaeopithecidae | Notoungulata order of the superorder Protoungulata (Soria 1988). |
| | | Campanorcidae | Asian and North American Arctostylopidae as a family of Notoungulata (Kondrashov and Lucas 2004). |
| | | Interatheriidae | Notoungulates classified in Paenungulata within Afrotheria (O'Leary *et al.* 2013). |
| | | Mesotheriidae | Notoungulata closely related to Litopterna forming a monophyletic unit with Perissodactyla called Panperissodactyla (Buckley 2015; Welker et al. 2015). |
| | | Oldfieldthomasiidae | |
| | Hegetotheria | Archaeohyracidae | |
| | | Hegetotheriidae | |
| Astrapotheria | | Astrapotheriidae | |
| | | Eoastrapostylopidae | Astrapotheria suborder of "Ungulata" (Lidekker 1893). |
| | | Trigonostylopidae | Astrapotheria suborder of the order Toxodontia (Notoungulata) within the cohort "Ungulata" (Osborn 1910). |

| | | |
|---|---|---|
| | | Astrapotheria as a suborder of the order Notoungulata (Schlosser 1911).<br>Astrapotheria order of the mirorder Meridiungulata, a subrank of grandorder Ungulata (McKenna 1975; McKenna and Bell 1997).<br>Astrapotheria order of the superorder Protoungulata (Soria 1988).<br>Astrapotheria closely related with North American periptychids (Horovitz 2004). |
| Pyrotheria | Colombitheriidae<br>Pyrotheriidae | Pyrotheria order of the superorder Notoungulata within the cohort "Ungulata" (Osborn 1910).<br>Pyrotheria as a suborder of the order Notoungulata (Schlosser 1911).<br>Pyrotheria is related to North American "condylarths" (Simpson 1945).<br>Pyrotheria order of the mirorder Meridiungulata, a subrank of grandorder Ungulata (McKenna 1975; McKenna and Bell 1997).<br>Pyrotheria order of the superorder Protoungulata (Soria 1988). |
| Xenungulata | Carodniidae | Xenungulata is related to North American "condylarths" (Simpson 1978, 1980).<br>Xenungulata order of the mirorder Meridiungulata, a subrank of grandorder Ungulata (McKenna 1975; McKenna and Bell 1997).<br>Xenungulata order of the superorder Protoungulata (Soria 1988).<br>Xenungulata closely related with Asian and North American Dinocerata (Tong and Lucas 1982).<br>Xenungulata classified in Paenungulata within Afrotheria (O'Leary *et al.* 2013). |

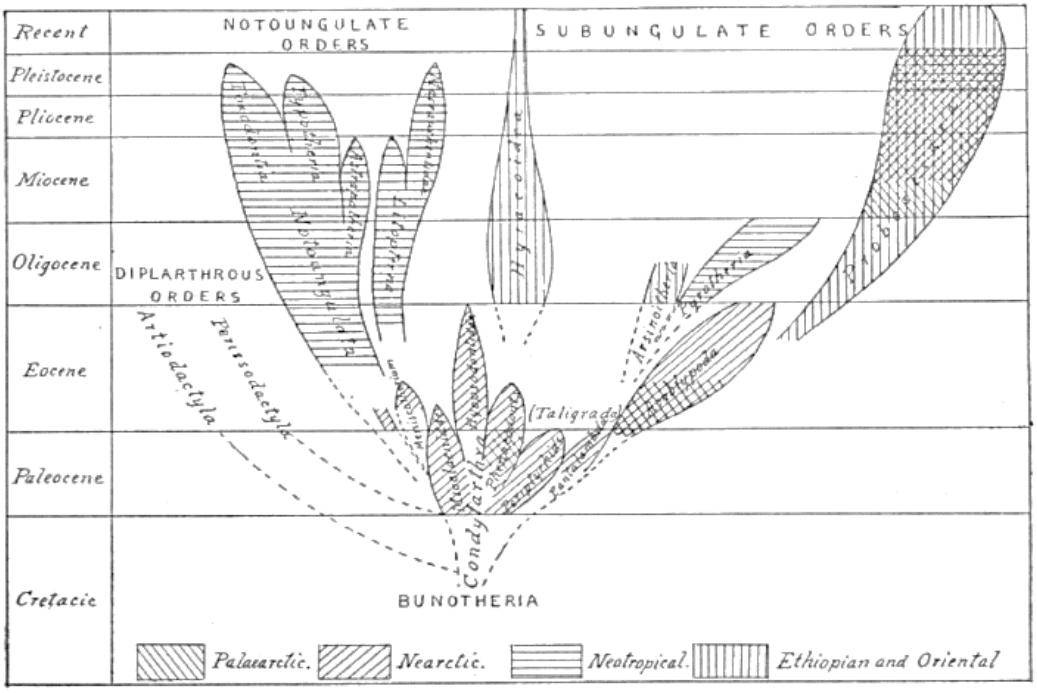



**Figure 1.2** Matthew's phylogenetic hypothesis of the origin of SANUs and their relationship with other ungulates. Note how he grouped SANUs very closely, although pyrotheres appear to be more closely related to other groups as Proboscidea (extracted and modified from Matthew 1915*a*).

As there is no evidence for a permanent land connection between North and South America during the late Cretaceous or early Palaeocene, current hypotheses involve the formation of transient volcanic islands that allowed a stepping stone migration of some faunas from north to south (Iturralde-Vinent 2006; Pascual and Ortiz-Jaureguizar 2007; Wilf *et al.* 2013; Figure 1.4a). Similarly, a late Cretaceous-early Eocene land connection between South America and Antarctica has been proposed based on geological evidence and the presence of early Eocene astrapotheres and sparnotheriodontid litopterns (Bond *et al.* 1989; Reguero *et al.* 2014; Gelfo *et al.* 2017; Figure 1.4b).

McKenna (McKenna 1975; McKenna & Bell 1997) taxonomically formalised the proposed monophyly of SANUs creating the mirorder Meridiungulata, a subrank of the grandorder Ungulata. This taxon comprises the orders Xenungulata, Notoungulata, Litopterna, Pyrotheria and Astrapotheria, the five orders of SANUs currently accepted. However, he/they did not provide any anatomical justification for the creation of this taxon apart from a shared geographical occurrence in South America. Even if the monophyly of this taxon is possible, clear derived characters shared by its members or synapomorphies are still not determined (Cifelli 1993). Cifelli (1983*a*), based on some dental features, argued instead for a common origin of Didolodontidae-Litopterna with Notoungulata from a mioclaenine hyopsodont-like ancestor, but excluding the other SANUs.

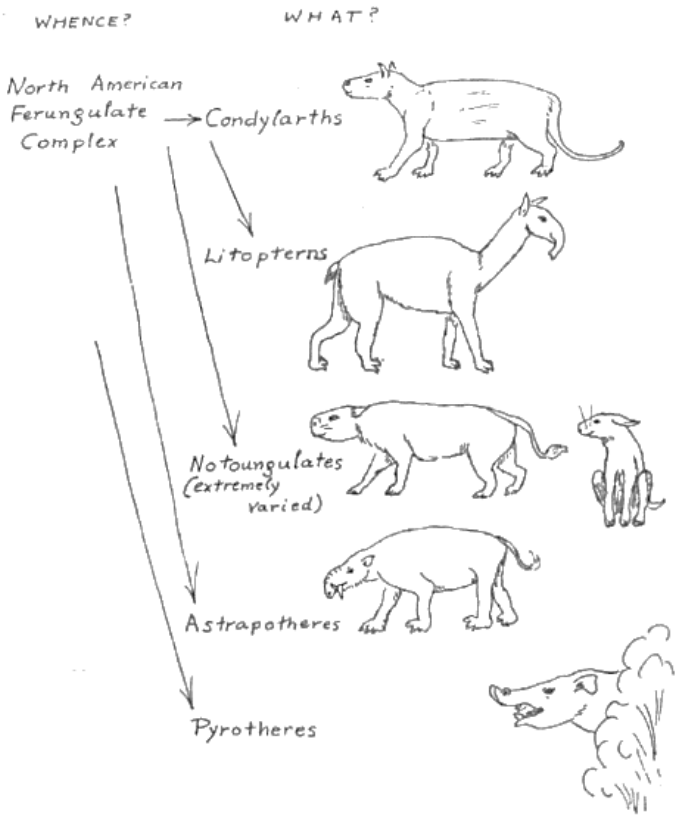



**Figure 1.3** Simpson's hypothesis about the origin of SANUs and simple reconstructions. He will later (Simpson 1978, 1980) include to this group Xenungulata (extracted and modified from Simpson 1951).

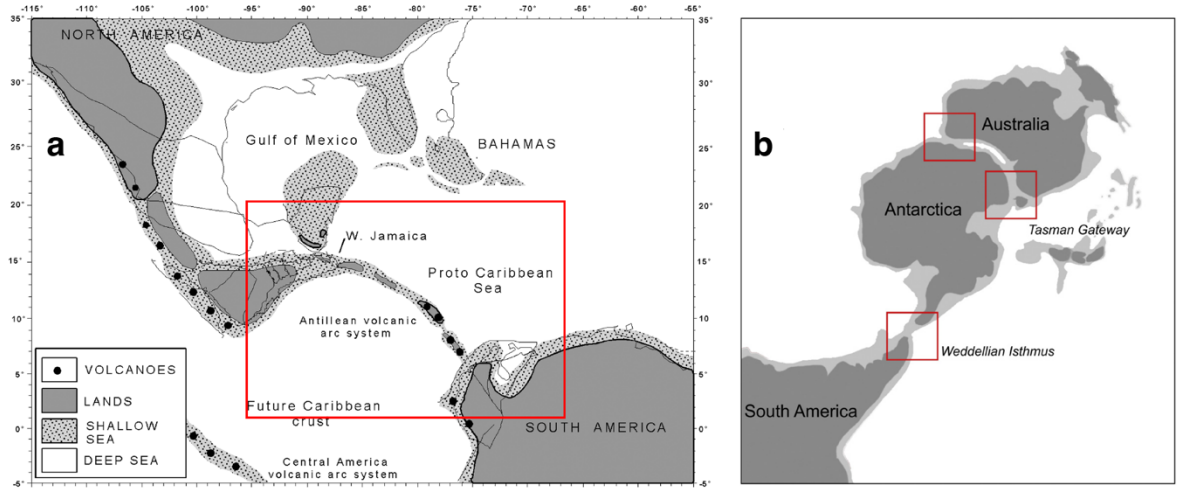



**Figure 1.4** Paleogeographic maps of the Caribbean (**a**) and the southern oceans (**b**) during the latest Cretaceous (70 Ma). Hypothesized land connections between continents are indicated by red squares. The "condylarth" migration from North America to South America would have been possible by the Antillean volcanic arc system, whereas the SANUs migration from South America to Antarctica would have been possible by the Weddellian Isthmus (extracted and edited from Iturralde-Vinent (2006) and Reguero et al. (2014).

In contrast, Soria (1988) proposed an alternative diphyletic origin for SANUs with two new superorders: Meridiungulata which includes Litopterna and "Condylarthra" in general, and Protoungulata (different from the Simpson (1945) concept), which includes Notoungulata,

Astrapotheria, Xenungulata, Pyrotheria and Notopterna. Notopterna is new order proposed by Soria (1989*a*), although considered by later authors within Litopterna (McKenna & Bell 1997). Soria (1988) based this classification on different anatomical features, including a possible phylogenetic connection previously established between the ear regions of Notoungulata and Pyrotheria (Patterson 1977).

Cifelli's (1983*a*) hypothesis was subsequently supported by early Palaeocene fossil findings in Tiupampa (Bolivia) in which "condylarths" of apparent mioclaenid affinities were found (Muizon & Marshall 1987*a*, *b*; Marshall & Muizon 1988). By studying the anatomy and using parsimony-based phylogenetic analyses, they proposed a new taxon, Panameriungulata, which includes Litopterna, Didolodontidae, Kollpaniinae (South American mioclaenids) and Mioclaeninae (North American mioclaenids), but excludes the other SANUs (Muizon & Cifelli 2000). This study provided the first robust link between a typical North American "condylarth" taxon with SANUs using modern phylogenetic analyses, although with a relatively limited taxon and character sampling.

Many later studies did not find support for the monophyly proposed by McKenna (1975). For instance, Tong and Lucas (1982) proposed that the Asian and North American Dinocerata and Xenungulata were closely related, and Kondrashov and Lucas (2004) classified the Asian and North American Arctostylopidae as a family of Notoungulata. Although these studies did not directly reject the proposed monophyly, they made it very difficult because they implied a most recent common ancestor with Palaeocene groups from other continents. However, other studies, based on the lack of common derived ankle and dental specializations between the supposed closely related groups, disagreed with those assertions (e.g. Cifelli 1985; Cifelli *et al.* 1989; Missiaen *et al.* 2006). Similarly, Horovitz (2004) performed a phylogenetic analysis using postcranial characters finding that Notoungulata and Litopterna were sister taxa closely related with the North American phenacodontid *Meniscotherium*, while Astrapotheria was closely related with North American periptychids. Most recently, O'Leary *et al.* (2013), using molecular and morphological information recovered a tree that supported a diphyletic scenario for SANUs. Notoungulates (represented by *Thomashuxleya externa*) and Xenungulata (represented by *Carodnia vieirai*) were classified in Paenungulata within Afrotheria, while Litopterna (represented by *Protolipterna ellipsodontoides*) was classified alongside "condylarths" including Didolodontidae (represented by *Didolodus multicuspis*) within Laurasiatheria as a stem eungulates. This hypothesis is consistent with a previous morphological-based study (Agnolin & Chimento 2011).

Nonetheless, the most recent studies have found some support for the hypothesized monophyly of SANUs (Westbury *et al.* 2017). First, a parsimony phylogenetic analysis using a comprehensive eutherian morphological matrix with representatives of the five SANU orders, found them forming a monophyletic group in their constrained analyses, which it was sister to the North American "condylarths" *Phenacodus*, *Hyopsodus* and *Meniscotherium* (Muizon *et al.* 2015). Similarly, Shelley (2017) recovered Meridiungulata in an unconstrained analyses, although some early artiodactyls were included possibly due to convergences or sampling issues. Additionally, two different studies that extracted collagen from specimens of the notoungulate *Toxodon platensis* and the litoptern *Macrauchenia patachonica* and that carried out protein-based phylogenetic analyses, found that they were closely related forming a monophyletic unit that is closely related to Perissodactyla (Buckley 2015; Welker *et al.* 2015). Welker *et al.* (2015) called this monophyletic group Panperissodactyla. Similarly, a molecular study in which aDNA was extracted from *M. patachonica*, found the same close relationship between Litopterna and Perissodactyla (Westbury *et al.* 2017). Even if these studies probe a phylogenetic relationship between Perissodactyla and two SANUs orders Litopterna and Notoungulata, it is still an open question whether the remaining three SANUs orders Xenungulata, Astrapotheria and Pyrotheria, and the two South American "condylarths", Didolodontidae and Kollpaniinae, are part of this monophyletic unit. It is also highly contentious how SANUs are related to North American "condylarths".

In total, SANUs include around 50 families and more than 250 genera that lived sometime during the Cenozoic (Croft *et al.* 2020). However, most of the familial diversity was during the Palaeogene, the most important period to consider if we want to enlighten their affinities and solve their position within Placentalia in the mammalian tree. Considering the enormous diversity of early SANUs, resolving their affinities and test their monophyly would probably need a very large morphological and molecular matrix that includes the earliest members of each placental order, extant and extinct. This is probably more than one student can achieve in a PhD thesis and requires a collaborative effort. Indeed, the origin and affinities of SANUs with other placentals is a key question that I have been aiming to solve as a member of the Palaeogene Mammal Working Group (PalM) directed by my main supervisor Stephen Brusatte. Part of this work has been included in this thesis as anatomical observations, but many aspects have been reserved for this future joint publication.

Therefore, in this thesis I focused in a more concise but not less relevant problem within the SANUs phylogeny, which is solving the interfamilial relationships of Litopterna. Even

though this is a relatively smaller problem than solving the interordinal affinities of SANUs, the anatomical disparity that early litopterns show and the scarce fossil record for the earliest Palaeogene in South America make this problem particularly challenging. Thus, I took a three-step sequential approach in order to tackle this problem: (1) test relatively new phylogenetic methods in a placental case study, (2) study the litoptern anatomy in detail and apply the similar methods of the step 1 in a small dataset, and (3) apply the methods and knowledge acquired in steps 2 and 3 in a new large litoptern and early SANUs matrix. These steps correspond to Chapters 2, 3 and 4 respectively, which I will now explain in detail.

## Outline of Research

The first section of this thesis, presented in Chapter 2, deals with estimation of divergence-times and trends in body mass and encephalization (brain mass relative to body mass) in human evolution. The timing of the divergence of our lineage from other African apes, and more importantly the antiquity and emergence of the genus *Homo* have been historically controversial in palaeoanthropology (Antón & Josh Snodgrass 2012; Harcourt-Smith 2016; Ruiter *et al.* 2017; Villmoare 2018). Dating cladogenetic events in human evolution is particularly relevant if we aim to understand evolutionary trends in key traits such as body mass and encephalization over time, and correlate these changes with both abiotic and biotic processes on geological timescales. Previous studies computed confidence intervals for the appearances and disappearances of several hominins (Bobe & Leakey 2009; Bobe & Carvalho 2019). However, their approach requires extensive palaeontological data about the relative abundance of each particular taxon among other collected fossil mammals from the same site, which hinders its application in hominin taxa with limited information available. In this chapter, I provided new insights in human evolution and the emergence of the genus *Homo* by conducting for the first time a Bayesian Total Evidence Dating approach (i.e., including molecular, morphological and stratigraphic evidence) using different topological hypotheses, and performing ancestral state reconstructions of body mass and phylogenetic encephalization quotient (PEQ).

Although the mammals studied in Chapter 2 (humans and close relatives) are different than those of the following chapters (SANUs), the Bayesian phylogenetic methods used are a key component of Chapters 3 and 4, as the they allow the estimation phylogenetic affinities and also of divergence-times of different lineages, which have not been applied to any SANU groups previously. Overall, this chapter achieves two objectives. First, it provides some

answers in longstanding questions in palaeoanthropology and future lines of research in this field. Second, it serves as a methodological chapter providing me with the tools necessary to solve important questions in the phylogeny of Litopterna. The methodological protocol followed in Chapter 2 allowed me to measure the impact that different phylogenetic hypotheses (i.e., tree topologies) have in divergence-time estimates, which is particularly important considering the uncertainty that exists around the early affinities of litopterns and SANUs in general. At this point it is important to mention that after the publication of this chapter as an article in the journal Nature Ecology & Evolution (Püschel *et al.* 2021*a*), a reply was published one year after, mainly criticising our calibration approach for the Total Evidence Dating analyses (Mongle *et al.* 2022). We responded to what we considered mostly unfair criticism with a reply article showing that even by using the calibration approach favoured by our detractors, the main results and conclusions of our original paper (i.e., Püschel *et al.* 2021*a*) are unaffected (Püschel *et al.* 2022). I included this reply article as the Appendix C2 Resource 4.

The second part of this thesis, presented in Chapter 3, deals with SANUs anatomy, in particular with the anatomy of macraucheniid litopterns. Here I present an anatomical description, with discussion on functional morphology, and phylogeny of a new small macraucheniid, *Micrauchenia saladensis* gen. et sp. nov. from late Miocene (Huayquerian SALMA) Bahía Inglesa Formation, Northern Chile. Since the detailed descriptions of early workers before the first half of the 20$^{th}$ century (e.g., Burmeister 1864; Scott 1910; Sefve 1925) there have been not many publications dealing with macraucheniid anatomy. Some excellent studies have been published since (e.g., Forasiepi *et al.* 2016), but these have been focused mainly on craniodental anatomy. Therefore, the postcranial anatomy of macraucheniids is well known only for the Santacrucian SALMA (early Miocene) with *Theosodon* and the late Pleistocene with *Macrauchenia* and *Xenorhinotherium*, but not much is known from species during the temporal gap between these two intervals. The description of the late Miocene *M. saladensis* aims to fill this gap in knowledge with detailed descriptions and illustrations of postcranial elements using a comparative anatomy perspective that includes earlier and later macraucheniids. In addition, following previous pioneering works in litoptern functional morphology (e.g., Shockey 1999; Shockey & Anaya 2008), I provide new interpretations in terms of the biology and locomotion of *M. saladensis* and macraucheniids. Functional aspects of the forelimb are treated in detail, in particular the peculiar aliform expansion of the radius which is only present in macraucheniine macraucheniids such as *M. saladensis* and

*Macrauchenia*, but absent in older macraucheniids like *Theosodon*. The postcranial anatomical information was then used to expand previous craniodental morphological matrices (Schmidt and Ferrero 2014; Forasiepi et al. 2016) adding postcranial chracters for the first time in macraucheniid phlyogenetics. Using Bayesian phylogenetic methods first presented in Chapter 2 and also maximum parsimony, I was able to place *M. saladensis* in the macraucheniid phylogeny with some degree of uncertainty, giving insights on the affinities of other macraucheniids and the timing of origin of the subfamily Macraucheniinae.

The third part of this thesis, presented in Chapter 4, deals with the phylogeny of Litopterna, focusing on determining whether Litopterna is a monophyletic group and resolving the interfamilial affinities within the order using maximum parsimony and Bayesian phylogenetic methods previously used in Chapters 2 and 3. Over the years there have been different taxonomic proposals for Litopterna (e.g., Cifelli 1983*a*; McKenna & Bell 1997; Soria 2001; Gelfo *et al.* 2016), although only one of these proposals (i.e., Cifelli 1983) has been partially supported with a subsequent phylogenetic analysis (Cifelli 1993). However, this analysis did not include other SANUs and it was based on an extremely reduced character matrix, which means that the monophyly of Litopterna was left untested. In a recent review, nine families of litopterns were recognised (Croft *et al.* 2020). Nonetheless, only four families can be considered firmly placed within Litopterna, whereas the phylogenetic affinities of the other five are still controversial. From these five families, three (Amilnedwardsiidae, Indaleciidae and Notonychopidae) have been previously classified in a different order (i.e., Notopterna) based on anatomical features in the dentition and the ear region (Soria 1989*a*, *b*). The inclusion of these three families in Litopterna was based on a phylogenetic analysis with an extremely reduced character matrix that only included litopterns in their sample (Bonaparte & Morales 1997). Another controversial family is Protolipternidae as its inclusion within Litopterna was based on an indirect assignment of tarsals with litoptern features (Cifelli 1983*a*, *b*) to dentitions that are undistinguishable from many members of the "condylarth" family Didolodontidae. The last controversial family is Sparnotheriodontidae that has been linked to didolodontids based on an indirect tarsal assignment (Cifelli 1983*a*, *b*), although dentally seems to show many similarities with the anisolambdid litopterns (Soria 2001). This tarsal association has been strongly criticized (Soria 2001; Lorente 2015). In addition, recently some authors have started considering the South American "condylarth" family Didolodontidae as part of Litopterna (e.g., Gelfo *et al.* 2020), which is problematic because it has not been tested empirically through a phylogenetic analysis.

It is clear that there are still important controversies in relation to the interfamilial affinities of Litopterna and the monophyly of this order. In consequence, in Chapter 4 I revisit these taxonomic problems using a new matrix with 954 dental and mandibular characters, that includes the earliest members of Litopterna, and also the some of the earliest members of each SANU order (except Pyrotheria) and also relevant South and North American "condylarths". I then ran maximum parsimony, and for the first time for litopterns and early SANUs, undated and tip-dated Bayesian phylogenetic analyses obtaining a set of phylogenies. By discussing the features these phylogenies share and the features in which they differ, important conclusions about litoptern taxonomy are advanced and a new definition for a monophyletic Litopterna is proposed, obtaining a better understanding of the interfamilial affinities of this important order. In addition, divergence-time estimates are obtained for important cladogenetic events in the early Litoptern evolution with implications for the placental ordinal origination and diversification. A date for the separation of the South American and Antarctic sparnotheriodontids is also estimated, which gives relevant information about major biogeographic processes in the Southern Hemisphere.

Chapter 5 provides a synthesis and general conclusions to my thesis, and suggests future directions of research. Each chapter is presented separately, with figures and tables imbedded in the text. The numbering of figures and tables was not continuous across the chapters; instead, the chapter number precedes the number of each table or figure. For example, Table 1.1 means Table 1 from Chapter 1 All references and appendices details are provided at the end of the text, and the numbering of the appendices is similar to the way figures and tables are numbered. That means that first the Appendix makes reference to the chapter number and then to the specific resource number. For instance, Table S1 in Appendix C2 Resource 1 means the Table S1 in the Resource 1 from Chapter's 2 Appendix.

# Chapter 2 Divergence-time estimates for hominins provide insight into encephalization and body mass trends in human evolution



*Australopithecus afarensis* | *Paranthropus boisei* | *Homo habilis* | *Homo erectus* | *Homo sapiens*

Some relevant hominins for our understanding of human evolution

# Introduction

Establishing an evolutionary timescale for human evolution is of essential relevance in palaeoanthropology (Finarelli & Clyde 2004; Du & Alemseged 2019; Du *et al.* 2020) because reliable estimates of the timing of speciation events across the hominin phylogeny facilitate the correlation of these events with both abiotic and biotic processes on geological timescales. An accurate timescale also provides a framework to test for associations between landmark evolutionary changes and different putative extrinsic causal factors such as changes in climate or other environmental influences (DeMenocal 2004, 2011). Despite recent relevant fossil findings, the antiquity and emergence of the genus *Homo*, as well as the timing of the divergence of our lineage with other African apes have not found a consensus (Antón & Josh Snodgrass 2012; Harcourt-Smith 2016; Ruiter *et al.* 2017; Villmoare 2018).

Traditionally, palaeoanthropologists have employed maximum parsimony analysis to infer hominin phylogenetic relationships (Skelton & McHenry 1992; Strait *et al.* 1997; Smith & Grine 2008), but this approach does not explicitly estimate divergence-times as part of the estimation of the phylogeny. Previous studies (Bobe & Leakey 2009; Bobe & Carvalho 2019) computed confidence intervals for the disappearances and appearances of several hominins. However, their approach is not easily applicable to several available hominin taxa, as it requires the availability of extensive palaeontological datasets. Additionally, this method only provides confidence intervals for local first and last appearance data, which do not correspond to the global origination and extinction dates of the taxa under analysis. Other studies have computed these values but their results have been limited by either focusing on a restricted number of hominin taxa (Du *et al.* 2020) or because the assumptions of their applied methods were not met (Maxwell 2018). Bayesian phylogenetic inference methods have also been applied to morphological data (Dembo *et al.* 2015, 2016) to provide divergence time estimates. However, these estimates were exclusively based on anatomical data, even though it is now widely known that the fragmentary nature of the fossil record is not enough to compute reliable divergence estimates (Donoghue & Benton 2007), and that it is necessary to consider the molecular information available for several hominin and ape taxa in the analyses.

There is currently a consensus that the most feasible way of determining an accurate evolutionary timescale is by using the molecular clock, a prospect that has progressively concretised with the development of Bayesian relaxed clock methods (Donoghue & Yang 2016; Dos Reis *et al.* 2016; Kumar & Blair Hedges 2016; Bromham *et al.* 2017). Bayesian

divergence-time estimates require the use of prior probability distributions to incorporate fossil evidence for calibrating the tree. Recently, a new approach known as 'total-evidence dating' (TED), 'tip-dating' or 'integrative dating'(Ronquist *et al.* 2016) has been developed (Pyron 2011; Ronquist *et al.* 2012*b*). TED complements the molecular sequence data derived from extant species with morphological information from both living and extinct species, which allows a more thorough inclusion of fossil data in the analysis and estimation of divergence-times.

Hence, in this work we applied this divergence-time estimation method to produce total evidence evolutionary timescales for the hominin clade. We considered four different topological hypotheses with alternative reasonable affinities for problematic hominin taxa (Fig. 2.1). This is highly relevant because these timescales can be used for dating the origin of *Homo* or any other hominin genus, inferring evolutionary rates and patterns, as well as providing a better understanding of the coevolution of hominins and their environment. Additionally, we subsequently used the dated trees to carry out ancestral state reconstruction (ACSR) of two evolutionary important phenotypic characters: body mass and phylogenetic encephalization quotient (PEQ). Body mass impacts almost every aspect of an animal's biology and ecology (Grabowski *et al.* 2015; Jungers *et al.* 2016), hence its importance in any palaeobiological inference, whilst an evolutionary trend of increasing encephalization is one of the hallmark processes in human evolution (Ni *et al.* 2019; Melchionna & Mondanaro 2020).

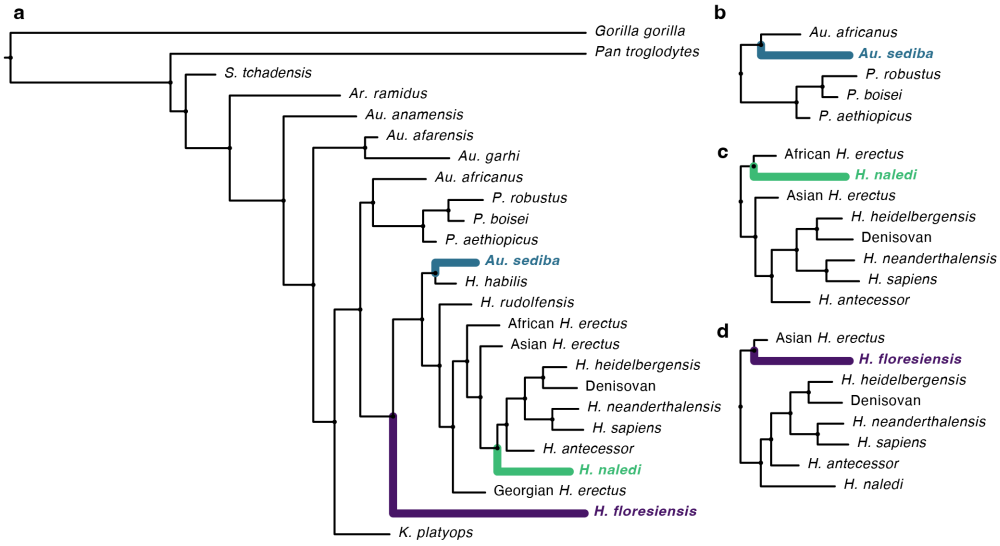



**Figure 2.1** Alternative topological hypotheses tested in the TED analyses. **a**. Similar to the phylogeny of Dembo *et al.* (2016). **b**. The same topology as a but moving *Au. sediba* from the *Homo* clade to be the sister taxon to *Au. africanus*. **c**. The same topology as a but changing the position of *H. naledi* from the stem of *H. antecessor* and its closest *Homo* relatives to be the sister taxon to the African *H. erectus*. **d**. The same topology as **a** but taking *H. floresiensis* from its basal position within the genus *Homo* to be the sister taxon to the Asian *H. erectus*.

# Methods

## Data collection and Total Evidence analyses

For the TED analysis, our taxon sampling was similar to previous published analyses (Dembo *et al.* 2016) but Denisovans were also included. The morphological data were obtained from the same study (Dembo *et al.* 2016), and comprised a supermatrix of 391 craniodental characters from matrices used in 13 previous studies (Cameron *et al.* 2004; Cameron & Groves 2004; Kimbel *et al.* 2004; Strait & Grine 2004; Chang 2005; Martinón-Torres *et al.* 2007; Gilbert 2008; Argue *et al.* 2009; Mounier *et al.* 2009; Zeitoun 2009; Berger *et al.* 2010; Irish *et al.* 2013; Lordkipanidze *et al.* 2013). Even though there are more recently published hominin phylogenetic analyses computed using different morphological matrices (Mongle *et al.* 2019; Martin *et al.* 2021), the morphological matrix used here (Dembo *et al.* 2016) is the most complete, to our knowledge, in terms of the number character states and hominin species included.

The molecular data were complete mtDNA genomes extracted from GenBank for the species for which it was available: *Gorilla gorilla* (KF914214.1), *Pan troglodytes* (JF727180.2), *Homo heidelbergensis* (KF683087.1), *Homo neanderthalensis* (MK123269.1), *Homo sapiens* (KC417443.1) and Denisovans (KX663333.1). Following previous analyses (Finstermeier *et al.* 2013; Meyer *et al.* 2014), we removed the D-loop region from the mtDNA due to the differential rate at which it acquires substitutions. We aligned the sequences with the MUSCLE algorithm in MEGA X (Kumar *et al.* 2018). Then, we analysed the alignment using PartitionFinder2 (Lanfear *et al.* 2017) using the "greedy" algorithm (Lanfear *et al.* 2012), in order to select the most appropriate models of molecular evolution for the different protein coding and non-coding regions of the mtDNA. The best partitioning scheme on the basis of AICc score included 16 partitions for the mtDNA (Table S1 in Appendix C2 Resource 1). We used these partitions for the mtDNA sequences, and the Mkv+ Γ model (Lewis 2001) for the morphological data, unlinking the model parameters across these partitions. In order to avoid a mismatch in our model, we used the dates associated with our data following the recommended procedure (Püschel *et al.* 2020), which meant that we did not necessarily calibrate a tip using the oldest or first fossil occurrence for a particular taxon. Hence, we calibrated the fossil tips of the tree using the age of the fossil specimen used for coding morphology in taxa without mtDNA available. If multiple specimens of different ages were used for coding the morphology of a taxon, the calibration bounds were based on the

radiometric uncertainty of the oldest specimen listed. This was based on the fact that simulations have shown that in cases of morphological stasis, more accurate and precise results are obtained by using the oldest stratigraphic occurrence of a lineage (Püschel *et al.* 2020).In taxa with mtDNA sequences available, the sequences were selected from individuals aged equally, or as close as possible, to the morphologically coded fossils, and the age associated with these sequences was used to calibrate the fossil tips. In all cases the radiometric age uncertainties were modelled using a uniform distribution between the maximum and minimum estimated ages for each fossil when available (O'Reilly *et al.* 2015; further information can be found in Table S2 in Appendix C2 Resource 1).

The selected outgroup was *Gorilla gorilla* and the root of the tree was calibrated using a uniform distribution between 10.00 and 12.5 Ma. The minimum age of 10 Ma and the maximum age of 12.5 were based on the appearance of the proposed stem member of the gorilla clade *Nakalipithecus nakayamai* (Kunimatsu *et al.* 2007; Katoh *et al.* 2016) and the probable crown pongine *Sivapithecus* (Begun 2010; Begun *et al.* 2012), respectively. Even though there is uncertainty regarding the exact phylogenetic placement of *N. nakayamai* (Kunimatsu *et al.* 2007; Katoh *et al.* 2016), we consider that the anatomical features linking it with gorillas are strong enough to use the age associated with this taxon as minimum divergence date for hominines, particularly when considering the possible ancestral-descendent relationship between *N. nakayamai* and the basal gorillin *Chororapithecus abyssinicus* (Suwa *et al.* 2007; Harrison 2012; Katoh *et al.* 2016).

We used a normally distributed clock rate prior, with a mean of 0.025 and standard deviation of 0.05, which is consistent with previous estimates of the mitochondrial rate of evolution in humans (Fu *et al.* 2013, 2014). The Independent Gamma Rate (IGR) relaxed clock model was used for modelling branch rate variation, employing a clock rate variance prior with an exponential distribution of rate 10. We used the FBD model as the prior on divergence times, using an exponential net diversification prior with rate 1, a beta turnover prior with shape parameters $\alpha=1$ and $\beta=1$, a beta fossil sampling proportion prior with shape parameters $\alpha=1$ and $\beta=1$ and an extant sampling proportion of 1. The priors employed in clock rate variance and the FBD model were intentionally diffuse, reflecting the general uncertainty in our prior expectation of the distribution of these parameters.

Even though our main focus was estimating hominin divergence-times, we are aware that that there is still controversy regarding the phylogenetic placement of some of the taxa

included in our matrix, particularly in the placement of *Australopithecus sediba* (Irish *et al.* 2013; Du & Alemseged 2019), *Homo floresiensis* (Brown *et al.* 2004; Dembo *et al.* 2015; Argue *et al.* 2017) and *Homo naledi* (Dembo *et al.* 2016; Berger *et al.* 2017). Therefore, we considered four different topological hypotheses for constraining four independent phylogenetic analyses (Fig. 2.1): a), a topology similar to the phylogeny of the analysis from which we extracted the morphological data (Dembo *et al.* 2016); b), the same topology as a) but moving *Au. sediba* from the *Homo* clade, to be the sister taxa of *Australopithecus africanus* as has been recently suggested (Kimbel & Rak 2017); c), the same topology as a) but changing the position of *Homo naledi* from the stem of *Homo antecessor* to be the sister taxa of the African *Homo erectus* as previously suggested (Berger *et al.* 2017; Schroeder *et al.* 2017); d), the same topology of a) but taking *H. floresiensis* from the base of the genus *Homo* to be the sister taxa of the Asian *Homo erectus* as was originally suggested (Brown *et al.* 2004). Nevertheless, we left *H. sapiens*, *H. neanderthalensis, H. heidelbergensis* and Denisovans unconstrained in the four analyses as they had mtDNA sequences which could also be informative of their phylogenetic relationships. Therefore, the constraints we used in all the analyses were soft, so the latter taxa could be accommodated in any position of the tree according their morphological, molecular and stratigraphic information.

We performed the analyses with MrBayes 3.2.7a (Ronquist *et al.* 2012*a*) using two runs of four chains and 60 million MCMC generations with the first 25% of samples discarded as burn-in. The analyses were run on CIPRES portal v3.3 (Miller *et al.* 2010). We ensured that the average standard deviation of split frequencies was below 0.01 and that all parameters had an effective sample size of more than 200. Additionally, we visually inspected that the two independent runs achieved convergence and stationarity using the program Tracer v1.7.1(Rambaut *et al.* 2018).

## Evaluating the prior sensitivity of divergence-time estimates

In order to evaluate the effect of alternative priors on our divergence-time estimates, we conducted sensitivity analyses in the first tree (i.e., Dembo *et al.*[Dembo *et al.* 2016] hypothesis) in which we changed the prior distribution of one important model parameter at a time into a reasonable alternative prior distribution, keeping the rest of the model parameters unchanged. This was done for the clock rate variance, the net diversification prior of the FBD model and root age prior. We did this in the former two cases because we wanted to test the effect of using more constrained priors, and in the latter, to account for the possibility that *N.*

*nakayamai* could be a stem hominid before the gorilla–human split (Kunimatsu *et al.* 2007; Katoh *et al.* 2016). Therefore, for the clock rate variance prior, we ran a strict clock and a non-clock analysis constrained to have the same topology. Then, following Ronquist's *et al.* (2012) methodology to estimate rate variance, the clock rate variance prior was estimated as 25.04. For the net diversification prior we followed Zhang *et al.* (2016) in using an exponential distribution of rate 100. In the case of the root age prior we used a uniform distribution changing the minimum to 8 but keeping the maximum in 12.5 Ma, because of the 8 Ma estimated for appearance of the proposed gorillin *C. abyssinicus* (Suwa *et al.* 2007; Katoh *et al.* 2016), which have been used to date the minimum age of the gorilla–human split in previous studies (Pozzi *et al.* 2014; Dos Reis *et al.* 2018).

## Estimating PEQ using a PGLS regression

The encephalization quotient (EQ) is commonly used to determine how brain size scales with respect to body size for a given individual (Jerison 1973, 1979; Cairó 2011; Grabowski *et al.* 2016). However, EQ does not take into account phylogenetic information, so a newly proposed measurement termed PEQ has been advanced as a way of considering the phylogenetic non-independence between data points (Ni *et al.* 2019).

Body mass and endocranial volume (ECV) were obtained from the literature (see Table S3 in Appendix C2 Resource 1 for further information). When more than one specimen was available, arithmetic averages for body mass and endocranial volume were used. Endocranial volume was converted into brain mass by dividing ECV by 1.036 (Stephan *et al.* 1981). We used R version 3.6.1 (R Core Team 2019) and the packages 'ape'(Paradis *et al.* 2004) and 'nlme'(Pinheiro *et al.* 2020) to compute phylogenetic correlations and to fit linear models, respectively. We log-scaled the data, and by assuming a Brownian motion model of evolution we calculated a correlation using the corBrownian() function to then fit a linear model (brain mass was the dependent variable, whilst body mass was the independent one) independently for each one of the four consensus trees obtained in the TED analysis (Fig. S8 in Appendix C2 Resource 2). $R^2$ were calculated using the R package rr2 v1.0.2 and the function R2.pred() (Ives 2019). The resulting equations were used to calculate the expected brain mass (E), and PEQ was calculated as the ratio between the actual estimated brain mass (A) and E (PEQ = A/E) for each one of the living and fossil taxa (Table S3 in Appendix C2 Resource 1).

## PEQ and body mass ancestral character state reconstructions

We used a ML approach to perform the ACSR at the internal nodes of the four consensus phylogenetic trees for 1) body mass and 2) PEQ (and brain mass) under a Brownian motion model. This procedure was performed using the fastAnc() and the contMap() functions from the package 'phytools' v 0.6-99(Revell 2012). *Kenyanthropus platyops* and *Australopithecus garhi* tips were dropped from the ACSR for body mass and PEQ as there were no body mass estimations for these taxa available due to their fragmentary fossil record. Similarly, Denisovans were removed from all ACSR analyses as there are no estimates available for their brain and body mass.

## Measuring uncertainty in the ML ancestral character state reconstructions

In order to measure the uncertainty in our ML ACSR we sampled every 10$^{th}$ time-calibrated tree from the posterior after discarding the first 25% as burn-in, which it meant a total of 9002 time-calibrated posterior trees sampled for each one of the four analyses. Then we ran ML ACSR analyses in all of these trees and their internal nodes for 1) body mass and 2) PEQ (and brain mass), using the same methods and R packages described in the previous section. For the PEQ ACSR, we previously ran the PGLS analysis for each one of the sampled trees, so the PEQ values in the trees' tips were independently estimated for each tree. This allowed us to incorporate uncertainty in our ACSR, and to analyse if the patterns observed in the ACSR for the consensus trees hold or not when we looked at different trees recovered from the posterior.

## Measuring the relationship between ACSR of brain mass and body mass

As brain size increase has been proposed as a driver of body size increase(Grabowski 2016), we carried out regressions between our ACSR of brain mass versus body mass in the four consensus trees to test if there was a pattern that could be consistent with that hypothesis. It is important to consider that we did not directly assess the hypothesis a brain size increase drove body mass evolution but rather evaluate if there was a general pattern that could provide further information about this issue. Both ACSR datasets were log-scaled before performing the regressions.

## Results

The TED analyses (Fig. 2.2, Table 2.1, and Fig. S1 in Appendix C2 Resource 2) show, in general, better-resolved divergence times for the nodes that have both morphological and molecular information available, in comparison with the nodes estimated with morphological information alone. The common ancestor of hominins and *P. troglodytes* (node 2) was dated at around 7.5 Ma with an uncertainty range of 8.59 – 6.61 Ma considering the 95% highest posterior density intervals (HPD) of all the trees. The common ancestor of the genus *Homo* (node 13 or 14 for *H. floresiensis* hypothesis) was dated at around 3.3 Ma with an uncertainty range of 4.30 – 2.56 Ma considering the 95% HPD of all the trees. In general, estimations for this node were consistent between the four trees, although the biggest difference resulted when *H. floresiensis* is removed from the base of *Homo*, making the node's age slightly younger (Fig. 2.2d). The prior sensitivity analysis (Fig. S2 in Appendix C2 Resource 2) shows mostly minor differences between divergence-times in the original analysis and analyses using different priors in relevant parameters, suggesting that the TED analyses are robust to changes in the employed priors.

The maximum likelihood (ML) ACSR based on the four consensus trees (Figs. 2.3, 2.4, and Figs. S3-6 in Appendix C2 Resource 2) are consistent with the ACSR based on samples of the posterior trees from these analyses (Fig. 2.5 and Fig. S7 in Appendix C2 Resource 2). The main difference is an apparent PEQ overestimation in the case of the ACSR based on the consensus trees versus the ACSR based on samples of the posterior trees (Fig. 2.5). These differences are explained because using equations based on PGLS regressions of the consensus trees (Fig. S8 in Appendix C2 Resource 2) returned lower expected brain masses calculated for the trees' tips on average than equations based on the sampled trees (Fig. S9 in Appendix C2 Resource 2). However, the general PEQ trends remain the same. Similarly, the brain mass ACSR versus body mass ACSR regressions results show a consistently similar pattern for the four analyses. When we analyse all the nodes together in the four trees, the slopes are slightly positive and the $R^2$ values are low (around 0.11; Fig. S10a-d in Appendix C2 Resource 2). However, when we split the data there are clearly two different trends. Before node 13/14 the slopes are negative with a moderate $R^2$ (around 0.46) (Fig. S10e-h in Appendix C2 Resource 2), whereas after node 13/14 the slopes are strongly positive with a high $R^2$ (around 0.96; Fig. S10i-l in Appendix C2 Resource 2).

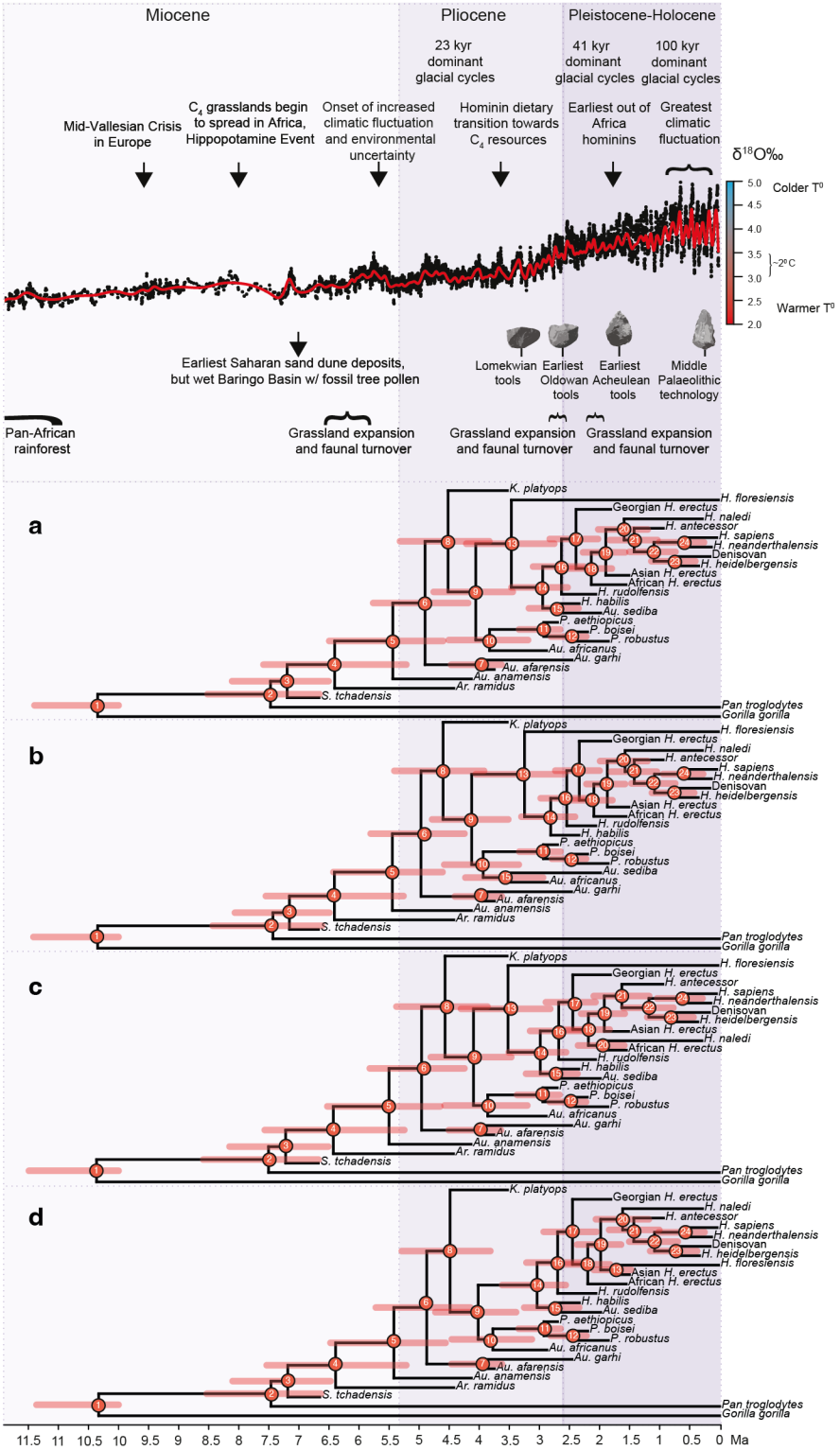



**Figure 2.2** Summary diagram of important palaeoclimatic and hominin evolution events plotted next to the four obtained consensus phylogenies and time divergence estimates. **a**. Dembo *et al.* (2016) hypothesis. **b**. *Au. sediba* hypothesis. **c**. *H. naledi* hypothesis. **d**. *H. floresiensis* hypothesis. Red node bars represent the 95% HPD for the estimated node ages. A composite benthic foraminifera oxygen isotope record previously obtained (Zachos *et al.* 2001) is displayed at the top of the figure to illustrate the evolution of high-latitude glacial cycles and dominant periodicity of glacial variability, as well as palaeotemperatures (the red line corresponds to a smoothing spline used to depict the main trend in δ18O values; smoothing parameter = 0.2).

The speciation events that occurred since the divergence from *G. gorilla* to the common ancestor of *Homo* (nodes 1-9 and 13/14), all occurred within the latest Miocene and Pliocene (Fig. 2.2 and Table 2.1). For that period, the body mass ACSR show that from a common ancestor of around 71 kg at 10.4 Ma, there is a trend of rapid decrease in body mass reaching around 38 kg by 3.3 Ma (Figs. 2.3, 2.5a-d, and Fig. S5 in Appendix C2 Resource 2). That is 1.87 smaller in 7.1 Myr. However, the PEQ ACSR show an opposite trend, increasing from around 0.87 to 1.88 in the same period (Figs. 2.4, 2.5e-h and Fig. S6 in Appendix C2 Resource 2), which is 2.16 times greater. The effect of removing of *H. floresiensis* from the base of *Homo* (Figs. 2.4d, 2.5h, and Fig. S6d in Appendix C2 Resource 2) is a higher estimated PEQ for the last common ancestor of this genus (i.e., 2.16) and the surrounding nodes. Following the path leading to *Au. africanus* and the members of the genus *Paranthropus* (nodes 1-10) the body mass tends to decrease to around 37 kg at node 10, which means a reduction of 1.92 times from the root in 6.6 Myr. Nevertheless, the path from nodes 9 to 10 does not indicate an increase in PEQ. Instead, it corresponds to the beginning of a slight reduction in PEQ in the lineage leading to *Paranthropus*. Interestingly, the last member of this genus*, P. robustus*, displays an increase in PEQ just before the extinction of the lineage. The incorporation of *Au. sediba* as the sister taxon of *Au. africanus* did not have a substantial influence on the ACSR of the neighbouring nodes.

Speciation events since the common ancestor of *Homo* start to occur around the mid-Pliocene at 3.3 Ma and end around the mid-Pleistocene at 0.6 Ma (Fig. 2.2 and Table 2.1). In contrast to the previous decreasing trend in body mass, the body mass ACSR show an increment from around 38 kg to 65 kg in this period (nodes 13/14-24; Figs. 2.3, 2.5a-d, and Fig. S5 in Appendix C2 Resource 2). This corresponds to an increase in body mass of 1.71 times in 2.7 Myr, which means a reversion in body size to similar levels as the one observed at the tree's root but in less than half of the time. In other words, the rate of body mass evolution approximately doubled in the genus *Homo* from what has been previously seen (10.0 kg/Myr vs 4.6 kg/Myr). However, these increments were not equal in all nodes and some groups even show a body mass reduction. For instance, the parallel branch that goes from node 14 to *Homo habilis* shows a decrease in body mass regardless of the position of *Au. sediba*. The effect of removing *Au. sediba* from *Homo* results in a slight increase in the reconstructed body mass at node 14. Similarly, *H. floresiensis* and *H. naledi* also displayed a considerable decrease in body mass from their ancestors in all the hypotheses. However, the decrease and its rate vary with the different hypotheses. When *H. floresiens*is is positioned at the base of *Homo*, the decrease

is around 10 kg (-3.0 kg/Myr), while when it is considered the sister taxon of the Asian *H. erectus* the decrease is approximately 22 kg (-13.0 kg/Myr). When *H. naledi* is at the stem of *H. antecessor* the decrease is around 13 kg (-10.1 kg/Myr), whereas when it is the sister taxon of the African *H. erectus* the decrease is approximately 5 kg (-3.0 kg/Myr).

**Table 2.1** Divergence times mean and 95% highest posterior density interval (HPD) in Ma for the different phylogenetic hypotheses in Fig. 1.1. The maximum and minimum bounds for the 95% HPD are in parentheses. Abbreviations: *Div.*, divergence-times mean; *d*, Dembo *et al.*(Dembo *et al.* 2016) hypothesis; *s*, *Au. sediba* hypothesis; *n*, *H. naledi* hypothesis; *f*, *H. floresiensis* hypothesis.

| Node* | Div. mean-d | Div. mean-s | Div. mean-n | Div. mean-f |
|---|---|---|---|---|
| 1 | 10.35 (11.40, 10.00) | 10.35 (11.42, 10.00) | 10.37 (11.49, 10.00) | 10.33 (11.36, 10.00) |
| 2 | 7.47 (8.52, 6.66) | 7.43 (8.43, 6.61) | 7.50 (8.59, 6.67) | 7.46 (8.53, 6.63) |
| 3 | 7.20 (8.11, 6.51) | 7.15 (8.06, 6.49) | 7.22 (8.15, 6.51) | 7.18 (8.10, 6.47) |
| 4 | 6.40 (7.59, 5.21) | 6.41 (7.55, 5.26) | 6.42 (7.57, 5.24) | 6.39 (7.54, 5.21) |
| 5 | 5.44 (6.49, 4.60) | 5.44 (6.42, 4.61) | 5.50 (6.52, 4.64) | 5.42 (6.47, 4.56) |
| 6 | 4.90 (5.76, 4.18) | 4.97 (5.80, 4.24) | 4.95 (5.82, 4.24) | 4.87 (5.72, 4.15) |
| 7 | 3.97 (4.47, 3.63) | 3.94 (4.40, 3.62) | 3.98 (4.50, 3.63) | 3.97 (4.46, 3.62) |
| 8 | 4.52 (5.32, 3.83) | 4.60 (5.41, 3.92) | 4.56 (5.37, 3.86) | 4.49 (5.29, 3.82) |
| 9 | 4.06 (4.76, 3.44) | 4.12 (4.78, 3.52) | 4.09 (4.80, 3.46) | 4.02 (4.73, 3.39) |
| 10 | 3.83 (4.51, 3.19) | 3.93 (4.58, 3.34) | 3.85 (4.57, 3.19) | 3.77 (4.46, 3.13) |
| 11 | 2.93 (3.34, 2.65) | 2.93 (3.33, 2.65) | 2.94 (3.36, 2.66) | 2.93 (3.34, 2.65) |
| 12 | 2.47 (2.81, 2.22) | 2.46 (2.79, 2.22) | 2.48 (2.82, 2.22) | 2.47 (2.81, 2.22) |
| 13 | 3.47 (4.21, 2.75) | 3.24 (4.05, 2.59) | 3.52 (4.30, 2.81) | **1.73 (2.09, 1.47)** |
| 14 | 2.94 (3.46, 2.53) | 2.81 (3.30, 2.40) | 2.98 (3.50, 2.55) | 3.04 (3.62, 2.56) |
| 15 | 2.70 (3.17, 2.35) | **3.57 (4.23, 2.94)** | 2.73 (3.21, 2.36) | 2.75 (3.25, 2.34) |
| 16 | 2.63 (3.10, 2.25) | 2.54 (2.97, 2.19) | 2.67 (3.15, 2.28) | 2.70 (3.21, 2.26) |
| 17 | 2.39 (2.83, 2.02) | 2.33 (2.73, 1.99) | 2.44 (2.88, 2.06) | 2.45 (2.93, 2.05) |
| 18 | 2.13 (2.54, 1.79) | 2.09 (2.47, 1.78) | 2.18 (2.58, 1.82) | 2.19 (2.63, 1.83) |
| 19 | 1.89 (2.27, 1.57) | 1.87 (2.21, 1.57) | 1.91 (2.30, 1.57) | 1.98 (2.37, 1.64) |
| 20 | 1.59 (2.02, 1.20) | 1.57 (1.99, 1.20) | **1.94 (2.35, 1.58)** | 1.61 (2.06, 1.18) |
| 21 | 1.42 (1.83, 1.04) | 1.42 (1.81, 1.04) | 1.62 (2.09, 1.17) | 1.43 (1.84, 1.01) |
| 22 | 1.09 (1.50, 0.73) | 1.08 (1.46, 0.74) | 1.17 (1.59, 0.76) | 1.08 (1.50, 0.70) |
| 23 | 0.77 (1.13, 0.40) | 0.77 (1.12, 0.42) | 0.80 (1.20, 0.43) | 0.76 (1.16, 0.38) |
| 24 | 0.60 (1.01, 0.26) | 0.59 (0.94, 0.27) | 0.63 (1.03, 0.28) | 0.59 (1.02, 0.25) |

*Node's ages that are not comparable due to the specific changes in the phylogenetic hypotheses are indicated in bold.

The PEQ ACSR for the period since the common ancestor of *Homo* (node 13/14) keeps the previously observed increasing trend, augmenting 1.53 times in 2.70 Myr, from around 1.88 in node 13/14 to 2.88 in node 24 (Figs. 2.4, 2.5e-h and Fig. S6 in Appendix C2 Resource

2). Even though the increase in PEQ is similar with the PEQ evolution before the common ancestor of *Homo* (1.00 and 1.01 respectively), its rate increased 2.64 times, going from 0.14 PEQ/Myr to 0.37 PEQ/Myr. Within this general PEQ evolutionary trend, there are three taxa that stand out from the rest: *H. floresiensis*, *H. naledi* and *H. sapiens*, although in the first two species the specific trends vary with the different hypotheses. When *H. floresiensis* is positioned is at the base of *Homo*, it displays a slight decrease or stasis in PEQ from its ancestor exhibiting a value around 1.7 for 3.4 Myr of evolutionary history, while when it is considered the sister taxon of the Asian *H. erectus* the decrease is 0.52 in 1.7 Myr (-0.30 PEQ/Myr). When *Homo naledi* is at the stem of *H. antecessor*, the PEQ decreases around 0.85 in 1.3 Myr (-0.65 PEQ/Myr), whereas when it is the sister taxon of the African *H. erectus* the decrease is approximately of 0.69 in 1.7 Myr (-0.42 PEQ/Myr). This strong decrease under different scenarios puts *H. naledi* very close to the PEQ values for *Au. afarensis*. In contrast, *H. sapiens* stands out due to its rapid increase in PEQ from its common ancestor with *H. neanderthalensis* (node 24), going from around 2.88 to 3.22 in approximately 0.55 Myr. That is 0.62 PEQ/Myr, which is 1.68 times greater compared to the rate observed since the common ancestor of *Homo* (nodes 13/14 to 24) between 3.3 Ma and 0.6 Ma, and 4.43 greater in comparison to the rate observed since the common ancestor of *G. gorilla* and the ancestor of *Homo* (nodes 1 to 13/14) between 10.4 Ma and 3.3 Ma.

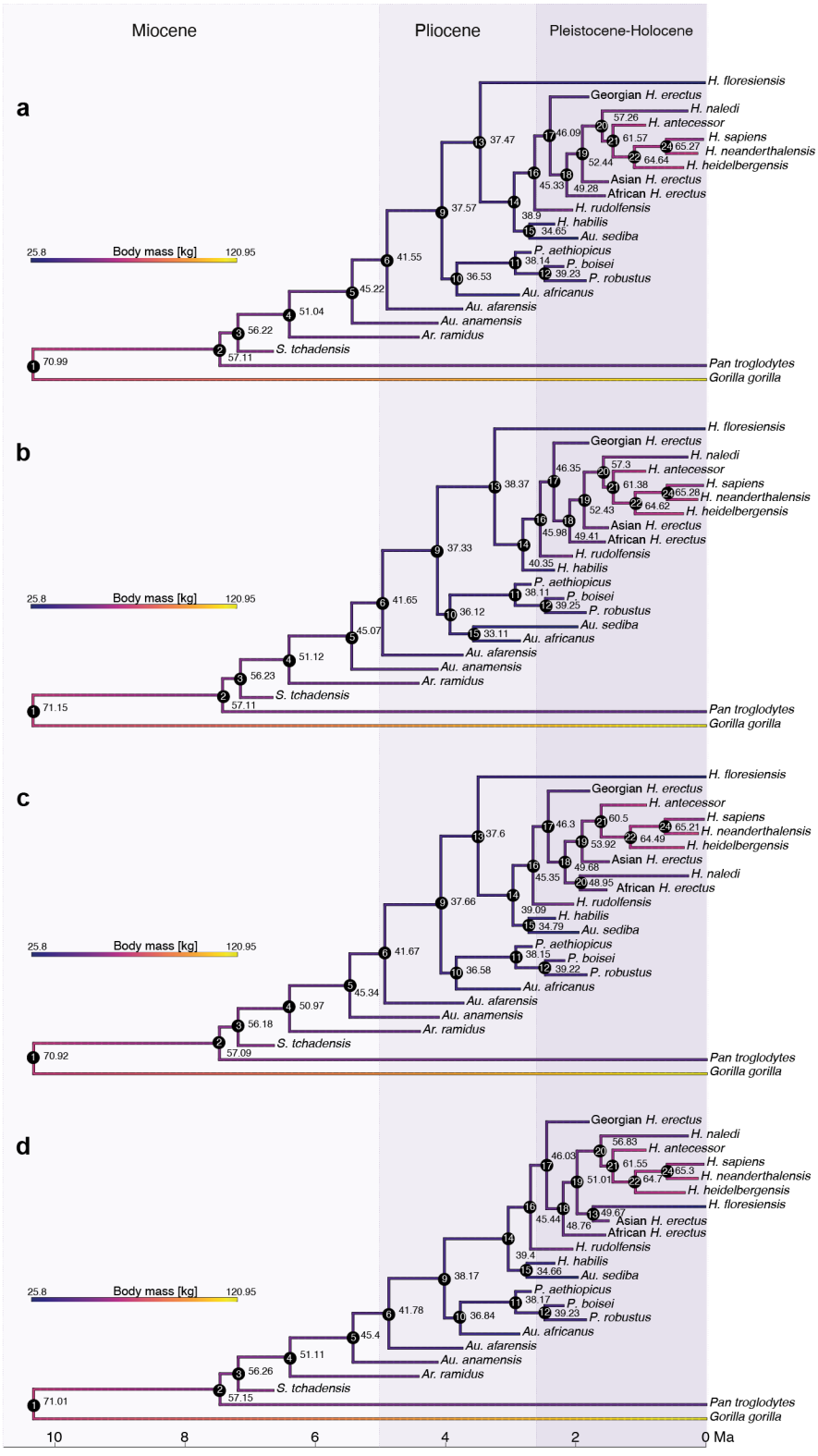



**Figure 2.3** Body mass ancestral character state reconstructions (ACSR) for each species mapped onto the four consensus time-calibrated phylogenies. **a**. Dembo *et al.* (2016) hypothesis. **b**. *Au. sediba* hypothesis. **c**. *H. naledi* hypothesis. **d**. *H. floresiensis* hypothesis. The values at nodes and branches were reconstructed using a maximum-likelihood ancestral character estimation method under a Brownian motion model.

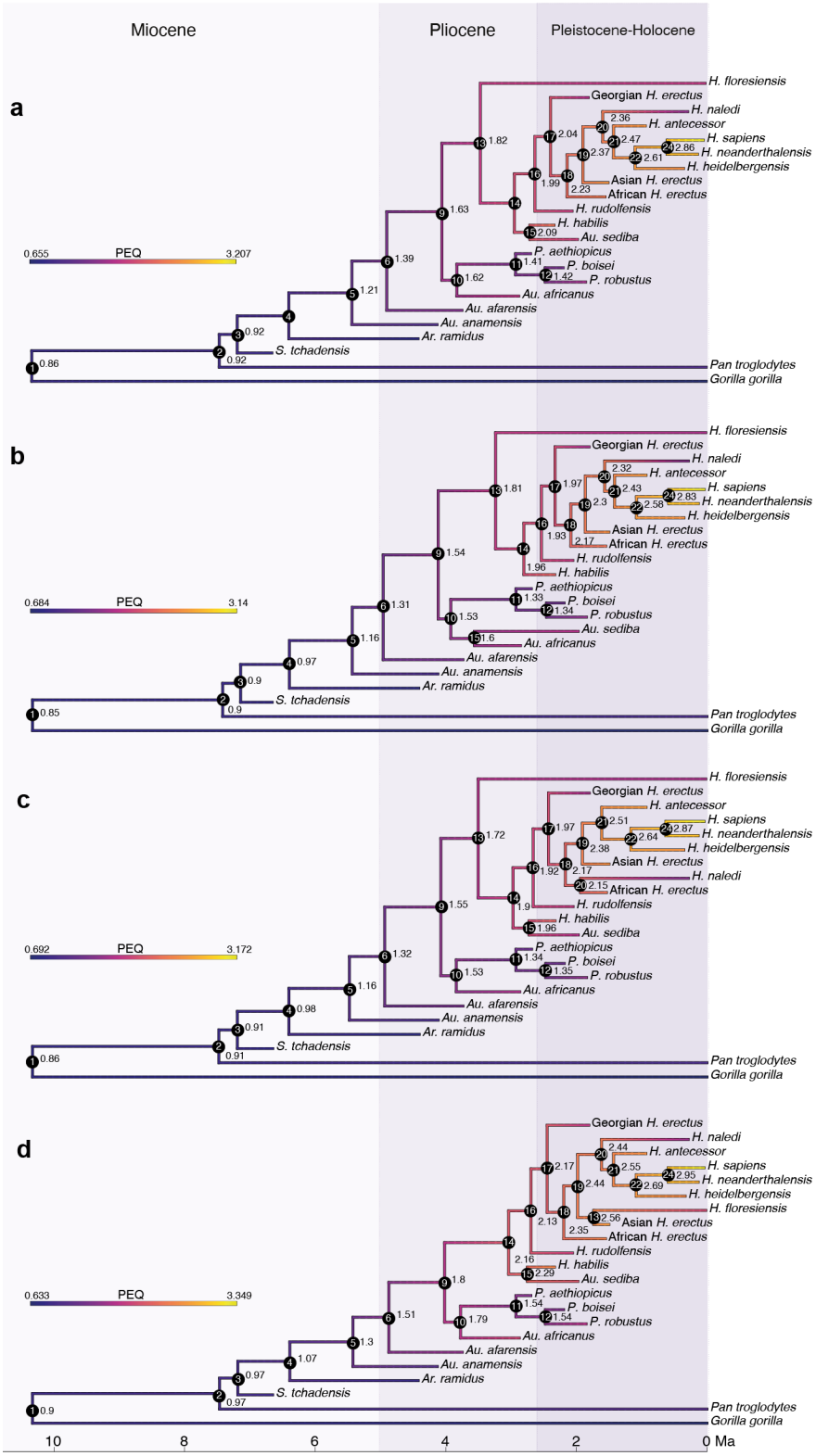



**Figure 2.4** PEQ ancestral character state reconstructions (ACSR) for each species mapped onto the four consensus time-calibrated phylogenies. **a**. Dembo *et al*. (2016) hypothesis. **b**. *Au. sediba* hypothesis. **c**. *H. naledi* hypothesis. **d**. *H. floresiensis* hypothesis. The values at nodes and branches were reconstructed using a maximum-likelihood ancestral character estimation method under a Brownian motion model.

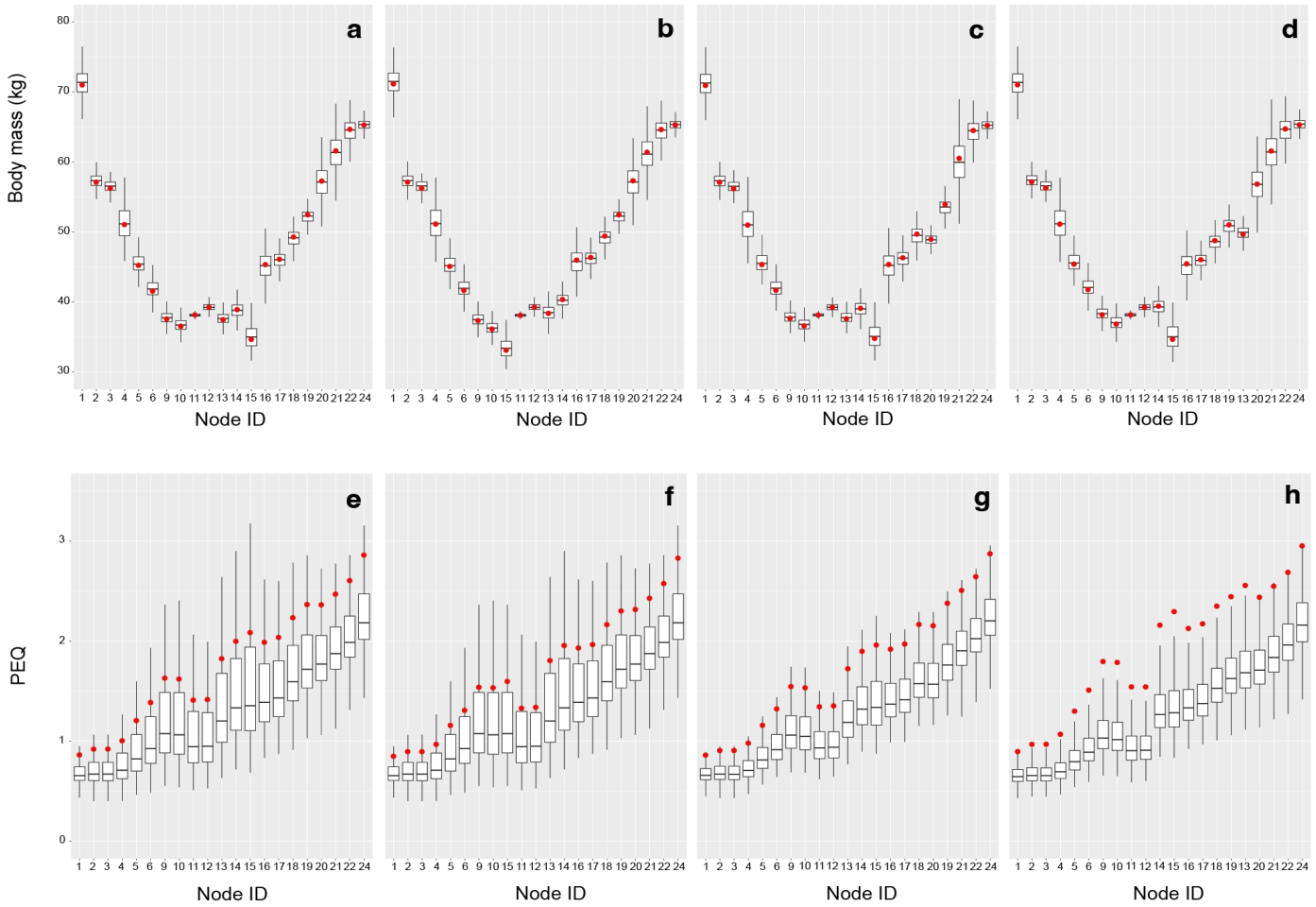



**Figure 2.5** Boxplots of (**a-d**) body mass (kg) and (**e-h**) PEQ ancestral character state reconstructions (ACSR) per node based on a sample of 9002 time-calibrated posterior trees for each of the tested hypothesis. **a**, **e**. Dembo *et al*. (2016) hypothesis, **b**, **f**. *Au. sediba* hypothesis, **c**, **g**. *H. naledi* hypothesis, and **d**, **h**. *H. floresiensis* hypothesis. The red dots indicate the ACSR conducted using the consensus trees. The median is indicated by the horizontal black line, the interquartile range (IQR) is the white box, and the whiskers indicate the minimum and the maximum (at 1.5 * IQR of the lower and upper hinge respectively).

## Discussion

We have presented here TED estimates of the divergence-times of most hominin taxa under different hypotheses. Our divergence estimates are in general agreement with previous molecular studies using fossil node-calibrations (Chatterjee *et al.* 2009; Dos Reis *et al.* 2012, 2018; Meyer *et al.* 2014; Pozzi *et al.* 2014), as well as with fossil calibration independent methods, such as those using generation times (Langergraber *et al.* 2012). The topology of our trees (Fig. 2.2) differs from the trees of Dembo *et al* (Dembo *et al.* 2015, 2016) in the position of *H. neanderthalensis* relative to *H. sapiens* and *H. heidelbergensis*, which is likely due to the influence of the mtDNA in our Total Evidence analysis. The position of these groups plus Denisovans is the same as obtained in a previous study (Meyer *et al.* 2014) using mtDNA but differs from studies using nuclear DNA (Meyer *et al.* 2016), probably related to a mtDNA introgression event that occurred ~270 ka (Posth *et al.* 2017). We think our divergence-time estimates are robust and consistent with the current evidence available. However, further refinements in some of the fossilized birth-death (FBD) model's assumptions, namely being able to consider a nonuniform fossil sampling among clades (Gavryushkina & Zhang 2020), and new fossil discoveries, could further improve these estimates.

Our ACSR results from the four different considered hypotheses are consistent between them, showing that refining the phylogenetic affinities of problematic taxa (e.g., *H. naledi*) would probably have a minor impact in major body size and encephalization trends in hominin evolution. Furthermore, our ACSR results are consistent with previous studies that show that body size in hominins has not been a simple linear increment since the divergence with *P. troglodytes* (Grabowski *et al.* 2015; Jungers *et al.* 2016; Will *et al.* 2017). The observed decreasing trend in body size from the root of the tree is in agreement with previous studies that suggest a chimpanzee-sized common ancestor with *P. troglodytes* (Grabowski & Jungers 2017; Grabowski *et al.* 2018). Our ACSR results also displayed a general trend towards greater body size that started after the emergence of the last common ancestor of *Homo*, contrary to a previous claim stating that there were no clear body mass temporal trends in hominin evolution (Grabowski *et al.* 2015). Instead, our results showed a complex history of body size changes that do not correlate linearly with brain size changes. It may be that after the emergence of the genus *Homo*, brain size carried body size increases as previously suggested (Grabowski 2016) (Fig. S10i-l in Appendix C2 Resource 2). However, before the emergence of *Homo*, brain size and body size seem to be decoupled or following opposite directions (Fig. S10e-h in Appendix

C2 Resource 2). Our results also agree with Pagel's (Pagel 2002) seminal work and other studies (e.g.,[Gómez-Robles *et al.* 2017; Diniz-Filho *et al.* 2019; Miller *et al.* 2019]) that showed a general trend of gradual but accelerating brain size evolution in hominins. However, some of them (i.e.,[Gómez-Robles *et al.* 2017; Diniz-Filho *et al.* 2019]) directly analysed endocranial volume without taking into account body mass estimations, which we considered in our PEQ estimations. This is problematic because it is only when body size is considered (McHenry & Coffing 2000) and phylogeny is included that we can consider whether observed brain size differences are significant in terms of encephalization (Montgomery *et al.* 2010; Grabowski *et al.* 2016; Ni *et al.* 2019). We are confident that our ACRS are reliable and consistent with the current evidence. Nevertheless, it is important to note that the inclusion of more fossils near the root could have an impact in the ACSR, in particular for the oldest nodes of the tree. Additionally, ACSR could be affected by the use of different methods and models of character evolution (Castiglione *et al.* 2020).

The fact that PEQ evolution tends to accelerate when moving from a relatively stable climate to more unstable climatic conditions (Fig. 2.2) appears to agree with the 'variability selection' hypothesis which correlates major adaptations in hominins with periods of high climatic variability (Potts 1996, 1998). Before the emergence of *Homo*, hominin evolution occurred in a mostly warm period although with a global cooling trend, which had started after the Mid-Miocene Climatic Optimum and the recovery of Antarctic ice-sheets around 10 Ma (Zachos *et al.* 2001). From a common ancestor with *P. troglodytes* at around 7.5 Ma, bipedalism started to emerge at least by 6 Ma (Crompton *et al.* 2008; Richmond & Jungers 2008; Almécija *et al.* 2013; Kuperavage *et al.* 2018) in the hominin lineage. This relatively stable period was interrupted by considerable temperature oscillations around the Miocene/Pliocene boundary at 5.3 Ma. Subsequently with the development of 23 kyr dominant glacial cycles, we observed the emergence of the genus *Homo* and an evolutionary shift, displaying the end of a general trend towards smaller body size and the beginning of an acceleration of the increase in PEQ and the start of a general trend towards larger body masses (Figs. 2.2-2.4). Even though the earliest member of *Homo* discovered so far was from 2.8 Ma (Hawks *et al.* 2015), our analysis allows us to predict the presence of early representatives of the *Homo* lineage not yet found (or identified) in the African fossil record around 3.3 Ma (i.e., 0.5 Myr earlier). Interestingly, 3.3 Ma is the age attributed to stone tools discovered in West Turkana (Harmand *et al.* 2015), which are commonly associated with *K. platyops* (Leakey *et al.* 2001) and *Au. afarensis*(Brown *et al.* 2001).

After the Pliocene-Pleistocene boundary at 2.58 Ma, the trend towards cooler temperatures and aridity continues, and 41 kyr dominant glacial cycles are established, with an intensification of climatic fluctuations. As PEQ continues to increase, so does the evidence of increasingly complex behaviours: tool innovations (Oldowan [2.6 Ma ;Braun *et al.* 2019], Acheulean [1.7-1.4 Ma; Lepre *et al.* 2011] and Aurignacian at [120–~50 ka; Gamble 2013], the use of fire (from 1.5 Ma onwards [Hlubik *et al.* 2017, 2019]) [strong evidence at 1.0–0.5 Ma; Gowlett 2016]), cooking and more frequent meat consumption (Wrangham *et al.* 1999; Carmody *et al.* 2011; Fonseca-Azevedo & Herculano-Houzel 2012) and the ability to produce art at ~540–430 ka (Joordens *et al.* 2015). By 300 ka Africa was inhabited by at least three *Homo* species, *H. sapiens*, *H. heidelbergensis* and *H. naledi*, and Eurasia by *H. neanderthalensis*, Denisovans, *H. floresiensis*, *H. luzonensis* and also possibly *H. erectus* and *H. heidelbergensis* (Grün *et al.* 2020). *H. sapiens* is the hominin species with the highest PEQ, so a possible explanation for its exclusive continuation would be that this difference in PEQ allowed *H. sapiens* to outcompete its contemporary relatives (McHenry & Coffing 2000; Banks *et al.* 2008; Kochiyama *et al.* 2018; Timmermann 2020). Even though it has been recently established that there was not a unique 'Out of Africa' event in *H. sapiens* history (Hovers 2006; Hershkovitz *et al.* 2018; Harvati *et al.* 2019; Scerri *et al.* 2019), it is widely accepted that Neanderthals were eventually displaced by *H. sapiens* in Europe by ~39 ka (Proctor *et al.* 2017). However, it is now understood that *H. neanderthalensis* was capable of very complex human behaviours (Villa & Roebroeks 2014; Galway-Witham *et al.* 2019).

Like *H. sapiens*, *H. neanderthalensis* was certainly a cultural niche constructor (Kendal *et al.* 2011; Downey & Lende 2012; Boivin *et al.* 2016) under harsh glacial-interglacial temperature fluctuations (Potts 2012). Nonetheless, *H. sapiens* not only displays a higher PEQ, but also a higher rate of change in PEQ compared to *H. neanderthalensis*. This probably means that within Hominini, PEQ selection was particularly strong within and between the metapopulations of *H. sapiens* (Scerri *et al.* 2018) in an arid-moist fluctuating Africa (Potts 2012). A larger relative brain mass has been associated in mammals with behavioural flexibility, adaptation and resilience in variable environmental conditions (Sol *et al.* 2008). Therefore in spite of the fact that the behavioural gap between the two species may have been minimal, even a small advantage in terms of behavioural flexibility and ability to adjust in a variable environment as it was during the late Pleistocene (Potts 2013), could have had enormous benefits in terms of fitness and successful competition for *H. sapiens* (Roberts &

Stewart 2018; Wedage *et al.* 2019). A similar explanation could also be applied for the demise of the rest of our contemporaneous relatives exhibiting an even lower PEQ.

Considering the evolution of *H. floresiensis*, it seems that selection was acting on body size by means of heterochrony (Van Heteren & Sankhyan 2009; Diniz-Filho & Raia 2017) favouring a reduction in body size as a mean of decreasing the energetic expenditure in a small island environment with limited resources as it also probably occurred for *Stegodon florensis* (Foster 1964; Kubo *et al.* 2013; Dennell *et al.* 2014). However, our results show that resolving the phylogenetic affinities of *H. floresiensis* would have important implications for the evolutionary trends on this taxon. The body size reduction in *H. floresiensis* is more spectacular if this taxon derives or is considered closely related to Asian *H. erectus* (Brown *et al.* 2004), a scenario that also implies a notorious encephalization reduction. Nevertheless, more recent studies favour the position of *H. floresiensis* at the base of *Homo* (Dembo *et al.* 2015, 2016; Argue *et al.* 2017), which would then favour a encephalization stasis scenario. Interestingly, if tool development can be associated with a certain level of cognition, considering the tools attributed to *H. floresiensis* (Brumm *et al.* 2006; Moore & Brumm 2009), we anticipate that the common ancestor of *Homo* with a similar PEQ value, was most likely able make stone tools as well.

Previous studies have described *H. naledi* as a small bodied and small brained hominin of the genus *Homo* (Garvin *et al.* 2017), with cranial (Laird *et al.* 2017), endocranial (Holloway *et al.* 2018) and postcranial features (Kivell *et al.* 2015; Marchi *et al.* 2017) that support this placement. There are two hypotheses which attempt to explain this small brain as either a (1) retention from the common ancestor from the genus *Homo*, or (2) a reduction from a later big-brained form of *Homo* (Holloway *et al.* 2018). The PEQ trends displayed by *H. naledi*'s ACSR supports the second hypothesis because there is an extraordinary reduction in PEQ from a big-brained ancestor in a relatively short time, although this reduction is faster if *H. naledi* is at the stem of *H. antecessor* as previously suggested (Dembo *et al.* 2016). *H. naledi* lived between 236 ka and 335 ka (Dirks *et al.* 2017) in South Africa, with a PEQ around 1.5, which is really close to *Au. afarensis* and other australopiths. This happened at a time in which big bodied and big brained hominins were the norm in continental landmasses, like *H. sapiens* and *H. neanderthalensis* both with a PEQ over 2.7. Even the insular small sized *H. floresiensis* had a higher PEQ. In a context of increasing PEQ over the hominin lineage at that time, the PEQ reduction in *H. naledi* could perhaps be explained, by the specialization in a niche of scarce and/or low energy food resources in which an expensive large brain would be prejudicial.

Hypotheses in relation to the cost of encephalization like the 'expensive tissue' (Aiello & Wheeler 1995; Isler & van Schaik 2009) and the 'energy trade off' hypotheses (Isler & Van Schaik 2006), could potentially explain this trend in *H. naledi*. Less energy expenditure could also explain the considerable body size reduction observed in *H. naledi* from its reconstructed bigger-brained ancestors. In fact, through dental topography comparisons it has been suggested that *H. naledi* was occupying a distinct ecological niche, which was different from previous and contemporaneous hominins (Berthaume *et al.* 2018).

In conclusion, our TED analyses and ACSR results showed that (1) the last common ancestor of the genus *Homo* most likely appeared around 3.3 Ma (between 4.30 and 2.56 Ma) with a body size close to that of *Au. afarensis* and an encephalization very similar to *H. floresiensis*, (2) hominin body mass evolution followed a general decreasing trend before the emergence of *Homo* and exhibited a general increasing trend afterwards, (3) hominins displayed a general trend of gradual but accelerating encephalization through time.

## Data availability

All data analysed in this study are available in the Appendix C2 Resource 1 (Tables S2 and S3) and in a permanent Zenodo (zenodo.org) repository at https://dx.doi.org/10.5281/zenodo.4537445(Püschel *et al.* 2021*b*). Additionally, the data is available in an open access repository at https://github.com/HansPueschel/Hominin-div-time-evolution (Püschel *et al.* 2021*b*).

## Code availability

The code and input files are available in a permanent Zenodo (zenodo.org) repository at https://dx.doi.org/10.5281/zenodo.4537445 (Püschel *et al.* 2021*b*). In addition, the code and input files are available in as an open access repository at https://github.com/HansPueschel/Hominin-div-time-evolution (Püschel *et al.* 2021*b*).

# Chapter 3 Anatomy and phylogeny of a new small macraucheniid (Mammalia: Litopterna) from the Bahía Inglesa Formation (late Miocene), Atacama Region, Northern Chile



*Micrauchenia saladensis* in the late Miocene coast of Bahía Salado, Chile. Art by Mauricio Álvarez

# Introduction

During most of the Cenozoic, South America was largely isolated from the rest of the continents, which allowed the independent evolution of a very particular mammalian fauna of South American ungulates (SANUs), xenarthrans and metatherians (Simpson 1980). This isolation was sporadically interrupted by mammalian immigrants arriving through rafting events during the Paleogene, probably from Africa (Antoine *et al.* 2012; Bond *et al.* 2015; Seiffert *et al.* 2020). The almost complete isolation of this fauna was finally put to an end by the gradual appearance of a terrestrial connection between South America and North America, the Isthmus of Panama, that fully connected both continents by 2.8 Ma (O'Dea *et al.* 2016), permitting immigration pulses from North America to South America and vice versa, in an event known as the Great American Biotic Interchange (GABI).

SANUs traditionally comprise five orders, Xenungulata, Notoungulata, Litopterna, Pyrotheria and Astrapotheria, with uncertain phylogenetic affinities. These orders were grouped in the mirorder Meridiungulata (McKenna 1975) probably due to biogeographic reasons and without any anatomical justification (Cifelli 1993). However, recent molecular studies have provided support for a close affinity between litopterns and notoungulates, which were both found to be closely related to perissodactyls (Buckley 2015; Welker *et al.* 2015; Westbury *et al.* 2017).

Among SANUs, litopterns were the most diverse order after notoungulates with 67 genera and 9 families (Pascual *et al.* 1996; Croft *et al.* 2020) currently recognized, including species ranging from the base of the middle Palaeocene (63.2 to 63.8 Ma, Peligran South American Land Mammal Age [SALMA]; Bonaparte and Morales 1997; Woodburne et al. 2014a, b) to the late Pleistocene/early Holocene (Tonni 1990; Bond 1999; Prado *et al.* 2015) in South America, and the Eocene in West Antarctica (Bond *et al.* 2006; Gelfo *et al.* 2017). Anatomically, litopterns tend to be the most similar SANUs to extant ungulates in terms of dental, cranial and postcranial proportions, and also present cursorial postcranial adaptations early in their evolutionary history (Scott 1910; Croft *et al.* 2020). Although most Paleogene taxa (e.g., Protolipternidae, Notonychopidae, Sparnotheriodontidae, Indaleciidae) have uncertain affinities (Cifelli 1993; Rose 2006; Croft *et al.* 2020), Neogene taxa are classified into three well-defined families: Macraucheniidae, Protherotheriidae and Adianthidae (Cifelli 1983*a*; Soria 2001; Gelfo *et al.* 2016). Of these families, macraucheniids were small to large-

sized litopterns (i.e., 53 - 1200 kg) with long necks, three-toed feet and a reduced nasal region, with a trend towards retraction of the nasals (Bond 1999; Vizcaíno *et al.* 2012).

Macraucheniids are distinguished from adianthids mostly based on dental features and size, as not much is known about the adianthids' postcranium. For instance, adianthids present a trilobed m3 and fossettes in P3-M3 formed by hypertrophied conular cristae (Cifelli & Soria 1983*a*; Cifelli 1993). Proterotheriids differ from macraucheniids in several dental features, such as the hypocone and protocone in the upper molars connected by a crest (Cifelli 1993), and postcranial features like a reduction (or loss) of lateral digits II and IV and an enlarged digit III, similar to modern horses. Considering previous taxonomic propositions (Cifelli 1983*a*; Soria 2001; Gelfo *et al.* 2016), the first occurrence for Macraucheniidae would be *Polymorphis* (Roth 1899) from the Mustersan (Late Eocene) of Patagonia, Argentina (Schmidt & Ferrero 2014), while the last occurrence is from the late Pleistocene/early Holocene, with the genera *Macrauchenia* (Bond 1999; Prado *et al.* 2015) and *Xenorhinotherium* (Cartelle & Lessa 1988). However, this age range excludes the poorly known *Victorlemoinea* and other sparnotheriodontids, the former previously considered within Macraucheniidae (Simpson 1945, 1948), which if proven correct, could imply an earlier origin for the family (early Eocene, Itaboraian SALMA).

Macraucheniidae is usually separated into two subfamilies: "Cramaucheniinae" (Eocene to middle Miocene) and Macraucheniinae (late Miocene to late Pleistocene/early Holocene), although only the latter has been shown to be monophyletic in phylogenetic analyses (Schmidt & Ferrero 2014; Forasiepi *et al.* 2016; McGrath *et al.* 2018). The most characteristic feature that distinguishes these two groups is that macraucheniines present a retracted nasal aperture to a more centrodorsal position, which suggests the presence of a proboscis (Burmeister 1864*b*; Scott 1910; Rusconi 1957; Bond 1999). Macraucheniines also have fused zeugopodial elements in the forelimbs (ulna-radius) and hindlimbs (tibia-fibula; Soria 1981).

Here we describe a new species *Micrauchenia saladensis* gen. et sp. nov. that represents the first macraucheniid (and SANU) from the Tortonian-Messinian levels (Huayquerian SALMA) marine deposits of the Bahía Inglesa Formation (middle Miocene-late Pliocene), Chile, and also the first late Miocene macraucheniid from the west coast of South America (Fig. 3.1). In addition, we expanded previous character-taxon matrices of macraucheniids with the addition of novel dental and postcranial characters in order to test the position

*Micrauchenia* within the family Macraucheniidae and also to better resolve the phylogenetic affinities of the different species of the family.

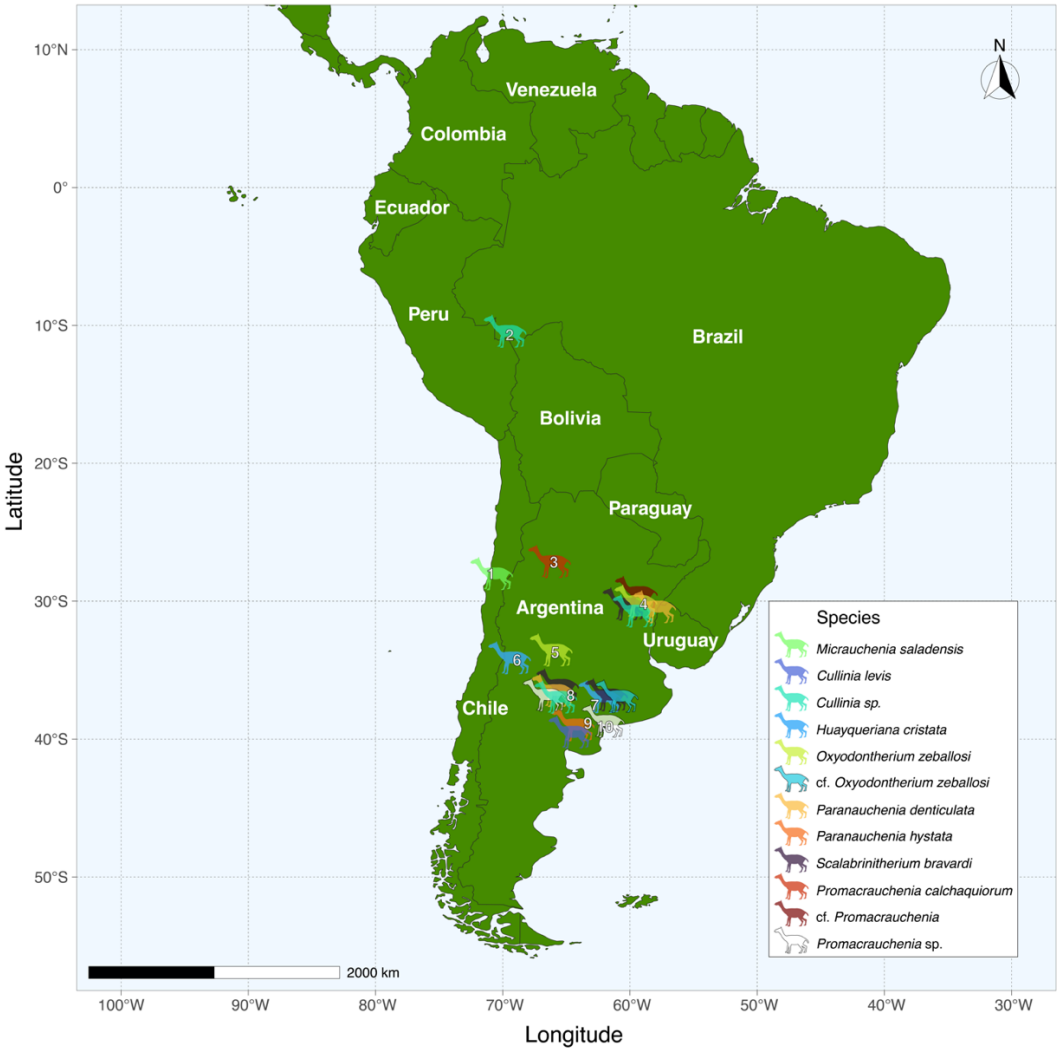



**Figure 3.1** Geographic distribution of late Miocene sites yielding macraucheniids. 1. Quebrada Remolón, Atacama region, Chile (Bahía Inglesa Formation, Huayquerian); 2. Acre region, southwestern Amazonia (Solimões Formation, "Mesopotamian" [Cozzuol 2006]); 3. Valle de Santa María, Catamarca, Argentina ("Estratos araucanos", Chasicoan to Montehermosan [Rovereto 1914; Forasiepi et al. 2016]); 4. Conglomerado osífero, Entre Ríos, Argentina (Ituzaingó Formation, "Mesopotamian" [Rusconi 1932; Schmidt 2013; Forasiepi et al. 2016]); **5**. Arroyo La Petra, San Luis, Argentina (Río Quinto Formation, "Mesopotamian" [Cerdeño et al. 2008]); **6**. Huayquerías de San Carlos, Mendoza, Argentina (Huayquerías Formation, Huayquerian [Soria 1986; Forasiepi et al. 2016]); **7**. Laguna Epecuén, and Laguna del Monte, Buenos Aires, Argentina (Cerro Azul Formation, Huayquerian [Soria 1986; Forasiepi et al. 2016; Schmidt et al. 2022]); **8**. Salinas Grandes de Hidalgo, Telén, Guatraché, and Laguna Chillhué, La Pampa, Argentina (Cerro Azul Formation, Huayquerian [Schmidt et al. 2022]). **9**. Arroyo Chasicó, Buenos Aires, Argentina (Chasicó Formation, Chasicoan [Bond and López 1995; Schmidt and Ferrero 2014]). **10**. Cantera Relleno Sanitario, Buenos Aires, Argentina (Cerro Azul Formation, Huayquerian [Schmidt et al. 2022]). The potentially late Miocene record of *Scalabrinitherium ferreriai* and ?*Oxyodontherium zeballosi* from "Barrancas de San Gregorio", Uruguay (Kraglievich 1932; Perea et al. 2013), has been here omitted as it does not have a good stratigraphic control (i.e., it was found washed out on the beach). Each taxon is represented with different colours. The silhouette used for the macraucheniid taxa was extracted from http://www.phylopic.org/ (by Zimices) and reproduced under a Creative Commons Attribution-ShareAlike 3.0 Unported (https://creativecommons.org/licenses/by-sa/3.0/)

## Geographic and geologic context

The specimen SGO.PV.21700 was collected in 2005 in Quebrada Remolón, a creek with an outcrop of the Bahía Inglesa Formation, located in the Bahía Salado area, ~ 70 km south of Caldera, Atacama Region, Chile (Figs. 3.1, 3.2a). The Bahía Inglesa Formation has a complex shallow marine to coastal depositional history, representing a shoreline affected by eustatic changes, and tectonic subsidence and uplift, reflected in a diverse array of deep to shallow marine facies and sub environments (Rojo 1985; Marquardt *et al.* 2000; Le Roux *et al.* 2016). The formation was deposited in a forearc Neogene basin, overlying in nonconformity to metamorphic and crystalline basements, or in disconformity to the continental lower Miocene Gravas de Angostura Beds. In addition, it often underlies in disconformity to the Quaternary Estratos de Caldera Beds or to recent unconsolidated Holocene deposits (Godoy *et al.* 2003). It also has a coquina facies, which create a conspicuous white ridge at the top of the main outcrops.

The Bahía Inglesa Formation has been dated as middle Miocene to late Pliocene based on its fossil content (e.g., Rojo 1985; Suárez et al. 2004), Sr stable isotopic data on fossil invertebrates (Achurra 2004; Henríquez 2006), and K/Ar absolute radiometric data (Marquardt 1999; Godoy *et al.* 2003). The type locality of the Bahía Inglesa Formation at Los Dedos, Los Negros and surroundings has been interpreted as littoral deposits. Farther south, at the Chorrillos locality, deep marine fan and channels were inferred (Carreño 2012; Le Roux *et al.* 2016). Near the Salado Bay and in Quebrada Remolón, ~ 50 km south of Chorrillos area, the main lithofacies represented are big lenticular diatomite levels overlaid by coquinas and a metric reddish phosphorite layer, which is used as regional guide (Cuitiño et al. 2021; Fig 3.2b). In a broad lithocorrelation, these lithofacies are equivalent to the Mina Fosforita Member present at the type locality, 7 m above an interbedded reworked crystalline tuff. K/Ar radiometric data of the interbedded tuff at the Mina Fosforita Member (*sensu* Le Roux et al. 2016), near the middle portion of the formation, indicates an age of 7.6 ± 1.3 Ma (Godoy *et al.* 2003), constraining this unit to the Tortonian-Messinian. As SGO.PV.21700 was found within a unit in Quebrada Remolón equivalent to the Mina Fosforita Member, we estimate its age to be ~ 8 – 6 Ma.

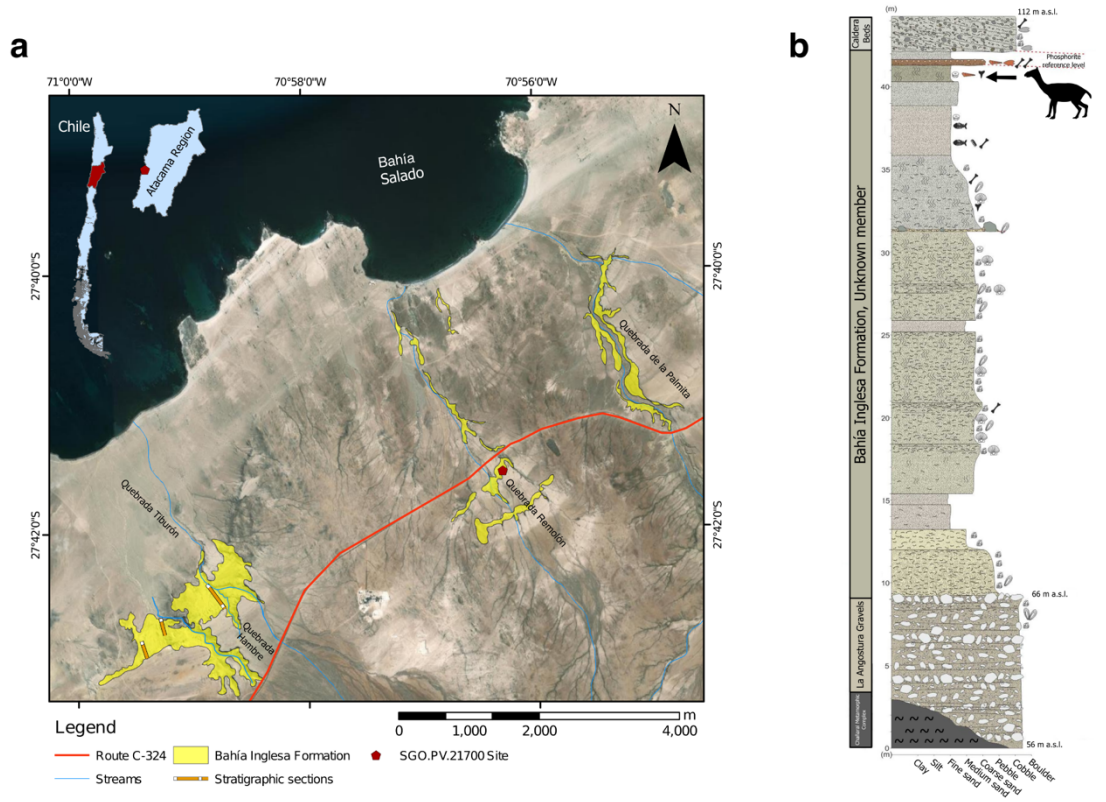



**Figure 3.2** Bahía Salado locality and stratigraphy. **a**. context map of the Bahía Salado locality, at the central coast of Atacama Region, Northern Chile. SGO.PV.21700 site at Quebrada Remolón and other relevant sites are highlighted. The main stratigraphic sections were made on the southwestern exposures. Geographic coordinates are in WGS84 datum. Basemap by ArcGIS 10.3 Geoeye/DigitalGlobe satellite composite of 2016; **b**. general stratigraphic section of Quebrada Hambre locality, with main contact relationships, topographic heights, and the correlative stratigraphic level of the SGO.PV.21700 remains, near the top of Bahía Inglesa Formation and below the local Phosphorite reference layer. The main facies are bioclastic conglomerates of coastal to closed shallow marine environments

## Paleoenvironmental conditions of Bahía Inglesa Formation

At the main classical phosphatic exposures of the Bahía Inglesa Formation more than 60 species of mostly marine vertebrates have been found, including chondrichtyan fishes (rays, chimeroids, and sharks), sea birds (penguins, cormorants, boobies, petrels, and albatrosses), reptiles (crocodiles), and marine mammals (dolphins, whales, dugongs, seals and marine sloths) (Le Roux *et al.* 2016). Findings of continental vertebrates in sediments of Bahía Inglesa Formation are rare. Remains of longirostrine crocodyliforms have been described in several localities of the unit (Walsh & Suárez 2005; Soto-Acuña *et al.* 2015). Today, the extant longirostrine crocodiles from the clade Gavialidae are restricted to freshwater environments (Grigg & Kirshner 2015). However, it is known that the Paleogene "thoracosaurs", which are considered putative stem-gavialoids, inhabited marine environments (Hua & Jouve 2004; Delfino *et al.* 2005). The same is also true for the early diverging gavialid *Sacacosuchus*

*cordovai* and the gryposuchine gavialid *Piscogavialis jugaliperforatus*, both from the Pisco Formation (Kraus 1998; Salas-Gismondi *et al.* 2022). Therefore, the crocodyliforms from Bahía Inglesa Formation are not necessarily reliable environmental indicators for terrestrial conditions. Nevertheless, a fragment of a capybara tooth conferred to *Cardiatherium* sp. was found in the Bahía Inglesa Formation, which constitutes the first non-marine vertebrate from this formation (Gutstein *et al.* 2007; Deschamps *et al.* 2013).

The complex lithofacies array of the succession suggest that the broad system was changing from closed shallow marine to littoral environments, in a relative short time span (Le Roux *et al.* 2016; Cuitiño *et al.* 2021). This condition allows the occurrence of typically continental vertebrates in coastal deposits. One of the best examples of shallow marine units bearing continental vertebrates in South America is the Camacho Formation (late Miocene) in Uruguay, which also contains a large assemblage of allochthonous Huayquerian vertebrate fossils in shallow marine to paralic environments (Perea & Martínez 2004; Perea *et al.* 2013; Soibelzon *et al.* 2019). Considering the similar general context, we suggest that the *Micrauchenia saladensis* remains are allochthonous in the clastic bearing levels, which is consistent with coquinas and very coarse sandstone to conglomerate layers bellow the phosphorite guide level. This depositional scenario occurred in a global eustatic high stage (Miller *et al.* 2005), but also with a local tectonic subsidence (Le Roux *et al.* 2016), both proper conditions for a significant variability in the former shoreline and the reworking of latter coastal to continental positions. *Micrauchenia saladensis* is the first record of Litopterna in this formation and the second record of a continental vertebrate in the Bahía Inglesa Formation.

# Material and methods

## Description and comparison

The anatomical descriptions were based on SGO.PV.21700, a specimen of a new macraucheniid from the Bahía Salado, Bahía Inglesa Formation, Chile. SGO.PV.21700 is deposited in the Paleontology Area of the National Museum of Natural History of Santiago de Chile. The specimen includes a mandible fragment with the right condylar and coronoid processes, an atlas fragment, an axis fragment, two cervical vertebrae fragments (fifth and seventh cervical vertebrae), one fragmentary thoracic vertebra (second thoracic vertebra), left scapula fragment, left ulna-radius fragment (mid-shaft to distal end preserved), seven carpal elements (partial left scaphoid, partial left and complete right lunate, left cuneiform, left

pisiform, left magnus and right unciform), three metapodials (right Mc II, a fragmentary left Mc III and a fragmentary Mc II or Mc IV) and six phalanges (two proximal of the right digit II and left digit III, and four intermediate, one of the digit III and three of the digits II and/or IV; Fig. 3.3). The fossil bones were mechanically prepared in the Red Paleontológica U-Chile Laboratory of the University of Chile. The preparation was carried out with airscribes ME 9100 and MicroJacks under trinocular microscopes and stabilized by consolidants such as paraloid (B-72) and cyanoacrylate.

Comparisons were made with fossil specimens described and photographed in literature and/or from direct observation/images from museum collections of taxa that have been recognized by anatomical features and/or phylogenetic studies as members of the family Macraucheniidae and that also preserve postcranial remains (e.g., Scott 1910; Sefve 1925; Parodi 1931; Cartelle and Lessa 1988). In particular, we compared SGO.PV.21700 with *Cramauchenia* (Ameghino 1902; late Oligocene to early Miocene, Deseadan to Colhuehuapian SALMAs), *Coniopternium* (Ameghino 1894a; late Oligocene, Deseadan SALMA), *Theosodon* (Ameghino 1887; early Miocene to late middle Miocene, Colhuehuapian-Laventan SALMAs), *Scalabrinitherium* (Ameghino 1883; Kraglievich 1932; late Miocene to early Pliocene, Huayquerian to Montehermosan SALMAs), *Cullinia* (Cabrera and Kraglievich 1931; late Miocene, Chasicoan to Huayquerian SALMAs), *Promacrauchenia* (Ameghino 1903-1904; late Miocene to early Pleistocene, Huayquerian to Marplatan SALMAs), *Macrauchenia* (Owen 1838; late Pliocene, Marplatan SALMA to late Pleistocene/early Holocene) and *Xenorhinotherium* (Cartelle and Lessa 1988; late Pleistocene/early Holocene). Most measurements were taken either manually using digital callipers, or digitally using Fiji (ImageJ v2.1.0; Schindelin et al. 2012), to the nearest two decimal places. Some measurements were taken directly from the literature for comparisons. A complete list of the comparison material, institutional numbers and measurements is given in the Appendix C3 Resource 1 (Tables S1-S7).

As the subfamily Cramaucheniinae has shown previously to be paraphyletic (Schmidt & Ferrero 2014; Forasiepi *et al.* 2016; McGrath *et al.* 2018), it cannot be considered a natural group. As such we used the term “cramaucheniines” throughout the article to talk about early macraucheniids that are outside the monophyletic subfamily Macraucheniinae.

We followed the Nomina Anatomica Veterinaria (International Committee on Veterinary Gross Anatomical Nomenclature 2017) for the anatomical terminology in general,

and for carpals terminology we followed (Rose 2006). When we made soft tissue inferences in anatomical descriptions, we mostly followed (Sisson 1914; Evans & Lahunta 2012; Constantinescu *et al.* 2018; Denoix 2019; Aurich *et al.* 2020) which contain anatomical information on some modern laurasiatheres, including perissodactyls, the closest living relatives of litopterns according to molecular evidence (Buckley 2015; Welker *et al.* 2015; Westbury *et al.* 2017). In some cases, we used additional references, and these we cite accordingly in the text.

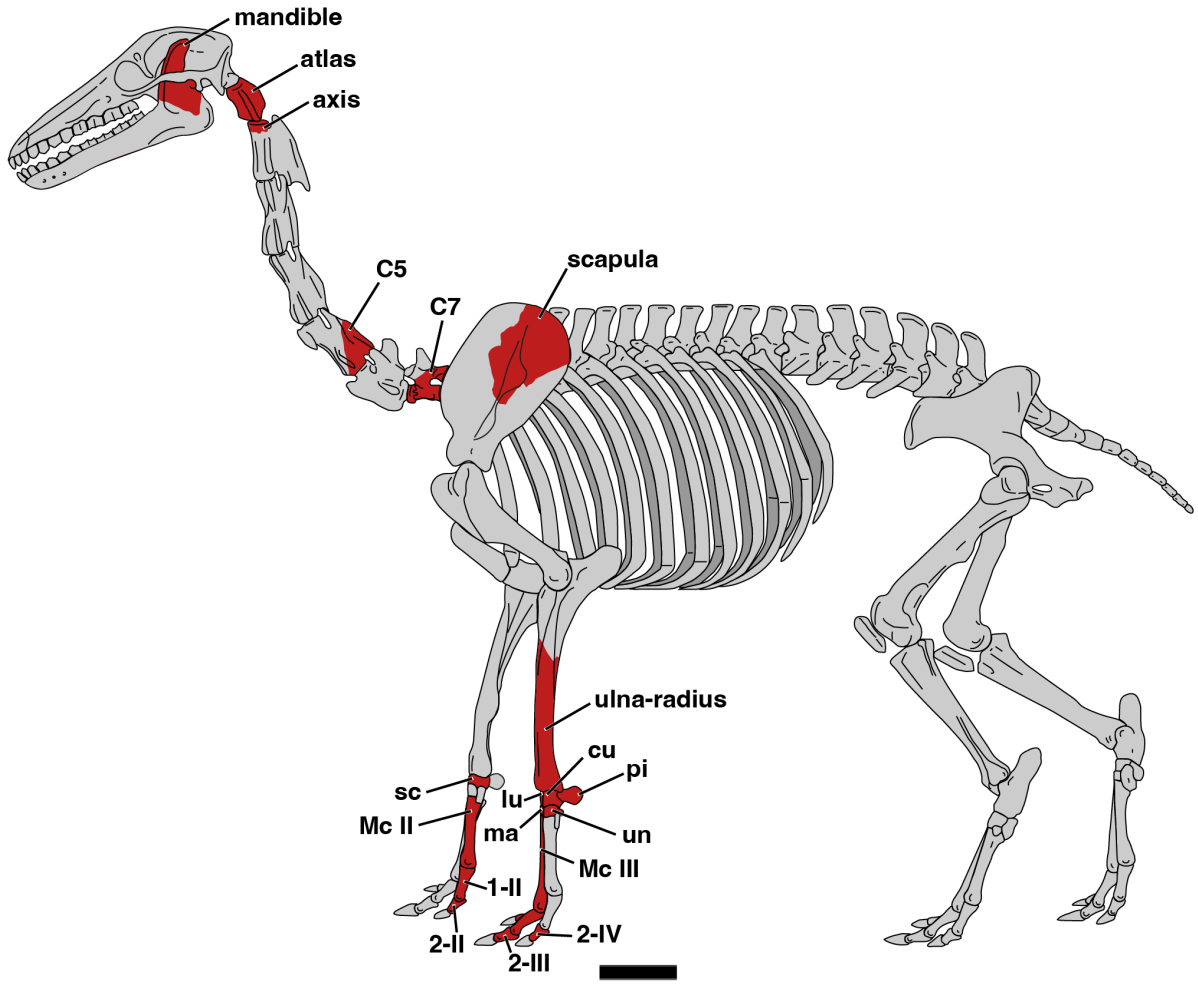



**Figure 3.3** Skeletal reconstruction of *Micrauchenia saladensis* (SGO.PV.21700) in left lateral view, with preserved elements in dark grey. The right portion of the mandible, right unciform and left scaphoid have been mirrored in order to be visible in the figure. The second thoracic vertebra (T2) is preserved but is not visible in the figure as it is behind the left scapula. The anatomy of the missing elements is based in other macraucheniids as *Theosodon* (Scott 1910), *Promacrauchenia* (Soria 1986), *Macrauchenia* (PIMUZ A/V 5700; MACN PV 2) and *Xenorhinotherium* (MCL 2643/03). At the limbs, Hindu-Arabic numerals indicate the phalanges position from proximal to distal (1 to 3), and Roman numerals indicate the digit position (II to IV). Abbreviations: *C5*, Fifth cervical vertebra; *C7*, seventh cervical vertebra; *cu*, cuneiform; *lu*, lunate; *ma*, magnum; *Mc*, metacarpal; *pi*, pisiform; *sc*, scaphoid; *un*, unciform. Scale bar equals 10 cm

## Character dataset and taxa included

To assess the phylogenetic affinities of SGO.PV.21700, we compiled a data matrix of 43 characters scored for 21 taxa. This dataset is modified from previous matrices (Schmidt & Ferrero 2014; Forasiepi *et al.* 2016) with the addition of a new craniodental character and eigth postcranial characters (Appendix C3 Resource 2). The matrix is available online on Morphobank (morphobank.org) under the project number 3933 and as Nexus files (Appendix C3 Resource 3 and 4). Even though the likely ancestral dental formula for litopterns is I1/i1 I2/i2 I3/i3 P1/p1 P2/p2 P4/p4 P5/p5 M1/m1 M2/m2 M3/m3 considering the probable loss of P3/p3 in the common ancestor of Placentalia (McKenna 1975; Novacek 1986; O'Leary *et al.* 2013), we kept the dental formula used by previous authors for macraucheniids of I1/i1 I2/i2 I3/i3 P1/p1 P2/p2 P3/p3 P4/p4 M1/m1 M2/m2 M3/m3 (e.g., Forasiepi et al. 2016) as it is more intuitive and does not have a negative impact in dental comparisons between litopterns (i.e., the comparisons are still homologous). We included the same taxa as Forasiepi et al. (2016) with the addition of *Llullataruca shockeyi* (McGrath *et al.* 2018). Additionally, we considered the small differences between *Huayqueriana cf. H. cristata* (Forasiepi *et al.* 2016) and *Huayqueriana cristata* (Rovereto 1914), as intraspecific variation of the latter taxon. Therefore, it was scored as a single taxon in the matrix, treating any contradictory scores as polymorphic. We chose *Tricoelodus* (Ameghino 1897) as the outgroup because is one the best-known and complete adianthids from the late Oligocene (Deseadan SALMA), and also it has been used in previous analyses (Schmidt & Ferrero 2014; Forasiepi *et al.* 2016; McGrath *et al.* 2018). However, in contrast to latter studies, we removed the adianthid *Proadiantus excavatus* (Ameghino 1897) because is poorly known, having considerably fewer scored characters than *Tricoelodus* (i.e., 11 vs 16). For the 34 craniodental characters of previous matrices (Schmidt & Ferrero 2014; Forasiepi *et al.* 2016) we used the character scores from McGrath et al. (2018), scoring additionally character 15 in *Polymorphis lechei* as it was possible to assess examining the holotype (MLP 12-2168). The nine new characters were scored based on direct observation of museum specimens, pictures of the specimens, and images/descriptions from the literature. Finally, we scored the Bahía Salado specimen (SGO.PV.21700) and also the dental and postcranial *Promacrauchenia* sp. material from Inchasi (Anaya & MacFadden 1995) into the matrix. The latter was included because its peculiar anatomy and the fact that its taxonomic assignment has been previously questioned (Schmidt 2013). Characters 1, 2, 3, 7 and 8 were treated as ordered, as they are part of a transformational sequence.

## Phylogenetic analyses

**Parsimony analysis** We use TNT v1.5 (Goloboff & Catalano 2016), setting the outgroup as *Tricoelodus* spp. and employing a "New Technology" driven search using sectorial search, ratchet, drift and tree fusing, set to find the minimum length tree (best score) 100 times. This was followed by an additional "traditional search" using tree bisection and reconnection (TBR) branch swapping algorithm. As a result, we obtained 36 most parsimonious trees (MPTs) of 89 steps with consistency index (CI) = 0.607 and retention index (RI) = 0.701. The MPTs were then used to compute a strict consensus tree and a 50% majority rule tree. The absolute Bremer supports and Jackknife resampling (1000 replicates, 36%-character removal) for the nodes were computed for the strict consensus tree. During these analyses, SGO.PV.21700 was identified as a wildcard taxon probably due the lack of scored craniodental characters, so it was removed a posteriori to analyse the topology of the strict consensus when this taxon is not present. As the topology excluding SGO.PV.21700 from the strict consensus tree was very similar to the 50% majority rule tree that included this taxon, we mapped apomorphies on the 50% majority rule tree.

**Undated Bayesian analysis** The undated Bayesian analysis was performed in MrBayes v3.2.7a (Ronquist *et al.* 2012*a*) setting the outgroup as *Tricoelodus* spp (Appendix C3 Resource 3). We used two partitions for analysing the morphological data: the Mkv + Γ model of morphological evolution (Lewis 2001) with four rate categories (Harrison & Larsson 2015) for the characters with three or more states, and the MkA + Γ model for the binary characters with four rate categories in order to consider asymmetrical forward and backward rates between character states (Pyron 2017). The analyses were run using two runs of four chains and 15 million Markov chain Monte Carlo (MCMC) generations, sampling every 1000 generations and discarding the 25% of the samples as burn-in. We ensured that the deviation of split frequencies was below 0.01 and that the effective sample size for the parameters was > 200.

**Tip-dated Bayesian analysis** The tip-dated Bayesian analysis was also performed in MrBayes v3.2.7a (Ronquist *et al.* 2012*a*) with the same model of morphological evolution and sampling settings as the undated Bayesian analysis (see above; Appendix C3 Resource 4). The root of the tree was calibrated using an exponential distribution with a minimum age of 42 Ma and a mean of 44 Ma. The minimum age for the root was based in the maximum age of the

most basal putative adianthid *Proectocion* (Barrancan SALMA, 42 – 39 Ma; Woodburne et al. 2014a).

Ideally, when defining calibration bounds for each taxon, these should be based on the radiometric age uncertainty associated to the specific specimens scored in the morphological matrix (Püschel *et al.* 2020). However, the institutional numbers of the specimens of the specimens used in the original matrices and their stratigraphic provenience has not been reported (Schmidt & Ferrero 2014; Forasiepi *et al.* 2016), and this information is not currently available (Schmidt 2021, personal communication). Therefore, the calibration bounds were based on the presence data of Croft et al. (2020) for each SALMA, and the radiometric information currently available for defining each time interval (Table S7 in Appendix C3 Resource 2). We used a uniform distribution between the maximum and minimum age associated with each taxon to represent the radiometric age uncertainties with one exception. As we only considered the Santacrucian specimens of *Theosodon* for character scoring, the age interval for the tip-dating Bayesian analysis for *Theosodon* spp. was the Santacrucian, instead of considering the whole-time interval of all the specimens included in this genus (i.e., Colhuehuapian to Laventan [21.0 – 11.8 Ma]). There is undoubtedly a need to revise the taxonomy of this genus, as previous authors have recognized (Cifelli & Guerrero Díaz 1997; Croft *et al.* 2004; Schmidt & Ferrero 2014; McGrath *et al.* 2018), with part of the problem being the number of species based on fragmentary remains from different time intervals, which generates a disagreement in the exact number of valid species between different authors (e.g., 10 [Croft et al. 2004], 7 [Cassini et al. 2012], 8 [McGrath et al. 2020]). However, a revision of this nature is beyond the scope of this work.

We used a gamma distributed clock rate prior, with a mean of 0.02462008 and standard deviation of 0.01095129. These priors were derived following the methodology of (Gunnell *et al.* 2018) using the previously obtained undated Bayesian consensus tree and the packages ape (Paradis *et al.* 2004) and fitdistrplus (Delignette-Muller & Dutang 2004) from R (R Core Team 2019). We selected the best model according to the Bayesian information criterion. Branch rate variation was modelled using the Independent Gamma Rate (IGR) relaxed clock model with an exponential distribution of rate 10 (default MrBayes setting). The FBD model was used as the prior on divergence times, using an exponential net diversification prior with rate 1, a beta turnover prior with shape parameters $\alpha=1$ and $\beta=1$, a beta fossil sampling proportion prior with shape parameters $\alpha=1$ and $\beta=1$ and an extant sampling proportion of 1. We use diffuse priors

for the clock rate variance and the FBD model, which reflect the uncertainty in our prior expectation of how these parameters are distributed.

The analyses were run using two runs of four chains and 45 million Markov chain Monte Carlo (MCMC) generations, sampling every 1000 generations and discarding the 25% of the samples as burn-in. We ensured that the deviation of split frequencies was below 0.01 and that the effective sample size for the parameters was > 200.

## Systematic palaeontology

**Mammalia** Linnaeus, 1758

**Eutheria** Huxley, 1880

**Panperissodactyla** Welker et al., 2015

**Litopterna** Ameghino, 1889

**Macraucheniidae** Gervais, 1855

**Macraucheniinae** Ameghino 1902*a*

**Emended diagnosis** (modified from Soria [1981] and Schmidt [2013]) small to large-sized macraucheniids (~53 to 1200 kg). Elongated rostrum. Nostrils in a dorsal position, close to the level of the orbits and posterior to dorsally projected maxillae. Nasals vestigial or absent. No sagittal crest. The coronal plane passing through infraorbital foramen is located in a position that varies between the anterior margin M2 and over M3. The left and right premaxillae and maxillae are sutured sagitally in dorsal view in contrast to earlier macraucheniids where the bones are separate. Palate narrows anteriorly at P2 or P3 level. Mesodont and selenodont molars. I1/i1-P1/p1 generally imbricated. P3-M3 with enamel fossettes in the trigon basin. Fused ulna and radius, and tendency towards the development of an aliform expansion on the radius. Tibia and fibula partially fused. Massive and less gracile calcaneus in comparison with earlier macraucheniids. Tridactyl manus and pes.

**Micrauchenia, gen. nov.**

LSID urn:lsid:zoobank.org:act:30B931AC-ED24-459D-A28A-DAE22EB7B9C1

Figures 3.4-3.19

**Type species** *Micrauchenia saladensis*

**Diagnosis** Small (53 – 103 kg) macraucheniid, similar in size to *Cramauchenia normalis* and *Coniopternium andinum*, and smaller than *Cullinia levis*, the previously smallest-known macraucheniine. The posteriormost border of the transverse processes of the atlas are posterior to the articular facets for the axis as in *Macrauchenia*, but in contrast to *Theosodon* where the transverse processes are anterior to the articular facets for the axis. The articular facets for the atlas of the axis are dorsoventrally low in relation to its mediolateral width (WA/HA > 0.9), more similar to *Macrauchenia* than to *Theosodon*, in which these facets are markedly relatively higher. The ulna and radius are completely fused, and the radius presents a well-developed medial aliform expansion or flange similar to *Promacrauchenia* in its degree of expansion. However, the ulna-radius is wider mediolaterally at this point than the width of this element measured at the level of the distal articular surfaces (URA/URD > 1) similar to *Macrauchenia* but in contrast to what is seen in *Promacrauchenia* where URA/URD < 1. The cuneiform and unciform extend over the magnum proximally as in *Macrauchenia*, but in contrast to *Theosodon* where the cuneiform-magnum and unciform-magnum articulations are entirely lateral. The pisiform is greatly proximodistally expanded at the posterior end as in *Cullinia*, *Promacrauchenia*, *Macrauchenia* and *Xenorhinotherium*. The robust metapodials are proportionally similar in terms of relative length and width to *Theosodon*, in contrast to *Cullinia levis*, in which they are proportionally more slender and elongated.

**Age and Distribution** Tortonian-Messinian, 8 – 6 Ma, Bahía Inglesa Formation, Chile, temporally within Huayquerian SALMA.

**Etymology** From the words “mikrós” and “aukhḗn”, meaning “small” and “neck” respectively in old Greek. The name refers to the small size of this macraucheniine in comparison to the Pleistocene genus *Macrauchenia*.

***Micrauchenia saladensis*, sp. nov.**

LSID urn:lsid:zoobank.org:act:1FB315E5-1908-444B-897A-E7C313EA3C6B

Figures 3.4-3.19

**Holotype** The specimen SGO.PV.21700 includes a right mandible fragment with the right condylar and coronoid processes, an atlas fragment, an axis fragment, two cervical vertebrae fragments (fifth and seventh cervical vertebrae), one fragmentary thoracic vertebra (second thoracic vertebra), left scapula fragment, left ulna-radius fragment (mid-shaft to distal end preserved), seven carpal elements (partial left scaphoid, partial left and complete right

lunate, left cuneiform, left pisiform, left magnus and right unciform), three metacarpals (right Mc II, a fragmentary left Mc III and a fragmentary Mc II or Mc IV) and six phalanges (two proximal of the right digit II and left digit III, and four intermediate, one of the digit III and three of the digits II and/or IV; Fig. 3.3).

**Etymology** From Bahía Salado, the locality in which the type and only specimen was found.

**Type locality** Quebrada Remolón, Bahía Salado, Copiapó Province, Atacama Region, Northern Chile.

**Age and Distribution** As for genus.

**Diagnosis** As for genus.

# Descriptions and comparisons

## Skull

**Mandible** The right mandible fragment preserves just the dorsal portion of the ramus with the coronoid and the condylar processes (Fig. 3.4, Table S1 on Appendix C3 Resource 1). The condylar process is small, cylindrical and posteriorly has a slightly convex articular facet where it articulates with the glenoid fossa *(fossa mandibularis*) on the squamosal. The mandibular notch (*incisura mandibulae*) is anteroposteriorly very narrow. The coronoid process is anteroposteriorly narrow, dorsoventrally elongated and mediolaterally slender. The apex of the coronoid process is tapered posteriorly and terminates posterior to the condylar process. Anteriorly, it presents a distinct coronoid crest that is very strong dorsally but as it continues ventrally it becomes more subtle. Laterally, the coronoid process is slightly concave near its tip for the attachment of the temporalis muscle (Evans & Lahunta 2012; Constantinescu *et al.* 2018). On the ramus portion, preserved below the level of the condylar process, there is a concavity laterally, which is probably part of the attachment area for the masseter (Evans & Lahunta 2012; Constantinescu *et al.* 2018).

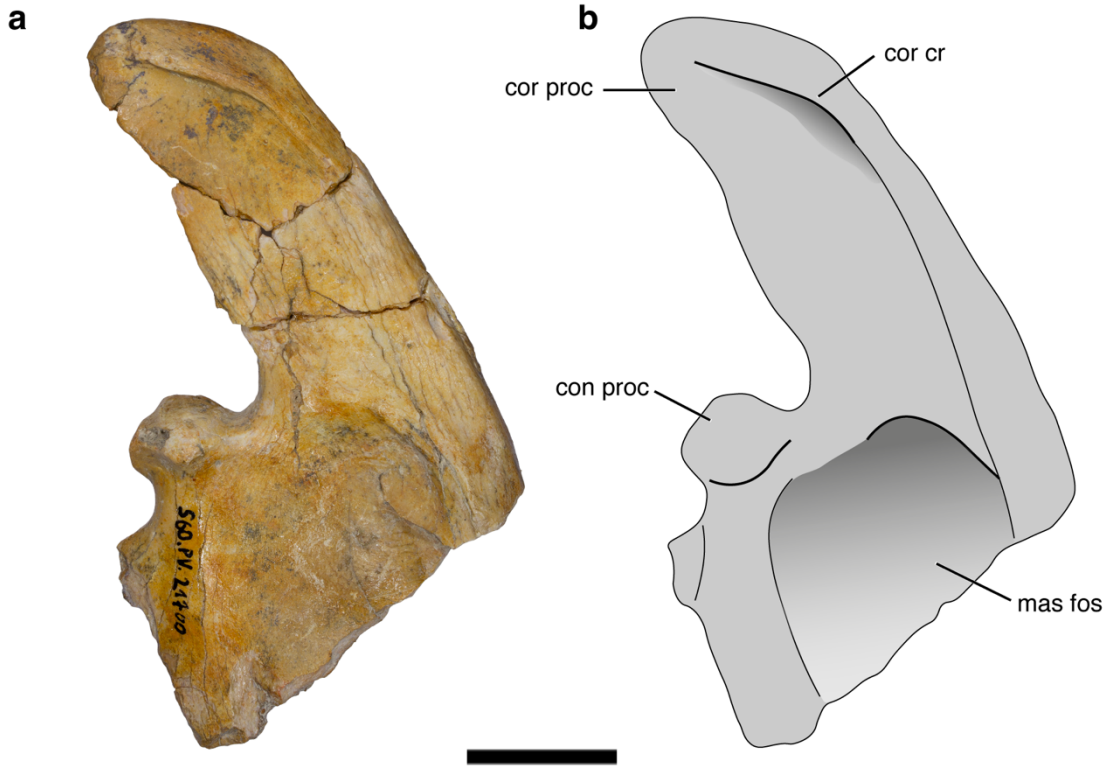



**Figure 3.4** Mandible of *Micrauchenia saladensis* (SGO.PV.21700). This corresponds to a fragment of the right dorsoposterior portion of the element. **a**. lateral view; **b**. annotated line drawing in lateral view. Abbreviations: *con proc*, condylar process; *cor cr*, coronoid crest; *cor proc*, coronoid process; *mas fos*, masseteric fossa. Scale bar equals 2 cm

There is no sign of a condyloid crest in contrast to *Cramauchenia normalis* (MNHN.F.COL181) and *Macrauchenia* (MACN PV 2), which present a subtle but noticeable condyloid crest dividing the masseteric fossa into two halves. In *Theosodon*, the condyloid crest may be variable, as there appears to be a very subtle ridge in *Theosodon garretorum* (YPM VPPU 015164; Scott 1910: Pl. XVII fig. 3.1) but this is absent in *Theosodon lydekkeri* specimens (MACN A 2490; MACN A 9269-88). *Llullataruca shockeyi* (UATF-V-001904) also seems to lack a condyloid crest (McGrath *et al.* 2018). Apart from differences in the development of the condyloid crest and differences in size, the general outline of this element is very similar to Miocene macraucheniids like *Theosodon* (YPM VPPU 015164) and *Llullataruca* (UATF-V-001904), and also to more derived Pleistocene macraucheniids like *Macrauchenia* (MACN PV 2), which indicates that over time this element has been mostly conserved within this family.

## Postcranial elements

### Vertebrae

The preserved elements of the vertebral column include the atlas, axis, two cervical vertebrae (fifth and seventh cervical vertebrae) and a thoracic vertebra (second thoracic vertebra) with different degrees of preservation (Figs. 3.5-3.8). In terms of absolute size, the vertebrae of *Micrauchenia saladensis* are on average of similar size than those of *Cramauchenia normalis*, ~27% smaller than *Theosodon* spp., and 2 – 3 times smaller than *Macrauchenia patachonica* and *Xenorhinotherium bahiense* (Table S2 in Appendix C3 Resource 1).

**Atlas** The atlas is broken preserving almost the entire left half and only part of the right half in fragments that are separated by a fracture in the dorsal arch; however, it is possible to infer its whole anatomy (Fig. 3.5a-f). Although part of the dorsal arch is missing, there is no indication of a marked dorsal tubercle (*tuberculum dorsale*), with the arch being moderately high but rounded. Positioned anteriorly are wide and mostly concave articular facets for the occipital condyles of the cranium or occipital facets which are closer ventrally to each other than dorsally, being convex in a small area at their ventromedial portion (Fig. 3.5a). Posteriorly, the atlas of *Micrauchenia saladensis* presents almost flat oval articular facets for the axis and in the ventral part of the neural arch there is a concave facet for the odontoid process of the axis (Fig. 3.5b). Just ventral to the facet for the odontoid process, on the ventral aspect of the atlas, there is a small but distinct ventral tubercle (*tuberculum ventrale*) that extends the length of the atlas becoming less prominent anteriorly (Fig. 3.5 d-e).

The transverse processes of the atlas or wings are moderately mediolaterally broad and anteroposteriorly elongated, ending anteriorly in an alar notch (*incisura alaris*) and posteriorly surpassing the articular facets for the axis terminating in a posteriorly projecting rounded lobe (Fig. 3.5c-e). Ventrally the transverse processes are moderately concave, and there is no atlantic fossa (*fossa atlantis*; Fig. 3.5d-e).

The alar notch of the atlas of *M. saladensis* is anteroposteriorly deep and mediolaterally narrow. The alar notch is similar to the same structure in the perissodactylamorph *Cambaytherium* (Rose *et al.* 2019), the perissodactyl *Hyracotherium* (Wood *et al.* 2011) and to *Canis* and other carnivorans (Evans & Lahunta 2012); in the case of the latter, it has been observed to be a point of passage of the vertebral artery, and homologous to the alar foramen

(*foramen alare*) observed in some modern artiodactyls such as *Bos* and perissodactyls as *Equus* (Aurich *et al.* 2020). The alar foramen is possibly derived from an alar notch that is closed anteriorly before reaching the occipital facets. In that sense, the illustration in (Evans and Lahunta 2012: fig. 4-50) of the atlas of *Canis* showing an alar foramen would be incorrect, and the foramen indicated as such is in reality the transverse foramen (*foramen transversarium*; König and Liebich 2020).

A transverse foramen is present in the atlas of *M. saladensis.* The posterior opening of transverse foramen is evident in posterior view (Fig. 3.5b), lateral to the facets for the axis. The anterior opening of the transverse foramen is positioned ventrally approximately at the anteroposterior midpoint of the atlas body where a small exit is visible (Fig. 3.5b, d-e). This anterior exit of the transverse canal is posterior to and distinct from the alar notch, and would likely give passage to vessels including the vertebral artery and veins as has been observed in several modern placental mammals including carnivorans like *Canis*, primates like *Homo*, and perissodactyls like *Equus* (Sisson 1914; Evans & Lahunta 2012; Standring 2015; Constantinescu *et al.* 2018). The posterior position of the posterior opening of the transverse foramen is similar to other ungulates like the perissodactylamorph *Cambaytherium* (Rose *et al.* 2019), the perissodactyl *Hyracotherium* (Wood *et al.* 2011), hegetotheriid notoungulates like *Hegetotherium* and *Pachyrukhos* (Sinclair 1909), the interatheriid notoungulate *Interatherium* (Sinclair 1909), the leontiniid notoungulate *Gualta cuyana* (Cerdeño & Vera 2015), the xenungulate *Carodnia vierai* (Paula Couto 1978*a*), the tylopod artiodactyl *Lama glama* (IMNH R-2392), among others. However, in *M. saladensis* the transverse canal is elongated in comparison to the abovementioned taxa, which generates an anteriorly located anterior opening of the transverse foramen. It is interesting to note that in modern ruminant artiodactyls, the transverse foramen is absent (Aurich *et al.* 2020).

Posterodorsal to the occipital facet there is a lateral foramen (*foramen vertebrale laterale*), for the first cervical spinal nerve and vertebral artery as in *Canis* and other mammals (Evans & Lahunta 2012; Aurich *et al.* 2020). In SGO.PV.21700, it is only possible to see the exit of the lateral foramina in the ventral aspect of the dorsal arch (Fig. 3.5f), as the dorsal entry is still covered in sediment (Fig. 3.5c). The vertebral foramen of the atlas is slightly mediolaterally wider than dorsoventrally higher (Table S2 in Appendix C3 Resource 1). However, the strong interior borders of the occipital facet invading the vertebral foramen, give the foramen a pyriform shape in anterior view (Fig. 3.5a-b).

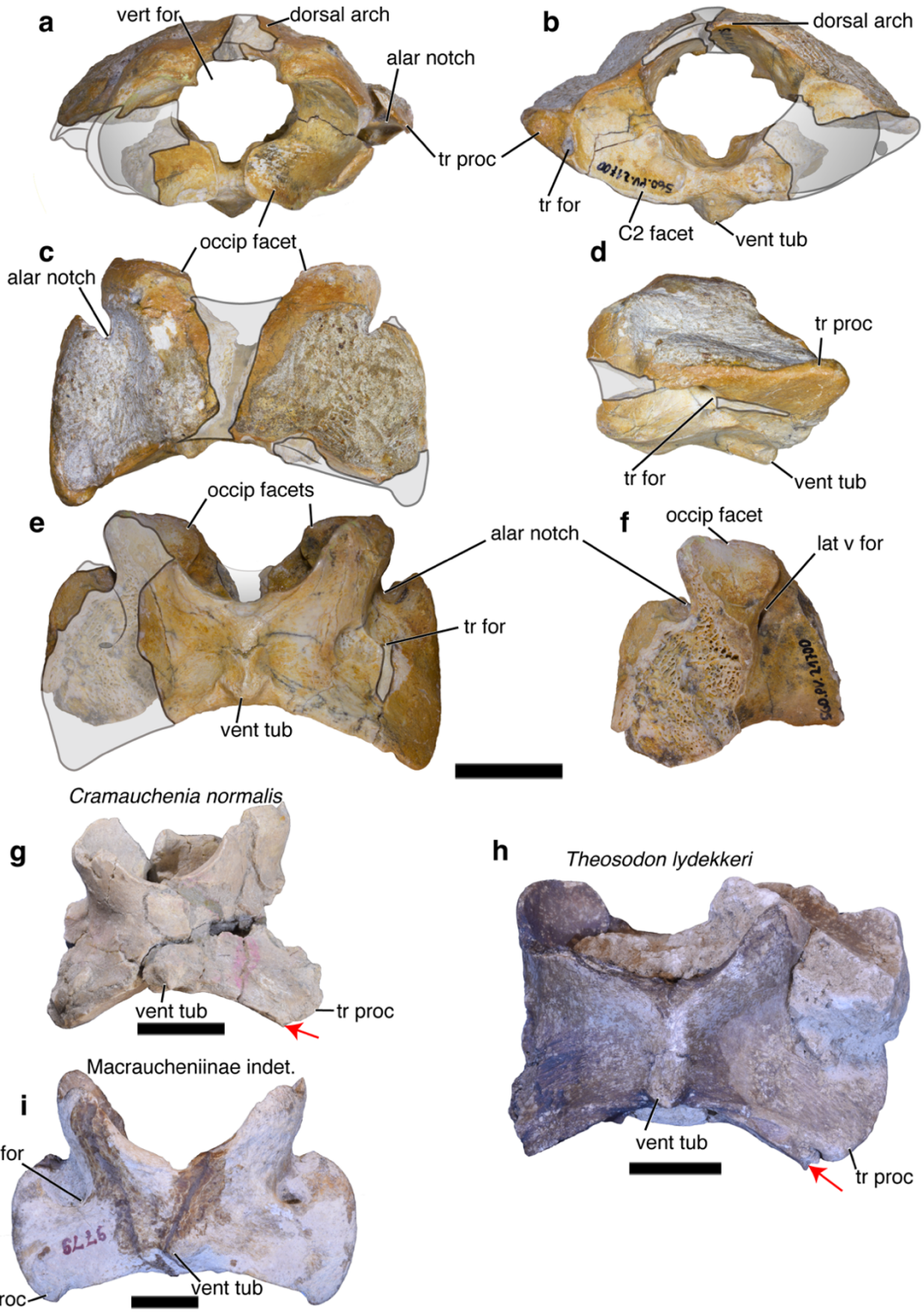



**Figure 3.5** Atlas of *Micrauchenia saladensis* compared with atlases of other macraucheniids. **a-f**. atlas of *Micrauchenia saladensis* (SGO.PV.21700) in anterior (**a**), posterior (**b**), dorsal (**c**), left lateral (**d**), ventral (**e**), and ventral (**f**; right fragment alone) views. **g**. atlas of a subadult *Cramauchenia normalis* (MLP 83-III-2-1) in ventral view. **h**. atlas of *Theosodon lydekkeri* (MACN A 9255) in ventral view. **i**. atlas of an early Pliocene macraucheniine indet. from Quequén Salado River (MACN PV 9779), possibly a subadult, in ventral view. The red arrows in **g** and **h** indicate the notch that separates the articular facet for the axis and the transverse process (absent in **c-d** and **i**). Abbreviations: *lat v for*, lateral vertebral foramen; *occip*, occipital; *tr for*, transverse foramen; *tr proc*, transverse process; *vent tub*, ventral tubercle; *vert for*, vertebral foramen. Scale bars equal 2 cm

When we compare the anatomy of the atlas of *M. saladensis* (SGO.PV.21700), with the atlas other macraucheniids like *Cramauchenia* (MLP 83-III-2-1), *Theosodon* (YPM VPPU 015164; MACN A 9255), an early Pliocene macraucheniine from Quequén Salado River (MACN PV 9779) and *Macrauchenia* (PIMUZ A/V 5700), most of the description given for the former fits with the anatomical features of the four latter (Fig. 3.5g-i). However, in *Cramauchenia* (MLP 83-III-2-1) and *Theosodon* (YPM VPPU 015164; MACN A 9255), the posteriormost portion of the articular facets for the axis are located posterior of the transverse processes and separated from them by a notch (Fig. 3.5g-h), which is different to the condition seen in *M. saladensis*, the Quequén Salado River macraucheniine (MACN PV 9779) and *Macrauchenia* (PIMUZ A/V 5700). In the latter three taxa, the transverse processes extend posterior to the articular facets for the axis (Fig. 3.5c-e, i).

At this point it is important to note a previous description and illustrations of the atlas of *Macrauchenia* (MACN PV 2) which describes it as similar to the atlas of ruminants because its general shape and the presence of two closely located vertebroarterial foramina (Burmeister 1864b: Pl. IV). However, this is not the case for *Macrauchenia* (PIMUZ A/V 5700), and close examination of this specimen suggests a misidentification in Burmeister (1864b) for several reasons. First, MACN PV 2 atlas and ruminant artiodactyls do not have a transverse foramen (König and Liebich 2020;Fig. S1a,d in Appendix C3 Resource 5), while a transverse foramen is clearly present in *Macrauchenia* (PIMUZ A/V 5700) and other macraucheniids (Fig. 3.5). Second, MACN PV 2 atlas shows a marked atlantic fossa (*fossa atlantis*) typical for modern ruminants (König and Liebich 2020; Fig S1b in Appendix C3 Resource 5), but absent in *Macrauchenia* (PIMUZ A/V 5700) and other macraucheniids such as *M. saladensis*, *Cramauchenia* (MLP 83-III-2-1) and *Theosodon* (MACN A 9255; Fig. 3.5e, g-i). Third, the transverse process in the MACN PV 2 atlas is anteroposteriorly extended anteriorly to the occipital facet of the atlas (Fig S1a-b in Appendix C3 Resource 5), whereas in *Macrauchenia* (PIMUZ A/V 5700) and other macraucheniids (Fig. 3.5), it terminates at the base of the process for the occipital facet, creating an alar notch which is absent in MACN PV 2 atlas. The foramina in the MACN PV 2 atlas include an alar foramen ventrally (Fig S1b in Appendix C3 Resource 5), and dorsally, the dorsal exit of the alar foramen and adjacent to it, the lateral vertebral foramen (Fig S1a in Appendix C3 Resource 5), which again is the observed condition in extant ruminants but not comparable to *Macrauchenia* (PIMUZ A/V 5700) and other macraucheniids. In addition, the MACN PV 2 atlas shows a very strong dorsal tubercle, closely appressed articular facets for the axis and a dorsoventrally compressed ovoid vertebral foramen (Fig. S1c

in Appendix C3 Resource 5), among other features clearly not present in *Macrauchenia* (PIMUZ A/V 5700). In sum, we assert that the MACN PV 2 atlas (also illustrated in Burmeister [1864-1869b]) is not from *Macrauchenia*, being instead of a ruminant, and likely, a bovid (possibly *Bos* or *Bison*) considering its specific anatomical features, size, and general shape (see Fig. S1 in Appendix C3 Resource 5). Furthermore, we think that the similarities found in Lessa (1992) between MACN PV 2 atlas and the atlas of *Xenorhinotherium* (MCL 2644\53), and the mention of both being similar to ruminants, is likely to be an error derived from following the misidentification in Burmeister (1864b). Indeed, when we look at a dorsoventral photograph of *Xenorhinotherium* (Lessa 1992: Pl. XIX), the atlas looks almost identical to *Macrauchenia* (PIMUZ A/V 5700), showing clear anterior exits of the transverse foramina in the transverse processes and alar notches posterior of the occipital facets. It is likely that Scott (1910) based his comparison for the atlas of *Theosodon* on the illustration of Burmeister (1864b) for *Macrauchenia*, because he mentions at least a couple of features like the absence of transverse foramina and anteriorly elongated traverse processes with alar foramina instead of alar notches, as key differences between both taxa. As we saw in *Macrauchenia* (PIMUZ A/V 5700), these alleged differences are incorrect.

In terms of relative size, when we compare the relative dorsoventral height versus the total length (ML/MH), the atlas of *M. saladensis* (SGO.PV.21700) is more similar to the atlas of *Macrauchenia* (PIMUZ A/V 5700) and the Quequén Salado River macraucheniine (MACN PV 9779), with values of 1.05, 0.99 and 1.18 respectively, being dorsoventrally higher than the atlas of *Theosodon garretorum* (YPM VPPU 015164) with a value of 1.43. Overall, considering shape, measurements proportions and anatomy, the atlas of *M. saladensis* is like a miniature version of the atlas of *Macrauchenia*. It is important to note here that the atlas of *Cramauchenia* (MLP 83-III-2-1; Fig. 3.5d) pertains to a subadult specimen as M2 was still erupting (not figured). The Quequén Salado River macraucheniine atlas (MACN PV 9779) could also be a subadult as its proportions seem to be a bit different to other macraucheniines as *M. saladensis* (SGO.PV.21700) and *Macrauchenia* (PIMUZ A/V 5700), in particular the relative length of its traverse processes (ML/TL) with a value of 1.58 versus 1.19 and 1.29 respectively for the two later (Table S2 in Appendix C3 Resource 1). In addition, it is interesting to note that considering the fossil records of the Quequén Salado River basin (Beilinson *et al.* 2017), the macraucheniid from Quequén Salado River found between Indio Rico and Cascada Cifuentes (early Pliocene, Prevosti et al. 2021) would be the first occurrence of this subfamily and of any litoptern recorded in that unit.

**Axis** The axis of *Micrauchenia saladensis* only preserves its anterior portion. The anterior articular facets for atlas are slightly mediolaterally broader than dorsoventrally deep, and strongly convex curving dorsoposteriorly (Fig. 3.6). On the midline of the axis, separated from the atlantic facets by sulci, there is a slightly elongated odontoid process or dens with a mediolaterally extended articular facet for the atlas. As in *Theosodon* and *Macrauchenia*, the odontoid process has a peg-like shape, which is uncommon for long-necked ungulates such as equids and camelids (Scott 1910). A keel is present on the dorsal surface of the body of the axis of *M. saladensis*, that runs posteriorly from the neck of the odontoid process towards the vertebral foramen (not preserved), a feature seen also in *Theosodon* (YPM VPPU 30601) and *Macrauchenia* (MUHNCAL-KM 004; PIMUZ A/V 5700; Fig. 3.6b).

The relative dimensions of the anterior articular atlantic facets of *M. saladensis* are more dorsoventrally compressed than *Theosodon* (YPM VPPU 30601) but less compressed than *Macrauchenia* (MUHNCAL-KM 004; PIMUZ A/V 5700) with a width to height ratio (WA/HA) of 0.96 for the ratio for *M. saladensis* versus 0.68 and 1.13 in *Theosodon* and *Macrauchenia* respectively (Table S2 in Appendix C3 Resource 1). This is evident in an anterior view of the anterior articular facets for the atlas: in *Theosodon*, the facets are ovoid or almost circularly shaped; in *Macrauchenia* the facets are rectangular in shape, and in *M. saladensis* the facets are also rectangular shaped although less dorsoventrally compressed than in *Macrauchenia* (Fig. 3.6a, d). In addition, the odontoid process of the axis of *M. saladensis* is relatively shorter than *Theosodon* (YPM VPPU 30601) with a ratio of 1.45 between the width of the atlantic facets and odontoid process length (WA/OL) versus 0.80 in *Theosodon* (Table S2 in Appendix C3 Resource 1). In contrast, the odontoid process of *Macrauchenia* has a similar relative length (WA/OL) to *M. saladensis* (MUHNCAL-KM 004 = 1.43; PIMUZ A/V 5700 = 1.57).

It is interesting to note that the specimen referred to *Theosodon* sp. from the middle Miocene Fitzcarrald area western Amazonia in Peru (Tejada-Lara *et al.* 2015), has noticeable differences to Santacrucian specimens of *Theosodon* in terms of the proportions of the anterior articular facets for the atlas and the relative length of the odontoid process, with more dorsoventrally compressed anterior articular facets for the atlas and a considerably shorter odontoid process (WA/HA = 0.84, WA/OL = 1.38; Table S2 in Appendix C3 Resource 1) when compared to YPM VPPU 30601, an early Miocene (Santacrucian SALMA) specimen of *Theosodon*. In fact, the relative length of the odontoid process (WA/OL) puts the Fitzcarrald specimen closer to *M. saladensis* and *Macrauchenia* than to *Theosodon*. This would suggest

that a taxonomic reinterpretation of the macraucheniid material from the Fitzcarrald area may be needed, although a taxonomic refinement could be difficult due to the limited and fragmentary condition of the material.

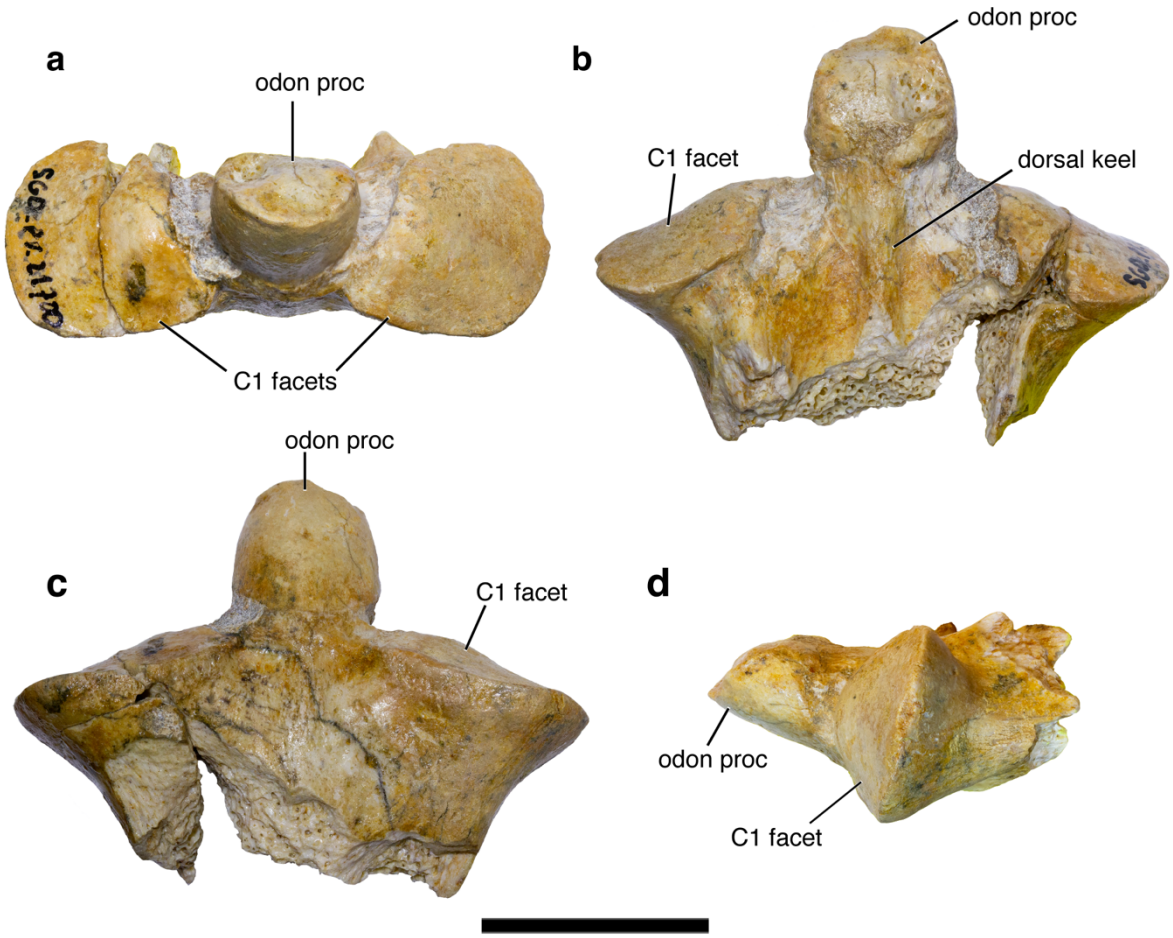



**Figure 3.6** Axis of *Micrauchenia saladensis* (SGO.PV.21700). **a**. anterior view; **b**. dorsal view; **c**. ventral view; **d**. left lateral view. Abbreviations: *odon proc*, odontoid process. Scale bar equals 2 cm

**Fifth cervical vertebra (C5)** C5 only preserves its posterior portion, so the prezygapophyses and the anterior transverse processes are missing (Fig. 3.7a-f). The C5 centrum is dorsoventrally compressed, and on its ventral surface, two oblique keels are present. Based on what is preserved it is likely the two keels converged anteriorly (Fig. 3.7e). It is interesting to mention that Scott (1910) noted that the fourth cervical vertebra (C4) of *Macrauchenia* presents a single ventral keel that does not diverge posteriorly into two sections in contrast to *Theosodon* that presents clear posteriorly divergent oblique keels that are connected anteriorly. However, close observation of *Macrauchenia* (PIMUZ A/V 5700, personal observation [H.P.P.]) shows that all these three cervical vertebrae (C3 – C5) present two posterior oblique keels, from which only C3 completely connects with the anterior central keel as in *Theosodon* (Scott 1910). The

postzygapophyses of C5 are prominent and projected posteriorly, forming a V-shaped profile in dorsal view (Fig. 3.7c).

Dorsally, it presents a mediolaterally thin and dorsoventrally low spinous process that increases in height anteriorly (Fig. 3.7a-d, f). The transverse processes are located approximately at the dorsoventral midpoint of the centrum, being slightly ventrally inclined. The lateral border of the transverse process is ventrally expanded (Fig. 3.7a-b). The transverse foramen (*foramen transversarium*) is not in the transverse process as in most mammals, being instead in the medial side of the wall of the neural arch (Fig. 3.7b, f). A similar position of the transverse foramina has been observed in other macraucheniids, *Theosodon* (YPM VPPU 015164) and *Macrauchenia* (NHMUK PV M 43402 A-B), and is also seen modern camelids (Owen 1838). From the two transverse foramina, only the right one was completely preserved in SGO.PV.21700. The vertebral foramen of C5 is circular in distal view (Fig. 3.7b).

All these features are in general terms consistent with the C3 – C5 in *Theosodon* (Scott 1910) and *Macrauchenia* (PIMUZ A/V 5700), which are the elongated vertebrae of the cervical series apart from the axis. However, there are some particular features that allow us to confidently assign it to C5. First, the ratio between the maximum mediolateral width at posterior end of vertebral body (WPB) and the mediolateral width between postzygapophyses (WPZ; WPB/WPZ) for the C5 of *Micrauchenia saladensis* is 1.30, which is similar to *Macrauchenia* (PIMUZ A/V 5700) which has a ratio 1.39, in contrast to the values of 1.60 and 1.54 for C3 and C4 of *Macrauchenia* (Table S2 in Appendix C3 Resource 1). Second, the V-shaped profile of the postzygapophyses in dorsal view is only present in C5 of *Macrauchenia* (PIMUZ A/V 5700). On C3 and C4 of *Macrauchenia* (PIMUZ A/V 5700), the postzygapophyses are not as broadly separated and therefore the incisure between the facets is not as deep. In *Theosodon* this feature seems to be present (Scott 1910: Pl. XVIII fig. 4a) although it is less developed than in *Macrauchenia* and *M. saladensis*, as the angle between the postzygapophyses is posterior to the beginning of the body. In addition, in the *M. saladensis* specimen the posterior transverse processes do not reach the posterior margin of the body, a feature present in C5 of *Theosodon* (see Scott (1910), Pl XVIII 4-4a) and *Macrauchenia* (PIMUZ A/V 5700). In C3 and C4 of the latter taxa, the posterior transverse processes reach the margin of the body posteriorly, and their lateral most tips even surpass the margin of the body posteriorly.

**Seventh cervical vertebra (C7)** C7 of *Micrauchenia saladensis* is short and robust (Fig. 3.7g-l). C7 is well preserved, although the anterior portion of the vertebral arch with the prezygapophyses is missing. In anterior view, the body is ovoid in shape being slightly dorsoventrally compressed (Fig. 3.7g), while in posterior view, the body is semilunar in shape with a flattened ventral border (Fig. 3.7h). The posterior end of the body is more strongly dorsoventrally compressed and relatively wider than the anterior portion. This is partially due to the presence of large and concave posterior costal foveae or demifacets (*Fovea costalis caudalis*; Fig. 3.7h) for the articular surface of the head of the first rib (*caput costae*). Ventrally, there is a strong keel that widens mediolaterally and dorsoventrally thickens as it approaches the anterior margin of the vertebral body, causing the anterior body face to be ventrally expanded at the level of the keel (Fig. 3.7g-h, k).

The postzygapophyses are widely separated and short (Fig. 3.7g-i), compared to the posterior position and closeness of the postzygapophyses on C5 (Fig. 3.7b-c). Anterior to the postzygapophyses, there is a low spinous process that appears to increase in height anteriorly (Fig. 3.7j, l). The transverse processes are dorsoventrally thick and anteroposteriorly short with the anterior margin projecting slightly anterior to the anterior end of the vertebral body (Fig. 3.7i-l). Dorsal of the main tubercle of the transverse process, there is a tiny tubercle pointing anteriorly (Fig. 3.7g, j). Similar to most mammals (Rose 2006), including *Macrauchenia* (PIMUZ A/V 5700), there is no transverse foramen on C7. In *Theosodon*, tiny transverse foramina were described at the base of the transverse processes, although too small to accommodate the major trunk of the vertebral artery (Scott 1910).

Overall, these features are comparable with the anatomy of C7 in *Macrauchenia* (PIMUZ A/V 5700) and what has been previously described for the C7 of *Theosodon* (Scott 1910). However, there are some subtle anatomical differences in the C7 of *M. saladensis* that differentiate it from *Macrauchenia* (PIMUZ A/V 5700). First, in the anteriormost portion of the vertebral body, the ventral keel of *Macrauchenia* is more mediolaterally compressed than in *M. saladensis*. Second, the transverse processes in *M. saladensis* have a small posterior projection (Fig. 3.7i-k), whereas in *Macrauchenia* a posterior projection is absent/reduced.

In terms of C7 general proportions, *M. saladensis* is very similar to *Macrauchenia* (PIMUZ A/V 5700) with a WPB/WPZ ratio of 1.08 and 1.07 respectively, which is substantially different from any other measured vertebrae of the cervical series (Table S2 in Appendix C3 Resource 1). The rest of the calculated ratios are fairly similar between these two

species, with the exception of the maximum anteroposterior vertebral body length versus maximum mediolateral width at anterior end of vertebral body ratio (LB/WAB), with values of 1.17 in *M. saladensis* and 1.05 in *Macrauchenia*, which means that C7 is relatively longer in the former than in the latter. *Theosodon lallemanti* (YPM VPPU 015216) and one specimen of *Xenorhinotherium bahiense* (MCL 2643/88) have a LB/WAB ratio of 1.16 and 1.18 respectively, and are very similar to *M. saladensis*. However, there seems to be some variation in the relative length even within the same genus or species, as *Theosodon garretorum* (YPM VPPU 015164) has a LB/WAB ratio of 1.07 which puts it closer to *Macrauchenia* (PIMUZ A/V 5700), and *Xenorhinotherium* shows a wide range of intraspecific variation with LB/WAB values between 1.18 and 1.49 (Table S2 in Appendix C3 Resource 1).

**Second thoracic vertebra (T2)** SGO.PV.21700 includes a vertebra that we tentatively identify as the T2 of *Micrauchenia saladensis* (Fig. 3.8). The postzygapophyses are not preserved, as the posterior part of the vertebral arch is missing. Only the left prezygapophysis is preserved. This vertebra is very similar to C7 in its general shape, although is considerably anteroposteriorly shorter (Fig. 3.8c-f). Apart from the length, the most notable difference is the presence of anterior costal foveae (*fovea costalis cranialis*) for the head of the second rib and costal foveae for the articular surface of the second rib tubercle (*tuberculum costae*) on the transverse process (*fovea costalis processus transversi*; Fig. 3.8a).

Overall, the vertebral body of T2 in *M. saladensis* is dorsoventrally compressed; however, the posterior aspect is slightly more compressed than the anterior aspect (Fig. 3.8a-b). The anterior costal foveae are mostly concave and located lateroventrally on the vertebral body (Fig. 3.8a). Adjacent to the medial margin of each fovea is a relatively small but deep foramen which it was likely a nutrient foramen for the entrance of blood vessels to innervate the vertebra (Evans & Lahunta 2012). Even though Scott (1910) did not mention this nutrient foramen for *Theosodon* on any of the thoracic vertebra, his drawing of the anterior view of T1 shows what it seems to be a couple of nutrient foramina in a similar position to *M. saladensis*. In *Macrauchenia* (PIMUZ A/V 5700) there seem to be similar canals in the same position on T2 although relatively smaller in size.

The posterior costal foveae of T2 in *M. saladensis* are also concave and located lateroventrally of the vertebral body, but they do not present nutrient foramina as the anterior coastal foveae (Fig. 3.8b). Ventrally, the anterior and posterior costal foveae are closely approximately each other due to the anteroposterior compression of the vertebral body (Fig.

3.8d). In the same ventral aspect, along the median plane of the vertebral body of T2, there is an anteroposterior keel. This keel is considerably weaker than the keel on C7. In contrast, T2 in *Macrauchenia* (PIMUZ A/V 5700) does not present a clear ventral keel.

The prezygapophysis of T2 in *M. saladensis* is concave and positioned dorsal to the transverse process, with its anteriormost portion slightly surpassing the anterior end of the vertebral body. Dorsally, there is a relatively developed spinous process which is poorly preserved, so it is not possible to estimate its total length and height (Fig. 3.8a-c, e, f). The spinous process is bent posteriorly and its basal width suggests that there is a substantial portion missing, and is likely that this missing portion extended well posterior of the posteriormost margin of the vertebral body. The posterior inclination and presumable large size of the spinous process suggests that this vertebra is T2 instead of the first thoracic vertebra (T1), considering that in *Theosodon* (YPM VPPU 015164) and *Macrauchenia* (PIMUZ A/V 5700) T1 has a base that is not inclined posteriorly. T3 and the following thoracic vertebrae can be discarded as in *Theosodon* (YPM VPPU 015164) and *Macrauchenia* (PIMUZ A/V 5700) they show clear differences with T1 and T2, having shorter traverse processes, very robust and high neural spines and laterally oriented costal foveae in the transverse processes.

The transverse processes are dorsoventrally higher and anteroposteriorly shorter than C7 (Table S2 in Appendix C3 Resource 1), presenting ventrally concave costal foveae for the for the second rib tubercles which have a slight anterolateral orientation (Fig. 3.8d-f). The transverse processes are continuously extended from their costal foveae ventrally to the prezygapophyses dorsally, which it also suggests a T2 identity, as this is similar to what is observed in this vertebra from *Macrauchenia* (PIMUZ A/V 5700). In contrast, T1 in *Macrauchenia* (PIMUZ A/V 5700) presents a mediolateral constriction that separates the transverse processes from the prezygapophysis. This constriction is also observed in the T1 of *Theosodon* (Scott 1910: Pl. XVIII fig. 6), although in this case the separation is even clearer as there is more distance between the transverse processes and the prezygapophyses. The oblique ventrolateral orientation of the costal foveae of the transverse processes in *M. saladensis* is similar to the same in T2 of *Macrauchenia* (PIMUZ A/V 5700) which it also supports a T2 identity, whereas in the latter genus, the costal foveae on T1 are oriented fully ventrally.

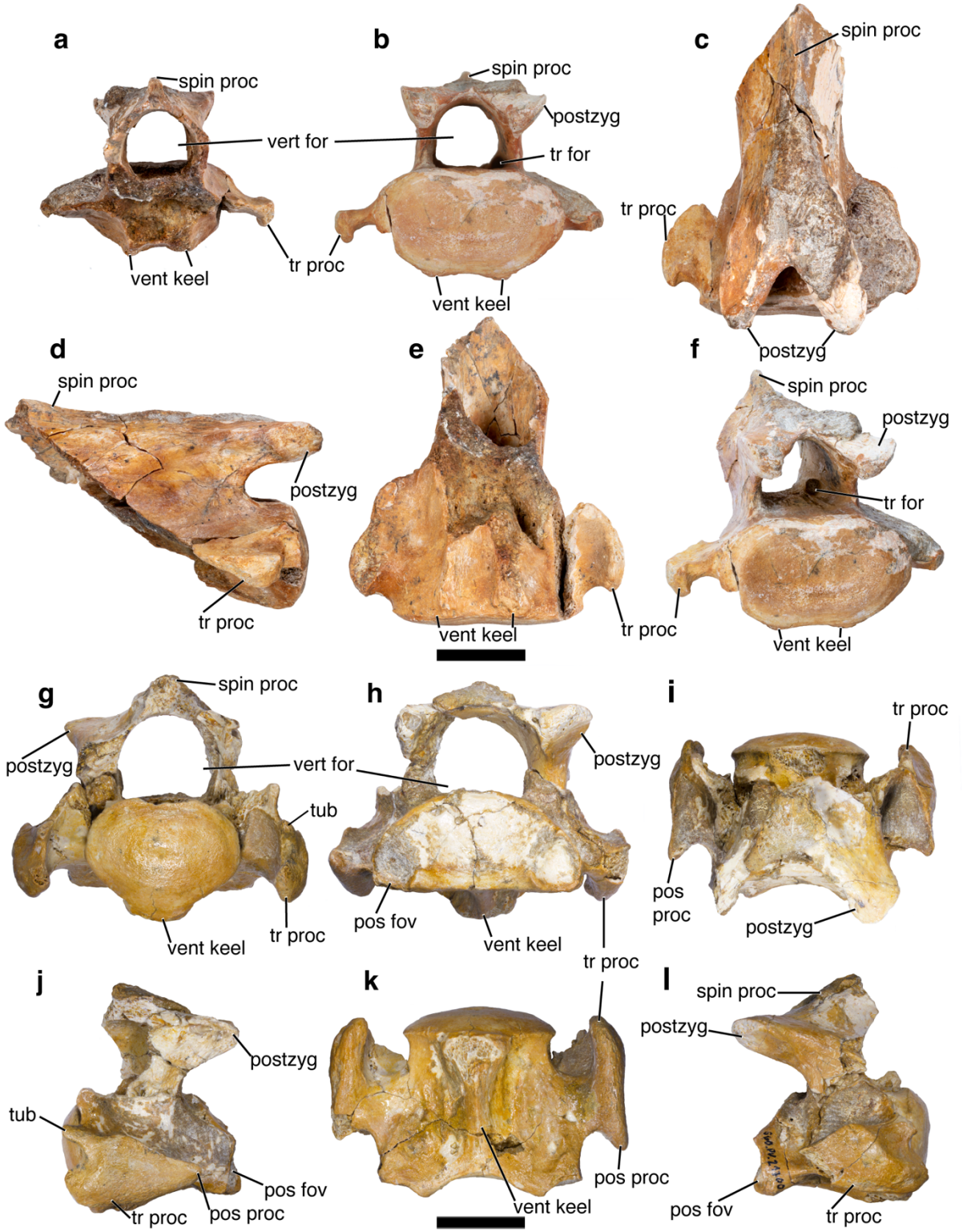



**Figure 3.7** Fifth and seventh cervical vertebrae (C5 and C7) of *Micrauchenia saladensis* (SGO.PV.21700). **a-f**. C5 in anterior (**a**), posterior (**b**), dorsal (**c**), left lateral (**d**), ventral (**e**), and posterolateral (**f**) views. **g-l.** C7 in anterior (**g**), posterior (**h**), dorsal (**i**), left lateral (**j**), ventral (**k**), and right lateral (**l**) views. Abbreviations: *pos fov*, posterior costal fovea; *pos proc*, posterior projection of the transverse process; *postzyg*, postzygapophysis; *spin proc*, spinous process; *tr for*, transverse foramen; *tr proc*, transverse process; *tub*, small anterior transverse process tubercle; *ven keel*, ventral keel; *vert for*, vertebral foramen. Scale bars equal 2 cm

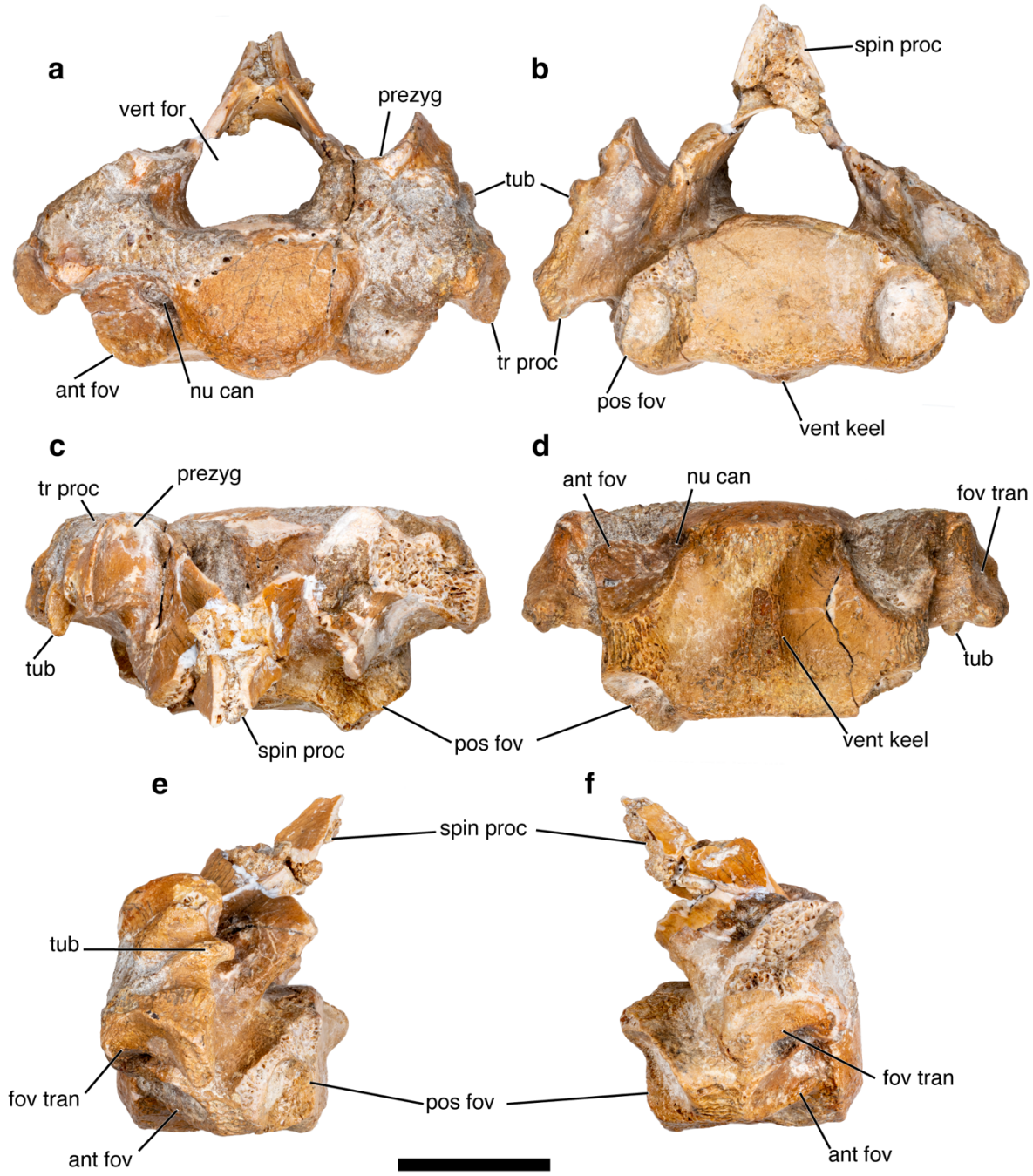



**Figure 3.8** Second thoracic vertebra (T2) of *Micrauchenia saladensis* (SGO.PV.21700). **a**. anterior view; **b**. posterior view; **c**. dorsal view; **d**. ventral view; **e**. left lateral view; **f**. right lateral view. Abbreviations*: ant fov*, anterior costal fovea; *fov tran*, Costal fovea of transverse process; *nu can*, nutrient canal; *prezyg*, prezygapophysis; *pos fov*, posterior costal fovea; *spin proc*, spinous process; *tr for*, transverse foramen; *tr proc*, transverse process; *tub*, small posterior transverse process tubercle; *ven keel*, ventral keel; *vert for*, vertebral foramen. Scale bar equals 2 cm

Interestingly, Scott (1910) describes T1 in *Theosodon* as having a ventrally oriented costal foveae of the transverse processes, although T1's drawing in his monograph (Pl. XVIII fig. 6) shows a anteriorly oriented costal foveae of the transverse processes.

In terms of relative proportions, T2 of *M. saladensis* is largely similar to *Macrauchenia* (PIMUZ A/V 5700) although some differences are evident due to the wider posterior end of vertebral body (WPB) in the latter (Table S2 in Appendix C3 Resource 1).

## Thoracic limbs

**Scapula** The left scapula of SGO.PV.21700 is fragmentary, only preserving part of its posterodorsal portion which is heavily damaged and eroded (Fig 3.9a). Only the lateral surface is exposed, and due to its fragility it is not possible to fully remove the sediment from the medial surface without compromising the entire element. The specimen preserves a section of the scapular spine (*spina scapulae*), in which the dorsal tubercle, as seen in other macraucheniids (e.g., *Theosodon* [YPM VPPU 015164]), has been probably eroded away. Anteriorly to the scapular spine, there is a small portion of the fossa supraspinata. Posteriorly to the scapular spine is a portion of the fossa infraspinata with part of the dorsal and posterodistal border of the scapula preserved. The preserved parts of this element are very similar to other macraucheniids, including *Theosodon* (Scott 1910, Pl XIX 1), *Macrauchenia* (PIMUZ A/V 5700), and *Xenorhinotherium* (Lessa 1992, Pl XXIV), although the state of preservation does not allow more detailed comparison.

**Ulna-radius** The ulna and radius of *Micrauchenia* are coosified, so they are here described as one element (Figs. 3.9b-e and 3.10a). The proximal end and part of the proximal portion of the diaphysis were not preserved, but the ulna and radius were likely fully coosified along their entire length considering this condition is observed in other macraucheniines (e.g., *Promacrauchenia* [MACN PV 5710] and *Macrauchenia* [MACN PV 2]).

The coosification or fusion of the ulna-radius strongly suggests that *M. saladensis* is a member of the subfamily Macraucheniinae *sensu* Soria (1981, 2001). Macraucheniids included in this subfamily in which these elements are known such as *Promacrauchenia*, *Macrauchenia* and *Xenorhinotherium* possess a fully fused ulna and radius in adult specimens (Gervais 1855; Parodi 1931; Cartelle & Lessa 1988), in contrast with earlier macraucheniids ("Cramaucheniinae") such as *Theosodon* and *Llullataruca*, that display the ulna and radius in close contact but without any coosification (Scott 1910; McGrath *et al.* 2018).

A well-developed medial aliform expansion is present on the radius diaphysis of *M. saladensis* (Fig. 3.9b-d), and proximal from it, there is marked bend towards the lateral aspect of the element. Both features further suggest an affinity between *M. saladensis* and

macraucheniines such as *Macrauchenia* (MACN PV 2) and *Promacrauchenia* (MACN PV 9526). The aliform expansion is formed by an arched medial thickening of the radius which is particularly rugose along its posterior aspect. This expansion has been observed to different degrees of development in *Promacrauchenia*, *Macrauchenia* and *Xenorhinotherium* (Parodi 1931; Lessa 1992). Considering its position, the rugose area on the aliform expansion could have provided attachment to the radial head (*caput radiale*) of the deep digital flexor muscle (*M. flexor digitorum profundus*; Sisson 1914; Denoix 2019; König and Liebich 2020; MacLaren and McHorse 2020; Blanco et al. 2021). This is different from the condition present in earlier macraucheniids as *Theosodon* (YPM VPPU 015164; MACN A 2569-2608; MACN A 9253), in which the radius does not exhibit this extreme protrusion in its diaphysis. However, *Theosodon gracilis* (MACN A 2569-2608) has a relatively subtle thickening in a similar area of the diaphysis, which could be considered a precursor of the aliform expansion seen in more derived macraucheniids.

*M. saladensis* shows a particularly broad aliform expansion, so much so that the maximum mediolateral width of the ulna-radius is greatest at the level of the aliform expansion, rather than the distal epiphysis (53.28 vs 43.95 mm respectively; Table S3 in Appendix C3 Resource 1). When we calculate the ratio between the maximum mediolateral width of the aliform expansion and the maximum mediolateral width of the distal epiphysis for different macraucheniids (URA/URD; Table S3 in Appendix C3 Resource 1) *M. saladensis* (SGO.PV.21700) has a value of 1.21, similar to *Macrauchenia patachonica* (MACN 2; PIMUZ A/V 5700; MNHN.F.PAM75) and MNHN-Bol-V 003372 described by Anaya and MacFadden (1995) as *Promacrauchenia* sp. with values of 1.08-1.31 and 1.12 respectively. In contrast, *Promacrauchenia antiquua* (MACN PV 5710) and *Promacrauchenia kraglievichi* (MACN PV 9526) have values below 1 of 0.83 and 0.93 respectively.

In *M. saladensis* the aliform expansion is positioned towards the distal end of the radius (Fig. 3.9b-d). The position of the expansion in *M. saladensis* is not as distal as the condition in *Macrauchenia patachonica* but is considerably more distal than that observed in *Promacrauchenia* sp (MNHN-Bol-V 003372) where the expansion is located on the proximal half of the radius (Anaya & MacFadden 1995). Due to the missing proximal half in the ulna-radius of SGO.PV.21700, it is not possible to quantify how far distal the aliform expansion is positioned in *M. saladensis* relative to the total radius length.

The distal radial epiphysis exhibits two articular facets for the scaphoid and the lunate (Fig. 3.10a). The scaphoid facet is positioned medially and is approximately twice the mediolateral width of the lunate facet. The maximum mediolateral width and anteroposterior length of the scaphoid facet are approximately subequal and the articular surface is anteriorly concave and posteriorly convex. The posterior margin of the scaphoid facets extends further posterior relative to the posterior margin of the lunate facet. The lunate facet is anteroposteriorly longer than mediolaterally wide. Similar to the scaphoid facet, the lunate facet is anteriorly concave and posteriorly convex. Lateral to the lunate facet, on the distal surface of the ulna, there is a concave cuneiform facet (Figs. 3.9e and 3.10a). The posterolateral part of the facet is damaged. The preserved has a similar mediolateral width than the lunate facet. The pisiform facet on the ulna, observed in other macraucheniids, was not preserved in SGO.PV.21700 due to damage.

In terms of absolute size, the ulna-radius of *M. saladensis* (SGO.PV.21700) is smaller *Theosodon garrettorum* (YPM VPPU 015164), *Promacrauchenia antiquua* (MACN PV 5710), *Promacrauchenia kraglievichi* (MACN PV 9526) and *Macrauchenia patachonica* (MACN 2; PIMUZ A/V 5700; MNHN.F.PAM75; Table S3 in Appendix C3 Resource 1), although due to the lack of the proximal end it was not possible to compare the total length of the element. Two specimens, MLP 57-X-10-157 and MLP 91-III-1-26 (Macraucheniinae indet.), from the late Miocene and early Pliocene respectively, are of similar size than SGO.PV.21700 (Table S3 in Appendix C3 Resource 1). However, they do not have a clear aliform expansion of the radius as in SGO.PV.21700.

### Carpals

The preserved elements of the carpus of *Micrauchenia saladensis* (SGO.PV.21700) include the scaphoid, lunate, cuneiform, magnum, and unciform and pisiform (Figs. 3.9b-c, 3.10b-c, 3.11a-f, 3.12a-f, 3.13a-f, 3.14a-f, 3.15a-f and 3.16a-f). The trapezium and trapezoid were present in life but are not preserved with the specimen described. The centrale is absent as a discrete bony element (i.e., probably fused with the scaphoid). Overall, the articulated carpus of *M. saladensis* is almost twice as mediolaterally wide than anteroposteriorly long (Fig. 3.10b-c; APL/MLW = 0.47; Table S4 in Appendix C3 Resource 1).

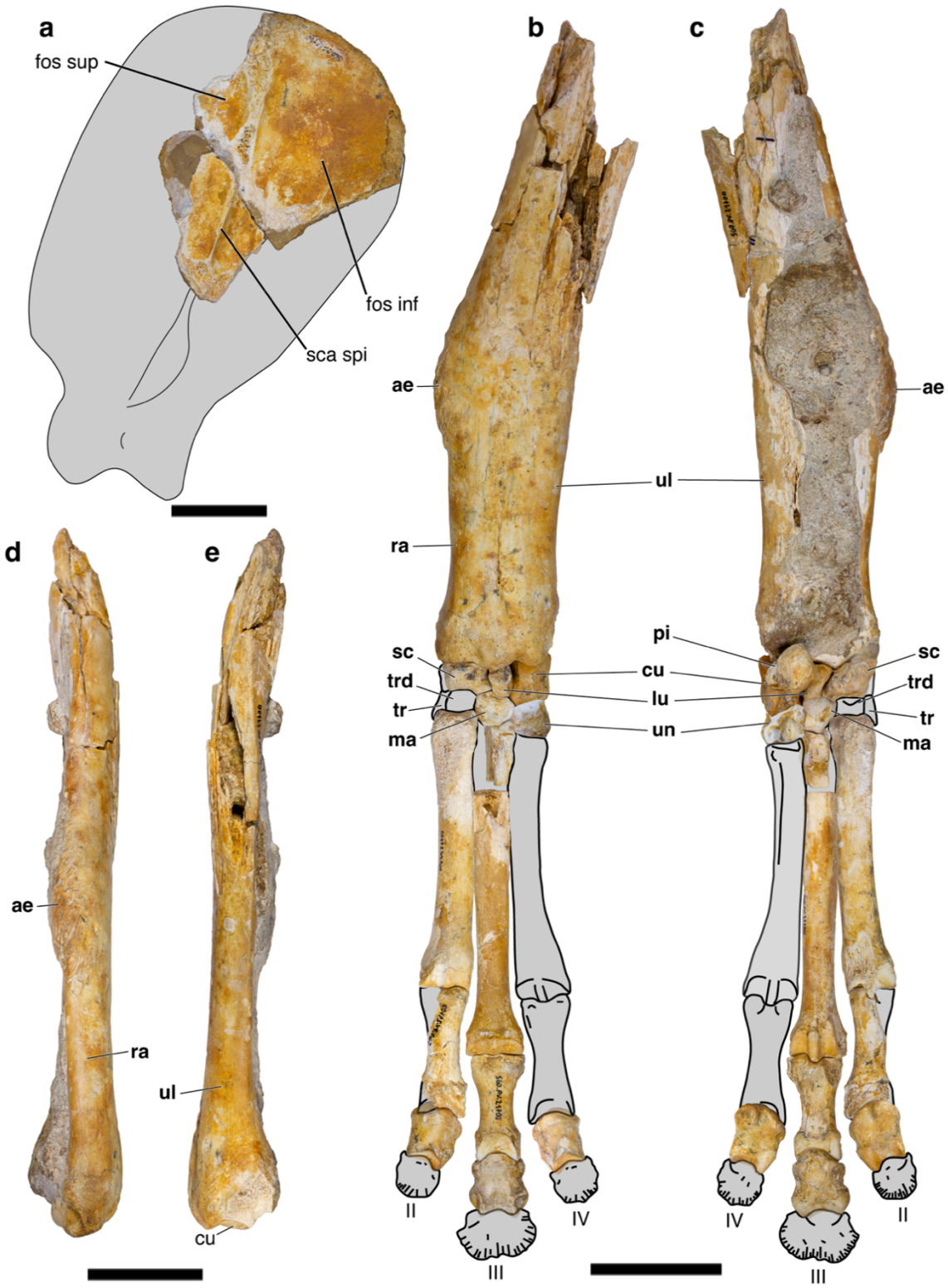



**Figure 3.9** Left scapula, and ulna-radius and manus articulated of *Micrauchenia saladensis* (SGO.PV.21700). **a.** scapula in lateral view. **b-c**. ulna-radius and manus articulated in anterior (**b**), and posterior (**c**) views. **d-e**. ulna-radius in medial (**d**), and lateral (**e**) views. The right digit II and the unciform were mirrored in **b-c**. Bones and facets are indicated in bold and regular font respectively. Abbreviations: *ae*, aliform expansion of the radius; *cu*, cuneiform; *fos inf*, fossa infraspinata; *fos sup*, fossa supraspinata; *lu*, lunate; *ma*, magnum; *pi*, pisiform; *ra*, radius; *sc*, scaphoid; *sca spi*, scapular spine; *tr*, trapezium; *trd*, trapezoid; *ul*, ulna; *un*, unciform. Scale bar equals 4 cm in **a** and **d**, and 5 cm in **b-c**

In terms of absolute size, the carpals of *M. saladensis* are of similar size than *Cramauchenia normalis*, considerably smaller than *Theosodon* (~31%; 8 – 60%), *Cullinia* cf *C. levis* (~40%), *Promacrauchenia antiquua* (~65%), *Macrauchenia patachonica* (132%), and *Xenorhinotherium bahiense* (123%; Table S4 in Appendix C3 Resource 1). Interestingly, the magnum of *Coniopternium primitivum* is slightly smaller but its lunate is slightly larger than in *M. saladensis*. However, considering our small sample for comparisons, it is entirely possible that in a bigger sample, the carpals' size distribution of *Coniopternium primitivum* and *M. saladensis* could overlap.

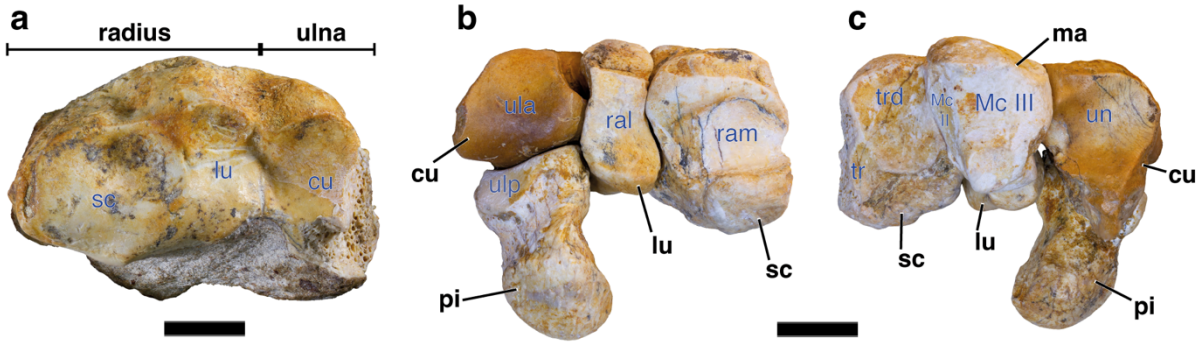



**Figure 3.10** Left ulna-radius and articulated carpals of *Micrauchenia saladensis* (SGO.PV.21700). **a**. left ulna-radius in proximal view. **b-c**. left articulated carpals in proximal (**a**), and distal (**c**) views. Bones and facets are indicated in black bold and dark blue regular font respectively. Abbreviations: *cu*, cuneiform; *lu*, lunate; *ma*, magnum; *Mc*, metacarpal; *pi*, pisiform; *ral*, radius lateral facet; *ram*, radius medial facet; *sc*, scaphoid; *tr*, trapezium; *trd*, trapezoid; *ula*, ulnar anterior facet; *ulp*, ulnar posterior facet; *un*, unciform. Scale bar equals 1 cm

In terms of general proportions *M. saladensis*'s articulated carpus falls within the range observed in other macraucheniids (APL/MLW = 0.46 - 0.51; Table S4 in Appendix C3 Resource 1), being most similar to *Macrauchenia patachonica* (MNHN.F.PAM75; APL/MLW = 0.46; Table S4 in Appendix C3 Resource 1).

**Scaphoid** Among the proximal row of carpals, the scaphoid (*os scaphoideum*) is proximodistally short, mediolaterally wide and anteroposteriorly deep, presenting a distinctive hook-shaped palmar tuberosity posteriorly (Figs. 3.9b-c, 3.10b-c and 3.11a-f; Table S4 in Appendix C3 Resource 1). There is a single proximal facet for the radius, which is largely convex on its anterior half, and concave in the posterior half towards the palmar tuberosity (Figs. 3.10b and 3.11a-c, e-f). The medial-most portion of this facet is missing due to the preservation of the element. Distally the scaphoid has three facets for the trapezium, trapezoid and magnum, ordered from medial to lateral (Figs. 3.10c and 3.11d-f). Only a posterior portion of the facet for the trapezium is preserved. The articular surface is concave and oriented distally. The trapezoid facet is the largest of the three facets. The articular surface faces distally

and is overall slightly concave. The magnum facet is weakly convex anteriorly and concave posteriorly. The articular surface of the magnum is oriented distolaterally (Fig. 3.11f). Given the shape and position of this distolateral portion that extends over the magnum, we hypothesize that the centrale has fused with the scaphoid (Holmgren 1952). On the lateral surface of the scaphoid there are two facets for the lunate, one proximal next to radius facet and, one distal next to the magnum facet. The distal facet is somewhat bigger than the proximal, and both facets are proximodistally thin but anteroposteriorly elongated.

The general configuration of the scaphoid in *M. saladensis* is overall similar to *Cramauchenia* (MNHN.F.COL188; MNHN.F.COL189), *Theosodon* (MLP 12-850; MLP 12-883; Fig. 3.11g-h), *Macrauchenia* (MLP 12-1660; MNHN.F.PAM75; Fig. 3.11k-l), *Xenorhinotherium* (MCL specimens), and also to the late Miocene macraucheniid MLP 57-X-10-157 (Macraucheniinae indet.; Fig. 3.11i-j). However, there are some differences between macraucheniines including *M. saladensis* with earlier macraucheniids (e.g., *Cramauchenia*). First, the trapezoid facet in *Cramauchenia* (MNHN.F.COL188; MNHN.F.COL189) and *Theosodon* (MLP 12-850; MLP 12-883) is divided into two concavities separated by a ridge of which the anterior concavity is mediolaterally wider (Fig. 3.11g). In contrast, in *M. saladensis*, *Macrauchenia* (MLP 12-1660; MNHN.F.PAM75) and MLP 57-X-10-157 (Macraucheniinae indet.) the trapezoid facet of the scaphoid is a continuous surface without any clear ridge separating the anterior and posterior portions of the facet (Fig. 3.11 d, i, k).

Another difference is that in *M. saladensis*, *Macrauchenia* (MLP 12-1660; MNHN.F.PAM75) and MLP 57-X-10-157 (Macraucheniinae indet.), the magnum facet in distal view has a similar mediolateral width throughout its length giving it a largely rectangular shape. In *Cramauchenia* (MNHN.F.COL188; MNHN.F.COL189) and *Theosodon* (MLP 12-883) the magnum facet is mediolaterally wider in its anterior aspect than its posterior aspect which confers it a pyriform shape. However, in *Cramauchenia* (MNHN.F.COL188; MNHN.F.COL189) the magnum facet is much shorter than in *Theosodon* (MLP 12-883), being most of the facet in the anterior half of the scaphoid. Additionally, in *M. saladensis* (SGO.PV.21700) and MLP 57-X-10-157 (Macraucheniinae indet.) the distal facet for the lunate in the scaphoid is anteroposteriorly elongated, having approximately the same length of the magnum facet (Fig. 3.11f, j), whereas in *Macrauchenia* (MNHN.F.PAM75) this facet is much shorter, being proximal to only the posterior portion of the magnum facet (Fig. 3.11l). In *Cramauchenia* (MNHN.F.COL188; MNHN.F.COL189) and *Theosodon* (MLP 12-883) the distal lunate facet has a fusiform-shaped expansion in the anterior margin of the scaphoid,

proximal to the anterior portion of the magnum facet (Fig. 3.11h). When comparing the proximal lunate facet of the scaphoid, *M. saladensis* (SGO.PV.21700) is more similar to *Macrauchenia* (MNHN.F.PAM75) as both have a very proximodistally thin facet (Fig. 3.11f, l). In contrast, *Theosodon* (MLP 12-883), and MLP 57-X-10-157 (Macraucheniinae indet.) have a proximal lunate facet more marked and proximodistally wider (Fig. 3.11h, j).

In terms of relatively size, the proportions of the scaphoid of SGO.PV.21700 are very similar and within the range of other macraucheniids here compared (Table S4 in Appendix C3 Resource 1).

**Lunate** Both the left and right lunate bones (*os lunatum*) of *M. saladensis* are preserved, although the left lunate is damaged and lacks the proximoanterior portion of the bone. The lunate is mediolaterally narrow, anteroposteriorly deep and proximodistally moderately tall (Figs. 3.9b-c, 3.10b-c and 3.12 a-f; Table S4 in Appendix C3 Resource 1). Proximally, the radial facet is anteroposteriorly elongate, being strongly convex in the anterior half and slightly concave in the posterior half (Figs. 3.10b and 3.12c, e-f). Medially, there are two proximodistally thin and anteroposteriorly elongate facets for the scaphoid (Fig. 3.12e). One of these facets is proximally located next to the radial facet, and the other is distally located next to the magnum facet. The outline of both facets is very subtle with poorly delimited margins probably due to some erosion of the element. Laterally, there is a proximodistally broad and slightly concave facet for the cuneiform located on the distal half of the lunate (Fig. 3.12f). When articulated with the cuneiform both elements are in close contact throughout their length, except at their proximoanterior aspect where a substantial gap opens up between them (Fig. 3.10b). On the distal surface of the lunate of *M. saladensis*, there is an anteroposteriorly elongate facet for the magnum. The facet is slightly constricted with a flat articular surface anteriorly and strongly concave posteriorly to form a saddle-shaped articular surface (Fig. 3.12d-e).

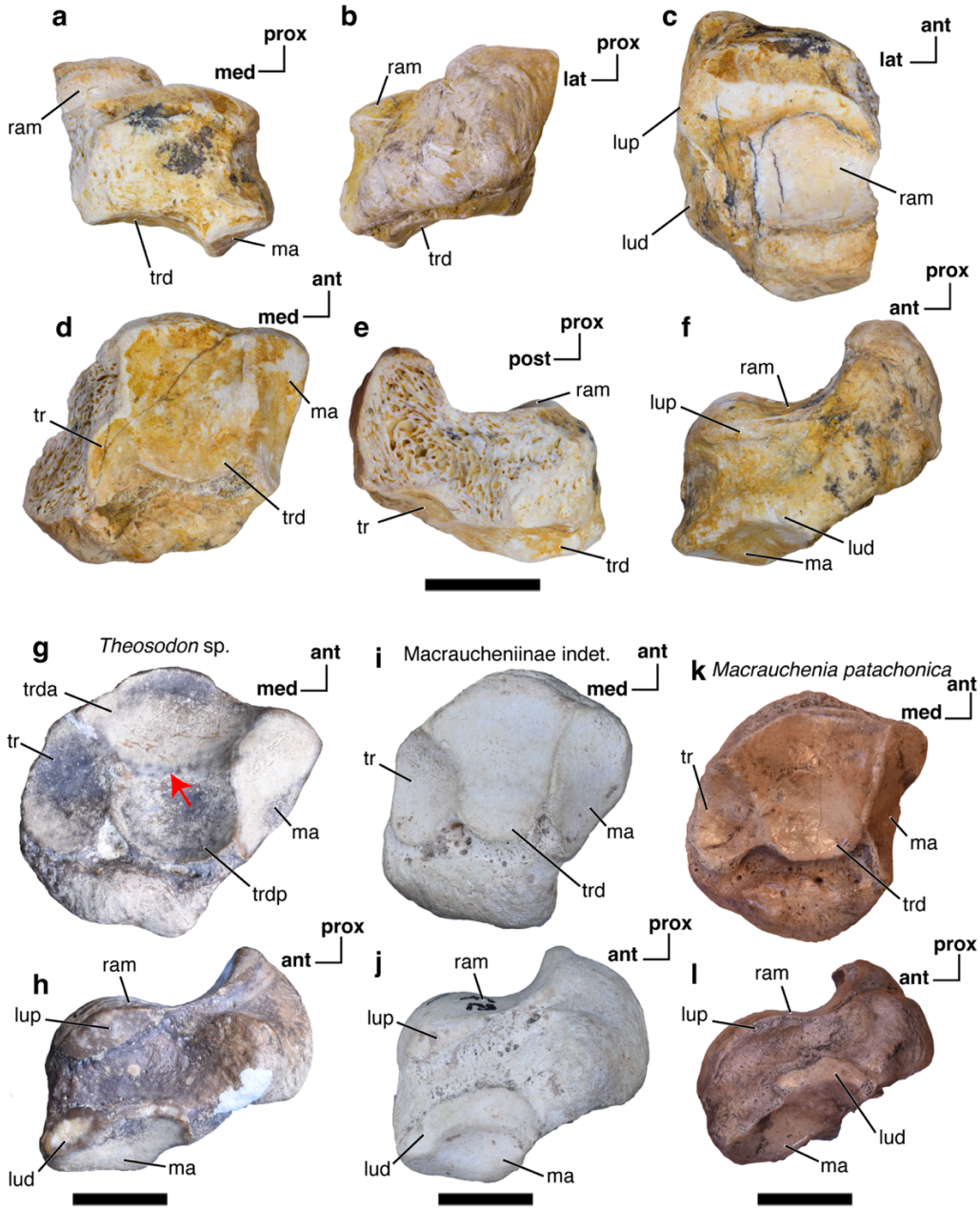



**Figure 3.11** Left scaphoid of *Micrauchenia saladensis* compared with scaphoids of other macraucheniids. **a-f**. scaphoid of *Micrauchenia saladensis* (SGO.PV.21700) in anterior (**a**), posterior (**b**), proximal (**c**), distal (**d**), medial (**e**), and lateral (**f**) views. **g-h**. scaphoid of *Theosodon* sp. (MLP 12-883) in distal (**g**), and lateral (**h**) views. **i-j**. scaphoid of a Pliocene Macraucheniinae indet. (MLP 57-X-10-157) in distal (**i**), and lateral (**j**) views. **k-l**, scaphoid of *Macrauchenia patachonica* in distal (**k**), and lateral (**l**) views. The red arrow indicates the ridge separating the anterior and posterior trapezoid facets. The scaphoids in **g-j** were mirrored to facilize comparisons. Abbreviations: *ant*, anterior; *lat*, lateral; *lud*, lunate distal facet; *lup*, lunate proximal facet; *ma*, magnum facet; *med,* medial; *post*, posterior; *prox*, proximal; *ram*, radius medial facet; *tr*, trapezium facet; *trd*, trapezoid facet; *trda*, trapezoid anterior facet; *trdp*, trapezoid posterior facet. Scale bar equals 1 cm in **a-j**, and 2 cm in **k-l**

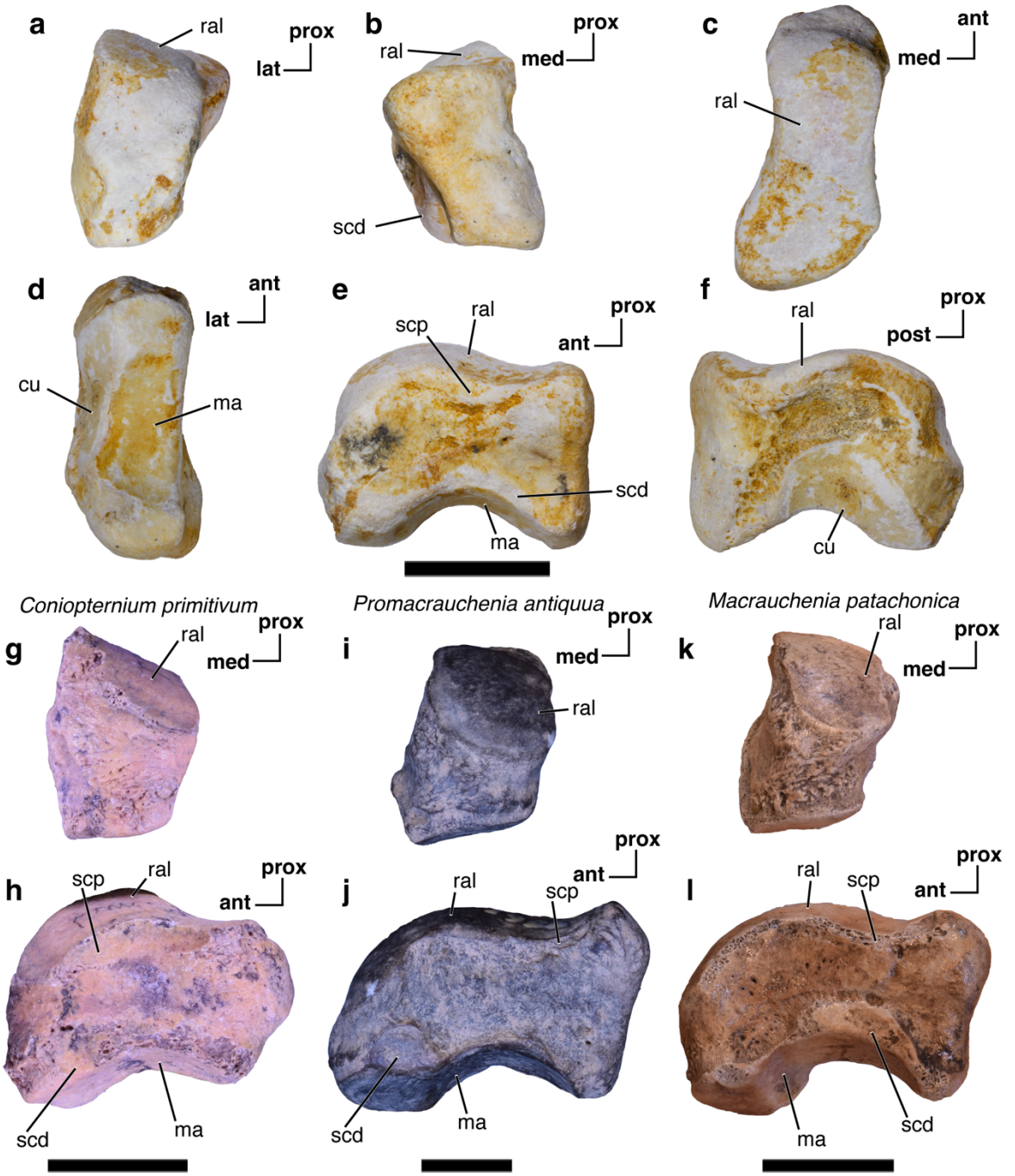



**Figure 3.12** Right lunate of *Micrauchenia saladensis* compared with lunates of other macraucheniids. **a-f**. lunate of *Micrauchenia saladensis* (SGO.PV.21700) in anterior (**a**), posterior (**b**), proximal (**c**), distal (**d**), medial (**e**), and lateral (**f**) views. **g-h**. lunate of *Coniopternium primitivum* (MNHN.F.SAL1051) in anterior (**g**), and medial (**h**) views. **i-j**. lunate of *Promacrauchenia antiquua* (MACN PV 7986) in anterior (**i**), and medial (**j**) views. **k-l**. lunate of *Macrauchenia patachonica* (MNHN.F.PAM75) in anterior (**k**), and medial (**l**) views. The lunates in **g-h** and **k-l** were mirrored to facilize comparisons. Abbreviations: *ant*, anterior; *cu*, cuneiform facet; *lat*, lateral; *ma*, magnum facet; *med,* medial; *prox*, proximal; *ral*, radius lateral facet; *scd*, scaphoid distal facet; *scp*, scaphoid proximal facet. Scale bar equals 1 cm in **a-j**, and 2 cm in **k-l**

Overall, the general configuration of this element is very similar to the lunate of *Coniopternium primitivum* (MNHN.F.SAL1051), *Cramauchenia normalis* (MNHN.F.COL187; MNHN.F.COL191), *Theosodon* (MLP 12-853), *Promacrauchenia*

*antiquua* (MACN PV 7986), and *Macrauchenia* (MLP 12-1660; MLP 12-1424; PIMUZ A/V 5700; MNHN.F.PAM75) and *Xenorhinotherium* (MCL specimens). However, there are some noticeable differences between the lunates of different macraucheniids (Fig. 3.12g-l). For instance, the proximal facet for the scaphoid is very marked and proximo-distally thick in *Coniopternium primitivum* (MNHN.F.SAL1051; Fig. 3.12h) and *Cramauchenia normalis* (MNHN.F.COL187; MNHN.F.COL191), in contrast to *M. saladensis* (SGO.PV.21700) *Promacrauchenia antiquua* (MACN PV 7986) and *Macrauchenia* (MNHN.F.PAM75) in which this facet extremely proximodistally thin (i.e., almost absent; Fig. 3.12e, j, l). A similar condition for this facet can be inferred for *Theosodon* sp. (MLP 12-883) considering the proximodistally thick proximal lunate facet present in its scaphoid (Fig. 3.11h).

In addition, there are some differences in the position of the distal scaphoid facet of the lunate among macraucheniids. In *Coniopternium* (MNHN.F.SAL1051), *Cramauchenia normalis* (MNHN.F.COL187; MNHN.F.COL191), and *Promacrauchenia antiquua* (MACN PV 7986) the distal scaphoid facet is located in the anterior margin being proximodistally thick (Fig. 3.12h, j), whereas in *Macrauchenia* (MNHN.F.PAM75) this is located posteriorly close to the posterior margin (Fig. 3.12l). Considering the position of the distal facet for the lunate in the scaphoid of *Theosodon* sp. (MLP 12-883; Fig 3.11h), we can infer that its lunate is similar to the three formers in the position of this facet. The proximodistally thin and anteroposteriorly elongate facet for the scaphoid in the lunate of *M. saladensis* (SGO.PV.217000) is different to both previous conditions (Fig. 3.12e). Considering its overall shape, the lunate of *M. saladensis* (SGO.PV.217000) is more similar to the lunate of *Macrauchenia* (MNHN.F.PAM75), particularly in the marked lateral curvature of their posterior end (Fig. 3.12a, k).

In terms of proportions, the lunate of *M. saladensis* is similar to *Promacrauchenia antiquua* (MACN PV 7986), but somewhat mediolaterally wider than the lunate in *Macrauchenia* (MNHN.F.PAM75) and *Xenorhinotherium* (MCL specimens), with a ratio between the maximum anteroposterior length and the maximum mediolateral width (MAPL/MMLW) of ~1.9 in contrast to *Xenorhinotherium* and *Macrauchenia* which have a consistently a greater ratio (MAPL/MMLW > 2.2; Table S4 in Appendix C3 Resource 1). In contrast, *Coniopternium* (MNHN.F.SAL1051 is somewhat mediolaterally wider than the lunate in *M. saladensis*, having a MAPL/MMLW of 1.75.

**Cuneiform** The cuneiform (*os triquetrum*) of *M. saladensis* is large and proximodistally elongate in comparison to other carpal bones (Figs. 3.9b-c, 3.10b-c and 3.13a-f). On the

proximal surface of the cuneiform there is an anteroposteriorly narrow and strongly convex articular facet for the ulna (Figs. 3.10b and 3.13a-c, e-f). On the posterior surface there is palmar tuberosity which has an enlarged pisiform facet on the proximal surface (Fig. 3.13b-c, e-f). The ulnar and pisiform facets are not well delimited from one another. On the distal surface of the cuneiform there is a wide concave facet for the unciform (Figs. 3.10c and 3.13d-f). On the medial surface, there are two anteroposteriorly elongate facets for the lunate and magnum (Fig. 3.13e). The facet for the lunate is positioned more proximally and oriented medially. The facet for the magnum is located distally and oriented mediodistally to form a trapezoid profile. In this regard, the cuneiform of *M. saladensis* (SGO.PV.21700) is more similar to other macraucheniines as *Promacrauchenia antiquua* (MACN PV 7986), and *Macrauchenia* (MNHN.F.PAM75; Fig. 3.13j, l), in contrast to *Cramauchenia normalis* (MNHN.F.COL186) and *Theosodon* sp. (MLP 12-877; MLP 12-850) in which the articular surface for the magnum is oriented medially (Fig. 3.13h). In addition, *Cramauchenia normalis* (MNHN.F.COL186) and *Theosodon* sp. (MLP 12-877; MLP 12-850) have an anteroposterior elongate ridge dividing the pisiform facet of the cuneiform (Fig. 3.13g) in contrast to the smooth surface seen in the pisiform facet of macraucheniines (Fig. 3.13c, i, k).

In terms of relative size, the cuneiform of *M. saladensis* is within the variation seen in other macraucheniids (Table S4 in Appendix C3 Resource 1).

**Pisiform** The pisiform of *M. saladensis* (*os piciforme*) is robust and anteroposteriorly elongate in comparison to the other carpal elements (Fig. 3.9c, 3.10b-c and 3.14a-f; Table S4 in Appendix C3 Resource 1). Anteriorly, on the proximal half of the bone, there is a crescent-shaped facet for the ulna, and on the distal half, a larger and elongate facet for the cuneiform (Figs. 3.10b and 3.14a, c-f). The pisiform is slightly mediolaterally constricted around the mid-point of its anteroposterior axis. The anterior end is proximodistally compressed in comparison with the posterior end which is strongly proximodistally expanded (Fig. 3.14e-f).

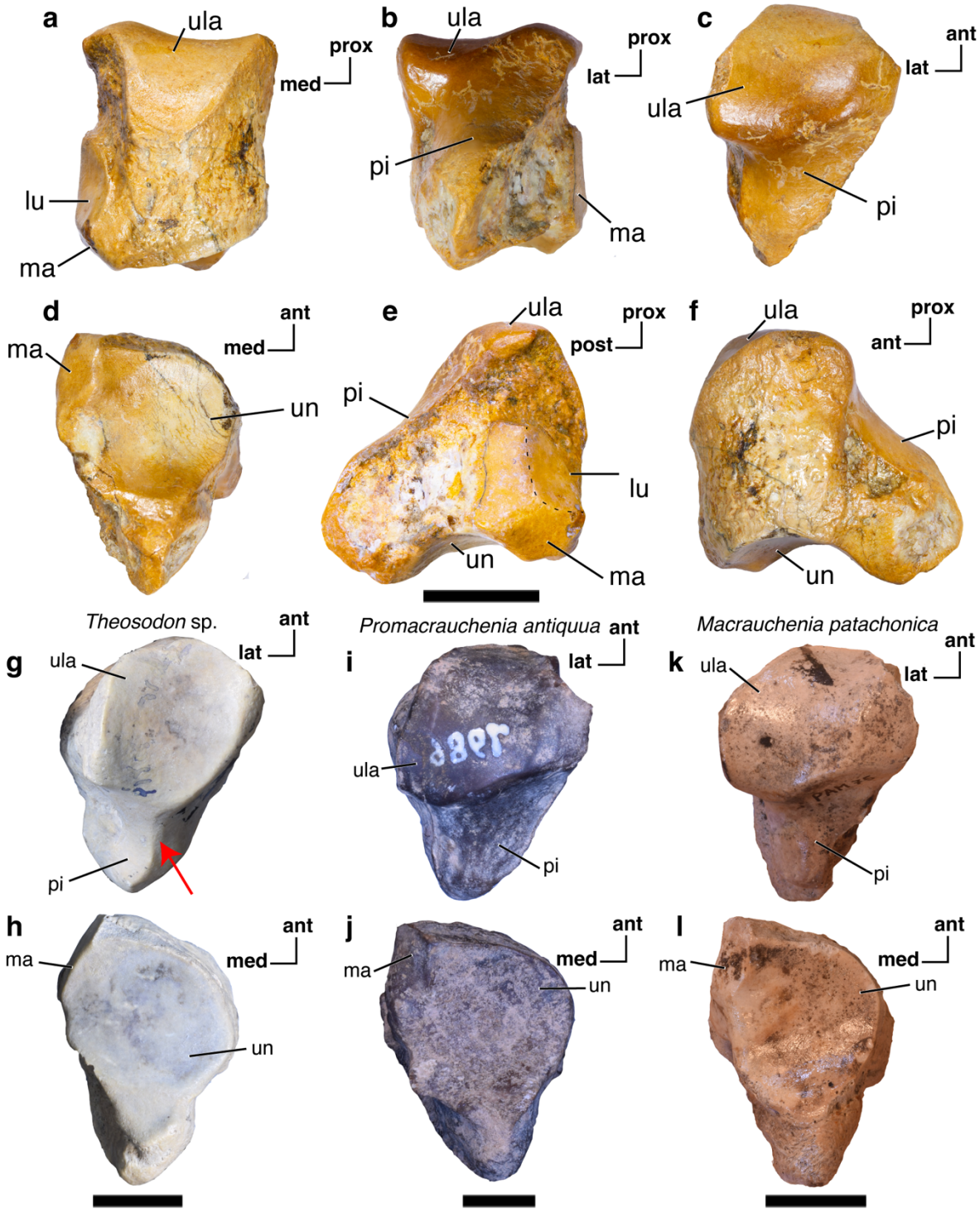



**Figure 3.13** Left cuneiform of *Micrauchenia saladensis* compared with cuneiforms of other macraucheniids. **a-f**. cuneiform of *Micrauchenia saladensis* (SGO.PV.21700) in anterior (**a**), posterior (**b**), proximal (**c**), distal (**d**), medial (**e**), and lateral (**f**) views. **g-h**. cuneiform of *Theosodon* sp. (MLP 12-877) in proximal (**g**), and distal (**h**) views. **i-j**. cuneiform of *Promacrauchenia antiquua* (MACN PV 7986) in proximal (**i**), and distal (**j**) views. **k-l**. cuneiform of *Macrauchenia patachonica* (MNHN.F.PAM75) in proximal (**k**), and distal (**l**) views. The cuneiform in **g-h** was mirrored to facilize comparisons. Black dashed lines indicate the limit between two facets. The red arrow indicates an anteroposterior elongate ridge dividing the pisiform facet in *Theosodon* sp.. Abbreviations: *ant*, anterior; *lat*, lateral; *lu*, lunate facet; *ma*, magnum facet; *med,* medial; *pi*, pisiform facet; *post*, posterior; *prox*, proximal; *ula*, ulnar anterior facet; *un*, unciform facet. Scale bar equals 1 cm in **a-j**, and 2 cm in **k-l**

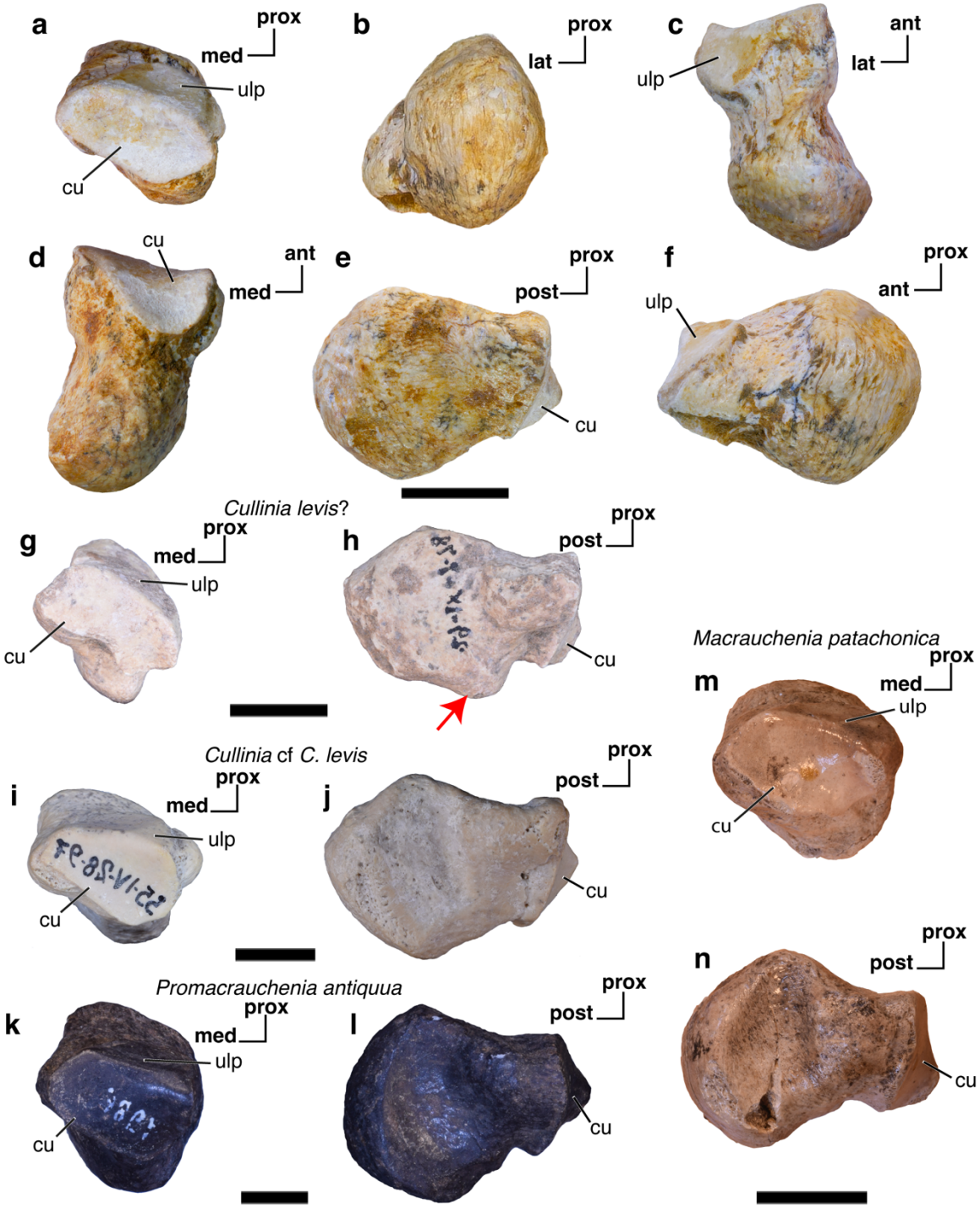



**Figure 3.14** Left pisiform of *Micrauchenia saladensis* compared with pisiforms of other macraucheniids. **a-f**. pisiform of *Micrauchenia saladensis* (SGO.PV.21700) in anterior (**a**), posterior (**b**), proximal (**c**), distal (**d**), medial (**e**), and lateral (**f**) views. **g-h**. pisiform of *Cullinia levis*? (MLP 29-IX-1-78; holotype) in anterior (**g**), and medial (**h**) views. **i-j**. pisiform of *Cullinia* cf *C. levis* (MLP 55-IV-28-97) in anterior (**i**), and medial (**j**) views. **k-l**. pisiform of *Promacrauchenia antiquua* (MACN PV 7986) in anterior (**k**), and medial (**l**) views. **m-n**. pisiform of *Macrauchenia patachonica* (MNHN.F.PAM75) in anterior (**m**), and medial (**n**) views. The red arrow is pointing to the distal swelling of the pisiform of *Cullinia levis*? (MLP 29-IX-1-78; holotype), not seen in other macraucheniines. The pisiforms in **g-l** were mirrored to facilize comparisons. Abbreviations: *ant*, anterior; *cu*, cuneiform facet; *lat*, lateral; *med*, medial; *post*, posterior; *prox*, proximal; *ulp*, ulnar posterior facet. Scale bar equals 1 cm in **a-l**, and 2 cm in **m-n**

Overall the pisiform of *M. saladensis* is very similar in shape to the pisiform of *Theosodon* (YPM VPPU 015164), *Cullinia* cf *C. levis* (MLP 55-IV-28-97), *Promacrauchenia antiquua* (MACN PV 7986), *Xenorhinotherium* (MCL specimens), and *Macrauchenia* (PIMUZ A/V 5700; MNHN.F.PAM75; Fig. 3.14a-f, i-n). The posterior expansion of the pisiform observed in *M. saladensis* is present in macraucheniines (i.e., *Promacrauchenia antiquua*, *Macrauchenia*, and *Xenorhinotherium*) but not *Theosodon*. However, even though the pisiform associate to the holotype of *Cullinia levis* presents a posterior expansion of the pisiform (MLP 29-IX-1-78; Fig. 3.14g-h), this element presents a swelling distally and anterior articular facets for the ulna and the cuneiform that differ noticeably from other macraucheniines including the pisiform of *Cullinia* cf *C. levis* (MLP 55-IV-28-97; Fig. 3.14i-j), which comes from the same site as the holotype (i.e., Arroyo Chasicó, Buenos Aires, Argentina). Considering these differences and also considerable difference in size between both specimens of *Cullinia*, it is possible that the pisiform associated to the holotype of *Cullina levis* (MLP 29-IX-1-78) belongs to a different taxon.

When considering relative proportions, the pisiform of *M. saladensis* has a relatively more proximodistally expanded posterior end than other macraucheniids (MMLW/Maximum proximodistal thickness [MPDT] = 0.77 versus MMLW/MPDT ≥ 0.82; Table S4 in Appendix C3 Resource 1).

**Magnum** The magnum of *M. saladensis* (*os capitatum*) articulates with scaphoid, lunate and cuneiform proximally, the trapezoid medially, the unciform laterally and metacarpals II and III distally (Figs. 3.9b-c, 3.10c, and 3.15a-f). The scaphoid facet is robust, being anteroposteriorly elongate and mediolaterally narrow (Fig. 3.15a-c, e). The posterior surface of the magnum is bulbous with a proximomedially oriented convexity that articulates, in part, with the mediodistal portion of the scaphoid. If our hypothesis about the fusion of the centrale with the scaphoid in *M. saladensis* (and other macraucheniids) is correct, this facet would have originally articulated with the centrale. The lunate facet has a similar general shape to the scaphoid facet, but it is slightly larger and its posterior portion is even more convex where it articulates with the proximal-most part of the posterior convexity of the magnum (Fig. 3.15a-c, f). On the lateral surface of the magnum, there are two articular facets for the cuneiform proximally and the unciform distally (Fig. 3.15f). The facet for the cuneiform is mostly concave. The facet for the unciform is strongly convex anteriorly and flat posteriorly. Both facets are oriented proximolaterally.

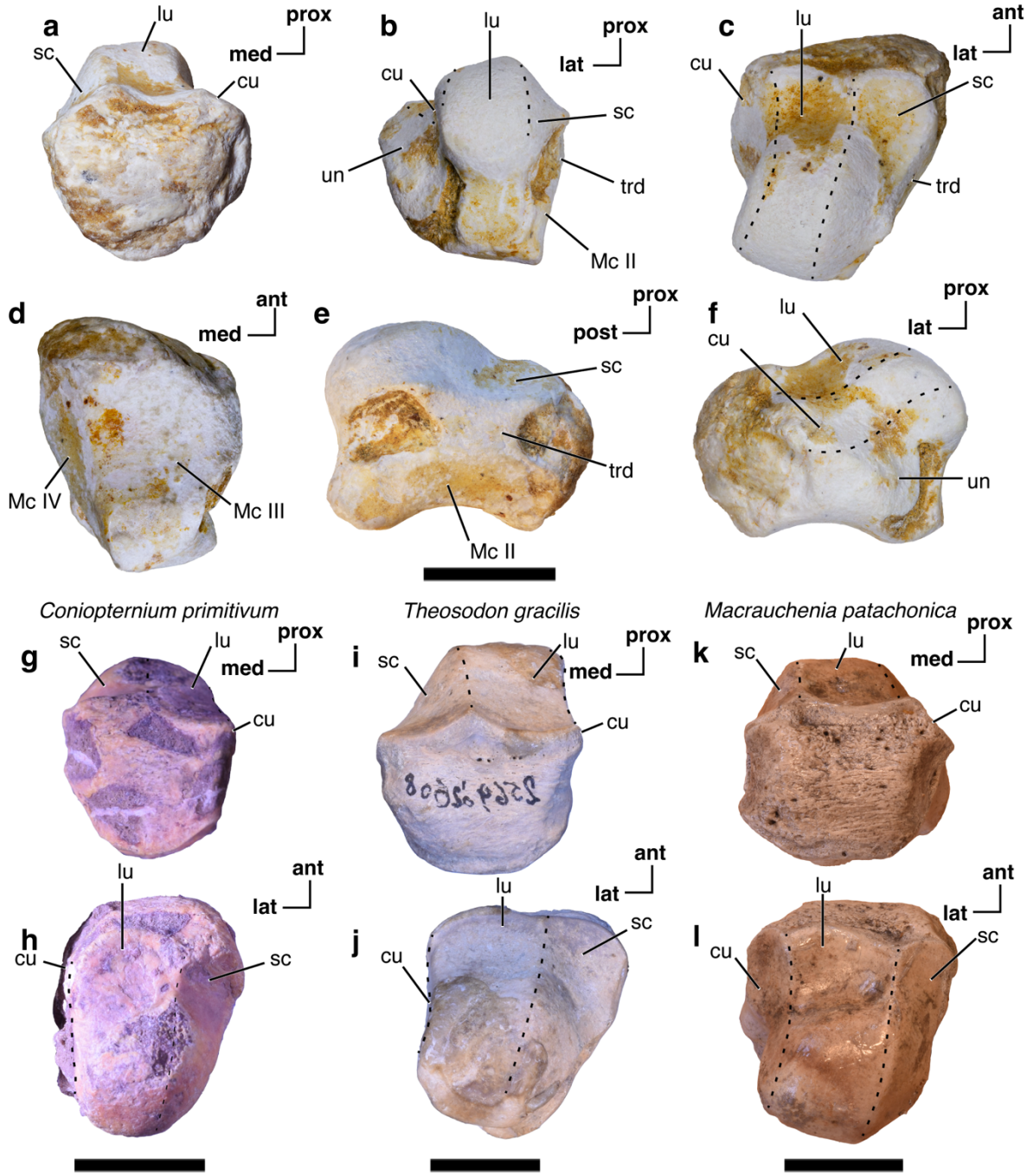



**Figure 3.15** Left magnum of *Micrauchenia saladensis* compared with magnums of other macraucheniids. **a-f**. magnum of *Micrauchenia saladensis* (SGO.PV.21700) in anterior (**a**), posterior (**b**), proximal (**c**), distal (**d**), medial (**e**), and lateral (**f**) views. **g-h**. magnum of *Coniopternium primitivum* (MNHN.F.SAL1050) in anterior (**g**), and proximal (**h**) views. **i-j**. magnum of *Theosodon gracilis* (MACN A 2569-2608) in anterior (**i**), and proximal (**j**) views. **k-l**. magnum of *Macrauchenia patachonica* (MNHN.F.PAM75) in anterior (**k**), and proximal (**l**) views. Black dashed lines indicate the limit between two facets. The magnum in **i-j** were mirrored to facilize comparisons. Abbreviations: *ant*, anterior; *cu*, cuneiform facet; *lat*, lateral; *lu*, lunate facet; *Mc*, metacarpal; *med*, medial; *post*, posterior; *prox*, proximal; *sc*, scaphoid facet; *trd*, trapezoid facet; *un*, unciform facet. Scale bar equals 1 cm in **a-j**, and 2 cm in **k-l**

On the distal surface of the magnum of *M. saladensis*, there is a wide, concave facet for Mc III (Figs. 3.10c and 3.15d). Medially adjacent to the facet for Mc III there is an

anteroposteriorly elongate and concave facet for the Mc II. The facet for Mc II is somewhat medially oriented and more proximally located than the facet for Mc III. Next to the Mc II facet, separated by a ridge, there is a medially oriented facet for the trapezoid which is anteroposteriorly narrow (Fig. 3.15e).

The magnum of *M. saladensis* is most similar to *Macrauchenia* (MNHN.F.PAM75) in that the cuneiform and unciform facets are oriented proximolaterally and present concavities/convexities (Fig. 3.15a-c, k-l) whereas in *Coniopternium primitivum* (MNHN.F.SAL1050), *Cramauchenia normalis* (MNHN.F.COL192), *Theosodon garretorum* (YPM VPPU 015164 [Scott 1910], *Theosodon* sp. (MLP 12-850) and *Theosodon gracilis* (MACN A 2569-2608) these facets face laterally with no proximal tilt so that the cuneiform and unciform do not overlay the magnum, being instead mostly flat facets (Fig. 3.15g-j). A similar magnum configuration as *M. saladensis* and *Macrauchenia* can be inferred for *Promacrauchenia antiquua* (MACN PV 7986), considering the mediodistal orientation of the facet for the magnum in its cuneiform (Fig. 3.13j). When comparing maximum width, length and depth ratios, the magnum of *M. saladensis* is very similar to other macraucheniids (Table S4 in Appendix C3 Resource 1).

**Unciform** The unciform of *M. saladensis* is proximodistally elongate and mediolaterally wide with a marked palmar process on the medial half of the posterior surface (Figs. 3.9b-c and 3.16a-f; Table S4 in Appendix C3 Resource 1). Proximally, there is a convex facet for the cuneiform which is subequal in anteroposterior and mediolateral dimensions (Fig. 3.16a-c, e-f). On the proximal half of the medial surface of the unciform there is the facet for the magnum, which is strongly concave anteriorly and flat posteriorly (Fig. 3.16e). A fragment of this posterior surface was not preserved. On the distal half of the medial surface of the unciform there is smaller and slightly concave facet for the Mc III. Both facets are oriented medially. Posterolaterally, adjacent to the palmar process, there is a small, shallowly concave articular facet a small that was likely for a vestigial Mc V (Fig. 3.16b, f). Among macraucheniids, a vestigial Mc V has been only described for *Xenorhinotherium* (Lessa 1992: Pl. XXIXa) to our knowledge, however, its presence can be inferred in *M. saladensis* given the presence of this well demarcated articular facet in the unciform as in *Xenorhinotherium*. A fifth metacarpal has been inferred in other macraucheniids including *Theosodon* and *Macrauchenia* based on the presence of a similar small facet on the posterior surface of Mc IV (Ameghino 1894*b*; Scott 1910; Sefve 1925). On the distal surface on the unciform of *M. saladensis*, there is a large and

almost flat facet for the Mc IV, which it is markedly mediolaterally narrower in its posterior half relative to the anterior half (Fig. 3.16d).

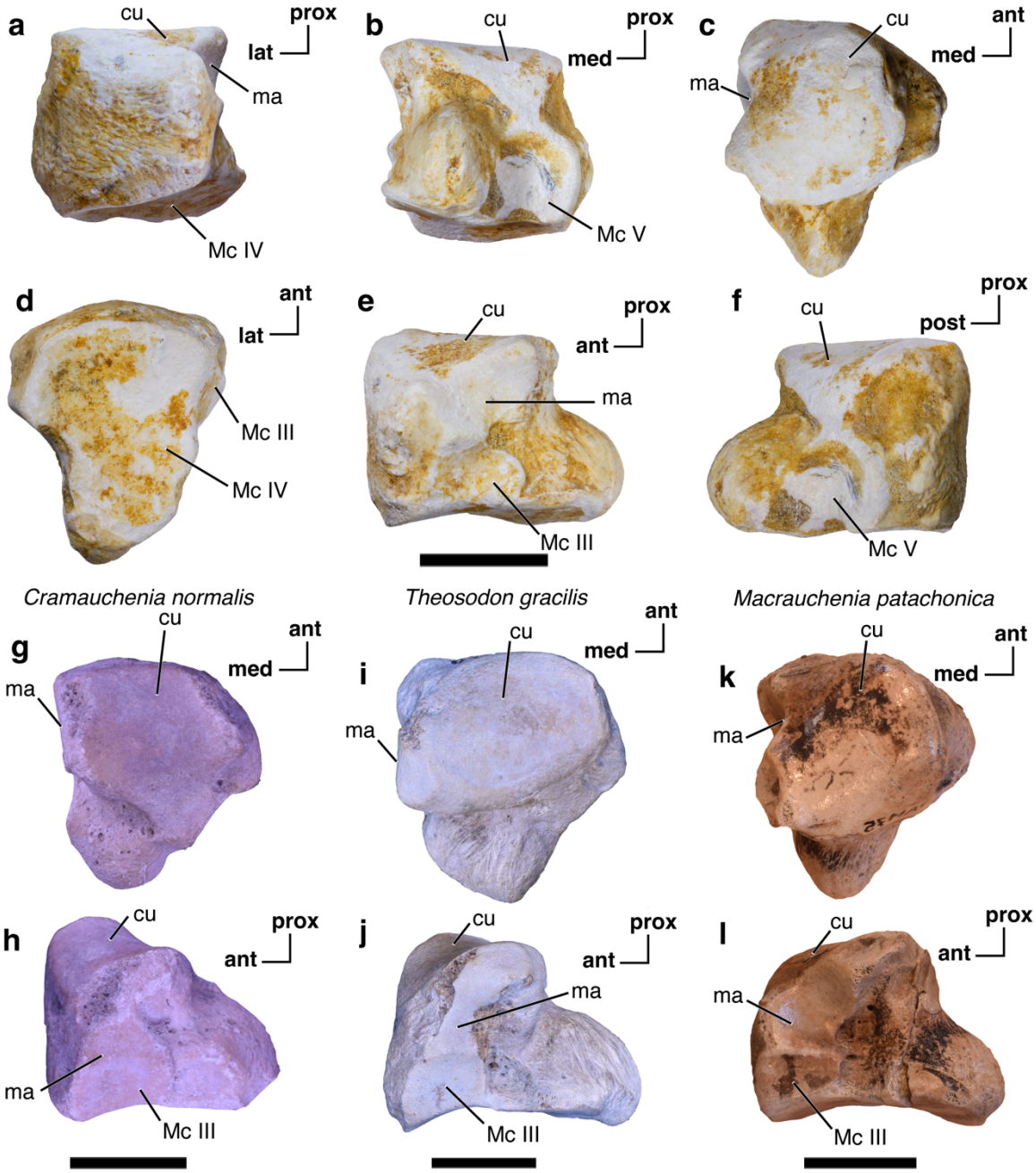



**Figure 3.16** Right unciform of *Micrauchenia saladensis* compared with unciforms of other macraucheniids. **a-f**. unciform of *Micrauchenia saladensis* (SGO.PV.21700) in anterior (**a**), posterior (**b**), proximal (**c**), distal (**d**), medial (**e**), and lateral (**f**) views. **g-h**. unciform of *Cramauchenia normalis* (MNHN.F.COL183) in proximal (**g**), and medial (**h**) views. **i-j**. unciform of *Theosodon gracilis* (MACN A 2569-2608) in proximal (**i**), and medial (**j**) views. **k-l**. unciform of *Macrauchenia patachonica* (MNHN.F.PAM75) in proximal (**k**), and medial (**l**) views. The unciform in **i-l** were mirrored to facilize comparisons. Abbreviations: *ant*, anterior; *cu*, cuneiform facet; *lat*, lateral; *ma*, magnum facet; *Mc*, metacarpal; *med*, medial; *post*, posterior; *prox*, proximal. Scale bar equals 1 cm in **a-j**, and 2 cm in **k-l**

Overall, the unciform of *M. saladensis* is very similar to the unciform of *Cramauchenia normalis* (MNHN.F.COL182; MNHN.F.COL183), *Theosodon* sp. (MLP specimens),

*Thesodon gracilis* (MACN A 2569-2608), *Macrauchenia* (MNHN.F.PAM75), and *Xenorhinotherium* (MCL specimens). However, in overall shape, *M. saladensis* is more similar to *Macrauchenia* (MNHN.F.PAM75; Fig. 3.16a-f, k-l). As *M. saladensis*, *Macrauchenia* has a facet for the magnum strongly convex anteriorly that overlays the unciform. In *Cramauchenia* and *Theosodon* facet for the magnum in the unciform is mostly flat and has a completely medial articulation with the magnum (Fig. 3.16g-h). Nevertheless, the facet for the magnum in the unciform of *Theosodon* is more anteroposteroirly elongate than in the unciform of *Cramauchenia*, being in this regard more similar to the unciform of macraucheniines like *M. saladensis* and *Macrauchenia*.

In terms of proportion the unciform of *M. saladensis* is very similar to other macraucheniids when comparing maximum width, length and depth ratios (Table S4 in Appendix C3 Resource 1).

### Metacarpals

Only three metacarpals are preserved in *Micrauchenia saladensis* (SGO.PV.21700), a right Mc II, a fragmentary left Mc III with part of the proximal epiphysis and diaphysis missing, and a fragmentary Mc II or Mc IV preserving only part of the distal epiphysis (Figs. 3.9b-c and 3.17a-i). In general, the metacarpals of *M. saladensis* are proximodistally elongated and mediolaterally narrow, overall, they are very similar in shape and proportion to the metacarpals known for other macraucheniids including *Theosodon* and *Macrauchenia* (Table S5 in Appendix C3 Resource 1). In terms of total length, the metacarpals of *M. saladensis* are the smallest in our sample, being slightly smaller than *Cramauchenia normalis* (~8%), and considerably smaller than *Theosodon* spp. (~15%), *Promacrauchenia antiquua* (~63%), *Promacrauchenia* sp. (Anaya and MacFadden 1995; ~37%), *Macrauchenia patachonica* (~83%), and *Xenorhinotherium bahiense* (~85%; Table S5 in Appendix C3 Resource 1).

**Metacarpal II** The second metacarpal of *M. saladensis* II is proximodistally elongate and mediolaterally narrow, being curved medially at its distal end (Figs. 3.9b-c and 3.17a-b, e-f). The proximal end is eroded as such the articular facets for the trapezoid, trapezium, magnum, and Mc III are not well preserved. However, proximally, there is part of the facet for the trapezoid, and laterally, a very eroded proximolaterally oriented facet for the magnum and distal to it, an eroded concave crescentic facet for the Mc III and a concavity that extends distally to receive Mc III (Fig. 3.17b, e). On the lateral side of the proximal end of Mc II the facet for the trapezium is not well demarcated because of its poor preservation (Fig. 3.17a, e).

These facets are very similar to *Macrauchenia patachonica* (MNHN.F.PAM75; Fig. 3.17j-k, n-o) and to earlier macraucheniids like *Cramauchenia normalis* (MNHN.F.DES305) and *Thesodon gracilis* (MACN A 2569-2608). The diaphysis of Mc II is robust when compared with Mc III. Medially, the diaphysis of Mc II it is slightly concave along its proximal half (Fig. 3.9b-c). The distal end of Mc II is asymmetric, whereby the medial portion of median keel is moderately mediolaterally wider than the lateral portion. The preservation of the distal end is in general good although a posterior fragment of the head is missing. On the medial and lateral sides of the distal end of Mc II there are well demarcated depressions for the attachment of the metacarpophalangeal collateral ligaments (Sisson 1914; Evans & Lahunta 2012; Denoix 2019). The lateral depression is wider and deeper than the medial one (Fig. 3.17a-b). These depressions are also present on the Mc II of *Macrauchenia patachonica* (Fig. 3.17j-k) showing the same morphology. The median keel is well-defined anteriorly and extends on to the posterior surface of the distal epiphysis (Figs. 3.9c and 3.17f). The posterior surface of the distal end of Mc II is not well preserved, however, it appears likely that median keel would have continued considerably to the posterior surface as observed in other macraucheniids allowing an extensive dorsopalmar movement of the toe (Owen 1838). This inference is further supported by the presence of a strong median keel on a poorly preserved fragment of a distal metacarpal. Considering the asymmetrical morphology of the bone and the development of the median keel it is likely Mc IV or Mc II (Fig. 3.17i). Overall, the general structure of Mc II in *M. saladensis* is very similar to other macraucheniids as *Cramauchenia normalis* (MNHN.F.DES305), *Thesodon gracilis* (MACN A 2569-2608) and *Macrauchenia patachonica* (MNHN.F.PAM75).

Comparing the relative length of Mc II using the distal mediolateral articular width (ratio DAW/TL) *M. saladensis* has a value of 0.18, which it is within the range observed in our sample of macraucheniids (0.13 – 0.23), being proportionally similar to *Cramauchenia normalis* (MNHN.F.DES305), *Theosodon garretorum* (YPM VPPU 015164) and a couple of specimens of *Xenorhinotherium bahiense* (MCL 3504 and MCL 3513; Table S5 in Appendix C3 Resource 1).

**Metacarpal III** The Mc III of *M. saladensis* is preserved in two parts: a fragment of the lateral side of the proximal end with the medial portion completely missing, and most of the shaft with a complete distal end (Figs. 3.9b-c and 3.17c-d, g-h). Even though the two fragments do not fit due to erosion between the contacting surfaces, the size and colour allow us to confidently assign them to the same element. The Mc III of *M. saladensis* is more elongate,

slender and straight than Mc II, being at least 17% longer (Table S5 in Appendix C3 Resource 1). The lateral side of the proximal end is worn but preserves two small articular facets for Mc IV, one closer to the anterior border and slightly concave and the other closer to the posterior border which is flat (Fig. 3.17d). Proximally, there is a convex facet for the magnum, and lateral to this surface and closer to the dorsal aspect, there is an oblique and extremely eroded facet for the unciform (Fig. 3.17d, g).

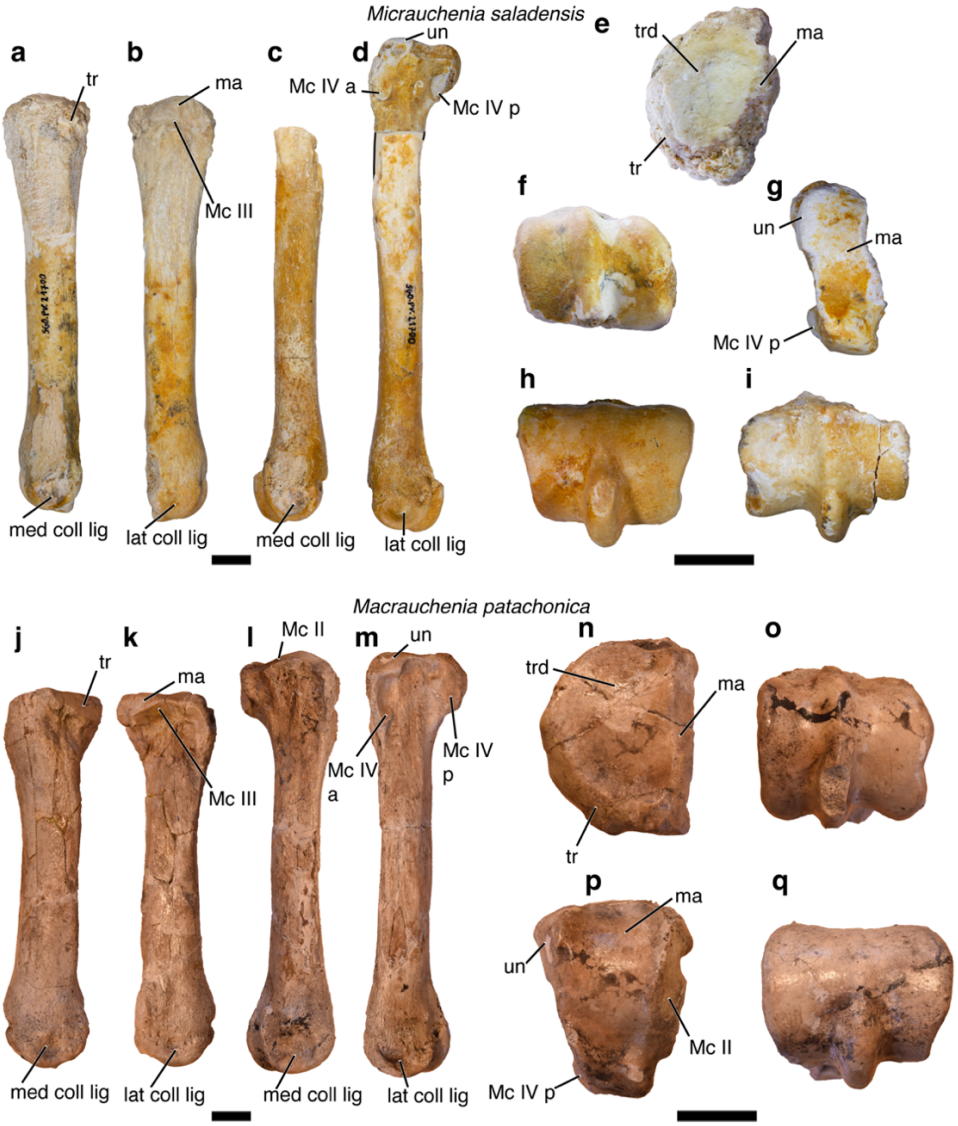



**Figure 3.17** Metacarpals of *Micrauchenia saladensis* (SGO.PV.21700) and *Macrauchenia patachonica* (MNHN.F.PAM75). **a-b, e-f**. right Mc II of *Micrauchenia saladensis* in medial (**a**), lateral (**b**), proximal (**e**), and distal (**f**) views. **c-d, g-h**. left Mc III of *Micrauchenia saladensis* in medial (**c**), lateral (**d**), proximal (**g**), and distal (**h**) views. **i.** Mc II or Mc IV? of *Micrauchenia saladensis* in distal view. **j-k, n-o.** left Mc II of *Macrauchenia patachonica* (mirrored) in medial (**j**), lateral (**k**), proximal (**n**), and distal (**o**) views. **l-m, p-q**. left Mc III of *Macrauchenia patachonica* in medial (**l**), lateral (**m**), proximal (**p**), and distal (**q**) views. Abbreviations: *a*, anterior facet; *coll lig*, metacarpophalangeal collateral ligaments; *lat*, lateral; *ma*, magnum facet; *Mc*, metacarpal; *med*, medial; *p*, posterior facet; *tr*, trapezium facet; *trd*, trapezoid facet; *un*, unciform facet. Scale bar equals 1 cm in **a-i**, and 2 cm in **j-q**

The Mc III diaphysis of *M. saladensis* is mediolaterally narrower than the Mc II, however, its distal articular end is considerably wider than the Mc II (14% wider; Table S5 in Appendix C3 Resource 1). In terms of proximodistal length of the head, Mc III only expands at the distal most end, consequently Mc II has a moderately longer head than Mc III. In addition, the head of Mc III is symmetrical (Figs. 3.9b-c and 3.17h), which is markedly different from the asymmetric head of Mc II (Figs. 3.9b-c and 3.17f). Furthermore, in contrast to Mc II, the Mc III median keel is very weak on the anterior surface of the bone but becomes stronger as it approaches the posterior side (Figs. 3.9b-c and 3.17c-d, h). On the posterior side it is strong and proximally elongate. A distinctively weak Mc III anterior medial keel has been previously observed in other macraucheniids including *Macrauchenia* and *Theosodon* (Gervais 1855; Scott 1910). As such the distal end of Mc III is easily distinguished from Mc II and Mc IV. It is important to note here that the strong anterior aspect of the median keel illustrated by Scott (1910: Pl. XIX fig. 6) for Mc III was probably mistakenly exaggerated as observations of the actual element (YPM VPPU 015164) show a very weak anterior keel (personal observation, H.P.P.), which is in agreement with Scott's actual description of this element and also with other specimens of *Theosodon* here examined (e.g., MACN A 2569-2608, MLP 12-850). Interestingly, the lack of a strong anterior component of the keel in Mc III, has also been observed in the Mt III of the late Oligocene macraucheniids (cf. ?*Coniopternium* spp.) from Salla, Bolivia (Shockey 1999).

On the medial and lateral sides of the head of Mc III, there are clear depressions for the attachment of the metacarpophalangeal collateral ligaments as inferred for Mc II (Sisson 1914; Evans & Lahunta 2012; Denoix 2019), although for this element the lateral and medial depressions are equally strongly pronounced. Overall, in terms of shape and general features, the Mc III of *M. saladensis* is very similar to other macraucheniids like *Theosodon gracilis*, (MACN A 2569-2608), *Theosodon* sp. (MLP 12-850), *Promacrauchenia antiquua* (MACN PV 7986) and *Macrauchenia patachonica* (MNHN.F.PAM75; Fig. 3.17l-m, p-q), and consistent with previous descriptions (e.g., Owen 1838; Scott 1910; Sefve 1925; Lessa 1992).

Comparing the relative length of Mc III*, M. saladensis* has a ratio DAW/TL of 0.18, which is within the range observed in our sample of macraucheniids (0.16 – 0.20; Table S5 in Appendix C3 Resource 1).

## Phalanges

*Micrauchenia saladensis* preserves six phalanges, of which there are two proximal, one from right digit II, and one from left digit III, and four intermediate, one from the left digit III and three from the digits II and/or IV (Figs. 3.9b-c, 3.18 and 3.19). The proximal phalanges are clearly distinguished from the intermediate phalanges, as they are considerably longer than the former having an elongated diaphysis (Figs. 3.9b-c and 3.18). Proximally, the proximal phalanges have a dorsopalmar concavo-convex articular surface for the metacarpals, which is interrupted at the ventral midpoint by a marked groove for receiving the medial keel of the associated metacarpal. Distally, the articular surface of the head of the proximal phalange is smooth and saddle-shaped extending dorsally and ventrally, which probably facilitated a range of dorsopalmar movement of the digits as in *Macrauchenia* (Owen 1838). On the lateral and medial sides of the distal end of the proximal phalanges there are well-demarcated depressions for the attachment of interphalangeal collateral ligaments (Sisson 1914; Evans & Lahunta 2012; Denoix 2019).

The intermediate phalanges of *M. saladensis* are short and robust, being around 40% more elongated in their mediolateral width than their proximodistal length (Figs. 3.9b-c and 3.19; Table S6 in Appendix C3 Resource 1). Apart from their length and shape, the main differences between the intermediate phalanges with the proximal phalanges are that the proximal articular surface is more markedly concavo-convex dorsopalmarly and also slightly convex mediolaterally, and there is no median groove on the proximal articular facet. Furthermore, posteriorly, close to the proximal articular surface, the intermediate phalanges have a thickened transverse flexor tuberosity with a well demarked groove that, considering its position, was likely a point of attachment for the sesamoidean ligament (*ligament sesamoideum rectum*) that in *Equus* connects the manus intermediate phalanx with the proximal sesamoid bones (Constantinescu *et al.* 2018; Aurich *et al.* 2020). As with the proximal phalanges, the distal articular surface for the proximal end of the distal phalanges is smooth and saddle-shaped, although more lengthened on the anterior side. Posteriorly, the distal end is smooth and concave where there was likely an articulation with the median or sagittal ridge of a distal sesamoid bone as in *Equus* (Denoix 2019; Aurich *et al.* 2020). In addition, the intermediate phalanges present well-demarcated depressions on the lateral and medial sides of the distal end for the attachment of interphalangeal collateral ligaments (Sisson 1914; Evans & Lahunta 2012; Denoix 2019). These are much more pronounced in digit III, and the side facing digit III of adjacent digits (i.e., the lateral side of digits II and the medial side of digit IV).

In terms of total length, the phalanges of *M. saladensis* are on average of similar size than *Cramauchenia normalis* (less than 2% difference), slightly smaller than *Coniopternium andinum* (~11%), and considerably smaller than *Theosodon* spp. (~18%), *Promacrauchenia antiquua* (~61%), *Promacrauchenia sp.* (Anaya and MacFadden 1995; ~20%), *Scalabrinitherium ferreriai* (20%), *Macrauchenia patachonica* (~87%), *Xenorhinotherium bahiense* (~81%), and *Macraucheniopsis ensenadensis* (106%; Table S6 in Appendix C3 Resource 1).

**Proximal phalanx of manual digit II** The proximal phalanx of digit II is elongate and slender, in particular along the shaft (Figs. 3.9b-c and 3.18a-d; Table S6 in Appendix C3 Resource 1). In terms of preservation, it is highly eroded on the palmar surface and the medial half of the proximal end of the bone is missing. The lateral portion of the proximal articular surface adjacent to the groove is anteroposteriorly elongate and mediolaterally narrow. The preserved part of the proximal articulation is near identical to the same portion in the same digit of *Macrauchenia* (PIMUZ A/V 5700; MNHN.F.PAM75; Fig. 3.18i). The diaphysis is constricted and approximately 30% mediolaterally narrower than the distal end (Fig. 3.9b-c; Table S6 in Appendix C3 Resource 1). Distally, the articular surface for the intermediate phalanx is not well-preserved, the medial portion is missing and the palmar surface is very eroded (Figs. 3.9b-c and 3.18d). On the medial side of the distal end there is a depression for the attachment of one of the interphalangeal collateral ligaments (Fig. 3.18b). Overall, in terms of general structure, the proximal phalanx of digit II in *M. saladensis* is extremely similar to that of *Macrauchenia* (PIMUZ A/V 5700; MNHN.F.PAM75).

Comparing the relative length of the proximal phalanx of digit II using its proximal mediolateral articular width to total length (ratio PAW/TL) and its distal mediolateral articular width to total length (ratio DAW/TL), *M. saladensis* has values of 0.36 for both measures, which are well within the range observed in our sample of macraucheniids (PAW/TL = 0.22 – 0.60; DAW/TL = 0.27 – 0.49; Table S6 in Appendix C3 Resource 1).

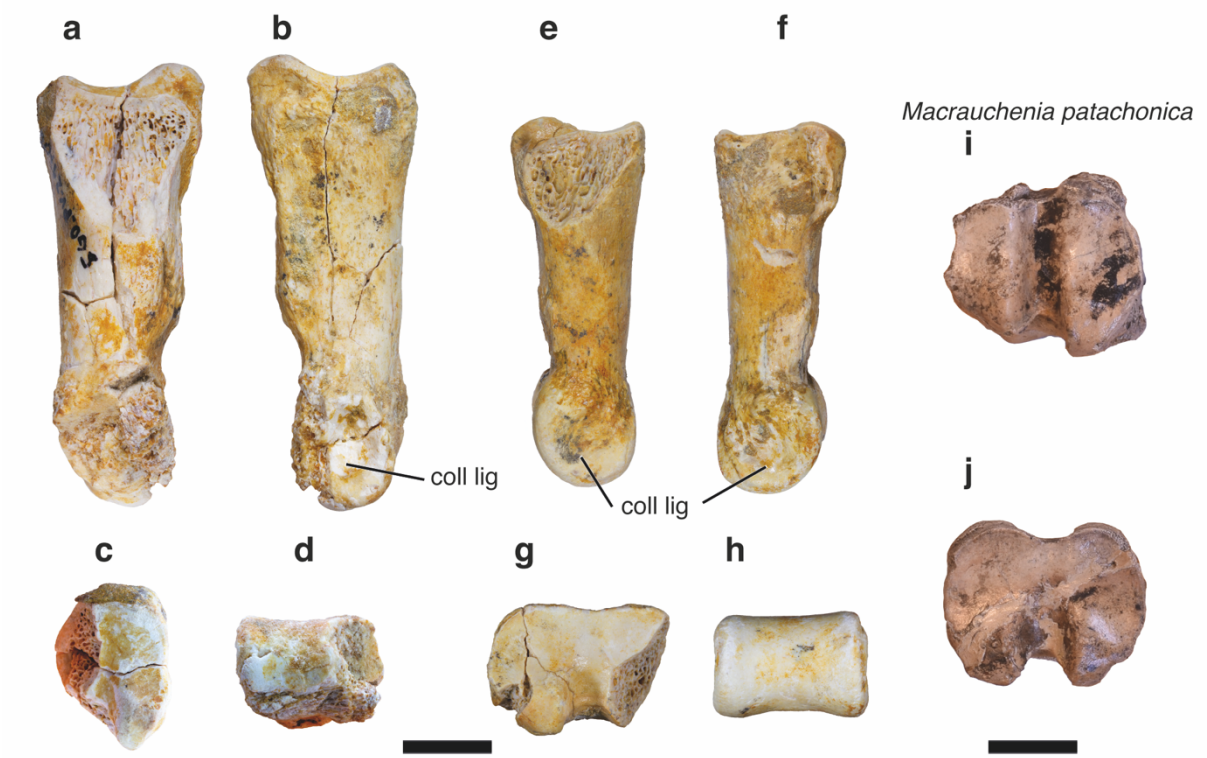



**Figure 3.18** Proximal phalanges of the manus of *Micrauchenia saladensis* (SGO.PV.21700). **a-d**. right proximal phalanx of digit II in medial (**a**), lateral (**b**), proximal (**c**), and distal (**d**) views; **e-h**. left proximal phalanx of digit III in medial (**e**), lateral (**f**), proximal (**g**), and distal (**h**) views. **i**. left proximal phalanx of digit II of *Macrauchenia patachonica* (MNHN.F.PAM75; mirrored) in proximal view. **j**. left proximal phalanx of digit III of *Macrauchenia patachonica* (MNHN.F.PAM75; mirrored) in proximal view. Abbreviation: *coll lig*, interphalangeal collateral ligament. Scale bar equals 1 cm in **a-i**, and 2 cm in **j-k**

**Proximal phalanx of manual digit III** The proximal phalanx of digit III is very similar to the proximal phalange of digit II, but less elongate and more symmetrical (Figs. 3.9b-c and 3.18e-h; Table S6 in Appendix C3 Resource 1). The bone is well preserved and only damaged on the medial part of the head and part of the proximal articular surface for Mc III. Proximally, the concavo-convex articular surface is symmetrical as also observed for *Macrauchenia* (PIMUZ A/V 5700; MNHN.F.PAM75; Figs.3.18g, j). Distally, the distal articular surface for the intermediate phalanx is more anteriorly extended than in the proximal phalanx of digit II (Fig. 3.9b), which is similar to what is observed in *Macrauchenia* (PIMUZ A/V 5700; MNHN.F.PAM75). On the medial and lateral sides of the distal head, there are depressions for the attachment of interphalangeal collateral ligaments (Fig. 3.18e-f).

Comparing the relative length of the proximal phalanx of digit III using the PAW/TL and DAW/TL ratios, *M. saladensis* has values of 0.49 and 0.39 respectively. and falls within the range observed in our sample of macraucheniids (PAW/TL = 0.32 – 0.71; DAW/TL = 0.30 – 0.56; Table S6 in Appendix C3 Resource 1), although *M. saladensis* is more slender than the biggest species *Macrauchenia* (PIMUZ A/V 5700; MNHN.F.PAM75; PAW/TL =0.64 – 0.66;

DAW/TL = 0.48 – 0. 51) and *Xenorhinotherium* (MCL specimens; PAW/TL =0.63 – 0.71; DAW/TL = 0.49 – 0. 56).

**Intermediate phalanges of manual digits II and IV** *M. saladensis* (SGO.PV.21700) preserves three intermediate phalanges (Figs. 3.9b-c and 3.19a-g). The intermediate phalanges for digits II and IV are described together below and they are near identical mirrored copies of one another. It is important to note at this point, that due to the striking morphological similarity between the phalanges of the fore and hind limbs in macraucheniids, and also the similarity between the phalanges of digits II and IV, previous workers have found it difficult to identify specific bones if they are not found in association with their respective metapodials (Scott 1910; Lessa 1992; Schmidt 2013). Therefore, the putative left intermediate phalange of digit IV could potentially be a pedal intermediate phalanx from digit II or IV. However, considering that SGO.PV.21700 does not preserve any unequivocal posterior element we consider this possibility to be unlikely.

The intermediate phalanges of digit II and IV are asymmetrical. The distal ends of are strongly asymmetric, having on the interior side (facing at the digit III) a marked angular process with a deep and concave depression for an interphalangeal collateral ligament attachment (Fig. 3.19c; Sisson 1914; Evans and Lahunta 2012; Denoix 2019). In the exterior surface of the distal end (facing away from digit III), there is subtle concavity for the attachment of an interphalangeal collateral ligament, although not as developed as in the medial side. (Fig. 3.19b). Overall, the general structure of the intermediate phalanges of digit II and IV is very similar to other macraucheniids as *Theosodon* sp. (e.g., MLP 12-757; MLP 12-758) and *Macrauchenia patachonica* (MNHN.F.PAM75; PIMUZ A/V 5700).

Comparing the relative length of the intermediate phalanges for digits II and IV using the PAW/TL and DAW/TL ratios, *M. saladensis* has values of 0.76 and 0.53 respectively and falls within the range observed in our sample of macraucheniids in terms of proximal mediolateral width but narrower in terms of distal mediolateral width (PAW/TL = 0.64 – 0.88; DAW/TL = 0.58 – 0.74; Table S6 in Appendix C3 Resource 1).

**Intermediate phalanx of manual digit III** The intermediate phalanx of digit III is distinguished from the intermediate phalanges of digit II and IV in that it exhibits a strong symmetry along its proximodistal axis (Fig 3.9b-c and 3.19h-l; Table S6 in Appendix C3 Resource 1). The distal end exhibits two marked angular processes each with a small concavity for the attachment of interphalangeal collateral ligaments (Fig. 3.19i-j; Sisson 1914; Evans and

Lahunta 2012; Denoix 2019). Overall, the general structure of the intermediate phalanges of digit III is very similar to other macraucheniids as *Theosodon* sp. (e.g., MLP 12-756) and *Macrauchenia patachonica* (MNHN.F.PAM75; PIMUZ A/V 5700).

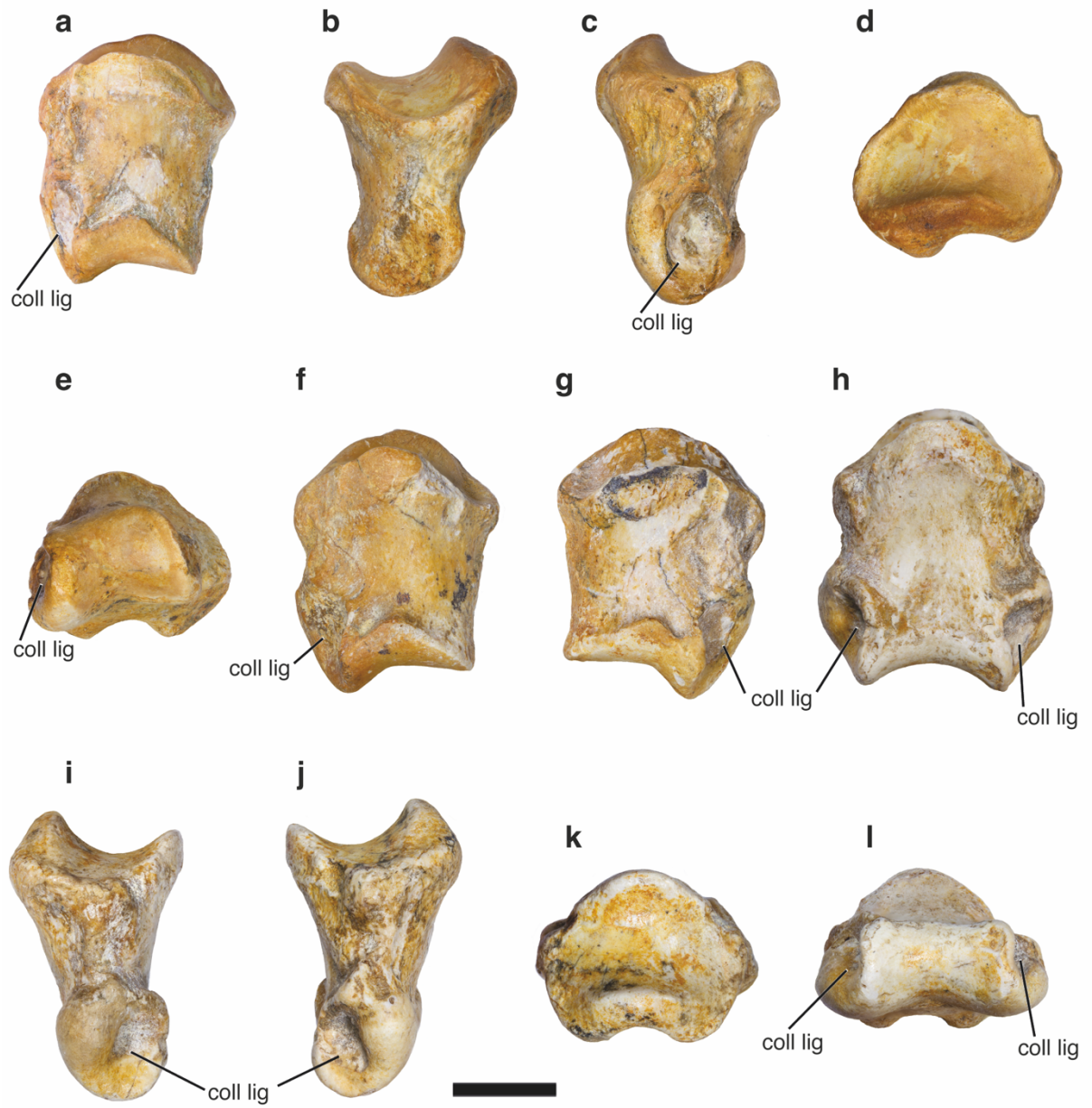



**Figure 3.19** Intermediate phalanges of *Micrauchenia saladensis* (SGO.PV.21700). **a-e**. right intermediate phalanx of digit II in dorsal (**a**), medial (**b**), lateral (**c**), proximal (**d**), and distal (**e**) views. **f**. left intermediate phalanx of digit IV in dorsal view. **g**. left intermediate phalanx of digit II or right intermediate phalanx of digit IV in dorsal view. **h-l**. left intermediate phalanx of digit III in dorsal (**h**), medial (**i**), lateral (**j**), proximal (**k**), and distal (**l**) views. Only the most demarcated depressions for the interphalangeal collateral ligament are pointed. *Abbreviation: coll lig*, interphalangeal collateral ligament. Scale bar equals 1 cm

Comparing the relative length of the intermediate phalanx of digit III using the PAW/TL and DAW/TL ratios, *M. saladensis* has values of 0.64 and 0.49, comparable to the values observed in our sample of macraucheniids (PAW/TL = 0.55 – 0.90; DAW/TL = 0.50 –

0.70; Table S6 in Appendix C3 Resource 1). The biggest species, *Macrauchenia patachonica* (e.g., MNHN.F.TAR813) and *Xenorhinotherium bahiense* (MCL specimens), tend to be in proportion mediolaterally wider than *M. saladensis*, being close to upper limit of both ratio ranges.

## Phylogenetic results

The strict consensus tree from the parsimony analysis recovers the subfamily Macraucheniinae as a monophyletic group in contrast with "cramaucheniines" which are paraphyletic (Fig. 3.20a). However, all the members of Macraucheniinae, including *Micrauchenia saladensis*, are part of an extensive polytomy that obscures assessment of the internal relationships within this group. The Bremer supports values are very low and the Jackknife resampling fails to recover all the nodes (Fig. 3.20a). The majority rule tree shows a much better resolved subfamily Macraucheniinae than the strict consensus tree, with *M. saladensis* nested in a polytomy that includes *Cullinia levis* and *Paranauchenia* spp. plus a clade of *Promacrauchenia calchaquiorum*, *Promacrauchenia antiquua*, *Windhausenia delacroixi*, *Xenorhinotherium bahiense*, *Promacrauchenia* sp. (Anaya & MacFadden 1995), and *Macraucheniopsis ensenadensis* (Fig. 3.20b, node 10). *Promacrauchenia* sp. (Anaya & MacFadden 1995) is part of a polytomy that includes *Macrauchenia patachonica* and *Macraucheniopsis ensenadensis* (Fig. 3.20b, node 16). The two species of *Promacrauchenia* form a monophyletic group in node 13, similar to the two species of *Paranauchenia* in node 11 (Fig. 3.20b). Among "cramaucheniids", *Cramauchenia normalis*, *Coniopternium* spp. and *Llullataruca shockeyi* are grouped in a polytomy (Fig. 3.20b, node 5), as was also recovered in the strict consensus tree (Fig. 3.20a). The effect of removing the wildcard taxon *M. saladensis* a posteriori from the strict consensus resolves the extensive polytomy in Macraucheniinae, returning a topology very similar to the majority rule consensus tree (Fig. S2 in Appendix C3 Resource 5).

When we mapped the apomorphies in the majority rule consensus tree, the subfamily Macraucheniinae is supported by the following eight unambiguous synapomorphies: (a) nasals vestigial or absent (char. 1), (b) the premaxillae and maxillae are sutured sagittally in dorsal view (char. 8), (c) the coronal plane that passes through infraorbital foramen is anterior to M3 (char. 9), (d) the caudal border of the nasal aperture is in level with the orbit (char. 10), (e) the anterior palatal shape narrows at P2 or P3 level (char. 11), (f) labially projected parastyle on P3-P4 (char. 17), (g) deep concavities between lingual styles (parastyle-mesostyle-metastyle)

on M1-M3 (char. 18) and (h) the absence of a sagittal crest (char. 31) (Table S8 in Appendix C3 Resource 2). The polytomy formed by *Promacrauchenia* sp. (Anaya & MacFadden 1995), *Macrauchenia patachonica* and *Macraucheniopsis ensenadensis* is supported by five unambiguous synapomorphies: (a) the absence of an entoconid on m1-m2 (char. 3), (b) a strongly compressed trigonid of m1 against the talonid of p4 (char. 4), (c) a rounded outline of the premaxillary area in palatal view (char. 12), (d) the presence of a diastema between I3-C (char. 16) and (e) the absence of an entolophid on m1-m2 (char. 23).

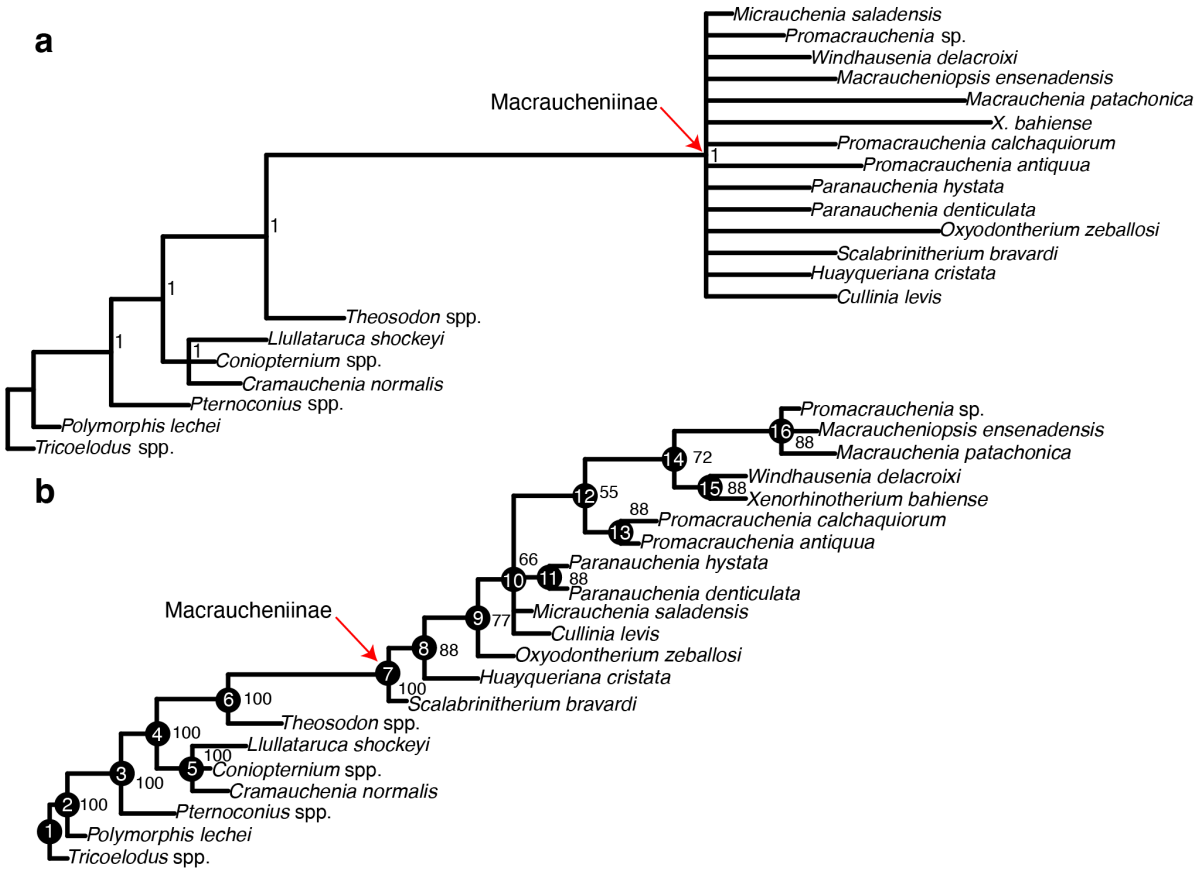



**Figure 3.20** Maximum parsimony phylogenies of Macraucheniidae. **a**. strict consensus tree. **b**, 50% majority rule consensus tree. The numbers next to the nodes in **a** are the absolute Bremer supports. The numbers next to the nodes in **b** indicate the percentage in which each node was recovered from the total number of most parsimonious trees (MPTs), and the numbers in the black circles are the nodes number. Node 7 corresponds to the subfamily Macraucheniinae, here recovered as a monophyletic group. *Promacrauchenia* sp. are the specimens previously attributed to this genus from Inchasi beds, Inchasi, Bolivia, mid-Pliocene, 4 – 3.3 Ma (MacFadden et al. 1993; Anaya and MacFadden 1995). Both phylogenies (**a**, **b**) summarise a total of 36 MPTs (89 steps; consistency index [CI] = 0.607; retention index [RI] = 0.701)

The consensus tree of the undated Bayesian analysis agrees with the parsimony strict consensus tree in also recovering the subfamily Macraucheniinae, although it shows a better resolution for the groups present within this subfamily (Fig. 3.21a). However, when we compare the undated Bayesian consensus tree with the parsimony majority rule tree, the former

is considerably less resolved, although in general terms they mostly agree in the position of most of the taxa with the exception of *M. saladensis*. This taxon is recovered in the Bayesian tree within a polytomy that includes *Promacrauchenia* sp. (Anaya & MacFadden 1995), *Macrauchenia patachonica* and *Macraucheniopsis ensenadensis*. Node support is generally low, with support for the node of the subfamily Macraucheniinae being strongest (0.94; Fig. 3.21a).

The consensus tree of the tip-dated Bayesian analysis shows in general similar phylogenetic affinities as the undated consensus tree (Fig 3.21b), the main difference being the position of *M. saladensis*, which is here more basally located within the subfamily Macraucheniinae in an extensive polytomy at the base of the subfamily (Fig 3.21b, node 4). *Promacrauchenia* sp. (Anaya & MacFadden 1995) is positioned in a polytomy with *Macrauchenia patachonica* and *Macraucheniopsis ensenadensis* (Fig. 3.21b, node 9), which is similar to what is seen in the parsimony majority rule consensus tree (Fig. 3.20b, node 16). Node support is generally higher than in the undated consensus tree, and in particular the subfamily Macraucheniinae is strongly supported (0.93; Fig 3.21b, node 4). In terms of divergence-times estimations, the origin of the subfamily Macraucheniinae (Fig 3.21b, node 4) was dated at 14.06 million years ago (Ma) with an uncertainty range of 19.05 – 10.52 Ma considering the 95% highest posterior density interval (HPD) (Table S9 in Appendix C3 Resource 2). The node including *Promacrauchenia* sp. (Anaya & MacFadden 1995), *Macrauchenia patachonica* and *Macraucheniopsis ensenadensis* (Fig 3.21b, node 9), was estimated at 4.62 Ma with an uncertainty range of 6.73 – 3.40 Ma considering the 95% HPD.

# Discussion

## Skeletal Anatomy, Locomotion, and Paleobiological Inferences

Macraucheniids are thought to have been cursorial animals *sensu* Stein and Casinos (1997) considering that they possess vertically oriented limbs that favoured movement in parasagittal planes. They possess a series of anatomical features considered adaptations for cursorial locomotion, these include: loss of the clavicle (allowing a greater range of parasagittal movement of the scapula), a short olecranon process on the ulna (restricts and stabilises against pronation-supination), interlocking keels and grooves in the limb joints (allowing a wide arc of parasagittal movement with reduced risk of dislocation), and block-like carpals and appressed metapodials (increases limb strength and directs loading through the limb), digit

reduction (i.e., loss/reduction of digits I and V; distal limb weight reduction, increasing locomotor economy [but see McHorse et al. 2019 for alternative interpretations]), elongated metapodials and proximal phalanges (increases length of stride), among other typical cursorial features (Hildebrand & Goslow 2001; Polly 2007). The zeugopodial elements are also fused in macraucheniines. The fusion of the radius and ulna, and in particular the radial head, further restricts pronation-supination movement, stabilizing the articulation in the parasagittal plane. Fusion of the tibia and fibula and reduction of the fibula further reduces the mass of the hindlimbs (Hildebrand & Goslow 2001; Polly 2007).

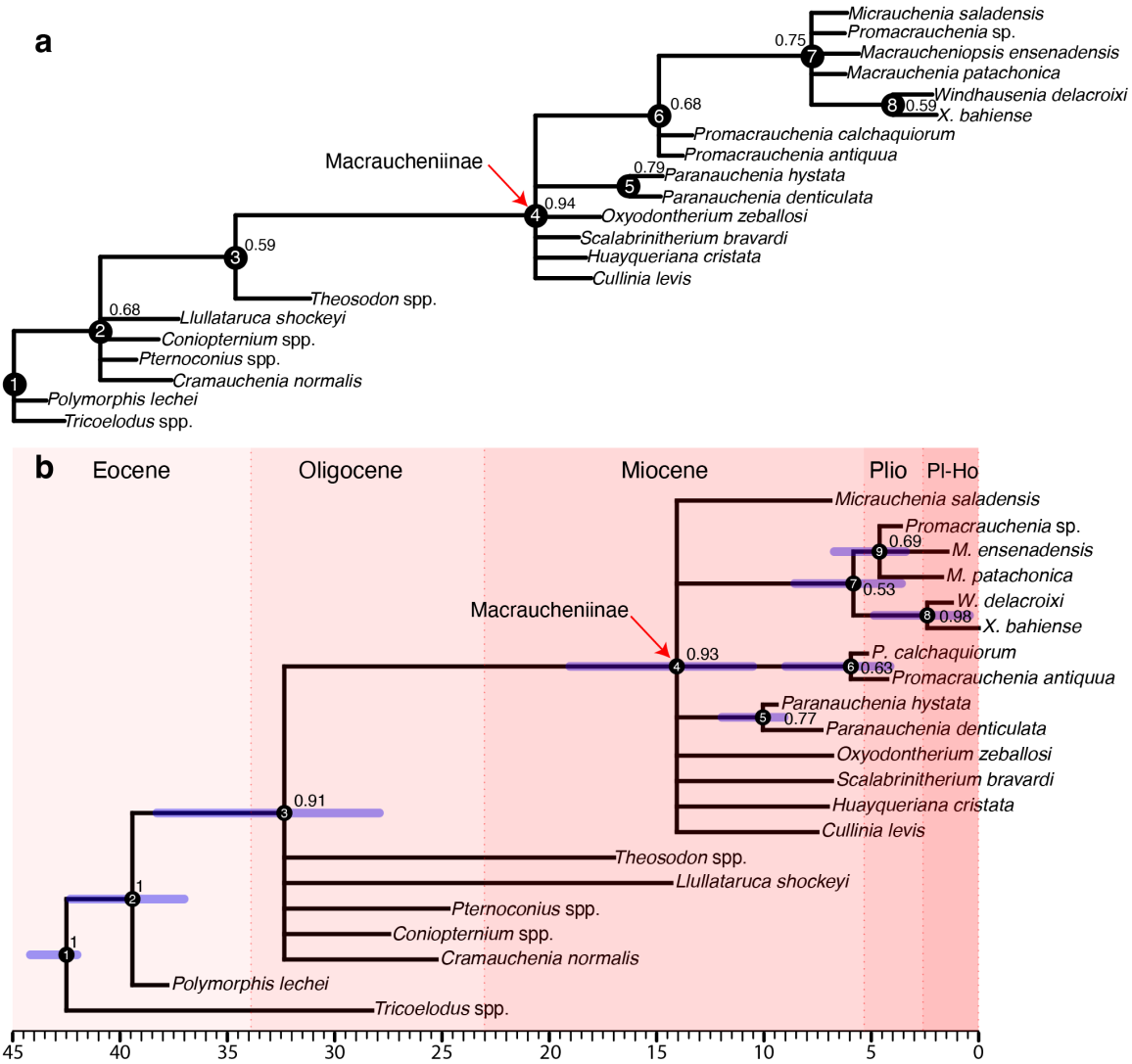



**Figure 3.21** Bayesian phylogenies of Macraucheniidae. **a**. undated Bayesian analysis. **b**. tip-dated Bayesian analysis calibrate in Ma. In **a-b** node support is indicated using Bayesian posterior probabilities, and in **b** the blue node bars represent the 95% highest posterior density (HPD) for the estimated node ages. In both phylogenies (**a, b**), node 4 corresponds to the subfamily Macraucheniinae recovered as a monophyletic group. *Promacrauchenia* sp. are the specimens previously attributed to this genus from Inchasi beds, Inchasi, Bolivia, mid-Pliocene, 4 – 3.3 Ma (MacFadden et al. 1993; Anaya and MacFadden 1995)

Cursorial locomotion of macraucheniids has been corroborated using biomechanical indices derived from limb measurements that suggest running capabilities for *Theosodon* (Cassini *et al.* 2012) and *Macrauchenia* (Carrano 1997; Fariña *et al.* 2005; Blanco *et al.* 2021), which are the most complete macraucheniids thus far found. *Micrauchenia*, with a vertically oriented forelimb, block-like carpals, elongate metacarpals, interlocking keels and grooves in the joints and additional stabilizing adaptations against non-parasagittal movements (more details below), is overall very similar to *Macrauchenia* and was most likely cursorial as well. Even macraucheniids older than *Theosodon*, like *Cramauchenia* and *Coniopternium* known from the Deseadan SALMA (late Oligocene) and with some associated postcranial remains (e.g., femur, tarsals and metatarsals), display postcranial features (e.g., elongated metatarsals) associated with cursorial locomotion (Shockey 1999; Dozo & Vera 2010). This suggests that the common ancestor of all macraucheniids was likely cursorial, which is not surprising if we consider that the probably pentadactyl *Protolipterna*, the earliest litoptern with relatively well-preserved postcranial remains, shows features consistent with cursoriality (Bastos and Bergqvist 2007; but see Cifelli 1983b for a saltatorial interpretation).

Macraucheniids have hooves which make them "ungulates" however, the possession of hooves is not necessarily the same as having a fully unguligrade foot posture. In a previous study (Carrano 1997), *Macrauchenia* was found to group with digitigrade mammals based on limb and tarsal measurements (i.e., femur, astragalus, calcaneum and metatarsals), in an analysis using only two categories: plantigrade (cruro-tarsal joint) and (b) digitigrade (metatarso-phalangeal joint), and excluding unguligrades. Within the digitigrade category, Carrano (1997) included subunguligrade animals that present a fleshy pad for support. When looking at the digital articular surfaces, it is possible to infer that in *Macrauchenia* (PIMUZ A/V 5700), *Theosodon* (YPM VPPU 015164) and *Micrauchenia* only the intermediate and ungual phalanges (unguals not preserved in *Micrauchenia*) were more horizontally positioned and in contact with the ground. Among these phalanges, the intermediate phalanx of digit III was probably the most horizontally positioned while in a neutral stance, considering the more dorsally extended articular surface of the proximal phalanx of digit III when compared with digits II and IV. The foot posture present in these macraucheniids would best be described as subunguligrade (*sensu* Carrano 1997). In the case of *Macrauchenia*, this hypothesis is further supported by ichnological evidence (i.e., footprints) suggesting that this taxon possessed thick palm and plantar pads in life, and a considerably more marked print for digit III (*Eumacrauchenichnus patachonicus*; Aramayo and de Bianco 2009; Aramayo et al. 2015).

Apart from macraucheniines, to our knowledge no other cursorial mammal, including modern and extinct ungulates, presents an aliform expansion in the distal part of the radius, which makes difficult a clear functional interpretation for this structure based on comparisons with modern taxa. Recently, Blanco et al. (2021) suggested that the mediolaterally wide radius in *Macrauchenia* was for the insertion of an enlarged deep digital flexor muscle (*M. flexor digitorum profundus*). Considering the muscular anatomy of some terrestrial extant artiodactyls and perissodactyls, such as *Equus*, *Tapirus*, *Bos* and *Babirusa* (Sisson 1914; Campbell 1936; Kneepkens *et al.* 1989; Denoix 2019; Aurich *et al.* 2020; MacLaren & McHorse 2020), we consider this a reasonable hypothesis with the caveat that none of these other taxa are particularly close relatives of litopterns.

The deep digital flexor muscle typically originates in four heads, two humeral (*caput humerale*), one ulnar (*caput ulnare*) and one radial (*caput radiale*) with different degrees of development depending on the taxon, and it inserts on the flexor surface of the distal phalanges (Campbell 1936; Aurich *et al.* 2020). We propose that the radial head of the deep digital flexor muscle was distally expanded in macraucheniines and originated from or in part from the medial aliform expansion of the radius. Functionally, the deep digital flexor muscle is a flexor of the forefoot (digital [metacarpo/interphalangeal] joint flexion; König and Liebich 2020; MacLaren and McHorse 2020; Etienne et al. 2021), which suggests that *Micrauchenia* and other macraucheniines such as *Promacrauchenia* and *Macrauchenia* had a strong musculature for flexing the forelimbs.

Blanco et al. (2021) suggested that this muscular development present in the radius of *Macrauchenia* was an adaptation for supporting a considerable part of the body weight on the forelimbs, specifically while running with the neck in a horizontal position. Considering the flexor function of the deep digital flexor muscle and the fact that *Macrauchenia* did not have naturally flexed forelimbs in neutral stance, we disagree with this interpretation. Moreover, *Camelus*, with an elongated neck and with a relatively large body mass (i.e., 400 – 657 kg (Köhler-Rollefson 1991; Makhdoomi *et al.* 2013)), does not show any particular expansion of the radius (e.g., IMNH R-1007) even though it is well known that it puts its neck in a horizontal position while running at fast speeds. An alternative hypothesis is that a strong flexor musculature was related to rapid and sudden changes of speed and/or direction, which could be useful, for instance, to avoid potential predators. Indeed, a previous study that used anteroposterior and transverse strength indicators estimated from the section modulus of the bone in parasagittal and transverse planes (i.e., IAC*ap* and IAC*t*), showed that the femur of

*Macrauchenia* was extremely resistant to transverse stress (Fariña *et al.* 2005). This was interpreted as an adaptation to cope with traverse stresses when veering in locomotion, particularly helpful to avoid predators by means of swerving and dodging (Fariña *et al.* 2005).

As observed for perissodactyls and most notoungulates, litopterns exhibit mesaxonic symmetry of the manus and pes through digit III (Scott 1910, 1912; Cifelli 1993). However, litopterns differ from perissodactyls and notoungulates in their specific carpal arrangement. In litopterns, the cuneiform is in contact with the magnum, which prevents contact between the lunate and the unciform. This litoptern carpal arrangement has been called "semi-taxeopod" (Scott 1910) or "reverse alternating" (Cifelli 1993), and it is present in macraucheniids and proterotheriids with further digital reduction (Scott 1910). As such, the carpal configuration and morphology of macraucheniids is highly conserved.

A reverse alternating carpus was present in earlier macraucheniids as *Cramauchenia*, *Coniopternium* (Fig. 3.15g-h), and it was probably present in *Polymorphis*, the oldest known macraucheniid, considering that proterotheriids have a similar carpal arrangement. It is unknown when this carpal arrangement was acquired as not much is known about the carpal arrangement of the earliest litopterns or even the earliest South American "condylarths" (Cifelli 1985; Bastos & Bergqvist 2007; Bergqvist 2008). Considering the carpal arrangement of early eutherians such as *Juramaia sinensis* (Middle–Late Jurassic; Luo et al. 2011) and *Eomaia scansoria* (Early Cretaceous; Ji et al. 2002) with a lunate-unciform articulation, a lunate unciform contact is likely the plesiomorphic placental condition. This inference is supported by the lunate-unciform articulation being present in different Paleogene placental ungulates such as *Arctocyon* (Argot 2013), *Hyopsodus* (Matthew 1915*b*), and *Peryptychus* (Shelley *et al.* 2018), among others. If we consider the proposed close relationship between litopterns, notoungulates and perissodactyls (Buckley 2015; Welker *et al.* 2015; Westbury *et al.* 2017) to be true, and the fact that notoungulates and perissodactyls (including stem perissodactyls like the anthracobunian *Cambaytherium* [Rose et al. 2019]) exhibit a lunate-unciform articulation, then the gaining of a cuneiform-magnum articulation with consequent loss of the lunate-unciform articulation could be considered a synapomorphy for Litopterna as previously suggested (Cifelli 1993). Far less clear, with the current fossil evidence, is if the mesaxonic symmetry of the manus and pes through digit III shared by these three orders is convergent or inherited from a common ancestor.

In terms of locomotion, the distinctive reverse alternating carpal arrangement of *Micrauchenia* and other macraucheniids entails that the scaphoid and cuneiform contact the magnum, and therefore it is possible that the medial and lateral loading during locomotion were transferred centrally towards digit III. The load increment in digit III would reduce the load on the outer digits so they could take on balance or stabilising role, a feature that could be useful in turning or swerving while running. The carpus of *Micrauchenia* also shows adaptations towards higher loadings during locomotion. In particular, the proximodistally expanded pisiform of *Micrauchenia* and other macraucheniines such as *Promacrauchenia*, *Macrauchenia* and *Xenorhinotherium* contrasts with the more slender pisiform in *Theosodon* could be related to with enlargement of muscles like the ulnar flexor muscle of the carpus (*m. flexor carpi ulnaris*) and the ulnar extensor muscle of the carpus (*m. extensor carpi ulnaris* [*m. ulnaris lateralis*]; König and Liebich 2020). Both muscles flex the wrist in large artiodactyls and in equids considering their caudal path and insertion on the pisiform (in tapirids as *Tapirus*, the ulnar extensor muscle of the carpus also supports extension due to its additional insertion on Mc V; Evans and Lahunta 2012; König and Liebich 2020; MacLaren and McHorse 2020; Etienne et al. 2021). A more distally prominent pisiform as observed in *Micrauchenia* and other macraucheniines, increases the lever arm of the ulnar flexor muscle of the carpus which exerts flexion during locomotion (Taylor 1974; Argot 2001).

The medial and lateral depressions on the distal ends of the metacarpals and phalanges inferred for the attachment of the metacarpophalangeal and interphalangeal collateral ligaments (Sisson 1914; Evans & Lahunta 2012; Denoix 2019) are symmetrical on digit III, but strongly asymmetrical in the digits II and IV, with the depressions on digits II and IV facing digit III being more pronounced. The medial and lateral depressions for the collateral ligaments are also observed in the metatarsals of different macraucheniids (Shockey 1999). Collateral ligaments provide lateral support and stability to the joints (Standring 2015). It is probable that more pronounced collateral ligaments facing digit III could also contributed to the stability of digit III, favouring dorsopalmar/plantar movements and preventing transverse stress. In addition, Mc II and Mc IV in macraucheniids have a stronger and more anteriorly elongate median keel than Mc III. It is likely that this strong and elongate median keel on Mc II and Mc IV allowed a wide arc of parasagittal movement and with a low risk of dislocation (Hildebrand & Goslow 2001), which in turn it could give more stability to digit III (Shockey 1999).

In sum, the aforementioned features of the forearm and digits in macraucheniids are indication of adaptations for cursorial locomotion, favouring parasagittal movement and

minimizing transverse stresses. The fusion of zeugopodial elements exhibited by macraucheniines can be seen as a further step towards specialization in cursorial locomotion, providing more economy of effort (Hildebrand & Goslow 2001). The same can be said about the interlocking happening between the cuneiform and unciform with the magnum in macraucheniines such as *Micrauchenia* and *Macrauchenia*, which increases limb strength and reduces risk of dislocation during locomotion. However, the aliform expansion of the radius and the well-demarcated depressions on the digits for the insertion of collateral ligaments (particularly in the marked angular processes present in the intermediate phalanges) observed in macraucheniines are unusual and lack an extant cursorial analogue, which suggests that these features could be connected to a particular behaviour that characterized this subfamily. In that context, the swerving hypothesis (Fariña *et al.* 2005) proposed as an adaptation of *Macrauchenia* against ambush predators such as *Smilodon*, is an interesting explanation for these macraucheniine anatomical structures. However, a small aliform expansion of the radius is present in some early macraucheniines from the late Miocene like *Micrauchenia, Promacrauchenia* sp. (Anaya & MacFadden 1995) and *Promacrauchenia*, and therefore predates the arrival of felids to South America during the GABI (Woodburne 2010; Cione *et al.* 2015), and long before the first appearance of large felids like *Smilodon* in the South American fossil record in the Ensenadan SALMA (~2.00 – ~0.70; Manzuetti et al. 2018). The only candidates for such predation pressure could be other predators from the late Miocene in South America like *Thylacosmilus atrox*, a marsupial sparassodont that due to its plantigrade pes posture, strong forelimbs and forwardly placed eyes has been inferred to be an ambush predator (Argot 2004; but see Ercoli et al. 2012 and Janis et al. 2020 for alternative locomotive and dietary interpretations). However, sparassodonts were already declining in the Huayquerian SALMA (~8.50 – 5.17 Ma), and *Thylacosmilus* (alongside the last sparassodonts) make their last appearance in the "middle" Pliocene (Chapadmalan SALMA; 3.74 – 3.04 Ma). This means that there is at least a ~1 Ma gap between the extinction of *Thylacosmilus* and the appearance of large hypercarnivore felids like *Smilodon* in the fossil record, a gap which is unlikely to be just a taphonomic and/or sampling bias (Prevosti & Forasiepi 2018). An alternative but not exclusive explanation for the aliform expansion of the radius and the extremely developed collateral ligaments in the digits is that these structures could be related to swerving and dodging due to intraspecific behaviours (e.g., competition and displays during mating season).

Considering that *Micrauchenia saladensis* is a terrestrial mammal that was preserved in marine rocks (see Paleoenvironmental conditions of Bahía Inglesa Formation section), we cannot directly infer the environment in which this macraucheniid was living from the rock unit in which it was found. However, vegetation modelling for the continental western side of southern South America during the late Miocene suggests the presence of a proto-Atacama Desert at 24–26°S and south of it, the presence of temperate xerophytic shrubland followed by sclerophyll woodland and shrubland (Pound *et al.* 2011, 2012). Paleosols further support the onset of the hyperaridity of the Atacama Desert during the late Miocene related to the formation of the Central Andean rain-shadow, although not as intense as during the late Pliocene and Pleistocene (Rech *et al.* 2019). Therefore, considering the latitude of the Bahía Salado area, it is likely that *M. saladensis* was living in a coastal environment with sclerophyll woodland and shrubland vegetation (Fig. 3.22).



**Figure 3.22** Restoration of *Micrauchenia saladensis* in the late Miocene coast of Bahía Salado, Northern Chile. Art by Mauricio Álvarez

## Body Mass

It is difficult to estimate the body mass for *Micrauchenia saladensis* using the known limited fossil material combined with the unique anatomy of macraucheniids, of which no extant mammals are clear analogues. For example, if we estimate body mass of *M. saladensis*

(SGO.PV.21700) and *Macrauchenia patachonica* (MACN PV 2) using the "all ungulates" radius R2 (log [body mass] = 2.7991 * log[R2] + 0.0890) and R4 (log[body mass] = 2.7703 * log[R4] – 0.0067) equations from Scott (1990); and we calculate the geometric mean of the estimates, we obtain 17.94 kg and 167.19 kg, respectively. These are both lower estimates than would be expected considering the overall dimensions of the different elements of the skeleton of both taxa (Tables S1-S6 in Appendix C3 Resource 1), and that previous body mass estimations of *Macrauchenia patachonica* which vary from 830 kg (Fariña *et al.* 1998) to 1100 kg (Fariña 1996). These previous estimations for *Macrauchenia* were based on 66 craniodental and postcranial equations, and the scaling up and averaging of modern South American camelids (considered "morphological analogues" by Fariña [1996]) respectively. If we use the ratio of the mass estimates between *Macrauchenia patachonica* and *M. saladensis* (i.e., 167.19 / 17.94 kg) and consider an estimation of 955.51 kg body mass for *Macrauchenia patachonica* (based on the geometric mean of the two previous estimations (Fariña 1996; Fariña *et al.* 1998)), *M. saladensis* would have had a body mass of around 102.52 kg. This is simply an estimate based on proportionality of two different body mass estimations, but it is consistent with previous body mass estimates for *Theosodon garretorum* and *Theosodon lydekkeri* of 158.04 kg and 130.94 kg, respectively, using craniodental equations (Cassini *et al.* 2012). These taxa were moderately but consistently bigger than *M. saladensis* considering linear measurements. However, even these and previous estimations have to be taken with caution as there is a considerable variation in body mass estimations depending in the method and equation used (McGrath *et al.* 2018), which is related to the unusual anatomy of macraucheniids when compared with the modern taxa used to generate these equations.

A different method for estimating body mass that is considered to be less affected by the potentially odd proportions of extinct taxa, is using occipital condyle width (OCW) regression equations (Engelman 2022). *Micrauchenia* (SGO.PV.21700) did not preserved a cranium, so measuring OCW directly is not possible. However, the interior width between the occipital facets of the atlas (i.e., 46 mm) can provide an estimation for OCW as the occipital condyles sit there. Using the regression equation for ungulates ($\ln(\text{body mass}) = 7.6451 \times \ln(\text{OCW})^{2/3} - 8.0565$), that included members of Artiodactyla, Perissodactyla, and Hyracoidea (Engelman 2022), we estimated a value of 42.35 kg for *Micrauchenia*. Using the same equation in other macraucheniids, we estimated the following body masses: *Cramauchenia normalis* (MPEF-PV 2524, OCW: 49.29 mm): 53.00 kg, *Huayqueriana cf. H. cristata* (IANIGLA-PV 29: 64.45 mm): 125.11 kg, *Scalabrinitherium bravardi* (MACN PV 13082: 66.77 mm): 139.92

kg, *Promacrauchenia antiquua* (MACN PV 7986, OCW: 72.12 mm): 178.36 kg, and *Macrauchenia patachonica* (MNHN.F.PAM69, OCW: 107.85 mm; MACN PV 2, OCW: 106.27 mm): 591.79 – 619.03 kg. These estimates are considerably lower than previous body mass estimations for *Huayqueriana* (154.39 – 721.18 kg; Forasiepi et al. 2016) and *Macrauchenia* (830 – 1100 kg; Fariña 1996; Fariña et al. 1998), although we consider them plausible taking into consideration the bizarre anatomy of macraucheniids.

## Macraucheniid Diversity in the Late Miocene

The presence of *Micrauchenia saladensis* in Bahía Salado increases the species richness and the diversity of body sizes of macraucheniids in the late Miocene, in particular of the Huayquerian SALMA (~8.50 – 5.17 Ma). Apart from *M. saladensis,* seven other macraucheniids species have been recognized for the late Miocene (i.e., *Cullinia levis*, *Huayqueriana cristata*, *Paranauchenia hystata*, *Paranauchenia denticulata*, *Oxyodontherium zeballosi*, *Scalabrinitherium bravardi,* and *Promacrauchenia calchaquiorum*). These are mostly medium-sized macraucheniids, except the small and gracile *Cullinia levis* (Fig. 3.1). Five of these (i.e., *Huayqueriana cristata*, *Paranauchenia denticulata*, *Oxyodontherium zeballosi*, *Scalabrinitherium bravardi*, and *Promacrauchenia calchaquiorum*) have been found within the Huayquerian SALMA.

The Huayquerian SALMA has been described as the highest diversity peak in macraucheniid evolution (McGrath *et al.* 2020*a*), and after this period, macraucheniids of small size disappear from the fossil record to never return. By the late Pleistocene, some macraucheniids reached enormous sizes like the 592 – 1100 kg *Macrauchenia patachonica* (Fariña 1996; Fariña *et al.* 1998), *Xenorhinotherium bahiense* inferred to be of a similar body size as *M. patachonica* considering its dimensions (Tables S2-S6 in Appendix C3 Resource 1) , and the colossal 1200 kg *Macraucheniopsis ensenadensis* (Vizcaíno et al. 2012, based in geometric similarity of a 988 kg estimation for *Macrauchenia patachonica*), which were part of the South American megafauna. It is unclear why the small bodied macraucheniids disappeared. A hypothesis on the disappearance of the smaller macraucheniids like *M. saladensis* and *Cullinia levis*, could be competition with the North American ungulates (i.e., equids, cervids, tayassuids, tapiroids) crossing into South America by the late Pliocene during the GABI. However, there was most likely a considerable gap between both events as these North American potential competitors are most likely absent from South America by most authors during the late Miocene (Woodburne 2010; Goin *et al.* 2012; Cione *et al.* 2015;

Gasparini *et al.* 2021). Even though some authors claim an earlier date for the GABI based on ungulates with North American affinities in supposed late Miocene deposits of Peruvian Amazon (Campbell *et al.* 2000; Frailey & Campbell 2012; Prothero *et al.* 2014), these have been recently questioned in terms of their taxonomy and provenance, being most likely Quaternary remains (Gasparini *et al.* 2021).

A more likely possibility that is consistent with the available evidence is that this particular disappearance of small macraucheniid species was a stochastic process within a general trend of reduction of diversity in macraucheniids. Indeed, beginning in the late Miocene, litopterns (i.e., macraucheniids and proterotheriids), and notoungulates started experiencing a steep reduction in diversity (i.e., number of genera; Marshall and Cifelli 1990; Bond et al. 1995; Croft et al. 2020), and therefore just by chance, the small forms of macraucheniids could have disappeared. There are currently no clear reasons for this general decline in diversity after the late Miocene and towards the Pliocene/Pleistocene, but it could be potentially related to the global cooling and climatic instability triggered by expansions of ice sheets in west-Antarctica and in the Arctic (Zachos *et al.* 2001) that, coupled with the uplift of the Andes creating rain shadow effects, led to an increase aridification and woodland retreat (Pascual *et al.* 1985; Pascual & Jaureguizar 1990; Rech *et al.* 2019). These environmental changes have been also argued as one of the potential causes for the sparassodont demise in the "middle" Pliocene (Chapadmalan SALMA; 3.74 – 3.04 Ma; Prevosti et al. 2013).

## Phylogenetic Considerations

The results of our phylogenetic analyses are consistent between the different methods here used, recovering similar positions for most of the taxa included in the phylogeny, although with a degree of uncertainty in particular regarding the affinities of the members of the subfamily Macraucheniinae. The newly described *Micrauchenia saladensis*, even though it always recovered within Macraucheniinae, varies from more basal in the tip-dated Bayesian and parsimony majority rule consensus trees, to more derived in the undated Bayesian consensus tree. These results reflect the degree of uncertainty of the phylogenetic placement of *M. saladensis* within Macraucheniinae, and can be attributed to the lack of craniodental characters scored for this taxon, and also the lack of postcranial information for most of the macraucheniids included. Indeed, the absence of detailed descriptions of the postcranial elements of macraucheniids, apart from *Theosodon* and *Macrauchenia*, make comparisons difficult. Even though there seems to be a striking overall anatomical uniformity of postcranial

characters between earlier macraucheniines (late Miocene-Pliocene) and later Pleistocene species like *Macrauchenia patachonica* as previous authors have noted (e.g., Parodi 1931), our postcranial descriptions of *M. saladensis* and comparisons with members of Macraucheniinae show that there are postcranial features that have potential to help untangle the phylogenetic affinities within this subfamily, and also the relationships of earlier macraucheniids. Here we included eight postcranial characters, although as more postcranial elements are found (either in the field or museum collections) and described, these could be potentially refined by dividing into more states, and new characters could be added, such as those that encapsulate vertebral elements, for example. This is important, in light of the fact the some of the dental characters employed here and in previous studies (Schmidt & Ferrero 2014; Forasiepi *et al.* 2016; McGrath *et al.* 2018) are prone to be affected by the level of tooth wear as macraucheniids increased their level of hypsodonty. Characters like the length of m2 (char. 6), the parastyle projection on P3-P4 (char. 17), position of the hypocone on M2 relative to the protocone (char. 20) and the relative position of the metaconid on m2 (char. 26) could be affected depending on degree of wear (Lobo 2015). This is problematic because the level of tooth wear tends to give more information about age and diet, instead of phylogenetic affinities.

Our maximum parsimony results broadly agree with previous parsimony studies using only craniodental characters (Schmidt & Ferrero 2014; Forasiepi *et al.* 2016; McGrath *et al.* 2018), and when *M. saladensis* is removed from the consensus, we had a comparable degree of resolution (Appendix C3 Resource 5 Fig. S2). In terms of the synapomorphies for the subfamily Macraucheniinae, our results are in general consistent with previous studies (Schmidt & Ferrero 2014; McGrath *et al.* 2018), although we found eight unambiguous synapomorphies, instead of five and six, respectively. The new synapomorphies were: (a) the premaxillae and maxillae are sutured sagitally in dorsal view (char. 8) and (b) the coronal plane passing through infraorbital foramen is anterior to M3 (char 9). We did not find mesodont dentition (char. 15) as an unambiguous synapomorphy for Macraucheniinae as in previous studies (Schmidt & Ferrero 2014; McGrath *et al.* 2018), although it is likely to be so, as this feature has not been found in early macraucheniids or "cramaucheniids" which are all brachyodont (i.e., HI < 1.45). The fusion of the ulna and radius is probably an additional synapomorphy for the subfamily Macraucheniinae considering that all late Miocene to late Pleistocene adult macraucheniids found so far possess this feature (Soria 2001). However, this feature was not found as an unambiguous synapomorphy in our analysis probably because of missing data, as most macraucheniids species are only known from craniodental remains.

Anaya and MacFadden (1995) assigned the macraucheniid material from Inchasi beds to *Promacrauchenia* sp. based on a clear size difference with the Pleistocene *Macrauchenia* and the presence of *Promacrauchenia* in other Pliocene localities. Contrary to this interpretation, the phylogenetic position of *Promacrauchenia* sp. (Anaya & MacFadden 1995) recovered in the Bayesian and parsimony phylogenetic analyses, strongly suggests that this is a different taxon from *Promacrauchenia calchaquiorum* and *Promacrauchenia antiquua* (*Promacrauchenia* spp.). Among the five unambiguous synapomorphies recovered from the parsimony-based majority rule consensus tree (Fig. 3.20b) that link *Promacrauchenia* sp. (Anaya & MacFadden 1995) with *Macrauchenia patachonica* and *Macraucheniopsis ensenadensis*, three of them are preserved in the *Promacrauchenia* sp. (Anaya & MacFadden 1995) specimens and are absent in the *Promacrauchenia spp.*: (a) the absence of an entoconid on m1-m2 (char. 3), (b) a strongly compressed trigonid of m1 against the talonid of p4 (char. 4), and (e) the absence of an entolophid on m1-m2 (char. 23). Indeed, the absence of entoconid and entolophid in the lower molar series of the macraucheniines from Inchasi was previously observed by Schmidt (2013), although the phylogenetic implications were never empirically tested until now. Apart from these dental features, there are postcranial characteristics that are not consistent with what is known from *Promacrauchenia*. One of the diagnostic features of the genus *Promacrauchenia* is that the width at the level of the distal articular surfaces of the ulna-radius is less than the width at the level of the aliform expansion (Pascual *et al.* 1966). *Promacrauchenia* sp. (Anaya & MacFadden 1995) shows the opposite condition, exhibiting a wider aliform expansion than the distal end of the ulna-radius, which is more similar to *Macrauchenia* and *M. saladensis*. However, a feature that clearly distinguishes *Promacrauchenia* sp. (Anaya & MacFadden 1995) from the latter two genera is that the aliform expansion is situated in a relatively more proximal position of the radius-ulna (Schmidt 2013). Taking all this evidence together in terms of size, dental and postcranial features, the macraucheniine specimens from Inchasi beds are probably a new and distinctive genus/species of macraucheniid, which merits a new detailed taxonomic revision.

Although we could not resolve the specific position of *M. saladensis* within Macraucheniinae, there are distinct anatomical features that allow us to confidently assign it to a new genus/species. Its size is particularly small for a macraucheniid from the late Miocene, being of a similar size of earlier macraucheniids like *Cramauchenia normalis* and *Coniopternium andinum*. The type specimen is not a juvenile, as it exhibits a complete fusion of the ulna and radius, and completely lacks epiphyseal plates in the distal end of the ulna and

radius and in the metacarpals and phalanges (Fig. 3.9b-c). Apart from the clear size difference, the relative level of development of its ulna-radius aliform expansion and position is different from *Promacrauchenia* spp. and *Promacrauchenia* sp. (Anaya & MacFadden 1995), being wider that the ulna-radius distal end (unlike *Promacrauchenia* spp.) and distally located (unlike *Promacrauchenia* sp. [Anaya and MacFadden 1995]). Unfortunately, not much is known about the postcranium of the earlier members of Macraucheniinae, but the smallest member of this subfamily so far described in terms of the dental and postcranial remains is *Cullinia levis* (Cabrera & Kraglievich 1931; Bond & López 1995). However, there are two main anatomical features that allow us to discard *Cullinia levis* as the species here described. First, *Cullinia levis* is consistently larger than *M. saladensis*. In the case of the pisiform, in which a direct comparison is possible, *Cullinia* cf *C. levis* (MLP 55-IV-28-97) is ~40% larger *M. saladensis* (SGO.PV.21700; Fig. 3.14a-f, i-j; Table S4 in Appendix C3 Resource 1). In addition, the size of *Cullinia levis* considering dental and postcranial remains is larger than *Coniopternium andinum* (Schmidt 2013; McGrath *et al.* 2020*a*). In contrast, *M. saladensis* tends to be slightly smaller than *Coniopternium andinum* considering linear measurements of its digits (Table S6 in Appendix C3 Resource 1). Second, one of the diagnostic features of *Cullinia levis* is that it is a very gracile macraucheniid, presenting metapodials that are proportionally longer than *Theosodon* or later macraucheniines (Cabrera & Kraglievich 1931; Pascual *et al.* 1966; Bond & López 1995). This feature can be clearly observed in the thin and elongated Mt II and Mt IV of *Cullinia levis* (MLP 71-IX-2-5; MLP 29-IX-1-78; Fig. S3e, g in Appendix C3 Resource 5). The relatively length of the metapodials of *M. saladensis* is similar to *Theosodon* spp., and within the range observed in our sample of macraucheniids (Table S5 in Appendix C3 Resource 1), contrary to what would be expected if these were remains of *Cullinia levis* (Table S7 in Appendix C3 Resource 1; Fig. S3 in Appendix C3 Resource 5). The metapodials of *Cullinia levis* (i.e., Mt II and Mt IV) are always proportionally mediolaterally thinner than the metapodials of *Theosodon* spp (i.e., considering total length). Other macraucheniids from the late Miocene from which not many postcranial materials are available or described, such as *Scalabrinitherium bravardi*, *Paranauchenia denticulata* or *Oxyodontherium zeballosi*, are just too large to be the SGO.PV.21700 materials considering that they are consistently larger than *Cullinia levis* when their dentition is compared (McGrath *et al.* 2020*a*). Taking all of this evidence together, we are confident that our taxonomic assignment of SGO.PV.21700 to the new species *Micrauchenia saladensis* is justified.

The description of *M. saladensis* provides important data on the postcranial anatomy of macraucheniids. The postcranial anatomy of the Santacrucian SALMA (early Miocene) specimens of *Theosodon* and the late Pleistocene *Macrauchenia* and *Xenorhinotherium* is well known, but not much is known (or described) about macraucheniid postcranial anatomy during the temporal gap between these two intervals. From anatomical comparisons between different macraucheniids, it can be argued that even though the general bauplan in macraucheniids is very conserved, there are clear anatomical trends in macraucheniid macroevolution: the retraction and atrophy of the nasal bones, nostrils becoming more dorsally positioned, increasing tooth crown height, the fusion of the ulna and radius, the fusion of the tibia and fibula, the development of the aliform expansion of the radius, among other features, some of which we identified as unambiguous synapomorphies in our parsimony analyses. These features appear to be ubiquitous and developed to a certain degree in all the macraucheniids found so far from the late Miocene to the late Pleistocene/Holocene, and are clearly absent in earlier macraucheniids.

# Conclusions

We describe a new macraucheniine macraucheniid *Micrauchenia saladensis* (SGO.PV.217000) from the late Miocene (Huayquerian SALMA), the first litoptern and SANU from the marine Bahía Inglesa Formation, Chile. With an estimated body mass of 53 – 102.52 kg, *M. saladensis* is also the smallest macraucheniine yet described, increasing the diversity of macraucheniid body sizes for the Huayquerian SALMA. The location of this specimen within the Bahía Inglesa Formation is curious, as the postcranial anatomy of *M. saladensis* is consistent with a terrestrial animal, likely one with a subunguligrade stance and a forelimb adapted for cursorial locomotion, as is seen in other macraucheniids. This suggests an allochthonous position for *Micrauchenia*, which probably died near the Bahía Salado coast, and was subsequently swept away by the tide to final its deposition site.

*M. saladensis* presents features that have been observed only in the subfamily Macraucheniinae, such as the fusion of the ulna and radius and the presence of a radial aliform expansion (Soria 1981). We consider the fusion of the ulna and radius as a cursorial specialization for restricting pronation-supination movement, favouring parasagittal motion. The radial aliform expansion provided a large area for the insertion of an enlarged deep digital flexor muscle which would have likely facilitated strong flexion of the forefoot and withstood higher transverse stresses (Fariña *et al.* 2005). We suggest that this unusual osteological feature

and its related muscular development was used for rapid flexion of the manus and aided in sudden movements, such as swerving and dodging, either to avoid predators, or for intraspecific behaviours (e.g., competition, mating).

Our phylogenetic analyses corroborate *M. saladensis* as member of subfamily Macraucheniinae, although with uncertain affinities within this subfamily. This is likely due to the lack of diagnostic craniodental remains in *Micrauchenia*, and also the lack of postcranial remains associated to most macraucheniid species. Indeed, apart from *Theosodon* and *Macrauchenia*, the postcrania of most other macraucheniids are insufficiently known. In that sense, *Micrauchenia* provides relevant anatomical information in macraucheniid evolution.

# Chapter 4 New phylogeny of Litopterna (Mammalia) and “archaic” Palaeogene ungulates enlightens their relationships and evolution



The litoptern *Macrauchenia patachonica* in the MACN exhibition. March 2019

# Introduction

During the Cenozoic, South America was mostly isolated from other continental landmasses, but experienced different sporadic faunal migration pulses, that culminated around 2.8 Ma with the full connection with North America through the Isthmus of Panama (O'Dea *et al.* 2016). The combined results of long-term isolation with sporadic immigration events define the modern South American mammalian fauna. The first one of these migration pulses, known as the South American Episode, is related with the arrival of therians from North America around the K/Pg boundary (Pascual & Ortiz-Jaureguizar 2007). Among the North American migrants, there were placental "ungulates" that after their arrival to South America, quickly diversified, giving rise to different groups of South American native ungulates (SANUs), such as the "condylarths" kollpanines and didolodontids, and the orders Astrapotheria, Litopterna, Notoungulata, Pyrotheria, and Xenungulata in a phase known as Stratum 1 of the mammalian faunal succession in South America (Simpson 1980; Croft *et al.* 2008). After Notoungulata, Litopterna is the second most diverse order of SANUs, with a outstanding temporal distribution of at least ~ 62.5 million years, from the early Palaeocene to the late Pleistocene/Holocene (Woodburne *et al.* 2014*b*). Litopterns are characterized by having cursorial and mesaxonic limbs and peculiar cranial and dental features. Most of them have quadrate-shaped upper molars with crescentic paracones and metacones, and increasingly bicrescentic lower molars. Their dentition ranges from bunodont to lophoselenodont, and varies from low-crowned to slightly hypsodont (i.e., mesodont; Croft *et al.* 2020). The biogeographic history of litopterns is also particularly interesting among SANUs, as they reached Antarctica during the Palaeogene with the genus *Notiolofos*, thus being the only SANU alongside with Astrapotheria with an Eocene fossil record on that continent (Gelfo *et al.* 2019).

In 1834, Charles Darwin discovered in southern Patagonia the first SANU known to science and the western world, the late Pleistocene/Holocene litoptern *Macrauchenia patachonica* (Darwin 1845). Ever since this discovery and the formal description of *M. patachonica* by Owen (1838), the phylogenetic affinities and taxonomic classification of litopterns have been controversial (Table 4.1). Ameghino (1889) included them within Perissodactyla creating the order Litopterna, probably because of anatomical similarities between litopterns and perissodactyls such as the mesaxonic limbs. Contrary to Ameghino's views, who considered litopterns within Perissodactyla throughout his life (e.g., Ameghino 1906), most authors around this time considered Litopterna as a distinct order within

"Ungulata", a wastebasket group that generally includes members of extant and fossil "ungulates" or hoofed mammals (Lydekker 1893; Osborn 1910; Scott 1910; Schlosser 1911). Lydekker (1896) considered that litopterns and the other orders of SANUs shared a "common ancestral stock" belonging to "Condylarthra" (i.e., wastebasket group of "archaic ungulates"), and likely with a North American origin, but not belonging to any particular order of modern ungulates such as Perissodactyla. Similarly, Scott (1910) concluded that litopterns were convergently similar to perissodactyls after making detailed anatomical observations of different litopterns. Later, Simpson (1945) proposed to include Litopterna in a superorder called Protoungulata, which also included the orders "Condylarthra" (North American "condylarths" plus didolodontids), Notoungulata, Astrapotheria and Tubulidentata. However, he later considered that litopterns alongside other SANUs derived from generalized North American "condylarths" that crossed to South America during the Late Cretaceous or early Palaeocene, although not necessarily originating from one ancestral form (Simpson 1948), a general view that he kept during his career (e.g., Simpson 1978, 1980). Most authors followed this interpretation (e.g., Paula Couto 1952; Cifelli 1983*a*), which was formalised by McKenna (1975), who used the mirorder Meridiungulata to include all the orders of SANUs. However, McKenna did not provide any anatomical justification for the creation of this taxon apart from a shared geographical occurrence in South America.

Even though most morphology-based phylogenetic studies failed to recover a monophyletic Meridiungulata (e.g., Horovitz 2004; O'Leary *et al.* 2013), recent molecular studies on *M. patachonica* have provided new insights. First, two independent molecular studies of collagen have shown that litopterns and notoungulates (i.e., *Toxodon platensis*) form a monophyletic unit that is closely related to Perissodactyla (Buckley 2015; Welker *et al.* 2015; Fig. 4.1a). Welker *et al.* (2015) named this monophyletic group Panperissodactyla. Similarly, a molecular study using *Macrauchenia*'s ancient mitochondrial DNA found the same close relationship between Litopterna and Perissodactyla (Westbury *et al.* 2017; Fig. 4.1 b), corroborating the close phylogenetic relationship between these two groups. Although these studies were a major breakthrough in the taxonomy of Litopterna by positioning this order within the placental tree, the interfamilial affinities within Litopterna, and whether various taxa assigned to Litopterna over the last 150+ years constitute a monophyletic unit or not, are still open questions. Indeed, even though a decent number of phylogenetic studies have included litopterns in their taxon sample (Billet *et al.* 2015; Muizon *et al.* 2015), in general this is limited to a small number of taxa that does not represent all of the different families of litopterns (Table 4.2).

**Table 4.1** Summary of the main taxonomic proposals for early SANUs ("condylarths"), Litopterna and Notopterna

| Lydekker (1893) | Ameghino (1899) | Ameghino (1904*a*) | Ameghino (1906) | Scott (1913) | Schlosser (1911) |
|---|---|---|---|---|---|
| **Order Ungulata** | **Ungulata** | **Order Condylarthra** | **Order Condylarthra** | **Order Litopterna** | **Order Ungulata** |
| **SO Litopterna** | **Perissodactyla** | Fam. Phenacodontidae | Fam. Pantostylopidae | Fam. Macraucheniidae | **Suborder Litopterna** |
| Fam. Macraucheniidae | **Order Litopterna** | Fam. Periptychidae | Fam. Phenacodontidae | Fam. Proterotheriidae | Fam. Bunolitopternidae |
| Fam. Proterotheriidae | Fam. Macraucheniidae | Fam. Pantolambdidae | Fam. Catathleidae | Fam. Didolodidae | Fam. Macraucheniidae |
| | Fam. Proterotheriidae | Fam. Pantostylopidae | Fam. Pantolambdidae | | Fam. Proterotheriidae |
| | Fam. Homalodontotheriidae | **Order Perissodactyla** | Fam. Arctocyonidae | | Fam. Adianthidae |
| | | Fam. Macrauchenidae | **Order Perissodactyla** | | |
| | | Subfam. Theosodontinae | Fam. Hyracotheriidae | | |
| | | Subfam. Macraucheninae | Fam. Palaeotheriidae | | |
| | | Fam. Adiantidae | Fam. Macraucheniidae | | |
| | | Fam. Proterotheriidae | Fam. Proterotheriidae | | |
| | | Fam. Hyracotheriidae | Fam. Adiantidae | | |
| | | Fam. Lophiodontidae | | | |
| Simpson (1945) | Cifelli (1983*a*) | McKenna & Bell (1997) | Soria (2001)& Soria (1989*b*) | Muizon & Cifelli (2000) | Gelfo *et al.* (2016) |
| **Order Condylartha** | **Order Condylarthra** | **Order Condylarthra** | **Order Condylarthra** | **Order Panameriungulata** | Panperissodactyla |
| Fam. Didolodontidae | **SF Didolodontoidea** | Fam. Didolodontidae | Fam. Didolodontidae | Fam. Mioclaenidae | **Order Panameriungulata** |
| **Order Litopterna** | Fam. Didolodontidae | **Order Litopterna** | **Order Litopterna** | Subfam. Kollpaniinae | Fam. Kollpaniinae |
| Fam. Macraucheniidae | Fam. Sparnotheriodontidae | Fam. Protolipternidae | **SO Eolitopterna** | Fam. Didolodontidae | Fam Didolodontidae?[1] |
| Subfam. Macraucheniinae | **Order Litopterna** | **SF Macrauchenoidea** | Fam. Anisolambdidae | **SO Litopterna** | **Order Litopterna** |
| Subfam. Adianthinae | Fam. Protolipternidae | Fam. Macraucheniidae | Fam. Sparnotheriodontidae | Fam. Protolipternidae | Fam. Didolodontidae? (= Protolipternidae)[1] |
| Fam. Proterotheriidae | **SO Lopholipterna** | Subfam. Sparnotheriodontinae | **SO Lopholipterna** | Fam. Macrauchenidae | Fam. Protolipternidae |
| Subfam. Polymorphinae | **SF Macrauchenoidea** | Subfam. Polymorphinae | Fam. Macraucheniidae | Fam. Adianthidae | Fam. Anisolambdidae |
| Subfam. Proterotheriinae | Fam. Macraucheniidae | Subfam. Cramaucheniinae | Subfam. Macraucheniinae | Fam. Proterotheriidae | Fam. Sparnotheriodontidae |
| | Subfam. Polymorphinae | Subfam. Macraucheniinae | Subfam. Cramaucheniinae | Fam. Notonychopidae | Fam. Macraucheniidae |
| | Subfam. Cramaucheniinae | Fam. Notonychopidae | Fam. Proterotheriidae | | Fam. Proterotheriidae |
| | Subfam. Macraucheniinae | Fam. Adianthidae | Fam. Adianthidae | | Fam. Adianthidae |
| | Fam. Adianthidae | Subfam. Indaleciinae | **Order Notopterna** | | Fam. Notonychopidae |
| | **SF Proterotherioidea** | Subfam. Adianthinae | Fam. Amilnedwarsiidae | | |
| | Fam Proterotheriidae | **SF Proterotherioidea** | Fam. Indaleciidae | | |
| | Subfam. Anisolambdinae | Fam. Proterotheriidae | Fam. Notonychopidae | | |
| | Subfam. Proterotheriinae | Subfam. Anisolambdinae | | | |
| | | Subfam. Proterotheriinae | | | |

[1] Gelfo *et al.* 2016 argued that Protolipternidae may be a junior synonym of Didolodontidae, which in turn it may be a form of bunodont litoptern. Orders and suborders are in bold. Abbreviations: *SF*, Superfamily; *SO*, Suborder.

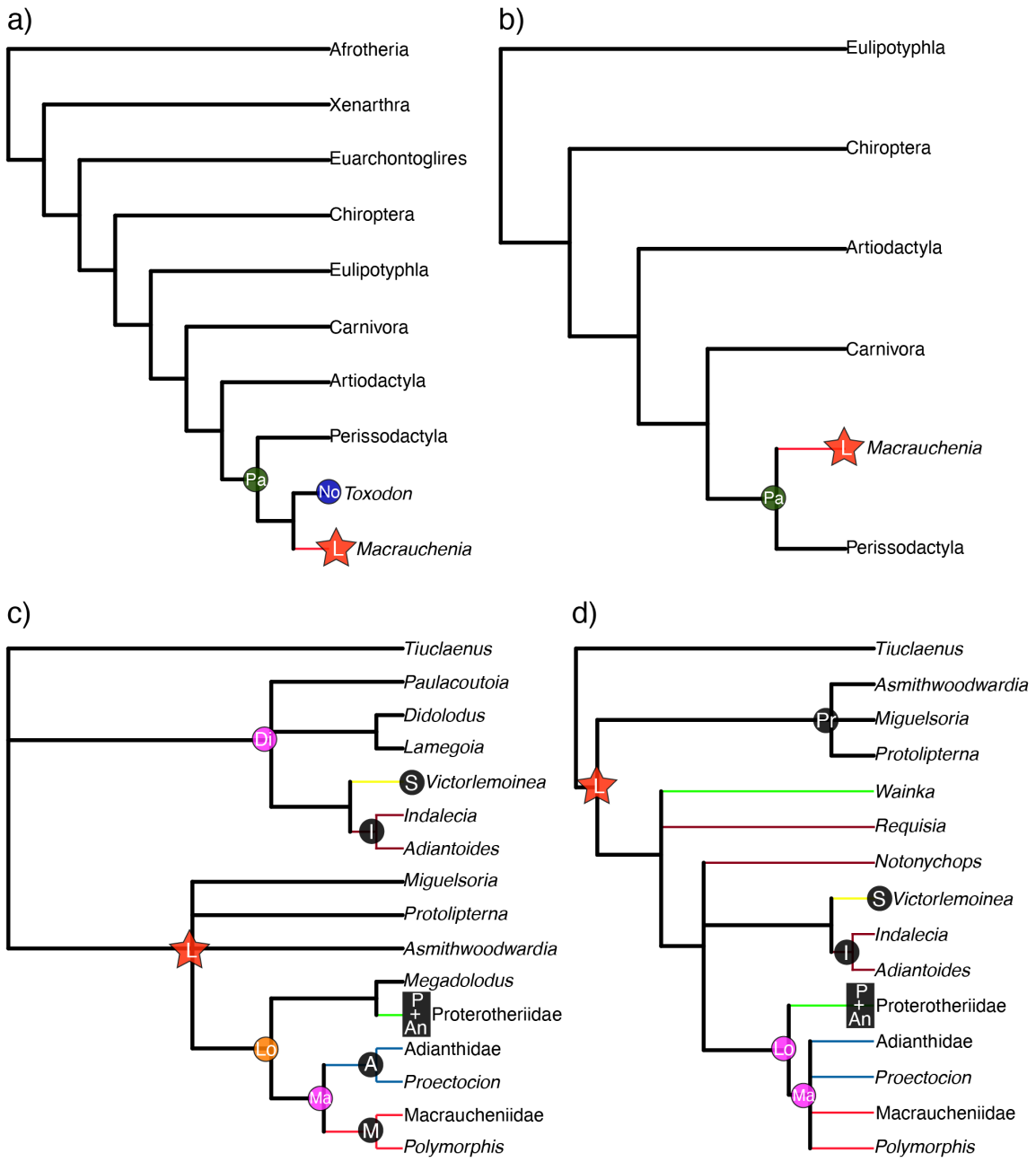



**Figure 4.1** Phylogenies of the order Litopterna illustrating its interordinal relationships (**a-b**) and its interfamilial relationships (**b-d**). **a**. (Buckley 2015) phylogeny; **b**. (Westbury et al. 2017) phylogeny; **c**. (Cifelli 1993); **d**. (Bonaparte & Morales 1997). Different colours in the branches are used for indicate different families or orders: blue Adianthidae; brown, Notopterna; green, Proterotheriidae; red, Macraucheniidae; yellow, Sparnotheriodontidae. Litopterna is indicated with a red star, but other nodes or tips of relevance are indicated in circles: blue, orders; orange, suborders; pink, superfamilies; black, families; green, non-defined rank. Abbreviations: *A*, Adianthidae; *An*, Anisolambdidae; *Di*, Didolodontidae; *I*, Indaleciidae; *L*, Litopterna; *Lo*, Lopholipterna; *No*, Notoungulata; *M*, Macraucheniidae; *Ma*, Macrauchenoidea; *S*, Sparnotheriodontidae; *P*, Proterotheriidae; *Pa*, Panperissodactyla.

Considering the relevance of litopterns as key component of the fauna during the Cenozoic of South America, it is frustrating that to date there has been only one study using

phylogenetic methods to resolve the interfamilial affinities of Litopterna (Cifelli 1993; Fig. 1.1 c). This study was followed up by another study by Bonaparte & Morales (1997), who built on the dataset by incorporating some taxa that Cifelli (1993) omitted, although it cannot be considered a totally independent study as they used practically the same matrix, characters and character states as Cifelli (1993). Considering that both studies only included 15 – 16 taxa of primitive South American ungulates and/or litopterns in a small matrix of 51 – 54 characters (Table 4.2), their conclusions should be considered as provisional. The results of these two studies have been the base of later familial taxonomic proposals for Litopterna (e.g., McKenna & Bell 1997; Muizon & Cifelli 2000), the most recent being the proposal of (Gelfo *et al.* 2016) which was partially based on Soria's (2001) taxonomic proposal (Table 4.1).

Considering the most recent familial taxonomic proposal for Litopterna (Gelfo *et al.* 2016) and the evidence from previous phylogenetic analyses (e.g., Cifelli 1993; Bonaparte & Morales 1997; Table 4.2) there are currently five uncontroversial families of litopterns: Anisolambdidae, Sparnotheriodontidae, Adianthidae, Macraucheniidae and Proterotheriidae. The two former families had a greater diversity during the Palaeogene, and the three latter with a greater diversity during the Neogene (Fig. 4.2). In addition, there are five other families of SANUs with controversial and mostly untested affinities that sometimes are included within Litopterna (e.g., Gelfo *et al.* 2016): Didolodontidae, Protolipternidae, Amilnedwardsiidae, Indaleciidae and Notonychopidae, all with a mostly Palaeogene distribution, and the three latter sometimes considered part of a different order, Notopterna (Soria 1989*b*). However, even for the five uncontroversial families of litopterns their interfamilial affinities are far from settled. It can be said that the difficulties in phylogenetically placing the Palaeogene early members of these families arise both from the generally incompleteness of the fossils so far found (i.e., mostly dental elements), and also from the bizarre, unique and diverse anatomy that they display. Indeed, when talking about early SANUs Simpson recognised this difficulty: "the Casamayoran [middle Eocene], presents the unusual and fascinating spectacle of such a great deployment still in its quantum phase, although nearing the end of it. Intragroup variation is enormous, intergroup variation is also unusually great in some cases, the ungulate population is protean almost beyond parallel, and there are so many transitional types, some of them quite plainly adaptively unstable, that the taxonomic problem seems almost hopeless." (Simpson 1944, p.214). Even though the taxonomic problem seems as difficult as in Simpson's time, in my view it is less hopeless as we now can use new phylogenetic tools such as the Bayesian methods that have never been applied to test the relationships of litopterns.

The main objectives of this work are to resolve the interfamilial affinities within the order Litopterna, test its monophyly, and put forward a new evidence-based taxonomic proposal for this order. To this end, I performed a phylogenetic analysis using maximum parsimony and for the first time for a litoptern matrix, both undated and tip-dated Bayesian methods, on a newly built morphological matrix of 954 characters. This matrix includes the earliest members of each litoptern family alongside early members of groups that have been linked to Litopterna in previous studies (i.e., North American Mioclaenidae, Kollpaninae, Didolodontidae, Xenungulata, Notoungulata and Astrapotheria), which total 35 taxa. In addition, by testing different hypotheses for the arrival of the ancestor/s of SANUs at South America, I was able to date important events in the evolutionary and biogeographic history of Litopterna, including the origin of the order and each family, and the timing of sparnotheriodontids arrival to Antarctica.

**Table 4.2** Previous phylogenetic analyses that included Litopterna and Didolodontidae

| Analysis | NT | NL | NC | CT | | | Litoptern families | | | | | Other families | | | | | | Orders | | | | Focus of the analysis |
|---|---|---|---|---|---|---|---|---|---|---|---|---|---|---|---|---|---|---|---|---|---|---|
| | | | | De | Cr | Po | A | An | M | P | S | Pr | D | K | I | Nt | Mi | As | No | X | Py | |
| Cifelli (1993) | 16[1] | 7 | 51 | X | | X | X | X | X | X | X | X | X | X | X | | | | | | | Primitive SA ungulates and interfamilial Litopterna |
| Bergqvist (1996) | 60 | 9 | 153 | | | X | X | X | X | X | X | X | X | | | | X | X | X | X | | Primitive SA ungulates and interordinal affinities of SANUs |
| Bonaparte & Morales (1997) | 15 | 7 | 54 | X | | X | X | X | X | X | X | X | | X[3] | X | X | | | | | | Affinities of *Requisia vidamari* within Litopterna |
| Muizon & Cifelli (2000) | 24 | 0 | 38 | X | | X | | | | | | X | X | X | | | X | | | | | Affinities of kollpanines with NA mioclaenids and SANUs |
| Gelfo (2004) | 19 | 0 | 27 | X | | | | | | | | X | X | X | | | X | | | | | Affinities of *Pascualodus patagoniensis* |
| Horovitz (2004) | 70 | 2 | 240 | | | X | | | X | X | | | | | | | X | X | X | | | Interordinal affinities of SANUs |
| Kramarz & Bond (2005) | 7 | 7 | 17 | X | | | | | | X | | | | | | | | | | | | Affinities of *Picturotherium migueli* |
| Gelfo (2006) | 26 | 0 | 88 | X | | X | | | | | | X | X | X | | | | | | | | Affinities of Didolodontidae with Protolipterna and Kollpaninae |
| Gelfo (2007) | 18 | 0 | 28 | X | | | | | | | | X | X | X | | | X | | | | | Affinities of *Raulvaccia peligrensis* |
| Gelfo *et al.* (2008) | 23 | 2 | 20 | X[2] | | | | X | | | X | | X | X | X | X | | X | X | X | X | Affinities of *Notoetayoa gargantuai* |
| Gelfo (2010) | 18 | 0 | 33 | X | | | | | | | | | X | X | | | | | | | | Affinities of Didolodontidae |
| Gelfo & Sigé (2011) | 20 | 0 | 41 | X | | | | | | | | | X | X | | | | | | | | Affinities of *Umayodus raimondi* within Proterotheriidae |
| Villafañe *et al.* (2012) | 16 | 16 | 21 | X | | | | | | X | | | | | | | | | | | | Affinities of *Thoatheriopsis mendocensis* within Proterotheriidae |
| Schmidt (2013) | 19 | 19 | 22 | X | | | | X[3] | | X | | | | | | | | | | | | Affinities within Proterotheriidae |
| Schmidt (2013) | 17 | 17 | 26 | X | X | | X[3] | | X | | | | | | | | | | | | | Affinities within Macraucheniidae |
| O'Leary *et al.* (2013) | 126 | 0 | 4541 | X | X | X | | | | | | X | X | | | | X | | X | X | | Interordinal affinities of living and fossil placental mammals |
| Schmidt & Ferrero (2014) | 18 | 18 | 25 | X | X | | X[3] | | X | | | | | | | | | | | | | Affinities of *Theosodon hystatus* within Macraucheniidae |
| Reguero *et al.* (2014) | 7 | 5 | 34 | X | | | | | | | X | | X | X[3] | | | | | | | | Affinities within Sparnotheriodontidae |
| Muizon *et al.* (2015) | 72 | 2 | 426 | X | X | X | | | X | X | | X | | | | | X | X | X | X | | Affinities of *Alcidedorbignya inopinata* in the placental tree |
| Billet *et al.* (2015) | 50 | 4 | 156 | X | X | | | | X | X | | X | X | | | | X | X | X | | X | Affinities of petrosals attributed to *Miguelsoria parayirunhor* |
| Schmidt (2015) | 20 | 20 | 22 | X | | | | X[3] | | X | | | | | | | | | | | | Affinities within Proterotheriidae |
| Buckley (2015)[4] | 46 | 1 | | | | | | | X | | | | | | | | | | X | | | Affinities of Litopterna and Notoungulata within Placentalia |
| Welker *et al.* (2015)[4] | 78 | 1 | | | | | | | X | | | | | | | | | | X | | | Affinities of Litopterna and Notoungulata within Placentalia |
| Forasiepi *et al.* (2016) | 20 | 20 | 34 | X | X | | X[3] | | X | | | | | | | | | | | | | Affinities of *Huayqueriana* cf. *H. cristata* within Macraucheniinae |
| Westbury *et al.* (2017)[4] | 95 | 1 | | | | | | | X | | | | | | | | | | | | | Affinities of Litopterna within Placentalia |
| McGrath *et al.* (2018) | 22 | 22 | 34 | X | X | | X[3] | | X | | | | | | | | | | | | | Affinities of *Llullataruca shockeyi* and *'Theosodon' arozquetai* within Litopterna |
| McGrath *et al.* (2020*b*) | 38 | 35 | 92 | X | X | X | | X | | X | | X[3] | X[3] | | X[3] | | | | | | | Affinities within Proterotheriidae |
| McGrath *et al.* (2020*a*) | 40 | 37 | 92 | X | X | X | | X | | X | | X[3] | X[3] | | X[3] | | | | | | | Affinities within Proterotheriidae |
| Chimento & Agnolin (2020)[5] | 79 | 7 | 214 | X | X | X | | | X | X | X | X | X | X | X | | X | | | | | Affinities of SA "condylarths" and Litopterna in a Perissodactyl matrix |
| Kramarz *et al.* (2021) | 78 | 7 | 214 | X | X | X | | | X | X | X | X | X | X | X | | X | | | | | Reply to Chimento & Agnolin 2020 paper |
| Macphee *et al.* (2021) | 41 | 4 | 146 | X | X | | | | X | X | | X | X | | | | X | X | X | | X | Affinities of *Trigonostylops wortmani* among SANUs |
| Avilla & Mothé (2021)[5] | 44 | 1 | 109 | X | | | | X | | | | X | X | | | | X | X | X | X | X | Interordinal affinities of SANUs |
| Kramarz & MacPhee (2022) | 44 | 1 | 109 | X | | | | X | | | | X | X | | | | X | X | X | X | X | Reply to Avilla & Mothé 2021 |
| Zimicz *et al.* (2022) | 30 | 1 | 43 | | | | | | | | X | X | X | X | X | | | | X | | | Affinities of *Kyraodus churcalensis* among SANUs |
| Püschel *et al.* (2023) | 21 | 21 | 43 | X | X | X | X[3] | | X | | | | | | | | | | | | | Affinities of *Micrauchenia saladensis* within Macraucheniidae |
| This study | 35 | 14 | 954 | X | | | X | X | X | X | X | X | X | X | X | X | X | X | X | X | | Interfamilial affinities of Litopterna |

[1]Three families assumed to be monophyletic: Proterotheriidae (probably including proterotheriids and the anisolambdids *Paranisolambda prodromus*, *Anisolambda amel*, *Anisolambda fissidens* and *Protheosodon coniferus*), Macraucheniidae (probably including *Cramauchenia normalis* and later macraucheniids) and Adianthidae (probably including *Proadiantus* and *Tricoelodus*).
[2]Only included characters of the lower dentition.
[3]Included as an outgroup.
[4]Molecular study.
[5]Study with important methodological problems, which raise questions about their conclusions. This was shown in a reply study
Abbreviations: *NT*, number of taxa; *NL*, number of uncontroversial litopterns; *NC*, number of characters; *CT*, character type; *De*, dental; *Cr*, cranial; *Po*, postcranial; *A*, Adianthidae; *An*, Anisolambdidae; *M*, Macraucheniidae; *P*, Proterotheriidae; *S*, Sparnotheriodontidae; *Pr*, Protolipternidae; *D*, Didolodontidae; *K*, Kollpaniinae; *I*, Indaleciidae; *Nt*, Notonychopidae; *Mi*, North American Mioclaenidae; *As*, Astrapotheria; *No*, Notoungulata; *X*, Xenungulata; *Py*, Pyrotheria.

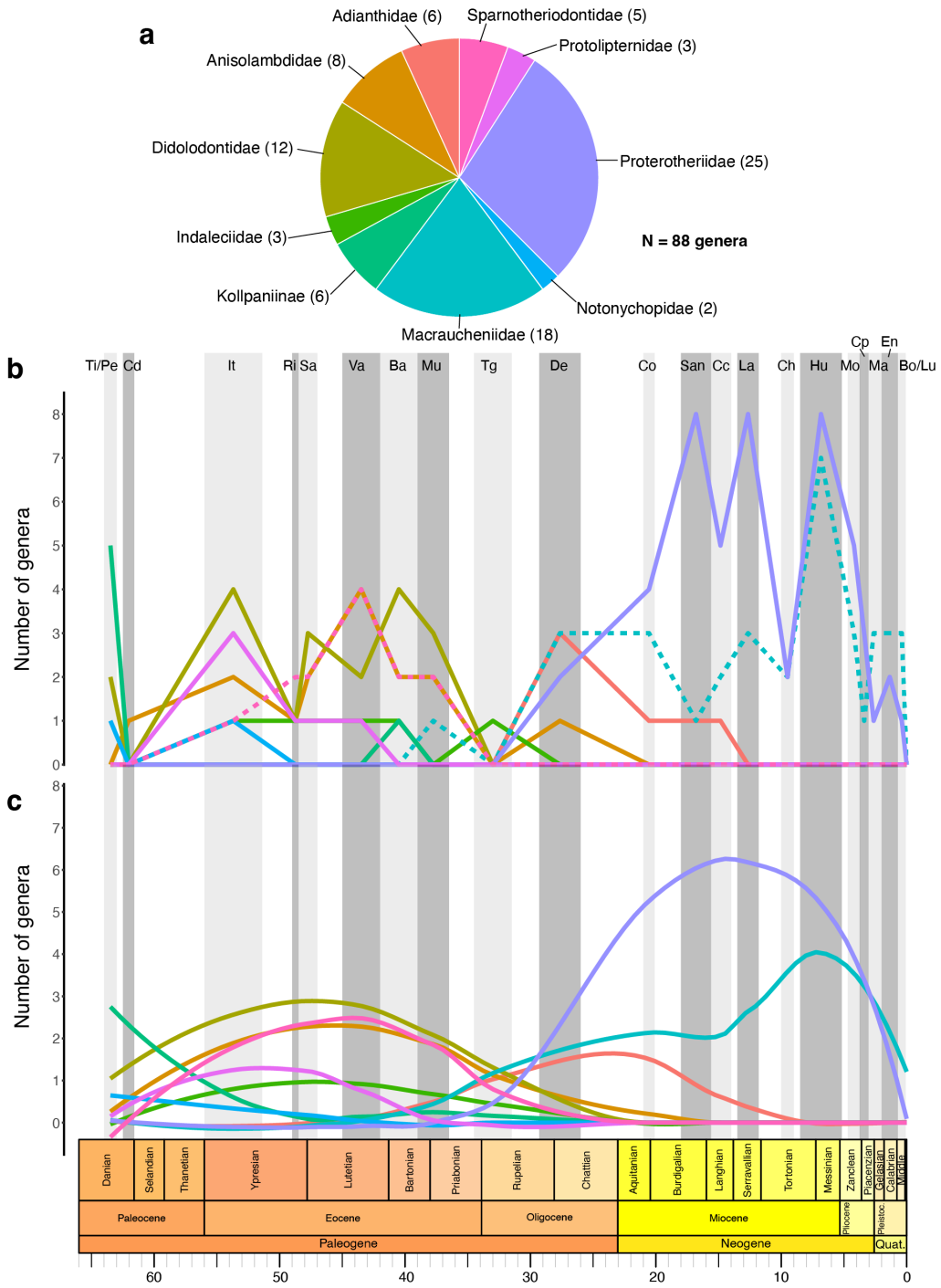



**Figure 4.2** Diversity of litoptern and associated early SANUs families expressed as the number of genera. **a**. Pie chart expressing with different the relative diversity of each family; **b**. Diversity over time of the different families of interest with colours corresponding to the families listed in **a**; **c**. same as **b** but using a smoothing function that averages the different occurrences aiding the eye in seeing patterns. In **a** the number of genera for each family is indicated next the name in between brackets. In **c** the function geom_smooth from the R package ggplot v3.4, method = loess and span = 0.5 was used. In c and d apart from the standard Periods, Epochs and Ages below, the SALMAs are indicated in grey boxes crossing the plots. The Tiupampan and Peligran SALMAs and the Bonaerian and Lujanian SALMAs are taken as only two temporal units instead of four for the plots**.** Abbreviations: *Ti/Pe*, Tiupampan and Peligran; *Cd*, *Carodnia* Zone; *It*, Itaboraian; *Ri*, Riochican; *Sa*, Sapoan; *Va*, Vacan; *Ba*, Barrancan; *Mu*, Mustersan; *Tg*, Tinguiririca n; *De*, Deseadan; *Co*, Colhuehuapian; *San*, Santacrucian; *Cc*, Colloncuran; *La*, Laventan; *Ch*, Chasicoan; *Hu*, Huayquerian; *Mo*, Montehermosan; *Cp*, Chapadmalalan; *Ma*, Marplatan; *En*, Ensenadan; Bo/Lu, Bonaerian and Lujanian.

## Families currently recognised of Litopterna and their phylogenetic relationships

### Macraucheniidae

With 18 currently accepted genera, Macraucheniidae is the second most diverse family of litopterns (Table S1 in Appendix C4 Resource 1), being particularly diverse during the Neogene alongside proterotheriids (Fig. 4.2 b-c). It was first proposed by Gervais (1855) as a member of the order Perissodactyla ("Ordre des Jumentés") to include one species, *Macrauchenia patachonica*. This taxon was discovered by Charles Darwin in 1834 (Darwin 1845) and later described by Owen (1838), being the first litoptern known to the world. Later Ameghino (1902*a*) based mostly on the position of the external nares in the cranium, subdivided this family into three subfamilies Cramaucheniinae, represented by *Cramauchenia* (Ameghino 1902*a*; Deseadan to Colhuehuapian SALMAs), Theosodontinae, represented by *Theosodon* (Ameghino 1887; Colhuehuapian to Laventan SALMAs), and Macraucheniinae, represented by *Macrauchenia* (Owen 1838; Pliocene to Holocene). Simpson (1945) reclassified Macraucheniidae into the subfamilies Macraucheniinae and Adianthinae, without giving an anatomical justification for this change. Macraucheniinae was composed of the members of the three subfamilies mentioned by Ameghino (1902*a*) and close Neogene relatives discovered since then (e.g., *Promacrauchenia* [Ameghino 1904*a*]), but also included *Paramacrauchenia* and *Victorlemoinea*, the former now considered a proterotheriid and the latter a sparnotheriodontid (Soria 2001; see Sparnotheriodontidae section for more details). The subfamily Adianthinae was composed of adianthids such as *Adianthus* (see Adianthidae section for more details). Similarly to Ameghino (1902*a*), Soria (1981) recognised important anatomical differences between macraucheniids before and after the Chasicoan SALMA (late Miocene) that justified a subfamilial division, separating Macraucheniidae into two subfamilies: Cramaucheniinae (pre the Chasicoan SALMA) and Macraucheniinae (post the Chasicoan SALMA or post Santacrucian SALMA). This separation was based in the fact that Macraucheniinae tends to have more derived features than Cramaucheniinae, possessing a nasal aperture retracted to a more centrodorsal position and fused zeugopodial elements in the forelimbs (ulna-radius) and hindlimbs (tibia-fibula; Soria 1981). However, of these two subfamilies only Macraucheniinae has been found to be monophyletic in phylogenetic analyses (Schmidt & Ferrero 2014; Forasiepi *et al.* 2016; McGrath *et al.* 2018; Püschel *et al.* 2023); Table 4.2).

Macraucheniids are clearly anatomically distinguished from the two other families, Adianthidae and Proterotheriidae. For instance, macraucheniids among other anatomical differences, lack the trilobed m3 characteristic of adianthids (Cifelli & Soria 1983*a*). Also, macraucheniids are functionally tridactyl in their fore and hind limbs, unlike proterotheriids which show a reduction (or loss) of lateral digits II and IV (Soria 2001). However, the origin of Macraucheniidae in the Palaeogene and the affinities of the family within Litopterna are still contentious topics. The oldest uncontroversial members of the family are *Coniopternium* (Ameghino 1894*a*), *Cramauchenia* (Ameghino 1902*a*) and *Pternoconius* (Cifelli & Soria 1983*b*), all with a first appearance datum (FAD) in the Deseadan SALMA (late Oligocene; Dozo & Vera 2010). These genera show dental and/or postcranial anatomical features that link them closely to later macraucheniids, like the presence of a mesolophid or crest that connects the cristid obliqua with the entoconid (=entolophid [Soria & Hoffstetter 1985]) in all or some of the lower molars. Before the Deseadan SALMA, *Polymorphis* (Roth 1899) from the Mustersan SALMA (Late Eocene) of Patagonia has been proposed as the earliest member of Macraucheniidae (Soria 1982; Cifelli 1983*a*), revalidating a previous proposal of Ameghino (1904*b*). Cifelli (1983*a*) even consider it as a member of a different subfamily, Polymorphinae, within Macraucheniidae. The key features for associating *Polymorphis* with macraucheniids are related to similarities in the upper molars, in particular in the presence of an oblique crest that connects the protocone with the metacone (Soria 1982); see also taxonomic comments in *Polymorphis* spp. section of the taxa list). In contrast, the lower molars of *Polymorphis* spp. show important differences with Deseadan SALMA macraucheniids such as the complete absence of a mesolophid. The proposal of *Polymorphis* as a macraucheniid was supported in an early computational phylogenetic analysis (Cifelli 1993; Fig. 4.1c), and since then most recent studies have considered this taxon as the earliest member of Macraucheniidae without any further testing (e.g., Dozo & Vera 2010; Croft *et al.* 2020; Table 4.2). In the same study (Cifelli 1993), Macraucheniidae was found as a sister group of Adianthidae (Macrauchenioidea), and both families closely related to Proterotheriidae (Lopholipterna; Fig 4.1c and Table 4.1c). Most additional phylogenetic studies with macraucheniids in the taxon sampling have either focused on the detailed relationships within the family (e.g., Püschel *et al.* 2022) or attempted to the determine the higher-level interordinal relationships within Placentalia (e.g., Buckley 2015) instead of the interfamilial affinities with other litopterns (Table 4.2).

Considering *Polymorphis* (Mustersan SALMA) as the first occurrence of the family and the Pliocene to Holocene *Macrauchenia* (Bond 1999; Prado et al. 2015) and the Holocene *Xenorhinotherium* (Cartelle and Lessa 1988) as the last occurrences of Macraucheniidae, the temporal interval for this family would be approximately 39.00 – 0.08 Ma (Fig. 4.2b and Table S1 in Appendix C4 Resource 1).

### Proterotheriidae

With 25 currently accepted genera, Proterotheriidae is the most diverse family of litopterns (Fig. 4.2a and Table S1 in Appendix C4 Resource 1), being particularly diverse during the Neogene alongside macraucheniids (Fig. 4.2b-c). Soria (2001) presented a major revision of this family, so in order to avoid unnecessary repetition, only the most important taxonomical aspects and the main advances since his revision are discussed here. Proterotheriidae was founded by Ameghino (1887) with the description of the genera *Proterotherium*, *Thoatherium*, *Diadiaphorus*, and *Licaphrium*. Simpson (1945) subdivided this family into two subfamilies, Polymorphinae and Proterotheriinae, the former including taxa mostly from the Palaeocene and Eocene (Peligran to Mustersan SALMAs) and the later the taxa since the late Oligocene (Deseadan SALMA). Even though this classification was followed by other authors (e.g., Lavocat 1958; Paula Couto 1979*a*), Simpson (1948) did not employ this subfamilial division and just used the family Proterotheriidae, without giving any explanation of this omission. Later Odreman-Rivas (1969) modified the subfamily Polymorphinae from Simpson (1945) keeping *Polymorphis* (including *Polyacrodon ligatus* [Roth 1899] and *Heteroglyphis* [Roth 1899]), and excluding the rest of the taxa such as genera now considered anisolambdids, namely *Wainka* (Simpson 1935) and *Anisolambda* (Ameghino 1901; including *Ricardolydekkeria* [Ameghino 1901] and *Josepholeidya* [Ameghino 1901]) and the didolodontid *Xesmodon* (Berg 1899). Cifelli (1983*a*) subdivided the family Proterotheriidae into two subfamilies, Anisolambdinae and Proterotheriinae, the former subfamily including mostly anisolambdids (see Anisolambdidae section for more details), and the latter the original definition of Simpson (1945). In addition, Cifelli (1983*a*), excluded the subfamily Polymorphinae from Proterotheriidae, placing it instead within the family Macraucheniidae (see Macraucheniidae section for more details). Soria (2001) later removed the subfamily Anisolambdinae from Proterotheriidae elevating its rank as a distinct family (see Anisolambdid section for more details), which leaves the concept of Proterotheriidae very similar to the subfamily Proterotheriinae from Simpson (1945), although with various new additions to the family since then (e.g., Corona *et al.* 2020; McGrath *et al.* 2020*a*).

Proterotheriidae has been included by some authors as part of Suborder Lopholipterna (Cifelli 1983*a*; Soria 2001; Table 4.1) which also includes the families Adianthidae and Macraucheniidae, a hypothesis that later found phylogenetic support (Cifelli 1993; Fig. 4.1c). Since then, most phylogenetic studies that included proterotheriids have focus either on resolving the affinities within Proterotheriidae (e.g., McGrath *et al.* 2020*b*) or studying interordinal relationships between SANUs (e.g., Macphee *et al.* 2021) instead of phylogenies looking at the interfamilial affinities of proterotheriids with other litopterns (Table 4.2).

Following Soria's (2001) concept of the family, the earliest proterotheriid is *Lambdaconus suinus* (Ameghino 1897) from different localities from Chubut, Sarmiento Formation, Argentina (Deseadan SALMA) and the last is *Neolicaphrium recents* from the late Pleistocene-Holocene from different localities in Argentina, Brazil and Uruguay (Gaudioso *et al.* 2017), giving a temporal interval of approximately 29.3 – 0.08 Ma for this family (Fig. 4.2b and Table S1 in Appendix C4 Resource 1).

### Adianthidae

Adianthidae currently includes six genera, being considerably less diverse than proterotheriids and macraucheniids during the Neogene (Fig. 4.2 and Table S1 in Appendix C4 Resource 1). Cifelli & Soria (1983*a*) did a major detailed revision of this family, so in order to avoid unnecessary repetition, only the most relevant taxonomic aspects are here discussed, along with the main advances since their revision. Known as the pygmy litopterns because of their reduced size, the family Adianthidae was founded by Ameghino (1891*a*) to place *Adianthus bucatus* (Santacrucian to Colloncuran SALMAs). Among other distinct anatomical features, they possess a trilobed m3 and enamel fossettes in P4-M3 formed by hypertrophied conular cristae (Cifelli & Soria 1983*a*). Following new fossil discoveries, Ameghino (1906) recognised three additional genera to the family Adianthidae: the Deseadan SALMA *Proadiantus* (Ameghino 1897) and *Tricoelodus* (Ameghino 1897), and the Barrancan to Tinguiririca SALMA *Pseudadiantus* (Ameghino 1901), the latter later excluded from the family and formally synonymized with the notopithecine interatheriid *Antepithecus* (Simpson 1967).

Bordas (1939) added the Colhuehuapian SALMA *Proheptaconus* (Bordas 1936) to what he considered the subfamily Adianthinae, a subfamily of Macraucheniidae, which was followed by other authors (Patterson 1940; Simpson & Minoprio 1949). However, Simpson *et al.* (1962) later changed this view and restored the family Adianthidae, but now including a

new taxon, *Adiatoides leali* (Simpson & Minoprio 1949) from the Divisadero Largo Formation, Argentina (Vacan to Barrancan SALMAs). Bond & Vucetich (1983) added to Adianthidae *Indalecia grandensis* from the Lumbrera Formation, Argentina (Itaboraian to Sapoan Fauna SALMAs), based on unique shared anatomical features with *Adiatoides leali* such as the absence of a postprotocrista connecting the protocone with the metaconule and a strong parastyle in M1-M2. These features are not present in other adianthids, so they grouped them in the new subfamily Indaleciinae keeping both species tentatively within the family Adianthidae, which was later followed with doubts by Cifelli & Soria (1983*a*). In the same work, Cifelli & Soria (1983*a*) added the genus *Thadanius* from the Deseadan SALMA of Bolivia to the family Adianthidae.

Cifelli (1983*a*) revisited the members of the family, and included *Proectocion* (previously considered a didolodontid by Simpson [1948]), as the earliest member of Adianthidae based on dental similarities. In addition, he proposed a new superfamily called Macrauchenioidea, to group adianthids and macraucheniids based on dental similarities such as an absent paraconid and the presence of a paralophid in the lower molars (Table 4.1). Soria (1984*a*), based on dental similarities with "amilnedwarsids", elevated the rank of the subfamily Indaleciinae to the family Indaleciidae, and later Soria (1989*a*) classified them as a family of the order Notopterna (see sections of Amilnedwardsiidae and the order Notopterna, and family Indaleciidae). Adianthidae has also been considered by some authors as part of Suborder Lopholipterna (Cifelli 1983*a*; Soria 2001) which includes the families Macraucheniidae and Proterotheriidae (Table 4.1), an hypothesis that later found phylogenetic support (Cifelli 1993; Fig. 4.1c). In the same study (Cifelli 1993), Macrauchenioidea was also supported, but only when indaleciids are excluded. Strikingly, there has not been a single study looking at the phylogenetic relationships within Adianthidae using modern phylogenetic methods, and most recent phylogenetic studies have include adianthids as outgroups for phylogenies of Macraucheniidae (e.g., Forasiepi *et al.* 2016; Table 4.2).

If we follow Cifelli (1983*a*) and consider *Proectocion* from the Barrancan SALMA of Argentina as the earliest member of Adianthidae and consider *Adianthus* from the Santacrucian and "Friasian" SALMAs of Argentina and Chile as the last member of this family (Cifelli 1991), the family Adianthidae encompasses a temporal interval of 42 – 14 Ma (Fig. 4.2b and Table S1 in Appendix C4 Resource 1).

### Sparnotheriodontidae

Sparnotheriodontidae has currently has five accepted genera, all with a fossil record exclusively in the Palaeogene (Fig. 4.2 and Table S1 in Appendix C4 Resource 1). The family Sparnotheriodontidae was initially proposed by Soria (1980*a*) to include *Sparnotheriodon epsilonoides* from Cañadon Vaca (Vacan SALMA), as was classified as *incertae sedis* within the order Notoungulata. The family was later removed from Notoungulata and incorporated to the order Litopterna, being expanded by Soria (1980*b*) by adding the genera *Victorlemoinea* (Ameghino 1901) and *Phoradiadus* (Simpson *et al.* 1962). *Victorlemoinea* was previously considered an early macraucheniid (Simpson 1945, 1948) and *Phoradiadus* was previously considered with doubts as a proterotheriid (Simpson *et al.* 1962). Soria's (1980*b*) grouping was based on shared similarities in the upper and lower molars such as the presence of a lophoid metaconule and a closed trigon basin in M2. *Phoradiadus* includes one species, *Phoradiadus divortiensis*, from Divisadero Largo Formation, Mendoza, Argentina (Vacan to Barrancan SALMAs; Woodburne *et al.* 2014*a*).

Simpson (1948) tentatively accepted three valid Patagonian species of the genus *Victorlemoinea* (Riochican to Vacan SALMAs; Woodburne *et al.* 2014*a*) previously named by Ameghino (1901), *V. labyrinthica*, *V. emarginata* and *V. longidens*, as they were represented only by isolated teeth, in the first two being represented by upper teeth, and in the latter by lower teeth. This means that *V. longidens* could potentially correspond to teeth from the lower dentition of either *V. labyrinthica* or *V. emarginata*, in particular the mandible fragment with m1-m2 of the holotype of *V. longidens* (MACN A-10670), as the allegedly associated premolars of this specimen seem to correspond to an isotemnid notoungulate (Bond *et al.* 2006). From the genus *Victorlemoinea*, Bond *et al.* (2006) only included *V. labyrinthica* in their list of formally recognised sparnotheriodontid species, and more recently some authors (e.g., Reguero *et al.* 2014; Gelfo 2016; Gelfo *et al.* 2019) have mentioned only *V. labyrinthica* for the Riochican and Vacan Patagonian faunas, omitting *V. emarginata* and *V. longidens*, which can be interpreted as implicitly synonymising them with *V. labyrinthica*. In addition, there is one *Victorlemoinea* species from Itaboraí, Brazil, *V. prototypica* (Paula Couto 1952; Itaboraian SALMA), also known mostly from dental material.

Cifelli (1983*b*) tentatively assigned some tarsals (i.e., calcaneum and astragalus) to *V. prototypica*, based on their relative size and abundance. These tarsals were large and scarce, so considering linear regressions with the dentition (m2 area) it could only correspond to either

the sparnotheriodontid *V. prototypica* or the didolodontid *Lamegoia conodonta*. Considering the similarities of the tarsals assigned to *V. prototypica* and others indirectly assigned to didolodontids, such as presenting a medial malleolar facet of astragalus extending onto the neck and the presence of a dorsal beak on the distal end of the calcaneum, Cifelli (1983*a*) grouped Sparnotheriodontidae and Didolodontidae under the superfamily Didolodontoidea in the order Condylarthra (Table 4.1). This hypothesis found some phylogenetic support (Cifelli 1993; Bergqvist 1996; Fig. 4.1c), and has been followed by some authors (e.g., Bergqvist 2008). However, other authors have questioned the indirect anatomical assignment of these tarsals to *V. prototypica* (e.g., Hoffstetter & Soria 1986; Soria 2001; Lorente 2015), and even suggested an affinity of these tarsals with Notoungulata (Soria 2001) or with Astrapotheria (Lorente 2015).

Among the different litoptern families, Soria (2001) considered that sparnotheriodontids were more closely related to the family Anisolambdidae due to overall dental similarities between both families, and also considering an isolated M1 (MNRJ 1479-V) from Itaboraí showing an intermediate anatomy between sparnotheriodontids and anisolambdids. Therefore, he created the suborder Eolitopterna to include both families (Table 4.1). In addition, Soria (2001) tentatively added *Heteroglyphis dewoletzky* (Roth 1899) to Sparnotheriodontidae without any detailed anatomical justification; this species is known from a broken upper molar probably from Cerro del Humo, Argentina (Mustersan SALMA). This taxon was previously referred to Proterotheriidae by Simpson (1948).

More recently, one genus and two new species from the lower Eocene La Meseta and Submeseta formations, Antarctica, have been added to the family Sparnotheriodontidae: *Notiolofos arquinotiensis* (Bond *et al.* 2006) and *Notiolofos regueroi* (Gelfo *et al.* 2017). They are differentiated mainly by their size and represented by isolated teeth (the latter species only by m3; Gelfo *et al.* 2019). *Notiolofos arquinotiensis* is particularly interesting as it is the most abundant land mammal in the Palaeogene of the La Meseta and Submeseta formations, presenting a continuous fossil record of at least 17.5 Ma (55.3 – 37.8 Ma), which has been interpreted as a case of morphological stasis (Gelfo 2016). The presence of the sparnotheriodontid *Notiolofos* in Antarctica raises important biogeographic questions, as no other litoptern lineage seems to have crossed to Antarctica, and among SANUs excluding *Notiolofos*, only the astrapothere *Antarctodon sobrali* (Bond *et al.* 2011) has been found on this continent so far.

Apart from early phylogenetic studies (Cifelli 1993; Bergqvist 1996; Bonaparte & Morales 1997; Fig. 4.1c-d), most recent phylogenetic studies have included one sparnotheriodontid in analyses that include a wide sample of different SANUs (e.g., Gelfo *et al.* 2008; Table 4.2) instead of solving their interfamilial relationships with other litopterns. In terms of the phylogenetic affinities within Sparnotheriodontidae, there is currently only one phylogenetic study that used a small taxon and character sample (Reguero *et al.* 2014; Table 4.2).

The earliest accepted member of Sparnotheriodontidae is *Victorlemoinea* with records in Argentina and Brazil (Itaboraian to Vacan SALMAs) and the last could be either *Notiolofos* from Antarctica (temporally equivalent to Riochican to Mustersan SALMAs) or *Heteroglyphis* from Argentina (Mustersan SALMA), giving a temporal interval of 56.0 – 36.5 Ma to this family (Fig. 4.2b and Table S1 in Appendix C4 Resource 1).

### Anisolambdidae

Anisolambdidae is currently represented by eight genera mostly with a Palaeogene distribution (Fig. 4.2 and Table S1 in Appendix C4 Resource 1). The family Anisolambdidae was proposed by Soria (2001) who elevated the rank of the subfamily Anisolambdinae. This subfamily was previously proposed by Cifelli (1983*a*) to group what he considered early members of the family Proterotheriidae with records in the early Eocene (Itaboraian SALMA) such as *Anisolambda* Ameghino (1901), distinctive from more derived proterotheriids (subfamily Proterotheriinae; Table 4.1). Anisolambdinae stands out for the presence of a strong paralophid ending in a large and distinct paraconid. Anisolambdinae (currently Anisolambdidae) and Proterotheriinae (currently Proterotheriidae) share a molarized P4 (P3 in Cifelli 1983*a*; see Methods section for tooth position criteria) with a well-developed metacone and mesostyle present, among other features. To a certain extent, Cifelli's (1983*a*) proposal was similar to previous arrangements (Simpson 1945, 1948). However, Simpson (1945, 1948) included anisolambdids in the subfamily Polymorphinae, a subfamily that also included the late Eocene (Mustersan SALMA) *Polymorphis* (Roth 1899), a taxon later included in Macraucheniidae (Cifelli 1983*a*; Soria 2001). In addition, Cifelli (1983*a*) renamed an anisolambdid from the early Eocene of Itaboraí, Brazil (Itaboraian SALMA) as *Paranisolambda prodromus* (previously known as *Anisolambda prodromus* (Paula Couto 1952), based on some dental differences with *Anisolambda* such as the absence of a postentocristid in m3, among other dental characters. Based on previous observations (Simpson

1948; Paula Couto 1952) and comparisons with *Paranisolambda*, Cifelli (1983*a*) synonymised the anisolambdids *Josepholeidya* and *Ricardolydekkeria*, taxa based on isolated upper teeth, with *Anisolambda*, which was based only on lower dentition. In addition, Cifelli (1983*a*) included *Wainka tshotshe* from Río Chico (Riochican SALMA), to the subfamily Anisolambdidae based on an m3 with an overall structure very similar to *Anisolambda*. *W. tshotshe* was previously assigned tentatively to Proterotheriidae (Simpson 1948).

Apart from elevating the rank of this subfamily to the family Anisolambdidae, Soria (2001) mostly followed Cifelli's (1983*a*) interpretations. However, Soria (2001) removed *Xesmodon* (Berg 1899) and *Heteroglyphis* (Roth 1899) from the family tentatively placing them in Didolodontidae and Sparnotheriodontidae respectively, as they showed important differences in their dentition compared to other anisolambdids. He also added *Lambdaconops* (Soria 2001) to Anisolambdidae due to close dental similarities to the late Oligocene (Deseadan SALMA) anisolambdid *Protheosodon coniferus* (Ameghino 1897), the latter being the only member of this family with associated tarsal remains (Loomis 1914). The validity of the different species of *Anisolambda* was not evaluated by Soria (2001). In addition, Soria (2001) erected the suborder Eolitopterna, to include the families Anisolambdidae and Sparnotheriodontidae due to overall dental similarities between both families (more details in Sparnotheriodontidae section; Table 4.1). Most recent authors have followed Soria's (2001) taxonomic proposal for Anisolambdidae (e.g., Gelfo 2006; Croft *et al.* 2020).

Early studies examining the interfamilial relationships of Litopterna assumed a monophyletic Proterotheriidae that included anisolambdids, without testing this hypothesis (Cifelli 1993; Bonaparte & Morales 1997); Fig. 4.1c-d). More recently, in phylogenetic studies evaluating phylogenetic affinities within Proterotheriidae including some anisolambdids as outgroups, anisolambdids were recovered nested within Proterotheriidae (McGrath *et al.* 2020*a*, *b*; Table 4.2). However, as not all families of litopterns were included in these analyses, the interfamilial affinities of anisolambdids remain to be tested. In addition, to this date there has been no study examining the phylogenetic relationships within Anisolambdidae.

The earliest accepted member of Anisolambdidae is *Wainka tshotshe* (Simpson 1935) from Cerro Redondo, Chubut, Argentina (Carodnia Zone) and the last is *Protheosodon coniferus* from Cabeza Blanca, Chubut, Argentina (Deseadan SALMA), giving a temporal interval of 62.5 – 26.0 Ma for this family (Fig. 4.2b and Table S1 in Appendix C4 Resource 1).

## Families of SANUs with controversial affinities and that are sometimes placed within Litopterna

### Didolodontidae

Didolodontidae currently includes 10 genera (or 12 if we include two unnamed genera [Tejedor *et al.* 2009]) with an exclusive Palaeogene distribution (Fig. 4.2b and Table S1 in Appendix C4 Resource 1). There has been recent major detailed revision of this family (Gelfo 2006, 2010), so in order to avoid unnecessary repetition, only the most relevant taxonomic aspects are here discussed, along with the advances since these revisions. The family Didolodontidae was proposed by Scott (1913) to classify a group of bunodont "condylarths" (see "Condylarthra" section) endemic to South America with a Palaeogene fossil record consisting mostly of isolated teeth. Initially, Ameghino (1897) described the first know Eocene didolodontid species *Didolodus multicuspis* as a phenacodontid. Osborn (1910) identified additional South American taxa as "Condylarthra" *incertae sedis* such as *Notoprotogonia* (Ameghino 1904*a*; later synonymised with *Ernestokokenia* [Simpson 1948]), *Lambdaconus* (Ameghino 1897; later considered an early proterotheriid [Soria 2001]), and *Proectocion* (Ameghino 1904*b*; later considered an early adianthid [Cifelli 1983*a*]). Scott (1913) later grouped these four taxa as part of the family Didolodidae within the order Litopterna (Table 4.1). Simpson (1934) subsequently corrected it to Didolodontidae, and grouped them again within "Condylarthra". After adding two new species from the Rio Chico formation (latest Danian–late Lutetian in age [Krause *et al.* 2017]) of the genus *Ernestokokenia* (*E. yirunhor* and *E. chaishoer*; Simpson 1935), Simpson (1948) revised the whole group giving new definition for Didolodontidae and emending many of Ameghino's (1906) taxonomic classifications of the Patagonian taxa, including the following genera in the family: *Didolodus*, *Ernestokokenia*, *Argyrolambda* (Ameghino 1904*a*), *Paulogervaisia* (Ameghino 1901), *Proectocion*, *Enneoconus* (Ameghino 1901), *Asmithwoodwarsia* (Ameghino 1901) and *Archaeohyracotherium* (Ameghino 1906). He soon recognised the close similarities between this group and North American "condylarths" including species of phenacodontid and mioclaenid, stating that they were impossible to separate on a pure morphological basis (Simpson 1948, 1980).

Paula Couto (1952) added two species of *Ernestokokenia* (*E. protocenica* and *E. parayiruhnor*) and the new genus *Lamegoia* from fissure fills in the Itaboraí Formation, Brazil (Itaboraian SALMA) to the family Didolodontidae. McKenna (1956) added *Megadolodus*

*molarijformis* from La Venta, Colombia (Laventan SALMA), which Cifelli & Villarroel (1997) later considered to be a bunodont proterotheriid. Paula Couto (1978*b*) added *Asmithwoodwardia scotti* from Itaboraí to the family, a taxon that he previously classified within the North American "Condylarthra" family Hyopsodontidae based on dental similarities (Paula Couto 1952). In a revision of the family Didolodontidae, (Cifelli 1983*a*) based on an indirect tarsal association, removed *Ernestokokenia parayirunhor* (renamed as *Miguelsoria parayirunhor*) and *Asmithwoodwardia scotti* from Didolodontidae and placed them in Litopterna (see Protolipternidae section for more information). This tarsal association was based on the fact that the relative size and abundance of these tarsals in the Itaboraí sites was what you would expect for the size and abundance of the dentition of *Miguelsoria parayirunhor* (Cifelli 1983*b*). Cifelli (1983*a*) reclassified *Ernestokokenia protocenica* as *Paulacoutoia protocenica* (now known as *Ricardocifellia protocenica* [Mones 2015]) because of preoccupation) because he considered it was distinct enough from the genus *Ernestokokenia*. According to Cifelli (1983*a*), didolodontids are characterised by having a primitive dentition very similar to mioclaenids, but possessing a hypocone on $M^3$ (absent in mioclaenids) and a primitive ankle structure similar to many South and North American "condylarths" (i.e., the astragalar facet for the medial malleolus is enlarged anteriorly and the calcaneal cuboid facet is dorsally expanded). Soria (2001), based on dental features, removed *Xesmodon* (Berg 1899) from Anisolambdidae and placed it within Didolodontidae.

In an detailed revision of Didolodontidae, Gelfo (2006) synonymised *Argyrolambda* with *Didolodus*, *Archaeohyracotherium* with *Asmithwoodwardia*, and *Enneoconus* with *Ernestokokenia* thus reducing the total number of valid didolodontid genera. Later, Gelfo (2007) based on dental similarities and a phylogenetic analysis, added *Escribania chubutensis* and *Raulvaccia peligrensis* from Punta Peligro, Argentina (Peligran SALMA) to Didolodontidae. *E. chubutensis* and *R. peligrensis* were previously classified within the "condylarth" North American family Mioclaenidae (Bonaparte *et al.* 1993). The most recent generic additions to Didolodontidae have been *Umayodus* (Gelfo & Sigé 2011) from Lower Muñani Formation (Itaboraian SALMA?), Peru and *Saltaodus* (Gelfo *et al.* 2020*b*) from the Lumbrera Formation (Itaborarian SALMA?), both of uncertain age (Gelfo & Sigé 2011; Zimicz *et al.* 2022).

In terms of the phylogenetic affinities of Didolodontidae, early phylogenetic analyses found a close relationship between didolodontids and sparnotheriodontids (Cifelli 1993; Bergqvist 1996; Fig. 4.1c), but these were based on tarsal associations that have been

questioned by later authors (e.g., Soria 2001; Gelfo & Sigé 2011; see also Sparnotheriodontidae and Protolipternidae sections). Muizon and Cifelli (2000), in a phylogenetic analysis that included North American mioclaenids, South American kollpanines, didolodontids and protolipternids, found that protolipternids were nested within Didolodontidae and that both groups together formed the sister group of kollpanines, a result that was also found in a later study (Gelfo 2006). This means that Didolodontidae excluding Protolipternidae is a paraphyletic group. Other phylogenetic studies that have included didolodontids in very small matrices have focused on their internal relationships, assuming their monophyly (e.g., Gelfo 2010; Table 4.2). When didolodontids have been included with a limited taxon sample (i.e., usually *Didolodus*) in broader analyses that include other SANUs, they have been found in a branch at the stem of some NA "condylarths" and other SANUs (e.g., Billet *et al.* 2015), or in a basal position in Laurasiatheria as a the sister group of Protolipternidae (O'Leary *et al.* 2013). When a larger sample of didolodontids has been included, they have found at the stem of litopterns but not forming a monophyletic Didolodontidae (Kramarz *et al.* 2021), or as a paraphyletic group among SANUs and North American "condylarths" (Zimicz *et al.* 2022). In sum, there is still a considerable uncertainty in the phylogenetic position of didolodontids and their relationship among SANUs, and whether they form a monophyletic group or not. In fact, there has not been any phylogenetic analysis that includes didolodontids alongside representatives of all litoptern families, protolipternids and the different SANUs' orders (Table 4.2). Part of the problem of resolving the didolodontids affinities is that their fossil record is limited mostly to dental remains. Nonetheless, recently some authors have started to consider the family Protolipternidae as a junior synonym of Didolodontidae, and Didolodontidae as a family of litopterns, but without any phylogenetic analysis supporting this new arrangement (Gelfo *et al.* 2016, 2020*b*; Croft & López 2020; see more in Protolipternidae section).

The earliest accepted members of Didolodontidae are *Escribania chubutensis* and *Raulvaccia peligrensis* from Punta Peligro, Argentina (Peligran SALMA) and the last would be *Ernestokokenia*, *Paulogervasia* and *Xesmodon* from different Patagonian localities of Mustersan SALMA age (Gelfo 2006, 2007, 2010), which gives a temporal interval to this family of 63.8 – 36.5 Ma (Fig. 4.2b and Table S1 in Appendix C4 Resource 1).

### Protolipternidae

Protolipternidae currently includes three genera (or two if we excluded *Asmithwoodwardia* as [Gelfo 2006] suggested) with an exclusively Palaeogene distribution

(Fig. 4.2 and Table S1 in Appendix C4 Resource 1). This family was proposed by Cifelli (1983*a*) to classify specimens from Itaboraí (Itaboraian SALMA) with bunodont didolodontid-like dentition and litoptern-like tarsals. The tarsals show specialisations that among SANUs are only present in litopterns, which include a spool-shaped astragalar body and a posterior astragalocalcaneal facets that allows rapid flexion of the crurotarsal joint (Cifelli 1983*a*). The taxonomic changes generated from this familiar proposal included the consideration of *Victorlemoinea prototypica* (a former litoptern [Paula Couto 1952]) as a "condylarth" closely related to didolodontids, and *Miguelsoria parayirunhor* (former didolodontid *Ernestokokenia parayirunhor* [Paula Couto 1952]) with *Asmithwoodwardia scotti* (a former didolodontid [Paula Couto 1978*b*]) as litopterns. Cifelli (1983*a*) grouped the latter two, plus a new species *Protolipterna ellipsodontoides*, within this family. However, the tarsals referred to *Protolipterna ellipsodontoides* and *Miguelsoria parayirunhor* were not found in association with their alleged dentition, being assigned indirectly by their relative size, abundance and expected morphology (Cifelli 1983*b*). Some authors have accepted this interpretation (e.g., Cifelli 1985, 1993; Muizon & Cifelli 2000; Bergqvist 2008), although others have questioned it (Hoffstetter & Soria 1986; Soria 2001; Gelfo 2010; Gelfo & Sigé 2011; Gelfo & Lorente 2012; Lorente 2015). For example, Soria (2001) suggested that the astragali and calcanea attributed by Cifelli (1983*b*) to didolodontids were most likely notoungulate elements. Indeed, a study that indirectly assigned isolated petrosals to the protolipternid *Miguelsoria* from Itaboraí failed to recover a monophyletic Litopterna when younger and better known litopterns (e.g., *Macrauchenia* & *Diadiaphorus*) were included (Billet *et al.* 2015). Considering that recent association models do not discard the association of litoptern-like tarsals to protolipternids (Lorente 2015) made by Cifelli (1983*b*), some authors have started to consider the family Protolipternidae as a junior synonym of Didolodontidae (Gelfo *et al.* 2016, 2020*b*; Croft & López 2020). This is problematic because this proposal has not been tested empirically with phylogenetic analyses. It is likely that the tarsal controversy would be resolved only when directly associated postcranial elements of these early SANUs are found alongside dental elements as previous authors have suggested (e.g., Gelfo & Sigé 2011). In addition, based on anatomical observations and a phylogenetic analysis, Gelfo (2006) considered that *Asmithwoodwardia scotti* should be generically renamed as is it not recovered as a sister taxon of the Patagonian *Asmithwoodwardia subtrigona* (Ameghino 1901).

Apart from early phylogenetic studies that found protolipternids closely related to other litopterns based on Cifelli's (1983*b*) tarsal associations (Cifelli 1993; Bergqvist 1996; Fig.

4.1c), other phylogenetic studies including protolipternids and didolodontids have usually failed to find them as distinctly separate groups (e.g., Muizon & Cifelli 2000); see also Didolodontidae section). Other phylogenetic studies with a wide taxon sampling have found Protolipternidae in a basal position in Laurasiatheria as a sister group of Didolodontidae (O'Leary *et al.* 2013), closely related to other more derived litopterns than to other SANUs (Muizon *et al.* 2015), among didolodontids at the at the stem of litopterns but not forming a monophyletic group (Kramarz *et al.* 2021), and forming a monophyletic group associated to a polytomy that includes didolodontids, sparnotheriodontids, indaleciids and North American phenacodontids (Zimicz *et al.* 2022). However, so far there has not been any phylogenetic analysis that includes protolipternids alongside representatives of all litoptern families, didolodontids and the different SANU orders (Table 4.2).

If we follow (Cifelli 1983*a*) and consider Protolipternidae as a valid family their earlier members are *Protolipterna* e*llipsodontoides*, *Miguelsoria parayirunhor* and *Asmithwoodwardia scotti* from Itaboraí, Brazil (Itaboraian SALMA), and the last member would be *Asmithwoodwardia subtrigona* with its last records in Cañadón Vaca, Argentina (Vacan SALMA; Gelfo 2006), which gives the family a temporal interval of 56 – 42 Ma (Fig. 4.2b and Table S1 in Appendix C4 Resource 1).

### Amilnedwardsiidae and the order Notopterna

Amilnedwardsiidae was founded preliminarily by Soria (1984*b*) and better justified in a later article (Soria 1989*a*). It is based on two genera (i.e., *Amilnedwarsia* and *Rutiyemeria*) and three species named after small bunodont isolated upper molars whose positions were assigned tentatively by Soria (1989*a*) by comparing them with the indaleciid *Indalecia grandensis*. Amilnedwardsiidae was considered to be the most basal family of the order Notopterna (Soria 1989*a*), which also includes the families Indaleciidae and Notonychopidae (Soria 1989*b*). Notopterna is defined by a well-developed and buccally projected parastyle and the absence of mesostyle in the upper molars, bicrescentic and selenodont lower molars, and anteriorly acuminate petrosals, among other anatomical features that distinguish them from other SANUs (Soria 1989*a*). Soria (1989*a*, *b*) argued that considering their dental similarities, "amilnedwarsids" could be the structural ancestor of both indaleciids and notonychopids. However, a phylogenetic analysis failed to recover the members of Notopterna as a monophyletic group (Bonaparte & Morales 1997), which has led to some authors to include its members tentatively within Litopterna (e.g., Gelfo *et al.* 2016; Croft *et al.* 2020; Goin *et al.*

2022). However, this is a problematic assumption as Bonaparte & Morales (1997) used a matrix that includes only litopterns, so the broader relationships of notopterns has not yet been tested in an analysis that includes other SANUs such as notoungulates and astrapotheres.

*Amilnedwardia* and *Rutimeyeria* were previously referred tentatively to the family Macraucheniidae and regarded as close to *Victorlemoinea* (Simpson 1945, 1948), although the latter now is now consider to be part of the family Sparnotheriodontidae. Cifelli (1983*a*) considered referred specimens of these taxa to be too fragmentary to allow the determination of a clear affinity, but suggested the referred specimens represent deciduous teeth of a henricosborniid notoungulate based on the presence of a metaconule-derived crest connecting with the ectoloph wall. Indeed, probably due to their limited fossil record, so far, no members of this family have ever been included in a phylogenetic analysis.

If we consider Amilnedwardsiidae to be a valid family, as its three species all come from Patagonian fossil localities of a similar age (Vacan SALMA), the temporal interval of this family is ~ 45 – 42 Ma (Fig. 4.2b and Table S1 in Appendix C4 Resource 1).

### Notonychopidae

Notonychopidae currently includes two accepted genera with an exclusively Palaeogene distribution (Fig. 4.2 and Table S1 in Appendix C4 Resource 1). Notonychopidae was founded to include *Notonychops powelli* from the Rio Loro Formation (age uncertain, although probably pre-Itaboraian SALMA age [Gelfo *et al.* 2020*a*], an ungulate with great development of the parastyle in M1-M3, which among other features, makes it anatomically distinctive from any other SANU previously described (Soria 1989*b*). Soria (1989*b*) considered that *N. powelli* was dentally convergently similar to members of the family Esthonychidae (Tillodonta), particularly with the lower molars being brachydont and selenodont with a subequal trigonid and talonid length. However, *N. powelli* shares important anatomical features with the dentition of "amilnedwarsids" and indaleciids, and of the ear region with indaleciids, which made Soria (1989b) place it within the order Notopterna (see Amilnedwardsidae and the order Notopterna section for more details). Key differences between notonychopids with indaleciids are the absence of enamel fossettes in P2-M3 and a greater development of the parastyle in the former, among other features (Soria 1989*b*). McKenna and Bell (1997) later classified Notonychopidae as a family within the order Litopterna albeit without any justification (Table 4.1). Bonaparte and Morales (1997) added to the Notonychopidae the taxon *Requisia vidmari* from Punta Peligro (Peligran SALMA) which they found it to be

phylogenetically close to *Wainka tshotshe* (Fig. 4.1d). However, since this analysis, an isolated m3 previously assigned to *Requisia vidmari* by Bonaparte & Morales (1997) has been called into question considering its bunodont features and how low and different its cristids are to what would be expected for a notonychopid, in particular in the talonid area (Goin *et al.* 2022).

Bonaparte & Morales (1997) failed to find a monophyletic Notonychopidae, as *N. powelli* and *R. vidmari* were not found closely related in their phylogeny (Fig. 4.1d). In addition, as notonychopids were found nested within Litopterna, most authors now consider them litopterns (e.g., Gelfo *et al.* 2016; Croft *et al.* 2020; Goin *et al.* 2022), which is problematic given Bonaparte & Morales (1997) used a matrix that includes exclusively litopterns and did not test alternative relationships. Since the early phylogenetic study of Bonaparte & Morales (1997), there has not been any attempt to test the monophyly of Notonychopidae and to resolve its position among litopterns and other SANUs (Table 4.2).

As the only two known members of Notonychopidae are the Peligran SALMA *R. vidmari* and the potentially pre-Itaboraian SALMA *N. powelli*, the temporal interval of this family is not well constrained with a current range of ~63.8 – 51.4 Ma, and is likely much narrower in range (Fig. 4.2b and Table S1 in Appendix C4 Resource 1).

### Indaleciidae

Indaleciidae currently includes three accepted genera with an exclusive Palaeogene distribution (Fig. 4.2 and Table S1 in Appendix C4 Resource 1). Indaleciidae was initially proposed by Soria (1984*a*) and better justified in a later article (Soria 1989*a*), in which he elevated the rank of the previously proposed subfamily Indaleciinae, which included *Indalecia grandensis* and *Adiantoides leali* (Bond & Vucetich 1983). Previously, *A. leali* from Divisadero largo Formation, Argentina (Vacan to Barrancan SALMAs [Woodburne *et al.* 2014*b*]) was placed tentatively in Adianthidae given dental similarities with the adianthid *Adianthus* (Simpson & Minoprio 1949; Simpson *et al.* 1962). Later, Bond and Vucetich (1983) described *Indalecia grandensis* from the Lumbrera Formation, Argentina (temporally equivalent to Itaboraian SALMA to Sapoan Fauna; [Fernicola *et al.* 2021]) that showed dental similarities with *Adiantoides leali* such as a buccolingually transverse crest connecting the hypocone with the metaconule, and the absence of a postprotocrista connecting the protocone with the metaconule on M1-M2, among other features that justified the proposal of a subfamily Indaleciinae within Adianthidae. Cifelli and Soria (1983*a*) tentatively followed Bond and Vucetich (1983) considering the shared presence of fossettes formed by hypertrophied conular

cristae in the upper molars in members of Indaleciinae and typical adianthids. However, they also noticed some important features that separated them such as the lack of mesostyle on the upper molars and the lack of entolophid (hypolophid in my matrix nomenclature; Appendix C4 Resource 2) on the lower molars, among other features. Cifelli and Soria (1983*a*) also added a new species *Adiantoides magnum* from Cañadon Vaca, Argentina (Vacan SALMA) to Indaleciinae. The differences between indaleciines and adianthids and also the dental similarities of the former with "amilnedwarsiids", led Soria (1989*a*) to propose the elevation of the subfamily Indaleciinae to the family Indaleciidae, including indaleciids, "amilnedwarsiids" and notonychopids under the same order Notopterna (see Amilnedwardsidae and the order Notopterna section). Apart from some common dental features, indaleciids share features of the ear region with notonychopids like anteriorly acuminate petrosals; however, they differentiate in the presence of enamel fossettes in P2-M3 and less developed parastyle in indaleciids, among other dental features (Soria 1989*b*).

Cifelli (1993) conducted a phylogenetic analysis that included indaleciids (i.e., *Indalecia* and *Adiantoides*) in a sample of different litoptern families and didolodontids, and found them to form a monophyletic group closely related to sparnotheriodontids (i.e., *Victorlemoinea*), and these three taxa were sister to didolodontids (Fig. 4.1c). This result was probably influenced by Cifelli's (1983*b*) indirect assignment of tarsals for *Victorlemoinea* (see Sparnotheriodontidae section). When Bonaparte and Morales (1997) repeated the analysis removing didolodontids and adding notonychopids, they similarly found this close relationship between indaleciids and sparnotheriodontids, without a close relationship with notonychopids (Fig. 4.1d). However, in a different analysis based only in lower molars, Gelfo *et al.* (2008) found indaleciids in a polytomy with *Notonychops powelli*, and this polytomy being sister of the sparnotheriodontid *Sparnotheriodon*. Probably because of the results of these previous analyses most authors have included Indaleciidae as family of Litopterna (e.g., Croft *et al.* 2020). Nevertheless, a preliminary study that included ear-region characters among other craniodental characters found the indaleciid *Indalecia* as a sister taxon to astrapotheres and notoungulates, instead of having a close relationship with Litopterna (García-López & Babot 2014). More recently, in a study that included litopterns, kollpanines and didolodontids, the indaleciid *Adiantoides* was found at the stem of litopterns, being more closely related to them than to didolodontids (Kramarz *et al.* 2021). In a different study that included also some early notoungulates, the indaleciid *Indalecia* was found in a polytomy that includes sparnotheriodontids, protolipternids, didolodontids and North American phenacodontids

(Zimicz *et al.* 2022). It is important to mention, that most of these studies have a relatively limited taxon and character sample, and none of them have included members of all the litoptern families and early members of the various SANU orders (Table 4.2). Therefore, the inclusion of Indaleciidae within the order Litopterna can only be considered as tentative.

The earliest member of Indaleciidae is *I. grandensis* which is temporally equivalent to Itaboraian SALMA to Sapoan Fauna (55 – 46.2; Fernicola *et al.* 2021) and the latest would be an undescribed indaleciid from the Abanico Formation, Chile (Tinguiririan SALMA; (Wyss *et al.* 1994), that gives the family a temporal interval of 55.0 – 34.5 Ma (Fig. 4.2b and Table S1 in Appendix C4 Resource 1).

## Other groups of interest

### "Condylarthra"

Cope (1881) first coined the group "Condylarthra" as a suborder of animals that he considered ancestral to Perissodactyla, in which initially included the Phenacodontidae, Hyopsodontidae and Periptychidae. This concept has been subsequently adopted and modified by many authors over the years, but essentially includes a diverse and likely polyphyletic assemblage of mainly Palaeogene ungulates usually from North America, Europe and Asia that made up a significant portion of the Palaeogene mammal faunas (Cope 1884; Simpson 1945; Van Valen 1978). It typically comprises the following six groups: Arctocyonidae, Periptychidae, Phenacodontidae, Hyopsodontidae, Mioclaenidae and Pleuraspidotheriidae (Archibald 1998; Rose 2006; Halliday *et al.* 2017). Some authors (e.g., Zack *et al.* 2005) consider that Mioclaenidae is synonymous with Hyopsodontidae. South American Didolodontidae is sometimes included in this grouping by some authors (e.g. Simpson 1945, 1948, 1980; Paula Couto 1952; Mckenna and Bell 1997; Rose 2006; Table 4.1) As many authors have noticed previously, "Condylarthra" is a "waste basket" taxon united mostly by plesiomorphies or ancestral characters instead of synapomorphies (Prothero *et al.* 1988; Archibald 1998). Therefore, considering the fact that it is likely a non-monophyletic group, I will follow Muizon and Cifelli (2000) in retaining the terms "Condylarthra" and "condylarths" with quotation marks when referring to this assemblage of archaic ungulates.

### Mioclaenidae and Kollpaniinae

Mioclaenidae was established as a family by Osborn and Earle (1895) and is composed by a group of primitive, small, largely bunodont "condylarths" with members in North

America, and potentially South America (Muizon & Cifelli 2000). Matthew (1909) observed clear similarities in some skeletal and dental features between Hyopsodontidae (then classified as Insectivora) and Mioclaenidae, which he later confirmed after studying Eocene hyopsodonts and reclassifying Hyopsodontidae within "Condylarthra" (Matthew 1915*c*). Considering these similarities, he later redefined these two groups as subfamilies, Mioclaeninae and Hyopsodontinae, within the family Hyopsodontidae (Matthew 1937), which was followed by Simpson (1937). However, Van Valen (1978) separated these two groups asserting they had different origins but did not provide any anatomical justification. Therefore, following authors have considered both interpretations, many supporting the division (e.g. Johnston and Fox 1984; Mckenna and Bell 1997; Archibald 1998; Muizon and Cifelli 2000; Rose 2006; Halliday *et al.* 2017), but some supporting their merging (e.g. Cifelli 1983*a*; Prothero *et al.* 1988). New arguments favouring the division are related to the fact that there are no undisputable apomorphies shared between the two taxa (Archibald 1998). Nevertheless, Zack *et al.* (2005) using phylogenetic analyses found evidence favouring the monophyly of Hyopsodontidae including *Hyopsodus* and Mioclaenidae, although excluding other typical "hyopsodontids" like apheliscines, which were grouped in another family, Apheliscidae.

Mioclaenidae has been historically associated with some South American ungulates. Simpson (1948) observed that the Patagonian *Asmithwoodwardia subtrigona* has some dental features in common with North American Mioclaeninae, such as the small or absent hypocone and triangular upper molars. Taking this a step further, Paula Couto (1952) included *Asmithwoodwardia* within Hyopsodontidae when describing *Asmithwoodwardia scotti* based on dental similarities. However, he later retracted this view in favour of Didolodontidae (Paula Couto 1978*b*)). Cifelli (1983*a*), trying to reconstruct a litoptern/didolodont ancestor, suggested that the most appropriate North American "condylarth" taxon was Mioclaenidae based mainly on shared dental features. His view found support a few years later with the findings of five genera of early Palaeocene "condylarths" *Andinodus*, *Molinodus*, *Pucanodus*, *Simoclaenus* and *Tiuclaenus*, from Tiupampa, Bolivia (Muizon & Marshall 1987*b*, *a*, 1991; Marshall & Muizon 1988; Muizon & Cifelli 2000), and of the Patagonian *Escribania chubutensis* and *Raulvaccia peligrensis* (Bonaparte *et al.* 1993) from Punta Peligro, Argentina. Bonaparte *et al.* (1993) noted the shared dental features between the Punta Peligran taxa and those from Tiupampa, thus proposing a new subfamily called Molinodinae within Mioclaenidae, which includes all the "condylarths" of both faunas. Muizon and Cifelli (2000) changed the subfamily name to Kollpaniinae due to taxonomic priority, and after conducting a phylogenetic analysis, found

support for a monophyletic group that contains South/North American Mioclaenidae and the endemic South American Litopterna and Didolodontidae, which they named as the order Panameriungulata (Table 4.1). As Kollpaniinae was found more closely related to Litopterna and Didolodontidae than to North American mioclaenids, when Muizon and Cifelli (2000) asserted on keeping Kollpaniinae within Mioclaenidae, they created a paraphyletic group. Even though Williamson and Carr (2007) found no close phylogenetic relation between South American Kollpaniinae and North American mioclaenids, most later studies have supported or recognized this connection (Gelfo 2004, 2007; Zack *et al.* 2005; Williamson & Weil 2011). More recently, the Barrancan (middle Eocene) mioclaenid *Pascualodus patagoniensis* from Argentina was added tentatively to Mioclaenidae (Gelfo 2004), and *Escribania chubutensis* and *Raulvaccia peligrensis* (synonym for *E. chubutensis* according to Muizon and Cifelli [2000]) were removed from Kollpaniinae and placed into Didolodontidae based on a phylogenetic analysis (Gelfo 2007).

The phylogenetic relationships of kollpanines have been explored mostly in studies with a limited taxon and character sampling (e.g., Gelfo 2007), being only recently incorporated into studies with a wider taxon sampling (Table 4.2). For instance, in a study including litopterns and didolodontids in a matrix with a focus on Perissodactyla, kollpanines were found forming a paraphyletic assemblage, with *Simoclaenus* closely related to some North American mioclaenids (e.g., *Promioclaenus*), but most at the stem of a group formed by mostly litopterns and didolodontids (Kramarz *et al.* 2021). In the same study, North American mioclaenids were found forming a polyphyletic assemblage, with *Protoselene* and *Litaletes* grouping with Perissodactyla, and Anthracobunia showing a basal position. More recently, a phylogenetic study found kollpanines closely related to the early notoungulate *Archaeogaia macachaae* in a monophyletic group, and well-separated from the North American mioclaenid *Mioclaenus* (Zimicz *et al.* 2022). However, kollpanines have been mostly omitted in studies with a wider taxon and character sampling (e.g., O'Leary *et al.* 2013; Muizon *et al.* 2015), and they have been never incorporated into a study with a wide character and taxon sampling with early representatives of all SANU orders (Table 4.2). In sum, there is still considerable uncertainty about the phylogenetic position of kollpanines in the placental tree, and the somewhat contradictory phylogenetic affinities among SANUs and North American mioclaenids that have been recovered so far in previous studies are tentative at best. As usual with many early SANUs, part of the reason of this uncertainty is their sparse fossil record,

limited mostly to teeth and some isolated and indirectly assigned tarsals (Muizon *et al.* 1998, 2019; Muizon & Cifelli 2000).

The earliest members of Kollpaninae are the seven species comprising five genera and from Tiupampa, Bolivia (Tiupampan SALMA) and the latest would be *Pascualodus patagoniensis* from Paso de Indios, Argentina (Barrancan SALMA) following Gelfo (2004), which would give kollpanines a temporal interval of 64.0 – 42.0 Ma (Fig. 4.2b and Table S1 in Appendix C4 Resource 1). However, considering that the only known specimen of *P. patagoniensis* is represented by only an isolated upper molar, its phylogenetic position in a polytomy with other kollpanines and a branch leading to didolodontids and protolipternids in the phylogeny of Gelfo (2004), the limited taxon and character sampling of this study, and the fact that there are no other known kollpaniines in the temporal interval between these two sites, it is entirely possible that *P. patagoniensis* is part of different group such as didolodontids, sharing only primitive features (plesiomorphies) with kollpaniines. If that is the case, kollpanines would be restricted only to the Tiupampan SALMA (64 – 63 Ma).

## Taxon sampling

As the main objectives of this chapter are resolving the interfamilial relationships of Litopterna and testing the monophyly Litopterna among other SANUs and early placental mammals, the taxon selection includes the earliest members of each litoptern family and also taxa of groups that have been linked to Litopterna in previous studies, which makes a total of 35 taxa.

The outgroup chosen was *Protungulatum donnae* as it is one the earliest archaic ungulate ("condylarths") known from the biochronologic zones Pu1 and Pu2 (Cifelli *et al.* 2004; Lofgren *et al.* 2004) in the earliest Puercan NALMA (early Palaeocene). The genus *Protungulatum* has also been found in deposits that are tentatively dated to the Late Cretaceous of North America, making it a potential survivor of the K/Pg extinction and the only current record of a "condylarth" in the Late Cretaceous (Archibald *et al.* 2011). Considering the proposed phylogenetic affinities of North American mioclaenids with early SANUs (e.g., Muizon & Cifelli 2000), I included four Palaeocene taxa of this group: *Mioclaenus turgidus*, *Protoselene opisthacus*, *Choeroclaenus turgidunculus* and *Promioclaenus* spp., which includes *Promioclaenus lemuroides* and *Promioclaenus acolytus*. The inclusion of the latter two species within *Promioclaenus* spp. serves to maximise the information on this genus, considering that both species have almost the same temporal distribution, and the species level differentiation

is based solely on a 20% size difference (Williamson 1996). For representing the earliest SANUs, I included two Tiupampan SALMA (early Palaeocene) kollpanines, *Molinodus suarezi* and *Tiuclaenus* spp. (*Tiuclaenus minutus*, *Tiuclaenus cotasi* and *Tiuclaenus robustus*), which have been previously included in Mioclaenidae (Muizon & Cifelli 2000). The inclusion of three species of *Tiuclaenus* under *Tiuclaenus* spp. was to maximise the information on this genus, considering that they have the same temporal distribution and that they differ mostly in their size and relatively minor features in their dentition (Muizon & Cifelli 2000; Muizon *et al.* 2019). In addition, considering the previously suggested close affinity between the "condylarth" South American family Didolodontidae and Litopterna (e.g., Simpson 1948), I included four taxa from this family: the Peligran SALMA (early Palaeocene) *Escribania chubutensis* and *Raulvaccia peligrensis*, the Itaboraian SALMA (early Eocene) *Ricardocifellia protocenica* and the Barrancan SALMA (middle Eocene) *Didolodus multicuspis*.

Considering the anatomical and molecular evidence supporting close affinities between litopterns and the other SANU orders (i.e., Notoungulata, Astrapotheria, Xenungulata) found in previous studies (Buckley 2015; Muizon *et al.* 2015; Welker *et al.* 2015), I included the middle to early Palaeocene notoungulate *Simpsonotus praecursor*, the Vacan to Barrancan SALMAs (middle Eocene) astrapothere *Trigonostylops wortmani*, and the Itaboraian SALMA xenungulates *Etayoa bacatensis* and *Carodnia vieirai*. I also included the early Eocene indaleciid *Indalecia grandensis* and two notonychopids, *Notonychops powelli* (probably early Eocene) and *Requisia vidmari* (Peligran SALMA, early Palaeocene), members of two families (i.e., Indaleciidae and Notonychopidae) included sometimes within Litopterna (e.g., Croft *et al.* 2020) and others in a separate order, Notopterna (Soria 1989*b*). Members of Amilnedwardsiidae were not included considering the that this family is only known from a few isolated upper molars whose positions are tentative (Soria 1989*a*) and because I was not able examine the specimens attributed to Amilnedwardsiidae in the MACN collections (they are possibly lost).

The order Pyrotheria was not included in the taxon sampling, as the assignment to this order of some of some its putative earliest representatives such as *Proticia* and *Colombitherium* have been challenged (Sánchez-Villagra *et al.* 2006; Billet *et al.* 2010) and the best known genus *Pyrotherium* is from the Deseadan SALMA (late Oligocene), and too derived dentally to make any meaningful dental comparisons with other taxa in the dataset (i.e., its molars are fully bilophodont). In addition, there is anatomical evidence that pyrotheres may be extremely derived notoungulates (Patterson 1977) which has been supported more recently by a

phylogenetic analysis (Billet 2010). Therefore, pyrotheres do not seem to be relevant in broader comparisons with Litopterna and its different families.

I included three members of the family Protolipternidae: the Itaboraian SALMA *Protolipterna ellipsodontoides*, *Asmithwoodwardia scotti* and *Miguelsoria parayiruhnor*, usually placed within Litopterna based on tarsal features (Cifelli 1993). In addition, I included members of the five relatively less controversial litoptern families (i.e., Adianthidae, Macraucheniidae, Proterotheriidae, Anisolambdidae and Sparnotheriodontidae). From Adianthidae I included three taxa: the Barrancan SALMA *Proectocion* spp. (*Proectocion argentinus* and *Proectocion precisus*) and the Deseadan SALMA (late Oligocene) species *Tricoelodus bicuspidatus* and *Proadiantus excavatus*. *Proectocion* spp. includes two species to maximise the information available for this genus, and also because both species are differentiated by relatively minor size differences (Simpson 1948). From Macraucheniidae I included four taxa: the Mustersan SALMA (late Eocene) *Polymorphis* spp., the Deseadan to Colhuehuapian SALMAs (late Oligocene to early Miocene) *Cramauchenia normalis*, the Santacrucian SALMA (early Miocene) *Theosodon* spp. (*Theosodon lydekkeri*, *Theosodon garretorum* and *Theosodon gracilis*) and the late Pleistocene to Holocene *Macrauchenia patachonica*. I used three species to represent the genus *Theosodon* in order to maximise the information on the genus, considering that these are all species from the same temporal distribution and that relatively minor differences in size and anatomical features distinguish them (Scott 1910). From Proterotheriidae I included 2 taxa: the Deseadan SALMA *Lambdaconus suinus* and the Santacrucian SALMA *Diadiaphorus majusculus*. From Anisolambdidae I included two taxa: the Itaboraian SALMA *Paranisolambda prodromus* and the Riochican to Barrancan SALMA (early to middle Eocene) *Anisolambda* spp. (*Anisolamda fissidens* and *Anisolamda amel*). I included two species for representing *Anisolambda* in order to maximise the information available for this genus, because these species differ mostly in size and because the upper dentition has not been clearly assigned to any of these species (see more in *Anisolambda* spp. taxonomic comments). From Sparnotheriodontidae I included three taxa: the Itaboraian SALMA *Victorlemoinea prototypica*, the early to late Eocene *Notiolofos arquinotiensis* from Antarctica, and the Vacan SALMA *Sparnotheriodon epsilonoides*.

It is important to highlight that the focus of this study are the phylogenetic affinities within Litopterna, and even though I include some early members of the SANU orders and some North American "condylarths" in the taxon sampling, I am not testing whether SANUs form a monophyletic group. In order to test the monophyly of SANUs, a phylogenetic analysis

with larger the taxon sampling that includes relevant early placental groups (e.g., perissodactyls, artiodactyls, afrotheres) should be performed. This work is currently underway and it is part of the objectives of the Palaeogene Mammal Working Group (PalM) to which I have been contributing during my PhD.

What follows is a detailed list of taxa with information about the types, specimens scored, known distribution, age and SALMA. The Age/SALMA reflects the stratigraphic uncertainty of the specimens scored, and it does not necessary reflect the first and last appearance datum (i.e., FAD and LAD) known for a particular taxon.

## Families currently recognised in the Order Litopterna (Ameghino 1889)

## Family Adianthidae (Ameghino 1891*a*)

### *Proectocion* spp. (Ameghino 1904*b*)

= *Proectocyon* (Ameghino 1906); spelling change)

= *Oxybunotherium* (Pascual 1965)

Included species in the scoring:

a) *Proectocion argentinus* (Ameghino 1904*b*)

b) *Proectocion precisus* (Ameghino 1904*a*)

**Holotypes and type localities:** *Proectocion argentinus*: MACN A 10673 (right M3) from Barranca south of Lago Colhué-Huapí, Sarmiento Formation, Chubut, Argentina (Simpson 1948); *Proectocion precisus*: MACN A 10679 from Barranca south of Lago Colhue-Huapi, Sarmiento Formation, Chubut, Argentina (Simpson 1948).

**Other specimens observed and scored:** MLP 59-II-28-107 (mandible fragment with talonid of m2 and complete m3; holotype of *Oxynobunotherium praecursor*); MLP 66-V-4-1 (mandible fragment with m1, root of m2 and fragment of p5).

**Known distribution:** Barranca south of Lago Colhue-Huapi (Simpson 1948): MACN A 10673 and MACN A 10679; Aguada Batistín (also known as "Tobas con mamíferos") (Pascual 1965), Sarmiento Formation, Chubut, Argentina: MLP 59-II-28-107 and MLP 66-V-4-1.

**Age/SALMA:** Middle Eocene/ Barrancan (42 – 39 Ma). Barranca south of Lago Colhue-Huapi and Aguada Batistín are both here considered to have a Barrancan SALMA age (Kramarz & Bond 2013).

**Taxonomic comments:** I followed Cifelli (1983*a*) in considering *Oxybunotherium* a junior synonym of *Proectocion*, being the former the lower molars, and the latter the upper molars of probably the same taxon, considering their size, morphology, temporal and geographic distribution.

### *Tricoelodus bicuspidatus* (Ameghino 1897)

= *Proadiantus* sp. (Patterson 1940)

**Holotype and type locality:** MACN A52-203 (right mandible fragment with P5-M2) of uncertain locality but probably from Cabeza Blanca, Sarmiento Formation, Chubut, Argentina considering its preservation (Cifelli & Soria 1983*a*).

**Other specimens observed and scored:** MACN A52-615 (left mandibular fragment with broken M3); FMNH P14698 (right P4-M2 and left P1?, P2-P4, and M1-M3), FMNH P14696 (right M2-M3); MLP 61-IV-11-65 (maxillary fragments with right P5-M3 and left P2-P5 and M2-M3).

**Known distribution:** Cabeza Blanca and El Pajarito, Sarmiento Formation, Chubut, Argentina (Patterson 1940; Cifelli & Soria 1983*a*).

**Age/SALMA:** Late Oligocene/Deseadan (29.3 – 26.0 Ma). Cabeza Blanca and El Pajarito are considered to have Deseadan age (Cifelli & Soria 1983*a*; Woodburne *et al.* 2014*b*)

**Taxonomic comments:** I agree with most of the descriptions of *Tricoelodus bicuspidatus* made by previous authors (Patterson 1940; Cifelli & Soria 1983*a*). However, I have a few anatomical discrepancies that have some impact on the scoring. First, I followed Patterson (1940) in his interpretation for the buccal aspect of P2 and P4 (P2 and P3 in his terminology) that present a prominent parastyle, paracone, metacone and a very small metastyle (*contra* Cifelli and Soria 1983). For P2 and P4, Cifelli and Soria (1983) considered the metacone to be absent and the distal cusp immediate to the paracone to be a prominent metastyle. However, close examination of specimens (FMNH P14698; MLP 61-IV-11-65) shows clearly a small metastyle in P2 and P4, which makes the prominent cusp distal to the paracone a metacone as Patterson (1940) observed.

Another feature in which I have a different interpretation is the mesialmost tooth in FMNH P14698. Patterson (1940) mentioned that this tooth was either a C or P1 considering the anatomy of those teeth in macraucheniids, but preferred the canine identification (C?). Cifelli and Soria (1983) later followed this interpretation. However, the lower canine (c) of *Proadiantus excavatus* (MACN A52-214), a close relative of *T. bicuspidatus* with a similar dental anatomy and age, is procumbent and incisiform being anteriorly directed. In contrast, P1 in *Proadiantus excavatus* (MACN A52-214) is small and erect considering its root (i.e., crown not preserved). Considering the anatomical features of c, you would expect that C would match its anatomy and orientation in a certain way in order to occlude properly. If we assume that the anatomy of the anterior dentition of *Tricoelodus bicuspidatus* is similar to *Proadiantus excavatus*, then the mesialmost tooth preserved is probably a P1 as it does not have an anatomy consistent with the c of the latter taxon. This is a working hypothesis considering the current fossil evidence available.

### ***Proadiantus excavatus*** **(Ameghino 1897)**

=*Proadianthus excavatus* (Loomis 1914)

=*Proadiantus pungidens* (Ameghino 1901)

**Holotype and type locality:** MACN A 52-213 (mandible fragment with p4-p5) of uncertain locality but probably from Cabeza Blanca, Sarmiento Formation, Chubut, Argentina considering its preservation (Cifelli & Soria 1983*a*).

**Other specimens observed and scored:** MACN A 52-214 (right mandible fragment with root of i1, i2-c, alveolus of p1 and p2-m2; holotype of *Proadiantus pungidens*); MACN A52-217 (right mandible fragment with p5-m1); MACN A52-215 (right mandible fragment with m1-m3).

**Known distribution:** Probably from Cabeza Blanca, Sarmiento Formation, Chubut, Argentina (Cifelli & Soria 1983*a*).

**Age/SALMA:** Late Oligocene/Deseadan (29.3 – 26.0 Ma). Cabeza Blanca is considered to have Deseadan age (Cifelli & Soria 1983*a*; Woodburne *et al.* 2014*b*).

**Anatomical comments:**

- *Proectocion* and *Proadiantus* share the presence in m1-m2 of a distolingual cingulid and a postcingulid (distobuccal cinguliud) that connects with the hypoconulid. In addition, in both taxa the hypoconulid is in contact with the entoconid in m1-m2.
- The canine in *Proadiantus* is incisiform and it has a conule at its base (margoconid?).
- In the lower molars (m1-m3) the precingulid seems to be connected as a continuous crest with the paraconid in *Proadiantus excavatus*, and the paraconid position is actually mesiolingual between the metaconid and protoconid. This is very similar to the condition seen in the m1-m3 of *Tricoelodus bicuspidatus*, in which the precingulid is connected with the paraconid in an almost continuous crest. However, in *Tricoelodus* the separation between paraconid and precingulid is clearer than in *Proadiantus excavatus*.

## Family Anisolambdidae (Soria 2001)

### *Anisolambda* spp. (Ameghino 1901)

= *Josepholeidya* (Ameghino 1901)

= *Ricardolydekkeria* (Ameghino 1901)

Included species in the scoring:

a) *Anisolamda fissidens* (Ameghino 1901)

b) *Anisolamda amel* (Simpson 1948)

**Holotypes and type localities:** *Anisolambda fissidens*: MACN A 10668 (right m1-m3 and left m1-m2 of different individuals from "Casamayoran" beds (Simpson 1948); *Anisolamda amel*: AMNH 28503 (left mandible fragment with m1-m3) from Cañadón Vaca, Sarmiento Formation, Chubut, Argentina (Simpson 1948).

**Other specimens observed and scored:** AMNH 28512 (right M3); AMNH 28516 (two not associated right and left M1 or M2); AMNH 28519 (left P4); AMNH 28520 (left P4); AMNH 28522 (right P4); MACN A 10682 (left M1 or M2); MACN A 10701 (right P4); MACN A 10705 (right P5); MLP 59-II-28-59 (right M1 or M2); MLP 59-II-24-453 (right M1 or M2); MLP 69-III-28-1 (right m1-m2); MLP 59-II-28-68 (left maxilla fragment with P4-P5 and left m3); MLP 59-II-24-580 (right P5); MNHN.F.CAS 486 (left M1 or M2); MNHN.F.CAS 485 (right P5); MNHN.F.CAS487 (right M3) and MNHN.F.CAS488 (left M3).

**Known distribution:** Cañadón Vaca, Sarmiento Formation, Chubut, Argentina (Simpson 1948): AMNH 28503, AMNH 28512, AMNH 28520, AMNH 28516, AMNH 28519 and AMNH 28522; Cerro Guacho, Sarmiento Formation, Chubut , Argentina: MLP 59-II-24-580, MLP 59-II-24-453; Bajo Palangana, Las Flores Formation, Chubut, Argentina (Simpson 1948; Vera & Krause 2020); Aguada Batistín, Sarmiento Formation, Chubut, Argentina: MLP 59-II-28-59, MLP 59-II-28-68 and MLP 69-III-28-1; Cerro Negro, Chubut, Argentina (Tournouër collection): MNHN.F.CAS 486, MNHN.F.CAS 485, MNHN.F.CAS487 and MNHN.F.CAS488.

**Age/SALMA:** Early to middle Eocene/Riochican to Barrancan SALMAs (49 – 39 Ma). Cañadón Vaca considered Vacan SALMA following Krause *et al.* (2017). Cerro Guacho and Aguada Batistín are considered Barrancan SALMA (Reguero & Prevosti 2010; Kramarz & Bond 2013). Considering the stratigraphic uncertainty of the specimens from Cerro Negro (Simpson 1948, 1964), an interval between the Vacan and Barrancan SALMA is here used. Bajo Palangana is here considered Riochican (Vera & Krause 2020). Even though there is no specimen in this list from Bajo Palangana, as there is uncertainty of the stratigraphic origin of certain individuals (e.g., MACN A 10668), the temporal interval used for *Anisolambda* includes the Riochican SALMA.

**Additional relevant references with descriptions and illustrations:** Gaudry (1904); Cifelli (1983*a*)

**Taxonomic comments:** In general, I followed Cifelli (1983*a*) interpretations about the synonymy of *Josepholeidya* and *Ricardolydekkeria* with *Anisolamda,* in which the former two are upper premolars of the latter. This is supported by MLP 59-II-28-68, which is an associated left P4-P5 and left m3 found in Aguada Batistín, Sarmiento Formation, Chubut, Argentina, and housed at the MLP collections. In particular, this specimen supports the synonymy of *Anisolambda* and *Ricardolydekkeria*. However, I disagree with (Cifelli 1983*a*) in relation to AMNH 28519 that I interpret as a left P4 instead of a left P5. The key for a correct interpretation of this tooth are the size and proportions of P4 in MLP 59-II-28-58, which are very similar to AMNH 28519 and AMNH 28520. In *Anisolambda*, P5 tends to be less quadrangular, being much wider than longer. In addition, *Anisolambda lunata* (MACN A 55-4) was excluded from the scoring as it has a very peculiar P4?. This P4 is completely squared in shape and presents a premetaconular crista, features unusual for a P4 of *Anisolambda*.

**Anatomical comments:**

- The presence of a marked premetaconular crista is variable in *Anisolambda* spp. AMNH28522 has a very marked premetaconular crista whereas in AMNH 28519, AMNH 28520 and MLP 59-II-2858 this crista is not present.
- The M3s of *Anisolambda* from the MNHN collections show variation of the extension of the preparaconular crista and the precingulum (see scores).
- The specimen MACN A 10705 of *Anisolambda* has a clear and small hypocone. In the other specimens the postcingulum is too worn to assess the presence of a hypocone.

### *Paranisolambda prodromus* (Cifelli 1983*a*)

= *Anisolambda prodromus* (Paula Couto 1952)

**Holotype and type locality:** DGM 262M (right mandible fragment with alveolus of c and dp2-dp5, m1 and erupting M2) from fissure fills in the Itaboraí Formation, near São José de Itaboraí, Rio de Janeiro, Brazil (Paula Couto 1952).

**Other specimens observed and scored:** DGM 310M (maxilla fragment with M2-M3, and fragment of posterior part of the skull; DGM 304M (maxilla fragment with dP4-DP5 and M1; paratype); DGM 307M (maxilla fragment with P2, dP4-dP5 and M1); MNRJ 1496V (left m2); MNRJ 1859V (left m3); DGM 273M (crushed maxilla with right P2 and dP4-dP5, and left P2, dP4-dP5 and erupting M1; paratype); AMNH 49818 (left m2).

**Specimens not observed:** Additional specimens listed in previous publications (Paula Couto 1952; Bergqvist 1996).

**Known distribution:** Fissure fills in the Itaboraí Formation, near São José de Itaboraí, Rio de Janeiro, Brazil (Paula Couto 1952).

**Age/SALMA:** Early Eocene/Itaboraian (56.0 – 51.4 Ma).

**Additional relevant references with descriptions and illustrations:** Bergqvist (2010).

**Taxonomic comments:** I followed Bergqvist (2010) interpretations for the loci of the teeth of *Paranisolambda* which were based in X-ray images, *contra* Cifelli's (1983*a*) interpretations for some of the loci. In addition, Cifelli (1983*a*) considered MNRJ 1479V as an M2 of *Paranisolambda*, which is 42% larger than other M2 (DGM 310M), attributed to same taxon. This size difference and also some features present in MNRJ 1479V (see Soria [2001]),

strongly suggest that MNRJ 1479V is a different taxon. Therefore I did not considered it for the scoring of *Paranisolambda* in my matrix. Soria (2001) hypothesised that MNRJ 1479V is a primitive Sparnotheriodontidae different from *Victorlemoinea prototypica*, and a key specimen for understanding the close affinities between anisolambdids and sparnotheriodontids.

**Anatomical comments:**

- *Paranisolambda* has a secondary postcingulum below the main one, a feature also seen in sparnotheriodontids (e.g., *Victorlemoinea prototypica* and *Notiolofos*).
- In the lower molars of *Paranisolambda* (m1-m3), the paracristid seems to be interrupted before arriving to the paraconid as Cifelli (1983*a*) previously observed.
- The P2 of *Paranisolambda* has a small metacone which was omitted in a previous description of this taxon (Paula Couto 1952).

## Family Macraucheniidae (Gervais 1855)

### *Polymorphis* spp. (Roth 1899)

Included species in the scoring:

**a) *Polymophis lechei*** (Roth 1899)

**b) *Polymorphis ligatus*** (Roth 1899), new combination

= *Polyacrodon ligatus* (Roth 1899)

= *Decaconus intricatus* (Ameghino 1901)

**Holotypes and type localities: *Polymophis lechei*:** MLP 12-2168 (left mandible fragment with symphysis and left i1-m3 and right i1-i3) from "Cretáceo superior de Lago Musters" Probably Musters formation of the Cerro del Humo, Chubut (Simpson 1948); ***Polymorphis ligatus*:** MLP 12-2169 (right M3) from "Cretáceo superior de Lago Musters" Probably Musters formation of the Cerro del Humo, Chubut (Simpson 1948).

**Other specimens observed and scored:** *Polymophis lechei*: AMNH 29480 (left mandible fragment with p2-m3); *Polymorphis ligatus*: MLP 12-2169 (right M3; holotype of *Polyacrodon ligatus* [Roth 1899]) and MACN A 10897 (right M3; holotype of *Decaconus intricatus* [Ameghino 1901]).

**Specimens not examined:** *Polymorphis*?: MLP 61-IV-9-26 (right M1 or M2); MLP 61-VIII-3-5 (right M3); MLP 67-II-27-6; MLP 67-II-27-7; MLP 67-II-27-8.

**Specimens not included:** *Polymorphis*?: AMNH 29481 (right M3; *Polyacrodon ligatus* according to Simpson [1948]).

**Known distribution:** "Cretáceo superior de Lago Musters" Probably Musters formation of the Cerro del Humo, Chubut, Argentina (Simpson 1948), and surroundings of Laguna del Mate, Argentina (Odreman-Rivas 1969).

**Age/SALMA:** Late Eocene/Mustersan (39.0 – 36.5 Ma). The age interval was based in the age of the Mustersan SALMA (Woodburne *et al.* 2014*b*).

**Additional relevant references with descriptions and illustrations:** Cifelli (1983*a*).

**Taxonomic comments:** Cifelli (1983) synonymised *Polyacrodon lanciformis* (Roth 1899) and *Polyacrodon ligatus* (Roth 1899) and included them within the genus *Polymophis* (Roth 1899) following a suggestion given previously by Simpson (1948), based in general anatomical similarities. However, *Polyacrodon lanciformis* has well developed conules (i.e., paraconule and metaconule) with strong mesial and distal cristae (i.e., preparaconule crista, postparaconule crista, premetaconule crista and postmetaconule crista). The same conules and cristae are less developed or even absent in *Polyacrodon ligatus*. The premetaconule crista which is connected with the metacone in *Polyacrodon ligatus* is directed to the paracone in *Polyacrodon lanciformis*. Indeed, *Polyacrodon lanciformis* (Roth 1899) has been considered a proterotheriid (Simpson 1948; Odreman-Rivas 1969; Gelfo 2006) or even a didolodontid (Soria 2001). Considering that the holotype of *Polyacrodon ligatus* (M3) is very similar to what is seen in the upper molars of macraucheniids, I followed the interpretation of Odreman-Rivas (1969) and Gelfo (2006), who consider *Polyacrodon* (Roth 1899) as a synonymous of *Polymophis* (Roth 1899), although I kept the species separation for caution. Gelfo (2006) suggested that *Polyacrodon lanciformis* should be referred as *Decaconus lanciformis*, due to the consideration that the type species of *Polyacrodon* is *Polyacrodon ligatus*, a junior synonym of *Polymorphis*. However, this decision carries the assumption that MACN A 10897 (holotype of *Decaconus intricatus* [Ameghino 1901]), is the same taxon as the holotype of *Polyacrodon lanciformis* (Roth 1899; MLP 12-2170) which I disagree based in their very different anatomy. The affinities of *Polyacrodon lanciformis* remain to be defined or tested, but it shows strong similarities with *Protheososon coniferus*, so it may well be an anisolambdid.

These dental similarities can be seen clearly in the specimens of *Polyacrodon lanciformis* MLP 12-2170 (left M2?) and AMNH 29482 (distal portion of P5, M1 and mesial portion of M2) when compared with *Protheosodon coniferus* (FMNH P 13418). Among other features, they share an expanded metastyle in P5 that is not seen in any other anisolambdid. In addition, considering the features of MACN A 10721 (M1 and lingual portion of M2), which is the holotype of *Lambdaconops* (Soria 2001), and its overall dental similarities with *Polyacrodon lanciformis* of a similar age, it could potentially be a synonym of the latter.

The upper molar specimens scored in this work are MLP 12-2169 (holoype of *Polyacrodon ligatus* (Roth 1899) and MACN A 10897 (holotype of *Decaconus intricatus* [Ameghino 1901]), both considered to be M3s considering the much more buccal parastylar lobe in comparison to the metastylar lobe, as it is seen in the M3 of macraucheniids such as *Cramauchenia normalis*. Considering the similar anatomy of the specimens referred to *Polyacrodon ligatus*, I grouped them as *Polymorphis ligatus* (Roth 1899), new combination, as at the present moment is not possible to be certain that they are effectively upper molars of *Polymophis lechei*. The reason for this uncertainty is that both taxa have not been found in association and there seems to be several morphotypes in the upper molars assigned by Odreman-Rivas (1969), which could indicate important polymorphism in one species or that there is more than one species. There are other upper molar specimens in the MLP collections listed by Gelfo (2006) with a morphology that apparently is similar to *Polymorphis ligatus* (MLP 61-IV-9-26; MLP 61-VIII-3-5; MLP 67-II-27-6; MLP 67-II-27-7; MLP 67-II-27-8). I have not been able to examine these specimens, so they have not been included in the present work. Two of these specimens were figured previously, MLP 61-IV-9-26 and MLP 61-VIII-3-5, both interpreted as M3s (Odreman-Rivas 1969). From the pictures, I agree that MLP 61-VIII-3-5 could be an M3 as its shape is very similar to both MLP 12-2169 and MACN A 10897, being their main difference that the premetaconule crista is not connecting with the metacone as in the latter two specimens, being more distally oriented. In consequence, MLP 61-VIII-3-5 was not scored. MLP 61-IV-9-26 has a more quadrangular shape and less asymmetry between the parastylar and metastylar lobes, which strongly suggests being a M1 or M2 considering the shape of these molars in macraucheniids such as *Cramauchenia normalis*. I excluded this specimen (MLP 61-IV-9-26) from the scoring because of two reasons. First, the presence of a strong postmetaconular crista which is absent in MLP 12-2169 and MACN A 10897. Second, there does not seem to be a mesial crista (predistocrista) going towards to metaconule area as in MLP 12-2169 and MACN A 10897. This could be just an artifact of the picture, but without

a close examination I prefer to abstain of scoring it for now. Even though I did not score MLP 61-IV-9-26 and MLP 61-VIII-3-5, I think they are probably closely related to *Polymorphis*.

In addition, there is another upper AMNH 29481 considered by Simpson (1948) a M3 of *Polyacrodon ligatus* and synonymised by Cifelli (1983*a*) as *Polymophis*. Even though I think this specimen is an M3 from a taxon closely related to *Polymorphis*, there are enough anatomical differences with in MLP 12-2169 and MACN A 10897 which suggest is a different taxon. For instance, it presents a postparaconule crista (absent in MLP 12-2169 and MACN A 108970) and the premetaconule crista is directed towards the paracone, instead of joining the metacone as in MLP 12-2169 and MACN A 108970. In addition, there is a weak crista (predistocrista) going from the distocone to the metaconule area, in contrast to the strong crista present in MLP 12-2169 and MACN A 10897.

### *Cramauchenia normalis* (Ameghino 1902*a*) *sensu* (Soria 1981)

= *Cramauchenia insolita* (Ameghino 1902*a*, 1904*b*)

= *Theosodon* (*Cramauchenia*) *normalis* (Gaudry 1904, 1906, 1908)

**Holotype and type locality:** MACN A-52-219 (cranium fragment with right maxilla and zygomatic arch fragment, with C-M3) from Gran Barranca, southern cliff of Colhué Huapí lake, Sarmiento Formation, Chubut, Argentina (Soria 1981; Dozo & Vera 2010).

**Other specimens observed and scored:** MACN A-52-220 (left mandible fragment, with the root of p1 and p2-m3 with part of the ramus; paralectotype); MACN A-52-232 (maxillary fragment with right M1-M2; type of *Cramauchenia insolita*); MACN A-52-233 (right mandible fragment with m2-m3; type of *Cramauchenia insolita*); MACN A-52-221 (right P5, and right and left M1, M2, and M3); MACN A-52-222 (left M1 or M2); MACN A-52-223 (left M3); MACN A-52-224 (left mandible fragment with p4-m2 and roots of p1-p2); MACN A-52-225 (mandibular symphysis with fragment with right p1-m2); MACN A-52-227 (left mandible fragment with p1); MACN A-52-229 (right P5); MACN A-52-235 (right mandible fragment with m1-m3); MACN A-52-236 (left mandible fragment with m2-m3); MACN A-52-237 (left and right m3, right p1, right p3 and 3 incisors); MACN A-52-238 (right calcaneum and left astragalus); MLP 83-III-2-1 (juvenile, complete crushed cranium and maxilla with dP2-dP5, M1 and erupting M2, right mandible fragment with dp2-dp5 and m1, and crushed atlas); MLP 85-VII-3-38a (cranium with almost complete right side and half of left side, right maxilla with I1-I2, root of I3 and C-M3 and left maxilla with root of I1 and I2-

M1; MPEF-PV 2524 (a nearly complete skull with left I3, C, and P1–M3, and right I2–3, C, and partial P1, right humerus, left metacarpal IV and three phalanges); AMNH 29753 (right M1 or M2); AMNH 15917 (right M1 or M2); AMNH 29726 (mandible fragment with root of p4 and p5-m3); MNHN.F.COL181 (mandible fragment missing the anterior portion and incisors, left mandible portion with condyle and almost complete condylar process with p1-m3 and right mandible portion with p2-m3; MNHN.F.COL multiple unnumbered specimens.

**Known distribution:** Gran Barranca, southern cliff of Colhué Huapí lake, Sarmiento Formation, Chubut, Argentina (Soria 1981; Dozo & Vera 2010): MACN A, MLP and MNHN.F.COL specimens; Cabeza Blanca, Sarmiento Formation, Chubut, Argentina (Dozo & Vera 2010): MPEF-PV 2524.

**Age/SALMA:** late Oligocene to early Miocene/Deseadan to Colhuehuapian (29.3 – 20.1 Ma). Gran Barranca, southern cliff of Colhué Huapí lake and Cabeza Blanca are here assigned a Colhuehuapian SALMA and a Deseadan SALMA age following Woodburne *et al.* (2014*b*). These determine the temporal interval given to *Cramauchenia*.

**Additional anatomical comments:**

- The upper molars of *Cramauchenia* have a buccally directed crista coming from the metaconule that connects with the metacone, which could be premetaconule crista or a postmetaconule crista. I think this is a postmetaconule crista and that the premetaconule crista is absent. I based this interpretation in the anatomy of *Polymorphis* (i.e., the putative earliest macraucheniid), that presents the same crista in M3 (MLP 12-2169 and MACN A 10897), although in *Polymorphis* this crista is more distally displaced than in *Cramauchenia.* Considering the position and direction of this crista in *Polymorphis*, it should be probably considered to be a postmetaconule crista, and thus in *Cramauchenia*, if we consider these cristae to be homologous in both taxa.

### *Theosodon* spp. (Ameghino 1887)

=*Pseudocoeloma* (Ameghino 1891*b*)

=*Oxyodontotherium* (Lydekker 1893)

Species included in the scoring:

**a) *Theosodon lydekkeri*** (Ameghino 1887)

=*Oxyodontherium lydekkeri* (Lydekker 1893)

**b) *Theosodon garretorum*** (Scott 1910)

**c) *Theosodon gracilis*** (Ameghino 1891*b*)

=*Theosodon patagonensis* (Mercerat 1891*a*)

= *Theosodon debilis* (Mercerat 1891*a*)

= *Oxyodontotherium angustidens* (Lydekker 1893)

**Holotype and type locality: *Theosodon lydekkeri***: MACN-A 2487–90 (Left side of the cranium with I3, P1-M3) from Corrigen Aike, Santa Cruz Formation, Santa Cruz, Argentina (Cassini *et al.* 2012); ***Theosodon garretorum***: YPM-VPPU 15164 (almost complete skeleton described in Scott [1910], relevant for the scoring is that it presents a well-preserved skull with left I1-I2, P1-M3 and right I2-M3, and a well preserved mandible with left i1-m3 and right p2-m3) from 10 miles of South Coy Inlet, Güer Aike Department, Santa Cruz Formation, Santa Cruz, Argentina (Scott 1910; Cassini *et al.* 2012). ***Theosodon gracilis*:** holotype and locality not reported (Scott 1910).

**Other specimens observed and scored: *Theosodon lydekkeri***: MACN-A 9269–88 (skull with left I1-P1, dP2-dP5, M1-M2, and right I2, brokenI3-C, P1, dP4-dP5, M1-2, and mandible with left p1, dp2-dp5, m1-m2, and right p1, dp2-dp5, m1-m2; subadult); MACN A 2490 (mandible with right and left i1-m3); YPM VPPU 015717 (skull with left and right P1, dP2-dP4, M1; juvenile); MLP 12-378 (p1, dp2-dp5, m1 and m2 erupting; juvenile); MLP 12-421 (dP5, M1-M2; juvenile); ***Theosodon garretorum***: FMNH P 13175 (skull with complete dentition [I1-M3]); ***Theosodon gracilis***: MACN A 2496 (skull with left i1-i2, M2-M3 and right I2-P1); MACN A 2496 (left mandible fragment with p1-p4, m1-m2); MACN A 9297 (right mandible fragment with p1, p4-m3); ***Theosodon* sp.**: PIMUZ A/V 4662 (left mandible fragment with i2–m3 and right mandible fragment with i3–m3, and right maxillary fragment with M1–M3)

**Known distribution:** Corrigen Aike, Santa Cruz Formation, Santa Cruz, Argentina: ***T. lydekkeri*** (MACN-A 2487–90, MACN-A 9269–88); 10 miles of South Coy Inlet, Güer Aike Department, Santa Cruz Formation, Santa Cruz, Argentina: ***T. lydekkeri*** (YPM VPPU 015717), ***T. garretorum*** (YPM-VPPU 15164, FMNH P 13175).

**Age/SALMA:** early Miocene/Santacrucian (18.0 – 15.6 Ma).

**Taxonomic comments:** I only scored specimens of *Theosodon* from the Santacrucian SALMA that showed certain anatomical consistency, instead of considering the whole-time interval of all the specimens included in this genus (i.e., Colhuehuapian to Laventan [21.0 – 11.8 Ma; Croft *et al.* 2020]). There is undoubtedly a need to revise the taxonomy of this genus, but revision of this nature is beyond the scope of this work.

**Anatomical comments:**

- The distolingual cusp in *Theosodon* spp. has been interpreted as the fusion of the hypocone with the metaconule by looking at the anatomy of earlier macraucheniids such as *Cramauchenia*, in which these cusps are closely located but clearly separated. The same idea was previously proposed by Soria (1981). In terms of scoring, the predistocrista/prehypocrista was scored as absent to avoid double scoring the cristae associated with the metaconule.
- The buccal crista coming originating from the metaconule-hypocone and connecting with the metacone has been interpreted as postmetaconule crista following the interpretation made for *Cramauchenia* (see above).

### *Macrauchenia patachonica* (Owen 1838)

=*Macrauchenia patagonica* (Lydekker 1893)

**Holotype and type locality:** NHMUK PV M 43402 (astragalus, femur, tibia-fibula, ulna-radius proximal fragment, vertebrae, metapodials, among other postcranial fragments described in Owen [1838]) from South side of San Julián port, Santa Cruz, Argentina (Owen 1838).

**Other specimens observed and scored:** MACN PV 2 (cranium with right M2-M3, and left P5-M1 and M3 preserved, mandible with left p5-m3 and right m1-m3 preserved, and many postcranial elements including: vertebrae, humerus, ulna-radius, femur, tibia, and almost complete pes with astragalus and calcaneum present); MACN PV 11361 (right M1-M3); MACN PV 11450 (left mandible fragment with i1-m3); MNHN.F.PAM75 (cranium with right P5-M3 preserved); MNHN.F.PAM339 (right P1, dP2, dP4 and dP5); MNHN.F.PAM69 (mandible with right p5-m3 and left m1 preserved); MNHN.F.PAM343 (mandible fragment with dp4-dp5, m1); MNHN.F.PAM83 (mandible with left dp4-dp5, m1-m2 and erupting m3, and right m1-m2 and erupting m3); MUHNCAL-KM 36 (right mandible fragment with p2-m3); MLP 12-1424 (cranium with right P1, P5-M3 and left P2-M3, mandible with left p5-m3

and right p2, p5-m3 and almost complete postcranium). MLP specimen from Ayacucho figured in (Sefve 1925) not found in my visit to the collection, includes maxilla fragment with left I1-M3 and right I1-C, P2-M3, mandible with left and right i1-m3, and postcranial elements);

**Known distribution:** Pleistocene/Holocene beds from Argentina, Brazil, Uruguay, Paraguay, Chile, Peru (Bond 1999; Scherer *et al.* 2009).

**Age/SALMA:** Pleistocene to Holocene/Ensenada to Lujanian (2 – 0.08 Ma). Occurrences based on (Bond 1999; Scherer *et al.* 2009).

**Additional relevant references with descriptions and illustrations:** Burmeister (1864*b*, *a*); Sefve (1925)**.**

**Anatomical comments:**

- *Macrauchenia patachonica* shows some level of hypsodonty, wearing quickly the cusps and crests (cristae and cristids) of the upper and lower molars (and some premolars), which have marked fossettes. These size and shape of these fossettes depends on the level of wear of the molars, which generally is tied with the ontogenetic stage of the specimen. Therefore, M1-M2 scores were mostly based on the M1-M3 of a relatively young specimen (MUHNCAL-KM 14), which has a limited wear in these molars. In addition, the unworn dP5 of a different specimen (MNHNPAM 339) helped in the interpretation for the molars. Lobo's *et al.* (2017) cusps interpretations for M1-M2 of *Xenorhinotherium* in unworn specimens are mostly similar to my own interpretations for the cusps in *Macrauchenia patachonica*. However, what he calls protocone I interpret it as a paraconule, and in the position of what he calls protocone-hypocone crest, I observed a cusp that I interpret as the protocone**.** This cusp can be seen more clearly in Lessa (1992; Estampa X). In addition, the interpretation I follow is consistent with the molar morphology seen in older macraucheniids such as *Theosodon*.

- The metastyle seems to be absent as a distinct cusp on the M3 of *Macrauchenia patachonica*. However, considering the *Macrauchenia*'s M3 morphology and the clear presence of this cusp in M1-M2, it is possible that the metastyle is present but appressed to the metacone, which makes difficult to distinguish both cusps. I followed this interpretation for the scoring of the metastyle in M3.

- In *Macrauchenia patachonica* the buccal cingulum was scored as "not presently available" (NPA), as technically it could be present but not visible due to the considerable portion of crown below the alveolar line (i.e., there is some degree of hypsodoncy). The same criterium was used for scoring the cingulids in the lower molars.

## Family Proterotheriidae (Ameghino 1887)

### *Lambdaconus suinus* (Ameghino 1897) *sensu* (Soria 2001)

= *Deuterotherium distichum* (Ameghino 1897, 1904*b*, 1906; Gaudry 1904; Loomis 1914; Roth 1927; Simpson 1932)

= *Deuterotherium distinctum* (spelling error; Paula Couto 1979*b*)

**Holotype and type locality:** MACN A-10718 (right mandibular fragment with p4 and p5 alveoli and m1) from the west of Bahía Sanguinetti, Punta Nava beds, Deseado, Santa Cruz, Sarmiento formation, Argentina (Soria 2001).

**Other specimens observed and scored:** MACN A-10718 (right mandibular fragment with m1, alveoli of p4-p5; holotype); MACN A-52-199 (right mandible fragment with i1-i2, c alveolus, p1, dp2-dp5 and m1-m2, left mandible fragment with dp5-m1 and m2); MACN A-52-198 (right maxillary fragment with P5-M3 and a left isolated buccal part of P4?); MACN A-52-801 (left maxillary fragment with P5-M3; type of *Deuterotherium distichum*); MNHN.F.DES159 (right mandible fragment with p5-m3); MNHN.F.DES158 (left mandible fragment with p5-m2); MNHN.F.DES162 (left M1); MNHN.F.DES163 (left M2); MNHN.F.DES164 (left M1); AMNH 29554 (fragmentary skull with C-M3).

**Known distribution:** Bahía Sanguinetti, Punta Nava beds and La Flecha, Deseado, Santa Cruz, and Cabeza Blanca, Escalante, Chubut, Sarmiento Formation, Argentina (Soria 2001).

**Age/SALMA:** Late Oligocene/Deseadan (29.3 – 26.0). The known locations for *Lambdaconus suinus* are all of Deseadan SALMA age (Woodburne *et al.* 2014*b*).

**Additional relevant references with descriptions and illustrations:** Schmidt *et al.* (2019)

**Taxonomic comments:**

- The specimen MACN A-52-801 was figured in Schmidt *et al.* (2019) under a different number (MACN A-12655). I was able to examine only pictures of this specimen, because is currently lost in the MACN collection.

- In the specimen AMNH 29559 of *Lambdaconus suinus* there is a small and worn mesial tooth that Simpson (1932) interpreted as a I3 or C. I interpreted it as C considering its position and the fact that in the mandible of a different specimen (MACN A-52-199) the c is small and separated from p1 and p2 by a diastema.

- In the specimen MACN 52-198 of *Lambdaconus suinus*, there is an isolated broken premolar previously described as right P4 (e.g., Schmidt *et al.* 2019). However, considering the morphology of P5 and the molars, which present a preparaconule crista almost continuous to the parastyle and the absence of a postmetaconule crista, the conule and crista seen in P4 are probably a paracone and a preparaconule crista. This means that this tooth corresponds to a left P4 instead of a right P4.

**Anatomical comments:**

- There is a discussion in relation to the presence or absence of an hypocone in P5 and P4. Simpson (1932) consider that the hypocone was present in P4 and P5 based on AMNH 29554, although there was considerable wear in these premolars. Examining specimens with less wear (MACN A-52-198; MACN A-52-801), Soria (2001) considered the hypocone to be absent in P4 and P5, although with the presence of a strong postcingulum that creates a talon in both premolars. I followed the latter interpretation for scoring.

- *Lambadaconus suinus* lacks a metaconule in M3 and M2. M1 presents one metaconule, like in the specimens MNHN DES 162 and 163 as observed previously (Soria 2001). Therefore, the presence of a metaconule in M1-M2 was scored as both present and absent (polymorphic).

### *Diadiaphorus majusculus* (Ameghino 1887)

= *Dradiaphorus diplinthius* (Ameghino 1891*b*)

= *Bunodontherium majusculum* (Mercerat 1891*b*)

= *Diadiaphorus robustus* (Ameghino 1894*c*)

= *Diadiaphorus coelops* (Ameghino 1904*b*)

**Holotype and type locality:** MLP 12-333 (right mandible fragment with p5 root, talonid of m1 and m2-m3; not observed/examined here) from the estuary of Santa Cruz, Corpen Aike, Santa Cruz formation, Argentina (Soria 2001).

**Specimens observed and scored:** AMNH FM 14499 (fragment of the cranium with left and right P1-M3, and well-preserved mandible with left p1-m3 and right p2-m3; cast); AMNH FM 14482 (cranium with basicranium preserved and left P2-M3 and right P1-M3; cast); MACN A 9180-82 (cranium and mandible with left talonid of p1 and p2-m3 and right p2-m3); MACN A 9118 (fragmentary cranium with left P2-M3 and right P1-M3); MACN 9137 (well preserved cranium with left and right I1-M3); MLP 12-304 (cranium with part of basicranium preserved and left I1-M3 and right P1-P5); MLP 12-306 (fragmentary cranium with left and right P1-M3); YPM PU 15751 (right maxilla fragment with I1-M3 and left mandible fragment with i1-m3); YPM PU 15752 (right maxilla fragment with I1-M3 and right mandible fragment with i2-m3); YPM PU 15799 (cranium with part of basicranium preserved and left P1-M3 and right I1-M3, and mandible with left i1-m3 and right i1-P2)

**Specimens not examined:** The holotype and additional specimens listed in Soria (2001).

**Known distribution:** Several locations in the Santa Cruz formation, Argentina (Soria 2001): Corrigen Aike: MACN A 9180-82; Monte Observación (=Cerro Observatorio): MACN-A 9137; Cañadón Corto; Sehuén; Monte León; La Cueva from Corpen Aike; Este de Rincón del Buque from Güer Aike.

**Age/SALMA:** Early Miocene/Santacrucian (18 – 15.6 Ma). This age was based in age estimated for the Santacrucian SALMA in (Cuitiño *et al.* 2016).

**Additional relevant references with descriptions and illustrations:** Scott (1910); Soria (2001); Cassini *et al.* (2012)**.**

**Anatomical comments:**

- The metaconule seems to be variably present in P4. From all the specimens I examined, it is present in YPM PU 15799 and absent in MLP 12-306.

- P2 presents a girthy paraconule. There is no character about this dental feature in the matrix, but it could have some importance for testing phylogenetic affinities within Proterotheriidae.

- There is one upper incisor in *Diadiaphorus majusculus* and it is difficult to establish if it is I1 or I2. In any case, for scoring, I considered it as the anteriormost incisor.

## Family Sparnotheriodontidae (Soria 1980*a*)

### *Victorlemoinea prototypica* (Paula Couto 1952)

**Holotype and type locality:** MNRJ 1470V (left M2) from fissure fills in the Itaboraí Formation, near São José de Itaboraí, Rio de Janeiro, Brazil (Paula Couto 1952).

**Other specimens observed and scored:** MNRJ 1471V (left M1 or M2; paratype); MNRJ 1472V (left M3); MNRJ 2484 (left M1); MNRJ 1482V (right m2). AMNH 49816 (left M3); DGM 268M (left mandible fragment with dp4-dp5, m1); AMNH 111963 (right M1; cast of MNRJ specimen).

**Known distribution:** Fissure fills in the Itaboraí Formation, near São José de Itaboraí, Rio de Janeiro, Brazil (Paula Couto 1952).

**Age/SALMA:** Early Eocene/Itaboraian (56.0 – 51.4 Ma). Based on (Krause *et al.* 2017).

**Additional relevant references with descriptions and illustrations:** Paula Couto (1978*b*).

**Taxonomic comments:**

- The position and orientation of the isolated molars of *Victorlemoinea prototypica* in the maxilla were inferred from other species of *Victorlemoinea* (MACN specimens), *Phoradiadus* specimens, and also *Paranisolambda* specimens to a certain extent.

**Anatomical comments:**

- In the upper molars, *Victorlemoinea prototypica* shows a secondary precingulum and postcingulum below the main one, similar to *Notiolofos* and the anisolambdid *Paranisolambda*. This feature has been observed previously (Bond *et al.* 2006; Gelfo *et al.* 2019).

### *Notiolofos arquinotiensis* (Bond et al. 2009)

=*Notolophus arquinotiensis* (preoccupied name; Bond *et al.* 2006)

**Holotype and type locality:** MLP 95-I-10-6 (left M3 incomplete, buccal part of paracone and metacone is missing) from DPV 16/84 locality, La Meseta Formation, Submeseta Member (TELM 7), Seymour Island, Antarctica (Bond *et al.* 2006).

**Other specimens observed and scored:** MLP 08-XI-30-43 (left p5); MLP 04-III-3-1 (right p5); MLP 12-XI-1-11 (left p4); MLP 90-I-20-5 (left P4); MLP 91-II-4-5 (left P1?); MLP 01-I-1-1 (right m3); MLP 91-II-4-1 (right m1); MLP 13-I-25-1 (talonid fragment of m1 or m2); MLP 90-I-20-1 (fragmentary left M1 with lingual portion and mesial part of the buccal portion preserved); MLP 96-I-5-9 (left i3); MLP 90-I-20-3 (right I3); MLP 96-I-5-10 (I3); MLP 94-III-15-3 (i2).

**Known distribution**: La Meseta (Acantilados II [Telm 3], Campamento [Telm 3], Cucullaea I [Telm 5] Allomembers) and Submeseta formations [Telms 6 and 7]. More details of all the localities in (Gelfo *et al.* 2019).

**Age/SALMA:** Middle Eocene to late Eocene/Itaboraian-Mustersan (44 – 34 Ma). Gelfo (2016) gives an approximate time interval between the oldest (MLP 13-I-25-1) and the youngest (MLP 95-I-10-6) records of *Notiolofos arquinotiensis* of 55.3 – 37.8 Ma based on previous isotopic dates of the La Meseta and Submeseta formations (Ivany *et al.* 2008; Montes *et al.* 2013). However, Douglas *et al.* (2014) based on dinoflagellates cyst samples suggest an age of 45 – 34 Ma for the La Meseta and Submeseta formations (from Telm 2 – Telm 7). More recently, Amenábar *et al.* (2019) complementing the ages proposed by Douglas *et al.* (2014), recovered an age of 44 – 40 Ma for Acantilados I to Cucullaea II Allomembers (from Telm 2 – Telm 6). As specimens of *Notiolofos arquinotiensis* here scored are recovered from strata representing Telms 3 to Telms 7, I consider an age of 44 – 34 Ma for this taxon following the latter interpretations (Douglas *et al.* 2014; Amenábar *et al.* 2019). This temporal interval could be narrowed in the future with a more precise estimation of Telm 2. It is important to mention that these estimates based on dinoflagellates (Douglas *et al.* 2014; Amenábar *et al.* 2019) contradict a recent age model based on magnetostratigraphy, isotopic data ($^{87}Sr/^{86}Sr$) and lithostratigraphy that suggests an age of ~58.4 – ~45.8 Ma for La Meseta formation (Montes *et al.* 2019). The reasons for this discrepancy require further studies (Amenábar *et al.* 2019) .

**Taxonomic comments:**

- I followed Gelfo's (2016) interpretations for the positions of the isolated teeth of *Notiolofos arquinotensis*, which was based on comparisons with the sparnotheriodontid *Sparnotheriodon epsilodonoides*.
- As Gelfo (2016) previously mentioned, the distal part of the buccal fragment of the M1 (MLP 90-I-20-1) of *Notiolofos arquinotensis* was broken and lost from the MLP collections. Therefore, some scores were based on a previous drawing of this specimen presented in Bond *et al.* (2006).
- I interpret MLP 91-II-4-5 to be a left P1 (*contra* Bond *et al.* [2006] and Gelfo [2016]) because of the distal shape of the lingual cingulid that resembles more what is seen in other litopterns such *Theosodon* and *Diadiaphorus*.

**Anatomical comments:**

- The paraconule of *Notiolofos arquinotensis* is not well preserved in any upper tooth due to wear. However, there is clearly a preprotocrista in the M1(MLP 90-I-20-1) and M3 (MLP 95-I-10-6), which tends to rise close to the area in which you would expect a paraconule. However, in both specimens that area is worn and parts of it are missing, so the exact position of this paraconule cannot be inferred. In any case, it is likely it was a very reduced cusp in terms of girth, maybe similar to the condition exhibited by the metaconule of this taxon.
- *Notiolofos* presents a secondary postcingulum as well in M3 (MLP 95-I-10-6), in M2 (MLP 90-I-20-1) and also in P4 (MLP 90-I-20-5). This is similar to *Victorlemoinea* and the anisolambdid *Paranisolambda*, as previous authors have observed (Bond *et al.* 2006; Gelfo *et al.* 2019).

### *Sparnotheriodon epsilonoides* (Soria 1980a)

**Holotype and type locality:** MACN 18225 (mandible fragment with symphysis and right and left i1-m3) from Cañadón Vaca, Sarmiento Formation, Chubut, Argentina (Soria 1980*a*).

**Known distribution:** Just the type locality.

**Age/SALMA:** Middle Eocene/Vacan (45 – 42 Ma). Based on the age of Cañadón Vaca (Vacan SALMA (Woodburne *et al.* 2014*b*).

## Families that are sometimes placed within Litopterna but that have been considered to be part of the order Notopterna (Soria 1984*b*)

### Family Indaleciidae (Soria 1989*b*)

#### *Indalecia grandensis* (Bond & Vucetich 1983)

**Holotype and type locality:** PVL 4186 (crushed skull with basicranium preserved and roots of I1-I2 and right and left I3-M3, and mandible with right c1-m3 and left i3-m3) from Faja Verde Inferior of the lower section of the Lumbrera Formation, Estancia Pampa Grande, Salta, Argentina (Bond & Vucetich 1983).

**Other specimens not examined:** There is another specimen PVL 6S- 12 (mandible fragment with m3) from the same locality as the holotype and mentioned previously (Bond & Vucetich 1983; Cifelli & Soria 1983*a*). However, this was not found in the PVL collection and thus not considered in the scoring of this taxon.

**Known distribution:** Just the type locality.

**Age/SALMA:** Early Eocene/Itaboraian to Sapoan Fauna (55 – 46.2 Ma). The specific age interval was based on an age estimation for the lower section of the Lumbrera Formation (Fernicola *et al.* 2021).

**Anatomical comments:**

- Because the level of wear of the postcingulum in *Indalecia*'s M3, it is difficult to evaluate the presence of a very small hypocone/distocone. I scored the distocone as present and much smaller than the protocone, as the postcingulum rises lingually.
- *Indalecia* seems to show a small and closely appressed metacone in P5. Therefore, I scored it as present even if some authors (Bond & Vucetich 1983; Cifelli & Soria 1983*a*) previously have said I that the P5 of *Indalecia* does not have a metacone.

### Family Notonychopidae (Soria 1989*a*)

#### *Requisia vidmari* (Bonaparte & Morales 1997)

**Holotype and type locality:** UNPSJB PV 944 (maxillary fragment with P4-P5, roots of M1-M2, and mesial portion of the alveolus of M3) from Banco Negro Inferior, Punta Peligro, Salamanca Formation, Chubut, Argentina (Bonaparte & Morales 1997).

**Other specimens observed and scored:** UNPSJB PV 945 (right maxillary fragment with P2-P4); UNPSJB PV 947 (right M1?); UNPSJB PV 948 (buccal portion of an upper premolar [?] with worn protocone preserved).

**Known distribution:** Just the type locality.

**Age/SALMA:** Early Palaeocene/Peligran (63.8 – 63.2 Ma). Based on the age of the Peligran SALMA (Woodburne *et al.* 2014*a*).

**Taxonomic comments:**

- Bonaparte & Morales (1997) considered the specimen UNPSJB PV 946 as m3 of *Requisia vidmari* because it was found close to the other remains attributed to this taxon in Punta Peligro. However, due to the marked bunodonty of its cusps, more recently Goin *et al.* (2022) considered that this m3 does not belong to *Requisia*, being probably of an m3 of a "didolodontid". I followed the latter interpretation for the scoring of this taxon, and therefore this m3 (UNPSJB PV 946) was no scored.

**Anatomical comments:**

- The *Requisia* specimen UNPSJB PV 947 was considered to be a left M1 by Bonaparte & Morales (1997). However, comparing this specimen with *Notonychops* (Soria 1989*b*) it is clear that is probably a right M1 or M2, considering the relative position of the protocone and the presence of a very worn hypocone which was previously omitted (Bonaparte & Morales 1997). *Notonychops* has an hypocone in M1 and M2 which is similar in position to the worn area considered by me to be a hypocone in *Requisia*.
- In the P5 and P4 of *Requisia* and also *Notonychops*, there is a postprotocrista that ends in the position of the metaconule, where instead of a clear cusp, there is crest. In terms of scoring, I considered the metaconule to be present but reduced to merged cristae.

### *Notonychops powelli* (Soria 1989*a*)

**Holotype and type locality:** PVL 4298 (crushed skull, with left P4-M3 and right alveolus of P1 with root and P2-P5, broken M1 and M1-M3, left mandible fragment with p2-m3 and right mandible fragment with p2-m3) from lower section of the Río Loro Formation, 30 kilometres of San Miguel de Tucumán, Argentina (Soria 1989*a*).

**Known distribution:** Just the type locality.

**Age/SALMA:** Age of the Río Loro Formation is uncertain, but based on its mammalian fauna it could be from early Palaeocene to early Eocene/Peligran to Itaboraian (Gelfo *et al.* 2020*a*). Therefore, for calibrating this tip, the interval used was 63.8 – 51.4 Ma to consider the uncertainty associated with the age of this formation.

**Anatomical comments**

- Soria (1989*a*) mentioned that there is no P1 alveolus in the right side of the maxilla. However, PVL 4298 presents a small P1 alveolus with its root present (i.e., no crown preserved).
- Soria (1989*a*) mentioned a lophoid metaconule (postmetacristula?) that divides the postcingulid into two parts in the M3 of *Notonychops powelli*. I interpret that the metaconule is a smaller cup located mesial to the cusp mentioned by Soria (1989*a*), which in my view is actually a small hypocone.
- Soria (1989*b*) considered that there is no paraconid in m1-m3 of *Notonychops powelli*. I consider that the paracristid ends in a small paraconid because there is a certain girth at the point you would expect to be a paraconid present.

## Other families that are sometimes placed within Litopterna

## Family Protolipternidae (Cifelli 1983a)

### *Protolipterna ellipsodontoides* (Cifelli 1983*a*)

**Holotype and type locality:** DNPM LE444A (mandibular fragment with c, alveoli of right and left p1-p2 and right and left p4-m3, and right maxillar fragment with M1-M3) from fissure fills in the Itaboraí Formation, near São José de Itaboraí, Rio de Janeiro, Brazil (Paula Couto 1952).

**Other specimens observed and scored:** DGM 1308M (left mandible fragment with p2-m3); DNPM LE 444C (right mandible fragment with p4-m3; DNPM LE 444D (left mandible fragment with p5-m3 and mandibular ramus preserved); DNPM LE 444E (right mandible fragment with m1-m3); DNPM LE 444F (left maxillar fragment with P5-M3); DNPM LE 444G (mandibular fragment with mandibular symphysis); DNPM LE 444H (left maxillar fragment with M1-M3); DNPM LE 444I (left maxilla fragment with P5-M3); DNPM LE 444B (right mandibular fragment with p4-m3); MCT 1392D (left mandible fragment with p5-m1 and complete ramus preserved); MCT 1635M (left p2); MCT 1456M (left p4); MCT

1647M (right p4); MCT 1547M (left p4); MCT 2114M (left p5); MCT 2308M (right p5); MCT 1317M (right m1); MCT 1618M (left m1 or right m1 [probably a duplicated specimen number)]); MCT 2194M (left m2); MCT 1445M (left m2); MCT 2192M (left m2); MCT 2170M (right m3); MCT 2162M (right m3); MCT 1615M (left m3); MCT 1628M (left P2); MCT 1626M (right P4); MCT 1135M (right P5); MCT 1622M (left P5); MCT 1396M (right P5); MCT 1429M (right M1); MCT 1777M (right M1); MCT 1772M (right M1); MCT 1783M (left M1); MCT 1806M (right M1); MCT 2117M (right M1); MCT 1438M (left M2); MCT 1765M (left M2); MCT 1774M (right M2); MCT 2151M (right M2); MCT 1627M (left M3); MCT 1689M (right M3); MCT 1708 (left M3); MCT 2152M (left M3). There were some mistakes in the tooth positions of the isolated teeth illustrated in Zanesco *et al*. (2019). In particular, there were some instances in which a right tooth was listed as left tooth (and vice versa). These errors were amended in this list.

**Known distribution:** Just the type locality.

**Age/SALMA:** Early Eocene/Itaboraian (56.0 – 51.4 Ma). Based on Krause *et al.* (2017).

**Additional relevant references with descriptions and illustrations:** Zanesco *et al.* (2019)

**Anatomical comments:**

- *Protolipterna*'s P2 in Zanesco *et al.* (2019) is misplaced. It should be rotated in 90 degrees clockwise to be better represented. Also, it is likely a left P2 instead of a right P2, if we follow the morphology of the P2 of *Didolodus* multicuspis (MACN 10690). Therefore, I considered it a left P2 for scoring.

### *Miguelsoria parayiruhnor* (Paula Couto 1952; Cifelli 1983*a*)

= *Ernestokokenia parayiruhnor* (Paula Couto 1952)

**Holotype and type locality:** MNRJ 1468V (right hemimandible with alveoli of i1-2, root of i3, alveoli of p1-p2, and with the c and p3-m3 present) from fissure fills in the Itaboraí Formation, near São José de Itaboraí, Rio de Janeiro, Brazil (Paula Couto 1952).

**Other specimens observed and scored:** MNRJ 1468V (holotype; right hemimandible with alveoli of i1-2, root of i3, alveoli of p1-p2, and with the c and p3-m3 present); DGM 305-M (maxilla fragment with M2-M3); MNRJ 4094V (maxilla fragment with p2, alveolus of p4-

p4, and m1-m3; DGM 249M (mandible fragment with m1-m2); DGM 296M (mandible fragment with m2-m3); DGM 330M (mandible fragment with symphysis, right c, p2-m2, and left p2); MNRJ 1466V mandible fragment with m1-m2); DGM 249M (left mandible fragment with condyle, coronoid process and m1-m3).

**Known distribution:** Just the type locality.

**Age/SALMA:** Early Eocene/Itaboraian (56.0 – 51.4 Ma). Based on Krause *et al.* (2017).

**Additional relevant references with descriptions and illustrations:** Paula Couto (1978*b*).

**Taxonomic comments:**

- There is variability in the presence of the paraconid in *Miguelsoria parayiruhnor*. In particular, this is absent in DGM 249M. The same specimen (DGM 249M) also has a preentoconulid. It is possible that DGM 249M is a different taxon from *M. parayiruhnor*, although more evidence is needed to discard intraspecific variation.

### *Asmithwoodwardia scotti* (Paula Couto 1952)

**Holotype and type locality:** DGM 358M (skull, with right P4, M1-M3, and left P4-M3, and mandible with i1-m3) from fissure fills in the Itaboraí Formation, near São José de Itaboraí, Rio de Janeiro, Brazil (Paula Couto 1952).

**Other specimens observed and scored:** DGM 410M (right mandible fragment with m1-m3); AMNH 49817 (right mandible fragment with p4-m2); MCT 2312M (left mandible fragment with p4-m3, alveolus of p2 and part of the symphysis).

**Known distribution** Just the type locality.

**Age/SALMA:** Early Eocene/Itaboraian (56.0 – 51.4 Ma). Based on Krause *et al.* (2017).

**Additional relevant references with descriptions and illustrations:** Paula Couto (1978*b*).

## Family Didolodontidae (Scott 1913)

### *Escribania chubutensis* (Bonaparte *et al.* 1993)

**Holotype and type locality:** UNPSJB PV 916 (left mandible fragment with m2–m3) from Banco Negro Inferior, Punta Peligro, Salamanca Formation, Chubut, Argentina (Bonaparte *et al.* 1993).

**Other specimens observed and scored:** MLP 93-XII-10-2 (left m2); MPEF-PV 1860 (right mandible fragment with m1-m2); MLP 93–XII-10–1 (right mandible fragment with m3); MLP 90–II-12–68 (maxillary fragment with M2); MPEF- PV 1860 (right mandible fragment with m1-m2); MLP 90–II-12–63 (right maxillary fragment with M2-M3).

**Known distribution:** Just the type locality.

**Age/SALMA:** Early Palaeocene/Peligran (63.8 – 63.2 Ma). Based on Woodburne *et al.* (2014*a*).

**Additional relevant references with descriptions and illustrations:** Gelfo *et al.* (2007); Kramarz *et al.* (2021).

**Anatomical comments:**

- The M2 of *Escribania chubutensis* (MLP-90-II-12-68) has a hypocone-metaconule crista, previously described as an entocrista (Goin *et al.* 2022). Also, the hypoconce seems to be connected to the protocone as in *Raulvaccia*'s M2 (although is too worn to be entirely sure). This is interesting because is similar to the condition seen in *Paranisolambda* and *Victorlemoinea* in which there is two cristae coming from the hypocone (distocone), one connecting with the protocone and the other with the metaconule. Interestingly, the M3 does not show this pattern, and the metaconule is connected to the protocone with a postprotocrista, which is the primitive condition (e.g., condition seen in *Protoungulatum*).

- Goin *et al.* (2022) mentioned a short metacristid (premetacristid) in m1-m2 of *Escribania chubutensis*, but previously Gelfo *et al.* (2007) stated that "There is no metacristid in occlusal view" for MPEF-PV 1860. I did not observe any premetacristid in m1-m2 when scoring this taxon. The m3 of the holotype (UNPSJB PV 916) seems to have a weak premetacristid.

### *Raulvacia peligrensis* (Bonaparte *et al.* 1993)

**Holotype and type locality:** UNPSJB PV 915 (left mandible fragment with part of m1) from Banco Negro Inferior, Punta Peligro, Salamanca Formation, Chubut, Argentina (Bonaparte *et al.* 1993).

**Other specimens observed and scored:** MLP 90−II−12−69 (left mandible fragment with talonid of m2 and m3); MLP 90-II-12- 70 (left M2).

**Known distribution:** Just the type locality.

**Age/SALMA:** Early Palaeocene/Peligran (63.8 – 63.2 Ma). Based on Woodburne *et al.* (2014*a*).

**Additional relevant references with descriptions and illustrations:** Gelfo (2007).

### *Ricardocifellia protocenica* (Paula Couto 1952; Cifelli 1983*a*; Cifelli & Ortiz-Jaureguizar 2014; Mones 2015)

**Holotype and type locality:** MNRJ 1430-V (left maxillary fragment with P4-M3) from fissure fills in the Itaboraí Formation, near São José de Itaboraí, Rio de Janeiro, Brazil (Paula Couto 1952).

**Other specimens observed and scored:** MNRJ 1431-V (left mandible fragment with m1-m3; paratype); MNRJ 1432-V (right mandible fragment with m3); MNRJ 1462-V (right M2-M3); MNRJ 1439-V (left m2); MNRJ 1434-V (right m3); MNRJ 1438-V (right m2); MNRJ 1454-V (right M2); MNRJ 1460-V (left P3); MNRJ 1461-V (left P3); MNRJ 1456-V (left M2); MNRJ 1457-V (right M1); MNRJ 1458-V (left M1); MNRJ 1459-V (left M1); MNRJ 1451-V (left M3); MNRJ 1452-V (left M3); MNRJ 1453-V (right M2); MNRJ 1441-V (right m1); MNRJ 1448-V (left p5?); MNRJ 1450-V (left p4?); MNRJ 1433-V (left m3); MNRJ 1449-V (left p4?); MNRJ 1444-V (left m1); AMNH 109553[DNPM 908M] (maxillary fragment with P5-M3); AMNH 49819 (right mandible fragment with m2-m3);

**Known distribution:** Just the type locality.

**Age/SALMA:** Early Eocene/Itaboraian (56.0 – 51.4 Ma). Based on Krause *et al.* (2017).

**Additional relevant references with descriptions and illustrations:** Paula Couto (1978*b*)

**Anatomical comments:**

- The premetaconule crista and the postparaconule are variably present in *Ricardocifellia*. For example, the holotype MNRJ 1430V and DNPM 908M do not have these cristae in M1-M2, but MNRJ 1453V (isolated M2) had them both.
- A very small mesostyle is variably present in the M3 of *Ricardocifellia protocenica*. From the specimens I examined, it is present only in the holotype MNRJ 1430V and in MNRJ1462V.
- The hypocone is always present in *Ricardocifellia protocenica*.

### *Didolodus multicuspis* (Ameghino 1897)

= *Didolodus crassicuspis* (Ameghino 1901)

= *Lonchoconus lanceolatus* (Ameghino 1901)

= *Didolodus colligatus* (Ameghino 1902*b*)

= *Cephanodus colligatus* (Ameghino 1902*c*)

=*Nephacodus latigonus* (Ameghino 1902*b*)

= *Didolodus dispar* (Ameghino 1904*a*)

=*Argyrolambda conidens* (Ameghino 1904*a*)

= *Argyrolambda conulifera* (Ameghino 1904*b*); typographic mistake)

= *Didalodus multicuspis* (Roth 1927); typographic mistake)

= *Didolodus latigonus* (Simpson 1948)

= *Didolodus conidens* (Simpson 1967)

**Holotype and type locality:** MACN 10690 (left maxillary fragment with P2-M3 and alveoli of P1 and C) from Casamayoran beds (Simpson 1948). No exact data of provenience is given by Ameghino (1897) for the holotype of *D. multicuspis*, and the same is true for the other synonymous types (Simpson 1948; Gelfo 2010).

**Other specimens observed and scored:** MACN A 10738 (right P1 and P2); MACN A 10720 (right mandible fragment with m3, roots of m2 and alveoli of i3-m1, and possibly associated M1 and C); MACN A 10689 (right p2-m3; type of *Didolodus crassicuspis*); MACN

A 10730 (left M1; type of *Lonchoconus lanceolatus*); MACN 10725 (left m2; type of *Didolodus latigonus*); MACN A 10736 (right m3, and left p4 and p5; type of *Didolodus colligatus*); MACN A 10733 (broken right M2; type of *Didolodus dispar*); MACN A 55-8 (broken right M1); AMNH 28475 (right mandible fragment with p5, alveolus of m1 and m2-m3); MLP 59-II-24-226 (left M3).

**Known distribution:** Cerro Guacho, Sarmiento Formation, Chubut, Argentina: MLP 59-II-24-226; The rest of the fossils do not have clear provenance, probably being most from the Barrancan SALMA in the Sarmiento Formation, but some materials from Río Chico Oeste could potentially have a Vaca SALMA age (Gelfo 2006)

**Age/SALMA:** Early to middle Eocene/Vacan to Barrancan (45 – 39 Ma). Considering the stratigraphic uncertainty of some of the fossils of *D. multicuspis* that I scored, I included the whole interval between the Vacan and Barrancan SALMAs for the temporal occurrence of this taxon. Cerro Guacho is considered Barrancan SALMA (Reguero & Prevosti 2010; Kramarz & Bond 2013).

**Additional relevant references with descriptions and illustrations:** Gelfo (2006, 2010).

## Other groups of interest

## Order Astrapotheria (Lydekker 1894)

### *Trigonostylops wortmani* (Ameghino 1897)

**Holotype and type locality:** MACN 10651 (probably M2, P4 and talonid of m3) with no locality data (Simpson 1948).

**Specimens observed and scored:** MACN A 10642 (maxilla fragment with M1-M3); MPEF PV 5483 (mandible with left i1-i3 alveoli, c, alveolus of p1 and p2-m3, and right alveoli of i1-i3, broken c, alveolus of p1 and p2-m3); MLP 52-X-5-98 (cranium fragment with left and right roots of C and P1, and P2-P5, M1, and M2); AMNH VP-28700 (skull with right P2-M3 and left P2-M2; young adult); MNHN.F.CAS1200 (cranium fragment with left C, alveolus of P1, P2-P5, and right C, alveoli of P1-P4); MNHN.F.CAS187 (right maxilla fragment with C, alveolus of P1, P2-M3); MNHN.F.CAS188 (mandible with left and right i1-m3).

**Known distribution:** Pampa de María Santísima, Sarmiento Formation, Chubut Argentina (Macphee *et al.* 2021): MLP 52-X-5-98; Barranca south of Lago Colhué-Huapí,

Sarmiento Formation, Argentina (Macphee *et al.* 2021): AMNH VP-28700; Río Chico, Chubut, Argentina(Simpson 1948): MACN A 10642; Cerro Negro, Chubut, Argentina (Tournouër collection 1903.24): MNHN.F.CAS1200; Casamayor, Chubut, Argentina (Tournouër collection 1903.3): MNHN.F.CAS187, MNHN.F.CAS188.

**Age/SALMA:** Middle Eocene/Vacan to Barrancan (45.0 – 39.0 Ma). The scored specimens have considerable uncertainty in relation to their age, in particular the "Casamayoran" specimens from Río Chico, Cerro Negro and Casamayor (Simpson 1948, 1964). Therefore, the interval here used is between the Vacan and Barrancan SALMA to include the uncertainty of their provenience, which is in agreement of the temporal distribution of *Trigonostylops wortmani* given by previous authors (Kramarz & Bond 2013).

**Anatomical comments:**

- Soria (1988) considers that the paraconid in *Trigonostylops wortmani* and *Tetragonostylops apthomasi* is not a true paraconid, but instead a neo-paraconid. He based this interpretation in the fact that the Palaeocene *Eoastrapostylops riolorense* does not have a paraconid (Soria & Powell 1981). In the matrix I consider this cusp as a true paraconid considering its position, and in order to make less assumptions about evolutionary processes.

## Order Notoungulata (Roth 1903)

### *Simpsonotus praecursor* (Pascual *et al.* 1978)

**Holotype and type locality:** MLP 73-VII-3-11 (flattened skull with left I2-M3 and right C-M3, and mandible with left i2?-m3 and right i2-c, alveolus of p1 and p2-m3) from the vicinity of the road between Tres Cruces and Mina Aguilar, Mealla Formation, Jujuy, Argentina (Pascual *et al.* 1978).

**Specimens observed and scored:** Just the holotype.

**Known distribution:** Just the type locality.

**Age/SALMA:** Middle to late Palaeocene/gap between Itaboraian and *Carodnia* Zone (61 – 57 Ma). This age for the Mealla Formation was based on a recent study of the biostratigraphy of the Santa Bárbara Subgroup (del Papa *et al.* 2022)**.**

**Anatomical comments:**

- In early notoungulates of different suborders there is a mesiolingual cusp, very close and mesial of the metaconid. Unlike Simpson (1967), this cusp has been interpreted by later authors (Soria 1989a; Bauzá et al. 2020) as a paraconid in which the connection with the paracristid is lost. The position of this mesiolingual cusp in notoungulates is consistent with the position and size of the paraconid in kollpanines, didolodontids and early litopterns.

- *Simpsonotus preacursor* has been scored as having two metaconules in M1-M2. This follows the interpretation that the distocone or hypocone of *Simpsonotus* arises from a metaconule duplication and shift of this secondary metaconule. This is supported from observations of unworn specimens of *Henricosbornia* (e.g., MACN A 10717, right M1 or M2), which show a clear metaconule, and very close and associate with it by a crista, a distocone as a secondary hypertrophied metaconule. In addition, the distocone in notoungulates does not originate from the postcingulum as it is commonly seen in Litopterns, Didolodontids, Xenungulates, and North American mioclaenids (in addition to other "condylarths"). This interpretation is *contra* Muizon *et al.* (2019) interpretation of the distocone in M1-M2 of notoungulates ("pseudohypocone") as a cusp originated from a protocone duplication event, as it is seen to be the case in the kollpanine *Molinodus* and some "didodolodontids".

## Order Xenungulata (Paula Couto 1952)

### *Carodnia vieirai* (Paula Couto 1952)

**Holotype and type locality:** DGM 333M (maxillae fragments with right P1-P5 and fragmentary M2-M3, and left C root, P1-P5, fragmentary M1-M2 and M3, two upper I and root of C, mandible with right i1, alveolus of c, roots of p1-p4, fragmentary p5-m1 and complete m2-m3, and left i1-i3, alveolus of c, and p1-m3, and other remains described in Paula Couto [1952]) from fissure fills in the Itaboraí Formation, near São José de Itaboraí, Rio de Janeiro, Brazil (Paula Couto 1952).

**Other specimens observed and scored:** DGM 334M (mandible of subadult with right and left i1-m3); DGM 335M (maxilla fragment with I3, C, and a different individual anterior skull fragment with right P1-P2 and left P1-P4, and fragment of left maxilla with P5-M2, and isolated left P4, P5, M1, M2 and right M3); AMNH 49828 (left M3).

**Known distribution:** Just the type locality.

**Age/SALMA:** Early Eocene/Itaboraian (56.0 – 51.4 Ma). The age for the Itaboraian was based on Krause *et al.* (2017).

**Anatomical comments:**

- *Carodnia vieirai* does not have a clear paraconid in the lower molars. It also presents a paracristid of variable degree of development depending on the individual and in the molar position. In DGM 334M there seems to be a low paracristid in m1-m3. In DGM 333M the paracristid is probably interrupted in m2 and m3, but it is complete in m1 reaching the metaconid. Previous authors (Antoine *et al.* 2015) have mentioned the presence of a premetacristid. Considering the complete paracristid observed in other Xenungulates as *Notoetayoa* (Gelfo *et al.* 2008) and *Etayoa* (Villarroel 1987) and the presence of a reduced paraconid, which is closely appressed to the metaconid, I consider this condition as the probable plesiomorphic condition for Xenungulates and the condition observed in *Carodnia* as derived. This interpretation is consistent with the position of the paraconid and its development in early SANUs. Therefore, it is likely that in *Carodnia vieirai* the paraconid was extremely reduced and completely fused to the metaconid, and that the premetacristid described by Antoine *et al.* (2015) is part of the original paracristid that got unattached in some molars of *Carodnia*, which occlusally generates a dividing sulcus (Vera *et al.* 2020).

- In the original description of *Carodnia vieirai*, Paula Couto (1952) when describing upper molars, especially M1 and M2, he described two main lophs: a paraloph (protoloph) and a metaloph. In his description, there was no mention of any potential conules present in these lophs. The specimen DGM 335-M preserves relatively unworn left P1-M2 which allow interpretations in relation to the potential cusps present. In the metaloph of DGM 335-M, both M1 and M2, have a small bump slightly risen and wider that could be considered an extremely weak metaconule. M2 in DGM 335-M also presents a small but clear bump in the paraloph that could be interpreted as a paraconule. In the M1 of DGM 335-M the presence of this putative paraconule is not as clear as in M2, and the pictures that I have did not allow me to establish with certainty the presence of a paraconule. There is some wear in the M1 of DGM 335-M that could also have an effect in its apparent

lack of a paraconule. However, even if is no longer distinguishable, part of the origin of the paraloph in *Carodnia*'s M1 could be a very reduced paraconule, and therefore this was scored as present for M1-M2. M3 also helps in the interpretation for the cusps in M1-M2, as it shows a more primitive condition, with a postprocrista still present and connecting the protocone, which presents a small metaconule. The wear pattern in the paraloph of M3 also suggests the presence of a relatively girthy paraconule. In M1 and M2, the postprotocrista is lost and the small metaconule is connected with a crista to the hypocone (i.e., true hypocone derived from postcingulum) which generates the metaloph and also bilophodont pattern seen in these molars. The same interpretation of a very reduced paraconule can be applied for *Carodnia*'s P5 and P4.

- There seems to be two morphotypes of *Carodnia* in Itaboraí considering the mandible size and shape of two of the specimens (DGM 333M and DGM 334M) referred to *Carodnia vierai*. p5 and p4 (p4 and p3 from Paula Couto [1952]) show some differences between these two specimens. In DGM 334M there is a paraconid, whereas in DGM 333M there is a paracristid that does not end in a cusp. p2 is also considerably different: in DGM 333M there is no paraconid and the protoconid is more mesially located, whereas in the p2 of DGM 334M, there is a paraconid and the protoconid is located considerably more distally. In the p2 of DGM 333M the metaconid is close to the protoconid and has a similar size to it, in contrast to DGM 334M, in which both cusps are more separated and the metaconid is considerably lower than the protoconid. In addition, there are some differences in the upper premolars of DGM 335M and DGM 334M. DGM 335M has a metacone in P2-P4 which is small and merged to the paracone. However, in DGM 333M the metacone is not present or extremely reduced. Some of the differences could be related to DGM 334M being a subadult as Paula Couto (1952) suggested. Potential alternative explanations are: (1) important dental variation (polymorphism) in *C. vierai*, (2) sexual dimorphism, and (3) the presence of two species of *Carodnia* in Itaboraí. More direct observations of the specimens are needed to confirm or reject each hypothesis.

- *Carodnia*'s m3 presents a clear hypoconulid, which is connected with postentocristid (=postcristid) to the entoconid, and the hypoconid in m3 does not connect with any of these cusps. In m1-m2 there is a transverse crest connecting the

hypoconid with the entoconid, and the hypoconulid is not present as a clear cusp, so if present, it has been fully integrated to the protolophid. The presence of the hypoconulid in m3 favours this interpretation. Another source of support comes from *Etayoa*, as it shows a clear distinct hypoconulid in m1-m2 participating in the protolophid which has led Villarroel (1987) to suggest a phylogenetic connection with Astrapotheria. However, Gelfo *et al.* (2008) found this feature to be convergent in a phylogenetic analysis based on a small lower molar matrix. Considering all the available evidence, I consider the hypoconulid to be present in *Carodnia* for scoring, even though it cannot be clearly distinguished from a crest.

### *Etayoa bacatensis* (Villarroel 1987)

**Holotype and type locality:** GM 32 (left mandible fragment with p2-m3) from Bogotá Formation, Colombia.

**Specimens observed and scored:** Just the holotype.

**Known distribution:** Just the type locality.

**Age/SALMA:** Early Eocene/Itaboraian (57.8 – 54.6 Ma). Age based in volcanic zircons recovered from an interbedded tiff that dates the Bogotá Formation as early Eocene in age (55.2 ± 1.6 Ma; Bayona *et al.* 2010; Morón *et al.* 2013).

## Subfamily Kollpaniinae (Marshall *et al.* 1990)

### *Molinodus suarezi* (Muizon & Marshall 1987*b*)

**Holotype and type locality:** YPFB Pal 6112 (left mandibular fragment with m1-3) from the site 2 of the locality of Tiupampa, Cochabamba Department, Bolivia (Muizon & Cifelli 2000).

**Specimens observed and scored:** MHNC 8280 (right maxilla fragment with dP5, M1-M2); MHNC 1247 (right maxilla fragment with P4-M3); MNHN 13870 (left maxilla fragment with M1-M3[M1-M2 lost their buccal portion]); MHNC 8330 (left M1 with broken protocone); YPFB Pal 6118 (right M2); MHNC 13867 (left mandible fragment with p4-m3); YPFB Pal 6113 (right mandible fragment with m1-m2 and erupting m3); MHNC 8344 (right mandible fragment with m1-m2); YPFB Pal 6114 (right mandible fragment with m2-m3); MHNC 8269 (left mandible with m1-m3); MHNC 1238 (left m3); MHNC 1243 (right mandible fragment with p2); YPFB Pal 6117 (left M1); MHNC 1248 (left M3); MHNC 1244 (right p5); MHNC

13883 (left mandible fragment with alveoli of incisors, c, p1, roots of p2, alveoli of p4 and alveolus of anterior root of p5).

**Known distribution:** All specimens except the holotype and MHNC 8344 are from from site 1 ("the quarry") at Tiupampa, Cochabamba Department, Bolivia. MHNC 8344 is from the same locality as the holotype (Muizon & Cifelli 2000).

**Age/SALMA:** Early Palaeocene/Tiupampan (64 – 63 Ma). The lower age was based on (Woodburne *et al.* 2014*a*) and the upper following (Flynn & Swisher 1995).

**Additional relevant references with descriptions and illustrations:** Muizon *et al.* (2019)**.**

**Anatomical comments:**

- P5 of *Molinodus suarezi* (MHNC 1247) has a small metacone (swelling) not mentioned in Muizon & Cifelli (2000). This is interesting, because Muizon & Cifelli (2000) considered this feature as a didolodontid-litoptern synapomorphy excluding kollpanines. Instead, I think this feature is probably shared between kollpanines, didolodontids and litopterns.

### *Tiuclaenus* spp. (Muizon & Marshall 1987*a*; Muizon & Cifelli 2000)

Included species in the scoring:

***Tiuclaenus minutus*** (Muizon & Marshall 1987*a*)

***Tiuclaenus cotasi*** (Muizon & Cifelli 2000)

***Tiuclaenus robustus*** (Muizon & Cifelli 2000)

**Holotypes and type localities: *Tiuclaenus minutus*:** YPFB Pal 6115 (left mandibular fragment with alveoli of i1 and i3, i2, c, alveolus of p1 and p2-m3) from site 1 ("the quarry") at Tiupampa, Cochabamba Department, Bolivia (Muizon & Cifelli 2000); ***Tiuclaenus cotasi*:** MHNC 1231 (left mandible fragment with p4-m3) from site 1 ("the quarry") at Tiupampa, Cochabamba Department, Bolivia (Muizon & Cifelli 2000); ***Tiuclaenus robustus*:** MHNC 1233 (left mandibular fragment with m2-m3) from site 1 ("the quarry") at Tiupampa, Cochabamba Department, Bolivia (Muizon & Cifelli 2000).

**Other specimens observed and scored: *Tiuclaenus minutus*:** YPFB Pal 6115 (left mandible fragment with alveoli of i1 and i3, i2, c, alveolus of p1, p2-m3; holotype); YPFB Pal

6119 (right M2); MHNC 8335 (left m3); MHNC 1252 (left m3); MHNC 1240 (right M1-M3); MHNC 13879 (right M1-M3); ***Tiuclaenus cotasi*:** MHNC 1231 (left mandible fragment with p4-m3; holotype); MHNC 8273 (left mandible fragment with condyle and part of coronoid preserved, and p5-m3); MHNC 8272 (right mandible fragment with m2); MHNC 1254 (right mandible fragment with m3); MHNC 1259 (right m1); MHNC 1255 (right m1); MHNC 1232 (left m3); MHNC 8341 (right maxillary fragment with P2-M2); MHNC 8347 (left P5); MHNC 8342 (left M2); MHNC 8342 (left M2); MHNC 1271 (right M3); ***Tiuclaenus robustus*:** MHNC 1233 (left mandible fragment with m2-m3; holotype); MHNC 1234 (right mandible fragment with m1-m2); MHNC 1246 (right p2); MHNC 1266 (right P4-P5); MHNC 1267 (right M1 lacking protocone); MHNC 1264 (right M2); MHNC 831 (left M3).

**Known distribution:** ***Tiuclaenus minutus*:** All specimens from the same locality as the type; ***Tiuclaenus cotasi*:** All specimens except MHNC 1236 are from the same locality as the type. MHNC 1236 is from site 5 at Tiupampa (Muizon & Cifelli 2000); ***Tiuclaenus robustus*:** All specimens from the same locality as the type.

**Age/SALMA:** Early Palaeocene/Tiupampan (64 – 63 Ma). The lower age was based on (Woodburne *et al.* 2014*a*) and the upper following (Flynn & Swisher 1995).

**Additional relevant references with descriptions and illustrations:** (Muizon *et al.* 2019)

**Anatomical comments:**

- The postmetaconular crista and the preparaconular crista are mostly absent in *Tiuclaenus* spp. However, the former is present in the M2 of *T. minutus* (MNHN 13879) and both are present in a M2 of the same taxon (YPFBPal6119).
- The parastyle and metastyle are particularly well-developed in the specimen MHNC13879 of *T. minutus* as Muizon *et al.* (2019) previously observed. The same specimen has a small hypocone in M2, not previously mentioned. It may be a different species of this genus.
- *Tiuclaenus* seems to have a variable development of the buccal cristae (i.e., preparacrista, postaparacrista, premetacrista and postmetacrista). *Tiuclaenus robustus* (MNHC 1264), *T. cotasi* (MHNC 8342) and *T. minutus* (YPFB.Pal6119) have some degree of development of them, but the specimens MHNC 13879 and MHNC 1240 of *Tiucleanus minutus* do not show any of these cristids.

- The postcristid is absent in the m3 of *Tiuclaenus minutus* (MHNC 1254). The m3s of other specimens of *Tiuclaenus* seem to have a very low postcristid, although is hard to judge considering the important level of wear that most of them have.
- In the m3 of *Tiuclaenus*, the ultimate m crest between the hypoconid and hypoconulid is always absent. Interestingly this is similar to the condition present in the m3 of different members of Xenungulata such as *Carodnia*.

## North American Mioclaenidae

### *Protoselene opisthacus* (Cope 1882*a*)

**Holotype and type locality:** AMNH 3275 (right p4, and mandible fragment with m1-m3, left mandible fragment with p2-4 and left mandible fragment with p5-m3) from San Juan Basin, Nacimiento Formation, New Mexico, USA.

**Specimens observed and scored:** NMMNH P-21503 (left mandible fragment with p5, m2-m3); TMM 40537-129 (left mandible fragment with m1-m3); NMMNH P-20920 (concreted cranium with left P4-M3 and right P4-M1); NMMNH P-53912 (concreted cranium with left P4-M3 and right P4-P5, M2); KU 13977 (right maxilla fragment with P4-M2, left maxilla fragment with P5-M3, right mandible fragment with p5-m3, and left mandible fragment with m1-m3); AMNH 15973 (left mandible fragment with m1-m3); AMNH 16618 (right maxilla fragment with M1-M3); AMNH 16614 (left maxilla fragment with M1-M3, right mandible fragment with p5-m3, and left mandible fragment with p4-m3); AMNH 2435; AMNH 3599; AMNH 3275.

**Known distribution:** P-E/Tj2 (Kutz Canyon and Chico Springs), E-A/Tj3 (Kutz Canyon [NMMNH P-21503; NMMNH P-53912; NMMNH P-20920]), A-P/Tj4 (Kutz Canyon, Torreon West and Torreon East), P-M/Tj5 (Kutz Canyon and Torreon West) and M/Tj6 (Escavada Wash, Torreon West and Torreon East; Williamson 1996; Flynn *et al.* 2020).

**Age/NALMA:** Early Palaeocene/To2-To3

**Exact age:** 63.49 – 62.25 Ma. This interval considers stratigraphic uncertainty because I scored specimens of unknown locality (e.g., AMNH 3599, KU 13977, AMNH 2435). Therefore, this interval represents the whole temporal interval from which *Protoselene opisthacus* is known.

### *Promioclaenus* spp. (Trouessart 1904)

Included species in the scoring:

**a) *Promioclaenus acolytus*** (Cope 1882*b*)

**b) *Promioclaenus lemuroides*** (Matthew 1897)

**Holotypes and type localities: *Promioclaenus acolytus*:** AMNH 3208 probably from San Juan Basin, Nacimiento Formation, New Mexico, USA (not examined in this work). ***Promioclaenus lemuroides*:** AMNH 2421 (left mandible fragment with p2-m3 and right p5-m2) from Torrejon Arroyo, San Juan Basin, Nacimiento Formation, New Mexico, USA.

**Other specimens observed and scored: *Promioclaenus acolytus*:** AMNH 15962 (left mandible fragment with p4-m3); AMNH 15949 (right mandible fragment with p1-m3); PU 17536 (right mandible fragment with p5-m3); AMNH 3294 (left mandible fragment with p4-m3; holotype of *Mioclaenus minimums*); NMMNH P-21985 (left mandible fragment with p5-m3); NMMNH P-59590 (right mandible fragment with p4-m3 and left mandible fragment with p5-m2); NMMNH P-47734 (ex_UniArizona 10971; crushed skull with left P4-M3 and right P5-M3); NMMNH P-72121 (concreted skull with left P5-M3 and right P4-M3); NMMNH P-38680 (concreted basicranium with right P4-M3 and left P5-M3); NMMMJ P-27792 (mandible fragments with left p2-m3 and p5-m2). ***Promioclaenus lemuroides*:** USNM 15747 (right maxilla fragment with M1-M3; holotype of *Jepsenia mantiensis*); NMMNH P-16269 (left mandible fragment with m1-m2, left maxilla fragment with M1-M2); NMMNH P-16349 (left mandible fragment with p4, m1-m3); AMNH 15952 (right mandible fragment with p2-m3 and left mandible fragment with p1-m3); AMNH 16636 (at least two individuals; right maxilla fragment with P5-M1, right maxilla fragment with M1-M3, left maxilla fragment with M1-M2, right mandible fragment with p5-m3, right mandible fragment with m1-m2 and left mandible fragment with p2-m2); USNM 15721 (right mandible fragment with m1-m3; holotype of *Promioclaenus shepherdi*); UALP 15790 (right maxilla fragment with MP5-M2); UALP 10902 (right mandible fragment with p5-m2); AMNH 15957 (left mandible fragment with p1-m2); AMNH 16638 (left mandible fragment with p2-m1); AMNH 5952 (right mandible fragment with p2-m3); AMNH 15952 (right mandible fragment with c-p4, broken p5, m1 and trigonid of m2 and left mandible fragment with p2-m3).

**Known distribution:** P-P/Tj1 (Head of Kimbeto Wash [only ***Promioclaenus lemuroides*]**), P-E/Tj2 (Kutz Canyon and Chico Springs), E-A/Tj3 (Kutz Canyon [NMMNH

P-59590]), A-P/Tj4 (Kutz Canyon, Torreon West and Torreon East), P-M/Tj5 (Kutz Canyon, Torreon West [NMMNH P-21985] and "Little Pocket" [NMMNH P-72121]) and M/Tj6 (Escavada Wash, Torreon West [NMMNH P-16269; NMMNH P-16349; UALP 10902] and Torreon East; Williamson 1996; Flynn *et al.* 2020).

**Age/NALMA:** Early Palaeocene/To1–To3

**Exact age:** 64.68 – 62.25 Ma. This interval considers stratigraphic uncertainty because I scored specimens of unknown locality (e.g., NMMNH P-38680, NMMNH P-47734). Therefore, this interval represents the whole temporal interval from which *Promioclaenus* spp. are known.

### *Choeroclaenus turgidunculus* (Cope 1888)

**Holotype and type locality:** AMNH 3291(left maxilla fragment with P5-M2) from San Juan Basin, Nacimiento Formation, New Mexico, USA.

**Other specimens observed and scored:** NMMMNH P-47232; NMMMNH P-47479; NMMMNH P-44396; NMMMNH P-15164; AMNN 16489; AMNH 16404.

**Known distribution:** H-T/Pc1(Betonnie Tsosie Wash [NMMMNH P-15164] and Kimbeto Wash [NMMMNH P-47232; AMNN 16489; AMNH 16404]), T-P/Pc2 (De-Na-Zin [NMMMNH P-47479; NMMMNH P-44396]; Williamson 1996; Flynn *et al.* 2020).

**Age/NALMA:** Early Palaeocene/Pu2 – Pu3

**Exact age:** 65.59 – 65.16 Ma. This interval considers stratigraphic uncertainty because of the scoring of specimens of uncertain stratigraphic provenience.

### *Mioclaenus turgidus* (Cope 1881*b*)

**Holotype and type locality:** AMNH 3135 (left P4-M2, left M1-M3, right p4-m1, and right p4-m3) from San Juan Basin, Nacimiento Formation, New Mexico, USA.

**Other specimens observed and scored:** KU 7828; NMMMNH P-62250; NMMMNH P-64935; NMMMNH P-69942; NMMMNH P-27795; NMMMNH P-47899; NMMMNH P-72182; NMMMNH P-48203; NMMMNH P-48204; NMMMNH P-21026; NMMMNH P-21086; AMNH 3154.

**Known distribution:** P-P/Tj1 (Kimbeto, Betonnie Tsosie, De-Na-Zin, Kutz Canyon), P-E/Tj2 (East Fork Kutz Canyon), E-A/Tj3 (Kutz Canyon [NMMMNH P-21086]), A-P/Tj4

(Kutz Canyon [KU 7828; NMMMNH P-62250; NMMMNH P-64935; NMMMNH P-27795; NMMMNH P-21026], Torreon West and Torreon East), P-M/Tj5 (Kutz Canyon and Torreon West) and M/Tj6 (Escavada Wash, Torreon West [NMMMNH P-69942; NMMMNH P-48203; NMMMNH P-48204]; Williamson 1996; Flynn *et al.* 2020).

**Age/NALMA:** Early Palaeocene/To1–To3

**Exact age:** 64.68 – 62.25 Ma. This interval incorporates stratigraphic uncertainty because I scored specimens of unknown locality (e.g., AMNH 3154, AMNH 3135). Therefore, this interval represents the whole temporal interval from which *Mioclaenus turgidus* is known.

### Arctocyonidae (Root of the tree)

#### *Protungulatum donnae* (Sloan & Van Valen 1965)

**Known distribution:** Pu1 and Pu2 (Cifelli *et al.* 2004; Lofgren *et al.* 2004).

**Holotype and type locality:** SPSM 62-2028, left mandible with P2-M3, type (Sloan & Van Valen 1965).

**Specimens observed and scored:** UMVP 1615 (left maxilla fragment with P5-M3); NMMNH C-253 (cast from UCM composite with left P4-M3 and right P5-M3); NMMNH C-254 (cast from UCM composite with left p5-m3 and right p4-m1); UCMP 112112 (left M2-M3); UCMP 112113 (right M1-M2); UCMP 112113 (left M2-M3); UMVP 5211 (left mandible fragment with m1-m3).

**Age/NALMA:** Early Palaeocene/ Puercan (66.06 – 65.31 Ma). This age was based on the occurrence of *Protungulatum donnae* in Pu1 and Pu2 (Cifelli *et al.* 2004; Lofgren *et al.* 2004) and the total temporal interval for these substages (Sprain *et al.* 2018; Flynn *et al.* 2020).

## Methods

### Dental nomenclature

In terms of tooth position, I used the ancestral dental formula for Placentalia of I1/i1 I2/i2 I3/i3 C/c P1/p1 P2/p2 P4/p4 P5/p5 M1/m1 M2/m2 M3/m3, and thus I used these positions for character scoring. This is justified because of the probable loss of P3/p3 in the common ancestor of Placentalia (McKenna 1975; Novacek 1986; O'Leary *et al.* 2013). As SANUs are placentals, most previous workers (e.g., Forasiepi et al. 2016) have considered a formula for SANUs counting the premolars anteroposteriorly from one to four (i.e., P1/p1 to P4/p4).

Therefore, attention must be given when reading about the last two premolars in the main text. The benefit of using the ancestral placental dental formula is to make easier homologous comparisons between different therians, and is useful for transposing the anatomical information presented in this thesis into larger scale projects that includes older members of Theria which retain P3/p3 present.

In relation to the dental nomenclature, I, in most cases, followed the terminology used in Nessov & Archibald (1998) although with some modifications and additions (see Fig. 4.3). In those cases, a definition is of the term is included as a comment in the character list (Appendix C4 Resource 2). In the text and also in the character list, the term hypocone unless stated otherwise is equivalent to the term distocone, and thus it does not contain any *a priori* assumption of the origin of this upper dentition distolingual cusp. The same was applied in the scoring, even though it seems that in Notoungulata the distocone does not arise from an inflation of the postcingulum, as in other SANUs, being instead potentially a duplicated protocone (Muizon *et al.* 2019) or a duplicated metaconule. In any case, even a postcingulum derived distocone (or a true hypocone) has been shown to have arisen independently in multiple lineages (Hunter & Jernvall 1995; Muizon *et al.* 2019), and therefore its presence or absence is not necessary a keystone character.

## Character sampling

Based on an inclusive matrix currently being built to test the affinities within Placentalia broadly, I built a new morphological matrix with 954 characters, of which 911 deal with dental anatomy and 43 with the mandibular anatomy. The character list is presented on Appendix C4 Resource 2.

In general, each tooth has a particular set of characters describing different anatomical aspects, the exception being M1/m1 and M2/m2, which have been grouped as M1-M2/m1-m2 characters in most cases, as predominantly these molar positions in SANUs and "condylarths" do not show much variation between them based on what I observed while scoring. In a M1-M2/m1-m2 character, in the case of a difference between M1/m1 and M2/m2, the character was scored as polymorphic. The scores were based on direct observation of museum specimens, pictures of the specimens, and images from the literature. As there are not evident morphoclines series on the dental and mandibular evolution on litopterns, I followed Brocklehurst & Haridy (2021) recommendations and treated all the characters as unordered in the phylogenetic analyses.

## Testing different hypotheses for the paraconid of notoungulates

In order to test the effect of two different anatomical hypotheses in relation to the paraconid in notoungulates, I scored the notoungulate *Simpsonotus praecursor* twice, and thus have two different matrix versions (Appendix C4 Resource 3 and Appendix C4 Resource 4). In early notoungulates of different suborders there is a mesiolingual cusp on the lower molars, very close to and mesial of the metaconid. Unlike Simpson (1967), most later authors have interpreted this cusp to be a paraconid in which the connection with the paracristid is lost (e.g., Bond 1988; Soria 1989*a*; Bauzá *et al.* 2020). This is consistent with the paraconid position and size in kollpanines, didolodontids, protolipternids and anisolambdids. In addition, the loss of contact between the paracristid and the paraconid has been seen in a lesser degree independently in the anisolambdid *Paranisolambda* (Cifelli 1983*a*), so it is known to happen in SANUs. In sum, the hypotheses to be tested are that (1) the mesiolingual cusp is a reduced paraconid and (2) the mesiolingual cusp is a twinned or duplicated metaconid. In one matrix *Simpsonotus praecursor* was scored following the former hypothesis, in a different matrix following the latter hypothesis. The objective is to test the influence of each hypothesis in the position of Litopterna among "condylarths" and other SANUs. Therefore, the following phylogenetic analyses were conducted twice, once for each hypothesis, and are denoted in the text as H1 and H2.

## Maximum parsimony analyses

I used TNT v1.6 (Goloboff & Catalano 2016), setting the outgroup as *Protungulatum donnae* and employing a "New Technology" driven search with sectorial search, ratchet, drift and tree fusing, using default settings for each search algorithm, and set to find the minimum length tree or best score 100 times. After completion, I used an additional "traditional search" using the tree bisection and reconnection (TBR) branch swapping algorithm on the trees obtained from the New Technology search. In each hypothesis (H1 and H2), the absolute Bremer supports (BS) and Jackknife resampling support (JS; 1000 replicates, 36%-character removal) for the nodes were calculated.

## Undated Bayesian analyses

The undated Bayesian analyses were conducted in MrBayes v3.2.7a (Ronquist *et al.* 2012*a*) using *Protungulatum donnae* as the outgroup. I set one partition for the morphological data using the Mkv + Γ model of morphological evolution (Lewis 2001) with four rate

categories (Harrison & Larsson 2015). The analyses were run using two independent runs of four chains for 10 million Markov chain Monte Carlo (MCMC) generations, removing the first 25% of the samples as burn-in. At the end of the analyses, the effective sample size for the parameters was > 200 and the deviation of split frequencies was below 0.01. In addition, the runs were visually inspected using Tracer v1.7.1 (Rambaut *et al.* 2018) to ensure convergence and stationarity were achieved. A 50% majority rule was computed at the end of the analyses and the posterior probabilities for the nodes (prob) were estimated. The same procedure using the same priors and parameters was conducted for H1 and H2.

## Tip-dated Bayesian analyses

The tip-dated Bayesian analyses were also conducted in in MrBayes v3.2.7a (Ronquist *et al.* 2012*a*) using the same outgroup, model of morphological evolution and sampling parameters as the undated Bayesian analyses (see above). To calibrate the root of tree a truncated normal prior was used with a minimum age of 66.061 Ma which is 0.001 Ma older than the maximum age of the oldest taxon *Protungulatum donnae* (66.06 Ma), a mean age 0.1 Ma older than maximum age of *Protungulatum donnae* (66.16 Ma) and a standard deviation of 1.0 Ma following an approach used in previous studies (Sallam & Seiffert 2020; Beck *et al.* 2023).

When defining the calibration bounds for each taxon, I used a uniform distribution that includes the minimum and maximum ages of the taxa that I scored in the matrix following previous recommendations (Püschel *et al.* 2020). This means that the temporal intervals may or may not correspond with the whole temporal interval between the first appearance datum (FAD) and last appearance datum (LAD) of a particular species, as the ages of specimens that I could not examine were excluded. In cases in which there was uncertainty about the stratigraphic location of a specific specimen (e.g., exact location not reported), this uncertainty was accounted by incorporating the whole known temporal interval for that taxon (between the FAD and LAD). In terms of the exact ages used for each taxon, priority was given to specific radiometric dates of the strata associated with the scored specimens. However, in most cases the age of a taxon is estimated from faunal correlations from sites with radiometric dates available and associated broadly with one or more SALMAs. In those cases, I used the age estimation of the SALMAs from previous authors (Table 4.3). See the Taxon sampling section for information of the specific temporal interval used for each taxon and its justification.

The prior distribution and the parameters of the clock rate were derived from the methodology of (Gunnell *et al.* 2018) using the packages ape (Paradis *et al.* 2004) and fitdistrplus (Delignette-Muller & Dutang 2004) from R (R Core Team 2019) and the undated Bayesian consensus trees previously obtained. I selected the best model considering the Bayesian information criterion, which it was lognormal distributed clock rate prior with a mean of -3.2153491 and a standard deviation of 0.5059051.

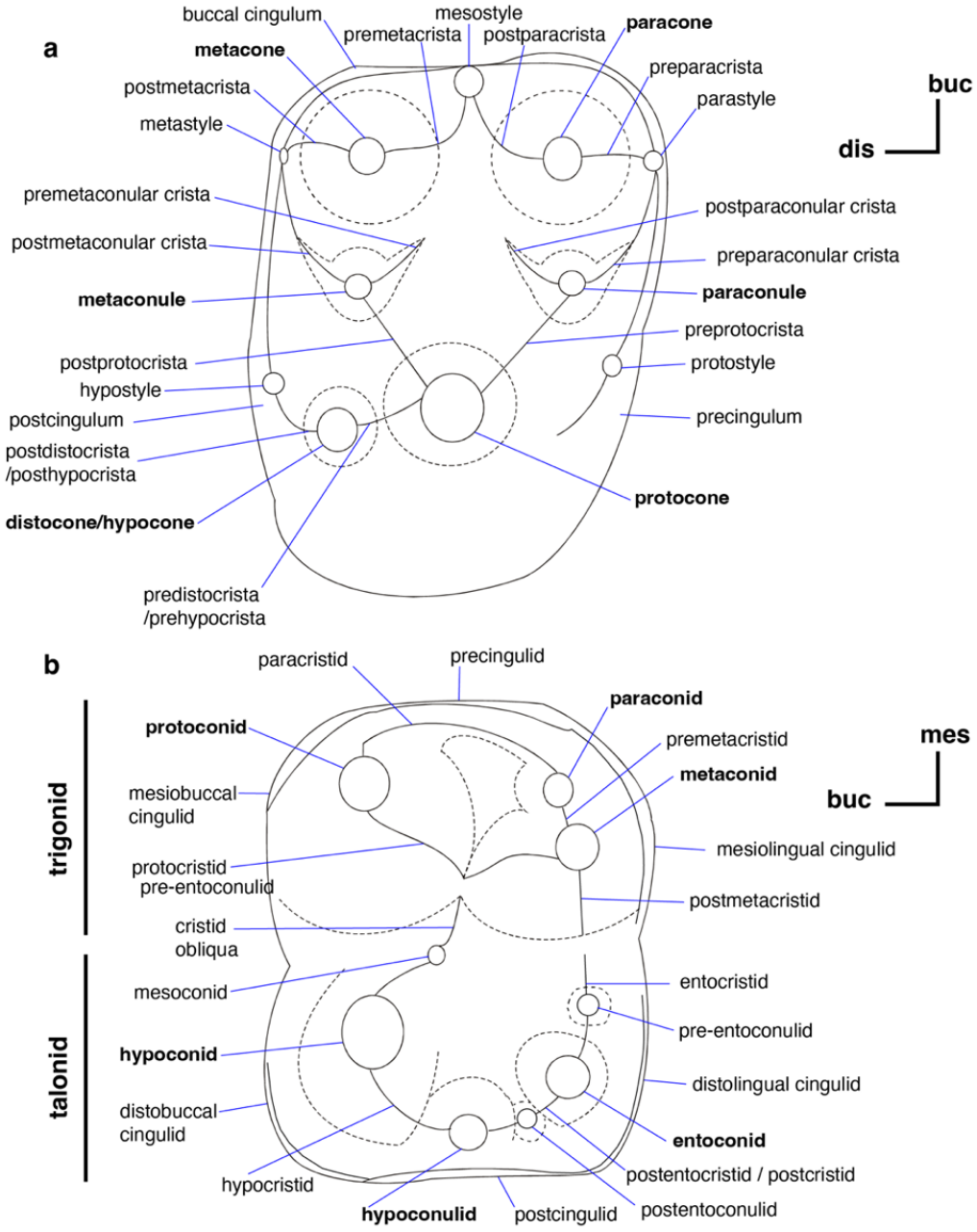



**Figure 4.3** Dental nomenclature used in the text and in the characters. **a**. upper molar; **b**. lower molar. The main cusps of the molars are highlighted in bold. The molars do not represent any particular SANUs' taxon. Molars edited from Gelfo (2006). Abbreviations: *buc*, buccal; *dis*, distal; *mes*, mesial.

**Table 4.3** SALMAs' lower and upper limits in Ma.

| SALMA | Lower limit (Ma) | Upper limit (Ma) | References |
|---|---|---|---|
| **Tiupampan** | 64.00 | 63.00 | Lower age following (Woodburne *et al.* 2014*a*) and upper following (Flynn & Swisher 1995) |
| **Peligran** | 63.80 | 63.20 | (Woodburne *et al.* 2014*a*) |
| **Carodnia Zone**[1] | 62.50 | 61.60 | (Krause *et al.* 2017) |
| **Itaboraian** | 56.00 | 51.40 | (Krause *et al.* 2017) |
| **Riochican**[2] | 49.00 | 48.50 | (Woodburne *et al.* 2014*a*) |
| **Sapoan Fauna**[3] | 48.50 | 47.00 | (Woodburne *et al.* 2014*a*) |
| **Vacan**[5] | ~45.00 | 42.00 | (Krause *et al.* 2017) |
| **Barrancan**[5] | 42.00 | 39.00 | (Woodburne *et al.* 2014*b*) |
| **Mustersan** | 39.00 | 36.50 | (Woodburne *et al.* 2014*b*) |
| **Tinguiririca**n | 31.50 | 34.50 | (Woodburne *et al.* 2014*b*) |
| **Deseadan** | 29.30 | 26.00 | (Woodburne *et al.* 2014*b*) |
| **Colhuehuapian** | 21.00 | 20.10 | (Dunn *et al.* 2013) |
| **Santacrucian**[4] | ~18.00 | ~15.60 | (Cuitiño *et al.* 2016) |
| **Colloncuran**[4] | 15.70 | 14.00 | (Madden *et al.* 1997) |
| **Laventan** | 13.50 | 11.80 | (Madden *et al.* 1997) |
| **Chasicoan** | ~10.00 | 9.00 | (Flynn & Swisher 1995) |
| **Huayquerian** | ~8.50 | 5.17 | Lower age following (Cione & Tonni 2001, 2005; Reguero & Candela 2011) and upper age following (Prevosti *et al.* 2021) |
| **Montehermosan** | 4.70 | 3.70 | (Prevosti *et al.* 2021) |
| **Chapadmalalan** | 3.74 | 3.04 | (Prevosti *et al.* 2021) |
| **Marplatan** | 3.27 | ~2.00 | Lower age following (Schultz *et al.* 1998) and upper age following (Cione & Tonni 1999; Woodburne *et al.* 2006) |
| **Ensenadan** | ~2.00 | ~0.70 | (Woodburne *et al.* 2006) |
| **Bonaerian** | ~0.70 | ~0.125 | (Woodburne *et al.* 2006) |
| **Lujanian** | ~0.125 | ~0.08 | (Woodburne *et al.* 2006) |

[1] Based on the age of the Peñas Coloradas Formation (62.5 - 61.6 Ma). The *Carodnia* Zone has been estimated to be ~62 Ma (Woodburne *et al.* 2014*a*; Krause *et al.* 2017).
[2] A different age interpretation for the Riochican SALMA is 46.70 - 42.20 Ma (Krause *et al.* 2017).
[3] The "Sapoan" as a unique biostratigraphic unit has been rejected by (Krause *et al.* 2017).
[4] The "Friasian" SALMA *sensu lato* should be somewhere between or within the Santacrucian and the Colloncuran SALMAs, although its specific age is still under debate (e.g., (Madden *et al.* 1997; Croft *et al.* 2016; Vera *et al.* 2019).
[5]The Divisaderan fauna has been here temporally considered within the Vacan and Barranca SALMAs as previously suggested (Woodburne *et al.* 2014*b*).

I modelled Branch rate variation employing the Independent Gamma Rate (IGR) relaxed clock model with an exponential distribution of rate 10 (default MrBayes setting). The fossilised birth-death (FBD) model was used as a prior on divergence times with an exponential net diversification prior with rate 1, a beta turnover prior with shape parameters $\alpha=1$ and $\beta=1$, a beta fossil sampling proportion prior with shape parameters $\alpha=1$ and $\beta=1$, extant sampling proportion of 1 and allowing fossil taxa to be sampled ancestors (samplestrat = random). The priors in the FBD model are diffuse priors that reflect the uncertainty in my prior expectation of how these parameters are distributed (Yang 2014).

I ran the analyses using two independent runs of four chains for 40 million Markov chain Monte Carlo (MCMC) generations, removing the first 25% of the samples as burn-in. At

the end of the analyses, the effective sample size for the parameters was > 200 and the deviation of split frequencies was below 0.01. Additionally, the runs were visually inspected using Tracer v1.7.1 (Rambaut *et al.* 2018) to make sure convergence and stationarity were achieved. The analyses were performed twice using the same priors and parameters for H1 and H2.

Preliminary results of the tip-dated Bayesian analyses showed that the node for the common ancestor of SANUS was potentially too old considering the fossil evidence, being dated around 68 Ma within the Maastrichtian. This is not impossible and it corresponds well with recent molecular studies that have posited that interordinal origination and diversification of Placentalia occurred prior the K/Pg boundary (long fuse model of placental diversification; Springer *et al.* 2017). However, most workers consider that SANUs arrived to South America in the earliest Palaeocene (e.g., Reguero & Goin 2021), considering that the Maastrichtian fossil localities in South America do not have any placental representatives (e.g., Martinelli *et al.* 2021). Therefore, it can be expected that the age of their common ancestor to be between the K/Pg boundary and the earliest Palaeocene, particularly if they are monophyletic, as the different SANUs orders diversify showing an enormous disparity particularly from the early Eocene (Croft *et al.* 2020). Accordingly, I repeated the analyses constraining the age of common ancestor of SANUs between 64 and 66 Ma, the minimum being the oldest age estimated for the kollpanines of Tiupampa (Flynn & Swisher 1995) and the maximum the age of the K/Pg boundary. For these new analyses I tried four different approaches: (a) using the H1 matrix with no constraints in the topology, (b) using H2 matrix with no constraints in the topology, (c) using the H1 matrix constraining the topology to be the same as in in the H1 undated tree, and (d) using the H2 matrix constraining the topology to be the same as in in the H2 undated tree. The last two approaches (c and d) were conducted in order to limit the influence of the fossil ages in the topology. This is because it is still an open question whether it is desirable to allow the age of fossils to have an influence in the topology of the tree (O'Reilly *et al.* 2015), particularly in cases of rapid diversification in which the ages of many taxa are very similar. Therefore, I used soft constraints in all cases except for the SANUs common ancestor node in which I used a hard constraint as it is required by MrBayes in order to time-calibrate a specific node. The rest of the parameters of the analyses were exactly the same as the other tip-dated Bayesian analyses (see above).

Finally, I repeated the approach in (c), but this time I used the oldest stratigraphic occurrence and its associated interval for taxa in which I observed morphological stasis when scoring. I tested this approach because simulations have shown that more accurate and precise

results are obtained by using the oldest stratigraphic occurrence in cases of morphological stasis (Püschel *et al.* 2020). Basing the calibration in the oldest stratigraphic occurrence was only possible in a few taxa because for most of South American fossil sites there is a great uncertainty in terms of its precise age, and also some of the scored specimens do not have a good record of their stratigraphic provenience. The taxa that suffer changes in terms of the calibration were the mioclaenids *Protoselene opisthacus*, *Promioclaenus* sp., *Choeroclaenus turgidunculus* and *Mioclaenus turgidus*, the sparnotheriodontid *Notiolofos arquinotiensis*, and the macraucheniid *Cramauchenia normalis* (see the ages in taxonomic sample). The objective of doing this was to test the effect of morphological stasis in divergence-time estimates in the phylogeny.

# Results

## Maximum parsimony analyses

In the maximum parsimony analyses, for H1, I obtained one most parsimonious tree (MPT) of 2161 steps and a consistency index (CI) = 0.397 and a retention index (RI) = 0.538. For H2, I obtained one most parsimonious tree (MPT) of 2162 steps and a consistency index (CI) = 0.401 and a retention index (RI) = 0.541. H1 and H2 converge on the same topology with a single MPT produced from each analysis, although with slightly different level of support for the nodes of the trees (Fig. 4.4a-b). North American Mioclaenidae is recovered as a polyphyletic group as *Mioclaenus turgidus* is positioned as a sister taxon of *Tiuclaenus* spp., nested within South American Kollpaninae in the most basal clade that includes SANUs, excluding the rest of North American mioclaenids in a group with relatively low support (BS = 3; JS = 23-25). *Protoselene opistachus*, *Choeroclaenus turgidunculus* and *Promioclaenus* spp. form a well-supported (BS = 7; JS = 85) monophyletic group at the base of the tree, just crownward of the outgroup *Protungulatum donnae*. Didolodontidae and Protolipternidae are not recovered as monophyletic groups; instead, the taxa composing these families form different clusters between them with relatively low support (BS ≤ 2; JS ≤ 52) and are all located in branches at the base of a monophyletic group mainly composed of the traditional SANU orders (i.e., Astrapotheria, Litopterna, Notoungulata and Xenungulata). The only exceptions are *Escribania chubutensis* and *Raulvaccia peligrensis* which form a well-supported basal monophyletic group (BS = 7; JS = 96-97).

The monophyletic cluster containing the traditional SANUs orders is strongly supported (BS = 20; JS = 99), and Xenungulata is found as the most basal position of this group showing *Carodnia vieirai* and *Etayoa bacatensis* as sister taxa (Fig. 4.4a-b). The orders Notoungulata and Astrapotheria, represented by *Simpsonotus praecursor* and *Trigonostylops wortmani* respectively, are found as sister taxa with moderate support (BS = 4-5; JS = 55-72) at the base of a different well-supported monophyletic group composed of litopterns and indaleciids and notonychopids (BS = 10-11; JS = 83-84). The notonychopids *Notonychops powelli* and *Requisia vidmari* form a well-supported sister group (BS = 5; JS = 97-98) which clusters with the indaleciid *Indalecia grandensis* forming a well-supported monophyletic group (hereinafter referred as Notopterna) at the base of Litopterna (BS = 3-6; JS = 78-90). The order Litopterna (excluding notonychopids and indaleciids) forms a robust monophyletic group (BS = 15; JS = 92), in which the most basal branch leads to the well-supported monophyletic family Macraucheniidae (BS = 9; JS = 98-99). Within Macraucheniidae, *Polymophis* spp. is found as the most basal macraucheniid, and *Macrauchenia patachonica* and *Theosodon* spp. are recovered as well-supported sister taxa (BS = 5; JS = 96). There is a poorly supported monophyletic group that includes the litoptern families Adianthidae, Proterotheriidae, Anisolambdidae and Sparnotheriodontidae (BS = 2; JS = 33; Fig. 4.4a-b). Adianthidae forms a well-supported monophyletic group (BS = 3-4; JS = 76-78) with *Proectocion* spp. as the most basal taxon and *Tricoelodus bicuspidatus* and *Proadianthus excavatus* found as strongly supported sister taxa (BS = 6; JS = 99). As sister group of Adianthidae, there is relatively well-supported group composed of the families Proterotheriidae, Anisolambdidae and Sparnotheriodontidae (BS = 4; JS = 70-79). The basal branch of this group is a well-supported monophyletic Proterotheriidae composed of *Diadiaphorus majusculus* and *Lambdaconus suinus* (BS = 12; JS = 84-86), which is a sister group of a strongly supported cluster consisting of the families Anisolambdidae and Sparnotheriodontidae (BS = 6-7; JS = 79-85). Anisolambdidae forms a strongly-supported monophyletic group composed of *Anisolambda* spp. and *Paranisolambda* (BS = 4; BJ = 85-89). Sparnotheriodontidae constitutes strongly supported monophyletic cluster (BS = 4; BJ = 77-79) with *Sparnotheriodon epsilonoides* as the most basal taxon, and *Notiolofos arquinotiensis* and *Victorlemoinea prototypica* as poorly supported sister taxa (BS = 1; BJ = 45-48).

In terms of the anatomical features supporting the well-supported groups, the group containing the traditional SANU orders (excludes kollpaniines, didolodontids and protolipternids) is supported by 47 unambiguous synapomorphies in H1 and H2 (Appendix C4

Resource 5) such as the presence of a metaconid in p2 (char. 168), a basined talonid in p2, a metaconid of p4 subequal in height in relation to the protoconid (char. 201), a cristid obliqua of p4 that attaches the trigonid mid-posterior the metaconid (char. 212), a hypoconid height in p4 being 30% or more higher than the protoconid height, a metaconule present in P4 (char. 371), a protocone in P4 with a similar size than the paracone (char. 378), a m1-m3 cristid obliqua contacting buccal to the midpoint between protoconid and metaconid (chars. 552 and 632), a slightly convex metacone and paracone labial edge in M1-M2 (char. 727), a M1-M3 width and length subequal (chars. 667 and 806), a distocone subequal in girth and height to the protocone (chars. 785 and 787), and several characters describing intermediate to high cristae and cristids in the lower (p4-m3; 188, 235, 265, 536, 549, 615 and 629) and upper teeth (P4-M3; chars. 348, 418, 735, 794 and 863). Xenungulata is supported by the same seven unambiguous synapomorphies in H1 and H2 (Appendix C4 Resource 5) such as a long talonid length relative to trigonid length in p5 (char. 262), an entoconid transverse and directly lingual relative to the hypoconid (char. 560), a metaconid directly opposite to protoconid (char. 613), a crest between the hypoconid and hypoconulid absent (char. 651). The group conformed by indaleciids and notonychopids (also called Notopterna (Soria 1989*b*) is supported by nine or 11 unambiguous synapomorphies in H1 and H2 respectively (Appendix C4 Resource 5) such as a large parastylar cusp in M1-M3 (chars. 685 and 823), a large parastylar lobe in M3 (char. 824) and a wider than long P4 and M1-M2 (chars. 331 and 667). The family Notonychopidae is supported the same six unambiguous synapomorphies in H1 and H2 (Appendix C4 Resource 5) such as a protocone in P4-P5 that in line with the paracone (chars. 380 and 469), the presence of an ectoflexus in P5, a talon and distocone more buccal than protocone (chars.784 and 789) and the presence of a protostyle in M1-M2 (char. 802).

Litopterna (excluding protolipternids, indaleciids and notonychopids) is supported by 26 common unambiguous synapomorphies in H1 and H2 (Appendix C4 Resource 5) such as a postparacrista angled distobuccally in P4, P5, M1-M2 and M3 (chars. 354, 425, 715 and 848), a mesostyle present in P5, M1-M2 and M3 (chars. 407, 693 and 829), a metacone in P4 (char. 357), a premetacrista angled mesiobuccally in P5, M1-M2 and M3 (chars. 428, 718 and 851) and a talon present in P5. Among litopterns, the family Macraucheniidae is supported by 16 common unambiguous synapomorphies in H1 and H2 (Appendix C4 Resource 5) such as a uniform depth in the dentary (char. 3), an absent entoconid in p4 (char. 213), a clear separation between the bases of the entoconid and the hypoconulid in m1-m2 (char. 561), a hypoconulid in m1-m2 that is lower than the entoconid (char. 576), a width of the hypoconulid in m3 being

less than 50% of the rest of the talonid width (char. 654), and a large talon in M3 being more than half of the total dimension of the trigon (char. 906). The family Adianthidae is supported by 14 shared unambiguous synapomorphies in H1 and H2 (Appendix C4 Resource 5) such as a very small mesostyle in P5 (char. 408), the presence of a postparaconular crista in P5-M3 (chars. 449, 749 and 876), a paraconid in m1-m2 mesiolingually located between the protoconid and the metaconid (char. 520), an absent postentocristid in m1-m3 (chars. 565 and 645), and a hypoconulid similar in length to the talonid mesial to hypoconulid (char. 658).

The monophyletic group composed of Proterotheriidae, Anisolambdidae and Sparnotheriodontidae is supported by 14 common unambiguous synapomorphies in H1 and H2 (Appendix C4 Resource 5) such as the presence of a hypoconulid in p2 (char. 176), a well-demarked entoconid in p4 (char. 214), a hypoconid of subequal girth that the protoconid (char. 222), a hypoconid in p4 distal to metaconid (char. 224), a mesostyle present in P4 (char. 344), a premetacrista angled mesiobuccally in P4 (char. 357) and a postprotocrista in M1-M2 oriented towards the distocone (char. 779). The family Proterotheriidae is supported by 20 common unambiguous synapomorphies in H1 and H2 (Appendix C4 Resource 5) such as the presence of two lower incisors (char. 44), the presence of a diastema between the anteriormost lower incisors (char. 46), a lower canine smaller than adjacent distal tooth (char. 100), a extremely reduced paraconid in p5 (char. 240), a postmetaconular crista absent on P5-M2 (chars. 463 and 765), a paracingulum not continuous with the precingulum in M1-M3 (chars. 671 and 810) and the presence of diastemata mesial and distal of the lower canine (chars. 931 and 933). The monophyletic group constituted by Anisolambdidae and Sparnotheriodontidae is supported by nine or 10 unambiguous synapomorphies in H1 and H2 respectively (Appendix C4 Resource 5) such as the presence of a protostyle in P4 (char. 386), a rounded distal surface of the paraconid (char. 518), a paraconid with a smaller girth than the girth of the metaconid but more than the half of its girth (char. 520), a secondary distal cingulum present in M1-M3 (chars. 677 and 816) and a well-developed protostyle in M1-M2 (char. 803). The family Anisolambdidae is supported by 10 shared unambiguous synapomorphies in H1 and H2 (Appendix C4 Resource 5) such as a rounded mesial surface in the paraconid of m1-m3 (chars. 517 and 596), a postentocristid absent in m1-m2 (char. 565), a paraconid of subequal height than the metaconid in m3 (char. 599), paraconid and metaconid with fused bases in m1-m3 (chars. 522 and 602), and a metacone shorter than the paracone in M1-M2 (723). The family Sparnotheriodontidae is supported by seven common unambiguous synapomorphies in H1 and H2 (Appendix C4 Resource 5) such as the presence of a distobuccal cingulid in m1-m2 (char.

506), the presence of a postmetacristid in m1-m3 (chars. 541 and 620), fused bases of the entoconid and hypoconulid creating a common base in m1-m2 (char. 561) and a hypoconulid width less than 50% of the rest of the talonid width in m3 (char. 654).

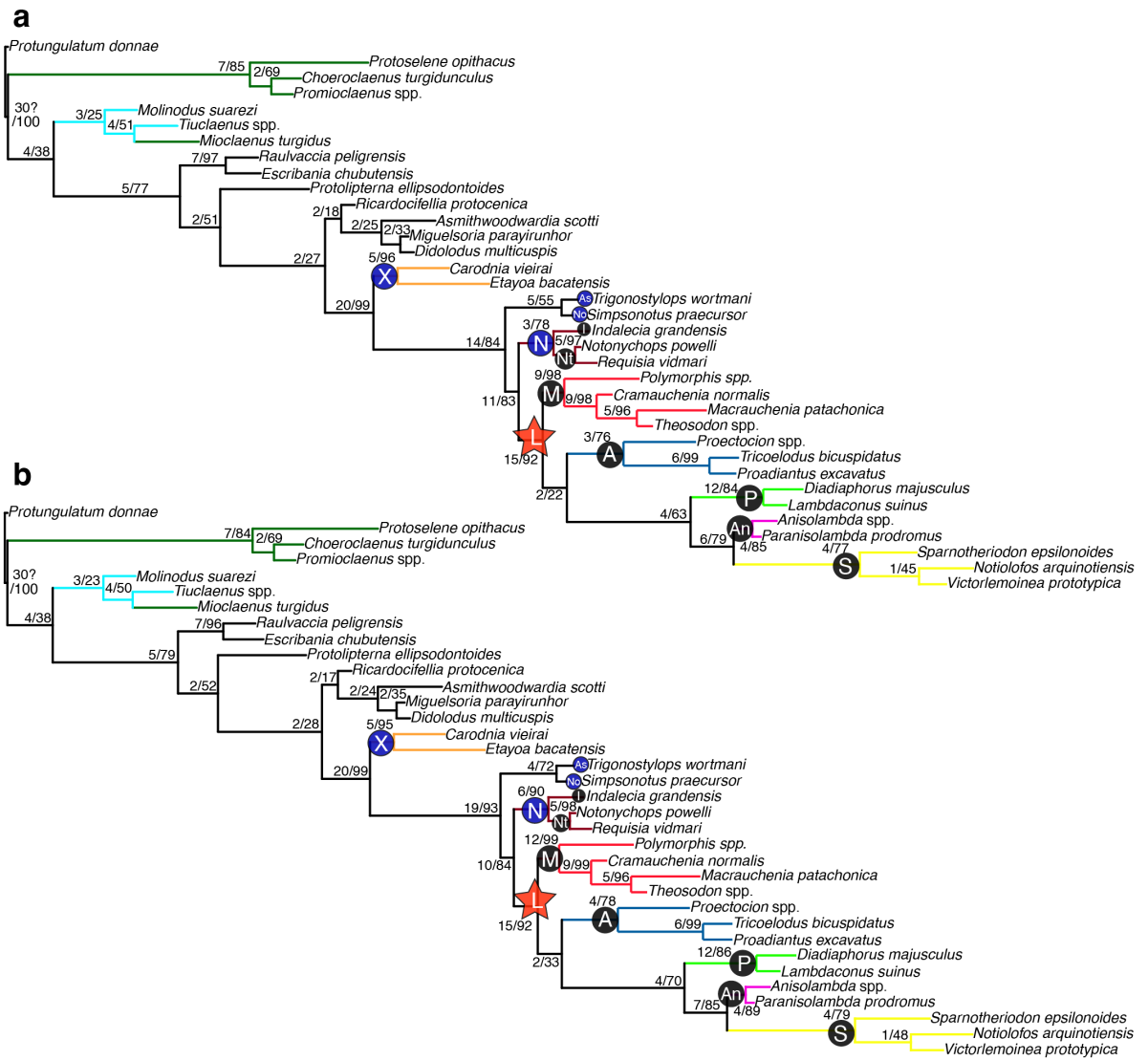



**Figure 4.4** Most parsimonious trees (MPTs) from the maximum parsimony analyses. **a**. Hypothesis 1 (H1). **b**. Hypothesis 2 (H2). H1 and H2 are different hypothesis for the paraconid of notoungulates (see main text). The numbers next to each node of tree are the absolute Bremer supports in the left side and the Jackknife resampling support values in the right side. Different colours in the branches are used for indicate different families or orders: blue, Adianthidae; brown, Notopterna; green, North American Mioclaenidae; light green, Proterotheriidae; light blue, Kollpaninae; red, Macraucheniidae; orange, Xenungulata; pink, Anisolambdidae; yellow, Sparnotheriodontidae. Litopterna is indicated with a red star, but other nodes or tips of relevance are indicated in circles of different colours: blue, orders; black, families. Abbreviations: *A*, Adianthidae; *An*, Anisolambdidae; *As*, Astrapotheria; *I*, Indaleciidae; *L*, Litopterna; *No*, Notoungulata; *Nt*, Notonychopidae; *M*, Macraucheniidae; *Ma*, Macrauchenoidea; *S*, Sparnotheriodontidae; *P*, Proterotheriidae; *X*, Xenungulata.

## Bayesian analyses

The 50% majority rule consensus tree of the undated Bayesian analyses for H1 and H2 are largely congruent and largely agree with the parsimony results (Fig. 4.5a-b). In the undated Bayesian trees, North American Mioclaenidae is recovered as a monophyletic group with *Mioclaenus turgidus* as its most basal taxon although with a relatively low support (prob = 0.57 – 0.58), in contrast to the polyphyletic Mioclaenidae in the parsimony trees (Fig. 4.4a-b). Similarly, Kollpaninae is recovered as a monophyletic group (Fig. 4.5a-b). Among didolodontids, only *Raulvaccia* and *Escribania* are recovered as a well-supported monophyletic group (prob = 1), but in contrast with the parsimony trees, there is no other monophyletic group among didolodontids and protolipternids (Fig. 4.5a-b). As in the parsimony trees, Notopterna and the traditional SANUs orders (i.e., Astrapotheria, Litopterna, Notoungulata and Xenungulata) are found as a strongly supported monophyletic group (prob = 1). However, the position of the orders Notoungulata, Astrapotheria and Notopterna varies between H1 and H2. In H1 *Simpsonotus* (Notoungulata) is found in a polytomy with Notopterna and a poorly supported (prob = 0.52) monophyletic group including *Trigonostylops* (Astrapotheria) and Litopterna (Fig. 4.5a). In contrast, in H2 Notopterna is sister taxon of a moderately supported monophyletic group (prob = 0.79) that includes Notoungulata and Astrapotheria as a sister group of Litopterna (Fig. 4.5a). Litopterna (excluding protolipternids and notopterns) is recovered as strongly supported group (prob = 1) and displaying the same internal topology H1 and H2 (Fig. 4.5a-b), which only differs with the parsimony trees in the position of the families Adianthidae and Macraucheniidae. In the undated Bayesian trees, Adianthidae is the most basal group of the family instead of Macraucheniidae, and Macraucheniidae is a moderately supported (prob = 0.75 – 0.78) sister group of the cluster of Proterotheriidae, Anisolambdidae and Sparnotheriodontidae. Another difference between the parsimony and undated Bayesian results regards the most basal sparnotheriodontid: *Victorlemoinea prototypica* in the undated Bayesian analyses (Fig. 4.5a-b) but *Sparnotheriodon epsilonoides* in the parsimony trees (Fig. 4.4a-b).

The unconstrained tip-dated Bayesian analyses for H1 and H2 are mostly consistent in terms of topology with the undated Bayesian analyses and the parsimony analyses, although there are some important differences (Figs. 4.6a and S1 in Appendix C4 Resource 6). The main differences are in the same nodes and groups with poor support in the undated Bayesian analyses and the parsimony analyses such as the exact affinities of "didolodontids" Astrapotheria, Notoungulata and Notopterna, and also the exact interfamilial affinities of

Macraucheniidae and Adianthidae within Litopterna. Constraining the age of the node for the common ancestor of SANUs between the K/Pg boundary and the oldest possible age for the kollpaniids of Tiumpampa (66 – 64 Ma) gives overall very similar results than the unconstrained tip-dated Bayesian analyses for both hypotheses, exhibiting only minor changes in the tree topology and node resolution (Figs. S2 and S3 in Appendix C4 Resource 6). Interesting common findings to all the unconstrained tip-dated Bayesian analyses are the recovery of a well-supported (prob = 0.93 – 0.96) monophyletic group made up of most didolodontids and protolipternids, only excluding the Peligran SALMA *Escribania* and *Raulvaccia* (Figs. 4.6a, S1, S2 and S3 in Appendix C4 Resource 6), and also that Notopterna is not recovered as a monophyletic group, finding the notonychopid *Notonychops* consistently in a polytomy with the notoungulate *Simpsonotus*. In addition, the cluster of Proterotheriidae, Anisolambdidae and Sparnotheriodontidae is not recovered, and Proterotheriidae is in most instances a low supported (prob = 0.53 – 0.68) sister group of the cluster of Macraucheniidae and Adianthidae. The tip-dated topology constrained Bayesian analyses return diverge-time estimations for nodes that sometimes are not recovered in the unconstrained analyses, being always consistent with the topology of the undated analyses (Figs.S4 and S5 in Appendix C4 Resource 6 and Table 4.4).

In terms of diverge-times estimations, the unconstrained tip-dated Bayesian analyses and the tip-dated Bayesian analyses constraining the age of the node for the common ancestor of SANUs are overall consistent between different analyses, having usually less than two million years of uncertainty between different divergence-time estimates in the means of the same nodes (Figs. 4.6, S1-S5 in Appendix C4 Resource 6 and Table 4.4). The age of the common ancestor of all SANUs is estimated in the Maastrichtian (~68.4 Ma) when this node is unconstrained, but when it is constrained, it is estimated very close to the K/Pg boundary (~65.9 Ma). The age of the common ancestor of the traditional SANUs orders (i.e., Astrapotheria, Litopterna, Notoungulata and Xenungulata) and Notopterna is estimated at ~64.3 Ma (67 – 63.4 Ma 95% highest posterior density [HPD]), the age of the order Xenungulata is estimated to be ~58.2 Ma (62.9 – 56.6 Ma 95% HPD) and the age Notopterna (when recovered) is estimated at ~ 63.5 Ma (63.9 – 63.3 Ma 95% HPD; Table 4.4). The age of Litopterna (excluding protolipternids and notopterns) is estimated to be ~ 57.4 Ma (62.1 – 53.7 Ma 95% HPD; Table 4.4), and the mean ages estimates for the families are following: Adianthidae ~ 44.7 Ma (53.5 – 39.6 Ma 95% HPD), Macraucheniidae ~ 40.8 Ma (41.9 – 37.1 Ma 95% HPD), Proterotheriidae ~ 33.2 Ma (41.8 – 27.5 Ma 95% HPD), Anisolambdidae ~

53.4 Ma (55.7 – 51.8 Ma 95% HPD) and Sparnotheriodontidae ~ 53.4 Ma (55.7 – 51.4 Ma 95% HPD; Table 4.4). In addition, the divergence-time estimate for the Patagonian *Sparnotheriodon epsilonoides* and the Antarctican *Notiolofos arquinotiensis* would be ~ 46.2 Ma (50.3 – 43.0 Ma 95% HPD) considering all the analysis, but in the analysis using the oldest occurrence of each taxon the mean is 46.41 Ma (50.1 – 44 Ma 95% HPD; Fig. 4.7 and Table 4.4).

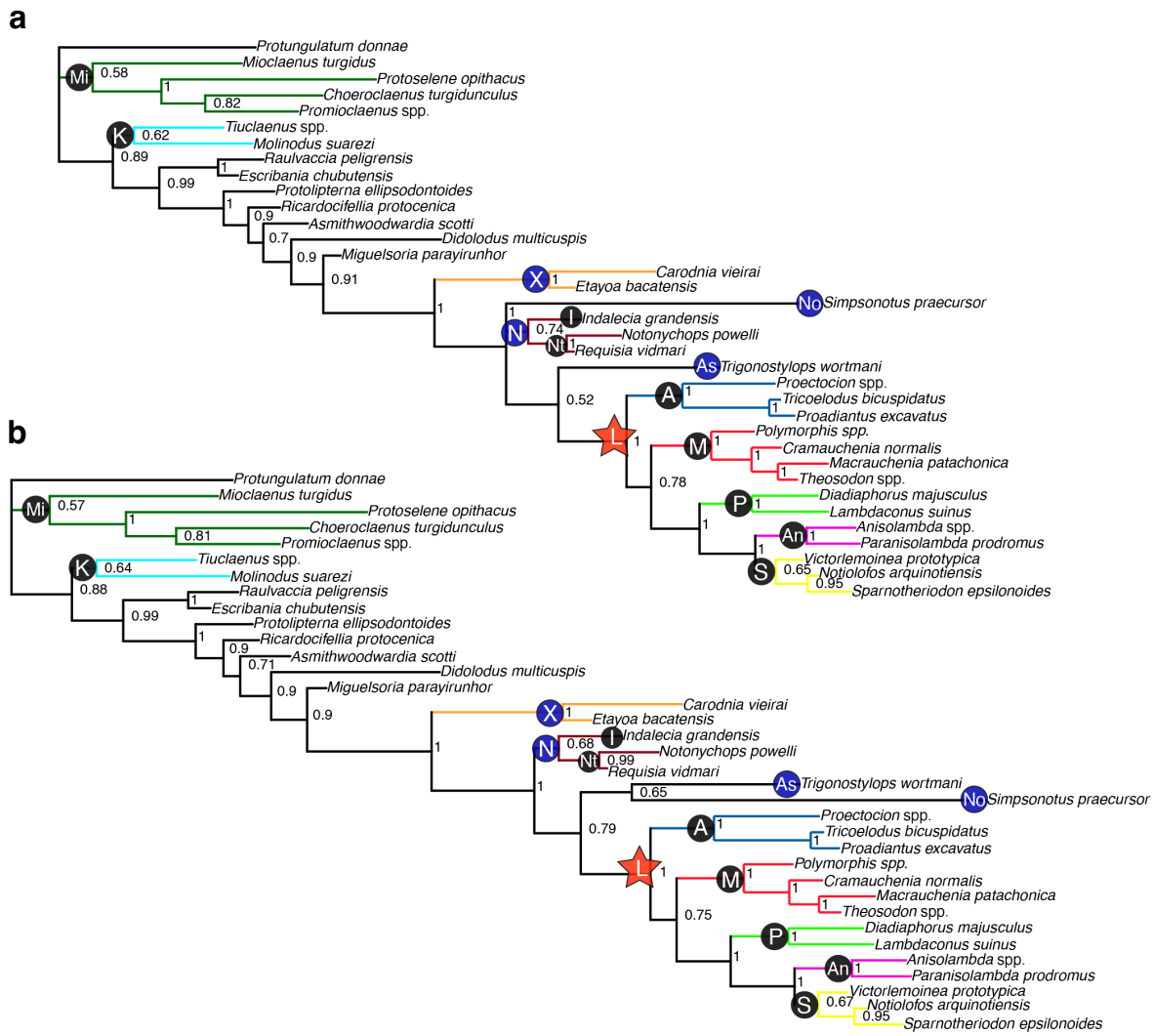



**Figure 4.5** Bayesian phylogenies of Litopterna from the undated analysis. **a**. Hypothesis (H1); **b**. Hypothesis 2 (H2). H1 and H2 are different hypothesis for the paraconid of notoungulates (see main text). In **a-b** node support is indicated using Bayesian posterior probabilities. Different colours in the branches are used for indicate different families or orders: blue, Adianthidae; brown, Notopterna; green, North American Mioclaenidae; light green, Proterotheriidae; light blue, Kollpaninae; red, Macraucheniidae; orange, Xenungulata; pink, Anisolambdidae; yellow, Sparnotheriodontidae. Litopterna is indicated with a red star, but other nodes or tips of relevance are indicated in circles of different colours: blue, orders; black, families. Abbreviations: *A*, Adianthidae; *An*, Anisolambdidae; *As*, Astrapotheria; *I*, Indaleciidae; *K*, Kollpaniinae; *L*, Litopterna; *No*, Notoungulata; *Nt*, Notonychopidae; *M*, Macraucheniidae; *Ma*, Macrauchenoidea; *Mi*, North American Mioclaenidae; *S*, Sparnotheriodontidae; *P*, Proterotheriidae; *X*, Xenungulata.

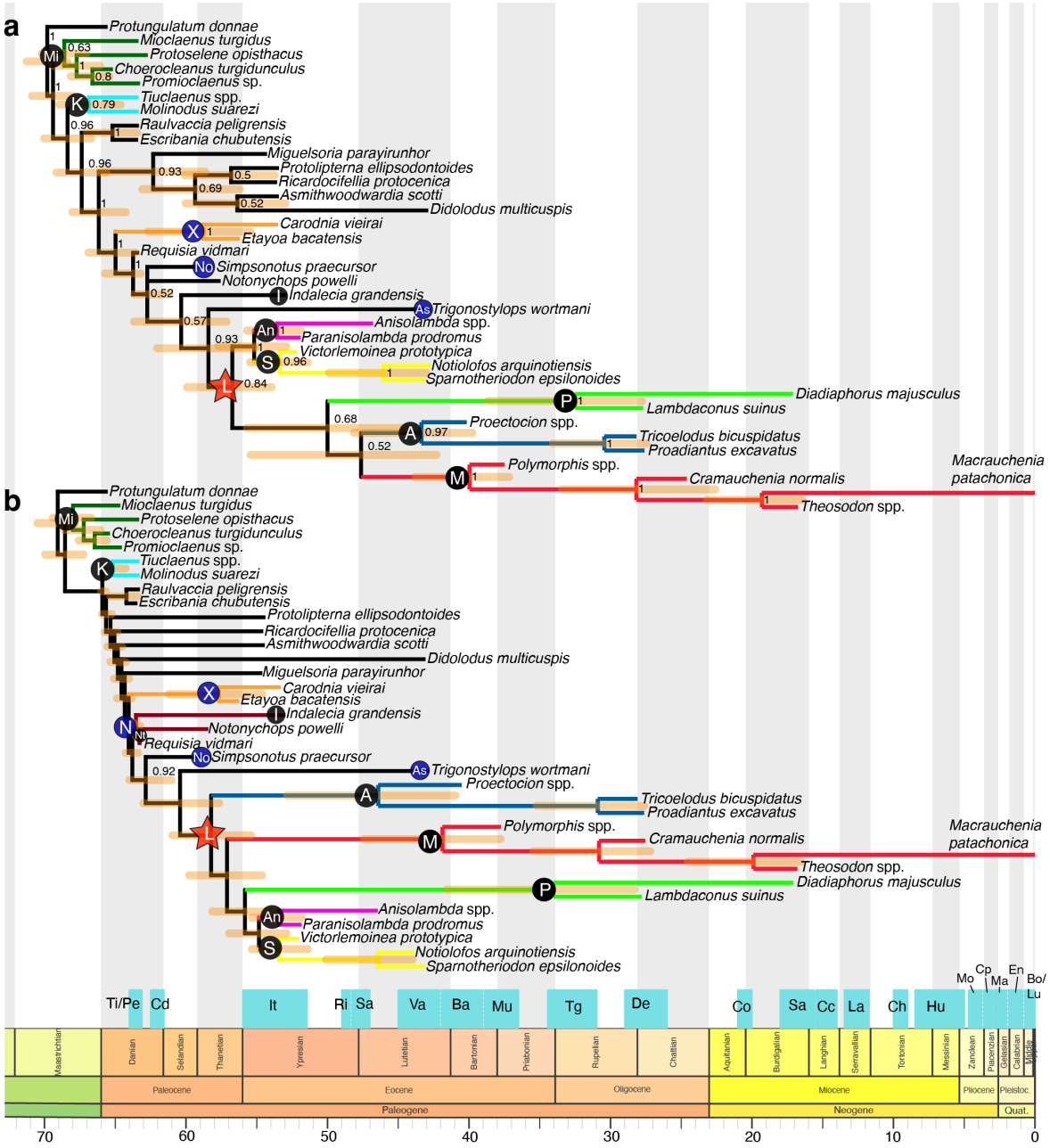



**Figure 4.6** Tip-dated Bayesian phylogenetic analyses. **a.** Unconstrained phylogeny using hypothesis 1 (H1) matrix. **b**. Tip-dated topology constrained Bayesian phylogeny using hypothesis 1 (H1) matrix and constraining the node for the common ancestor of SANUS between the K/Pg boundary and the oldest age for the kollpaniids of Tiumpampa (66 – 64 Ma), and also using the minimum possible ages for the tree tips. The topological constraint in **b** was based on the topology of the undated Bayesian tree for H1. The trees in **a** and **b** represents a 50% majority rule in which tree support is indicated using Bayesian posterior probabilities in the nodes and the node bars represent the 95% highest posterior density (HPD) for the estimated node ages. In b node support is only indicated for then node that was unconstrained (the undated tree presented a polytomy for that node). Different colours in the branches are used for indicate different families or orders: blue, Adianthidae; brown, Notopterna; green, North American Mioclaenidae; light green, Proterotheriidae; light blue, Kollpaninae; red, Macraucheniidae; orange, Xenungulata; pink, Anisolambdidae; yellow, Sparnotheriodontidae. Litopterna is indicated with a red star, but other nodes or tips of relevance are indicated in circles of different colours: blue, orders; black, families. Abbreviations: *A*, Adianthidae; *An*, Anisolambdidae; *As*, Astrapotheria; *I*, Indaleciidae; *K*, Kollpaniinae; *L*, Litopterna; *No*, Notoungulata; *Nt*, Notonychopidae; *M*, Macraucheniidae; *Ma*, Macrauchenoidea; *Mi*, North American Mioclaenidae; *S*, Sparnotheriodontidae; *P*, Proterotheriidae; *X*, Xenungulata.

**Table 4.4** Divergence-times mean for each Bayesian analysis, the total mean and total maximum and minimum ages.

| Taxonomic groups | H1 | H2 | H1N | H2N | H1N top | H2N top | H1N top ma | Total mean | Max | Min |
|---|---|---|---|---|---|---|---|---|---|---|
| Root | 69.81 | 69.80 | 68.77 | 68.8 | 68.92 | 68.91 | 69.07 | 69.15 | 71.34 | 67.47 |
| SANU-CA | 68.37 | 68.41 | 65.85 | 65.85 | 65.92 | 65.92 | 65.92 | 66.61 | 70.92 | 65.4 |
| Family Kollpaniinae | 66.86 | 66.86 | 65.06 | 65.07 | 65.17 | 65.14 | 65.17 | 65.62 | 70.22 | 64.09 |
| SANUs orders-CA | 64.98 | 65.04 | 64.05 | 64.03 | 64.05 | 64.05 | 64.06 | 64.32 | 67 | 63.37 |
| Order Xenungulata | 58.76 | 58.77 | 58.21 | 58.25 | 57.7 | 57.69 | 57.67 | 58.15 | 62.88 | 54.61 |
| Order Notopterna | - | - | - | - | 63.53 | 63.54 | 63.54 | 63.54 | 63.93 | 63.26 |
| Family Notonychopidae | - | - | - | - | 63.29 | 63.29 | 63.29 | 63.29 | 63.56 | 63.2 |
| Order Litopterna | 56.73 | 56.86 | 56.29 | 56.19 | 58.17 | 59.29 | 58.23 | 57.39 | 62.14 | 53.65 |
| Family Adianthidae | 43.36 | 43.84 | 43.03 | 43.24 | 46.55 | 46.59 | 46.42 | 44.72 | 53.52 | 39.62 |
| Family Macraucheniidae | 39.96 | 40.31 | 39.75 | 39.91 | 41.68 | 41.77 | 41.87 | 40.75 | 41.87 | 37.09 |
| Suborder Proterotheria | - | - | - | - | 55.79 | 56.39 | 55.84 | 56.01 | 59.13 | 53.56 |
| Family Proterotheriidae | 32.5 | 32.97 | 31.93 | 32.28 | 34.2 | 34.31 | 34.03 | 33.17 | 41.82 | 27.45 |
| Superfamily Eolitopternoidea | 55.18 | 54.99 | 55.02 | 54.72 | 54.76 | 55.2 | 54.84 | 54.96 | 57.71 | 52.68 |
| Family Anisolambdidae | 53.55 | 53.44 | 53.45 | 53.29 | 53.35 | 53.59 | 53.4 | 53.44 | 55.7 | 51.84 |
| Family Sparnotheriodontidae | 53.37 | 53.35 | 53.25 | 53.13 | 53.36 | 53.66 | 53.43 | 53.36 | 55.66 | 51.4 |
| Sparnotheriodon-Notiolofos-CA | 46.05 | 46.11 | 45.91 | 45.91 | 46.29 | 46.37 | 46.41 | 46.15 | 50.33 | 42.97 |

**Abbreviations**: **H1**, hypothesis 1 for the notoungulate paraconid (see methods); **H2**, hypothesis 2 for the notoungulate paraconid (see methods); **N**, constraint in the node for the common ancestor of SANUS between the K/Pg boundary and the oldest age for the kollpaniids of Tiumpampa (66 – 64 Ma); **top**, topological constraint in the analysis to make the topology similar to the one in the undated Bayesian analysis; **ma**, analysis using for calibrating the taxa ages based in the oldest occurrence or minimum age of each taxon (see methods). **Max**, maximum age based in the 95% HPD of the same node in different analyses; **Mi**n, minimum ages were based in the 95% HPD of the same node in different analyses.

# Discussion

## Early origins of SANUs, kollpanines, didolodontids and protolipternids

Whether SANUs form a monophyletic entity or not has been a long-standing question in South American palaeontology. As Simpson (1944) recognised, SANUs' disparity was at its highest early in their evolution during the Palaeogene, being a key example in his concept of "quantum evolution". This exceptional disparity, reflected in the current number of families accepted in the Palaeogene, coupled with the scarcity of the fossil record over this period, particularly in the earliest Palaeocene, hinders efforts to resolve SANUs affinities in the placental tree. Considering the great diversity of placental groups during the early Paleocene and a complex and a still poorly understood paleobiogeographic history in latest Cretaceous and earliest Palaeocene (Reguero & Goin 2021), efforts to test SANUs monophyly need to include a wide placental taxonomic sample in the line of studies such as O'Leary *et al.* (2013). My study does not include a wide taxonomic sample of all the placentals known for the Palaeocene, so any results in relation to the wider relationships of SANUs within Placentalia have to be taken with caution as not all the potential affinities of SANUs have been tested. However, even with this limitation, interesting inferences and hypotheses about the early affinities of SANUs can still be made.

When we consider the dental anatomy of kollpaniines, the earliest and probably most primitive SANUs known in the South American fossil record, there are anatomical similarities shared with North American mioclaenids that depart from what it is seen in *Protungulatum donnae*, as previous workers have suggested (e.g., Muizon & Cifelli 2000) such as a reduced stylar shelf and parastyle in M1-M2. However, my results do not support a particularly strong relationship between North American mioclaenids and kollpaniines, as they are not recovered in a monophyletic subgroup in all the Bayesian analyses (Figs. 4.5, 4.6 and S1-S5 in Appendix C4 Resource 6). Even though in the parsimony analyses, *Mioclaenus turgidus* was recovered as a sister taxon of *Tiuclaenus* spp. (Fig. 4.4), this position could be due to shared plesiomorphic dental features and some convergences, considering the low support for this node and the fact that in all Bayesian analyses *M. turgidus* was recovered as the most basal taxon of North American Mioclaenidae, with Kollpaninae forming a different monophyletic group (Figs. 4.5, 4.6 and S1-S5 in Appendix C4 Resource 6). The position of North American Mioclaenidae in the Bayesian analyses is consistent with previous phylogenetic studies that failed to recover kollpaniines as part of a monophyletic Mioclaenidae (Muizon & Cifelli 2000;

Williamson & Carr 2007; Kramarz *et al.* 2021; Zimicz *et al.* 2022). As clustering Kollpaninae and North American mioclaenids within Mioclaenidae involves the exclusion of other SANUs, this is by definition a paraphyletic group and therefore its usage should be avoided. Considering the relatively primitive and unspecialised dental anatomy of kollpaniines, they could potentially diversify in any of the SANU orders. Consequently, in a monophyletic Meridiungulata scenario, it is entirely possible that they are closely related to the common ancestor of the more derived SANU orders (i.e., Astrapotheria, Litopterna, Notoungulata and Xenungulata). In light of the current evidence, I propose to remove kollpaniines from Mioclaenidae, and group them under the family Kollpaniidae, new rank. Considering its phylogenetic position, this family for now should be considered *incertae sedis* in terms of its broader relationships, until more evidence is available and may serve to link them to a particular SANU order.

Unrelated to the exclusion of kollpaniids, it is still an open question as to whether among "condylarths", North American mioclaenids are the closest relatives of SANUs. Anatomical evidence seems to suggest this scenario in some studies (Muizon & Cifelli 2000; Kramarz *et al.* 2021), although a recent phylogenetic study favours a closer phylogenetic affinity of some SANUs with North American Phenacodontidae (Zimicz *et al.* 2022). However, some of these studies rely on very small data matrices (<50 characters; Muizon & Cifelli 2000; Zimicz *et al.* 2022), and in all of them the taxon sampling may be insufficient to answer this question. Nevertheless, the current consensus is that one or more North American "condylarth" lineages emigrated to South America in the latest Cretaceous or earliest Palaeocene, potentially through stepping-stone island hopping in an Antillean volcanic arc system (Iturralde-Vinent 2006), to later diversify into the SANU orders. Even though a recent phylogenetic study found kollpaniids, didolodontids and litopterns nested in a panperissodactyl lineage that excluded North American "condylarths" and instead suggested South American-Indian biogeographic connections during this period (Chimento & Agnolin 2020), this has been criticised in the light of anatomical, phylogenetic and biogeographic evidence (Kramarz *et al.* 2021). More importantly to determine a more robust connection between mioclaenids or any particular "condylarth" group with early SANUs, we need better fossils of both groups that include more evidence than dental material alone, which has shown in some instances to recover inaccurate phylogenies probably due to homoplasy (Sansom *et al.* 2017). However, this happens also with other scored anatomical regions apart from the dentition (Brocklehurst & Benevento 2020), so

probably it is better to use a variety of sources of anatomical evidence in phylogenetic analyses when possible.

as recovered in the unconstrained tip-dated Bayesian analyses and the constrained tip-dated Bayesian analyses constraining the age of the node for the common ancestor of SANUs

In relation to the age estimated for a putative SANU common ancestor in the tip-dated Bayesian analyses, a Maastrichtian age (~68.4 Ma) or an age just after the to K/Pg boundary (~65.9 Ma) are both plausible (Figs. 4.6, S1-S5 in Appendix C4 Resource 6 and Table 4.4), but in the light of the current palaeontological evidence for the Late Cretaceous and early Palaeocene of South America the latter is more likely. In Maastrichtian fossil sites from South America there are no eutherian mammals preserved; instead, these faunas are dominated by members of Gondwanan lineages such as gondwanatheres and meriodiolestids (Rougier *et al.* 2021). If the SANU common ancestor migrated from North America in the Maastrichtian, it is expected that during this age some of these "condylarths" or early SANUs would be present in the South American fossil record. Instead, SANUs are first recorded in the early Palaeocene of Tiupampa in Bolivia and Punta Peligro in the Argentinean Patagonia (Tiupampan and Peligran SALMAs), and because they are not particularly diverse, it suggests a relatively recent migration (Woodburne *et al.* 2014*b*). In that context, constraining the SANUs common ancestor node in the Bayesian analysis is probably more appropriate than leaving this node unconstrained. It is likely that in cases of great concurrent diversification within a lineage and in the absence of prior information added to time-constrain the node of interest, MrBayes would tend to accommodate these nodes by pushing them back in time instead of considering great rates of evolution in a short period of time. My estimation for the age of the putative SANUs common ancestor is somewhat younger than previous molecular studies. Welker *et al.* (2015) estimated a divergence-time estimate for the separation between SANUs (Litopterna + Notoungulata) and Perissodactyla of 88.7 – 73.9 Ma (95% HPD), and Westbury *et al.* (2017) estimated 66.15 Ma (77.8 – 56.6 Ma 95% HPD) for the same divergence event.

## About the status of the families Didolodontidae and Protolipternidae

All the phylogenetic analyses conducted here failed to recover Didolodontidae and Protolipternidae as distinct monophyletic groups (Figs. 4.4, 4.5, 4.6 and S1-S5 in Appendix C4 Resource 6). Members of both families were found consistently outside Litopterna and at the stem of the more derived SANUs orders. Previous studies have found, in general, a close phylogenetic relationship between Didolodontidae and Protolipternidae. When both groups are

included in the same analysis, a monophyletic Protolipternidae is usually recovered nested within Didolodontidae, which makes the latter family paraphyletic (Muizon & Cifelli 2000; Gelfo 2006). In a different study, the opposite situation is seen with a monophyletic Didolodontidae nested within a paraphyletic Protolipternidae (Gelfo 2004). This is not surprising as both families share dental features such as a distocone on M1-M2 and a well-developed metacone on P5 almost as high as the paracone and connate to it, among other dental characteristics that do not allow separating them based on their dentition (Cifelli 1993; Muizon & Cifelli 2000). The problem with these studies (e.g., Muizon & Cifelli 2000; Gelfo 2004, 2006) is that they base their conclusions on a very limited character and taxonomic sample, which means that any conclusions about the wider affinities of these families are not well-supported. A different phylogenetic study with a wider character and taxonomic sample that included indirectly assigned isolated petrosals to the protolipternid *Miguelsoria*, failed to recover Protolipternidae within Litopterna (Billet *et al.* 2015). It is worth mentioning that this study did not include any postcranial characters.

The only apparent justification for separating Protolipternidae from Didolodontidae and including it within Litopterna is based on tarsal features such as a spool-like astragalar body with subequal tibial and fibular crests and an anteroposteriorly concave sustentacular facet of the calcaneus, which were found as two of the nine tarsal synapomorphies of the order Litopterna in a phylogenetic analysis (Cifelli 1993). Bergqvist (1996) recovered similar results in a phylogenetic analysis based on postcranial characters. However, as the putative protolipternid and didolodontid tarsals scored in the previous phylogenetic studies were not found in association with their alleged dentition, being only indirectly associated (Cifelli 1983*b*), most authors have questioned some of these associations, in particular, those made between didolodontids and notoungulate-like tarsals (Hoffstetter & Soria 1986; Soria 2001; Gelfo 2010; Gelfo & Sigé 2011; Gelfo & Lorente 2012; Lorente 2015); see also Protolipternidae section in the Introduction).

As the tarsals and postcranial material of the protolipternid *Protolipterna* comes from the same fissure fills in the Itaboraí Formation as the dental specimens, this association seems to be more robust than tarsal-tooth associations made for didolodontids, which led Soria (2001) to tentatively suggest that all didolodontids should have a litoptern-like tarsal considering their dental similarities with protolipternids. More recently, as association models do not discard the association of litoptern-like tarsals to protolipternids (Lorente 2015), some authors have started to consider the Didolodontidae as a family within Litopterna, implying that Protolipternidae

should be considered a junior synonym of Didolodontidae, but for some reason have not formalised it (Gelfo *et al.* 2016, 2020*b*; Croft & López 2020). This is problematic because keeping both families, and at the same time considering Didolodontidae within Litopterna is contradictory, and more importantly, there is no strong phylogenetic evidence to support this arrangement. My results disagree with this interpretation showing that at least dentally there is no evidence that (a) Protolipternidae and Didolodontidae are monophyletic groups, and (b) that they are more closely related to Litopterna than to any other SANU order. The dentition of both families is in general plesiomorphic and not very different from that of the early "condylarth" *Protungulatum donnae*, but differs in sharing some derived dental features with kollpaniids such a strongly arched paracristid in m1-m3 (i.e., mesiobuccally oriented at paraconid) and a metaconid located distolingually from the protoconid in m1-m3, as previously noted (Muizon & Cifelli 2000). Protolipternids and didolodontids are probably dentally anatomically close to the structural ancestor of any of the more derived SANU orders (i.e., Astrapotheria, Litopterna, Notoungulata). Therefore, for the moment it seems more reasonable use the term "didolodontids" when referring to these early SANUs (i.e., didolodontids and protolipternids) without grouping them within any particular family, in a similar fashion to how the term "condylarth" is used to refer to archaic ungulates. In the future, more complete associated specimens of future findings could potentially link some of these "didolodontid" taxa with one or more SANU orders. It is likely that the tarsal controversy will only be resolved when directly associated postcranial elements of these early SANUs are found alongside dental elements as others have previously noted (e.g., Gelfo 2010; Gelfo & Sigé 2011). In relation, to Protolipternidae, if we believe the tarsal association for *Protolipterna* (Cifelli 1983*a*, *b*) to be correct, and more comprehensive phylogenetic analyses that include postcranial evidence support this relationship, then this taxon could be included within Litopterna and Protolipternidae may be considered as a valid family.

The phylogenetic affinities of *Escribania chubutensis* and *Raulvaccia peligrensis* as recovered here are particularly interesting. All of the phylogenetic analyses found these two taxa forming a well-supported monophyletic group among SANUs, more derived than kollapaniids but less than "didolodontids", the latter being phylogenetically more related to the common ancestor of the more derived SANU orders (Figs. 4.4, 4.5, 4.6 and S1-S5 in Appendix C4 Resource 6). Previous phylogenetic analyses usually find *E. chubutensis* and *R. peligrensis* closely related, but their position varies within Didolodontidae, being sometimes in a more basal position Gelfo (2006) and in others, variably more closely related to different

"didolodontids" like *Ricardocifellia* or *Didolodus* (Gelfo 2004, 2007, 2010; Gelfo & Sigé 2011). Again, these were phylogenies based on very limited character and taxonomic samples, so they do not give many hints about broader affinities of these taxa. When looking in detail at their dental anatomy, *E. chubutensis* and *R. peligrensis* shared some derived features not seen in other "didodolodontids" and kollpaniids, recovered among the 10 unambiguous synapomorphies in the parsimony analyses for their common node, such as the presence of two cristae in the distocone of M1-M2, one connecting the distocone with the protocone and the other connecting the distocone with the metaconule, and a premetacrista oriented towards the paracone or postparacrista, among other features (Appendix C4 Resource 5). This suggests that among early SANUs, *E. chubutensis* and *R. peligrensis* may be part of a different lineage distinct from other "didodolodontids". However, the scarce material known for both taxa hinders more refined assertions about their broader affinities.

## Interordinal affinities among the SANU orders

All the phylogenetic analyses performed here strongly support a monophyletic group that includes members of the traditional SANUs orders (i.e., Astrapotheria, Litopterna, Notoungulata and Xenungulata) and Notopterna (Figs. 4.4, 4.5, 4.6 and S1-S5 in Appendix C4 Resource 6). Indeed, they share many dental features, some of them recovered among the 47 unambiguous synapomorphies in the parsimony analyses that in general are associated with more molarised premolars, a greater development of the distocone on the upper molars, and higher cristae and cristids connecting different cusps on the upper and lower dentition (Appendix C4 Resource 5). In terms of the affinities between orders, only the position of Xenungulata and Litopterna was consistently the same among the different phylogenetic analyses, which suggests that there is a considerable uncertainty in the position of Astrapotheria, Notoungulata and Notopterna (when recovered). There were clearly differences in phylogenies generated by different phylogenetic methods and also by those generated assuming two different hypotheses about the paraconid in notoungulates (H1 and H2). Therefore, no firm conclusions about interordinal affinities of the SANUs orders can be advanced from these results. Although my results strongly suggest the monophyly of a clade including all the traditional SANU orders, they should be taken with caution as some of these features could have potentially arisen independently in different lineages. A good example is of this is the independent origin and development of the hypocone in different groups (Hunter & Jernvall 1995; Muizon *et al.* 2019). Consequently, the monophyly of the SANU orders has to be tested ideally in a larger matrix including craniodental and postcranial characters,

molecular evidence for the more recent groups, and a broad taxon sample of early placentals. This work is currently underway and it is part of the objectives of the Palaeogene Mammal Working Group (PalM) to which I have been contributing during my PhD. Indeed, so far there has not been a study of this kind that included members of all SANU orders (Table 4.2). In terms of the divergence age of this monophyletic group monophyletic group containing the SANUs' traditional orders and Notopterna, I consider that the age given in the tip-dated Bayesian analyses of ~64.3 Ma for the putative SANU common ancestor is in agreement with the fossil evidence (Table 4.4). This age consistent with a previous Bayesian molecular analysis that estimated an age of 69.2 – 64.3 Ma (95% HPD) for the common node of Litopterna and Notoungulata (Welker *et al.* 2015).

Notopterna was found across all the phylogenetic analyses as a group outside the order Litopterna except in the tip-dated topology constrained Bayesian where it was not recovered as a monophyletic group (Figs. 4.4, 4.5, 4.6, and S1, S4 and S5 in Appendix C4 Resource 6). Notopterns share important anatomical features some of which were recovered as the 9 or 11 unambiguous synapomorphies in my parsimony analyses (Appendix C4 Resource 5), such as a distinctive large and buccally projected parastylar cusp in M1-M3. These and additional features have been previously recognised and used to justify the proposal of the distinct order Notopterna (Soria 1984*b*, 1989*a*, *b*), composed of the families Amilnedwardsiidae, Indaleciidae and Notonychopidae. Only one phylogenetic study has been conducted in the past test the existence of this order, and it failed to recover a monophyletic Notopterna (Bonaparte & Morales 1997), which led most authors to include them in Litopterna (e.g., Gelfo *et al.* 2016; Croft *et al.* 2020; Goin *et al.* 2022). However, the analysis of Bonaparte and Morales (1997) has its shortcomings: it used a small matrix limited to only 54 characters and 15 taxa, and more importantly, among SANUs, it only included litopterns in the analysis, which precludes any possibility of testing whether they are effectively part of Litopterna or not. With the inclusion of astrapotheres, notoungulates and xenungulates, my analyses effectively tested the monophyly of the order Notopterna and a moderate support for it as it was recovered in most of the phylogenetic analyses. Similarities in the ear region of indaleciids and notonychopids previously observed (Soria 1989*b*) also support a close relationship between indaleciids and notonychopids. In addition, a preliminary analysis incorporating the indaleciid *Indalecia grandensis* in a matrix that included craniodental characters including features of the ear region, recovered it as sister taxon of astrapotheres and notoungulates instead of being closely related to , or nested within, litopterns (García-López & Babot 2014). In sum, considering the

available evidence, I propose to tentatively restore the order Notopterna as a distinct order from Litopterna and composed of the families Indaleciidae and Notonychopidae (Table 4.5). Following phylogenetic taxonomy methods (De Queiroz & Gauthier 1992), Notopterna could be defined as the clade composed of the indaleciid notoptern *Indalecia* (Bond & Vucetich 1983) and all SANUs more closely related to it than to the xenungulate *Carodnia* (Simpson 1935), the litoptern *Macrauchenia patachonica* (Owen 1838), the notoungulate *Simpsonotus* (Pascual *et al.* 1978) and the astrapothere *Trigonostylops* (Ameghino 1897); node N in Figs. 4.4, 4.5 and 4.6).

In relation to the family Amilnedwardsiidae, considering that its members are only known from isolated upper molars whose positions are tentative (Soria 1989*a*) and as some of the material is currently lost, I suggest to exclude this group from the order Notoptena, and consider this family as *incertae sedis* until there is more fossil evidence in association to support or reject their inclusion, and to test whether this is a valid family or not. In addition, *contra* the phylogeny of Bonaparte and Morales (1997; Fig. 4.1d), I found in most of the phylogenetic analyses, the family Notonychopidae as a monophyletic group (Figs. 4.4, 4.5, 4.6 and S4-S5 in Appendix C4 Resource 6), although in the topology-unconstrained tip-dated Bayesian analysis this family was not recovered as a monophyletic group (S1-S3 in Appendix C4 Resource 6). The monophyly of the family Notonychopidae is justified by multiple dental similarities some of which were recovered among the six unambiguous synapomorphies in the parsimony analyses (Appendix C4 Resource 5). The monophyly of the family Indaleciidae was not tested here as I only included *I. grandensis* in my matrix. However, considering the many similarities between *I. grandensis* and *Adiantoides leali* previously exposed (Bond & Vucetich 1983), the monophyly of Indaleciidae is very likely. My phylogenetic analyses also consistently reject the inclusion of indaleciids as a family within Adianthidae as it was originally proposed (Bond & Vucetich 1983) and some authors have recently followed (Zimicz *et al.* 2022). The age of Notopterna at ~63.5 Ma (Table 4.4) puts it as the earliest diversification among the SANU orders, being ~6 Ma earlier than Litopterna.

Even though I found evidence for the existence of the order Notopterna as a monophyletic group in most of the phylogenetic analyses, the interordinal affinities with other SANU orders still need to be resolved. In order to do so, phylogenetic analyses that include craniodental and postcranial characters, and members of all the early representatives of the SANU orders are imperative. The ear region of the indaleciid *Indalecia grandensis* and the notonychopid *Notonychops powelli* should be revisited and incorporated in such analyses.

## Interfamilial affinities of Litopterna: Macraucheniidae and Adianthidae

Litopterna (excluding notopterns and "didolodontids") was consistently found as a strongly supported monophyletic group in all the phylogenetic analyses (Figs. 4.4, 4.5, 4.6 and S1-S5 in Appendix C4 Resource 6). This is not a surprising result as litopterns share many dentally derived features not seen in other SANU orders, some of which were recovered among the 26 common unambiguous synapomorphies, such as a distobuccally oriented postparacrista, a mesiobuccally oriented premetacrista, and a mesostyle in the upper molars (Appendix C4 Resource 5). Considering the phylogenetic position of notopterns (notonychopids and indaleciids) and "didolodontids" among other SANUs, my results suggest that the use of Litopterna should be restricted for now to only the families Macraucheniidae, Adianthidae, Proterotheriidae, Anisolambdidae and Sparnotheriodontidae (Table 4.5). Following phylogenetic taxonomy methods (De Queiroz & Gauthier 1992), Litopterna can be defined as the clade composed of *Macrauchenia patachonica* (Owen 1838) and all taxa more closely related to it than to the xenungulate *Carodnia feruglioi* (Simpson 1935), the indaleciid notoptern *Indalecia grandensis* (Bond & Vucetich 1983), the notoungulate *Simpsonotus praecursor* (Pascual *et al.* 1978) and the astrapothere *Astrapotherium magnum* (Owen 1853); node L in Figs. 4.4, 4.5 and 4.6).

Considering the interfamilial affinities between the different families of litopterns my results show a considerable uncertainty in the exact position of the families Adianthidae and Macraucheniidae. At the same time Proterotheriidae, Anisolambdidae and Sparnotheriodontidae are found forming a monophyletic group in which Anisolambdidae and Sparnotheriodontidae are sister taxa in most of the analyses (Figs. 4.4, 4.5, 4.6b and S4-S5 in Appendix C4 Resource 6)., although in topology-unconstrained tip-dated Bayesian analyses Proterotheriidae groups with a cluster formed by Adianthidae and Macraucheniidae (Figs. 4.6a and S1-S3 in Appendix C4 Resource 6). Consequently, I did not find support for the suborder Lopholitopterna and the superfamily Proterotherioidea proposed by Cifelli (1983*a*; Table 4.1) as Sparnotheriodontidae was consistently found within Litopterna, instead of being linked to didolodontids. The topology-unconstrained tip-dated Bayesian analyses support Soria's (2001) definition of the suborder Lopholitopterna, as Proterotheriidae is found closely related to Adianthidae and Macraucheniidae, and also the suborder Eolitopterna, as Anisolambdidae and Sparnotheriodontidae are found closely related. However, all the rest of the analyses, including undated Bayesian and parsimony, does not support these definitions as Anisolambdidae and Sparnotheriodontidae are found closely related to Proterotheriidae forming a monophyletic

group. Cifelli's (1983*a*) superfamily Macrauchenoidea (Macraucheniinae and Adianthidae; Table 4.1) found support only in most of the unconstrained tip-dated Bayesian analyses (Fig. 4.6 and Figs. S1, S3 in Appendix C4 Resource 6) probably because of the influence of the tip-calibrations on the topology of the tree. Considering the variation in the phylogenetic position of Adianthidae and Macraucheniidae among different analyses, resolving their exact interfamilial affinities may need other sources of evidence apart from the dental features used here.

The family Macraucheniidae was found consistently found as a monophyletic group in all the analyses here performed (Figs. 4.4, 4.5, 4.6 and Figs. S1-S5 in Appendix C4 Resource 6). There are multiple anatomical features that support the monophyly of this family, some of which were recovered among the 16 unambiguous synapomorphies of the parsimony analyses (Appendix C4 Resource 5), such as having a clear separation between the bases of the entoconid and the hypoconulid in m1-m2 and an upper buccolingually narrow hypoconulid in m3. Following phylogenetic taxonomy methods (De Queiroz & Gauthier 1992), Macraucheniidae can be defined as the clade composed of *Macrauchenia patachonica* (Owen 1838) and all the taxa more closely related to it than to the adianthid *Adianthus bucatus* (Ameghino 1891*a*), the proterotheriid *Proterotherium cervioides* (Ameghino 1883*b*), the sparnotheriodontid *Sparnotheriodon epsilonoides* (Soria 1980*a*) and the anisolambdid *Anisolambda fissidens* (Ameghino 1901).

The Mustersan SALMA *Polymorphis* spp. was consistently found near the base of Macraucheniidae, supporting Cifelli's (1983*a*) inclusion of this genus in the family (Table 4.1) and in agreement with a previous phylogenetic analysis (Cifelli 1993; Fig. 4.1c). There are still many unsolved questions in relation to the upper dentition of *Polymorphis* (see taxonomic comments for *Polymorphis* spp.), in which a new revision of the available material and new fossil findings could help to resolve. However, considering that my conservative approach in the scoring of this genus still allowed the phylogenetic analyses to firmly place it within Macraucheniidae, it is likely that the inclusion of more character evidence in the scoring should only reinforce its placement in the family. In addition, I did not find support for the subfamily Cramaucheniinae (Soria 1981) in any of our analyses, as the "cramaucheniine" *Theosodon* spp. was found to be more closely related to the macraucheniine *Macrauchenia patachonica* than to the "cramaucheniine" *Cramauchenia normalis*. Therefore this subfamily is paraphyletic, a result consistent with previous analyses testing the phylogenetic affinities within Macraucheniidae (Schmidt & Ferrero 2014; Forasiepi *et al.* 2016; McGrath *et al.* 2018; Püschel

*et al.* 2023). Taking all this evidence into consideration, I recommend to stop using the name Cramaucheniinae, as its members do not form a monophyletic group. A potential alternative could be to use the informal term "early macraucheniids", when referring to the taxa typically included in this subfamily. The validity of the subfamily Macraucheniinae (Ameghino 1902*a*) was not tested here as among its members only *M. patachonica* was included in my analyses. However, its validity seems likely as the most recent study of Macraucheniidae found strong anatomical and phylogenetic evidence supporting it, while updating also the diagnosis of this subfamily (Püschel *et al.* 2023). In terms of the divergence date recovered for the family Macraucheniidae of ~ 40.8 Ma (41.9 – 37.1 Ma 95% HPD; Table 4.4), this is consistent across the different tip-dated Bayesian analyses and implies a common ancestor for the family around the Barrancan SALMA (middle Eocene).

The family Adianthidae was found consistently forming a monophyletic group under different phylogenetic approaches (Figs. 4.4, 4.5, 4.6 and Figs. S1-S5 in Appendix C4 Resource 6). Several anatomical features support the monophyly of this family, some of which were recovered among the 14 unambiguous synapomorphies in the parsimony analyses such as the presence of a postparaconular crista in P5-M3 and a hypoconulid similar in length to the talonid mesial to hypoconulid in m3 (Appendix C4 Resource 5). Following phylogenetic taxonomy methods (De Queiroz & Gauthier 1992), Adianthidae can be defined as the clade composed of *Adianthus bucatus* (Ameghino 1891*a*) and all the taxa more closely related to it than to the macraucheniid *Macrauchenia patachonica* (Owen 1838), the proterotheriid *Proterotherium cervioides* (Ameghino 1883*b*), the sparnotheriodontid *Sparnotheriodon epsilonoides* (Soria 1980*a*) and the anisolambdid *Anisolambda fissidens* (Ameghino 1901).

**Table 4.5** New taxonomic proposal for the orders Litopterna and Notopterna.

| | |
|---|---|
| Order Litopterna | |
| | Family Adianthidae |
| | Family Macraucheniidae |
| | *Suborder Proterotheria, new rank |
| | Family Proterotheriidae |
| | Superfamily Eolitopternoidea, new rank |
| | Family Anisolambdidae |
| | Family Sparnotheriodontidae |
| *Order Notopterna | |
| | Family Indaleciidae |
| | *Family Notonychopidae |

*Taxonomic ranks tentatively proposed as they were not supported consistently in all the phylogenetic analyses.

In all the analyses, the Barrancan SALMA *Proectocion* spp. was consistently found in a basal position within the family, and the Deseadan SALMA *Tricoelodus bicuspidatus* and *Proadiantus excavatus* as sister taxa. These results support the inclusion of *Proectocion* within

the family Adianthidae as Cifelli (1983*a*) previously proposed and later supported in a phylogenetic analysis (Cifelli 1993; Fig. 4.1c). Including indaleciids within Adianthidae as some authors have suggested (Simpson *et al.* 1962; Bond & Vucetich 1983; Cifelli 1983*a*; Zimicz *et al.* 2022) is not supported in my analyses, as I found the indaleciid *Indalecia grandensis* in most cases closely related to notonychopids (Notopterna). It is important to mention, that the intrafamilial affinities of Adianthidae still remain to be tested using modern phylogenetic methods. The morphological matrix used in this study could be expanded for such a purpose. The divergence estimate recovered for Adianthidae of ~ 44.7 Ma (53.5 – 39.6 Ma 95% HPD; Table 4.4) is overall consistent across the different tip-dated Bayesian analyses an implies a common ancestor for the family around the Sapoan Fauna SALMA (middle Eocene).

## Interfamilial affinities of Litopterna: Proterotheriidae, Anisolambdidae and Sparnotheriodontidae

The monophyletic group composed of Proterotheriidae, Anisolambdidae and Sparnotheriodontidae was found in most phylogenetic analyses with a strong support (Figs. 4.4, 4.5, 4.6b and Figs. S1-S3 in Appendix C4 Resource 6), the exception being the topology-unconstrained tip-dated Bayesian analyses (Fig. 4.6a and Figs. S4-S5 in Appendix C4 Resource 6). This group is supported by various anatomical features some of which were recovered as one of 14 unambiguous synapomorphies in the parsimony analyses, such as the presence of a hypoconulid on p2 and a postprotocrista in M1-M2 oriented towards the distocone (see Results section and Appendix C4 Resource 5). Even though these three families have been previously associated, a taxonomic rank for this grouping has never been proposed probably because previous phylogenetic studies including members of these families did not recovered them forming a monophyletic group (Cifelli 1993; Bonaparte & Morales 1997; Fig. 4.1c-d). Cifelli's (1983) superfamily Proterotherioidea includes anisolambdids and proterotheriids as subfamilies, but excludes sparnotheriodontids (Table 4.1). Soria's (2001) suborder Eolitopterna includes anisolambdids and sparnotheriodontids, but excludes proterotheriids (Table 4.1). Consequently, I propose the suborder Proterotheria new rank to include the family Sparnotheriodontidae alongside the families Anisolambdidae and Proterotheriidae, considering the important anatomical features that these families share (Table 4.5). Following phylogenetic taxonomy methods (De Queiroz & Gauthier 1992), Proterotheria can be defined as the clade composed of the most recent ancestor of the proterotheriid *Proterotherium cervioides* (Ameghino 1883*b*), the sparnotheriodontid *Sparnotheriodon epsilonoides* (Soria 1980*a*) and

the anisolambdid *Anisolambda fissidens* (Ameghino 1901), and all of its descendants. The composition of each family is based on my results and also in Soria (2001) for the taxa not scored in my study (Table S1 in Appendix C4 Resource 1). Considering the tip-dated Bayesian analyses the origin age of Proterotheria is ~ 56.0 Ma (59.13 – 53.56 Ma 95% HPD; Table 4.4) which implies a common ancestor living around the Itaboraian SALMA.

The family Proterotheriidae consistently formed a well-supported monophyletic group in all the phylogenetic analyses (Figs. 4.4, 4.5, 4.6 and Figs. S1-S5 in Appendix C4 Resource 6). Different anatomical features support the monophyly of this family, some of which were recovered among the 20 unambiguous synapomorphies in the parsimony analyses (see Results section and Appendix C4 Resource 5), such as the possession of two lower incisors and a postmetaconular crista absent on P5-M2. McGrath *et al.* (2020*b*) proposed a stem-based definition of Proterotheriidae, as the clade composed of *Tetramerorhinus lucarius* (Ameghino 1894*c*); *sensu* Soria 2001) and all litopterns more closely related to it than to *Macrauchenia patachonica* (Owen 1838), *Tricoelodus bicuspidatus* (Ameghino 1897) or *Protolipterna ellipsodontoides* (Cifelli 1983*a*). However, McGrath's *et al* (2020*b*) definition of Proterotheriidae presents some problems. First, it uses *Tetramerorhinus lucarius* and *Tricoelodus bicuspidatus* instead of *Proterotherium cervioides* (Ameghino 1883*b*) and *Adianthus bucatus* (Ameghino 1891*a*) respectively as internal specifiers of Proterotheriidae and Adianthidae, which is the standard practice. Also, McGrath's *et al* (2020*b*) definition does not mention the families Anisolambdidae and Sparnotheriodontidae, which means that considering the phylogenetic position close to Proterotheriidae here recovered, under this definition members of these families would be proterotheriids. In addition, it includes the "didolodontid" *Protolipterna*, which has uncertain affinities among SANUs. Therefore, I propose to update this stem-based definition of the family in the light of my results. In that sense, Proterotheriidae can be redefined as the clade composed of the proterotheriid *Proterotherium cervioides* (Ameghino 1883*b*) and all taxa more closely related to it than to the anisolambdid *Anisolambda fissidens* (Ameghino 1901), the sparnotheriodontid *Sparnotheriodon epsilonoides* (Soria 1980*a*), the macraucheniid *Macrauchenia patachonica* (Owen 1838) and the adianthid *Adianthus bucatus* (Ameghino 1891*a*).

The Deseadan SALMA *Lambdaconus suinus* was consistently found as being closely related to the more derived Santacrucian SALMA *Diadiaphorus majusculus*, which supports the inclusion of the former as the earliest member of Proterotheriidae as Soria (2001) previously suggested. My results differ from a previous phylogenetic analysis that found the

indaleciid *Adiantoides leali* and the anisolambdids *Anisolambda* spp., *Paranisolambda prodromus* and *Protheosodon coniferus* within Proterotheriidae (McGrath *et al.* 2020*b*). However, their study was based on a relatively small list of characters and a small matrix and that did not include any members of the litoptern families Adianthidae, Macraucheniidae, Sparnotheriodontidae and Notonychopidae. Therefore, their analysis was inadequate for testing interfamilial relationships of these groups. I did not try to assess the internal relationships within Proterotheriidae in this study, but more taxa and postcranial characters could be added to my matrix for such a purpose, corroborating or rejecting previous phylogenetic hypotheses for this family (Kramarz & Bond 2005; Villafañe *et al.* 2012; Schmidt 2015; McGrath *et al.* 2020*b*). In a future study, it would be particularly interesting to determine the position of the Laventan SALMA (middle Miocene) bunodont *Megadolodus molariformis* which was found as a member of Proterotheriidae in previous analyses that, contrary to my study, failed to recover a distinct and monophyletic family Anisolambdidae (Cifelli 1993; McGrath *et al.* 2020*b*). The tip-dated Bayesian analyses gave an origin age for the family Proterotheriidae of ~ 33.2 Ma (41.8 – 27.5 Ma 95% HPD; Table 4.4), implying a common ancestor living around the Mustersan and Tinguiririan SALMAs (late Eocene to Early Oligocene). This makes Proterotheriidae the youngest family of the order Litopterna.

The families Anisolambdidae and Sparnotheriodontidae form a strongly supported monophyletic group consistently across different phylogenetic analyses (Figs. 4.4, 4.5, 4.6 and Figs. S1-S5 in Appendix C4 Resource 6). This is not particularly surprising, as they share many anatomical features, some of them recovered among the nine or 10 unambiguous synapomorphies in the parsimony analyses such as the presence of a secondary distal cingulum in M1-M3 and a well-developed protostyle in M1-M2 (see Results section and Appendix C4 Resource 5). The strong relationship between these two families supports Soria's (2001) proposal of the suborder Eolitopterna for grouping both families based on shared dental features. Here I propose to change the rank of this monophyletic group to superfamily Eolitopternoidea, as this group would be within the suborder Proterotheria. Following phylogenetic taxonomy methods (De Queiroz & Gauthier 1992), Eolitopternoidea can be defined as the clade composed of the most recent common ancestor of the sparnotheriodontid *Sparnotheriodon epsilonoides* (Soria 1980*a*) and the anisolambdid *Anisolambda fissidens* (Ameghino 1901), and all its descendants. The tip-dated Bayesian analyses gave an origin age for the superfamily Eolitopternoidea of ~ 54.9 Ma (57.7 – 52.7 Ma 95% HPD; Table 4.4), which places a common ancestor for this group between the *Carodnia* Zone and Itaboraian

SALMAs (late Palaeocene to early Eocene) which is close to the age of the earliest anisolambdid *Wainka tshotshe* (*Carodnia* Zone SALMA).

The family Anisolambdidae was recovered as a well-supported monophyletic group in all the phylogenetic analyses here performed (Figs. 4.4, 4.5, 4.6 and Figs. S1-S5 in Appendix C4 Resource 6). Anisolambdids share multiple anatomical features some of which were retrieved among the 10 unambiguous synapomorphies in the parsimony analyses, such as the absence of a postentocristid on m1-m2 (see Results section and Appendix C4 Resource 5). Following phylogenetic taxonomy methods (De Queiroz & Gauthier 1992), Anisolambdidae can be defined as the clade composed of the anisolambdid *Anisolambda fissidens* (Ameghino 1901) and all the taxa more closely related to it than to the proterotheriid *Proterotherium cervioides* (Ameghino 1883*b*), the sparnotheriodontid *Sparnotheriodon epsilonoides* (Soria 1980*a*), the macraucheniid *Macrauchenia patachonica* (Owen 1838) and the adianthid *Adianthus bucatus* (Ameghino 1891*a*). It is important to note that Soria (2001), in his revision of Anisolambdidae, did not evaluate in detail the different species of the Riochican to Barrancan SALMAs *Anisolambda*, so their validity remains to be investigated, an issue hindered by the incompleteness of their remains. In the present analyses, apart from *Anisolambda* spp. I only included the Itaboraian *Paranisolambda prodromus*, so the affinities of other anisolambdids remain to be tested (Table S1 Appendix C4 Resource 1).

Even though I did not score the earliest putative anisolambdid *Wainka tshotshe*, I think its general features do correspond to it being an anisolambdid, in particular the preserved m3 (AMNH 28505) as it shares many distinctive features with *P. prodromus* and *Anisolambda* spp. such as a well-developed and rounded paraconid with its base fused with the metaconid base. The affinities of the holotype (AMNH 28505) are less clear, as it is a worn upper premolar (probably P5 or P4) without a mesostyle and with an appressed paracone and metacone, which are features completely different to the P4 and P5 of *Anisolambda* spp. The latter has a distinct mesostyle and separated paracone and metacone in P4 and P5. In my view, it is entirely possible that the holotype of *W. tshotshe* may be a different taxon than the preserved m3, with potentially different affinities among litopterns or even among SANUs, contrary to previous assertions (Cifelli 1983*a*; Soria 2001). Indeed, Soria (2001) justified the inclusion of the holotype of *W. tshotshe* within Anisolambdidae based on dental similarities to the Deseadan SALMA anisolambdid *Protheosodon coniferus*. However, the affinities of *Protheosodon coniferus* are still controversial, as in the most recent analysis it is nested within Proterotheriidae (McGrath *et al.* 2020*b*). Resolving the affinities of *Protheosodon coniferus* is

particularly important also because of the fact it is potentially the only member of this family with associated tarsal remains (Loomis 1914; but see Simpson [1948] for a different interpretation).

In my taxonomic list for Anisolambdidae (Table S1 Appendix C4 Resource 1) I mostly followed Soria (2001), with some modifications. I tentatively included the genus *Polyacrodon* within Anisolambdidae considering similarities with *Protheosodon* (see *Polymorphis* spp. in taxon sampling section for more details). *Eolicaphrium* (Ameghino 1902*b*) and *Guilielmofloweria* (Ameghino 1901) are only tentatively included in the taxonomic list, as they could correspond to a juvenile specimen of *Anisolambda* and a premolar of a sparnotheriodontid respectively (Soria 2001). The origin age of Anisolambdidae ~ 53.4 Ma (55.7 – 51.8 Ma 95% HPD; Table 4.4) estimated with the Bayesian tip-dated analyses implies a common ancestor for the group around the Itaboraian SALMA (early Eocene). This date is somewhat late if the *Carodnia* Zone (middle Palaeocene) *W. tshotshe* is actually an anisolambdid, in which case this taxon would probably be close temporally to the common ancestor of the entire family.

## Sparnotheriodontidae and an Antarctic voyage

The family Sparnotheriodontidae was consistently recovered as a strongly supported monophyletic group in different phylogenetic analyses (Figs. 4.4, 4.5, 4.6 and Figs. S1-S5 in Appendix C4 Resource 6). Sparnotheriodontids share many anatomical features that distinguish them from other litopterns, some were recovered among the seven unambiguous synapomorphies in the parsimony analyses, like the presence of a postmetacristid in m1-m3 (see Results section and Appendix C4 Resource 5). Following phylogenetic taxonomy methods (De Queiroz & Gauthier 1992), Sparnotheriodontidae can be defined as the clade composed of the sparnotheriodontid *Victorlemoinea prototypica* (Paula Couto 1952) and all the taxa more closely related to it than to the anisolambdid *Anisolambda fissidens* (Ameghino 1901), the proterotheriid *Proterotherium cervioides* (Ameghino 1883*b*), the macraucheniid *Macrauchenia patachonica* (Owen 1838) and the adianthid *Adianthus bucatus* (Ameghino 1891*a*).

The Patagonian species of the genus *Victorlemoinea* (*V. labyrinthica*, *V. emarginata* and *V. longidens*) were not included in my analyses, as the specimens are in general very fragmentary and there is uncertainty about the validity of each species. Even though most recent authors (e.g., Reguero *et al.* 2014; Gelfo 2016; Gelfo *et al.* 2019) have mentioned only

*V. labyrinthica* for the Riochican and Vacan Patagonian faunas indirectly implying a synonymy with the other two taxa, at the present these taxa should not be synonymised until a formal revision of the Patagonian material of *Victorlemoinea* is conducted. The position of the family Sparnotheriodontidae as a sister family of Anisolambdidae (superfamily Eolitopternoidea) and deeply nested within Litopterna, argues strongly against grouping them with "didolodontids" as Cifelli (1983*b*) suggested. This suggestion was based on an indirect tarsal assignment for the Itaboraian SALMA *Victorlemoinea prototypica* and later found some phylogenetic support (Cifelli 1993; Bergqvist 1996; Fig. 4.1c). Considering that the tarsal association for *V. prototypica* has been questioned by several authors on anatomical grounds (e.g., Hoffstetter & Soria 1986; Soria 2001; Lorente 2015), and also the strong phylogenetic support for a family Sparnotheriodontidae within Litopterna and its close relationship with Anisolambdidae in my phylogenetic analyses, I consider it unlikely that Cifelli's (1983*b*) tarsal association was correct as it would imply major anatomical convergences between sparnotheriodontids and the rest of litopterns such as the 9 or 10 unambiguous synapomorphies that support the superfamily Eolitopternoidea (see above and Appendix C4 Resource 5). Particularly important is the presence of a secondary distal cingulum in M1-M3 (double cingulum mentioned by previous authors [Bond *et al.* 2006; Gelfo *et al.* 2019]), a unique feature among litopterns and only shared with anisolambdids. Nevertheless, in a future study it would be interesting to add tarsal characters to my matrix and test the effect of incorporating Cifelli's (1983*b*) tarsal referral for *V. prototypica* to see how it affects the affinities of sparnotheriodontids with other litoptern families and with early SANUs.

A difference between the parsimony and the Bayesian phylogenies is the identity of the most basal sparnotheriodontid: *Sparnotheriodon epsilonoides* in the former analyses and *V. prototypica* in the latter analyses. This is probably related to the lack of known upper dentition for *S. epsilonoides*, which increases the uncertainty of its exact placement among sparnotheriodontids. These results also differ from a previous phylogenetic analysis of a smaller dataset (i.e., 34 dental characters) that found the Antarctican early to middle Eocene *Notiolofos arquinotiensis* as the most basal sparnotheriodontid (Reguero *et al.* 2014). Considering the age and stratigraphic provenience of each taxon, I think a basal position for *V. prototypica* is more likely, leaving *S. epsilonoides* and the Antarctican *N. arquinotiensis* as sister taxa. The divergence-time estimates between these two taxa in the Bayesian analyses are overall consistent across different constraints and calibration approaches (Table 4.4). It is important to mention that Gelfo (2016) gives an approximate time interval between the oldest

(MLP 13-I-25-1) and the youngest (MLP 95-I-10-6) records of *Notiolofos arquinotiensis* of 55.3 – 37.8 Ma based on previous isotopic dates of the La Meseta and Submeseta formations (Ivany *et al.* 2008; Montes *et al.* 2013), arguing that this species displays 17.5 Ma of morphological stasis. However, I consider an age of 44 – 34 Ma for this taxon following later interpretations of La Meseta and Submeseta formations (Douglas *et al.* 2014; Amenábar *et al.* 2019; for more details see also *Notiolofos arquinotiensis* in the Taxon sampling section), which implies instead 10 Ma of morphological stasis in this taxon. As *N. arquinotiensis* displays a considerable morphological stasis over time (Gelfo 2016), I consider it more appropriate to use the divergence-time estimate given by the calibration approach that used the age of the oldest specimen (Püschel *et al.* 2020), although in this the difference between divergence-time estimates among different calibration approaches were consistent (Table 4.4), giving an estimate of ~46.1 Ma (50.3 – 43.0 Ma 95% HPD). An estimation of 46.1 Ma is considerably younger than previous estimations using ghost lineages of 58 – 59 Ma for the common ancestor of *N. arquinotiensis* and the rest of the sparnotheriodontids (Reguero *et al.* 2014). The older age estimated by Reguero *et al.* (2014) is probably a product of the different age interpterion for the La Meseta formation and also the relatively more basal phylogenetic position of *N. arquinotiensis* recovered in their phylogeny. The diverge-time estimate 46.1 Ma (50.3 – 43.0 Ma 95% HPD) for the clade of *S. epsilonoides* and *N. arquinotiensis* also gives a minimum age for the crossing of sparnotheriodontids to Antarctica. This estimation (46.1 Ma) is temporally close to the earliest record of *N. arquinotiensis* at 44.0 Ma (Gelfo 2016; Amenábar *et al.* 2019), which suggests a probable widespread distribution of sparnotheriodontids in South America and Antarctica during the early/middle Eocene (Itaboraian, Riochican and Sapoan Fauna SALMAs). This hypothesis is consistent with the distribution of the different species of sparnotheriodontids during the Eocene: Patagonian *Victorlemoinea* spp. present from the Riochican and Vacan faunas of Patagonia (early to middle Eocene), *Phoradiadius divoertensis* from Divisadero Largo Formation, Mendoza, Argentina (middle Eocene) and *Sparnotheriodon epsilodonoides* from the Patagonian Vacan fauna (middle Eocene).

Another group with a widespread distribution in the early Eocene is Astrapotheria, which included different genera during the early Eocene: *Eoastrapostylops*? (maybe a basal as a basal "meridiungulate" [Kramarz *et al.* 2017; Macphee *et al.* 2021]), *Shecenia*, *Tetragonostylops* and *Trigonostylops* . Sparnotheriodontids and astrapotheres are not known in the early Palaeocene fossil record of the Patagonian Punta Peligro (Peligran SALMA) and Bolivian Tiupampa (Tiupampan SALMA), nor in the middle Palaeocene of Patagonia

*Carodnia* Zone (Woodburne *et al.* 2014*b*). This implies that these lineages likely had not evolved yet during the early Palaeocene, or perhaps that they had a marginal distribution in South America at that time. It is possible that these groups achieve a widespread distribution between the *Carodnia* Zone and the Riochican/Sapoan Fauna SALMAs, a time in which a land bridge (i.e., Weddellian Isthmus) allowed them to cross to the Antarctic Peninsula (Reguero *et al.* 2014). Then the connection was lost and a marine gap was generated between South America and Antarctica potentially at the middle Eocene, considering the absence of evidence that suggest an new influx of mammalian crossings during the whole temporal interval ( ~10 Myr) that encompasses the La Meseta and Submeseta formations, Antarctic Peninsula (Reguero & Goin 2021).

During the Palaeocene, there is no evidence of physical barriers that could have limited mammal dispersion events from South America to the Antarctic Peninsula (and vice versa), and even though there is controversy about the exact opening of the Drake passage, the earliest estimation for its onset is during the middle Eocene (Livermore *et al.* 2005; Scher & Martin 2006). Consequently, the current consensus is that there was a continuous causeway between both continents through the Late Cretaceous (Campanian) and late Palaeocene (Reguero *et al.* 2014; Reguero & Goin 2021). However, there are some palaeontological considerations that suggest otherwise. Xenungulates were widespread in South American from the early Palaeocene and to the early Eocene, known from fossil sites from Colombia to Patagonia (Vera *et al.* 2020). Considering the ease of dispersal of this order, particularly of the genus *Carodnia*, in the presence of a continuous land bridge such as the Weddellian Isthmus, it might be expected that *Carodnia* would have crossed the land bridge without problems. However, so far there is no evidence of any xenungulate fossil in the Antarctic Peninsula. Similarly, there is no evidence of any "didolodontids" or notonychopids in Antarctica, which were present in the early Palaeocene Patagonian Punta Peligro. In that context, an interesting possibility is that there could have been some barrier limiting the dispersion between both landmasses between the Peligran SALMA and the *Carodnia Zone* during the early Palaeocene. This barrier—whether physical, climatic, or otherwise—must have been lifted at some point between the *Carodnia* Zone and the end Itaboraian SALMA—that is between the late Palaeocene and the early Eocene. This could explain the absence of notonychopids and xenungulates on the Antarctic Peninsula, as they disappear from the Patagonian fossil record around the early Eocene (Itaboraian SALMA).

An interesting question is also why only sparnotheriodontid litopterns and astrapotheres were the only SANUs able to cross to the Antarctic Peninsula during this timeframe. In the case of notoungulates, it has been proposed that they experienced a delayed radiation in the southern portion of South America, based on the early Palaeogene fossil record of this group, but its absence in the Salamanca Formation of Punta Peligro (Reguero *et al.* 2014; Reguero & Goin 2021). If so, notoungulates may not have been present in the southern regions of South America, adjacent to Antarctica, before the migration corridors closed. This is a promising explanation, although the same "delayed radiation" scenario may be true for litopterns and astrapotheres, as among SANUs, only "didolodontids" and notoptern notonychopids are present at Punta Peligro in the early Palaeocene. I suggest that an important part of the answer is related to body size. In macroecological studies of modern ungulates, the scaling between body mass and home range size is well known and larger species tend to occupy larger home ranges than smaller species, and browsers have larger home ranges compared with grazers (Ofstad *et al.* 2016). Both sparnotheriodontids and astrapotheres were among the biggest mammals in their faunal communities during the Eocene (Vizcaíno *et al.* 1998, 2012) and were most likely browsers, so they may have been more liable to migrate widely. The early Palaeocene to early Eocene cosmopolitan xenungulate *Carodnia*, with browsing capabilities and a large body mass (Bergqvist & Koenigswald 2017), also fits this pattern, which makes its absence in Antarctica even more enigmatic, supporting the hypothesis of a dispersal barrier during the early Palaeocene (see above). In a future study it would be interesting to expand the astrapothere sample including *Antarctodon sobrali* and perform tip-dating Bayesian analyses to see if the divergence-time estimates correspond to the pattern seen in sparnotheriodontids. The same could be done for Metatheria—another mammal group that spanned South America and Antarctica at this time—using a metatherian phylogeny including the Palaeogene Patagonian and Antarctic species.

## Macroevolutionary trends in litoptern evolution

The first half of the Palaeogene was a time of global warm climate and little seasonality, which peaked in the early Eocene Climatic Optimum (Zachos *et al.* 2001). In North America, bunodont "archaic" ungulates were an important part of the fauna during this period. However, following this peak, there was a global trend towards cooler temperatures and a drop in ungulate diversity during the late Eocene (Janis 2000). This process ended with the extinction of these "archaic" ungulates by the Eocene-Oligocene transition (EOT) and the growing predominance of more semi-lophed or lophed taxa (Janis 2000). An analogous faunal turnover

is known to have occurred in Europe with the *Grande Coupure* event (Hooker 2000; Hooker *et al.* 2004). However, although these global changes were synchronous and of similar magnitude in the sea (Zachos *et al.* 2001), terrestrially there were differences in magnitude and timing between the turnover in North America and Europe (Eronen *et al.* 2015). This is explained by the heterogeneity of responses in terms of vegetation and climate during the EOT in different parts of the world (Pound & Salzmann 2017).

South American climate proxy data shows a more complicated record during the EOT, with some studies showing no change across this boundary in Patagonia (Kohn *et al.* 2004, 2015) and more recently, others showing a cooling similar to the Northern Hemisphere in this period (Colwyn & Hren 2019). Even so, South American ungulates evolved following an analogous narrative to those in North America and Europe. "Didolodontids" diversified generically during the Palaeocene, keeping the "primitive" bunodont pattern first seen in Kollpaniidae (Fig. 4.2b-c), whereas litopterns, astrapotheres and notoungulates tended to develop a more lophed pattern during this period. After the EOT the latter three SANU orders survived and "didolodontids" went extinct (Gelfo 2010), just as most primitive bunodont "condylarths" went extinct in the north and were superseded by more derived lophed taxa. However, this turnover seems to be more complex than just the extinction of bunodont SANUs and later blossoming of lophed taxa, as also anisolambdids and sparnotheriodontids litopterns, and indaleciid notopterns with lophed dentition, were greatly affected by the EOT, with none of them surviving to the Neogene. Among litopterns only three families made it to the Neogene and diversified: Adianthidae, Macraucheniidae and Proterotheriidae (Fig. 4.2b-c). The origin dates for each of these three families were estimated consistently during the Eocene (Table 4.4), a period in which there are not many fossils of these groups, which suggests they were not particularly abundant (i.e., proterotheriids are only known since the Oligocene). This makes the question of their survival among litopterns more puzzling, and more studies, and probably more fossil material, will be needed for resolve this controversy.

# Conclusions

Litopterna was the second most diverse order of SANUs after Notoungulata and a key component of the South American fauna during most of the Cenozoic (Croft *et al.* 2020). Considering the importance of litopterns among the terrestrial fauna of South America, the lack of studies using modern phylogenetic methods to test its monophyly and interfamilial affinities hinders the possibility of a better understanding of how and when this group evolved and

diversified in South America in the earliest Palaeogene, and how it relates to the earliest SANUs and placental ungulates that lived just after the K/Pg mass extinction. An important part of the problem is the limited fossil record of this period and in particular of the early Palaeocene in South America, which is limited in most cases of isolated dental elements (Simpson 1948; Muizon & Cifelli 2000; Goin *et al.* 2022).

In that sense, my study is particularly relevant as I used all the available evidence of the earliest litopterns and their putative ungulate relatives and place it in a phylogenetic framework. I used, for the first time, undated and tip-dated Bayesian analyses to compare with the results from the most traditional maximum parsimony analyses under different anatomical and temporal hypotheses in order to test their influence in the topology of the trees. Although there were some differences, important general patterns in the phylogeny of Litopterna and early SANUs emerged: (1) "Didolodontids" (including "protolipternids"), kollpaniids and North American mioclaenids were found consistently at the stem of a monophyletic group composed of the SANUs' orders, with "didolodontids" always being phylogenetically closer to the SANUs' orders than to kollpanines and North American mioclaenids, (2) Indaleciidae and Notonychopidae form in most phylogenetic analyses a monophyletic group (order Notopterna) whose exact affinities among the SANU orders are still undetermined, although they were recovered consistently phylogenetically closer to astrapotheres, litopterns and notoungulates than to xenungulates, (3) the order Litopterna is composed of the families Adianthidae, Anisolambdidae, Macraucheniidae, Proterotheriidae and Sparnotheriodontidae, (4) Although the placement of Adianthidae and Macraucheniidae within Litopterna is very robust, their exact interfamilial relationships are still uncertain, (5) Anisolambdidae, Proterotheriidae and Sparnotheriodontidae form in most analyses a monophyletic unit within Litopterna, here named as the suborder Proterotheria new rank, and (6) Anisolambdidae and Sparnotheriodontidae form consistently a monophyletic unit, here named as the superfamily Eolitopternoidea new rank.

In terms of the timing for important events in SANUs evolutions it can be said: (1) The age of the putative common ancestor of SANUs is likely to be ~ 65.9 Ma in the earliest Palaeocene and close to the K/Pg boundary , (2) the age of the common ancestor of the orders of SANUs is likely to be ~ 64.3 Ma, (3) the age of the order Litopterna is close to ~ 57.3 Ma being well placed in the late Palaeocene with all the interfamilial diversification happening in the Eocene (Table 4.4), and (4) the timing of the crossing to Antarctica of sparnotheriodontid litopterns was likely ~46.1 Ma during the Eocene.

Even though I am confident that these results are robust, it is important to note that some of these conclusions might change in the light of new fossil evidence, and the inclusion of cranial and postcranial characters. In particular, associated postcranial characters could have a major impact in the "didolodontid"/"protolipternid" controversy (Gelfo *et al.* 2016), and effectively probe if these groups can be linked more closely with litopterns based in their postcranium. In future studies, cranial and postcranial characters could be added to the matrix for the taxa with those elements preserved, and test whether their inclusion generates changes in the topology of the tree. In addition, the timing of the cladogenetic events here recovered could be refined in the future when better radiometric dates are available for the different SALMAs and relevant fossil localities in the South American Palaeogene.

# Chapter 5 Synthesis & Conclusions



Portrait of Florentino Ameghino working in mammalian fossils. MACN collections, March 2019

## Summary of Key Findings

Through the use of modern phylogenetic methods, my thesis provides new insights about the tempo and mode of evolution of relevant placental lineages during the Cenozoic. What follows is a summary of the most important findings.

In Chapter 2 I generated relevant new knowledge on human evolution applying for the first time a Bayesian Total Evidence dating (TED) analyses for obtaining a set of hominin plausible trees, which were then used to explore body mass and encephalisation trends. Applying TED analyses in a hominin phylogeny in order to date important cladogenetic events in human evolution was a novel application of the method, so this study opened new paths of research in palaeoanthropology. I showed that (1) the last common ancestor of the genus *Homo* most likely appeared around 3.3 Ma (between 4.30 and 2.56 Ma) with a body size close to that of *Australopithecus afarensis* and an encephalization very similar to *Homo floresiensis*, (2) hominin body mass evolution followed a general trend of decreasing size before the emergence of *Homo* and exhibited a general trend of increasing size afterwards, (3) hominins displayed a general trend of gradual but accelerating encephalization through time, (4) *Homo sapiens* is the most encephalized hominin species possessing the greatest encephalization positive rate and (5) *Homo floresiensis* and *Homo naledi* did not follow these encephalization and body mass general trends. Different phylogenetic hypotheses have an important effect on interpretations of *H. floresiensis* evolutionary trends, although if we consider a basal position of this taxon within *Homo* (Argue *et al.* 2017), then an encephalization stasis scenario is favored. In the case of *H. naledi*, its phylogenetic position and age suggest a strong reduction in encephalization in a relatively short time. Although these conclusions are not directly related to SANUs and litoptern evolution, the phylogenetic methods employed provide a foundation for the methods used in Chapter 3 and Chapter 4.

In Chapter 3 I described a new litoptern, the macraucheniine macraucheniid *Micrauchenia saladensis* (SGO.PV.217000) from the marine late Miocene (Huayquerian SALMA) Bahía Inglesa Formation, Chile, I analysed the function of its forelimbs through the examination of their morphology and performed new maximum parsimony and Bayesian undated and tip-dated phylogenetic analyses incorporating postcranial characters for the first time in this group. The description of *M. saladensis* provides important data on the postcranial anatomy of macraucheniids as not much postcranial has been described previously for this group, particularly for the temporal interval between the early Miocene *Theosodon* and the late

Pleistocene *Macrauchenia*. I showed that (1) the body mass of *M. saladensis* was 53 – 102.52 kg, making it the smallest macraucheniine yet described, (2) *M. saladensis* was a terrestrial animal, likely one with a subunguligrade stance and a forelimb adapted for cursorial locomotion which suggests an allochthonous position for this taxon in this marine formation, (3) the fusion of the ulna and radius in *M. saladensis* was probably a cursorial specialization for restricting pronation-supination movement and favouring parasagittal motion, (4) the radial aliform expansion of *M. saladensis* and other macraucheniines most likely provided a large area for the insertion of an enlarged deep digital flexor muscle which would have likely facilitated strong flexion of the forefoot and maybe aided in sudden movements, such as swerving and dodging, (5) the phylogenetic analyses corroborate *M. saladensis* as member of subfamily Macraucheniinae, although with uncertain affinities within this subfamily, and (6) the origin of the subfamily Macraucheniinae was probably around 14.06 Ma (between 19.05 and 10.52 Ma. The detailed comparative anatomical examination of litopterns and other SANUs performed in Chapter 3 served as the foundation of the anatomical observations made in Chapter 4 for building a morphological matrix of early litopterns and some early SANUs.

In Chapter 4 I ran maximum parsimony and for the first time undated and tip-dated Bayesian phylogenetic analyses in a new litoptern matrix with 954 dental and mandibular characters to test the interfamilial relationships of Litopterna and its monophyly. This matrix includes the earliest members of Litopterna, and also the some of the earliest members of each SANU order (except Pyrotheria) and also relevant South and North American "condylarths". This is the first time that the affinities within Litopterna have been tested with a matrix that also includes some of the earliest members of the most important lineages of SANUs (Table 4.2). From the set of phylogenies obtained in the phylogenetic analyses in relation to Litopterna I showed that (1) the order Litopterna is composed of the families Adianthidae, Anisolambdidae, Macraucheniidae, Proterotheriidae and Sparnotheriodontidae, (2) the placement of Adianthidae and Macraucheniidae within Litopterna is very robust, but their exact interfamilial relationships are still uncertain, (3) Anisolambdidae, Proterotheriidae and Sparnotheriodontidae form in most instances a monophyletic unit within Litopterna, here named as the suborder Proterotheria new rank, and (4) Anisolambdidae and Sparnotheriodontidae form a monophyletic unit, here named as the superfamily Eolitopternoidea new rank. In relation to SANUs that have been previously linked to Litopterna I demonstrated that (1) "Didolodontids" (including "protolipternids") are phylogenetically closer to the SANU orders (Astrapotheria + Litopterna + Notoungulata + Xenungulata +

Notopterna) than to kollpanines and North American mioclaenids, so a special phylogenetic relationship between "didolodontids" and litopterns is discarded and (2) Indaleciidae and Notonychopidae form in most analyses a monophyletic group (order Notopterna) whose exact affinities among the SANU orders are still undetermined. In addition, the divergence-time estimations from the tip-dated analyses allowed me to advance the following proposals for SANU and litoptern evolution: (1) The age of the putative common ancestor of all SANUs (including kollpaniids and didolodontids) is likely to be ~ 65.9 Ma in the earliest Palaeocene and close to the K/Pg boundary , (2) the age of the common ancestor of the SANU orders (Astrapotheria, Litopterna, Notoungulata and Xenungulata) is likely to be ~ 64.3 Ma, (3) the age of the order Litopterna is close to ~ 57.3 Ma being well placed in the late Palaeocene with all the interfamilial diversification happening in the Eocene, and (4) the timing of the crossing to Antarctica of sparnotheriodontid litopterns was likely ~46.1 Ma during the Eocene.

Altogether, these three chapters provided important progress in placental mammalian evolution through the use of cutting-edge phylogenetic methods. Crucially, this thesis as a whole represents a major step in our understanding of the anatomy and phylogenetic affinities of litopterns and early SANUs.

# Future directions

## Hominin phylogenetics

Although Chapter 2 represents an important advancement in our understanding of hominin evolution, there are still relevant aspects that could be addressed in future studies. In particular, the most comprehensive matrix of hominins (Dembo *et al.* 2016) seem to have some problems of character redundancy probably derived from the way it was built as a supermatrix of previous studies (Mongle *et al.* 2022). Even though collaborators and I showed that the impact of this redundancy is negligible in terms of diverge-time estimations (Püschel *et al.* 2022), it is possible it can still have significant effects for the affinities obtained in the hominin phylogeny when conducting phylogenetic analyses. Therefore, I think a new hominin matrix should be built and maybe expanded in a way that allows the incorporation of other extant and fossil simians (Simiiformes) which could permit to study of evolutionary trends in primate evolution in a broader taxonomic and temporal scale. In addition, considering the taxonomic uncertainty of some hominin taxa and the problems it can generate for defining the maximum and minimum bonds for calibration, an option could be to estimate the hominin phylogeny at

specimen level. In this case, more than one specimen could be potentially included per taxon but only if it comes from the same stratigraphic position.

## Anatomy, biology and phylogeny of Macraucheniidae

Chapter 3 contributes new information on macraucheniid postcranial anatomy as I not only described *Micrauchenia saladensis*, but I also compared it with the anatomy of stratigraphically younger and older macraucheniids, including multiple illustrations. However, there is still a lot to do and study in terms of the postcranial anatomy of macraucheniids. Although there are important early contributions in terms of the study of the postcranial anatomy of macraucheniids (e.g., Scott 1910; Sefve 1925), most recent studies tend to give much more importance to the study of dental remains (e.g., Schmidt & Ferrero 2014; Forasiepi *et al.* 2016; Schmidt *et al.* 2022) probably because of their greater abundance and their taxonomic relevance (i.e., most fossil mammals species are based on them). Even in recent macraucheniid studies that include postcranial material the descriptions tend to be very brief, with few images, and with limited comparisons with other macraucheniids (e.g., McGrath *et al.* 2018).

A better understanding of the postcranial anatomy of macraucheniids could also lead to an expansion of the macraucheniid morphological matrix that I used in Chapter 3, and potentially help to disentangle the exact position of *M. saladensis* and other problematic taxa in the macraucheniid phylogeny. In order to achieve this, more attention has to be given to postcranial elements when found in the field, and also by restudying museum collections with SANU material, in which in many cases postcranial elements are understudied (or not studied at all).

In Chapter 3 I used a functional morphology perspective in order to interpret the palaeobiology and locomotion of *M. saladensis* and other macraucheniids in line with the observations of previous workers in extinct (e.g., Shockey 1999; Shockey & Anaya 2008) and extant ungulates (e.g., (Hildebrand & Goslow 2001). However, there is still much to be done in terms of studying form and function in macraucheniids. In particular, the application of geometric morphometrics and finite element analyses in a phylogenetic and evolutionary framework (Polly *et al.* 2016) could bring important new information about the biology of these extinct ungulates.

## Phylogeny of Litopterna and early SANUs phylogeny

Chapter 4 represents an important effort towards a better understanding of the early evolution of litopterns and SANUs in general, being the first phylogenetic study such a diverse sample of early litopterns and SANUs and applying Bayesian phylogenetic methods. Even though I am confident that the results obtained in Chapter 4 are robust, it is important to note that some of these conclusions might change in light of new fossil evidence, and the inclusion of cranial and postcranial characters. In particular, the finding of associated cranial and postcranial elements could have a major impact on the "didolodontid"/"protolipternid" controversy (Gelfo *et al.* 2016), and address whether these groups can be linked more closely with litopterns based in their postcranium.

In future studies, cranial and postcranial characters could be added to the matrix for the taxa with those elements preserved, and test whether their inclusion generates changes in the topology of the tree. The inclusion of cranial characters and in particular those related to the ear region, could have a major impact in solving the controversial affinities of notopterns and testing more thoroughly their monophyly, considering the importance that these characters seem to have in defining this order (Soria 1984*b*; García-López & Babot 2014). In addition, the taxonomic sampling could be expanded in order to include a couple of more taxa for the SANU orders Notoungulata and Astrapotheria, such as the early Eocene notoungulate *Thomashuxleya externa* which has several postcranial elements known and described (e.g., Carrillo & Asher 2017), and the early Palaeocene or early Eocene *Eoastrapostylops riolorense* which has been considered a basal astrapothere (Soria & Powell 1981) but that has been found as a basal "meridiungulate" of uncertain position in previous phylogenetic analyses (Kramarz *et al.* 2017; Macphee *et al.* 2021). Future analyses could also include additional Palaeogene North American "condylarths" such as the phenacodontid *Tetraclaenodon puercensis*, and early members or stem taxa of the orders Perissodactyla and Artiodactyla. By expanding the matrix with early members of different relevant placental orders, the research question could be easily expanded towards solving the interordinal affinities of SANUs and their exact phylogenetic position in the placental tree, and also test if SANUs form a monophyletic group (Meridiungulata). This work is currently underway and it is part of the objectives of the Palaeogene Mammal Working Group (PalM) to which I have been contributing during my PhD.

The timing of the cladogenetic events here recovered could be refined in the future when better radiometric dates are available for the different SALMAs and relevant fossil localities in the South American Palaeogene. A refinement of these dates could have an impact in the dating of important events in litoptern and SANU evolution, having biogeographic implications such as when the first SANUs ancestors arrived in South America. In addition, with the incorporation of cranial and postcranial characters it would be possible to evaluate the impact that alternative models of partitioning have on the topology of the obtained trees and the divergence-time estimates.

# References


ACHURRA, L. E. 2004. Cambios del nivel del mar y evolución tectónica de la cuenca neógena de Caldera, III Región.'Dissertation', Universidad de Chile, 138pp.

AGNOLIN, F. L. and CHIMENTO, N. R. 2011. Afrotherian affinities for endemic South American 'ungulates'. *Mammalian Biology*, **76**, 101–108.

AIELLO, L. C. and WHEELER, P. 1995. The Expensive-Tissue Hypothesis: The Brain and the Digestive System in Human and Primate Evolution. *Current Anthropology*, **36**, 199–221.

ALMÉCIJA, S., TALLMAN, M., ALBA, D. M., PINA, M., MOYÀ-SOLÀ, S. and JUNGERS, W. L. 2013. The femur of *Orrorin tugenensis* exhibits morphometric affinities with both Miocene apes and later hominins. *Nature Communications*, **4**, 1–12.

ALROY, J. 1998. Cope's rule and the dynamics of body mass evolution in North American fossil mammals. *Science*, **280**, 731–734.

———. 1999. The Fossil Record of North American Mammals: Evidence for a Paleocene Evolutionary Radiation. *Systematic Biology*, **48**, 107–118.

AMEGHINO, F. 1883*a*. Sobre una colección de mamíferos fósiles del piso Mesopotámico de la formación Patagónica recogidos en las barrancas del Paraná por el profesor Pedro Scalabrini. *Boletín de la Academia Nacional de Ciencias en Cordoba*, **5**, 101–116.

———. 1883*b*. Sobre una nueva colección de mamíferos fósiles recogidos por el profesor Scalabrini en las barrancas del Paraná. *Boletín de la Academia Nacional de Ciencias en Cordoba*, **5**, 257–306.

———. 1887. Enumeración sistemática de las especies de mamíferos fósiles coleccionados por Carlos Ameghino en los terrenos Eocenos de la Patagonia Austral y depositados en el Museo de La Plata. *Boletín del Museo de La Plata*, **1**, 1–26.

———. 1889. Contribución al conocimiento de los mamíferos fósiles de la República Argentina. *Actas de la Academia Nacional de Ciencias de la República Argentina en*

*Córdoba*, **6**, 1–1027.

———. 1891*a*. Caracteres diagnósticos de cincuenta especies nuevas de mamiferos fósiles argentinos. *Revista Argentina de Historia Natural*, **1**, 129–167.

———. 1891*b*. Nuevos restos de mamíferos fósiles descubiertos por Carlos Ameghino en el Eoceno inferior de la Patagonia austral. - Especies nuevas, adiciones y correcciones. *Revista Argentina de Historia Natural*, **1**, 289–328.

———. 1894*a*. Sur les oiseaux fossiles de Patagonie et la faune mammalogique des couches à *Pyrotherium*. *Boletín del Instituto Geográfico Argentino*, **15**, 501–660.

———. 1894*b*. Sur les ongulés fossiles de l'Argentine. *Revista del Jardín Zoológico de Buenos Ayres*, **Tomo II**, 193–303.

———. 1894*c*. Enumération synoptique des espèces de mammifères fossiles des formations éocènes de Patagonie. *Boletín de la Academia de Ciencias de Córdoba*, **13**, 1–196.

———. 1897. Mammiféres crétacés de l'Argentine (Deuxième contribution à la connaissance de la fauna mammalogique de couches à *Pyrotherium*). *Boletín del Instituto Geográfico Argentino*, **18**, 406–521.

———. 1901. Notices préliminaires sur des ongulés nouveaux des terrains crétacés de Patagonie. *Boletín de la Academia de Ciencias de Córdoba*, **16**, 349–426.

———. 1902*a*. Première contribution à la connaissance de la faune mammalogique des couches à *Colpodon*. *Boletín de la Academia Nacional de Ciencias en Córdoba*, **17**, 71–138.

———. 1902*b*. Notices préliminaires sur des mammifères nouveaux des terrains Creétacés de Patagonie. *Boletín de la Academia Nacional de Ciencias en Córdoba*, **17**, 5–70.

———. 1902*c*. Línea filogenética de los proboscídeos. *Anales del Museo Nacional de Buenos Aires*, **3**, 19–43.

———. 1904*a*. Nuevas especies de mamíferos cretáceos y terciarios de la República Argentina. *Anales de la Sociedad Científica Argentina*, **56**–**58**, 1–142.

———. 1904*b*. Recherches de morphologic phylogénétique sur les molaires supérieures des ongulés. *Anales del Museo Nacional de Buenos Aires*, **3**, 1–541.

———. 1906. Les formations sedimentaires du cretace superieur et du tertiaire de Patagonie avec un parallele entre leurs faunes mammalogiques et celles de l'ancien continent. *Anales del Museo Nacional de Buenos Aires*, **15**, 1–568.

AMENÁBAR, C. R., MONTES, M., NOZAL, F. and SANTILLANA, S. 2019. Dinoflagellate cysts of the la Meseta Formation (middle to late Eocene), Antarctic Peninsula: Implications for biostratigraphy, palaeoceanography and palaeoenvironment. *Geological Magazine*, **157**, 351–366.

ANAYA, F. and MACFADDEN, B. J. 1995. Pliocene Mammals from Inchasi, Bolivia: the endemic fauna just before the great American interchange. *Bulletin of the Florida Museum of Natural History*, **39**, 87–140.

ANTOINE, P.-O., BILLET, G., SALAS-GISMONDI, R., TEJADA LARA, J., BABY, P., BRUSSET, S., ESPURT, N., ANTOINE, O. and SALAS-GISMONDI, R. 2015. A New Carodnia Simpson, 1935 (Mammalia, Xenungulata) from the Early Eocene of Northwestern Peru and a Phylogeny of Xenungulates at Species Level. *Journal of Mammalian Evolution*, **22**, 129–140.

ANTOINE, P. O., MARIVAUX, L., CROFT, D. A., BILLET, G., GANERØD, M., JARAMILLO, C., MARTIN, T., ORLIAC, M. J., TEJADA, J., ALTAMIRANO, A. J., DURANTHON, F., FANJAT, G., ROUSSE, S. and GISMONDI, R. S. 2012. Middle Eocene rodents from Peruvian Amazonia reveal the pattern and timing of caviomorph origins and biogeography. *Proceedings of the Royal Society B: Biological Sciences*, **279**, 1319–1326.

ANTÓN, S. C. and JOSH SNODGRASS, J. 2012. Origins and evolution of genus *Homo*: New perspectives. *Current Anthropology*, **53**, S479–S496.

ARAMAYO, S. A. and DE BIANCO, T. M. 2009. Late Quaternary palaeoichnological sites from the Southern Atlantic coast of Buenos Aires Province, Argentina: mammal, bird and hominid evidence. *Ichnos*, **16**, 25–32.

ARAMAYO, S. A., DE BIANCO, T. M., BASTIANELLI, N. V and MELCHOR, R. N. 2015. Pehuen Co: Updated taxonomic review of a late Pleistocene ichnological site in Argentina. *Palaeogeography, Palaeoclimatology, Palaeoecology*, **439**, 144–165.

ARCHIBALD, J. D. 1998. Archaic ungulates ("Condylarthra"), Volume 1. In Janis C. M., Scot

K. M. & Jacobs L. L. (eds), Evolution of Tertiary Mammals of North America. Terrestrial Carnivores, Ungulates, and Ungulate-like Mammals. Cambridge University Press. 292–331.

——— and DEUTSCHMAN, D. H. 2001. Quantitative Analysis of the Timing of the Origin and Diversification of Extant Placental Orders. *Journal of Mammalian Evolution*, **8**, 107–124.

ARCHIBALD, J. D., ZHANG, Y., HARPER, T. and CIFELLI, R. L. 2011. Protungulatum, Confirmed Cretaceous Occurrence of an Otherwise Paleocene Eutherian (Placental?) Mammal. *Journal of Mammalian Evolution*, **18**, 153–161.

ARGOT, C. 2001. Functional-adaptive anatomy of the forelimb in the Didelphidae, and the paleobiology of the Paleocene marsupials *Mayulestes ferox* and *Pucadelphys andinus*. *Journal of Morphology*, **247**, 51–79.

———. 2004. Functional-adaptive features and palaeobiologic implications of the postcranial skeleton of the late Miocene sabretooth borhyaenoid *Thylacosmilus atrox* (Metatheria). *Alcheringa*, **28**, 229–266.

———. 2013. Postcranial analysis of a carnivoran-like archaic ungulate: the case of *Arctocyon primaevus* (Arctocyonidae, Mammalia) from the Late Paleocene of France. *Journal of Mammalian Evolution*, **20**, 83–114.

ARGUE, D., GROVES, C. P., LEE, M. S. Y. and JUNGERS, W. L. 2017. The affinities of *Homo floresiensis* based on phylogenetic analyses of cranial, dental, and postcranial characters. *Journal of Human Evolution*, **107**, 107–133.

ARGUE, D., MORWOOD, M. J., SUTIKNA, T., JATMIKO and SAPTOMO, E. W. 2009. *Homo floresiensis*: a cladistic analysis. *Journal of Human Evolution*, **57**, 623–639.

AURICH, C., BRAGULLA, H., BUDRAS, K.-D., FORSTENPOINTNER, G., HAGEN, J., KNEISSL, S., KÖNIG, H. E., LATORRE, R., LIEBICH, H.-G., LUDEWIG, E., MAIERL, J., MÜLLING, C., PAULSEN, P., PEHAM, C., PÉREZ, W., REESE, S., RUBERTE, J., SCHÖPPER, H., SEEGER, J., SORA, M.-C., SÓTONYI, P., WEISSENGRUBER, G. and WITTER, K. 2020. *Veterinary Anatomy of Domestic Animals*. *In* KÖNIG, H. E. and LIEBICH, H.-G. (eds.) Georg Thieme Verlag, Stuttgart · New York.

AVILLA, L. S. and MOTHÉ, D. 2021. Out of Africa: A New Afrotheria Lineage Rises From Extinct South American Mammals. *Frontiers in Ecology and Evolution*, **9**, 1–14.

BANKS, W. E., D'ERRICO, F., PETERSON, A. T., KAGEYAMA, M., SIMA, A. and SÁNCHEZ-GOÑI, M. F. 2008. Neanderthal extinction by competitive exclusion. *PLoS ONE*, **3**, e3972.

BASTOS, A. C. F. and BERGQVIST, L. P. 2007. A postura locomotora de *Protolipterna ellipsodontoides* Cifelli, 1983 (Mammalia: Litopterna: Protolipternidae) da Bacia de São José de Itaboraí, Rio de Janeiro (Paleoceno superior). *Anuário do Instituto de Geociências*, **30**, 58–66.

BAUZÁ, N., GELFO, J. N. and LÓPEZ, G. M. 2020. Phylogenetics Implications of Dental Characters in Henricosborniidae (Mammalia, Notoungulata). *Ameghiniana*, **57**, 90–102.

BAYONA, G., MONTENEGRO, O., CARDONA, A., JARAMILLO, C., LAMUS, F., MORÓN, S., QUIROZ, L., RUIZ, M., VALENCIA, V., PARRA, M. and STOCKLI, D. 2010. Estratigrafía, procedencia, subsidencia y exhumación de las unidades Paleógenas en el Sinclinal de Usme, sur de la zona axial de la Cordillera Oriental. *Geología Colombiana*, **35**, 5–35.

BECK, R. M. D., VRIES, D. De, JANIAK, M. C., GOODHEAD, I. B. and BOUBLI, J. P. 2023. Total evidence phylogeny of platyrrhine primates and a comparison of undated and tip-dating approaches. *Journal of Human Evolution*, **174**, 103293.

BEGUN, D. R. 2010. Miocene Hominids and the Origins of the African Apes and Humans. *Annual Review of Anthropology*, **39**, 67–84.

BEGUN, D. R., NARGOLWALLA, M. C. and KORDOS, L. 2012. European Miocene Hominids and the Origin of the African Ape and Human Clade. *Evolutionary Anthropology*, **21**, 10–23.

BEILINSON, E., GASPARINI, G. M., TOMASSINI, R. L., ZÁRATE, M. A., DESCHAMPS, C. M., BARENDREGT, R. W. and RABASSA, J. 2017. The Quequén Salado river basin: Geology and biochronostratigraphy of the Mio-Pliocene boundary in the southern Pampean plain, Argentina. *Journal of South American Earth Sciences*, **76**, 362–374.

BENEVENTO, G. L., BENSON, R. B. J. and FRIEDMAN, M. 2019. Patterns of mammalian jaw ecomorphological disparity during the Mesozoic/Cenozoic transition. *Proceedings of*

*the Royal Society B: Biological Sciences*, **286**, 20190347.

BENTON, M. J. 1999. Early origins of modern birds and mammals: Molecules vs. morphology. *BioEssays*, **21**, 1043–1051.

BERG, C. 1899. Substitución de nombres genéricos. III. *Comunicaciones del Museo Nacional de Buenos Aires*, **1**, 77–80.

BERGER, L. R., HAWKS, J., DIRKS, P. H. G. M., ELLIOTT, M. and ROBERTS, E. M. 2017. *Homo naledi* and Pleistocene hominin evolution in subequatorial Africa. *ELife*, **6**, e24234.

BERGER, L. R., DE RUITER, D. J., CHURCHILL, S. E., SCHMID, P., CARLSON, K. J., DIRKS, P. H. G. M. and KIBII, J. M. 2010. *Australopithecus sediba*: A New Species of Homo-Like Australopith from South Africa. *Science*, **328**, 195–204.

BERGQVIST, L. P. 1996. Reasociaçao de pós-crânio às espécies de ungulados da Bacia de S.J. Itaboraí (Paleoceno), Estado do Rio de Janeiro, e Filogenia dos "Condylarthra," e ungulados Sul-Americanos com base no póscranio.Ph.D. Dissertation, Universidade Federal do Rio Grande do Sul, 1–400pp.

BERGQVIST, L. P. 2008. Postcranial skeleton of the upper Paleocene of Itaboraí Basin, Brazil. *In* SARGIS, E. J. and DAGOSTO, M. (eds.) *Mammalian Evolutionary Morphology: A Tribute to Frederik S. Szalay.*, Springer-Verlag, New York, 107–133 pp.

BERGQVIST, L. P. 2010. Deciduous Premolars of Paleocene Litopterns of São José De Itaboraí Basin, Rio De Janeiro, Brasil. *Journal of Paleontology*, **84**, 858–867.

——— and KOENIGSWALD, W. von. 2017. The dentition of Carodnia vieirai (Mammalia: Xenungulata): enamel microstructure and mastication pattern. *Palaeontologia Electronica*, **20.2.30A**, 1–15.

BERTHAUME, M. A., DELEZENE, L. K. and KUPCZIK, K. 2018. Dental topography and the diet of *Homo naledi*. *Journal of Human Evolution*, **118**, 14–26.

BILLET, G. 2010. New Observations on the Skull of *Pyrotherium* (Pyrotheria, Mammalia) and New Phylogenetic Hypotheses on South American Ungulates. *Journal of Mammalian Evolution*, **17**, 21–59.

———, ORLIAC, M., ANTOINE, P. O. and JARAMILLO, C. 2010. New observations and reinterpretation on the enigmatic taxon *Colombitherium* (?Pyrotheria, Mammalia) from

Colombia. *Palaeontology*, **53**, 319–325.

———, DE MUIZON, C., SCHELLHORN, R., RUF, I., LADEVÈZE, S. and BERGQVIST, L. 2015. Petrosal and inner ear anatomy and allometry amongst specimens referred to Litopterna (Placentalia). *Zoological Journal of the Linnean Society*, **173**, 956–987.

BININDA-EMONDS, O. R. P., CARDILLO, M., JONES, K. E., MACPHEE, R. D. E., BECK, R. M. D., GRENYER, R., PRICE, S. A., VOS, R. A., GITTLEMAN, J. L. and PURVIS, A. 2007. The delayed rise of present-day mammals. *Nature*, **446**, 507–12.

BLANCO, R. E., JONES, W. W., YORIO, L. and RINDERKNECHT, A. 2021. *Macrauchenia patachonica* Owen, 1838: Limb bones morphology, locomotory biomechanics, and paleobiological inferences. *Geobios*, **68**, 61–70.

BOBE, R. and LEAKEY, M. G. 2009. Ecology of Plio-Pleistocene Mammals in the Omo—Turkana Basin and the Emergence of Homo. *In* GRINE, F. E., FLEAGLE, J. G. and LEAKEY, R. E. (eds.) *The First Humans: Origins of the Genus Homo*, Dordrecht: Springer, 173–184 pp.

——— and CARVALHO, S. 2019. Hominin diversity and high environmental variability in the Okote Member, Koobi Fora Formation, Kenya. *Journal of Human Evolution*, **126**, 91–105.

BOIVIN, N. L., ZEDER, M. A., FULLER, D. Q., CROWTHER, A., LARSON, G., ERLANDSON, J. M., DENHAMI, T. and PETRAGLIA, M. D. 2016. Ecological consequences of human niche construction: Examining long-term anthropogenic shaping of global species distributions. *Proceedings of the National Academy of Sciences of the United States of America*, **113**, 6388–6396.

BONAPARTE, J. F. and MORALES, J. 1997. Un primitivo Notonychopidae (Litopterna) del Paleoceno inferior de Punta Peligro, Chubut, Argentina. *Estudios Geológicos*, **274**, 263–274.

———, VAN VALEN, L. and KRAMARZ, A. G. 1993. La fauna local de Punta Peligro, Paleoceno inferior, de la provincia del Chubut, Patagonia, Argentina. *Evolutionary Monographs*, **14**, 3–61.

BOND, M. 1988. Consideraciones sobre la morfología de los molariformes inferiores de los Notoungulata. *Resúmenes de las V Jornadas Argentinas de Paleontología de*

*Vertebrados*, 76–77.

———. 1999. Quaternary native ungulates of southern South America. A synthesis. *In* RABASSA, J. and SALEMME, M. (eds.) *Quaternary of South America and Antarctic Península, 12*, Rotterdam, 177–205 pp.

——— and VUCETICH, M. G. 1983. *Indalecia grandensis* gen. et sp. nov. del Eoceno temprano del noroeste argentino, tipo de una nueva subfamilia de los Adianthidae. *Revista de la Asociación Geológica Argentina*, **38**, 107–117.

——— and LÓPEZ, G. M. 1995. Los Macraucheniidae (Mammalia, Litopterna) de la Formación Arroyo Chasicó (Partido de Vallarino, Pcia. de Buenos Aires). *Actas, IV Jornadas Geológicas y Geofísicas Bonaerenses*, **1**, 23–27.

———, CERDEÑO, E. and LOPEZ, G. 1995. Los ungulados nativos de América del Sur. *In* ALBERDI, M., LEONE, G. and TONNI, E. (eds.) *Evolución Biológica y Climática de La Región Pampeana Durante Los Últimos Cinco Millones de Años. Un Ensayo de Correlación Con El Mediterráeno Occidental*, Museo Nacional de Ciencias Naturales, Madrid, 260–275 pp.

BOND, M., REGUERO, M. A., VIZCAÍNO, S. F. and MARENSSI, S. A. 2006. A new 'South American ungulate' (Mammalia: Litopterna) from the Eocene of the Antarctic Peninsula. *In* FRANCIS, J. E., PIRRIE, D. and CRAME, J. A. (eds.) *Cretaceous-Tertiary High-Latitude Palaeoenvironments, James Ross Basin, Antarctica. Geological Society of London, London, Special Publications 258*, 163–176 pp.

BOND, M., KRAMARZ, A., MACPHEE, R. D. E. and REGUERO, M. 2011. A New Astrapothere (Mammalia, Meridiungulata) from La Meseta Formation, Seymour (Marambio) Island, and a Reassessment of Previous Records of Antarctic Astrapotheres. *American Museum Novitates*, **3718**, 1–16.

———, PASCUAL, R., REGUERO, M. A., SANTILLANA, S. and MARENSSI, S. A. 1989. Los primeros "ungulados" extinguidos sudamericanos de la Antártida. *Ameghiniana*, **26**, 240.

———, REGUERO, M. A., VIZCANO, S. F., MARENSSI, S. A. and ORTIZ-JAUREGUIZAR, E. 2009. *Notiolofos*, a replacement name for *Notolophus* Bond, Reguero, Vizcaíno and Marenssi, 2006, a preoccupied name. *Journal of Vertebrate*

*Paleontology*, **29**, 979.

———, TEJEDOR, M. F., CAMPBELL, K. E., CHORNOGUBSKY, L., NOVO, N. and GOIN, F. 2015. Eocene primates of South America and the African origins of New World monkeys. *Nature*, **520**, 538–541.

BORDAS, A. F. 1936. Un nuevo mamífero del *Colpodon* de Gaiman (*Proheptaconus trelewense*, gen.et sp. nov.). *Physis*, **12**, 110–112.

———. 1939. Diagnosis sobre algunos mamíferos de las capas con *Colpodon*, del valle del río Chubut (República Argentina). *Physis*, **14**, 413–433.

BRAUN, D. R., ALDEIAS, V., ARCHER, W., ARROWSMITH, J. R., BARAKI, N., CAMPISANO, C. J., DEINO, A. L., DIMAGGIO, E. N., DUPONT-NIVET, G., ENGDA, B., FEARY, D. A., GARELLO, D. I., KERFELEW, Z., MCPHERRON, S. P., PATTERSON, D. B., REEVES, J. S., THOMPSON, J. C. and REED, K. E. 2019. Earliest known Oldowan artifacts at >2.58 Ma from Ledi-Geraru, Ethiopia, highlight early technological diversity. *Proceedings of the National Academy of Sciences of the United States of America*, **116**, 11712–11717.

BROCKLEHURST, N. and BENEVENTO, G. L. 2020. Dental characters used in phylogenetic analyses of mammals show higher rates of evolution, but not reduced independence. *PeerJ*, **8**, e8744.

——— and HARIDY, Y. 2021. Do Meristic Characters Used in Phylogenetic Analysis Evolve in an Ordered Manner? *Systematic biology*, **70**, 707–718.

BROMHAM, L., PHILLIPS, M. J. and PENNY, D. 1999. Growing up with dinosaurs: Molecular dates and the mammalian radiation. *Trends in Ecology and Evolution*, **14**, 113–118.

———, DUCHÊNE, S., HUA, X., RITCHIE, A. M., DUCHÊNE, D. A. and HO, S. Y. W. 2017. Bayesian molecular dating: opening up the black box. *Biological Reviews*, **93**, 1165–1191.

BROWN, B., BROWN, F. H. and WALKER, A. 2001. New hominids from the Lake Turkana Basin, Kenya. *Journal of Human Evolution*, **41**, 29–44.

BROWN, P., SUTIKNA, T., MORWOOD, M. J., SOEJONO, R. P., JATMIKO, SAPTOMO, E. W. and DUE, R. A. 2004. A new small-bodied hominin from the Late Pleistocene of

Flores, Indonesia. *Nature*, **431**, 1055–1061.

BRUMM, A., AZIZ, F., VAN DEN BERGH, G. D., MORWOOD, M. J., MOORE, M. W., KURNIAWAN, I., HOBBS, D. R. and FULLAGAR, R. 2006. Early stone technology on Flores and its implications for *Homo floresiensis*. *Nature*, **441**, 624–628.

BUCKLEY, M. 2015. Ancient collagen reveals evolutionary history of the endemic South American 'ungulates'. *Proceedings of the Royal Society B: Biological Sciences*, **282**, 20142671.

BURGIN, C. J., COLELLA, J. P., KAHN, P. L. and UPHAM, N. S. 2018. How many species of mammals are there? *Journal of Mammalogy*, **99**, 1–14.

BURMEISTER, G. 1864*a*. Descripción de la *Macrauchenia patachonica*. *In Anales Del Museo Público de Buenos Aires Para Dar a Conocer Los Objetos de Historia Natural Nuevos o Poco Conocidos Conservados En Este Establecimiento. Tomo I*, Vol. 1. Imprenta de 'La Tribuna', Buenos Aires, 32–66 pp.

———. 1864*b*. Beschreibung der Macrauchenia patachonica Owen (Opisthorhinus falkoneri Brav.) nach A. Bravard's Zeichnungen und den im Museo zu Buenos Aires vorhandenen Resten entworfen. *Abhandlung der Naturforscher Gesellschaft zu Halle*, **1**, 75–112.

CABRERA, Á. and KRAGLIEVICH, L. 1931. Diagnosis previas de los ungulados fósiles del Arroyo Chasicó. *Notas Preliminares del Museo de La Plata*, **Tomo 1**, 107–113.

CAIŘO, O. 2011. External measures of cognition. *Frontiers in Human Neuroscience*, **5**, 108.

CAMERON, D., PATNAIK, R. and SAHNI, A. 2004. The phylogenetic significance of the middle pleistocene Narmada hominin cranium from central India. *International Journal of Osteoarchaeology*, **14**, 419–447.

CAMERON, D. W. and GROVES, C. P. 2004. *Bones, Stones and Molecules: Out of Africa and Human Origins*. Elsevier, San Diego.

CAMPBELL, B. 1936. The comparative myology of the forelimb of the hippopotamus, pig and tapir. *American Journal of Anatomy*, **59**, 201–247.

CAMPBELL, K. E. J., FRAILEY, C. D., PITTMAN, L. R. and ROMERO-PITTMAN, L. 2000. The late Miocene gomphothere *Amahuacatherium peruvium* (Proboscidea: Gomphotheriidae) from Amazonian Peru: implications for the Great American Faunal

Interchange. *Boletín Estudios Regionales, Instituto Geológico, Minero y Metalúrgico*, **23**, 1–152.

CARMODY, R. N., WEINTRAUB, G. S. and WRANGHAM, R. W. 2011. Energetic consequences of thermal and nonthermal food processing. *Proceedings of the National Academy of Sciences of the United States of America*, **108**, 19199–19203.

CARRANO, M. T. 1997. Morphological indicators of foot posture in mammals: A statistical and biomechanical analysis. *Zoological Journal of the Linnean Society*, **121**, 77–104.

CARREÑO, C. 2012. Ambiente deposicional de la Formación Bahía Inglesa (Neógeno) en la Cuenca de Caldera, III Región, Chile.'Dissertation', Universidad de Chile, Facultad de Ciencias Físicas y Matemáticas. 98 pp., 1–98pp.

CARRILLO, J. D. and ASHER, R. J. 2017. An exceptionally well-preserved skeleton of Thomashuxleya externa (Mammalia, Notoungulata), from the Eocene of Patagonia, Argentina. *Palaeontologia Electronica*, **20.2.34A**, 1–33.

CARROLL, R. L. 1997. Patterns and processes of vertebrate evolution. Cambridge University Press, Cambridge. .

CARTELLE, C. and LESSA, G. 1988. Descrição de um gênero e espécie de Macraucheniidae (Mammalia, Litopterna) do Pleistoceno final do Brasil. *Paula-Coutiana*, **3**, 3–26.

CASSINI, G. H., CERDEÑO, E., VILLAFAÑE, A. L. and MUÑOZ, N. A. 2012. Paleobiology of Santacrucian native ungulates (Meridiungulata: Astrapotheria, Litopterna and Notoungulata). *In* VIZCAÍNO, S. F., KAY, R. F. and BARGO, M. S. (eds.) *Early Miocene Paleobiology in Patagonia*, Cambridge University Press, New York, 243–286 pp.

CASTIGLIONE, S., SERIO, C., MONDANARO, A., MELCHIONNA, M., CAROTENUTO, F., DI FEBBRARO, M., PROFICO, A., TAMAGNINI, D. and RAIA, P. 2020. Ancestral State Estimation with Phylogenetic Ridge Regression. *Evolutionary Biology*, **47**, 220–232.

CERDEÑO, E. and VERA, B. 2015. A new Leontiniidae (Notoungulata) from the Late Oligocene beds of Mendoza Province, Argentina. *Journal of Systematic Palaeontology*, **13**, 943–962.

CHANG, M. L. 2005. Neandertal origins, Middle Pleistocene systematics, and tests of current

taxonomic and phylogenetic hypotheses. Ph.D. Dissertation, University of Pennsylvania. .

CHATTERJEE, H. J., HO, S. Y., BARNES, I. and GROVES, C. 2009. Estimating the phylogeny and divergence times of primates using a supermatrix approach. *BMC Evolutionary Biology*, **9**.

CHIMENTO, N. R. and AGNOLIN, F. L. 2020. Phylogenetic tree of Litopterna and Perissodactyla indicates a complex early history of hoofed mammals. *Scientific Reports*, **10**, 13280.

CIFELLI, R. L. 1983*a*. The origin and affinities of the South American Condylarthra and early Tertiary Litopterna (Mammalia). *American Museum Novitates*, **2772**, 1–49.

———. 1983*b*. Eutherian tarsals from the late Paleocene of Brazil. *American Museum Novitates*, **2761**, 1–31.

———. 1985. South American ungulate evolution and extinction. *In* STEHLI, F. G. and WEBB, S. D. (eds.) *The Great American Biotic Interchange*, Springer US, 249–266 pp.

———. 1991. A new Adianthid Litoptern (Mammalia) from the Miocene of Chile. *Revista Chilena de Historia Natural*, **64**, 119–125.

CIFELLI, R. L. 1993. The phylogeny of the native South American ungulates. *In* SZALAY, F. S., NOVACEK, M. J. and MCKENNA, M. C. (eds.) *Mammal Phylogeny: Placentals*, Springer-Verlag, New York, 195–216 pp.

CIFELLI, R. L. and SORIA, M. F. 1983*a*. Systematics of the Adianthidae (Litopterna , Mammalia). *American Museum Novitates*, **2771**, 1–25.

——— and ———. 1983*b*. Notes on Deseadan Macraucheniidae. *Ameghiniana*, **20**, 141–153.

——— and GUERRERO DÍAZ, J. 1997. Litopterns. *In* KAY, R. F., MADDEN, R. H., CIFELLI, R. L. and FLYNN, J. J. (eds.) *Vertebrate Paleontology in the Neotropics: The Miocene Fauna of La Venta, Colombia*, Smithsonian Institution Press, Washington and London, 289–302 pp.

——— and VILLARROEL, C. 1997. Paleobiology and affinities of Megadolodus. *In Vertebrate Paleontology in the Neotropics: The Miocene Fauna of La Venta, Colombia, ed. RF Kay, RH Madden, RL Cifelli, JJ Flynn*, 265–288.

——— and ORTIZ-JAUREGUIZAR, E. 2014. Depaulacoutoia , a replacement name for Paulacoutoia Cifelli, 1983, a preoccupied name. *Journal of Vertebrate Paleontology*, **34**, 730–730.

CIFELLI, R. L., SCHAFF, C. R. and MCKENNA, M. C. 1989. The relationships of the Arctostylopidae ( Mammalia ): new data and interpretation. *Bulletin of The Museum of Comparative Zoology*, **152**, 1–44.

———, EBERLE, J. J., LOFGREN, D. L., LILLEGRAVEN, J. A. and CLEMENS, W. A. 2004. Mammalian biochronology of the latest Cretaceous. *In* WOODBURNE, M. O. (ed.) *Late Cretaceous and Cenozoic Mammals of North America*, Columbia University Press, New York, 21–42 pp.

CIONE, A. L. and TONNI, E. P. 1999. Biostratigraphy and chronological scale of upper-most Cenozoic in the Pampean Area, Argentina. *Quaternary of South America and Antarctic Peninsula*, 23–51.

CIONE, A. L. and TONNI, E. P. 2001. Correlation of pliocene to holocene southern South American and European vertebrate-bearing units. *Bollettino della Societa Paleontologica Italiana*, **40**, 167–173.

CIONE, A. L. and TONNI, E. P. 2005. Bioestratigrafía basada en mamíferos del Cenozoico superior de la provincia de Buenos Aires, Argentina. *In Geología y Recursos Minerales de La Provincia de Buenos Aires. Relatorio Del XVI Congreso Geológico Argentino*, 183–200 pp.

CIONE, A. L., GASPARINI, G. M. and SOIBELZON, E. 2015. *The Great American Biotic Interchange: a South American Perspective*. Dordrecht : Springer.

COLWYN, D. A. and HREN, M. T. 2019. An abrupt decrease in Southern Hemisphere terrestrial temperature during the Eocene–Oligocene transition. *Earth and Planetary Science Letters*, **512**, 227–235.

CONSTANTINESCU, G. M., HABEL, R. E., HILLEBRAND, A., SACK, W. O., SCHALLER, O., SIMOENS, P. and VOS, N. R. de. 2018. *Illustrated Veterinary Anatomical Nomenclature*. *In* CONSTANTINESCU, G. M. (ed.) Georg Thieme Verlag, Stuttgart.

COPE, E. D. 1881*a*. A new type of Perissodactyla. *The American Naturalist*, **15**, 1017–1023.

———. 1881*b*. On some Mammalia of the lowest Eocene beds of New Mexico. *Proceedings of the American Philosophical Society*, **19**, 484–495.

———. 1882*a*. Some new forms from the Puerco Eocene. *The American Naturalist*, **16**, 833–834.

———. 1882*b*. Synopsis of the Vertebrata of the Puerco Eocene epoch. *Proceedings of the American Philosophical Society*, **20**, 461–471.

———. 1884. The Condylarthra. *American Naturalist*, **18**, 790–805.

———. 1888. Synopsis of the vertebrate fauna of the Puerco series. *Transactions of the American Philosophical Society*, **16**, 298–361.

CORONA, A., BADÍN, A. C., PEREA, D., UBILLA, M. and SCHMIDT, G. I. 2020. A new genus and species and additional reports of the South American native ungulates Proterotheriidae (Mammalia, Litopterna) in the Late Miocene of Uruguay. *Journal of South American Earth Sciences*, **102**, 102646.

CROFT, D. A. and LÓPEZ, G. M. 2020. Gondwanan Perspectives: Evolution, Biogeography, and Paleoecology of the Native Ungulates of South America. *Ameghiniana*, **57**, 71–79.

———, FLYNN, J. J. and WYSS, A. R. 2004. Notoungulata and Litopterna of the Early Miocene Chucal fauna, northern Chile. *Fieldiana, Geology*, **50**, 1–52.

CROFT, D. A., GELFO, J. N. and LÓPEZ, G. M. 2020. Splendid Innovation: The Extinct South American Native Ungulates. *Annual Reviews*, **48**, 11.1-11.32.

CROFT, D. A., CARLINI, A. A., CIANCIO, M. R., BRANDONI, D., DREW, N. E., ENGELMAN, R. K. and ANAYA, F. 2016. New mammal faunal data from Cerdas, Bolivia, a middle-latitude Neotropical site that chronicles the end of the Middle Miocene Climatic Optimum in South America. *Journal of Vertebrate Paleontology*, **36**.

CROFT, D. a, FLYNN, J. J. and WYSS, A. R. 2008. The Tinguiririca fauna of Chile and the early stages of "modernization" of South American mammal faunas. *Arquivos do Museu Nacional*, **1**, 191–211.

CROMPTON, R. H., VEREECKE, E. E. and THORPE, S. K. S. 2008. Locomotion and posture from the common hominoid ancestor to fully modern hominins, with special reference to the last common panin/hominin ancestor. *Journal of Anatomy*, **212**, 501–543.

CUITIÑO, J. I., GUTSTEIN, C. S., UGALDE, R. and MUÑOZ, F. 2021. Variaciones de paleoambientes marinos de alta bioproductividad: el caso de la Formación Bahía Inglesa, Neógeno de Atacama, Chile. *Actas XVII Reunión Argentina de Sedimentología*, 131.

———, FERNICOLA, J. C., KOHN, M. J., TRAYLER, R., NAIPAUER, M., BARGO, M. S., KAY, R. F. and VIZCAÍNO, S. F. 2016. U-Pb geochronology of the Santa Cruz Formation (early Miocene) at the Río Bote and Río Santa Cruz (southernmost Patagonia, Argentina): Implications for the correlation of fossil vertebrate localities. *Journal of South American Earth Sciences*, **70**, 198–210.

DARWIN, C. 1839. Journal of Researches into the Geology and Natural History of the Various Countries Visited by H.M.S. Beagle under the Command of Captain Fitzroy, R.N. from 1832 to 1836 (London, Colburn). .

———. 1845. *Journal of Researches into the Natural History and Geology of the Countries Visited during the Voyage of H.M.S. Beagle Round the World, under the Command of Capt. Fitz Roy*. JOHN MURRAY, ALBEMARLE STREET, London.

DAVIES, T. W., BELL, M. A., GOSWAMI, A. and HALLIDAY, T. J. D. 2017. Completeness of the eutherian mammal fossil record and implications for reconstructing mammal evolution through the Cretaceous/Paleogene mass extinction. *Paleobiology*, **43**, 521–536.

DELFINO, M., PIRAS, P. and SMITH, T. 2005. Anatomy and phylogeny of the gavialoid crocodylian *Eosuchus lerichei* from the Paleocene of Europe. *Acta Palaeontologica Polonica*, **50**, 565–580.

DELIGNETTE-MULLER, M. L. and DUTANG, C. 2004. fitdistrplus: an R package for fitting distributions. *Journal of statistical software*, **64**, 1–34.

DEMBO, M., RADOVČIĆ, D., GARVIN, H. M., LAIRD, M. F., SCHROEDER, L., SCOTT, J. E., BROPHY, J., ACKERMANN, R. R., MUSIBA, C. M., DE RUITER, D. J., MOOERS, A. and COLLARD, M. 2016. The evolutionary relationships and age of *Homo naledi*: An assessment using dated Bayesian phylogenetic methods. *Journal of Human Evolution*, **97**, 17–26.

———, MATZKE, N. J., MOOERS, A. and COLLARD, M. 2015. Bayesian analysis of a morphological supermatrix sheds light on controversial fossil hominin relationships. *Proceedings of the Royal Society B: Biological Sciences*, **282**, 20150943.

DEMENOCAL, P. B. 2004. African climate change and faunal evolution during the Pliocene-Pleistocene. *Earth and Planetary Science Letters*, **220**, 3–24.

———. 2011. Climate and human evolution. *Science*, **331**, 540–542.

DENNELL, R. W., LOUYS, J., O'REGAN, H. J. and WILKINSON, D. M. 2014. The origins and persistence of *Homo floresiensis* on Flores: Biogeographical and ecological perspectives. *Quaternary Science Reviews*, **96**, 98–107.

DENOIX, J.-M. 2019. *Essentials in Clinical Anatomy of the Equine Locomotor System*. Taylor & Francis Group.

DESCHAMPS, C. M., VUCETICH, M. G., MONTALVO, C. I. and ZÁRATE, M. A. 2013. Capybaras (Rodentia, Hydrochoeridae, Hydrochoerinae) and their bearing in the calibration of the late Miocene-Pliocene sequences of South America. *Journal of South American Earth Sciences*, **48**, 145–158.

DINIZ-FILHO, J. A. F. and RAIA, P. 2017. Island rule, quantitative genetics and brain-body size evolution in *Homo floresiensis*. *Proceedings of the Royal Society B: Biological Sciences*, **284**, 20171065.

———, JARDIM, L., MONDANARO, A. and RAIA, P. 2019. Multiple Components of Phylogenetic Non-stationarity in the Evolution of Brain Size in Fossil Hominins. *Evolutionary Biology*, **46**, 47–59.

DIRKS, P. H., ROBERTS, E. M., HILBERT-WOLF, H., KRAMERS, J. D., HAWKS, J., DOSSETO, A., DUVAL, M., ELLIOTT, M., EVANS, M., GRUN, R., HELLSTROM, J., HERRIES, A. I., JOANNES-BOYAU, R., MAKHUBELA, T. V, PLACZEK, C. J., ROBBINS, J., SPANDLER, C., WIERSMA, J., WOODHEAD, J. and BERGER, L. R. 2017. The age of *Homo naledi* and associated sediments in the Rising Star Cave, South Africa. *ELife*, **6**, e24231.

DONOGHUE, P. C. J. and BENTON, M. J. 2007. Rocks and clocks: calibrating the Tree of Life using fossils and molecules. *Trends in Ecology and Evolution*, **22**, 424–431.

——— and YANG, Z. 2016. The evolution of methods for establishing evolutionary timescales. *Philosophical Transactions of the Royal Society B: Biological Sciences*, **371**, 20160020.

DOUGLAS, P. M. J., AFFEK, H. P., IVANY, L. C., HOUBEN, A. J. P., SIJP, W. P., SLUIJS,

A., SCHOUTEN, S. and PAGANI, M. 2014. Pronounced zonal heterogeneity in Eocene southern high-latitude sea surface temperatures. *Proceedings of the National Academy of Sciences of the United States of America*, **111**, 6582–6587.

DOWNEY, G. and LENDE, D. H. 2012. Evolution and the brain. *In* LENNDE, D. H. and DOWNEY, G. (eds.) *The Encultured Brain: An Introduction to Neuroanthropology*, MIT Press: Cambridge, 103–138 pp.

DOZO, M. T. and VERA, B. 2010. First skull and associated postcranial bones of Macraucheniidae (Mammalia, Litopterna) from the Deseadan SALMA (Late Oligocene) of Cabeza Blanca (Chubut, Argentina). *Journal of Vertebrate Paleontology*, **30**, 1818–1826.

DU, A. and ALEMSEGED, Z. 2019. Temporal evidence shows *Australopithecus sediba* is unlikely to be the ancestor of Homo. *Science Advances*, **5**, eaav9038.

———, ROWAN, J., WANG, S. C., WOOD, B. A. and ALEMSEGED, Z. 2020. Statistical estimates of hominin origination and extinction dates: A case study examining the *Australopithecus anamensis–afarensis* lineage. *Journal of Human Evolution*, **138**.

DUNN, R. E., MADDEN, R. H., KOHN, M. J., SCHMITZ, M. D., STRÖMBERG, C. A. E., CARLINI, A. A., RÉ, G. H. and CROWLEY, J. 2013. A new chronology for middle Eocene-early Miocene South American Land Mammal Ages. *Bulletin of the Geological Society of America*, **125**, 539–555.

EIZIRIK, E. 2001. Molecular Dating and Biogeography of the Early Placental Mammal Radiation. *Journal of Heredity*, **92**, 212–219.

ENGELMAN, R. K. 2022. Occipital condyle width (OCW) is a highly accurate predictor of body mass in therian mammals. *BMC Biology*, **20:37**, 1–44.

ERCOLI, M. D., PREVOSTI, F. J. and ÁLVAREZ, A. 2012. Form and function within a phylogenetic framework: Locomotory habits of extant predators and some Miocene Sparassodonta (Metatheria). *Zoological Journal of the Linnean Society*, **165**, 224–251.

ERONEN, J. T., JANIS, C. M., CHAMBERLAIN, C. P. and MULCH, A. 2015. Mountain uplift explains differences in palaeogene patterns of mammalian evolution and extinction between north America and Europe. *Proceedings of the Royal Society B: Biological Sciences*, **282**.

ETIENNE, C., HOUSSAYE, A. and HUTCHINSON, J. R. 2021. Limb myology and muscle architecture of the Indian rhinoceros *Rhinoceros unicornis* and the white rhinoceros *Ceratotherium simum* (Mammalia: Rhinocerotidae). *PeerJ*, **9**, e11314.

EVANS, H. and LAHUNTA, A. de. 2012. *Miller's Anatomy of the Dog*. Saunders.

FARIÑA, R. A. 1996. Trophic relationships among Lujanian mammals. *Evolutionary Theory*, **11**, 125–134.

FARIÑA, R. A., VIZCAÍNO, S. F. and BARGO, M. S. 1998. Body mass estimation in Lujanian (Late Pleistocene-Early Holocene of South America) mammal megafauna Pleistocene megafauna. *Mastozoología Neotropical*, **5**, 87–108.

———, BLANCO, R. E. and CHRISTIANSEN, P. 2005. Swerving as the escape strategy of *Macrauchenia patachonica* Owen (Mammalia; Litopterna). *Ameghiniana*, **42**, 751–760.

FERNICOLA, J. C., ZIMICZ, A. N., CHORNOGUBSKY, L., DUCEA, M., CRUZ, L. E., BOND, M., ARNAL, M., CÁRDENAS, M. and FERNÁNDEZ, M. 2021. The Early Eocene Climatic Optimum at the Lower Section of the Lumbrera Formation (Ypresian, Salta Province, Northwestern Argentina): Origin and Early Diversification of the Cingulata. *Journal of Mammalian Evolution*, **28**, 621–633.

FINARELLI, J. A. and CLYDE, W. C. 2004. Reassessing hominoid phylogeny: evaluating congruence in the morphological and temporal data. *Paleobiology*, **30**, 614–651.

FINSTERMEIER, K., ZINNER, D., BRAMEIER, M., MEYER, M., KREUZ, E., HOFREITER, M. and ROOS, C. 2013. A Mitogenomic Phylogeny of Living Primates. *PLoS ONE*, **8**, 69504.

FLYNN, A. G., DAVIS, A. J., WILLIAMSON, T. E., HEIZLER, M., WILLIAM FENLEY, C., LESLIE, C. E., SECORD, R., BRUSATTE, S. L. and PEPPE, D. J. 2020. Early Paleocene magnetostratigraphy and revised biostratigraphy of the Ojo Alamo Sandstone and lower Nacimiento Formation, San Juan Basin, New Mexico, USA. *Bulletin of the Geological Society of America*, **132**, 2154–2174.

FLYNN, J. and SWISHER, C. C. 1995. Cenozoic South American land mammal ages: correlation to global geochronologies. *In* BERGGREN, W. A., KENT, D. V., AUBRY, M.-P. and HARDENBOL, J. (eds.) *Geochronology, Time Scales and Stratigraphic Correlation: Framework for an Historical Geology*, Peligran, 317–333 pp.

FOLEY, N. M., SPRINGER, M. S. and TEELING, E. C. 2016. Mammal madness: Is the mammal tree of life not yet resolved? *Philosophical Transactions of the Royal Society B: Biological Sciences*, **371**, 20150140.

FONSECA-AZEVEDO, K. and HERCULANO-HOUZEL, S. 2012. Metabolic constraint imposes tradeoff between body size and number of brain neurons in human evolution. *Proceedings of the National Academy of Sciences of the United States of America*, **109**, 18571–18576.

FOOTE, M., HUNTER, J. P., JANIS, C. M. and SEPKOSKI, J. J. 1999. Evolutionary and preservational constraints on origins of biologic groups: Divergence times of eutherian mammals. *Science*, **283**, 1310–1314.

FORASIEPI, A. M., MACPHEE, R. D. E., HERNÁNDEZ DEL PINO, S., SCHMIDT, G. I., AMSON, E. and GROHÉ, C. 2016. Exceptional skull of *Huayqueriana* (Mammalia, Litopterna, Macraucheniidae) from the late Miocene of Argentina: anatomy, systematics, and paleobiological implications. *Bulletin of the American Museum of Natural History*, **404**, 1–76.

FOSTER, J. B. 1964. Evolution of mammals on Islands. *Nature*, **202**, 234–235.

FRAILEY, C. D. and CAMPBELL, K. E. 2012. Two new genera of peccaries (Mammalia, Artiodactyla, Tayassuidae) from upper Miocene deposits of the Amazon Basin. *Journal of Paleontology*, **86**, 852–877.

FU, Q., MITTNIK, A., JOHNSON, P. L. F., BOS, K., LARI, M., BOLLONGINO, R., SUN, C., GIEMSCH, L., SCHMITZ, R., BURGER, J., RONCHITELLI, A. M., MARTINI, F., CREMONESI, R. G., SVOBODA, J., BAUER, P., CARAMELLI, D., CASTELLANO, S., REICH, D., PÄÄBO, S. and KRAUSE, J. 2013. A revised timescale for human evolution based on ancient mitochondrial genomes. *Current Biology*, **23**, 553–559.

———, LI, H., MOORJANI, P., JAY, F., SLEPCHENKO, S. M., BONDAREV, A. A., JOHNSON, P. L. F., AXIMU-PETRI, A., PRÜFER, K., DE FILIPPO, C., MEYER, M., ZWYNS, N., SALAZAR-GARCÍA, D. C., KUZMIN, Y. V, KEATES, S. G., KOSINTSEV, P. A., RAZHEV, D. I., RICHARDS, M. P., PERISTOV, N. V, LACHMANN, M., DOUKA, K., HIGHAM, T. F. G., SLATKIN, M., HUBLIN, J. J., REICH, D., KELSO, J., VIOLA, T. B. and PÄÄBO, S. 2014. Genome sequence of a 45,000-year-old modern human from western Siberia. *Nature*, **514**, 445–449.

GALWAY-WITHAM, J., COLE, J. and STRINGER, C. 2019. Aspects of human physical and behavioural evolution during the last 1 million years. *Journal of Quaternary Science*, **34**, 355–378.

GAMBLE, C. S. 2013. *Settling the Earth: the Archaeology of Deep Human History*. Cambridge University Press: New York.

GARCÍA-LÓPEZ, D. A. and BABOT, J. 2014. The auditory region of the middle Eocene Litopterna Indalecia grandensis Bond & Vucetich 1983: anatomical and phylogenetic approach. *IV International Paleontological Congress*, 183.

GARVIN, H. M., ELLIOTT, M. C., DELEZENE, L. K., HAWKS, J., CHURCHILL, S. E., BERGER, L. R. and HOLLIDAY, T. W. 2017. Body size, brain size, and sexual dimorphism in *Homo naledi* from the Dinaledi Chamber. *Journal of Human Evolution*, **111**, 119–138.

GASPARINI, G. M., DUTRA, R. P., PERINI, F. A., CROFT, D. A., COZZUOL, M. A., MISSAGIA, R. V and LUCAS, S. G. 2021. On the supposed presence of Miocene Tayassuidae and Dromomerycinae (Mammalia, Cetartiodactyla) in South America. *American Museum Novitates*, **3968**, 1–27.

GAUDIOSO, P. J., GASPARINI, G. M., HERBST, R. and BÁRQUEZ, R. M. 2017. First record of the Neolicaphrium recens Frenguelli, 1921 (Mammalia, Litopterna) in the Pleistocene of Santiago del Estero Province, Argentina. *Papéis Avulsos de Zoologia. Museu de Zología da Universidade de São Paulo, Brasil*, **57**, 23–29.

GAUDRY, A. 1904. Fossiles de Patagonie: dentition de quelques mammifères. *Mémoires de la Société Géologique de France, Paléontologie 12, Mémoire*, **31**, 1–27.

———. 1906. Fossiles de Patagonie: étude sur une portion du monde antartique. *Annales de Paléontologie*, **2**, 101–143.

GAUDRY, M. A. 1908. Fossiles de Patagonie: de l'économie dans la nature. *Annales de paléontologie*, **3**, 6–60.

GAVRYUSHKINA, A. and ZHANG, C. 2020. Total-Evidence Dating and the Fossilized Birth–Death Model. *In* HO, S. Y. W. (ed.) *The Molecular Evolutionary Clock: Theory and Practice*, Springer International Publishing, 175–193 pp.

GELFO, J. N. 2004. A new South American mioclaenid (Mammalia: Ungulatomorpha) from

the Tertiary of Patagonia, Argentina. *Ameghiniana*, **41**, 475–484.

GELFO, J. N. 2006. Los Didolodontidae (Mammalia: Ungulatomorpha) del Terciario Sudamericano. Sistemática, origen y evolución.472pp.

———. 2007. The ‘Condylarth’ <I>Raulvaccia peligrensis</I> (Mammalia: Didolodontidae) from the Paleocene of Patagonia, Argentina. *Journal of Vertebrate Paleontology*, **27**, 651–660.

GELFO, J. N. 2010. The ‘condylarth’ Didolodontidae from Gran Barranca: history of the bunodont South American mammals until the Eocene-Oligocene transition. In R. H. Madden, A. A. Carlini, M. G. Vucetich, R. F. Kay (eds.), The Paleontology of Gran Barranca: evolution and en. 130–142.

———. 2016. Considerations about the evolutionary stasis of *Notiolofos arquinotiensis* (Mammalia: Sparnotheriodontidae), Eocene of Seymour Island, Antarctica. *Ameghiniana*, **53**, 316–332.

GELFO, J. N. and SIGÉ, B. 2011. A New Didolodontid Mammal from the Late Paleocene—Earliest Eocene of Laguna Umayo, Peru. *Acta Palaeontologica Polonica*, **56**, 665–678.

GELFO, J. N. and LORENTE, M. 2012. The alleged astragalar remains of Didolodus Ameghino, 1897 (Mammalia, Panameriungulata) and a critic of isolated bone association models. *Bulletin of Geosciences*, **87**, 249–259.

GELFO, J. N., ORTIZ-JAUREGUIZAR, E. and ROUGIER, G. W. 2007. New remains and species of the ‘condylarth’ genus Escribania (Mammalia: Didolodontidae) from the Palaeocene of Patagonia, Argentina. *Earth and Environmental Science Transactions of the Royal Society of Edinburgh*, **98**, 127–138.

———, LÓPEZ, G. M. and BOND, M. 2008. A new Xenungulata (Mammalia) from the Paleocene of Patagonia, Argentina. *Journal of Paleontology*, **82**, 329–335.

GELFO, J. N., LÓPEZ, G. M. and LORENTE, M. 2016. Los ungulados arcaicos de América del Sur: “Condylarthra” y Litopterna. *Contribuciones Científicas Del Museo Argentino de Ciencias Naturales “Bernardino Rivadavia"*, **6**, 285–291.

GELFO, J. N., LÓPEZ, G. M. and SANTILLANA, S. N. 2017. Eocene ungulate mammals from West Antarctica: Implications from their fossil record and a new species. *Antarctic Science*, **29**, 445–455.

———, GARCÍA-LÓPEZ, D. A. and BERGQVIST, L. P. 2020*a*. Phylogenetic relationships and palaeobiology of a new xenungulate (Mammalia: Eutheria) from the Palaeogene of Argentina. *Journal of Systematic Palaeontology*, **18**, 993–1007.

GELFO, J. N., GOIN, F. J., BAUZA, N. and REGUERO, M. A. 2019. The fossil record of Antarctic land mammals : commented review and hypotheses for future research. *Advances in Polar Science*, **30**, 274–292.

GELFO, J. N., ALONSO, R. N., MADDEN, R. H. and CARLINI, A. A. 2020*b*. An Eocene Bunodont South American Native Ungulate (Didolodontidae) from the Lumbrera Formation, Salta Province, Argentina. *Ameghiniana*, **57**, 132–145.

GERVAIS, M. P. 1855. Recherches sur les mammifères fossiles de l'Amérique Méridonale. *In* CASTELNAU, F. de (ed.) *Animaux Nouveaux Ou Rares Recueillis Pendant l'expedition Dans Les Parties Centrales de l'Amérique Du Sudde Rio de Janeiro á Lima, et de Lima Au Para*, P. Bertrand, Libraire-Éditeur, Paris, 1–63 pp.

GILBERT, W. H. 2008. *Homo erectus* cranial anatomy. *In* GILBERT, W. H. and ASFAW, B. (eds.) *Homo Erectus: Pleistocene Evidence from the Middle Awash, Ethiopia*, University of California Press, Berkeley, 265–311 pp.

GODOY, E., MARQUARDT, C. and BLANCO, N. 2003. Carta Caldera, Región de Atacama. *In Serie Geología Básica*, Vol. 76. Servicio Nacional de Geología y Minería, Santiago, 38 pp.

GOIN, F. J., GELFO, J. N., CHORNOGUBSKY, L., WOODBURNE, M. O. and MARTIN, T. 2012. Origins, radiations, and distribution of South American mammals. *In* PATTERSON, B. D. and COSTA, L. P. (eds.) *Bones, Clones, and Biomes: The History and Geography of Recent Neotropical Mammals*, The University of Chicago Press, Chicago, 20–50 pp.

———, ———, ORTIZ-JAUREGUIZAR, E., FORASIEPI, A. M., CANDELA, A. M., VIEYTES, C. E. and CLADERA, G. 2022. Mamíferos del Banco Negro Inferior, Formación Salamanca, Cuenca del Golfo de San Jorge. *In* GIACOSA, R. E. (ed.) *Geología y Recursos Naturales de La Provincia de Chubut*, 1029–1053 pp.

GOLOBOFF, P. A. and CATALANO, S. A. 2016. TNT version 1.5, including a full implementation of phylogenetic morphometrics. *Cladistics*, **32**, 221–238.

GÓMEZ-ROBLES, A., SMAERS, J. B., HOLLOWAY, R. L., POLLY, P. D. and WOOD, B. A. 2017. Brain enlargement and dental reduction were not linked in hominin evolution. *Proceedings of the National Academy of Sciences of the United States of America*, **114**, 468–473.

GOWLETT, J. A. J. 2016. The discovery of fire by humans: A long and convoluted process. *Philosophical Transactions of the Royal Society B: Biological Sciences*, **371**, 1–12.

GRABOWSKI, M. 2016. Bigger brains led to bigger bodies?: The correlated evolution of human brain and body size. *Current Anthropology*, **57**, 174–196.

——— and JUNGERS, W. L. 2017. Evidence of a chimpanzee-sized ancestor of humans but a gibbon-sized ancestor of apes. *Nature Communications*, **8**, 1–10.

———, VOJE, K. L. and HANSEN, T. F. 2016. Evolutionary modeling and correcting for observation error support a 3/5 brain-body allometry for primates. *Journal of Human Evolution*, **94**, 106–116.

———, HATALA, K. G. and JUNGERS, W. L. 2018. Body mass estimates of the earliest possible hominins and implications for the last common ancestor. *Journal of Human Evolution*, **122**, 84–92.

———, ———, ——— and RICHMOND, B. G. 2015. Body mass estimates of hominin fossils and the evolution of human body size. *Journal of Human Evolution*, **85**, 75–93.

GRIGG, G. and KIRSHNER, D. 2015. *Biology and evolution of crocodylians*. Cornell University Press, New York.

GROSSNICKLE, D. M. and NEWHAM, E. 2016. Therian mammals experience an ecomorphological radiation during the Late Cretaceous and selective extinction at the K–Pg boundary. *Proceedings of the Royal Society B: Biological Sciences*, **283**, 1–8.

———, SMITH, S. M. and WILSON, G. P. 2019. Untangling the Multiple Ecological Radiations of Early Mammals. *Trends in Ecology & Evolution*, 1–14.

GRÜN, R., PIKE, A., MCDERMOTT, F., EGGINS, S., MORTIMER, G., AUBERT, M., KINSLEY, L., JOANNES-BOYAU, R., RUMSEY, M., DENYS, C., BRINK, J., CLARK, T. and STRINGER, C. 2020. Dating the skull from Broken Hill, Zambia, and its position in human evolution. *Nature*, **580**, 372–375.

GUNNELL, G. F., BOYER, D. M., FRISCIA, A. R., HERITAGE, S., MANTHI, F. K., MILLER, E. R., SALLAM, H. M., SIMMONS, N. B., STEVENS, N. J. and SEIFFERT, E. R. 2018. Fossil lemurs from Egypt and Kenya suggest an African origin for Madagascar's aye-aye. *Nature Communications*, **9**, 1–12.

GUTSTEIN, C. S., CHEREM, J. J., COZZUOL, M. A. and SUÁREZ, M. 2007. Primer registro de capibara (Hydrochoeridae, Rodentia) de Chile (Fm. Bahía Inglesa). *Biological Research*, **40**.

HALLIDAY, T. J. D. and GOSWAMI, A. 2016*a*. Eutherian morphological disparity across the end-Cretaceous mass extinction. *Biological Journal of the Linnean Society*, **118**, 152–168.

HALLIDAY, T. J. D. and GOSWAMI, A. 2016*b*. The impact of phylogenetic dating method on interpreting trait evolution: A case study of Cretaceous-Palaeogene eutherian body-size evolution. *Biology Letters*, **12**.

HALLIDAY, T. J. D., UPCHURCH, P. and GOSWAMI, A. 2016. Eutherians experienced elevated evolutionary rates in the immediate aftermath of the Cretaceous-Palaeogene mass extinction. *Proceedings of the Royal Society B: Biological Sciences*, **283**.

HALLIDAY, T. J. D., UPCHURCH, P. and GOSWAMI, A. 2017. Resolving the relationships of Paleocene placental mammals. *Biological Reviews*, **92**, 521–550.

HALLIDAY, T. J. D., DOS REIS, M., TAMURI, A. U., FERGUSON-GOW, H., YANG, Z. and GOSWAMI, A. 2019. Rapid morphological evolution in placental mammals post-dates the origin of the crown group. *Proc. R. Soc. B*, **286**.

HARCOURT-SMITH, W. E. H. 2016. Early hominin diversity and the emergence of the genus *Homo*. *Journal of Anthropological Sciences*, **94**, 19–27.

HARMAND, S., LEWIS, J. E., FEIBEL, C. S., LEPRE, C. J., PRAT, S., LENOBLE, A., BOËS, X., QUINN, R. L., BRENET, M., ARROYO, A., TAYLOR, N., CLÉMENT, S., DAVER, G., BRUGAL, J. P., LEAKEY, L., MORTLOCK, R. A., WRIGHT, J. D., LOKORODI, S., KIRWA, C., KENT, D. V and ROCHE, H. 2015. 3.3-million-year-old stone tools from Lomekwi 3, West Turkana, Kenya. *Nature*, **521**, 310–315.

HARRISON, L. B. and LARSSON, H. C. E. 2015. Among-character rate variation distributions in phylogenetic analysis of discrete morphological characters. *Systematic*

*Biology*, **64**, 307–324.

HARRISON, T. 2012. Dendropithecoidea, Proconsuloidea, and Hominoidea. *In* WERDELIN, L. and SANDERS, W. (eds.) *Cenozoic Mammals of Africa*, University of California Press, Berkeley, 429–470 pp.

HARVATI, K., RÖDING, C., BOSMAN, A. M., KARAKOSTIS, F. A., GRÜN, R., STRINGER, C., KARKANAS, P., THOMPSON, N. C., KOUTOULIDIS, V., MOULOPOULOS, L. A., GORGOULIS, V. G. and KOULOUKOUSSA, M. 2019. Apidima Cave fossils provide earliest evidence of *Homo sapiens* in Eurasia. *Nature*, **571**, 500–504.

HAWKS, J., DE RUITER, D. J. and BERGER, L. R. 2015. Comment on 'Early Homo at 2.8 Ma from Ledi-Geraru, Afar, Ethiopia'. *Science*, **348**, 1326–1326.

HENRÍQUEZ, A. A. 2006. Variaciones locales del nivel del mar en las cuencas neógenas de Caldera, III Región y Arauco, VIII Región: deducción de tasas de alzamiento y subsidencia tectónica.'Dissertation', Universidad de Chile, 170pp.

HERSHKOVITZ, I., WEBER, G. W., QUAM, R., DUVAL, M., GRÜN, R., KINSLEY, L., AYALON, A., BAR-MATTHEWS, M., VALLADAS, H., MERCIER, N., ARSUAGA, J. L., MARTINÓN-TORRES, M., DE CASTRO, J. M. B., FORNAI, C., MARTÍN-FRANCÉS, L., SARIG, R., MAY, H., KRENN, V. A., SLON, V., RODRÍGUEZ, L., GARCÍA, R., LORENZO, C., CARRETERO, J. M., FRUMKIN, A., SHAHACK-GROSS, R., MAYER, D. E. B. Y., CUI, Y., WU, X., PELED, N., GROMAN-YAROSLAVSKI, I., WEISSBROD, L., YESHURUN, R., TSATSKIN, A., ZAIDNER, Y. and WEINSTEIN-EVRON, M. 2018. The earliest modern humans outside Africa. *Science*, **359**, 456–459.

VAN HETEREN, A. H. and SANKHYAN, A. R. 2009. Hobbits and pygmies:trends in evolution. *In* SANKHYAN, A. R. (ed.) *Asian Perspectives on Human Evolution*, Serials Publications, New Delhi, India, 172–187 pp.

HILDEBRAND, M. and GOSLOW, G. E. 2001. *Analysis of Vertebrate Structure*. John Wiley & Sons, Inc., New York,.

HLUBIK, S., BERNA, F., FEIBEL, C., BRAUN, D. and HARRIS, J. W. K. 2017. Researching the nature of fire at 1.5 Mya on the site of FxJj20 AB, Koobi Fora, Kenya, using high-

resolution spatial analysis and FTIR spectrometry. *Current Anthropology*, **58**, S243–S257.

———, CUTTS, R., BRAUN, D. R., BERNA, F., FEIBEL, C. S. and HARRIS, J. W. K. 2019. Hominin fire use in the Okote member at Koobi Fora, Kenya: New evidence for the old debate. *Journal of Human Evolution*, **133**, 214–229.

HOFFSTETTER, R. and SORIA, M. F. 1986. Neolodus colombianus gen. et sp. nov., un noveau Condylarthre (Mammalia) dans le Miocene de Colombie. *Comptes Rendus de la Academie de Sciences, Paris, 303*, **série II**, 1619–1622.

HOLLOWAY, R. L., HURST, S. D., GARVIN, H. M., SCHOENEMANN, P. T., VANTI, W. B., BERGER, L. R. and HAWKS, J. 2018. Endocast morphology of *Homo naledi* from the Dinaledi Chamber, South Africa. *Proceedings of the National Academy of Sciences of the United States of America*, **115**, 5738–5743.

HOLMGREN, N. 1952. An embryological analysis of the mammalian carpus and its bearing upon the question of the origin of the tetrapod limb. *Acta Zoologica*, **33**, 1–115.

HOOKER, J. J. 2000. Paleogene mammals: crises and ecological change. *In Biotic Response to Global Change*, ed. SJ Culver, PF Rawson, pp. 333–49. New York: Ca.

HOOKER, J. J., COLLINSON, M. E. and SILLE, N. P. 2004. Eocene-Oligocene mammalian faunal turnover in the Hampshire Basin, UK: Calibration to the global time scale and the major cooling event. *Journal of the Geological Society*, **161**, 161–172.

HOROVITZ, I. 2004. Eutherian mammal systematics and the origins of South American ungulates. *Bulletin of Carnegie Museum of Natural History*, 63–79.

HOVERS, E. 2006. Neandertals and modern humans in the middle Palaeolithic of the Levant: what kind of interaction? *In* CONARD, N. (ed.) *When Neandertals and Moderns Meet*, Kerns Verlag, Tübingen, 65–85 pp.

HUA, S. and JOUVE, S. 2004. A primitive marine gavialoid from the Paleocene of Morocco. *Journal of Vertebrate Paleontology*, **24**, 341–350.

HUNTER, J. P. and JERNVALL, J. 1995. The hypocone as a key innovation in mammalian evolution. *Proceedings of the National Academy of Sciences of the United States of America*, **92**, 10718–10722.

INTERNATIONAL COMMITTEE ON VETERINARY GROSS ANATOMICAL NOMENCLATURE. 2017. *Nomina Anatomica Veterinaria*. Editorial Committee Hanover (Germany), Ghent (Belgium), Columbia, MO (U.S.A.), Rio de Janeiro (Brazil).

IRISH, J. D., GUATELLI-STEINBERG, D., LEGGE, S. S., DE RUITER, D. J. and BERGER, L. R. 2013. Dental morphology and the phylogenetic 'place' of *Australopithecus sediba*. *Science*, **340**, 1233062.

ISLER, K. and VAN SCHAIK, C. P. 2006. Metabolic costs of brain size evolution. *Biology Letters*, **2**, 557–560.

——— and VAN SCHAIK, C. P. 2009. The Expensive Brain: A framework for explaining evolutionary changes in brain size. *Journal of Human Evolution*, **57**, 392–400.

ITURRALDE-VINENT, M. A. 2006. Meso-Cenozoic Caribbean Paleogeography: Implications for the Historical Biogeography of the Region. *International Geology Review*, **48**, 791–827.

IVANY, L. C., LOHMANN, K. C., HASIUK, F., BLAKE, D. B., GLASS, A., ARONSON, R. B. and MOODY, R. M. 2008. Eocene climate record of a high southern latitude continental shelf: Seymour Island, Antarctica. *Bulletin of the Geological Society of America*, **120**, 659–678.

IVES, A. R. 2019. R 2 s for Correlated Data: Phylogenetic Models, LMMs, and GLMMs. *Systematic Biology*, **68**, 234–251.

JANIS, C. M. 2000. Patterns in the evolution of herbivory in large terrestrial mammals: the Paleogene of North America. *In Evolution of Herbivory in Terrestrial Vertebrates*, Cambridge University Press, 168–222 pp.

———, FIGUEIRIDO, B., DESANTIS, L. and LAUTENSCHLAGER, S. 2020. An eye for a tooth: *Thylacosmilus* was not a marsupial 'saber-tooth predator'. *PeerJ*, **2020**, 1–36.

JERISON, H. J. 1973. *Evolution of the Brain and Intelligence*. Academic Press, New York.

———. 1979. Brain, body and encephalization in early primates. *Journal of Human Evolution*, **8**, 615–635.

JI, Q., LUO, Z. X., YUAN, C. X., WIBLE, J. R., ZHANG, J. P. and GEORGI, J. A. 2002. The earliest known eutherian mammal. *Nature*, **416**, 816–822.

JOHNSTON, P. A. and FOX, R. C. 1984. Paleocene and late Cretaceous mammals from Saskatchewan, Canada. *Palaeontographica Abteilung A*, **186**, 163–222.

JONES, K. E. and SAFI, K. 2011. Ecology and evolution of mammalian biodiversity. *Philosophical Transactions of the Royal Society B: Biological Sciences*, **366**, 2451–2461.

JOORDENS, J. C. A., D'ERRICO, F., WESSELINGH, F. P., MUNRO, S., DE VOS, J., WALLINGA, J., ANKJÆRGAARD, C., REIMANN, T., WIJBRANS, J. R., KUIPER, K. F., MÜCHER, H. J., COQUEUGNIOT, H., PRIÉ, V., JOOSTEN, I., VAN OS, B., SCHULP, A. S., PANUEL, M., VAN DER HAAS, V., LUSTENHOUWER, W., REIJMER, J. J. G. and ROEBROEKS, W. 2015. *Homo erectus* at Trinil on Java used shells for tool production and engraving. *Nature*, **518**, 228–231.

JUNGERS, W. L., GRABOWSKI, M., HATALA, K. G. and RICHMOND, B. G. 2016. The evolution of body size and shape in the human career. *Philosophical Transactions of the Royal Society B: Biological Sciences*, **371**.

KATOH, S., BEYENE, Y., ITAYA, T., HYODO, H., HYODO, M., YAGI, K., GOUZU, C., WOLDEGABRIEL, G., HART, W. K., AMBROSE, S. H., NAKAYA, H., BERNOR, R. L., BOISSERIE, J. R., BIBI, F., SAEGUSA, H., SASAKI, T., SANO, K., ASFAW, B. and SUWA, G. 2016. New geological and palaeontological age constraint for the gorilla-human lineage split. *Nature*, **530**, 215–218.

KENDAL, J., TEHRANI, J. J. and ODLING-SMEE, J. 2011. Human niche construction in interdisciplinary focus. *Philosophical Transactions of the Royal Society B: Biological Sciences*, **366**, 785–792.

KIMBEL, W. H. and RAK, Y. 2017. *Australopithecus sediba* and the emergence of *Homo*: Questionable evidence from the cranium of the juvenile holotype MH 1. *Journal of Human Evolution*, **107**, 94–106.

———, ——— and JOHANSON, D. C. 2004. *The skull of Australopithecus afarensis*. Oxford University Press, New York.

KIVELL, T. L., DEANE, A. S., TOCHERI, M. W., ORR, C. M., SCHMID, P., HAWKS, J., BERGER, L. R. and CHURCHILL, S. E. 2015. The hand of *Homo naledi*. *Nature Communications*, **6**, 1–9.

KNEEPKENS, A. F. L. M., BADOUX, D. M. and MACDONALD, A. A. 1989. Descriptive

and comparative myology of the forelimb of the babirusa (*Babyrousa babyrussa* L. 1758). *Anatomia, Histologia, Embryologia*, **18**, 349–365.

KOCHIYAMA, T., OGIHARA, N., TANABE, H. C., KONDO, O., AMANO, H., HASEGAWA, K., SUZUKI, H., PONCE DE LEÓN, M. S., ZOLLIKOFER, C. P. E., BASTIR, M., STRINGER, C., SADATO, N. and AKAZAWA, T. 2018. Reconstructing the Neanderthal brain using computational anatomy. *Scientific Reports*, **8**, 1–9.

KÖHLER-ROLLEFSON, I. U. 1991. Camelus dromedarius. *Mammalian Species*, **375**, 1–8.

KOHN, M. J., JOSEF, J. A., MADDEN, R., KAY, R., VUCETICH, G. and CARLINI, A. A. 2004. Climate stability across the Eocene-Oligocene transition, southern Argentina. *Geology*, **32**, 621–624.

KOHN, M. J., STRÖMBERG, C. A. E., MADDEN, R. H., DUNN, R. E., EVANS, S., PALACIOS, A. and CARLINI, A. A. 2015. Quasi-static Eocene-Oligocene climate in Patagonia promotes slow faunal evolution and mid-Cenozoic global cooling. *Palaeogeography, Palaeoclimatology, Palaeoecology*, **435**, 24–37.

KONDRASHOV, P. E. and LUCAS, S. G. 2004. Palaeostylops iturus from the upper Paleocene of Mongolia and the status of Arctostylopida (Mammalia, Eutheria). *New Mexico Museum of Natural History and Science Bulletin*, **26**, 195–203.

KRAGLIEVICH, L. 1932. Nuevos apuntes para la geología y paleontología uruguayas. *Anales del Museo de Historia Natural de Montevideo*, **3**, 257–321.

KRAMARZ, A. and BOND, M. 2013. On the status of *Isolophodon* Roth, 1903 (Mammalia, Astrapotheria) and other little-known Paleogene astrapotheres from central Patagonia. *Geobios*, **46**, 203–211.

KRAMARZ, A. G. and BOND, M. 2005. Los Litopterna (Mammalia) de la Formación Pinturas, Mioceno Temprano-Medio de Patagonia. *Ameghiniana*, **42**, 611–625.

KRAMARZ, A. G. and MACPHEE, R. D. E. 2022. Did some extinct South American native ungulates arise from an afrothere ancestor? A critical appraisal of Avilla and Mothé's (2021) Sudamericungulata–Panameridiungulata hypothesis. *Journal of Mammalian Evolution*.

KRAMARZ, A. G., BOND, M. and ROUGIER, G. W. 2017. Re-Description of the Auditory Region of the Putative Basal Astrapothere (Mammalia) Eoastrapostylops riolorense Soria

and Powell, 1981. Systematic and Phylogenetic Considerations. *Annals of Carnegie Museum*, **84**, 95–164.

———, ——— and MACPHEE, R. D. E. 2021. On the alleged perissodactyl affinities of the "condylarth" Escribania chubutensis and other endemic South American ungulate-like placentals. *Journal of Vertebrate Paleontology*, **41**, e1986716.

KRAUS, R. 1998. The cranium of *Piscogavialis jugaliperforatus* n.gen., n.sp. (Gavialidae, Crocodylia) from the Miocene of Peru. *Paläontologische Zeitschrift*, **72**, 389–405.

KRAUSE, J. M., CLYDE, W. C., IBAÑEZ-MEJÍA, M., SCHMITZ, M. D., BARNUM, T., BELLOSI, E. S. and WILF, P. 2017. New age constraints for early Paleogene strata of central Patagonia, Argentina: Implications for the timing of South American Land Mammal Ages. *Bulletin of the Geological Society of America*, **129**, 886–903.

KUBO, D., KONO, R. T. and KAIFU, Y. 2013. Brain size of *Homo floresiensis* and its evolutionary implications. *Proceedings of the Royal Society B: Biological Sciences*, **280**.

KUMAR, S. and HEDGES, S. B. 1998. A molecular timescale for vertebrate development. *Nature*, **392**, 917–920.

——— and BLAIR HEDGES, S. 2016. Advances in time estimation methods for molecular data. *Molecular Biology and Evolution*, **33**, 863–869.

———, STECHER, G., LI, M., KNYAZ, C. and TAMURA, K. 2018. MEGA X: Molecular evolutionary genetics analysis across computing platforms. *Molecular Biology and Evolution*, **35**, 1547–1549.

KUNIMATSU, Y., NAKATSUKASA, M., SAWADA, Y., SAKAI, T., HYODO, M., HYODO, H., ITAYA, T., NAKAYA, H., SAEGUSA, H., MAZURIER, A., SANEYOSHI, M., TSUJIKAWA, H., YAMAMOTO, A. and MBUA, E. 2007. A new Late Miocene great ape from Kenya and its implications for the origins of African great apes and humans. *Proceedings of the National Academy of Sciences of the United States of America*, **104**, 19220–19225.

KUPERAVAGE, A., POKRAJAC, D., CHAVANAVES, S. and ECKHARDT, R. B. 2018. Earliest known hominin calcar femorale in *Orrorin tugenensis* provides further Internal anatomical evidence for origin of human bipedal locomotion. *Anatomical Record*, **301**, 1834–1839.

LAIRD, M. F., SCHROEDER, L., GARVIN, H. M., SCOTT, J. E., DEMBO, M., RADOVČIĆ, D., MUSIBA, C. M., ACKERMANN, R. R., SCHMID, P., HAWKS, J., BERGER, L. R. and DE RUITER, D. J. 2017. The skull of *Homo naledi*. *Journal of Human Evolution*, **104**, 100–123.

LANFEAR, R., CALCOTT, B., HO, S. Y. W. and GUINDON, S. 2012. PartitionFinder: Combined selection of partitioning schemes and substitution models for phylogenetic analyses. *Molecular Biology and Evolution*, **29**, 1695–1701.

———, FRANDSEN, P. B., WRIGHT, A. M., SENFELD, T. and CALCOTT, B. 2017. Partitionfinder 2: New methods for selecting partitioned models of evolution for molecular and morphological phylogenetic analyses. *Molecular Biology and Evolution*, **34**, 772–773.

LANGERGRABER, K. E., PRÜFER, K., ROWNEY, C., BOESCH, C., CROCKFORD, C., FAWCETT, K., INOUE, E., INOUE-MURUYAMA, M., MITANI, J. C., MULLER, M. N., ROBBINS, M. M., SCHUBERT, G., STOINSKI, T. S., VIOLA, B., WATTS, D., WITTIG, R. M., WRANGHAM, R. W., ZUBERBUḦLER, K., PÄÄBO, S. and VIGILANT, L. 2012. Generation times in wild chimpanzees and gorillas suggest earlier divergence times in great ape and human evolution. *Proceedings of the National Academy of Sciences of the United States of America*, **109**, 15716–15721.

LAVOCAT, R. 1958. Litopterna. *In Traite de Paleontologie*, 31–59 pp.

LEAKEY, M. G., SPOOR, F., BROWN, F. H., GATHOGO, P. N., KIARIE, C., LEAKEY, L. N. and MCDOUGALL, I. 2001. New hominin genus from eastern Africa shows diverse middle Pliocene lineages. *Nature*, **410**, 433–440.

LEPRE, C. J., ROCHE, H., KENT, D. V., HARMAND, S., QUINN, R. L., BRUGAL, J. P., TEXIER, P. J., LENOBLE, A. and FEIBEL, C. S. 2011. An earlier origin for the Acheulian. *Nature*, **477**, 82–85.

LESSA, G. M. 1992. Estudo descritivo de *Xenorhinotherium bahiense* Cartelle & Lessa, 1998 e comparação com outras espécies de Macraucheniidae (Litopterna, Mammalia).'Dissertation', Universidade Federal do Rio de Janeiro, 1–121pp.

LEWIS, P. 2001. A likelihood approach to estimating phylogeny from discrete morphological character data. *Society of Systematic Biologists*, **50**, 913–925.

LIVERMORE, R., NANKIVELL, A., EAGLES, G. and MORRIS, P. 2005. Paleogene opening of Drake Passage. *Earth and Planetary Science Letters*, **236**, 459–470.

LOBO, L. S. 2015. Estudo da morfologia dentária de *Xenorhinotheirum bahiense* Cartelle & Lessa, 1988 (Litopterna, Macraucheniidae).'Dissertation', Universidade Federal de Viçosa, 175pp.

———, LESSA, G., CARTELLE, C. and ROMANO, P. S. R. 2017. Dental eruption sequence and hypsodonty index of a Pleistocene macraucheniid from the Brazilian Intertropical Region. *Journal of Paleontology*, **91**, 1083–1090.

LOFGREN, D. L., LILLEGRAVEN, J. A., CLEMENS, W. A., GINGERICH, P. D. and WILLIAMSON, T. E. 2004. Paleocene Biochronology: The Puercan Through Clarkforkian Land Mammal Ages. *In* WOODBURNE, M. O. (ed.) *Late Cretaceous and Cenozoic Mammals of North America*, Columbia University Press, New York, 43–105 pp.

LOOMIS, F. B. 1914. *The Deseado formation of Patagonia*. Amherst, Massachusett, Amherst College.

LORDKIPANIDZE, D., DE PONCE LEÓN, M. S., MARGVELASHVILI, A., RAK, Y., RIGHTMIRE, G. P., VEKUA, A. and ZOLLIKOFER, C. P. E. 2013. A complete skull from Dmanisi, Georgia, and the evolutionary biology of early *Homo*. *Science*, **342**, 326–331.

LORENTE, M. 2015. Desarrollo de modelos de asociación y clasificaciones de restos postcraneanos aislados de ungulados nativos del Paleoceno-Eoceno de América del Sur.'Dissertation' Universidad Nacional de La Plata, La Plata, 1–576pp.

LUO, Z. X., YUAN, C. X., MENG, Q. J. and JI, Q. 2011. A Jurassic eutherian mammal and divergence of marsupials and placentals. *Nature*, **476**, 442–445.

LYDEKKER, R. 1893. Contributions to knowledge of the fossil vertebrates of Argentina, 3. A study of the extinct ungulates of Argentina. *Anales del Museo de La Plata. Paleontología Argentina*, **2**, 1–91.

———. 1894. Contributions to a knowledge of the fossil vertebrates of Argentina. *Anales del Museo de La Plata. Paleontología Argentina*, **3**, 1–118.

LYDEKKER, R. 1896. A geographical history of mammals, University Press, Cambridge. .

LYSON, T. R., MILLER, I. M., BERCOVICI, A. D., WEISSENBURGER, K., FUENTES, A. J., CLYDE, W. C., HAGADORN, J. W., BUTRIM, M. J., JOHNSON, K. R., FLEMING, R. F., BARCLAY, R. S., MACCRACKEN, S. A., LLOYD, B., WILSON, G. P., KRAUSE, D. W. and CHESTER, S. G. B. 2019. Exceptional continental record of biotic recovery after the Cretaceous-Paleogene mass extinction. *Science (New York, N.Y.)*, eaay2268.

MACLAREN, J. A. and MCHORSE, B. K. 2020. Comparative forelimb myology and muscular architecture of a juvenile Malayan tapir (*Tapirus indicus*). *Journal of Anatomy*, **236**, 85–97.

MACPHEE, R. D. E., HERNÁNDEZ DEL PINO, S., KRAMARZ, A., FORASIEPI, A. M., BOND, M. and SULSER, R. B. 2021. Cranial morphology and phylogenetic relationships of *Trigonostylops wortmani*. *Bulletin American Museum of Natural History*, 1–183.

MADDEN, R. H., GUERRERO, J., KAY, R. F., FLYNN, J. J., SWISHER, C. C. and WALTON, A. H. 1997. The Laventan stage and age. *In* KAY, R. F., MADDEN, R. H., CIFELLI, R. L. and FLYNN, J. J. (eds.) *Vertebrate Paleontology in the Neotropics: The Miocene Fauna of La Venta, Colombia,* Smithsonian Instituion Press, Washington and London, 499–519 pp.

MAKHDOOMI, D. M., GAZI, M. A., UL NABI, S. and AHMED, S. 2013. Morphometric studies on adult double humped camel of Ladakh, India. *Emirates Journal of Food and Agriculture*, **25**, 544–548.

MANZUETTI, A., PEREA, D., UBILLA, M. and RINDERKNECHT, A. 2018. First record of *Smilodon fatalis* Leidy, 1868 (Felidae, Machairodontinae) in the extra-Andean region of South America (late Pleistocene, Sopas Formation), Uruguay: Taxonomic and paleobiogeographic implications. *Quaternary Science Reviews*, **180**, 57–62.

MARCHI, D., WALKER, C. S., WEI, P., HOLLIDAY, T. W., CHURCHILL, S. E., BERGER, L. R. and DESILVA, J. M. 2017. The thigh and leg of *Homo naledi*. *Journal of Human Evolution*, **104**, 174–204.

MARQUARDT, C. 1999. Neotectónica de la franja costera y aportes a la geología regional entre Caldera y Caleta Pajonal (27°–27°4′), III Región de Atacama.‘Dissertation’, Universidad de Chilepp.

———, BLANCO, N., GODOY, E., LAVENU, A., ORTLIEB, L., MARCHANT, M. and GUZMÁN, N. 2000. Estratigrafía del Cenozoico Superior en el área de Caldera (26°45′28″S), III Región de Atacama, Chile. *IX Congreso Geológico Chileno*, **1**, 504–508.

MARSHALL, L. G. and MUIZON, C. de. 1988. The dawn of the Age of Mammals in South America. *Nat.Geogr.Res.\rNational Geographic Research J1 - NGR*, **4**, 23–55.

MARSHALL, L. G. and CIFELLI, R. L. 1990. Analysis of changing diversity patterns in Cenozoic land mammal age faunas, South America. *Palaeovertebrata*, **19**, 169–210.

———, CASE, J. A. and WOODBURNE, M. O. 1990. Phylogenetic relationships of the families of marsupials. *Current Mammalogy*, **2**, 433–505.

MARTIN, J. M., LEECE, A. B., NEUBAUER, S., BAKER, S. E., MONGLE, C. S., BOSCHIAN, G., SCHWARTZ, G. T., SMITH, A. L., LEDOGAR, J. A., STRAIT, D. S. and HERRIES, A. I. R. 2021. Drimolen cranium DNH 155 documents microevolution in an early hominin species. *Nature Ecology & Evolution*, **5**, 38–45.

MARTINELLI, A. G., SOTO-ACUÑA, S., GOIN, F. J., KALUZA, J., BOSTELMANN, J. E., FONSECA, P. H. M., REGUERO, M. A., LEPPE, M. and VARGAS, A. O. 2021. New cladotherian mammal from southern Chile and the evolution of mesungulatid meridiolestidans at the dusk of the Mesozoic era. *Scientific Reports*, **11**, 7594.

MARTINÓN-TORRES, M., BERMÚDEZ DE CASTRO, J. M., GÓMEZ-ROBLES, A., ARSUAGA, J. L., CARBONELL, E., LORDKIPANIDZE, D., MANZI, G. and MARGVELASHVILI, A. 2007. Dental evidence on the hominin dispersals during the Pleistocene. *Proceedings of the National Academy of Sciences of the United States of America*, **104**, 13279–13282.

MATTHEW, W. D. 1897. A revision of the Puerco fauna. *Bulletin of American Museum of Natural History*, **9**, 259–323.

———. 1909. The Carnivora and Insectivora of the Bridger Basin, Middle Eocene. *Memoirs of the AMNH*, **9**, 293–576.

———. 1915*a*. Climate and Evolution. *Annals of the New York Academy of Sciences*, **24**, 171–318.

———. 1915*b*. A revision of the lower Eocene Wasatch and Wind River faunas. Part II. Order

Condylarthra, Family Hyopsodontidae. *Bulletin of American Museum of Natural History*, **9**, 311–328.

———. 1915*c*. A revision of the lower Eocene Wasatch and Wind River faunas. Part IV. Entelonychia, Primates, Insectivora (Part). *Bulletin of the American Museum of Natural History*, **34**, 429–483.

MATTHEW, W. D. 1937. Paleocene Faunas of the San Juan Basin, New Mexico. *Transactions of the American Philosophical Society*, **30**, 1–510.

MAXWELL, S. J. 2018. The quality of the early hominin fossil record: Implications for evolutionary analyses. PhD, University College London - Birkbeck, London. .

MCGRATH, A. J., ANAYA, F. and CROFT, D. A. 2018. Two new macraucheniids (Mammalia: Litopterna) from the late middle Miocene (Laventan South American Land Mammal Age) of Quebrada Honda, Bolivia. *Journal of Vertebrate Paleontology*, **38**, e1461632.

———, ——— and CROFT, D. A. 2020*a*. New proterotheriids from the middle Miocene of Quebrada Honda, Bolivia, and body size and diversity trends in proterotheriid and macraucheniid litopterns (Mammalia). *Ameghiniana*, **57**, 159–188.

———, FLYNN, J. J. and WYSS, A. R. 2020*b*. Proterotheriids and macraucheniids (Litopterna: Mammalia) from the Pampa Castillo Fauna, Chile (early Miocene, Santacrucian SALMA) and a new phylogeny of Proterotheriidae. *Journal of Systematic Palaeontology*, **18**, 717–738.

MCHENRY, H. M. and COFFING, K. 2000. *Australopithecus* to *Homo*: Transformations in Body and Mind. *Annual Review of Anthropology*, **29**, 125–146.

MCHORSE, B. K., BIEWENER, A. A. and PIERCE, S. E. 2019. The evolution of a single toe in horses: causes, consequences, and the way forward. *Integrative and Comparative Biology*, **59**, 638–655.

MCKENNA, M. C. 1956. Survival of primitive notoungulates and condylarths into the Miocene of Colombia. *American Journal of Science*, **254**, 736–743.

MCKENNA, M. C. 1975. Toward a phylogenetic classification of the Mammalia. *In* LUCKETT, W. P. and SZALAY, F. S. (eds.) *Phylogeny of the Primates*, Plenum Press, New York, 21–46 pp.

MCKENNA, M. C. and BELL, S. K. 1997. Classification of mammals above the species level. *Columbia University Press, New York*, 1–631.

MELCHIONNA, M. and MONDANARO, A. 2020. Macroevolutionary trends of brain mass in Primates. *Biological Journal of the Linnean Society*, **129**, 14–25.

MERCERAT, A. 1891*a*. Caracteres diagnósticos de algunas especies del gen. *Theosodon* conservadas en el Museo de la Plata. *Revista del Museo de la Plata*, **1**, 47–49.

———. 1891*b*. Sinopsis de la Familia de los Bunodontheridae (Eoceno de Patagonia), conservados en el Museo de La Plata. *Revista del Museo de la Plata*, **1**, 447–468.

MEREDITH, R. W., JANEČKA, J. E., GATESY, J., RYDER, O. A., COLLEEN, A., TEELING, E. C., GOODBLA, A., EIZIRIK, E., SIMÃO, T. L. L., STADLER, T., RABOSKY, D. L., HONEYCUTT, R. L., FLYNN, J. J., INGRAM, C. M., WILLIAMS, T. L., ROBINSON, T. J., BURK-HERRICK, A., AYOUB, N. A., SPRINGER, M. S., MURPHY, W. J., MEREDITH, R. W., JANEČKA, J. E., GATESY, J., RYDER, O. A., FISHER, C. A., TEELING, E. C., GOODBLA, A., EIZIRIK, E., SIMÃO, T. L. L., STADLER, T., RABOSKY, D. L., HONEYCUTT, R. L., FLYNN, J., INGRAM, C. M., STEINER, C., WILLIAMS, T. L., ROBINSON, T. J., BURK-HERRICK, A. and WESTERMAN, M. 2011. Impacts of the Cretaceous Terrestrial Revolution and KPg extinction on mammal diversification. *Science*, **334**, 521–524.

MEYER, M., FU, Q., AXIMU-PETRI, A., GLOCKE, I., NICKEL, B., ARSUAGA, J. L., MARTÍNEZ, I., GRACIA, A., DE CASTRO, J. M. B., CARBONELL, E. and PÄÄBO, S. 2014. A mitochondrial genome sequence of a hominin from Sima de los Huesos. *Nature*, **505**, 403–406.

———, ARSUAGA, J. L., DE FILIPPO, C., NAGEL, S., AXIMU-PETRI, A., NICKEL, B., MARTÍNEZ, I., GRACIA, A., DE CASTRO, J. M. B., CARBONELL, E., VIOLA, B., KELSO, J., PRÜFER, K. and PÄÄBO, S. 2016. Nuclear DNA sequences from the Middle Pleistocene Sima de los Huesos hominins. *Nature*, **531**, 504–507.

MILLER, I. F., BARTON, R. A. and NUNN, C. L. 2019. Quantitative uniqueness of human brain evolution revealed through phylogenetic comparative analysis. *ELife*, **8**.

MILLER, K. G., KOMINZ, A., BROWNING, J. V, WRIGHT, J. D., MOUNTAIN, G. S., KATZ, M. E., SUGARMAN, P. J., CRAMER, B. S., CHRISTIE-BLICK, N. and PEKAR,

S. F. 2005. The Phanerozoic record of sea level change. *Science*, **310**, 1293–1298.

MILLER, M. A., PFEIFFER, W. and SCHWARTZ, T. 2010. Creating the CIPRES Science Gateway for inference of large phylogenetic trees. *In Proceedings of the Gateway Computing Enviroments Workshop (GCE)*, New Orleans,LA, 1–8 pp.

MISSIAEN, P., SMITH, T., GUO, D. Y., BLOCH, J. I. and GINGERICH, P. D. 2006. Asian gliriform origin for arctostylopid mammals. *Naturwissenschaften*, **93**, 407–411.

MONES, A. 2015. *Ricardocifellia* , a replacement name for *Paulacoutoia* Cifelli, 1983, and *Depaulacoutoia* Cifelli and Ortiz-Jaureguizar, 2014 (Mammalia, 'Condylarthra,' Didolodontidae), and the status of *Depaulacoutoia* Kretzoi and Kretzoi, 2000 . *Journal of Vertebrate Paleontology*, **35**, e973571.

MONGLE, C. S., STRAIT, D. S. and GRINE, F. E. 2019. Expanded character sampling underscores phylogenetic stability of *Ardipithecus ramidus* as a basal hominin. *Journal of Human Evolution*, **131**, 28–39.

———, PUGH, K. D., STRAIT, D. S. and GRINE, F. E. 2022. Modelling hominin evolution requires accurate hominin data. *Nature Ecology and Evolution*, **6**, 1090–1091.

MONTES, M., BEAMUD, E., NOZAL, F. and SANTILLANA, S. 2019. Late Maastrichtian-Paleocene chronostratigraphy from Seymour (Marambio) Island (James Ross Basin, Antarctic Peninsula). Eustatic controls of sedimentation. *Advances in Polar Science*, **30**, 303–327.

———, NOZAL, F., SANTILLANA, S., MARENSSI, S. and OLIVERO, E. 2013. Mapa Geológico de la Isla Marambio (Seymour); escala 1:20.000. *Serie Cartográfica Geocientífica Antártica. Con texto complementario. Madrid: Instituto Geológico y Minero de España; Buenos Aires: Instituto Antártico Argentino*.

MONTGOMERY, S. H., CAPELLINI, I., BARTON, R. A. and MUNDY, N. I. 2010. Reconstructing the ups and downs of primate brain evolution: Implications for adaptive hypotheses and *Homo floresiensis*. *BMC Biology*, **8**.

MOORE, M. W. and BRUMM, A. 2009. Homo floresiensis and the African Oldowan. 9781402090592. *In* HOVERS, E. and BRAUN, D. R. (eds.) *Interdisciplinary Approaches to the Oldowan*, Springer, New York, 61–69 pp.

MORÓN, S., FOX, D. L., FEINBERG, J. M., JARAMILLO, C., BAYONA, G., MONTES, C.

and BLOCH, J. I. 2013. Climate change during the Early Paleogene in the Bogotá Basin (Colombia) inferred from paleosol carbon isotope stratigraphy, major oxides, and environmental magnetism. *Palaeogeography, Palaeoclimatology, Palaeoecology*, **388**, 115–127.

MOUNIER, A., MARCHAL, F. and CONDEMI, S. 2009. Is *Homo heidelbergens* is a distinct species? New insight on the Mauer mandible. *Journal of Human Evolution*, **56**, 219–246.

MUIZON, C. de and MARSHALL, L. G. 1987*a*. Deux nouveaux conylarthres (Mammalia) du Maastrichtien de Tiupampa (Bolivie). *Comptes Rendus des Séances de l'Académie des Sciences [Paris], Série II*, **304**, 947–950.

——— and MARSHALL, L. G. 1987*b*. Le plus ancien Condylarthre (Mammalia) sud-américain (Crétacé supérieur, Bolivie). *Comptes rendus hebdomadaires des séances de l'Académie des sciences*, **13**, 771–774.

——— and MARSHALL, L. G. 1991. Nouveaux Condylarthres du Paléocène inférieur de Tiupampa (Bolivie). *Bulletin du Muséum national d'Histoire naturelle*, **13**, 201–227.

——— and CIFELLI, R. L. 2000. The "condylarths" (archaic Ungulata, Mammalia) from the early Palaeocene of Tiupampa (Bolivia): implications on the origin of the South American ungulates. *Geodiversitas*, **22**, 47–150.

———, CIFELLI, R. L. and BERGQVIST, L. P. 1998. Eutherian tarsals from the early Paleocene of Bolivia. *Journal of Vertebrate Paleontology*, **18**, 655–663.

———, BILLET, G. and LADEVÈZE, S. 2019. New remains of kollpaniine "condylarths" (Panameriungulata) from the early Palaeocene of Bolivia shed light on hypocone origins and molar proportions among ungulate-like placentals. *Geodiversitas*, **41**, 841–874.

———, ———, ARGOT, C., LADEVÈZE, S. and GOUSSARD, F. 2015. *Alcidedorbignya inopinata*, a basal pantodont (Placentalia, Mammalia) from the early Palaeocene of Bolivia: Anatomy, phylogeny and palaeobiology. *Geodiversitas*, **37**, 397–631.

NESSOV, L. A. and ARCHIBALD, J. D. 1998. Ungulate-like mammals from the Late Cretaceous. *Bulletin of Carnegie Museum of Natural History*, **34**, 40–88.

NI, X., FLYNN, J. J., WYSS, A. R. and ZHANG, C. 2019. Cranial endocast of a stem platyrrhine primate and ancestral brain conditions in anthropoids. *Science Advances*, **5**.

NOVACEK, M. J. 1986. The primitive eutherian dental formula. *Journal of Vertebrate Paleontology*, **6**, 191–196.

O'DEA, A., LESSIOS, H. A., COATES, A. G., EYTAN, R. I., RESTREPO-MORENO, S. A., CIONE, A. L., COLLINS, L. S., DE QUEIROZ, A., FARRIS, D. W., NORRIS, R. D., STALLARD, R. F., WOODBURNE, M. O., AGUILERA, O., AUBRY, M. P., BERGGREN, W. A., BUDD, A. F., COZZUOL, M. A., COPPARD, S. E., DUQUE-CARO, H., FINNEGAN, S., GASPARINI, G. M., GROSSMAN, E. L., JOHNSON, K. G., KEIGWIN, L. D., KNOWLTON, N., LEIGH, E. G., LEONARD-PINGEL, J. S., MARKO, P. B., PYENSON, N. D., RACHELLO-DOLMEN, P. G., SOIBELZON, E., SOIBELZON, L., TODD, J. A., VERMEIJ, G. J. and JACKSON, J. B. C. 2016. Formation of the Isthmus of Panama. *Science Advances*, **2**, e1600883.

O'LEARY, M. A., BLOCH, J. I., FLYNN, J. J., GAUDIN, T. J., GIALLOMBARDO, A., GIANNINI, N. P., GOLDBERG, S. L., KRAATZ, B. P., LUO, Z. X., MENG, J., NI, X., NOVACEK, M. J., PERINI, F. A., RANDALL, Z. S., ROUGIER, G. W., SARGIS, E. J., SILCOX, M. T., SIMMONS, N. B., SPAULDING, M., VELAZCO, P. M., WEKSLER, M., WIBLE, J. R. and CIRRANELLO, A. L. 2013. The placental mammal ancestor and the Post-K-Pg radiation of placentals. *Science*, **339**, 662–667.

O'REILLY, J. E., DOS REIS, M. and DONOGHUE, P. C. J. 2015. Dating Tips for Divergence-Time Estimation. *Trends in Genetics*, **31**, 637–650.

ODREMAN-RIVAS, O. E. 1969. Los Polymorphinae, un diferente tipo adaptativo de los Proterotheriidae (Mammalia, Litopterna). *Ameghiniana*, **VI**, 57–64.

OFSTAD, E. G., HERFINDAL, I., SOLBERG, E. J. and SÆTHER, B. E. 2016. Home ranges, habitat and body mass: Simple correlates of home range size in ungulates. *Proceedings of the Royal Society B: Biological Sciences*, **283**, 20161234.

OSBORN, H. F. 1910. *The Age of Mammals in Europe, Asia, and North America*. Macmillan.

——— and EARLE, C. 1895. Fossil mammals of the Puerco beds: collection of 1892. *Bulletin of the American Museum of Natural History*, **7**, 1–70.

OWEN, R. 1837. A description of the Cranium of the Toxodon platensis, a gigantic extinct mammiferous species, referrible by its dentition to the Rodentia, but with affinities to the Pachydermata and the Herbivorous Cetacea. *Proceedings of the Geological Society of*

*London*, **2**, 541–542.

———. 1838. Part 1: Fossil Mammalia. *In* DARWIN, C. R. (ed.) *The Zoology of the Voyage of H. M. S. Beagle, under the Command of Captain Fitz Roy during the Years 1832 to 1836*, Smith, Elder and Co, London, 1–111 pp.

———. 1853. Description of some species of the extinct genus *Nesodon* with remarks of the primary group (Toxodontia) of the hoofed quadrupeds to which the genus is referable. *Philosophical Transactions of the Royal Society of London*, **143**, 291–309.

PAGEL, M. 2002. Modelling the evolution of continuously varying characters on phylogenetic trees: The case of Hominid cranial capacity. *In* MACLEOD, N. and FOREY, P. L. (eds.) *Morphology, Shape and Phylogeny*, Taylor and Francis, London, 269–286 pp.

DEL PAPA, C., BABOT, J., DAHLQUIST, J., LÓPEZ, D. G., DERACO, V., HERRERA, C., BERTELLI, S., ROUGIER, G. W. and GIANNINI, N. P. 2022. Toward a chronostratigraphy of the Paleocene-Eocene sedimentary record in northwestern Argentina. *Journal of South American Earth Sciences*, **113**, 103677.

PARADIS, E., CLAUDE, J. and STRIMMER, K. 2004. APE: Analyses of phylogenetics and evolution in R language. *Bioinformatics*, **20**, 289–290.

PARODI, L. J. 1931. Huesos de los miembros de los macroquénidos neoterciarios. *Physis*, **10**, 294–304.

PASCUAL, R. 1965. Un nuevo Condylarthra (Mammalia) de Edad Casamayorense de Paso de los Indios (Chubut, Argentina). Breves consideraciones sobre la edad Casamayorense. *Ameghiniana*, **4**, 57–65.

——— and JAUREGUIZAR, E. O. 1990. Evolving climates and mammal faunas in cenozoic South America. *Journal of Human Evolution*, **19**, 23–60.

——— and ORTIZ-JAUREGUIZAR, E. 2007. The Gondwanan and South American episodes: Two major and unrelated moments in the history of the South American mammals. *Journal of Mammalian Evolution*, **14**, 75–137.

———, VUCETICH, M. G. and FERNÁNDEZ, J. 1978. Los primeros mamíferos (Notoungulata, Henricosborniidae) de la formacion Mealla (Grupo Salta, subgrupo Santa Bárbara). Sus implicancias filogenéticas, taxonómicas y cronológicas. *Ameghiniana*, **15**, 366–390.

———, ORTIZ JAUREGUIZAR, E. and PRADO, J. L. 1996. Land mammals: Paradigm for Cenozoic South American geobiotic evolution. *Münchner Geowissen Abhand (A)*, **30**, 265–319.

———, VUCETICH, M. G., SCILLATO-YANÉ, G. J. and BOND, M. 1985. Main pathways of mammalian diversification in South America. *In* STEHLI, F. G. and WEBB, S. D. (eds.) *The Great American Biotic Interchange*, Springer US, 219–239 pp.

———, CATTOI, N. V, FRANCIS, J. C., GONDAR, D., ORTEGA HINOJOSA, E. J., TONNI, E. P., PISANO, J. A., RINGUELET, A. and ZETTI, J. 1966. *Paleontografía Bonaerense, Fascículo IV, Vertebrata*. *In* BORRELLO, A. (ed.) Comisión de Investigación Científica, La Plata.

PATTERSON, B. 1940. An Adianthinae litoptern from the Deseado Formation of Patagonia. *Geological Series of Field Museum of Natural History*, **8**, 13–19.

———. 1977. A Primitive Pyrothere (Mammalia, Notoungulata) From the Early Tertiary of Northwestern Venezuela. *Fieldiana, Geology*, **33**, 397–422.

——— and PASCUAL, R. 1972. The Fossil Mammal Fauna of South America. In: A. Kerst, F. C. Erk, and B. Glass, editors, Evolution, Mammals, and Southern Continents. (Albany, State Univ. of New York Press). 247–309.

PAULA COUTO, C. 1952. Fossil mammals from the beginning of the Cenozoic in Brazil. Condylarthra, Litopterna, Xenungulata and Astrapotheria. *Bulletin of American Museum of Natural History*, **99**, 355–394.

———. 1978*a*. Ungulados fosseis do Riochiquense de Itaborai, RJ, Brasil. I - Xenungulata. *Anais da Academia Brasileira de Ciencias*, **50**, 203–207.

———. 1978*b*. Ungulados fosseis do Riochiquense de Itaboraí, R. J., Brasil. II- Condylarthra e Litopterna. *Anais da Academia Brasileira de Ciencias*, **50**, 209–218.

———. 1979*a*. Ungulados fósseis do Riochiquense de Itaboraí, R. J., Brasil. IV- Retificação sobre os Notoungulata. *Anais da Academia Brasileira de Ciencias*, **51**, 345–348.

PAULA COUTO, C. de. 1979*b*. *Tratado de Paleomastozoologia. Academia Brasileira de Ciencias, Río de Janeiro*. .

PEREA, D. and MARTÍNEZ, S. 2004. Estratigrafía del Mioceno-Pleistoceno en el litoral sur-

oeste de Uruguay. *In* VEROSLAVSKY, G., UBILLA, M. and MARTÍNEZ, S. (eds.) *Cuencas Sedimentarias de Uruguay: Geología, Paleontología y Recursos Naturales – Cenozoico*, DIRAC, 105–124 pp.

———, RINDERKNECHT, A., UBILLA, M., BOSTELMANN, E. and MARTÍNEZ, S. 2013. Mamíferos y estratigrafía del Neógeno de Uruguay. *In* BRANDONI, D. and NORIEGA, J. I. (eds.) *El Neógeno de La Mesopotamia Argentina*, Asociación Paleontológica Argentina, Publicación Especial 14, 192–206 pp.

PHILLIPS, M. J. 2016. Geomolecular dating and the origin of placental mammals. *Systematic Biology*, **65**, 546–557.

——— and FRUCIANO, C. 2018. The soft explosive model of placental mammal evolution. *BMC Evolutionary Biology*, **18**, 1–13.

PIMM, S. L., JENKINS, C. N., ABELL, R., BROOKS, T. M., GITTLEMAN, J. L., RAVEN, P. H., ROBERTS, C. M. and SEXTON, J. O. 2014. The biodiversity of species and their rates of extinction, distribution, and protection. *Science*, **344**, 1246752.

PINHEIRO, J., BATES, D., DEBROY, S. and SARKAR, D. 2020. nlme: Linear and Nonlinear Mixed Effects Models. R package version 3.1-147. .

POLLY, P. D. 2007. Limbs in mammalian evolution. *In* HALL, B. K. (ed.) *Fins into Limbs: Evolution, Development, and Transformation*, Vol. 15. University of Chicago Press, Chicago, 245–268 pp.

———, STAYTON, C. T., DUMONT, E. R., PIERCE, S. E., RAYFIELD, E. J. and ANGIELCZYK, K. D. 2016. Combining geometric morphometrics and finite element analysis with evolutionary modeling: towards a synthesis. *Journal of Vertebrate Paleontology*, **36**.

POSTH, C., WISSING, C., KITAGAWA, K., PAGANI, L., VAN HOLSTEIN, L., RACIMO, F., WEHRBERGER, K., CONARD, N. J., KIND, C. J., BOCHERENS, H. and KRAUSE, J. 2017. Deeply divergent archaic mitochondrial genome provides lower time boundary for African gene flow into Neanderthals. *Nature Communications*, **8**.

POTTS, R. 1996. Evolution and climate variability. *Science*, **273**, 922–923.

———. 1998. Environmental hypotheses of hominin evolution. *American Journal of Physical Anthropology*, **107**, 93–136.

———. 2012. Evolution and Environmental Change in Early Human Prehistory. *Annual Review of Anthropology*, **41**, 151–167.

———. 2013. Hominin evolution in settings of strong environmental variability. *Quaternary Science Reviews*, **73**, 1–13.

POUND, M. J. and SALZMANN, U. 2017. Heterogeneity in global vegetation and terrestrial climate change during the late Eocene to early Oligocene transition. *Scientific Reports*, **7**.

POUND, M. J., HAYWOOD, A. M., SALZMANN, U. and RIDING, J. B. 2012. Global vegetation dynamics and latitudinal temperature gradients during the Mid to Late Miocene (15.97-5.33Ma). *Earth-Science Reviews*, **112**, 1–22.

———, ———, ———, ———, LUNT, D. J. and HUNTER, S. J. 2011. A Tortonian (Late Miocene, 11.61-7.25Ma) global vegetation reconstruction. *Palaeogeography, Palaeoclimatology, Palaeoecology*, **300**, 29–45.

POZZI, L., HODGSON, J. A., BURRELL, A. S., STERNER, K. N., RAAUM, R. L. and DISOTELL, T. R. 2014. Primate phylogenetic relationships and divergence dates inferred from complete mitochondrial genomes. *Molecular Phylogenetics and Evolution*, **75**, 165–183.

PRADO, J. L., MARTINEZ-MAZA, C. and ALBERDI, M. T. 2015. Megafauna extinction in South America: A new chronology for the Argentine Pampas. *Palaeogeography, Palaeoclimatology, Palaeoecology*, **425**, 41–49.

PREVOSTI, F. J., ROMANO, C. O., FORASIEPI, A. M., HEMMING, S., BONINI, R., CANDELA, A. M., CERDEÑO, E., CAROLINA, M., JAÉN, M., ORTIZ, P. E., PUJOS, F., RASIA, L., SCHMIDT, G. I., TAGLIORETTI, M., MACPHEE, R. D. E. and PARDIÑAS, U. F. J. 2021. New radiometric 40Ar-39Ar dates and faunistic analyses refine evolutionary dynamics of Neogene vertebrate assemblages in southern South America. *Scientific Reports*, **11**, 1–14.

PREVOSTI, F. J. and FORASIEPI, A. M. 2018. The fossil record of mammalian carnivores in South America: Bias and limitations. *In Evolution of South American Mammalian Predators During the Cenozoic: Paleobiogeographic and Paleoenvironmental Contingencies*, Springer International Publishing, 137–154 pp.

PREVOSTI, F. J., FORASIEPI, A. and ZIMICZ, N. 2013. The evolution of the Cenozoic

terrestrial mammalian predator guild in South America: competition or replacement? *Journal of Mammalian Evolution*, **20**, 3–21.

PROCTOR, C., DOUKA, K., PROCTOR, J. W. and HIGHAM, T. 2017. The Age and Context of the KC4 Maxilla, Kent's Cavern, UK. *European Journal of Archaeology*, **20**, 74–97.

PROTHERO, D. R., MANNING, E. M. and FISCHER, M. 1988. The phylogeny of the ungulates. In Benton M. J. (ed.), The Phylogeny and Classification of the Tetrapods, Volume 2: Mammals. Clarendon Press, Oxford. 201–234.

PROTHERO, D. R., CAMPBELL, K. E., BEATTY, B. L. and FRAILEY, C. D. 2014. New late Miocene dromomerycine artiodactyl from the Amazon Basin: implications for interchange dynamics. *Journal of Paleontology*, **88**, 434–443.

PÜSCHEL, H. P., O'REILLY, J. E., PISANI, D. and DONOGHUE, P. C. J. 2020. The impact of fossil stratigraphic ranges on tip-calibration, and the accuracy and precision of divergence time estimates. *Palaeontology*, **63**, 67–83.

———, BERTRAND, O. C., O'REILLY, J. E., BOBE, R. and PÜSCHEL, T. A. 2021*a*. Divergence-time estimates for hominins provide insight into encephalization and body mass trends in human evolution. *Nature Ecology & Evolution*, **5**, 808–819.

———, ———, ———, ——— and ———. 2021*b*. Divergence-time estimates for hominins provide insight into encephalization and body mass trends in human evolution: Data and Code. GitHub. https://github.com/HansPueschel/Hominin-div-time-evolution; https://dx.doi.org/10.5281/zenodo.4537445. .

PÜSCHEL, H. P., BERTRAND, O. C., REILLY, J. E. O., BOBE, R. and PÜSCHEL, T. A. 2022. Reply to: Modelling hominin evolution requires accurate hominin data. *Nature Ecology and Evolution*, **6**, 1092–1094.

PÜSCHEL, H. P., ALARCÓN-MUÑOZ, J., SOTO-ACUÑA, S., UGALDE, R., SHELLEY, S. L. and BRUSATTE, S. L. 2023. Anatomy and phylogeny of a new small macraucheniid (Mammalia: Litopterna) from the Bahía Inglesa Formation (late Miocene), Atacama Region, Northern Chile. *Journal of Mammalian Evolution*.

PYRON, R. A. 2011. Divergence time estimation using fossils as terminal taxa and the origins of lissamphibia. *Systematic Biology*, **60**, 466–481.

———. 2017. Novel approaches for phylogenetic inference from morphological data and total-

evidence dating in squamate reptiles (Lizards, Snakes, and Amphisbaenians). *Systematic Biology*, **66**, 38–56.

DE QUEIROZ, K. and GAUTHIER, J. 1992. Phylogenetic taxonomy. *Annual Review of Ecology and Systematics*, **23**, 449–480.

R CORE TEAM. 2019. *R: A language and environment for statistical computing*. R Foundation for Statistical Computing, Vienna, Austria. URL http://www.R-project.org/.

RAMBAUT, A., DRUMMOND, A. J., XIE, D., BAELE, G. and SUCHARD, M. A. 2018. Posterior Summarization in Bayesian Phylogenetics Using Tracer 1.7. *Systematic Biology*, **67**, 901–904.

RECH, J. A., CURRIE, B. S., JORDAN, T. E., RIQUELME, R., LEHMANN, S. B., KIRK-LAWLOR, N. E., LI, S. and GOOLEY, J. T. 2019. Massive middle Miocene gypsic paleosols in the Atacama Desert and the formation of the Central Andean rain-shadow. *Earth and Planetary Science Letters*, **506**, 184–194.

REEDER, D. M., HELGEN, K. M. and WILSON, D. E. 2007. Global trends and biases in new mammal species discoveries. *Occasional Papers, Museum of Texas Tech University*, **269**, 1–35.

REGUERO, M. A. and PREVOSTI, F. J. 2010. Rodent-like notoungulates (Typotheria) from Gran Barranca, Chubut Province, Argentina: phylogeny and systematics. *In* MADDEN, R. H., CARLINI, A. A., VUCETICH, M. G. and KAY, R. F. (eds.) *The Paleontology of Gran Barranca: Evolution and Environmental Change through the Middle Cenozoic of Patagonia*, Cambridge University Press, New York, 152–162 pp.

REGUERO, M. A. and CANDELA, A. M. 2011. Late Cenozoic mammals from the northwest of Argentina. *Cenozoic Geology of the Central Andes of Argentina*, 411–426.

——— and GOIN, F. J. 2021. Paleogeography and biogeography of the Gondwanan final breakup and its terrestrial vertebrates: New insights from southern South America and the "double Noah's Ark" Antarctic Peninsula. *Journal of South American Earth Sciences*, **108**, 1–23.

———, GELFO, J. N., LÓPEZ, G. M., BOND, M., ABELLO, A., SANTILLANA, S. N. and MARENSSI, S. A. 2014. Final Gondwana breakup: The Paleogene South American native ungulates and the demise of the South America-Antarctica land connection. *Global*

*and Planetary Change*, **123**, 400–413.

DOS REIS, M., DONOGHUE, P. C. J. and YANG, Z. 2014. Neither phylogenomic nor palaeontological data support a Palaeogene origin of placental mammals. *Biology Letters*, **10**.

———, ——— and ———. 2016. Bayesian molecular clock dating of species divergences in the genomics era. *Nature Reviews Genetics*, **17**, 71–80.

DOS REIS, M., INOUE, J., HASEGAWA, M., ASHER, R. J., DONOGHUE, P. C. J. and YANG, Z. 2012. Phylogenomic datasets provide both precision and accuracy in estimating the timescale of placental mammal phylogeny. *Proceedings of the Royal Society B: Biological Sciences*, **279**, 3491–3500.

DOS REIS, M., GUNNELL, G. F., BARBA-MONTOYA, J., WILKINS, A., YANG, Z. and YODER, A. D. 2018. Using phylogenomic data to explore the effects of relaxed clocks and calibration strategies on divergence time estimation: Primates as a test case. *Systematic Biology*, **67**, 594–615.

RENFREE, M. B. 2010. Review: Marsupials: Placental Mammals with a Difference. *Placenta*, **24**, S21–S26.

REVELL, L. J. 2012. phytools: An R package for phylogenetic comparative biology (and other things). *Methods in Ecology and Evolution*, **3**, 217–223.

RICHMOND, B. G. and JUNGERS, W. L. 2008. *Orrorin tugenensis* femoral morphology and the evolution of hominin bipedalism. *Science*, **319**, 1662–1665.

ROBERTS, P. and STEWART, B. A. 2018. Defining the 'generalist specialist' niche for Pleistocene Homo sapiens. *Nature Human Behaviour*, **2**, 542–550.

ROJO, M. A. 1985. Un aporte al conocimiento del Terciario marino: Formación Bahía Inglesa. *IV Congreso Geológico Chileno*, **1**, 514–533.

RONQUIST, F., TESLENKO, M., VAN DER MARK, P., AYRES, D. L., DARLING, A., HÖHNA, S., LARGET, B., LIU, L., SUCHARD, M. A. and HUELSENBECK, J. P. 2012*a*. MrBayes 3.2: Efficient Bayesian phylogenetic inference and model choice across a large model space. *Systematic Biology*, **61**, 539–542.

———, LARTILLOT, N. and PHILLIPS, M. J. 2016. Closing the gap between rocks and

clocks using total-evidence dating. *Philosophical Transactions of the Royal Society B: Biological Sciences*, **371**, 20150136.

———, KLOPFSTEIN, S., VILHELMSEN, L., SCHULMEISTER, S., MURRAY, D. L. and RASNITSYN, A. P. 2012*b*. A total-evidence approach to dating with fossils, applied to the early radiation of the hymenoptera. *Systematic Biology*, **61**, 973–999.

ROSE, K. D. 2006. *The Beginning of the Age of Mammals*. The Johns Hopkins University Press, Baltimore.

ROSE, K. D., HOLBROOK, L. T., KUMAR, K., RANA, R. S., AHRENS, H. E., DUNN, R. H., FOLIE, A., JONES, K. E. and SMITH, T. 2019. Anatomy, relationships, and paleobiology of *Cambaytherium* (Mammalia, Perissodactylamorpha, Anthracobunia) from the lower Eocene of western India. *Journal of Vertebrate Paleontology*, **39**, 1–147.

ROTH, S. 1899. Aviso preliminar sobre mamíferos mesozóicos encontrados en Patagonia. *Revista del Museo de la Plata*, **9**, 381–388.

———. 1903. Los ungulados sudamericanos. *Anales del Museo de La Plata. Sección Paleontológica. Talleres de publicaciones del Museo*, **V**, 1–40.

———. 1927. La diferenciación del sistema dentario en los ungulados, notoungulados y primates. *Revista del Museo de La Plata*, **30**, 171–255.

ROUGIER, G. W., MARTINELLI, A. G. and FORASIEPI, A. M. 2021. Chapter 2: The Fossil Record of South American Mesozoic Mammals and Their Close Relatives. *In Mesozoic Mammals from South America and Their Forerunners*, 25–126 pp.

LE ROUX, J. P., ACHURRA, L., HENRÍQUEZ, Á., CARREÑO, C., RIVERA, H., SUÁREZ, M. E., ISHMAN, S. E., PYENSON, N. D. and GUTSTEIN, C. S. 2016. Oroclinal bending of the Juan Fernández Ridge suggested by geohistory analysis of the Bahía Inglesa Formation, north-central Chile. *Sedimentary Geology*, **333**, 32–49.

ROVERETO, C. 1914. Los estratos araucanos y sus fósiles. *Anales del Museo Nacional de Historia Natural de Buenos Aires*, **25**, 1–250.

RUITER, D. J. de, CHURCHILL, S. E., HAWKS, J. and BERGER, L. R. 2017. Late Australopiths and the Emergence of *Homo*. *Annual Review of Anthropology*, **46**, 99–115.

RUSCONI, C. 1957. Evolución de la trompa en las macrauquenias. *Revista del Museo de*

*Historia Natural de Mendoza*, **10**, 111–118.

SALAS-GISMONDI, R., OCHOA, D., JOUVE, S., ROMERO, P. E., CARDICH, J., PEREZ, A., DEVRIES, T., BABY, P., URBINA, M. and CARRÉ, M. 2022. Miocene fossils from the southeastern Pacific shed light on the last radiation of marine crocodylians. *Proceedings of the Royal Society B: Biological Sciences*, **289**, 20220380.

SALLAM, H. M. and SEIFFERT, E. R. 2020. Revision of Oligocene 'Paraphiomys' and an origin for crown Thryonomyoidea (Rodentia: Hystricognathi: Phiomorpha) near the Oligocene–Miocene boundary in Africa. *Zoological Journal of the Linnean Society*, **190**, 352–371.

SÁNCHEZ-VILLAGRA, M. R., BURNHAM, R. J., CAMPBELL, D. C., FELDMANN, R. M., GAFFNEY, E. S., KAY, R. F., LOZSÁN, R., PURDY, R. and THEWISSEN, J. G. M. 2006. A new near-shore marine fauna and flora from the early Neogene of northwestern Venezuela. *Journal of Paleontology*, **74**, 957–968.

SANSOM, R. S., WILLS, M. A. and WILLIAMS, T. 2017. Dental data perform relatively poorly in reconstructing mammal phylogenies: Morphological partitions evaluated with molecular benchmarks. *Systematic Biology*, **66**, 813–822.

SCERRI, E. M. L., THOMAS, M. G., MANICA, A., GUNZ, P., STOCK, J. T., STRINGER, C., GROVE, M., GROUCUTT, H. S., TIMMERMANN, A., RIGHTMIRE, G. P., D'ERRICO, F., TRYON, C. A., DRAKE, N. A., BROOKS, A. S., DENNELL, R. W., DURBIN, R., HENN, B. M., LEE-THORP, J., DEMENOCAL, P., PETRAGLIA, M. D., THOMPSON, J. C., SCALLY, A. and CHIKHI, L. 2018. Did Our Species Evolve in Subdivided Populations across Africa, and Why Does It Matter? *Trends in ecology & evolution*, **33**, 582–594.

———, CHIKHI, L. and THOMAS, M. G. 2019. Beyond multiregional and simple out-of-Africa models of human evolution. *Nature Ecology and Evolution*, **3**, 1370–1372.

SCHER, H. D. and MARTIN, E. E. 2006. Timing and climatic consequences of the opening of drake passage. *Science*, **312**, 428–430.

SCHERER, C., PITANA, V. and RIBEIRO, A. M. 2009. Proterotheriidae and Macraucheniidae (Litopterna, Mammalia) from the Pleistocene of Rio Grande do Sul State, Brazil. *Revista Brasileira de Paleontologia*, **12**, 231–246.

SCHINDELIN, J., ARGANDA-CARRERAS, I., FRISE, E., KAYNIG, V., LONGAIR, M., PIETZSCH, T., PREIBISCH, S., RUEDEN, C., SAALFELD, S., SCHMID, B., TINEVEZ, J. Y., WHITE, D. J., HARTENSTEIN, V., ELICEIRI, K., TOMANCAK, P. and CARDONA, A. 2012. Fiji: An open-source platform for biological-image analysis. *Nature Methods*, **9**, 676–682.

SCHLOSSER, M. 1911. Klasse. Mammalia. Säugetiere. *In* ZITTEL, K. A. (ed.) *Grundzüge Der Paläontologie (Paläozoologie). II. Abteilung: Vertebrata*, 325–550 pp.

SCHMIDT, G., HERNÁNDEZ DEL PINO, S., MUÑOZ, N. and FERNÁNDEZ, M. 2019. Litopterna (Mammalia) From the Santa Cruz Formation (Early-Middle Miocene) At the Río Santa Cruz, Southern Argentina. *Publicación Electrónica de la Asociación Paleontológica Argentina*, **19**, 170–192.

SCHMIDT, G. I. 2013. Litopterna y Notoungulata (Mammalia) de la Formación Ituzaingó (Mioceno tardío) de la provincia de Entre Ríos: sistemática, bioestratigrafía y paleobiogeografía.'Dissertation', Facultad de Ciencias Naturales y Museo, Universidad Nacional de La Plata, Buenos Aires, Argentina, 423pp.

SCHMIDT, G. I. 2015. Actualización sistemática y filogenia de los Proterotheriidae (Mammalia, litopterna) del "Mesopotamiense" (Mioceno tardío) de Entre Ríos, Argentina. *Revista Brasileira de Paleontologia*, **18**, 521–546.

SCHMIDT, G. I. and FERRERO, B. S. 2014. Taxonomic reinterpretation of *Theosodon hystatus* Cabrera and Kraglievich, 1931 (Litopterna, Macraucheniidae) and phylogenetic relationships of the family. *Journal of Vertebrate Paleontology*, **34**, 1231–1238.

———, MONTALVO, C. I., CERDEÑO, E., SOSTILLO, R., TOMASSINI, R. L. and BONINI, R. A. 2022. Updated data on Litopterna from the Huayquerian Stage/Age (Late Miocene-Early Pliocene) of central-east Argentina. *Comptes Rendus Palevol*, **21**, 721–743.

SCHROEDER, L., SCOTT, J. E., GARVIN, H. M., LAIRD, M. F., DEMBO, M., RADOVČIĆ, D., BERGER, L. R., DE RUITER, D. J. and ACKERMANN, R. R. 2017. Skull diversity in the *Homo* lineage and the relative position of *Homo naledi*. *Journal of Human Evolution*, **104**, 124–135.

SCHULTZ, P. H., ZARATE, M., HAMES, W., CAMILIÓN, C. and KING, J. 1998. A 3.3-Ma

impact in Argentina and possible consequences. *Science*, **282**, 2061–2063.

SCOTT, K. M. 1990. Postcranial dimensions of ungulates as predictors of body mass. *In* DAMUTH, J. and MACFADDEN, B. J. (eds.) *Body Size in Mammalian Paleobiology: Estimation and Biological Implications*, Cambridge University Press, Cambridge University, UK, 301–377 pp.

SCOTT, W. B. 1910. Mammalia of the Santa Cruz beds: Litopterna. *In* SCOTT, W. B. (ed.) *Reports of the Princeton University Expeditions to Patagonia, 1896-1899, Vol 7, Paleontology 4*, Vol. 7. Princeton University, E. Schweizerbart'sche Verlashandlung. Stuttgart, 1–156 pp.

SCOTT, W. B. 1912. Toxodonta and Entelonychia of the Santa Cruz Beds. *In* SCOTT, W. B. (ed.) *Reports of the Princeton University Expeditions to Patagonia, 1896–1899, Vol. 6, Paleontology 3. Mammalia of the Santa Cruz Beds, Part 2–3*, Princeton University, E. Schweizerbart'sche Verlashandlung. Stuttgart, 111–300 pp.

SCOTT, W. B. 1913. *A History of Land Mammals in the Western Hemisphere*. The McMillan Co., New York.

SEFVE, I. 1925. Macrauchenia patagonica. *Bulletin of the Geological Institution of the University of Upsala*, **19**, 1–21.

SEIFFERT, E. R., TEJEDOR, M. F., FLEAGLE, J. G., NOVO, N. M., CORNEJO, F. M., BOND, M., DE VRIES, D. and CAMPBELL, K. E. 2020. A parapithecid stem anthropoid of African origin in the Paleogene of South America. *Science*, **368**, 194–197.

SHELLEY, S. L. 2017. The rise of placental mammals: the anatomy, palaeobiology and phylogeny of *Periptychus* and the Periptychidae. Unpublished PhD Thesis, University of Edinburgh. .

SHELLEY, S. L., WILLIAMSON, T. E. and BRUSATTE, S. L. 2018. The osteology of *Periptychus carinidens*: A robust, ungulate-like placental mammal (Mammalia: Periptychidae) from the Paleocene of North America. *PLoS ONE*, **13**, e0200132.

SHOCKEY, B. J. 1999. Postcranial osteology and functional morphology of the Litopterna of Salla, Bolivia (Late Oligocene). *Journal of Vertebrate Paleontology*, **19**, 383–390.

——— and ANAYA, F. 2008. Postcranial osteology of mammals from Salla, Bolivia (late Oligocene): Form, function, and phylogenetic implications. 9781402069963. *In*

*Mammalian Evolutionary Morphology: A Tribute to Frederick S. Szalay*, 135–157 pp.

SIMPSON, G. G. 1932. New or little-known ungulates from the Pyrotherium and Colpodon beds of Patagonia. *American Museum Novitates*, **576**, 1–13.

SIMPSON, G. G. 1934. Provisional classification of extinct South American hoofed mammals. *American Museum Novitates*, **750**, 1–10.

———. 1935. Descriptions of the oldest known South American mammals, from the Río Chico Formation. *American Museum Novitates*, 1–26.

———. 1937. The Fort Union of the Crazy Mountain Field, Montana, and its mammalian faunas. *Bulletin of the United States National Museum*, **169**, 1–287.

———. 1944. *Tempo and Mode in Evolution*. Columbia University Press, New York.

———. 1945. The principles of classification and a classification of mammals. *Bulletin of the American Museum of Natural History*, **85**, 1–350.

SIMPSON, G. G. 1948. The beginning of the age of mammals in South America, Part 1. *Bulletin of the American Museum of Natural History*, **91**, 1–232.

SIMPSON, G. G. 1951. History of the Fauna of Latin America. In: G. A. Baitsell, editor, Science in Progress (7th Series) (New Haven, Yale University Press), pp. 369-408. 369–408.

———. 1964. Los mamíferos casamayorenses de la Colección Tournouër. *Revista del Museo Argentino de Ciencias Naturales 'Bernardino Rivadavia' e Instituto Nacional de Investigación de Ciencias Naturales, Paleontología*, **1**, 1–21.

SIMPSON, G. G. 1967. The Beginning of the Age of Mammals in South America, Part II. *Bulletin of the American Museum of Natural History*, **137**, 1–260.

SIMPSON, G. G. 1978. Early Mammals in South America: Fact, Controversy, and Mystery. *Proceedings of the American Philosophical Society*, **122**, 318–328.

———. 1980. *Splendid Isolation: the Curious History of South American Mammals*. Yale University Press, New Haven.

——— and MINOPRIO, J. L. 1949. A new Adianthine litoptern and associated mammals from a Deseadan faunule in Mendoza, Argentina. *American Museum Novitates*, **1434**, 1–27.

———, ——— and PATTERSON, B. 1962. The mammalian fauna of the Divisadero Largo Formation, Mendoza, Argentina. *Bulletin of the Museum of Comparative Zoology*, **127**, 239–293.

SINCLAIR, W. J. 1909. Typotheria of the Santa Cruz Beds. *In* SCOTT, W. B. (ed.) *Reports of the Princeton University Expeditions to Patagonia, 1896–1899, Vol. 6, Paleontology. Mammalia of the Santa Cruz Beds, Part 1*, Princeton University, E. Schweizerbart'sche Verlashandlung. Stuttgart, 1–110 pp.

SISSON, S. 1914. *The Anatomy of the Domestic Animals*. W. B. Saunders Company, Philadelphia & London.

SKELTON, R. R. and MCHENRY, H. M. 1992. Evolutionary relationships among early hominids. *Journal of Human Evolution*, **23**, 309–349.

SLATER, G. J. 2013. Phylogenetic evidence for a shift in the mode of mammalian body size evolution at the Cretaceous-Palaeogene boundary. *Methods in Ecology and Evolution*, **4**, 734–744.

SLOAN, R. E. and VAN VALEN, L. 1965. Cretaceous mammals from Montana. *Science*, **148**, 220–227.

SMITH, F. A., BOYER, A. G., BROWN, J. H., COSTA, D. P., DAYAN, T., ERNEST, S. K. M., EVANS, A. R., FORTELIUS, M., GITTLEMAN, J. L., HAMILTON, M. J., HARDING, L. E., LINTULAAKSO, K., LYONS, S. K., MCCAIN, C., OKIE, J. G., SAARINEN, J. J., SIBLY, R. M., STEPHENS, P. R., THEODOR, J. and UHEN, M. D. 2010. The evolution of maximum body size of terrestrial mammals. *Science*, **330**, 1216–1219.

SMITH, H. F. and GRINE, F. E. 2008. Cladistic analysis of early *Homo* crania from Swartkrans and Sterkfontein, South Africa. *Journal of Human Evolution*, **54**, 684–704.

SOIBELZON, E., SOIBELZON, L. H., GASPARINI, G. M. and TONNI, E. P. 2019. El Pleistoceno de la provincia de Buenos Aires y sus mamíferos. *Opera Lilloana*, **52**, 606–637.

SOL, D., BACHER, S., READER, S. M. and LEFEBVRE, L. 2008. Brain size predicts the success of mammal species introduced into novel environments. *American Naturalist*, **172**, 63–71.

SORIA, M. F. 1980*a*. Una nueva y problematica forma de ungulado del Casamayorense. *Actas del Segundo Congreso Argentino del Paleontologia y Bioestratigrafia y Primer Congreso Latinoamericano de Paleontologia. Tomo II*, 193–203.

———. 1980*b*. Las afinidades de *Phoradiadus divortiensis* Simpson, Minoprio y Patterson, 1962. *Circular informativa Asociación Paleontológica Argentina 4*, 20.

———. 1981. Los Litopterna del Colhuehuapense (Oligoceno Tardío) de la Argentina. *Revista del Museo Argentino de Ciencias Naturales 'Bernardino Rivadavia'*, **III**, 1–54.

———. 1982. Ubicación sistemática de *Polymorphis* Roth, 1899 y su significado filogenético. *Circular informativa Asociación Paleontológica Argentina 10*, 7.

———. 1984*a*. Noticia preliminar sobre los Amilnedwardsidae, fam. nov. (Mammalia) del Eoceno temprano de Patagonia, República Argentina. *Primeras Jornadas Argentinas de Paleontología de Vertebrados*, 19.

———. 1984*b*. Notopterna: un nuevo orden de mamíferos ungulados del Terciario inferior de Sudamérica. *Resúmenes de las 1as Jornadas Argentinas de Paleontología de Vertebrados*, 23.

———. 1988. Estudios sobre los Astrapotheria (Mammalia) del Paleoceno y Eoceno. Parte II: Filogenia, origen y relaciones. *Ameghiniana*, **25**, 47–59.

———. 1989*a*. Notopterna: un nuevo orden de mamíferos ungulados Eógenos de América del Sur. Parte I. Los Amilnedwardsidae. *Ameghiniana*, **25**, 245–258.

———. 1989*b*. Notopterna: un nuevo orden de mamíferos ungulados Eógenos de América de Sur. Parte II. *Notonychops powelli* gen. et sp. nov. (Notonychopidae nov.) de la formación Río Loro (Paleoceno Medio), Provincia de Tucumán, Argentina. *Ameghiniana*, **25**, 259–272.

———. 2001. Los Proterotheriidae (Litopterna, Mammalia), sistemática, origen y filogenia. *Monografias del Museo Argentino de Ciencias Naturales*, **1**, 1–167.

——— and POWELL, J. E. 1981. Un primitivo Astrapotheria (Mammalia) y la edad de la Formación Río Loro, Provincia de Tucumán, República Argentina. *Ameghiniana*, **18**, 155–168.

——— and HOFFSTETTER, R. 1985. Pternoconius tournoueri, una nueva especie de

Macraucheniidae (Mammalia; Litopterna) de Edad Colhuehuapense (Oligoceno Tardío); provincia del Chubut, República Argentina. *Ameghiniana*, **22**, 149–158.

SOTO-ACUÑA, S., OTERO, R. A., RUBILAR-ROGERS, D. and VARGAS, A. O. 2015. Arcosaurios no avianos de Chile. *In* RUBILAR-ROGERS, D., OTERO, R., VARGAS, A. and SALLABERRY, M. (eds.) *Vertebrados Fósiles de Chile, Publicación Ocasional Del Museo Nacional de Historia Natural, N° 63*, 209–263 pp.

SPRAIN, C. J., RENNE, P. R., CLEMENS, W. A. and WILSON, G. P. 2018. Calibration of chron C29r: New high-precision geochronologic and paleomagnetic constraints from the Hell Creek region, Montana. *Bulletin of the Geological Society of America*, **130**, 1615–1644.

SPRINGER, M. S. 1997. Molecular clocks and the timing of the placental and marsupial radiations in relation to the cretaceoustertiary boundary. *Journal of Mammalian Evolution*, **4**, 285–302.

SPRINGER, M. S., FOLEY, N. M., BRADY, P. L., GATESY, J. and MURPHY, W. J. 2019. Evolutionary Models for the Diversification of Placental Mammals Across the KPg Boundary. *Frontiers in Genetics*, **10**, 1–22.

———, EMERLING, C. A., MEREDITH, R. W., JANEČKA, J. E., EIZIRIK, E. and MURPHY, W. J. 2017. Waking the undead: Implications of a soft explosive model for the timing of placental mammal diversification. *Molecular Phylogenetics and Evolution*, **106**, 86–102.

STANDRING, S. 2015. *Gray's Anatomy, the Anatomical Basis of Clinical Practice*. Elsevier.

STEIN, B. R. and CASINOS, A. 1997. What is a cursorial mammal? *Journal of Zoology*, **242**, 185–192.

STEPHAN, H., FRAHM, H. D. and BARON, G. 1981. New and revised data on volumes of brain structures in insectivores and primates. *Folia Primatologica*, **35**, 1–29.

STRAIT, D. S. and GRINE, F. E. 2004. Inferring hominoid and early hominid phylogeny using craniodental characters: The role of fossil taxa. *Journal of Human Evolution*, **47**, 399–452.

———, ——— and MONIZ, M. A. 1997. A reappraisal of early hominid phylogeny. *Journal of Human Evolution*, **32**, 17–82.

SUÁREZ, M. E., LAMILLA, J. and MARQUARDT, C. 2004. Peces Chimaeriformes (Chondrichthyes, Holocephali) del Neógeno de la Formación Bahía Inglesa (Región de Atacama, Chile). *Revista Geologica de Chile*, **31**, 105–114.

SUWA, G., KONO, R. T., KATOH, S., ASFAW, B. and BEYENE, Y. 2007. A new species of great ape from the late Miocene epoch in Ethiopia. *Nature*, **448**, 921–924.

TARVER, J. E., DOS REIS, M., MIRARAB, S., MORAN, R. J., PARKER, S., O'REILLY, J. E., KING, B. L., O'CONNELL, M. J., ASHER, R. J., WARNOW, T., PETERSON, K. J., DONOGHUE, P. C. J. and PISANI, D. 2016. The Interrelationships of Placental Mammals and the Limits of Phylogenetic Inference. *Genome biology and evolution*, **8**, 330–44.

TAYLOR, M. E. 1974. The functional anatomy of the forelimb of some African Viverridae (Carnivora). *Journal of Morphology*, **143**, 307–335.

TEJADA-LARA, J. V., SALAS-GISMONDI, R., PUJOS, F., BABY, P., BENAMMI, M., BRUSSET, S., DE FRANCESCHI, D., ESPURT, N., URBINA, M. and ANTOINE, P. O. 2015. Life in proto-Amazonia: Middle Miocene mammals from the Fitzcarrald Arch (Peruvian Amazonia). *Palaeontology*, **58**, 341–378.

TEJEDOR, M. F., GOIN, F. J., GELFO, J. N., LÓPEZ, G., BOND, M., CARLINI, A. A., SCILLATO-YANE, G. J., WOODBURNE, M. O., CHORNOGUBSKY, L., ARAGÓN, E., REGUERO, M. A., CZAPLEWSKI, N. J., VINCON, S., MARTIN, G. M. and CIANCIO, M. R. 2009. New early Eocene mammalian fauna from western Patagonia, Argentina. *American Museum Novitates*, **3638**, 1–43.

TIMMERMANN, A. 2020. Quantifying the potential causes of Neanderthal extinction: Abrupt climate change versus competition and interbreeding. *Quaternary Science Reviews*, **238**, 106331.

TONG, Y. and LUCAS, S. G. 1982. A review of Chinese uintatheres and the origin of the Dinocerata (Mammalia, Eutheria). *Third North American Paleontological Convention. Proceedings*, **2**, 551–556.

TONNI, E. P. 1990. Mamíferos del Holoceno en la provincia de Buenos Aires. *Paula-Coutiana*, **4**, 3–21.

TROUESSART, E. L. 1904. *Catalogus Mammalium Tam Viventium Quam Fossilium.*

*Supplement. Pts. 1–2,*. .

VAN VALEN, L. 1978. The beginning of the Age of Mammals. *Evolutionary Theory 4*, **4**, 45–80.

VERA, B. and KRAUSE, J. M. 2020. New insights into the *Kibenikhoria* and *Ernestokokenia* faunas and the implications for the early Eocene of Patagonia, Argentina. *Journal of Vertebrate Paleontology*, e1772801.

———, FORNASIERO, M. and FAVERO, L. Del. 2020. New Data on Carodnia feruglioi (Carodniidae, Xenungulata) from the Early Eocene of Patagonia (Argentina). *Ameghiniana*, **57**, 566–581.

———, GONZÁLEZ RUIZ, L., NOVO, N., MARTIN, G., REATO, A. and TEJEDOR, M. F. 2019. The Interatheriinae (Mammalia, Notoungulata) of the Friasian *sensu stricto* and Mayoan (middle to late Miocene), and the fossils from Cerro Zeballos, Patagonia, Argentina. *Journal of Systematic Palaeontology*, **17**, 923–943.

VILLA, P. and ROEBROEKS, W. 2014. Neandertal demise: An archaeological analysis of the modern human superiority complex. *PLoS ONE*, **9**, 96424.

VILLAFAÑE, A. L., SCHMIDT, G. I. and CERDEÑO, E. 2012. Consideraciones sistemáticas y bioestratigráficas acerca de *Thoatheriopsis mendocensis* Soria, 2001 (Litopterna, Proterotheriidae). *Ameghiniana*, **49**, 365–374.

VILLARROEL, C. 1987. Caracteristicas y afinidades de *Etayoa* n. gen., tipo de una nueva familia de Xenungulata (Mammalia) del Paleoceno Medio (?) de Colombia. *Comunicaciones Paleontologicas del Museo de Historia Natural de Montevideo*, **1**, 241–253.

VILLMOARE, B. 2018. Early *Homo* and the role of the genus in paleoanthropology. *American Journal of Physical Anthropology*, **165**, 72–89.

VIZCAÍNO, S. F., CASSINI, G. H., TOLEDO, N. and BARGO, S. 2012. On the evolution of large size in mammalian herbivores of Cenozoic faunas of southern South America. *In* PATTERSON, B. and COSTA, L. P. (eds.) *Bones, Clones, and Biomes: The History and Geography of Recent Neotropical Mammals.*, The University of Chicago Press, Chicago, 76–101 pp.

VIZCAÍNO, S. F., REGUERO, M. A., GOIN, F. J., TAMBUSSI, C. P. and NORIEGA, J. I.

1998. Community structure of Eocene terrestrial vertebrates from Antarctic Peninsula. *Paleogene in South America and the Antarctic Pennisula*, **5**, 177–183.

WALSH, S. A. and SUÁREZ, M. 2005. First post−Mesozoic record of Crocodyliformes from Chile. *Acta Palaeontologica Polonica*, **50**, 595–600.

WEDAGE, O., AMANO, N., LANGLEY, M. C., DOUKA, K., BLINKHORN, J., CROWTHER, A., DERANIYAGALA, S., KOURAMPAS, N., SIMPSON, I., PERERA, N., PICIN, A., BOIVIN, N., PETRAGLIA, M. and ROBERTS, P. 2019. Specialized rainforest hunting by *Homo sapiens* ~45,000 years ago. *Nature Communications*, **10**, 1–8.

WELKER, F., COLLINS, M. J., THOMAS, J. A., WADSLEY, M., BRACE, S., CAPPELLINI, E., TURVEY, S. T., REGUERO, M., GELFO, J. N., KRAMARZ, A., BURGER, J., THOMAS-OATES, J., ASHFORD, D. A., ASHTON, P. D., ROWSELL, K., PORTER, D. M., KESSLER, B., FISCHER, R., BAESSMANN, C., KASPAR, S., OLSEN, J. V., KILEY, P., ELLIOTT, J. A., KELSTRUP, C. D., MULLIN, V., HOFREITER, M., WILLERSLEV, E., HUBLIN, J. J., ORLANDO, L., BARNES, I. and MACPHEE, R. D. E. 2015. Ancient proteins resolve the evolutionary history of Darwin's South American ungulates. *Nature*, **522**, 81–84.

WESTBURY, M., BALEKA, S., BARLOW, A., HARTMANN, S., PAIJMANS, J. L. A., KRAMARZ, A., FORASIEPI, A. M., BOND, M., GELFO, J. N., REGUERO, M. A., LÓPEZ-MENDOZA, P., TAGLIORETTI, M., SCAGLIA, F., RINDERKNECHT, A., JONES, W., MENA, F., BILLET, G., DE MUIZON, C., AGUILAR, J. L., MACPHEE, R. D. E. and HOFREITER, M. 2017. A mitogenomic timetree for Darwin's enigmatic South American mammal *Macrauchenia patachonica*. *Nature Communications*, **8**, 1–8.

WIBLE, J. R., ROUGIER, G. W., NOVACEK, M. J. and ASHER, R. J. 2007. Cretaceous eutherians and Laurasian origin for placental mammals near the K/T boundary. *Nature*, **447**, 1003–1006.

WIBLE, J. R., ROUGIER, G. W., NOVACEK, M. J. and ASHER, R. J. 2009. The Eutherian Mammal Maelestes gobiensis from the Late Cretaceous of Mongolia and the phylogeny of cretaceous eutheria. *Bulletin of the American Museum of Natural History*, **327**, 1–123.

WILF, P., CÚNEO, N. R., ESCAPA, I. H., POL, D. and WOODBURNE, M. O. 2013. Splendid and seldom Isolated: the paleobiogeography of Patagonia. *Annual Review of Earth and*

*Planetary Sciences*, **41**, 561–603.

WILL, M., PABLOS, A. and STOCK, J. T. 2017. Long-term patterns of body mass and stature evolution within the hominin lineage. *Royal Society Open Science*, **4**.

WILLIAMSON, T. E. 1996. The beginning of the age of mammals in the San Juan Basin, New Mexico: Biostratigraphy and evolution of Paleocene mammals of the Nacimiento Formation. *New Mexico Museum of Natural History and Science Bulletin*, **8**, 1–141.

——— and CARR, T. D. 2007. Bomburia and Ellipsodon (Mammalia: Mioclaenidae) from the early Paleocene of New Mexico. *Journal of Paleontology*, **81**, 966–985.

WILLIAMSON, T. E. and WEIL, A. 2011. A new Puercan (early Paleocene) hyopsodontid 'condylarth' from New Mexico. *Acta Palaeontologica Polonica*, **56**, 247–255.

WILSON, G. P. 2013. Mammals across the K/Pg boundary in northeastern Montana, U.S.A.: dental morphology and body-size patterns reveal extinction selectivity and immigrant-fueled ecospace filling. *Paleobiology*, **39**, 429–469.

WOOD, A. R., BEBEJ, R. M., MANZ, C. L., BEGUN, D. L. and GINGERICH, P. D. 2011. Postcranial functional morphology of *Hyracotherium* (Equidae, Perissodactyla) and locomotion in the earliest horses. *Journal of Mammalian Evolution*, **18**, 1–32.

WOODBURNE, M., CIONE, A. L. and TONNI, E. P. 2006. Central American provincialism and the Great American biotic interchange. *In Advances in late Tertiary vertebrate paleontology in Mexico and the Great American Biotic Inerchange, Carranza-Castañeda, Óscar, and Lindsay, E.H., eds*, 73–101.

WOODBURNE, M. O. 2010. The Great American Biotic Interchange: dispersals, tectonics, climate, sea level and holding pens. *Journal of Mammalian Evolution*, **17**, 245–264.

WOODBURNE, M. O., GOIN, F. J., RAIGEMBORN, M. S., HEIZLER, M., GELFO, J. N. and OLIVEIRA, E. V. 2014*a*. Revised timing of the South American early Paleogene land mammal ages. *Journal of South American Earth Sciences*, **54**, 109–119.

———, ———, BOND, M., CARLINI, A. A., GELFO, J. N., LÓPEZ, G. M., IGLESIAS, A. and ZIMICZ, A. N. 2014*b*. Paleogene land mammal faunas of South America; a response to global climatic changes and indigenous floral diversity. *Journal of Mammalian Evolution*, **21**, 1–73.

WRANGHAM, JONES, LADEN, PILBEAM and CONKLIN-BRITTAIN. 1999. The Raw and the Stolen: Cooking and the Ecology of Human Origins. *Current Anthropology*, **40**, 567–594.

WYSS, A. R., FLYNN, J. J., NORELL, M. a, SWISHER, C. C., NOVACEK, M. J., MCKENNA, M. C. and CHARRIER, R. 1994. Paleogene mammals from the Andes of central Chile: a preliminary taxonomic, biostratigraphic, and geochronologic assessment. *American Museum Novitates*, **3098**, 1–31.

YANG, Z. 2014. *Molecular evolution: a statistical approach*. Oxford University Press, Oxford.

ZACHOS, J., PAGANI, H., SLOAN, L., THOMAS, E. and BILLUPS, K. 2001. Trends, rhythms, and aberrations in global climate 65 Ma to present. *Science*, **292**, 686–693.

ZACK, S. P., PENKROT, T. A., KRAUSE, D. W. and MAAS, M. C. 2005. A new apheliscine 'condylarth' mammal from the late Paleocene of Montana and Alberta and the phylogeny of hyopsodontids. *Acta Palaeontologica Polonica*, **50**, 809–830.

ZANESCO, T., BERGQVIST, L. P. and PEREIRA, Á. A. 2019. Intraspecific Variation of One of the Oldest Litopterna (Mammalia), *Protolipterna ellipsodontoides*, and Redescription of the Species. *Ameghiniana*, **56**, 380–401.

ZEITOUN, V. 2009. *The Human Canopy: Homo erectus, Homo soloensis, Homo pekinensis and Homo floresiensis*. *In* HEDGES, J. and HEDGES, E. (eds.) B.A.R. S1937.

ZIMICZ, N., FERNÁNDEZ, M., BOND, M., CHORNOGUBSKY, L. and FERNICOLA, J. C. 2022. A new SANU (Mammalia, Panperissodactyla) from the early Eocene levels of the Lumbrera Formation at Los Cardones National Park (Salta Province, Northwestern Argentina). *Historical Biology*.

# Appendices

## Appendix C2

### Resource 1: Supplementary Tables

**Table S1.** mtDNA partitions and models selected.

**Table S2.** Radiometric age estimates for the analysed fossil hominins.

**Table S3.** Species used in the present study with their associated relevant data.

### Resource 2: Supplementary Figures

**Figure S1** Consensus trees with Bayesian posterior probabilities showing the support for the nodes

**Figure S2** Prior sensitivity analysis.

**Figure S3** Brain mass ACSR for each species mapped onto the four consensus time-calibrated phylogenies.

**Figure S4** Brain mass (g) ACSR traitgram for each species mapped onto the four consensus time-calibrated phylogenies.

**Figure S5** Body mass (kg) ACSR traitgram for each species mapped onto the four consensus time-calibrated phylogenies.

**Figure S6** PEQ ACSR traitgram for each species mapped onto the four consensus time-calibrated phylogenies.

**Figure S7** Boxplots of brain mass (g) ACSR per node based on a sample of 9002 time-calibrated posterior trees for each one of the plots.

**Figure S8** PglS models of ln(body mass) on ln(brain mass) based on the different consensus trees. a. Dembo *et al*. (2016) hypothesis.

**Figure S9** Boxplots of expected brain mass (a–d) and PEQ (e–h) for all the tips based on a sample of 9002 time-calibrated posterior trees for each one of the hypotheses.

**Figure S10** Brain mass ACSR versus body mass ACSR regressions from the consensus trees for each one of hypotheses. a–d. Regressions considering nodes 1 to 24.

### Resource 3: Püschel *et al.* (2021) article "Divergence-time estimates for hominins provide insight into encephalization and body mass trends in human evolution"

### Resource 4: Püschel *et al.* (2022) article "Reply to: Modelling hominin evolution requires accurate hominin data"

## Appendix C3

### Resource 1: Supplementary Tables

**Table S1.** Measurements of the mandible (in mm)

**Table S2.** Measurements of the vertebrae (in mm)

**Table S3.** Measurements of the ulna-radius (in mm)

**Table S4.** Measurements of the carpals (in mm)

**Table S5.** Measurements of the metacarpals (in mm)

**Table S6.** Measurements of the phalanges (in mm)

**Table S7.** Measurements of the metatarsals to compare with *Cullinia levis* (in mm)

### Resource 2: Character list and supplementary tables in relation to the phylogenetic aspect of this study

**List of characters and character states used in the phylogenetic analysis**

**Table S7.** SALMAs' lower and upper limits in Ma.

**Table S8.** List of apomorphies of groups recovered in the majority rule consensus tree in Fig. 3.19b.

**Table S9.** Divergence-times mean and 95% highest posterior density interval (HPD) for the tree in Fig. 3.20b.

### Resource 3: Nexus file with the script for the undated Bayesian analysis

### Resource 4: Nexus file with the script for the tip-dated Bayesian analysis

### Resource 5: Additional figures.

**Figure S1** Atlases classified as *Macrauchenia patachonica* in the MACN collections, here reinterpreted as ruminant atlases possibly from a species of *Bos*.

**Figure S2** Maximum parsimony strict consensus tree of Macraucheniidae excluding *Micrauchenia saladensis*.

**Figure S3** Mc II of *Micrauchenia* in comparison with Mc II, Mt IV and Mt II of other macraucheniids.

## Appendix C4

### Resource 1: Table S1. Valid genera of Litopterna and relevant South American native ungulate (SANU) recorded during the South American land mammal ages (SALMAs) in the Cenozoic

### Resource 2: List of characters and character states

### Resource 3: Matrix with scores for hypothesis 1 regarding *Simpsonotus* paraconid

### Resource 4: Matrix with scores for hypothesis 2 regarding *Simpsonotus* paraconid

### Resource 5: List of synapomorphies and autapomorphies

**Figure S1** Most parsimonious tree with node numbers for H1 and H2.

**List of synapomorphies and autapomorphies for H1**

**List of synapomorphies and autapomorphies for H2**

### Resource 6: Additional tip-dated Bayesian phylogenetic analyses results

**Figure S1** Tip-dated unconstrained Bayesian phylogeny using H2 matrix.

**Figure S2** Tip-dated Bayesian phylogeny using H1 matrix and constraining the node for the common ancestor of SANUS between the latest Cretaceous (Maastrichtian) and the earliest Palaeocene (64.0 and 72.1 Ma).

**Figure S3** Tip-dated Bayesian phylogeny using H2 matrix and constraining the node for the common ancestor of SANUS between the latest Cretaceous (Maastrichtian) and the earliest Palaeocene (64.0 and 72.1 Ma).

**Figure S4** Tip-dated topology constrained Bayesian phylogeny using H1 matrix and constraining the node for the common ancestor of SANUS between the latest Cretaceous (Maastrichtian) and the earliest Palaeocene (64.0 and 72.1 Ma).

**Figure S5** Tip-dated topology constrained Bayesian phylogeny using H2 matrix and constraining the node for the common ancestor of SANUS between the latest Cretaceous (Maastrichtian) and the earliest Palaeocene (64.0 and 72.1 Ma).